The hybrid electric vehicle

I. Forster

The Hybrid Electric Vehicle

A Thesis Submitted for

the Degree of Doctor of Philosophy

by I. Forster

Department of Engineering

University of Durham

1985

ACKNOWLEDGEMENTS

The author would like to express thanks to all for the help and advice given in the course of the work presented here.

Particular thanks are given to Dr.J.R.Bumby and Dr.P.H.Clarke of the Department of Engineering of the University of Durham for their guidance; and to Shell Research Limited, the Ford Motor Company and B.L. Cars for their interest shown in the project.

Summary

With the background of an impending price increase of petroleum based fuels in the near-term due to decreasing availability, the hybrid-electric vehicle has been shown to offer a solution to the problem of road transport dependency on this energy source without the range limitations of the pure-electric vehicle.

The technique of computer simulation has been shown to be the most feasible way in terms of cost and speed of assessing novel and complex drive-train configurations, and within this context a road-vehicle simulation program developed at the University of Durham - named JANUS - has been described.

Both pure-electric and hybrid-electric drive-trains have been assessed separately using JANUS - in terms of the effects of their respective vehicle parameters. A comparison has then been made between the pure-electric, hybrid-electric and conventional i.c. engined drive-trains in terms of primary energy consumption and on-board energy consumption (as the user sees it). It has been subsequently shown that although the hybrid-electric vehicle will be unlikely to save primary or on-board energy it may in the future present an energy cost benefit to the user relative to the i.c. engined vehicle, whilst allowing the user infinite range compared to the electric vehicle, if the cost of petroleum relative to wall-plug energy increases in the near-term - as is predicted.

Contents

Chapter 1

Introduction to the Hybrid Electric Vehicle

Chapter 2

Chapter 3

Chapter 4

Chapter 5

Chapter 6

Chapter 7

Chapter 8

Appendices

Appendix I

Appendix III

Appendix IV

Appendix VI

Appendix VII

Appendix VIII

Appendix IX

List of Tables

Chapter 1

Chapter 2

Chapter 3

Chapter 4

Chapter 5

Chapter 7

Chapter 8

Appendices

Appendix IV

Appendix V

Appendix VI

List of Abbreviations and Symbols

English Abbreviations and Symbols

A - Piston Crown Area (m^2)

ACL - Vehicle Acceleration (m/s^2)

AC - Alternating Current

CAL - Liquid fuel calorific value (arbitrary units)

CC - I.C. Enmgine Capacity (con^3)

Cd - Vehicle Drag Coefficient

Cdyn - Dynamic rolling loss term

CRl - Total Rolling loss term

Cstatio- Static Rolling loss term

Cl-C3 - Traction motor mechanical loss constants

CVT - Continuously Variable Transmission

d - Armature diameter (m)

DC - Direct Current

DOD _ Battery Depth of Discharge (%)

E - Back e.m.f. (volts)

El - Primary Source Energy consumption (Kwhr)

E2 - Secondary Source Energy consumption (Kwhr)

ED5 - 5 hr Battery Energy Density (whr/Kg)

ETV-l - Electric Test vehicle l

EUT - Eindhoven University of Technology

F - Ojective function (Kwhr)

FA - Vehicle Frontal Area (m^2)

FCS - Instantaneous liquid fuel consumption (arbitrary units)

g - Acceleration due to gravity (m/s^2)

GE - General Electric Co.Ltd.

GR - Primary Gear ratio

GR1 - Secondary Gear ratio

H - Cycle Time step (seconds)

hr - hours

Ia - Armature Current (Amps)

Iamax,Imax - Maximum Armature Current (Amps)

IAV - Average Armature current (Amps)

If - Field Current (Amps)

Ifmax - Maximum Field current (Amps)

Ifpu - Field current Fraction of Maximum

IRD - International Research & Development Co.Ltd.

JPL - Jet Propulsion Laboratory

J - Joules

K - General Braking constant

Ki - Motor torque constant

K2 - Motor Back e.m.f. constant

K2L-Ks - Motor saturation constants

K3-K4 - Chopper controller efficiency equation constants

K5-K8 - Mechanical transmission torque and power loss equation constants

KI - Rotor inertia equation constant

Km - Kilometres

Kw - Kilowatts

l - Armature length (m)

m - Transmission speed dependent torque and power loss polynominal index

mpg - Fuel consumption in miles per gallon

mph - Vehicle speed in miles per hour

m/s - Speed in metres per second

N - Rolling loss model speed index

n - Motor/i.c.engine shaft speed (rad/sec)

nb - Motor break speed (rad/sec)

nb1 - Upper break speed (rad/sec)

nb2 - Lower break speed (rad/sec)

nch - Chopper efficiency voltage dependent term polynominal index

nc - Polytropic index of compression

ne - Polytropic index of expansion

niN - Transmission input speed (rpm)

Ni/Fe - Nickel-Iron

Ni/Zn - Nickel-Zinc

nmax - Maximum Shaft speed (rad/sec)

NP - Number of Vehicle Parameters

NV - Number of values for each vehicle parameter

P - Pressure (N/M^2)

Pa - Armature Power (Kw)

Pag - Air Gap Power (Kw)

PB - Power Removed in Friction Braking (Kw)

$\bar{P}$ - Average pressure above piston (N/m^2)

PDEC - Decelerative Power Available (Kw)

PE - Power at the i.c. engine shaft (Kw)

PFRAC - Fraction at Total loss at Break point to mechanical losses

PF - Field Power (Kw)

PG, Po - Power at the motor shaft (Kw)

Pi,PI - Terminal Power (Kw)

PICE - I.C. engine rated power (Kw)

PIMAX - Maximum terminal power (Kw)

PIN - Transmission input power (Kw)

PLOSS - Power loss in a mechanical transmission (Kw)

Pmax- Maximum i.c. engine power (kw)

PMOT - Motor rated power (Kw)

PML - Mechanical loss power (Kw)

Pamax - Maximum motor shaft power (Kw)

Prated - Rated power (Kw)

PTOT - Total Installed power (Kw)

PW - Power available at the wheels for regeneration (Kw)

r - Crank radius (m)

$\bar{r}$ - Average Crank radius (m)

R - CVT output speed (rad/sec)

Ra - Armature Resistance (Ohms)

RE - Generator Set speed (rpm)

Rf - Field Resistance (ohms)

RG - Motor Armature Inertia (Kgm^2)

rm - Armature radius (m)

RMIN - I.C. Engine minimum speed (rad/sec)

RSW - Motor speed corresponding to voltage (rad/box)

S - Piston Stroke (m)

SAE - Society of Automotive Engineers

SCT - South Coast Technology

SFC - Specific fuel consumption (arbitrary units)

SI - System International

SOC - Battery state of charge (%)

t - Cycle time (seconds)

T - Torque (Nm)

$\bar{T}$ - Average Torque (Nm)

Ta - Ambient temperature (°C)

TAg - Air Gap Torque (NM)

TE - I.C.Engine torque (Nm)

TG - Clutch/torque converter output torque (Nm)

TIN - Transmission Input torque (Nm)

TLOSS - Torque loss in a mechanical transmission (Nm)

Tm - Mechanical loss torque (Nm)

To - Motor shaft torque (Nm)

Tomax - Maximum motor shaft torque (Nm)

Trol - Tractive effort to overcome rolling losses (N)

TR - Road load torque at torque split point (Nm)

V - Volume of cylinder (m^3)

Va - Armature voltage (volts)

Vamax, Vmax - Maximum armature voltage (volts)

VaV - Average armature voltage (volts)

VDEM - Motor Demand voltage from the battery (volts)

Ve - Vehicle velocity (mph)

Vf - Field voltage (volts)

VFmax - Maximum field voltage (volts)

VHW - Head Wind (mph)

VSW - Battery switch voltage (volts)

W - Work done in a cylinder process (J)

WBATT - Battery weight (Kg)

WT - Component weight (Kg)

WPR - Weight to power ratio (Kg/Kw)

Wv - Vehicle weight (Kg)

x - Distance travelled (miles)

X - Primary source fraction of road load

Ycold - Cold start penalty as a fraction of fully warmed-up fuel consumption - at 0°C

Yhot - Cold start penalty as a fraction of fully warmed-up fuel consumption - at 20°C

YTA - Cold start penalty as a fraction of fully warmed-up fuel consumption - at Ta°C

Greek Symbols

$\Delta\chi$	-	Increment of torque/power split fraction
Δ SOC	-	Increment of battery state of charge (%)
η	-	General Efficiency (%)
γ	-	Index of Insentropic compression/expansion
λ_1	-	Primary source Weighting factor
λ_2	-	Secondary source Weighting factor
ν	-	Arbitrary Hybrid Electric Vehicle control variable
ρ	-	Density (Kg/m^3)
θ	-	Angular Displacement (arbitrary units)
$\ddot{T}$	-	Time to discharge (arbitrary units)

CHAPTER 1

Introduction to the Hybrid Electric Vehicle

1.1 Future Energy Supply and Demand

Future world energy supply will depend upon the availability, the rate of extraction and the rate of production of the various primary energy sources. World energy demand, on the other hand, will depend to a large extent on the consumer's expectations of supply. Therefore any predictions of future energy supply and demand can be many and varied due to the different senarios forseeable.

Of the numerous energy supply and demand predictions, covering various senarios, there is general agreement that energy demand will increase steadily into the next century. However, the total energy supplied will depend upon the availability (and hence price) of the world's individual energy resources at any given point in time, due to their respective rates of consumption (D.O.E. 1979).

Of all the primary energy sources, petroleum (or crude oil) forms the largest single source upon which the world depends at present to meet demand, and, given future predictions of supply and price, it seems likely that it will continue to do so at least up to the turn of the next century (Ford Energy Report Vol.1) (D.O.E. 1979).

At its predicted rate of usage and availablity, and assuming no significant new finds, the world's oil resources will last until the early part of the next century (Ford Energy Report Vol.1). If, however, new and significant finds of petroleum are made then this time scale will obviously lengthen - depending upon any associated production difficulties (and hence price).

Because petroleum forms such a large proportion of the total world energy supplied - a picture echoed in Europe and the U.K. (D.O.E.1979)

(Ford Energy Report Vol.1) (Bumby et al.,1982), shown in Figure 1.1, it seems appropriate that in order to avert any long-term energy supply crisis the dependence on petroleum must be reduced in the various sections of usage: i.e. power generation, transport, domestic and industrial heating, lubrication and chemicals.

1.2 Petroleum Usage Trends

Figure 1.1 also shows how the supply of petroleum, if broken down into the aforementioned areas of use in the U.K., the road transport sector forms the largest single sector (40%). Furthermore, because other crude oil fractions are being replaced by alternatives (also shown in Figure 1.1), in the foreseeable future it is likely that the percentage used in transport will increase (Bumby et al.,1982). It is therefore reasonable to assume that the largest reductions in the rate of consumption and in dependency will come from this one area, although reductions from the other areas can only help also.

1.2.1 Petroleum Usage Trends in the Road Transport Sector

The road transport sector as a petroleum user was broken down into the various forms of road transport (Bumby et al.,1982), and was observed that the largest single market (the passenger car market - being 92% of the total) is also the largest single user of petroleum (60% - and in particular, gasoline or petrol).

The passenger car market was also broken down to show precisely, by engine size or capacity, present and predicted market size and petroleum usage trends - and these are given in Figure 1.2 and Table 1.1 respectively. It was found that at present a passenger car with an engine capacity of between 1200cc and 1800cc forms by far the largest single market (70% of the total vehicle market), and hence fuel user (46% of the road transport sector usage); and also that this market is tending to increase. This class of vehicle in European terms is regarded as a "medium sized passenger car".

Of the other classes of road-transport vehicle : the small car (1000cc) consumes only 7% of the fuel used in road transport but has 10% of the road transport vehicle market. As Figure 1.2 shows, the market for this vehicle is surprisingly on the decline. A similar picture is drawn for the large car (>2000cc). Light goods vehicles or delivery vans, consume 11% of the road transport fuel usage and have a market share of 7%; and heavy goods vehicles (lorries) consume 21% of the road transport fuel usage, but have only 4% of the total vehicle market.

It is clear that none of the classes of vehicle other than the medium passenger car offers ,either the potential for significant reductions in petroleum usage and dependency in the road transport market, or a sufficiently large vehicle market to be able to justify any fundamental changes in vehicle design that may be necessary to achieve these ends.

However, as far as the operator is concerned running cost reductions as a result of fuel savings must also be considered along with any possible increases in vehicle purchase cost. The increase in initial purchase cost would usually be spread over the lifetime of the vehicle in order to assess any benefit or penalty to the user when compared with fuel savings. So, although it may seem for classes of vehicle other than the medium passenger car not worthwhile from an energy consumption point of view to introduce new and novel drive-train configurations, from the point of view of the costs to the user it still may be justified.

As the medium passenger car clearly offers the potential for petroleum dependency reductions and for possible running cost reductions to the user, then it would appear that it is in this area of the road transport market that efforts should definitely be concentrated.

1.3 Conservation of Petroleum Resources by Reducing Consumption and Dependency in the Road Transport Sector

Under the heading conservation will come the headings of dependency reduction and reduction in the rate of consumption. The methods to be discussed here will cover both aims.

1.3.1 Reducing Fleet Miles

One of the ways of reducing vehicle fleet miles is to increase the price of petroleum based fuels (which may occur as they become more scarce), but as experience with the 1973 and 1979 oil shortages has shown, although an initial reduction in fleet miles is achieved, the market place will then stablise back to the situation before the upheaval (Bumby et al.,1982) (Bumby et al.,1984).

Another way of reducing fleet miles would be to induce a system of rationing. This would have the effect of reducing the consumption rate and of conserving the petroleum resources.

1.3.2 Increased Vehicle Efficiency

By increasing vehicle efficiency, if the vehicle fleet still covers the same number of miles, because the vehicles are now burning fuel more efficiently the consumption rate will reduce and petroleum will be conserved. If, however, the tendency is for fleet miles to increase then the consumption rate may remain the same or even increase.

Increases in vehicle efficiency can be achieved by reductions in vehicle aerodynamic drag and rolling losses, improved transmission efficiency, reductions in vehicle weight for a given vehicle class, better i.c. engine/transmission matching and improved i.c. engine efficiency. Reductions in vehicle aerodynamic drag losses are being achieved by greater attention to body design, and reductions in rolling losses due to recent advances in tyre technology. Transmission efficiency can be improved by using new lubricants to reduce oil churning losses.

Vehicle weight reductions can and are being achieved by substituting new materials for the 'traditional' materials - such as high strength steel (HSS), aluminium alloys and glass and carbon fibre materials. Finally, improvements in i.c. engine efficiency may come from the incorporation of electronic controls, variable valve timing and also the reduction of thermodynamic and friction losses. Other areas such as engine/ transmission matching and fuel cut-off at idle and/or overrun come under a more general heading of overall vehicle control, but must also be considered as they are both significant.

Trends in present day road and vehicle designs show that all of the above areas are being explored (Ford Energy Report vols.I, II and III) in order to increase overall vehicle efficiency - although it is the manufacturers themselves through competition who have conditioned the potential buyer to expect an efficient road vehicle.

An additional method of increasing overall vehicle efficiency is to recover energy that would otherwise be lost in vehicle braking by means of either a flywheel (Beachley et al.,1978)(Frank et al.,1984) (Bumby et al.,1977), a hydraulic pneumatic accumulator (Bumby et al.,1977) or an electric motor/generator/storage battery combination (Bumby et al.,1977).

This energy can then be used again during the acceleration phase of the vehicle to supplement the main power source, enabling this power source to be reduced in size for a given acceleration requirement, so increasing its average 'load-factor' and hence its average efficiency.

This concept will come under the additional heading of the 'hybrid vehicle' but it must also be stated here as a means of improving vehicle efficiency (particularly as regards i.c. engine efficiency).

Finally, moving to more efficient heat-engine cycles (that approach the Carnot cycle) must also be considered, but past and present experience has shown that the most promising (in terms of efficiency) cycles are the most difficult to achieve mechanically.

However, the Stirling cycle gives the best compromise on thermal efficiency and complexity as experience stands to date. It has found several applications, although not in the road-transport area as yet, despite studies (Curtis,1984) for city buses with a view to reducing emissions, noise and petroleum dependency rather than increasing efficiency.

The reductions in vehicle fuel consumption due to possible improvements in the areas discussed can be broken down as Table 1.2 shows.

Increasing vehicle efficiency to the extent shown in Table 1.2 may only serve to increase vehicle fleet miles travelled, if to the user running costs remain the same. Hence, the consumption of petroleum will continue along its present trend. Even if fleet miles were to remain constant, petroleum dependence would still be present - i.e. there still would be an energy crisis, only further into the future than is predicted at present. To reduce petroleum dependence, petroleum based fuels must be displaced or substituted by some alternative energy source (s).

1.3.3 Total Substitution by Alternative Fuels

Substitution of petroleum fuels can be achieved in either one of two ways. Firstly, the fuel used in existing prime-movers such as the spark-ignition and compression-ignition engines can be derived from other sources such as oil shale, tar sands and coal (House of Lords,1980), and secondly, by adopting alternative prime-movers such as the gas-turbine, the stirling engine, the Rankin engine and the electric traction motor, a much broader base of fuels can be used for road transport (including the less refined distillates of petroleum if required).

To consider existing prime-movers, first of all, the techniques of deriving existing fuels from new sources have not been perfected, and in the case of deriving gasoline from coal, the process is considerably less efficient than the petroleum-gasoline route - typically 50-60% and 90% respectively (House of Lords,1980). Other alternative fuels such as hydrogen, that offer similar properties already enjoyed by using petroleum fuels, suffer from storage problems in that they can only remain in liquid form at very low temperatures and/or very high pressures. However LPG is extensively used in vehicles at present, but mainly in 'dual-fuelled' vehicles, gasoline plus LPG, where the fuel system is only optimised for one (usually gasoline) fuel. Another gaseous fuel alternative for total substitution is methane.

As well as the storage problems associated with gaseous fuels, at present there is no infrastructure for fuelling on the scale of gasoline or diesel. Therefore any move in this direction would require a significant expenditure in developing such an infrastructure.

In the case of alternative prime-movers, all of the types described suffer from serious drawb acks that have not been satisfactorily overcome when compared to existing prime movers.

The gas turbine suffers from poor part-load efficiency which would be a serious drawback for road-vehicle applications (JPL-Shall we have a new engine) (Bumby et al.,1982).

The Stirling engine, because of its mechanical complexity, has not been perfected as yet, and designs always suffer from thermal inertia due to the comparatively tortuous heat-transfer path (JPL-Shall we have a new engine) (Bumby et al.,1982).

Finally, the electric motor, although being simple in design and high in efficiency, relies in one form, on the road vehicle having an on-board energy storage medium (the traction battery) which at its

present state of development has neither the energy density (energy stored per unit mass of storage medium) of liquid or gaseous fuels, or an energy density/power density characteristic in which energy stored is independent of power drawn/demanded per unit mass at storage medium - a characteristic of liquid fuels. For the application of the electric motor in another form the vehicle may be connected to the mains supply by overhead lines or live rail with no limitation on range and performance but now having restricted 'movement' and the requirement for a complex and expensive infrastructure of power supply (if not already in existence) with all of the safety and environmental problems associated. Movement can be improved by a combination of on-board battery storage and overhead lines - sometimes called the 'Combat' trolley bus (Bradford et al.1978) - or by a combination at a heat engine plus overhead lines - sometimes called the 'duo-bus' (Collie 1979).

Although the electric vehicle range performance and/or movement tends to be restricted when compared with vehicles powered by existing prime movers, the poor power density of the traditional lead-acid cell can be overcome by using a device capable of high power density in its place during short-term high power (hence current) drains, and simply leaving the lead-acid battery to deal with the low power long-term drains. This can be achieved by using either a flywheel, a hydraulic/pneumatic accumulator or a more advanced cell (Ni/Zn...etc) - sometimes called the 'Electric hybrid' (Chang,1978)(Kugler 1973).

In the event of the on board storage medium being adopted for the electric traction motor, an infrastructure of 'refuelling' stations would have to be provided if only to allow vehicle ranges to match what can be achieved by a conventional vehicle on a tank full of gasoline or diesel fuel. Because of the slow battery charging time, some method of battery exchange would be required, with the inherent problems of introducing the required infrastructure (Hoffman,1969)(Gurley 1977) (Hagen,1974).

1.3.4 Partial Substitution by Alternative Fuels

Partial substitution can be achieved in one of three ways. Firstly by direct substitution of petroleum fuels using fuels derived from alternative sources such as methanol and ethanol - commonly referred to as 'extenders'. Secondly, by indirect substitution of alternative fuels such as stored electrical energy (derived from coal, oil, nuclear...etc). Or thirdly, partial substituion by recovering what would be otherwise wasted energy during vehicle deceleration by regenerative braking into a flywheel, a pneumatic or hydraulic device or an electric storage device. This energy then being used during the acceleration phase of the vehicle once again.

Direct substituion by alternative fuels such as methanol, ethanol and alcohol can only be achieved up to a certain proportion (5%), because of existing prime-mover tolerance without considerable modification (Bumby et al.,1982) (Ford Energy Report,1981).

Indirect substitution by in board stored electrical energy uses existing electric vehicle technology and combines the benefits of both the electric vehicle and the i.c. engine vehicle whilst substituting petroleum for an energy source derived from a broad base such as coal, oil, nuclear, hydro-electric and in the future, solar, wind and wave.

Finally, for the recovery of otherwise wasted vehicle energy - so effectively making the vehicle more efficient - the most popular methods appear to be either the flywheel, the pneumatic/hydraulic and the electrical types. The flywheel method has the advantage of being simple in principle, although designs tend to become complex with the need to reduce bearing and windage losses. In order to minimise weight ($\propto$ diameter^2) rotational speeds tend to be high to achieve adequate energy storage(up to an order of magnitude higher than for the prime mover); and, because the flywheel speed must be matched to the transmission under all conditions to control the flow of power, a CVT is

required for this component also (Beachley et al.,1978) (Frank et al.1984). Also, at least with respect to the hydraulic/pneumatic method, the flywheel tends to be 'bulky' -i.e., difficult to install without restricting payload and generally heavier (Hamerstrom, 1984). However, one particular advantage it has is the capability of high power density, limited only by the handling capacity of the transmission. However, because the flywheel does suffer from relatively low energy density, the vehicle would be unable to depend upon this energy source for significant periods if required. The hydraulic/pneumatic accumulator systems echo the advantages and disadvantages of the flywheel system in terms of power and energy density, but with the advantage over the flywheel of easier component displacement, made possible by the flexible hydraulic connections between. The result is that the hydraulic/pneumatic system has tended to be favoured - at least when applied to commercial vehicles - over the flywheel system (Hamerstrom,1984) (Martini,1984) (Dorey et al.,1984).

Finally, the electrical system, although suffering from lower power density (power delivered and received per unit mass of storage medium) than the aforementioned system, because of a substantial improvement in energy density (energy stored per unit mass of storage medium) enables the vehicle to depend upon this power/energy source alone for significant distances if required.

Thus the "hybrid-electric" vehicle offers the advantage of the electric vehicle in terms of being able, when required, to totally displace petroleum by the second on board energy source, but without the restricted range and/or movement associated.

It is for this reason, and the fact that the concept uses components that at least in Europe (as far as electric vehicle experience is concerned) are well developed over a number of years, that the "hybrid-electric" vehicle has tended to be favoured as a possible means of reducing petroleum consumption or dependence.

1.4 The Hybrid Electric Vehicle

Hybrid vehicles - whether a heat-engine electric traction motor/generation combination or the heat-engine hydrostatic pump/motor combination - can be either of 'series' or 'parallel' configurations.

In the series configuration the two on board power sources - be they the heat-engine and hydraulic motor/pump or heat-engine electric motor/generator - are connected in series. Figure 1.3 shows for the heat-engine traction motor/generator (hybrid-electric) combination how this is achieved.

For the parallel configuration the two on board power sources are connected in parallel and Figure 1.4 shows, again for the hybrid-electric case, how this is achieved.

When comparing the 'series' and 'parallel' configurations, the result is that for the parallel configuration fewer energy conversions are apparent. In addition, one of the two power sources for the series configuration is required to be rated to meet the full vehicle

requirement, whereas for the parallel configuration the combined output of the two power sources can be rated to meet this demand. For the series configuration, however, because of the 'soft' electrical connection between certain components, the i.c. engine may be totally decoupled from the road conditions (effectively an electrical or hydrostatic CVT) and also component displacement is made easier.

Both hybrid-electric and mechanical-hybrid alternatives can be designed to 'load-level' the primary or heat-engine power source in that the deceleration energy of the vehicle can be recovered regeneratively into the on-board storage device (battery, flywheel or accumulator) and then used to assist the heat-engine during the next vehicle acceleration phase. The aim of load-levelling the heat-engine is to enable a smaller unit to be used at higher average load-factors and hence efficiency (as was discussed in section 1.2), so allowing the hybrid to save energy - the 'energy saving aim'.

In the case of the flywheel and hydraulic accumulator storage devices, energy can only be held for a comparatively short period of time - due to windage and bearing losses for the flywheel and heat losses for the accumulator - so necessitating the use of the stored energy immediately. Because this is not the case for the battery storage device, and because the energy storable per unit mass is greater, this medium can be used to propel the vehicle for significant periods other than acceleration.

Here petroleum based fuels that would otherwise have been consumed are displaced by mains electricity and its attendant broader energy base. This effect can therefore be called for the "petroleum displacement" or "petroleum substitution" aim and although an energy

consumption analysis can be performed, it requires values for energy conversion efficiency of the petroleum to gasoline and coal to battery energy routes. These are not required for the aforementioned "energy saving" aim as there is a direct comparison possible between the hybrid and the conventional i.c. engined vehicle since no wall plug energy is consumed.

Studies into the 'hybrid-electric vehicle' alternative during the initial period of interest in the 1960s and early part of the 1970s were almost exclusively achieved by means of vehicle construction, with computer simulation - if used at all - forming a final design tool. Now, with vehicle construction still, obviously, a necessary part of any hybrid-vehicle study, the emphasis has changed in that with the advent of sophisticated and flexible simulation packages, computer simulation is being employed, to varying extents, during the initial concept stage also.

1.4.1 Hybrid-Electric Vehicle Construction

During the 1960s and early 1970s the main aim of the hybrid vehicle was emission control (Bumby et al.,1977) which was (and still is) of considerable importance in the U.S.A. and Japan and is of growing importance in Europe and the U.K.

Now the emphasis of hybridisation has firmly shifted to improving vehcile fuel economy (spurred on by the 1973 and 1979 oil shortages). Experience has also spread further afield - from the U.S.A. to Europe and Japan (Humphreys et al.,1978).

Although in Europe emissions and noise regulations are becoming as tight as those in the U.S.A. and Japan, the emphasis is still (and will be for the near-term) on improvements to vehicle design to reduce fuel consumption.

Both the 'series' and 'parallel' hybrid-electric vehicle configurations discussed in section 1.4 have been studied in the past. These configurations have tended to find very different applications in the road-transport market, in that during early hybrid work in the U.S.A. with the emphasis firmly on emissions the 'series' configuration with its ability to allow the i.e. engine to run at optimum conditions for minimum emissions was commonly adopted. Now with vehicle efficiency of considerable importance, at least for the passenger car the 'parallel' configuration, with its inherent efficiency advantage over the series configuration, is now tending to be favoured - both in the U.S.A. and in other markets now involved in hybridisation.

1.4.1.1 Series Configurations

Series hybrid-electrical vehicle configurations have tended to be applied to city buses (Brusaglino, 1981) where the advantages of component displacement and potential for reducing emissions outweigh the shortfall in efficiency compared to the parallel configuration (Sampson, et al 1972) For bus applications, minimising intrusion into the passenger carrying area is important, and this has made the hybrid drive train an alternative to the electric drive-train. The traction battery for the electric case tends to become so large in order to meet average daily ranges, that useful payload has to be significantly reduced within the confines of the 16 tonnes GVW. Although Fiat (Brusaglino, 1981) have demonstrated significant fuel economy improvements over the conventional bus, a true comparison was not made because the conventional vehicle was of current design, whereas the hybrid bus could only realistically be considered as a near-term development.

Hence, the i.c. engine control features for the hybrid (such as fuel off at idle and overrun) plus general improvements in component efficiency, could also just as easily be applied to the conventional vehicle.

A second hybrid bus project had also been proposed as a design to primarily reduce emissions, and utilizes a gas-turbine running at the optimum conditions for low emissions (Brusaglino et al.,1974).

Although the series configuration has generally found favour more with larger vehicles in the past, a number of smaller vehicles have also been constructed. One partcular example, the 'Stirlec' passenger car (Agarwal et al.,1967) combined the advanced features of a stirling engine and a.c. induction motor into an existing vehicle design (Opel Kaddet).

This vehicle was essentially intended as an electric vehicle with the small generator-set provided to extend all-electric range. Performance was therefore comparable with that of an electric vehicle.

Modifications to an existing vehicle chassis to incorporate the hybrid drive-train has proved common practice-especially where a comparison was to be made with the conventioal drive-train in that design (as was the case for the bus (Brusaglino,1981)). However, modifying an existing vehicle does not optimise hardware and may even dictate how the actual drive-train is designed. This may not be the case for the larger vehicles, because of the increased scope for installation. Thus, a purpose designed hybrid bus, say, may look very much like its conventional counterpart.

Recently in the U.K., Lucas Chloride have developed a hybrid car (Harding et al.,1983), which although essentially a parallel configuration, has the ability to run as a series configuration. So, although purpose designed, is not fully optimised in terms of hardware.

A purely parallel or series configuration, alone, may adopt either the front-engine/motor/generator- front wheel drive arrangement, or the rear engine/motor/generator - rear wheel drive arrangement - so making battery displacement simpler, reducing weight, frontal area and drag coefficient.

1.4.1.2 Parallel Configurations

With the parallel configuration, particularly for small vehicles (passenger cars), component installation is made more difficult than with the series configuration due to the mechanical connections between components. However, despite this drawback, the parallel configuration has tended to be applied to passenger cars because of the inherently higher energy conversion efficiencies than for the series. Such was the case for all 4 design proposals in phase I of the DOE Near-Term-Hybrid-Vehicle program in the US - submitted by G.E..,South Coast Technology (SCT), Minicars and Fiat (Sandberg 1980). In phase II, GE were selected to implement their design (Burke, et al.,198) (Trummel et al., 1983). All 4 of the phase I proposals were modifications of existing vehicle chassis designs, with improvements (where possible) to reduce drag and rolling losses and to save weight (Sandberg,1980).

As discussed in section 1.4.1.1 the Lucas hybrid car is primarily intended as a parallel configuration, although the front engine/motor/ generator - rear wheel drive arrangement appears to have made battery displacement difficult, caused body line to rise, probably resulted in a heavy design and also increased vehicle frontal area.

For example, a power train installation at the front with a front-wheel-drive arrangement would have resulted in no central drive-shaft. The traction batteries could then be installed either totally or at least partly in this position, and because the passengers may not now be sitting upon the batteries, it might be possible to lower the seat-level, roof line and hence reduce frontal area. The absence of the central drive-shaft would also have the additional effect of reducing weight which is a common practice with conventional i.c. engine vehicle designs at present.

In Italy, as well as the work performed on buses, Fiat have also built a parallel configuration passenger car (Morello et al.,1979) following computer simulation work on the design. Little has been published on the experimental work, except to validate the mathematical modelling. A comparison was possible, however, between the hybrid and the conventional vehicle upon which it was based but the conventional vehicle results were not considered over the hybrid vehicle time-scale.

In the USA, the Universty of Wisconsin (Beachley et al.,1973) designed and built a hybrid electric car power plant consisting of the i.c. engine and the traction motor/generator driving through a novel drive-train consisting of an epicyclic gear train. Although again, a modification of an existing vehicle chassis, it was primarily built to study the control options possible with this drive-train.

In the U.K. a joint effort by the University of Swansea and Dragonfly Research Ltd., (Watson and Lee) resulted in the construction of a hybrid delivery van - again, based on an existing vehicle design, employing a parallel configuration and including the unusual feature of discs motors as the electric traction devices.

1.4.1.3 Hybrid - Electric Vehicle Assessment by Vehicle Construction

The advantage of performance assessment of a hybrid-electric or any other type of road vehicle as a result of vehicle construction is that energy consumption over realistic driving cycles (actual road conditions) can be determined. However, short of building a fleet of vehicles that will embody all of the necessary drive-train configuration, component size and component type variations required of a comprehensive study, the assessment will be committed to a single configuration with fixed component sizes and types. Furthermore, if a large number of hardware variations were to be possible, then there would arise the question of driving cycle repeatabilty in order to make a valid comparison between alternatives and this would clearly depend upon the driver(s).

Clearly, in terms of both cost and consistency of results an exhaustive study based on hardware construction would be undesirable. A cheaper and also faster method would be by the use of a computer simulation program, where although the assessments would be made over arbitrary driving cycles, because of the accurate repeatability of the cycle, a valid comparison between the different options can be made.

1.4.2 Computer Simulation Studies of Hybrid-Electric Vehicles

The advantages of the computer simulation method of studying the energy consumption of novel as opposed to conventional drive-train configurations are relatively fast and relatively inexpensive compared with, say, building vehicles or rig-testing. Providing adequate attention has been devoted to component modelling, it will aso provide reasonable accurate 'absolute' as well as relative results. Furthermore, results can be projected forward in time to account for the timescale of developing and implementing these 'novel' configurations with relative ease.

However, as a given configuration can only be simulated over prescribed driving duties, unless data for a particular vehicle has been gathered empirically and the cycle is repeated consistently for the vehicle, then this cycle can only approximate to what will occur in practice and 'absolute' results will suffer.

Nevertheless, when comparing drive-train configurations, component types and component sizes, it is the trends in results that are important and so simulation over a realistic duty cycle would only be a final design consideration with hardware construction imminent.

1.4.2.1 Studies Undertaken

The simulation studies regarding hybrid-electric vehicles, have not all employed the use of simulation programs capable of a 'general' approach.

Indeed, a study performed by the Ford Motor Co.(Unnerwehr et al.1976) opted for the parallel configuration with a definite arrangement of components and furthermore used a Nickel-Cadmium battery when comparing with the conventional i.c. engine powered drive-train. No weight increase for the hybrid configruation was assumed and a current conventional i.c. engine vehicle was used for comparison (considering the near-term time scale, at least, for the hybrid). These factors must be taken into consideration when studying the 30-100% improvement over the conventional vehicle that was quoted.

A study by the Aerospace Corp. (Sampson et al.1972) considered a fixed parallel and a fixed series configuration when considering exhaust emissions.

Both of the above studies looked at several vehicle applications for the configurations under consideration : the former considered a large car and a delivery vehicle; whilst the latter covered a range of vehicles, from commuter car to city bus. Although the latter study found the parallel configuration 10-20% more efficient than the series, because the emphasis was on the reduction of emissions - concluding points were contrary to energy reduction aims generally.

Another emissions study, by General Motors (Liddle,1973 (a) and (b)) studied both parallel and series configurations and compared them with a conventional vehicle. However, as with the Unnewehr study, no weight increase was assumed for the hybrid case.

Several points raised by the Unnewehr study regarding hybrid vehicle control are consistently raised by other computer simulation based studies considered here, and indeed have been features of studies featuring vehicle construction. These points are : the i.c. engine only to be used for heavy loading conditions (acceleration); and fuel to be cut from the i.c. engine when not in use. However, the control strategy was not optimised in the Unnewehr study in order to reach those conclusions.

As far as the Near-Term Hybrid Vehicle program was concerned, the submitting contractors (G.E., S.C.T., Minicars and Fiat) all relied to varying extents on computer simulation for their respective design studies (Sandberg,1980). All participants studied the series and parallel configurations, with and without flywheels in drivetrains, and compared them with conventional and electric vehicles in terms of cost, weight and performance. The HYVEC and HYVELD programs (Burke et al.,1982) (Burke et al.,1980) were used for the G.E.design study. SCT (South Coast Technology) merely used computer simulation to determine component sizes (Schwarz,1980) after first opting for the parallel

configuration. Fiat, however, (Traversi et al.,1980) used simulation to study several parallel configurations: the torque split point up and down stream of the transmission (a CVT); no transmission at all; and the effect of decoupling the electric motor when not in use.

At Fiat there has also been the work on the hybrid passenger car prototype (Morello et al.,1979) and here a comparison between series and parallel configurations was possible, as well as between the parallel configuration selected and the conventional vehicle upon which the hybrid was based. However, this conventional vehicle was not projected into the future to include conventional i.c. engined vehicle energy consumption improvements.

A study by the Aerospace Corp.(Lapedes,1971) into low-speed and high-speed buses, considered both energy consumption and emissions. Configurations were selected for each bus type and the study proceeded to look at the effects of different i.c. engine types on the conflicting requirements of fuel consumption and emission reduction.

The HEAVY simulation program (Hammond et al.,1981) has been used in two studies into hybrid-electric vehicles. At the University College Swansea (Watson et al,1984) a light goods vehicle already built was the subject of a simulation study intended to both improve the vehicle design and also the mathematical modelling. The original vehicle building program was the result of a previous simulation study using a purpose written program - looking at both the delivery van and the small city bus (Watson and Lee). At Boeing (McGehee et al.1981) the effects of control strategy on vehicle energy consumption have been studied using a fixed parallel configuration over a fixed cycle (J227aD).

A recent study in the UK (Nightingale et al.,1984) compared a hybrid and conventional i.c. engined vehicle by considering the

hybrid's electrical system purely as a load-leveller in that the traction motor would assist the heat engine during acceleration, recover braking energy regeneratively and convert excess energy from the heat energy into stored battery energy. As the battery would experience no discharge per driving cycle when in this mode, this would correspond to the energy saving aim.

Although a single parallel configuration was used to study the effects of one power source size relative to the other (motor fraction) the battery size was not studied, nor did the study project the results for the conventional vehicle forward in time. Furthermore, although the power split between the two power sources was optimised, ECE-15 gear shift points were adhered to throughout and since the vehicle could only meet the acceleration requirements of the ECE-15, performance was therefore not of present-day expectations.

1.5 Units of Measurement for Road Vehicles

Whilst it is desirable to express the results of any study into road vehicles in units that are consistent - be they S.I., British or U.S. - practice in the automotive industry is to use a mixture of units that are appropriate to the physical conditions.

Not only is this the case for the conventional i.c. engined vehicle, but, in order to make sensible comparisons, has also been the case for the hybrid-electric vehicle studies, described in section 1.4, and also the electric vehicle.

The physical conditions that determine the units used for road vehicles are largely due to the environment in which the road-vehicle operates but also due to the influence of historical practice.

Because the road-vehicle covers distances that are more easily expressed and grasped in units such as kilometers or miles, KM/hr or mph as measures of vehicle speed have been preferred to the S.I. equivalent of m/s.

Similarly as regards energy consumption, because of the need to express results in units that have meaning to the user, as far as liquid fuel consumption is concerned the units of volume, such as gallons or litres, have been adopted, whereas for mains electricity the domestic units of Kwhr have been preferred to the S.I. equivalent of J.

As a result for the conventional i.c.engined vehicle it is common to find vehicle speed expressed in mph or Km/hr and for energy consumption in mpg or ℓ/100Km. Although vehicle speed is expressed also in mph or Km/hr for the electric vehicle, energy consumption is usually expressed in Kwhr/mile, Kwhr/Km or even Kwhr/tonne/Km. Energy consumption for the hybrid-electric vehicle, therefore has tended to be expressed in units appropriate to both energy supply routes.

Therefore despite it being possible for any study to express all results in a consistent set of units, it has been found necessary for both hardware construction and computer simulation to retain the aforementioned mixture of units in order to give physical meaning to the results.

In the results presented here, liquid fuel energy consumption will be presented in the aforementioned miles per gallon (mpg), whereas battery (wall-plug) energy consumption will be presented as either Kwhr, Kwhr/mile or Kwhr/tonne/Km. As far as vehicle velocity is concerned, the single units of mph will be adhered to throughout in order to achieve a degree of consistency between this and energy consumption.

1.6 Conclusions

Of the alternative ways discussed in this chapter of both conserving (i.e. reducing the rate of consumption) and reducing the dependence upon, petroleum based fuels what route is eventually taken will be determined by the future road-vehicle technological developments in the areas covered, the possibility of new and significant finds of

petroleum or the development of a total substitute and the various political pressures that may be brought to bear.

Using computer simulation, results can be projected forward in time with relative ease in order to assess the impact of the aforementioned technological advances. What is important to bear in mind here is that only the developments possible to a particular vehicle (hybrid-electric, pure-electric or conventional vehicle) need be considered and developments applicable to each in the same proportions fixed as a common base. Similarly, the effects of the various energy supply senarios - such as producing gasoline from alternative primary sources such as coal - can also be included.

Political pressures such as those affecting future energy prices and taxation will be difficult to both predict and to quantify, and although cannot be realistically included in a computer simulation study at this stage, must nevertheless be born in mind.

From the discussion in section 1.3, the most feasible method of petroleum displacement at this point in time, and probably for the foreseeable future, is the "hybrid-electric vehicle" both in terms of performance and in terms of market acceptance (unlike the electric vehicle with the inherent restrictions on range and/or movement).

It has been the hybrid-electric vehicle that has been the focus of the most attention in the past, but mainly as a result of actual hardware construction.

Despite the inherently narrow approach of vehicle construction - which is usually committed to a particular solution - there have been valuable lessons learned, not least of which is the need to broaden the approach. To achieve this by hardware construction would be expensive and time-consuming, but by the use of computer simulation a vast range of possibilities can be studied before commital to either a rig-test phase, vehicle installation of a drive-train or vehicle design from scratch.

The current trend in road-vehicle assessment is for computer simulation techniques to be used more and more, but the majority of computer simulation programs available have been written with particular drive-train configurations in mind - so narrowing the approach once more. The few computer simulation based studies that have employed the use of a program capable of a general approach have either tended not to go far enough in considering all of the possible alternatives, have opted for a solution on the basis of previous work or have produced results that are only applicable to a particular market in terms of vehicle weight, general power source sizes, emission constraints, aerodynamic characteristics and so forth. Because the most detailed studies produced using computer simulation to date have been based on market conditions in the U.S., the latter case is certainly true. But all simulation studies have been guilty to varying extents of taking too many short-cuts on the basis of previous work in order to reduce the computational burden.

There is therefore a need for a more detailed computer simulation based study into the hybrid-electric vehicle concept based on European market conditions, and here at least it would appear that the most likely market sector to aim for is the "medium sized passenger car".

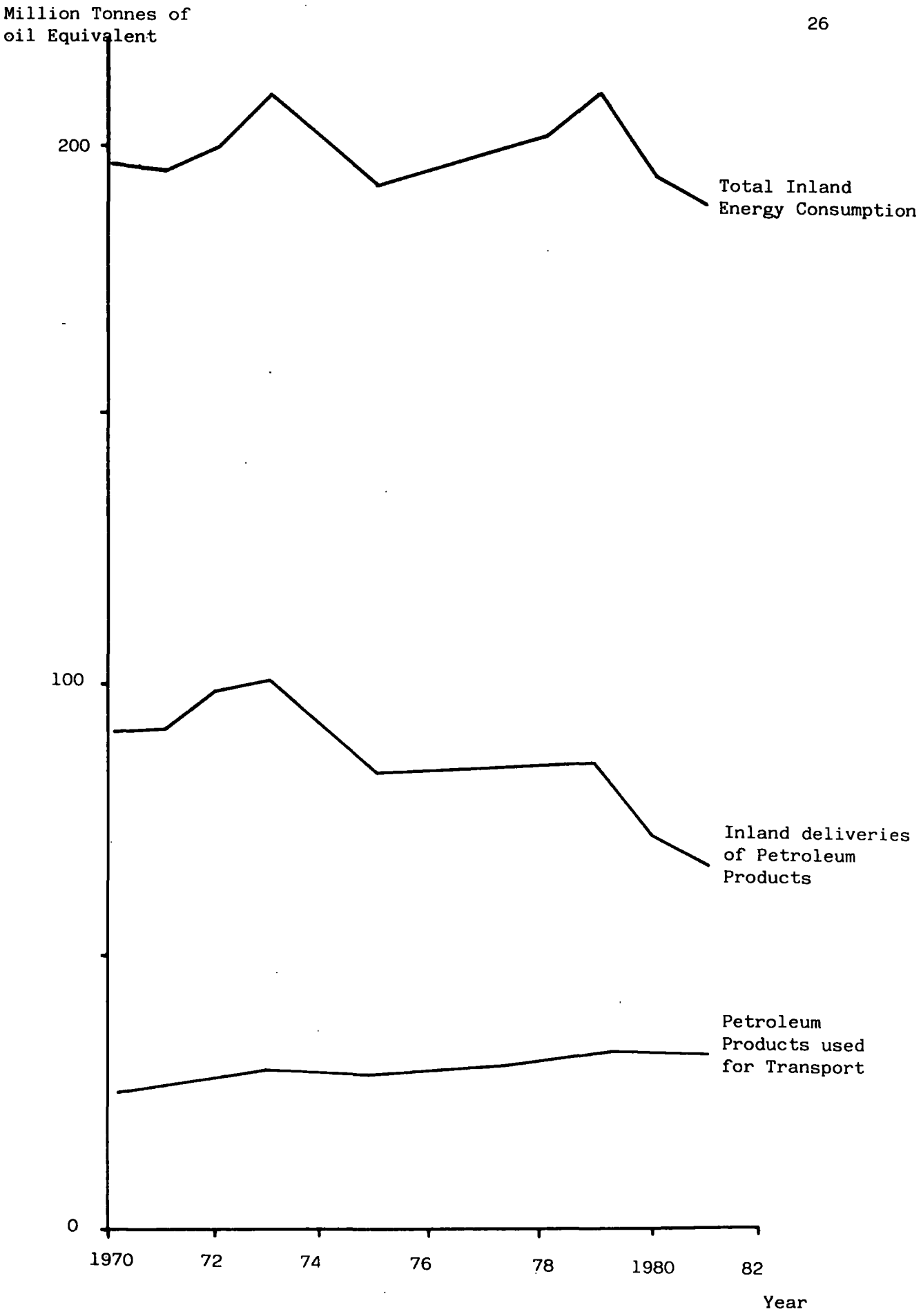

FIGURE 1.1 Energy Supply and Demand in the U.K.
(Bumby et al, 1982)

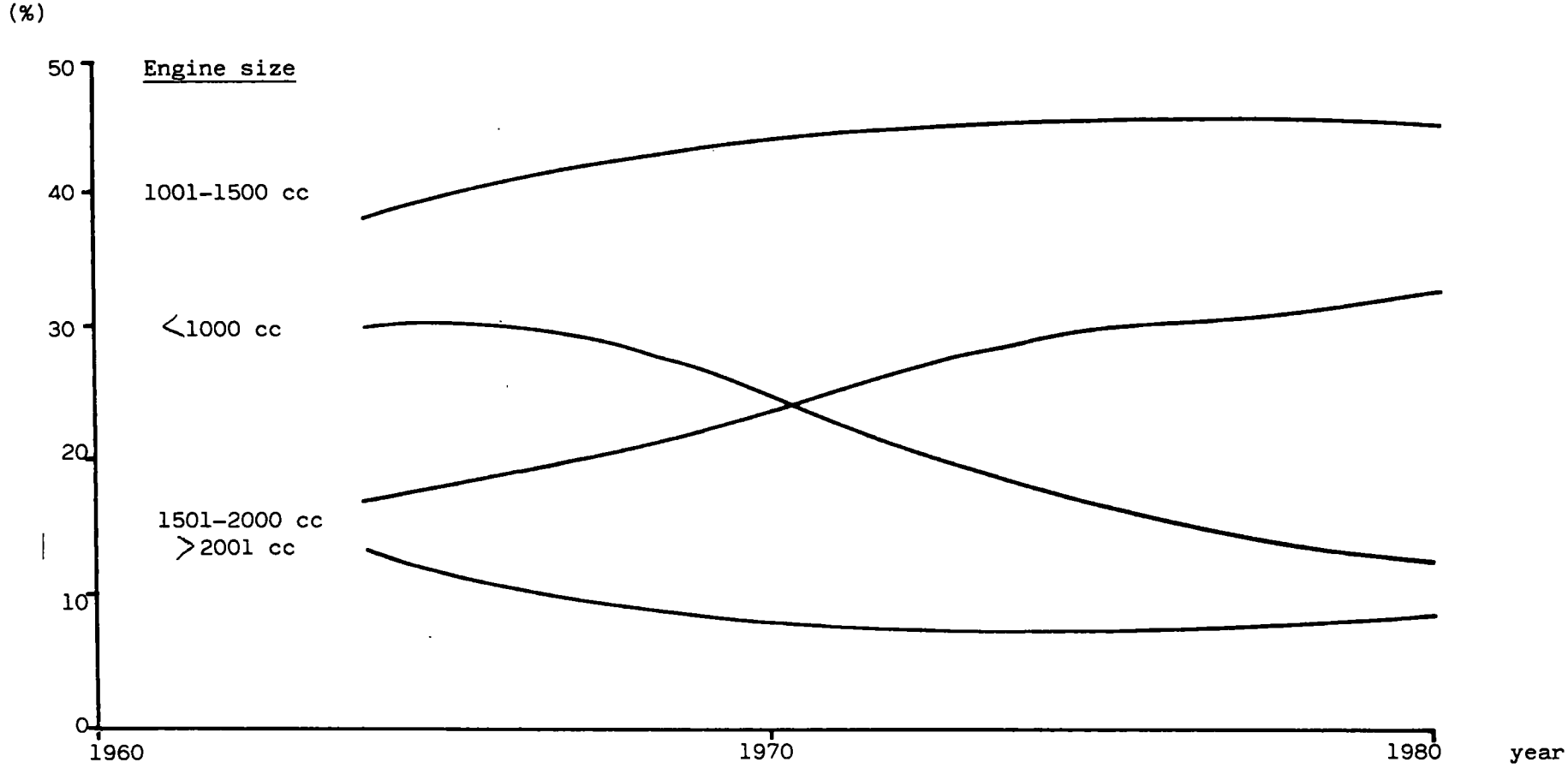

FIGURE 1.2: Passenger Car markets in the U.K. (Bumby et al,1982)

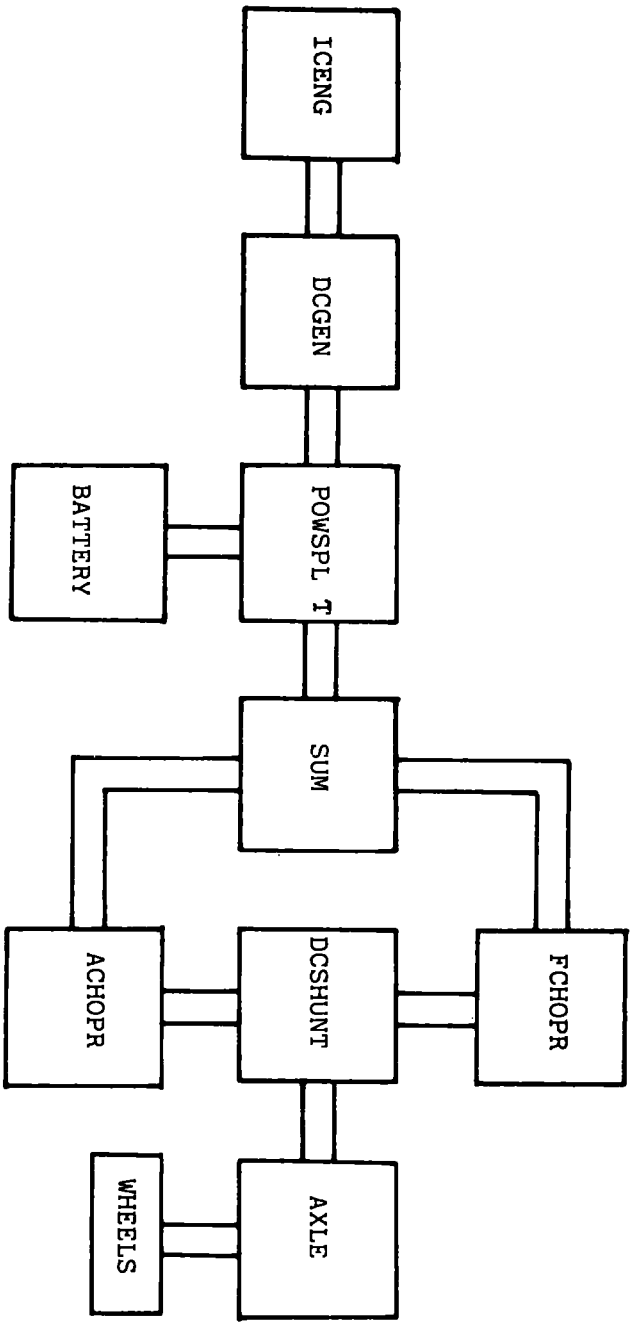

FIGURE 1.3: Series Hybrid - Electric Configuration

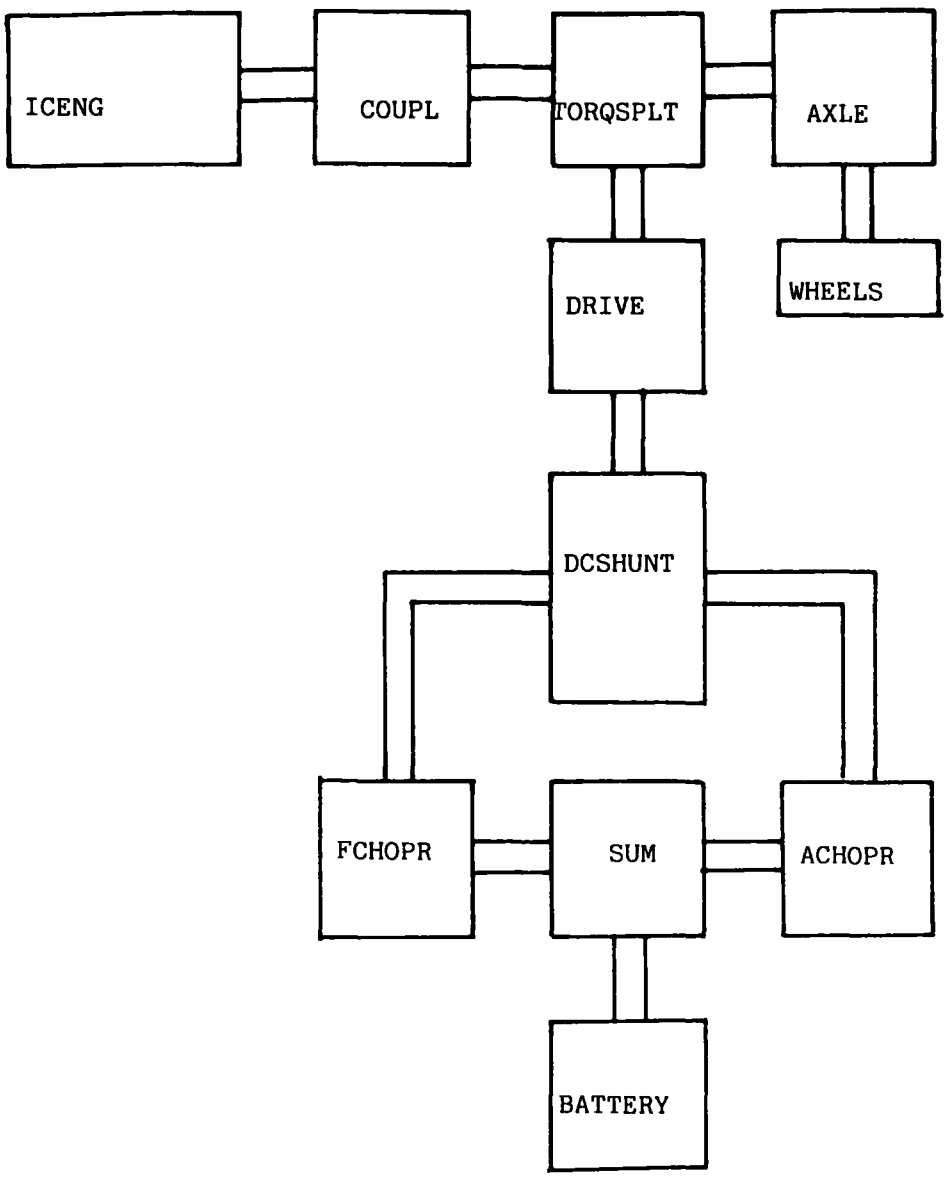

FIGURE 1.4: Parallel Hybrid-Electric Configuration

Vehicle Class	Energy used (1976) (PJ*)
Passenger Cars	
1000 cc	78
1000-1500 cc	274
1501-2000 cc	212
2000 cc	82
Goods Vehicles	
Light-Medium	118
Heavy	223
Taxi	10
Bus	43

TABLE 1.1: Passenger Car Energy Usage in the U.K. (Bumby et al,1982)

* 1PJ = 1 x 10^{15} Joules

Vehicle Design Improvement	Percent Reduction in Fuel Consumption
Transmission -	5-6
Engine/Transmission matching -	10-37
I.C.Engine Design -	7-20
I.C.Engine Electronic Controls -	3-5
I.C.Engine Fuel Cut-off	20-40
Reductions in Drag	2-6
Reductions in Rolling Losses -	2-10
Reductions in Weight (9% plastics,6% HSS)	10
Recovery of Braking Energy -	4-10
Total	63-154
Average	109

TABLE 1.2: Predicted Improvements to Conventional I.C.Engined Vehicle Efficiency (Bumby et al, 1984) (Ford Energy Report VOL.I) (Magee,1982) (Peterson et al.,1983)

CHAPTER 2

Background and Development of a Road Vehicle Simulation Program at the University of Durham

2.1 Road Vehicle Simulation Programs

In chapter 1, the need for, and application of, road vehicle simulation programs was discussed when studying novel and sometimes complex drive-train arrangements.

Road vehicle simulation programs generally fall into one of two categories:

(i) highly specific programs;

(ii) more general programs.

Highly specific programs are written with a specific drive-train configuration in mind. They may be written to study parameteric variations on a drive-train not yet in existence, or may be designed to study some aspect of behaviour (not necessarily energy consumption) of an existing drive-train.

More fundamentally, the difference between a highly specific program and a more general program lies in the 'user friendliness' i.e., it may be possible to model more drive-train options using the specific program but this will tend to require additional programming; whereas for the latter case, because of inherent user friendliness, simple commands will be all that is required to change configurations. In other words, configuration changes can be relatively easily made by any user for the general case but only by the principal writers or a user who is familiar with the language and program for the specific case.

In a survey of Hybrid and Electric Vehicle simulation programs (Bevan et al.,1978) over 100 were noted of varying complexity, with the majority capable of electric and conventional i.c. engined vehicle simulations, but few capable of i.c. engined, electric and hybrid-electric drive-trains.

A more recent study (Wolfson et al.,1983) as well as covering the points made by the above study highlighted the existence of very few 'general' simulation packages.

2.1.1 Highly Specific Programs

Highly specific programs have been written to model a small number of drive-train configurations to be the subject of a comparative study into exhaust emissions (Sampson et al.1972) or energy consumption (Blumberg,1972 and Unnewehr et al.,1976); or even a single drive-train configuration intended to model some aspect of behaviour - such as gear shifting transients (Jones et al.,1984) (Koch,1972).

The programs intended to study energy consumption or the production of exhaust emissions generally are of the type that assume pseudo-steady-state conditions at each driving cycle time-step, and employ look-up tables or equations to define component efficiencies. However, the programs intended to study transient behaviour, use differential equation techniques to model components, and, as a result are considerably heavier on computer time.

There have been programs written using the differential equation approach to study energy consumption (Dorey et al.,1984); but at least in this case, a mechanical hybrid was the intended configur ation (having a pneumatic storage device), with the transient behaviour of the storage device of particular importance.

In Japan a simulation program was written to perform studies around a Daihatsu light-truck (Honda et al.,1979) when driven over several driving cycles.

Although very little information is given, the Aerospace company have used a simulation to compare series and parallel configurations (Lapedes,1971). It is assumed that because only two configurations were considered, that this program was purpose written and therefore specific to the study.

In the UK, at Queen Mary College (Nightingale, et al.,1984) a simulation to study a specific parallel configuration has been written.

Although it is common practice for programs intended for energy studies to use 'look-up' tables of experimental data to model components, here the experimental data had been converted into defining equations for each component. In practice there may be a combination of defining equations for simpler components and look-up tables for components that are more complex to represent mathematically (i.e. the heat engine).

General Motors (Watens,1972) have developed their own simulation program, but it is directed only at the conventional i.c. engined vehicle configurations. This was also the case for the program developed at the Oakridge National Laboratory (Roberts et al.,1982), only in this case the program was designed to receive its component efficiency data directly from an actual vehicle test and then perform 'what-if' studies on that vehicle.

As far as electric vehicle simulation programs are concerned, at the University of Eindhoven (EUT) (Van Donger et al.,1981) a progam has been written and developed specifically to study a particular electric vehicle application - i.e., a modified VW Rabbit (or Golf).

Another purely electric vehicle simulation program was developed at the Air Force Institute of Technology (Stafford,1980), however, little else has been published as regards any applications of this program.

2.1.2 More General Programs

Of all of the road vehicle simulation programs available, several can be classfied as more general programs, i.e., drive-train configuration alterations can be made by relatively simple commands.

Perhaps the most user-friendly simulation program available at present is 'HEAVY' (Hammond et al.,1981). The model generation features of this program means that the user does not need to be familiar with the language used. However, in its most basic form, the program will run only in "batch" form, so offsetting, to a certain extent, the user friendliness. The program has, however, been modified to run interactively by a user in the UK. at the University of Bristol.

Another program from the USA (the Jet Propulsion Laboratory) is 'ELVEC' (Chapman et al.,1981). This program appears to share several component models (essentially data) with the HEAVY program, but unlike the HEAVY program is available for interactive as well as batch use. Although it does not share the user-friendly model generation features of HEAVY, drive-train configurations can be varied (covering i.c. engined, electric and hybrid configurations) but over a narrower range than for HEAVY.

Again, from the USA are the 'HYVELD' and 'HYVEC' simulation programs (Burke et al.,1980) (Burke et al.,1982) that have also been developed at the Jet Propulsion Laboratory (JPL), have been applied to the G.E. design work for the Near-Term Hybrid Vehicle Program (Burke et al.,1980).

None of the aforementioned general programs have optimisation algorithms available to the user. In the case of the HEAVY program, the user is left to assemble vehicle control by means of "logic" building blocks within the simulation; whereas for the ELVEC program several pre-defined control strategies are built into the program and can be selected by the user.

Generally, the i.c. engine data used in the American simulation programs tends to be applicable to the US market only, as there is still a wide acceptance of larger vehicles than in Europe, and also because of the considerably tighter emissions regulations. This results in i.c. engine data (in performance map form) that covers power ranges above that which is typical of Europe and SFC data that is significantly higher than would be experienced for European engines.

2.2.0 The Road Vehicle Simulation Program at the University of Durham

With the need to perform road vehicle simulation studies into hybrid-electric vehicles using a program written with European market conditions in mind, a general simulation package has been written and developed within the department of Engineering at the Universty of Durham.

Because the package requires component models in order to model hybrid-electric vehicles, that are also common to both conventional i.c.

engined and pure electric vehicles, it is therefore also possible to model and simulate those types of vehicle. This feature is important when making comparisons between the hybrid-electric drive-train and the drive-train alternatives that the hybrid electric concept is intended to compete against.

2.2.1 Program Description

The simulation approach at Durham from the outset has been to develop a package that is user-friendly, whilst at the same time being capable of modelling a discrete but wide range of drive-train configurations.

The fundamental concept chosen has been to take driving cycle conditions at the vehicle road-wheels (velocity, acceleration, gradient and head wind) and reflect these 'upstream' to the power source(s) and from then to their respective energy sources to determine energy usage. The process of reflection upstream accounts for each component's efficiency which, where data is available, tends to vary with load and speed.

An alternative approach is to begin at driver demand (accelerator pedal position) and work 'down stream' to the road-wheels and determine the resulting vehicle acceleration and velocity. Here a known pattern of empirically derived accelerator position/time data must be known, whereas for the former case an empirically derived set of velocity/time data is required. As data for the latter case are more readily available, this aproach has tended to be favoured in the published sources.

The simulation program (named JANUS) uses a 'block-by-block' vehicle modelling technique, in that the basic components that go to make up a particular vehicle drive-train configuration (Axle, transmission, i.c.

engine....etc) are modelled in FORTRAN subroutines. These subroutines form the basic building blocks of the simulation program, and the user simply 'links' them together to form the desired drive-train by writing a 'master program'. In the Master program, an example of which is shown in Figure 2.1 for the conventional i.c. engined vehicle, the blocks are selected and linked together by a series of FORTRAN subroutine CALL statements. The user must write a master program to model each different drive-train arrangement - i.c. engined, hybrid or pure electric.

The simulation program allows the user to select any one of a series of pre-defined driving cycles (including an acceleration test and a cruise condition), and in execution, steps through the given driving cycle in discrete and equal time intervals (defaulting to 1 second), assuming steady-state conditions at each step. Effects such as fuel consumpton transients due to the i.c. engine carburettor accelerator pump and battery current transients are small over typical urban driving cycles where acceleration rates from one time-step to the next are low, and are not considered. During gear-shifting, transients may not be small within a given time-step, but as they will cover such a small proportion of the total driving cycle, the only purpose of including them would be to study the effects of, say, battery current transients on the electrical system hardware. Similarly, for an acceleration test, the transients may not be small and may be significant throughout the test, but as the purposes of such a test is to study the acceleration time and not energy consumption, the practical advantage of including them could, again, be to assess the affects of transients on hardware design.

At each time-step, calculations are performed from the road-wheels, where linear velocity and acceleration (plus any other environmental conditions such as gradient and head/tail winds) are converted to the shaft torque requirement and rotation. This is then reflected 'upstream' through the drive-train to the prime-mover (two in the case of the hybrid-electric case), taking account of each component's efficiency. From there the operating condition is reflected to prime mover's energy source and the energy consumption is determined for this one time-step.

The basic road load equation used in the simulation program, including the environmental conditions is for the tractive effort at the road wheels:

$$T_E = W_v.g.CR1 + W_v.AC_L + W_v.\sin\theta + 1/2.\rho_{air}.C_d.FA.(V_e \pm V_{HW})^2 \quad (N) \quad - (1)$$

Here, the 1st term represents the tractive effort required to overcome rolling loss; the 2nd term, the tractive effort required to meet vehicle acceleration requirement; the 3rd term, the tractive effort to overcome any gradient; and the 4th term the tractive effort to overcome the aerodynamic drag on the vehicle, which includes a term for vehicle velocity (V_e) and also head/tail winds ($\pm$ VHW).

From the user's point of view, the program operation is divided into 3 sections:

(i) the initial or input section;

(ii) the dynamic section;

(iii) and the output section

The initial and dynamic sections are further subdivided and there is a user option for the output section.

The user chooses a driving cycle and inputs vehicle parameters in the 1st initial section in the order the building blocks appear in the master program (see Figure 2.1). Any additional vehicle parameters that cannot be calculated until all of the data has been input are determined in the 2nd initial section - which the user does not see. For example, in the case of the calculation of vehicle weight by the program (see section 2.3.2.8), on the 1st initial section pass the user will input power source ratings which may be upstream (after) components such as the transmission and axle (Figure 2.1). In order to determine the transmission components' weights (which are a function of the power/torque they have to transmit) the 2nd initial section is necessary to pass the required rating to these components.

In the 1st dynamic section,as has been described,for each time step, the program will move through each component building block included, calculating variables, iteratively if necessary (see 2.3.1), until a stable operating condition is reached. Once a stable operating condition has been achieved, the energy usage, component by component, is calculated in the 2nd dynamic section. The next cycle time-step is then selected and the process is repeated. When all of the cycle time steps have been passed through, the program will select the output section, and either a detailed, component by component, breakdown of energy usage, or just the overall vehicle energy usage (in mpg and/or range in miles) is displayed to the user.

A block diagram of the overall program operation is given in Figure 2.2.

The simulation uses a mixture of defining equations and look-up tables to model component efficiencies. The inherently simpler components have efficiency defined using euqations derived by curve fitting published data.

Such is the case for the variable and fixed ratio transmissions (not including the CVT model) and the DC motor controller. More complex components such as the prime-mover and CVT models have efficiency defined in 2-dimensional arrays/matrices/look-up tables in terms of load and speed. An array search and linear interpolation at any given load and speed will enable the component efficiency to be found (SFC in the case of the i.c. engine).

Whereas for the CVT and traction motor models there are a set of maps to cover each CVT type (traction, hydrostatic, hydrodynamic...etc) and each motor type (DC shunt, DC series, DC switched reluctance, AC induction), in the case of the i.c. engine (gasoline and diesel) there are also a number of maps to span a range of power ratings.

This is explained by the mechanical changes necessary in practice when an i.c. engine power rating (capacity) is altered - particularly for gasoline engines where cylinder diameter is limited. This mechanical change, such as the number of cylinders, will obviously affect efficiency, and it is recommended by manufacturers that engines be scaled or stretched only realistically up to 10-20% of their norminal rating. The traction motor on the other hand, because rating changes do not result in fundamental mechanical changes, maps can be stretched considerably further from the nominal without affecting the validity of the results.

As far as the storage battery is concerned, because of its extremely complex nature, which is mainly due to the electrochemistry, but also because some of the characteristics, such as recuperation, are not fully understood, three methods of modelling are available. All three are well described in the literature and are the Shepherd model (Shepherd,1965), the fractional discharge model (Chapman et al.,1981) and the generic model (Chapman et al.,1982).

The Shepherd model uses a voltage-current-time relationship for a given battery to define battery performance. The battery is said to be discharged when the terminal voltage drops below a pre-defined cut-off value - Figure 2.3.

The fractional discharge model simply uses the power density/energy density characteristic for a given battery to determine a time to discharge at a given power density (loading condition) (τ) - Figure 2.4. A 'theoretical' mass of battery is then incremented or decremented (power density negative and positive respectively) in the ratio of the cycle time step to τ. When no 'theoretical' mass is left, the battery is said to be discharged.

Finally, a battery model that relies on empirical data to a lesser extent than the aforementioned models is the generic model. This model relates instantaneous discharge current and capacity (current x discharge time) to the actual capacity left in the battery by means of a defining equation.

The fractional discharge model is used throughout the studies presented here to model battery performance.

A list of all of the component 'hardware' building blocks available to the user is given in table 2.1. Similarly, a list of 'software' component building blocks (control strategy algorithms) is given in table 2.2. For several building blocks there are a number of options available to the user and these, along with several program operational features are shown in tables 2.3 and 2.4 respectively.

A more detailed description of hardware and software building blocks is given in the user's manual (currently an in-house document at the University of Durham) and alternative descriptions of the program operation are offered in the available litereature (Bumby et al.,1984 (a)), (Bumby et al,1985).

2.2.1.1 Conventional i.c. engined Vehicle Simulation

A block diagram of the vehicle configuration to be modelled is given in Figure 2.5 and the corresponding master program containing the relevant building blocks in Figure 2.1. The order of the components in the master program runs from the road wheels to the energy source. Here the energy source is the vehicle fuel tank, which, because it can be regarded as infinite (easily replenished) and because it has no load dependent characteristics, does not require a separate building block.

2.2.1.2 Electric Vehicle Simulation

The block diagram of the configuration to be modelled is shown in Figure 2.6, and the master program is shown in Figure 2.7. Again, the order of components runs from the road-wheels to the energy source. The energy source in this case is the traction battery, which, because it cannot be regarded as infinite (i.e. it is not easily or quickly replenished) and also because it has load dependent characteristics, needs to be modelled as a separate component block.

2.2.1.3 Hybrid-Electric Vehicle Simulation

In the case of a hybrid-electric vehicle simulation (here a parallel configuration - Figures 2.8 and 2.9) the order of components runs from the road wheels, and then to each of the two energy sources in turn after the torque/power splitting module (TORQSPLT).

The hybrid-electric simulation, for both parallel or series configurations (Figures 2.10 and 2.11) requires additional modules or

blocks - namely CONTROLP, CONTROLS, POWSPLT and TORQSPLT. These blocks go to make up, in these cases, pre-defined overall vehicle control required when operating the two power sources. In these examples, the control strategies decided upon are not ideal and are only included to show the hybrid layouts. The control blocks for the parallel configuration, CONTROLP and TORQSPLT, are the control blocks that go to make up a simple velocity control strategy. CONTROLP simply decides upon the vehicle driving mode (all-electric,all i.c. engine hybrid...etc) according to vehicle speed, and then passes this information to TORQSPLT which then decides how the torque/power will split between the two power sources. In a similar fashion, the control blocks for the series configuration, CONTROLS and POWSPLT, perform similar functions except the control variable is battery state of charge (SOC) instead of velocity.

The simulation package does have building blocks available for both parallel and series configurations that will optimise the control strategy at each cycle time step for a particular requirement - which in this case is the minimisation of energy consumption. The master programs take on a very similar form as Figure 2.12 shows. The building blocks (OPTCONT, OPTQSPLT and OPTIMISE) used in this example, along with the control blocks for other configurations will be described more fully in section 2.3.3 and their implementation in chapters 5, 6 and 7.

2.3 Program Development

From the basic program operation described in section 2.2, development has covered 3 broad areas:

(i) operational improvements;

(ii) component modelling developments;

(iii) hybrid vehicle simulation and control

2.3.1 Operational Improvements

To increase the flexibility and general usefulness of the program, the following features have been added - see table 2.4.

(i) program multirun capability;

(ii) program multicycle capability;

(iii) Simulation output options;

(iv) program checking when component peformance limits are exceeded.

As far as program multi-runs are concerned, the user is given the choice at the end of each simulation run (at the end of the output section) of either running again with no data changes, running again but with some or all of the data to be changed or not to run again - in which case the program will end (Figure 2.2).

The program has the ability to run through a number of driving cycles consecutively (between 1 and 100) as certain performance assessments, such as cold starting and aspects of hybrid vehicle control, can only be performed after a significant distance has been covered by the vehicle (typical pre-defined cycles cover short distances to be repeated). This aspect of the program is also shown in Figure 2.2.

In addition, the user is given the option of directing simulation output to either the VDU for interactive viewing, or to send both numerical and graphical output data to hard-copy devices.

As was mentioned in section 2.2., the 1st dynamic section pass performs all calculations for component variables until a stable operating condition has been reached. In other words, the program checks to see if the operating condition/point is wthin component limits - particularly for the prime-movers. If the operating condition is outside these fixed

limits (maximum speed and/or maximum torque - the latter of which will also vary with speed) then the program will progressively reduce the severity of the driving cycle at this time step (velocity and/or acceleration), iteratively until the new operating condition falls within prime-mover limits. This 'actual', rather than 'theoretical' cycle is recorded as the theoretical cycle is driven, and is displayed to the user, along with the theoretical cycle during the program output section.

When the torque limit of a prime-mover (i.c. engine or electrical machine) is exceeded, the vehicle acceleration rate at the given time-step is reduced by an amount corresponding to how much the prime-mover limit was exceeded, and reflected back through the drive-train (taking account of drive-train efficiency). This leads to a fast convergence of the iteration to bring the operating point within component limits. If the iteration brings the operating point too far inside the torque limit, then for the next iteration, the acceleration rate is increased by an amount corresponding to the excess power available at the prime-mover and reflected back through the drive-train.

When the maximum speed limit of the prime-mover is exceeded, however, the vehicle velocity at the given time step is simply reduced in small steps regardless of by how much the speed limit was exceeded, in order to reduce the number of 'flags', and hence, complexity of the program.

During an acceleration test (a driving cycle option which is available to the user) a similar procedure occurs in order to find the maximum vehicle acceleration rate possible at a given time-step. Here, the vehicle acceleration rate is progressively increased (according to how much excess power is available at the prime-mover, and reflected back through the drive-train) until the performance limit is reached or exceeded. If the latter case occurs, then (as before) the acceleration rate is reduced.

If speed limits are exceeded during an acceleration test, the program will prompt the user to modify transmission ratios and/or gear change points (according to vehicle speed) and perform the test again. If the gear change points were according to engine speed, then, providing that reasonable values for transmission ratio were input, the speed limit would not be exceeded. However, it is perhaps easier to visualise gear shifting with vehicle speed, and the effects of changing shift points can be studied.

The basic interface of the driving cycle iteration for normal cycle conditions into the main simulation program is shown in the program flow chart of Figure 2.2.

2.3.2 Component Modelling Developments

Component modelling development covers areas in the simulation software where improvements have been made to improve the absolute accuracy of results and to improve the flexibility of the program by increasing the number of options available to the user - in some cases involving the extension of the simulation package by the addition of new building blocks.

To a certain extent, program verification, to be described in chapter 3, and program development, have gone hand-in-hand as any shortfalls are quickly highlighted when comparing simulation with actual hardware results.

2.3.2.1 The Electric Traction Motor Models

In the general program description of section 2.2 it was stated that the more complex component building blocks were represented, in terms of efficiency, by look-up tables. For the traction motor models the same applies, and efficiency is represented in a 2-dimensional table of shaft speed and torque.

The simulation package has been extended by the inclusion of traction motor models to supplement the DC series machine model which originally formed the only electric traction option. These models represent the DC shunt, the DC switched reluctance and the AC induction motor types.

The DC switched reluctance and AC induction motors as a result of the efficiency data obtained are very similar in that efficiency includes both motor and controller. As a result modelling is relatively straightforward in that there is a single terminal input and a single shaft output.

However, the data obtained for the DC shunt motor type describes motor efficiency only, and, because armature and field are independent, this model requires two terminal inputs and one shaft output.

2.3.2.1.1 The D.C.Shunt Wound Motor Model

The D.C. shunt motor model uses efficiency data in terms of shaft torque and speed (output conditions) for two current machines: a General Electric motor and a Siemens motor. The 2-dimensional tables, or efficiency maps, for these types are shown in Figures 2.13 and 2.14 respectively.

Figure 2.15 shows how the overall efficiency data of Figures 2.13 and 2.14 is broken down into the various losses in the machine, from terminal inputs (2) to shaft output (the reverse being the case during regeneration but with the field still positive).

Mechanical losses in the machine need to be represented in the model because the vehicle braking model (to be described in section 2.3.2.4) requires the prime mover to still provide an absorbing loss when no regeneration is present. They are modelled in terms of the polynomial equation (47) shown in appendix I - to account for the 3 sources of loss: brush and bearing coulomb friction; bearing rolling losses; and rotor windage losses. The equation constants are determined from other motor

constants input by the user, but the polynomial indices are derived from published sources (Nasar et al.,1983)(Steven et al.,1983). The first term of the equation, representing coulomb friction is linear with speed; the second term, representing bearing rolling friction is given as varying with speed to the 1st or 2nd power; and the 3rd term, representing rotor windage is given as varying with speed to the 2nd or 3rd power. Although brush friction is regarded as the largest of the 3 terms (Nasar et al.,1983) (Steven et al.,1983) when the equation constants are determined, because no proportions have been quoted, it is assumed that all 3 are equal at the break point. Mechanical losses are also used, as Figure 2.1.5 shows, to calculate air-gap torque (shaft torque plus mechanical losses when motoring and shaft torque minus mechanical losses when regenerating).

The electrical losses shown in Figure 2.15, although not needing to be represented in the model (as efficiency covers shaft output to terminal input) consist of field and armature resistance losses, brush to commutator resistance losses, field and armature iron losses and hysteresis losses (due to changing magnetic fields with time). The latter two losses are extremely difficult to model as they vary with both the magnetic field and some polynomial of rotor speed.

Because the Shepherd and Generic battery models require current and voltage inputs (only power is required for the fractional discharge model - see section 2.2) then the terminal input power must be broken down into its constituent voltages and currents for a given operating condition - shown in Figure 2.16.

To do this, the motor performance map is divided up to 2 'motoring' regions and 2 'regeneration' regions - shown in Figure 2.17 - and full mathematical power, current and voltage relationships for each region are given in appendix I.

In region 1, below the motor break speed, full field voltage is applied (hence full field current) and armature current is determined from the shaft torque. Then armature voltage can be found from the terminal input power (determined from the overall efficiency on the look-up table) field power and armature current.

In region 2, above the motor break speed, full armature voltage is applied. By assuming that the operating point lies on a line of constant back e.m.f. (hence armature current and therefore torque), back e.m.f at the break point can be found and so field current at the operating point can be found. Terminal input power is again determined from shaft power and overall efficiency, armature current from the shaft torque. In this region the field is weakened as the motor speed is increased to maintain back e.m.f.

Region 3 is now a regenerating region, the field is strengthened as motor speed decreases in order to maintain back e.m.f. Terminal power is now represented by the armature power (i.e., actual terminal power before subtraction of the field loss). The calculation procedure is similar to that of region 2.

Finally in region 4, regeneration below the break speed, full field is now applied having been gradually increased as the speed decreased in region 3. Armature current is determined from the shaft torque, terminal power from the overall efficiency and shaft power and hence armature voltage can be found.

Although shaft or 'output' conditions are used to 'look-up' efficiency when the machine is motoring, it is unclear from the published literature what conditions should be used to look-up efficiency when the machine is regenerating - or if indeed the motoring map will still apply. If 'output' conditions are assumed then these will correspond to the motor

terminals. An 'equivalent electrical torque' must be used (along with shaft speed) to look up efficiency, and since terminal power cannot be determined until overall efficiency has been found, this must be determined iteratively.

The motor model uses this approach, but the differences between this and simply using shaft torque for the look-up have been found to be small.

The motor model also includes the effects of rotor inertia by simply adding the torque and power on to the steady state shaft torque and power, and also the effects of saturation shown in Figure 2.18 where a non-linear relationship between field current and magnetic field strength is assumed.

All motor model defining equations have constants that are calculated from parameters such as motor power, speed and voltage ratings, and this procedure is also described in appendix I.

2.3.2.1.2 The D.C. Switched Relutance and A.C.Induction Motor/Controller Models

The D.C. switched reluctance and A.C. induction motor types, although not new ideas, have only recently, with the developments in power electronics and micro-electronics, become a viable alternative to the well established D.C. series and D.C. shunt machines in the field of automotive traction. Both types have the significant advantage of simple rotor construction, but requiring more complex control electronics.

Because the data representing efficiency for both types includes both motor and controller, there is only one terminal input and therefore no need to divide the performance maps into operating regions with individual control strategies - as was the case for the D.C. shunt motor.

Despite this, the modelling procedure is similar to that of the D.C. shunt motor. Mechanical losses are determined in exactly the same way, as is rotor inertia.

Efficiency data for the motor/controller types is shown in Figures 2.19 and 2.20. For low speeds, data was not complete and extrapolation of data into this region was necessary. Because of the large gap between the lowest speed values and zero it was preferable to plot efficiency variation with speed and do an extrapolation by eye, rather than do a linear extrapolation. Figures 2.21 and 2.22 show for both types, the effects of both methods of extrapolation. Also, in a similar fashion to the D.C shunt motor model a loss diagram for the switched reluctance and induction motor model can be produced, and this is shown in Figure 2.23.

2.3.2.2 D.C. Motor Controller Model

As the D.C. shunt motor model, described in 2.3.2.1, did not include any controller (as is also the case for the D.C. series motor model), separate building blocks to represent the controller loss were required.

Currently the most popular method of D.C. motor control, due to its smooth voltage control and high efficiency when compared to other methods, is the 'chopper' type. (JPL - Should we have a New Engine 1975).

Because it is a relatively simple component to model, efficiency is defined in terms of equations derived by curve-fitting published data.

Figure 2.24 shows a diagramatic representation of a D.C. chopper, whilst Figure 2.25 shows the current and voltage variation during the switching or chopping process. Typical waveforms are shown both on the battery side and on the motor side of the controller.

As the duty cycle (t_{on}/t_{cycle}) increases (having a maximum value of 1.0 when full battery voltage is applied across the motor) motor voltage will increase.

Because the motor circuit (and to a lesser extent the battery circuit) will have inductance, current will 'lag' behind voltage - as shown in Figure 2.25. As far as the battery circuit is concerned, when the motor voltage is chopped, the current will drop to zero almost immediately. For the motor circuit, however, due to the presence of the free-wheeling diode, the current will decay slowly through the motor inductance. When the voltage is re-applied, both battery and motor sides of the choppper will see the same current wave-form.

Power losses in a D.C. chopper can be broken down into 3 areas:

(i) the resistive losses of the circuitry;

(ii) the parasitic losses of the thyristor or transistor firing circuits;

(iii) and resistance losses associated with the switching process

The first loss route is fairly self-explanatory in that the power lost will be dependent on the chopper circuit resistance and increaseswith the current being passed. As far as the parasitic losses are concerned, these will increase as the degree of switching increases (load current decreases).

The third loss route is seen in Figure 2.25 during the part of the switching cycle when the free-wheeling diode circuit is used. The current decay through this circuit will depend upon the back e.m.f and the circuit resistance. For a given back e.m.f the decay period is going to be less than if there was no resistance present - so resulting in an average current loss. As the duty cycle (t_{on}/t_{cycle}) decreases the proportion of the average current lost will increase.

Including the chopper circuit resistance during the t_{on} or conduction period serves to reduce motor voltage relative to battery voltage, and this is shown for the 'rise' period in Figure 2.25. Although varying with

load, the absolute value of resistance loss will be small in practice since resistance values are small, and so can be represented as a constant loss at full load.

The chopper efficiency may therefoe be represented by a single equation which basically comprises of two terms. The first term represents the parasitic loss, and is linear with the degree of switching. The second term represents the chopper circuit resistance loss associated with the free-wheeling diode circuit and will vary as some polynomial of the average current being passed since resistance loss in a simple circuit varies as the current squared.

The published data available yielded chopper efficiency variation with both average (motor) voltage to represent the switching resistance loss and average (motor) current to represent the parasitic switching loss.

$$\eta = K_3 \left(\frac{IAV}{IMAX} \right) + K_4 \left(\frac{VAV}{VMAX} \right)^{Nch} \qquad (2)$$

By curve fitting published data for thyristor and transistor-type choppers (Wilson et al.,1982) (JPL - Shall we Have a New Engine 1975), constants K_3 and K_4 and the polynomial index N_{ch} could be found.

For the thyristor-type, substituting for K_3 and K_4 in (2):

$$\eta = 0.05 \left(\frac{IAV}{IMAX} \right) + 0.93 \left(\frac{VAV}{VMAX} \right)^{0.045} \qquad (3);$$

and for the transistor type in a similar fashion:

$$\eta = 0.0053 \left(\frac{IAV}{IMAX} \right) + 0.9747 \left(\frac{VAV}{VMAX} \right)^{0.06} \qquad (4)$$

The above curve fits are presented in Figure 2.26.

During regeneration, because circuitry is generally significantly different from that used for motoring (Collie,1979), a different efficiency model is assumed.

The chopper functions during regeneration by short circuiting the motor armature/inductance, so allowing the current to build up. When the current has reached a certain level the short circuit is broken, upon which the induced voltage opposing the rate of change of current, when added to the back e.m.f. of the motor, causes the armature voltage to rise above the battery voltage. The motor armature is then reconnected to battery terminals and current passes into the battery until the motor armature voltage drops to equal battery voltage, upon which the process is repeated (Collie,1979).

The model is based on data from rig-tests of the ETV-1 drive-train (Sargent, et al.,1981) and uses two equations to fit the experimental data:

for $VAV/_{VMAX} < 0.4$,

$$\eta = 1.12 \left(\frac{VAV}{VMAX} \right)^{0.35} \quad - \quad (5);$$

and for $VAV/_{VMAX} \geq 0.4$,

$$\eta = 0.95 \quad (VAX/_{VMAX})^{0.1} \quad - \quad (6)$$

The curve-fit and experimental data are presented in Figure 2.27.

Efficiency during regeneration is generally lower than for motoring due to the additional circuitry brought into play.

Although the regeneration experimental data was from an 'overall' controller for a D.C. shunt motor (armature plus field controller), the

model assumes that when $VAV/V_{MAX} > 1.0$, the field chopper will control regeneration with the armature chopper bypassed. When $VAV/V_{MAX} < 1.0$, the field chopper output voltage is at a maximum and regeneration is controlled by the armature chopper only using the equations discussed.

2.3.2.3 Mechanical Transmission Efficiency Modelling

Modelling of mechanical transmission components has covered three areas: variable ratio transmissions (but not including CVTs as they are the subject of an MSc thesis at the University of Durham), fixed ratio transmission components (such as the final drive unit of a road vehicle) and starting devices, such as the friction clutch and torque convertor.

2.3.2.3.1 Variable Ratio Transmission

Because discrete variable ratio transmissions for automotive applications have tended to employ gear drives, so modelling development has been concentrated in this area.

As with the D.C. chopper controller of section 2.3.2.2, because the gearbox is relatively simple to represent in terms of losses, efficiency is defined by an equation obtained by curve fitting published data.

Torque losses in a gearbox can be divided into speed dependent losses and load dependent losses. The speed dependent loss is mainly associated with lubrication oil churning (assuming that the gearbox is sump, and not jet, lubricated), viscous losses associated with the rolling elements in the bearings and due to the rolling contact between gear teeth. This latter loss route is due to the hydrodynamic pressure built-up between gear teeth and bearing rolling elements in the lubricant but is small by comparison to the churning loss (Martin,1980) (Anderson et al,1980). The load dependent losses are associated with the tooth contact forces and the

bearing rolling element contact forces, resulting from the transmitted torque. This loss mechanism is explained by the small amount of 'sliding' between gear teeth and bearing rolling elements, rather than the ideal 'rolling' which should occur over all of the respective contact paths (Anderson et al,1980).

The load dependent losses are therefore directly proportional to the transmitted torque (Anderson et al.,1980), whereas the speed dependent losses will vary as some polynomial of speed:

$$TLOSS = K_5 T_{IN} + K_6 \cdot n_{IN}^{\ m} \ (Nm) \qquad - \qquad (7)$$

Alternatively, this can be written as:

$$PLOSS = K_7 P_{IN} + K_8 \ n_{IN}^{\ (m+1)} \ (KW) \ - \qquad (8)$$

where K_5 to K_8 are constants.

Using empirically obtained data from several sources, the two constants K_7 and K_8, and the speed index m + 1 can be found by curve fitting this data (Blumberg,1976) (Van Donger et al.,1981) (Aston et al.,1981) (Bujold,1981) (Morello et al.,1979)

The speed dependent constant K_8 of equation (8) was found to be 1.14 x 10^{-8}, so giving a small speed dependent term at low to medium speeds, and only becoming significant at very high speeds.

Constant K_7 in (8), associated with the load dependent term, depends upon the type of gearing employed in the transmission (spur or bevel types) and also any parasitic losses that may be present, for example, due to the presence of a hydraulic pump in an automatic transmission. The overwhelming majority of discrete ratio transmissions for automotive use

employ 'spur' gears with their lower sliding losses than 'bevel' gears (having a 90° change in transmission direction). From the published data, typical values of K_7 are:

0.02 - spur gears;

0.02 - bevel gears

Also in terms of parasitic losses:

0.02 - no parasitic loss (manual gearbox)

0.03 - parasitic losses (automatic gearbox)

As far as the parasitic losses are concerned, these will be mainly associated with the transmitted torque (i.e, the effort required to 'hold' a gear in the case of an automatic gearbox), and although there will be a speed dependent effect due to flow losses, those will be small. Modification of the load dependent constant is all that is required.

The speed polynomial index value, m + 1, was studied for a variety of driving conditions - shown in Figure 2.28. Above a value of about 2.1 efficiency starts to fall away sharply. Because the model was intended to be typical and since the empirical data suggested not moving above this value (particularly at part loads), this value was selected.

The final basic relationship is therefore:

$$PLOSS = K_7 PIN + 1.14 \times 10^{-8} n_{IN}^{2.1} \ (kw) \quad - \quad (9)$$

where $K_7 = 0.02$ for a manual transmission and

$K_7 = 0.03$ for an automatic transmission.

PIN and n_{IN} refer to power and speed at the input (i.c. engine input) to the gearbox.

The value of K_7 will be altered further for a manual gearbox where it is common for 4th gear (in both 4 and 5 speed units) to be a direct drive with no meshing gears. In this case the speed dependent term will

remain unchanged since the drive gears still remain churning in the oil, but the load dependent term needs to be modified as only bearing losses will be present. For such non-meshing gears data from Ford Motor Co.(UK) gives a value of K_7 of 0.01. Figure 2.29 shows how the transmission efficiency model is displayed graphically. When compared with the empirical data from which it was derived it shows good approximation but tending to be slightly pessimistic for part-load high speed cases.

The EUT transmission efficiency data (van Donger et al.,1981) also shows efficiency variation occurring between the various gears selected at a given load and speed (1st - 4th, shown in Figure 2.30) - progressively becoming lower (shown by the Pin/p_{max} = 0.1 (load-line)). Although not a large variation this may be explained by the practical consideration, that, in order to reduce noise and vibration at high rotational speeds for prolonged periods (say, 4th gear), a large 'helix' angle may be cut on this gear set. For 1st gear, although rotational speeds may still be high, the percentage time spent in this gear will be extremely small, with the result that quite often no helix angle is cut on this gear set (characterised by a 'whine' that some gearbox designs emit when the vehicle pulls away from rest). The result is that a lower efficiency for the gears with a helix angle cut on the gear set will occur compared with the gear whose gear set has no helix angle ,due to increased tooth sliding losses at a given load and speed. The progressive reduction in efficiency from 1st - 4th in Figure 2.30 may indicate a gradually increasing helix angle - 1st-4th.

The efficiency model in JANUS assumes no such varition between gears at the same speed and load conditions (other than the consideration when no gear set is used to transmit the torque for a 1:1 ratio - no meshing gears), as it is a 'typical' model, and such effects are due to particular gearbox designs.

2.3.2.3.2 Fixed Ratio Transmission

Unlike the variable ratio transmission, because the ratio is fixed, a fixed ratio transmission can be any one of several types that are popular and well tried. These types are gear drives, belt drives (toothed, vee and flat) and chain drives, and all are available in the two fixed ratio transmission building blocks (AXLE and DRIVE) as user options.

For the gear drive option, the efficiency variation is assumed to be as for the variable ratio unit, with the exception that K_7 in (8) now varies due to the different gear types that are possible (spur gears and bevel gears), depending upon whether the drive direction is to be turned through 90° or to remain parallel. In the case of the AXLE module this will depend upon whether the vehicle is of a front transverse engine/front wheel drive or a front in line engine/front or rear wheel drive arrangement.

The loss equation (8) therefore becomes:

$$PLOSS = K_7 PIN + 1.14 \times 10^{-8} \quad IN^{2.1} \ (KW) \qquad - \qquad (10)$$

where $K_7 = 0.02$ for spur gears;

and $K_7 = 0.03$ for bevel gears. (assumed to be hypoid or curved tooth bevel gears).

Belt drive efficiency will also vary with speed and load. Speed effects are due to circumferential belt slip for 'vee' and 'flat' belts, radial slip due to 'wedging in and out' in the case of the 'vee' belt only and for all three belt types ('flat', 'toothed' and 'vee') due to the centrifugal effect tending to throw the belt radially off the pulley. Load effects are simply due to belt stretching under the applied torque.

The limited efficiency data available (Firbank 1976) (Breig et al 1980) suggests that the speed dependent term is negligibly small and that the loss equation can therefore be written:

$$PLOSS = K_5 \, TIN \quad (Nm) \qquad - \qquad (11)$$

and

$$PLOSS = K_7 \, PIN \quad (KW) \qquad - \qquad (12)$$

This implies that a constant efficiency model is acceptable for these drive-types. Typical efficiency valus are: (Firbank 1976) (Breig et al., 1980)

vee belt	-	90-96%
flat belt	-	96-98%
toothed belt	-	90-96%

Chain drive efficiency variation depends upon the type of lubrication method employed. If sump lubricated, there is a more significant speed dependent term than for jet lubrication, where a parasitic loss now exists (hence a greater load dependent term).

Automotive chain drives tend to be sump lubricated (Lucas Chloride) but the amount of Lubricant to be transferred by a sprocket dipping into the sump will be less than for a gear drive. This is because of the geometry of the chain/sprocket contact and the number of contacts sharing the load, contact pressures are lower than for mating gear teeth. In addition, the cooling requirement is less for a chain unit due to the inherently slacker running tolerances (hence seizure will not be so critical).

Again, the limited amount of empirical data available suggests that the above argument of the load dependent term dominating over the speed

dependent term (Mechanical Power Transmission,1971). Also, when compared to the belt drives, because of the higher stiffness of the chain when compared to the belt, stretching losses will be lower. A typical constant efficiency value is 98-99% (Mechanical Power Transmission 1971).

2.3.2.3.3 Friction Clutch

The friction clutch in automotive applications is used as both a disconnect device on the drive-line (for changing gear) and also as a starting device to enable the i.c. engine to operate at road speeds that correspond to engine speeds below the minimum for the i.c. engine. The latter course is achieved by slipping the clutch with the i.c. engine set some speed at or above its minimum value, and the gearbox input speed at some speed between zero and the i.c. engine speed.

To simulate this effect it is assumed that clutch slipping occurs when the transmission input speed, R_G is below a predetermined minimum (RMIN) value for the particular engine map selected. In this situation torques on both sides of the clutch are assumed to be equal, giving a linear variation in efficiency.

Clutch efficiency simply becomes:

$$\eta_{CLUTCH} = \frac{TG}{T_E} \times \frac{RG}{R_E} \times 100 \quad - \quad (13)$$

$$\eta_{CLUTCH} = \frac{RG}{R_E} \times 100 \ (\%) \quad - \quad (14);$$

$$R_G < R_{min}$$

2.3.2.3.4 Torque Convertor

The torque convertor in automotive applications fulfills a similar function to that of the friction clutch - particulary during vehicle starting or 'take-off'. The torque convertor is a fluid or

hydrodynamic device, however, and differs from the friction clutch in that torque multiplication can be achieved by suitable design of the stator vanes between the 'pump' and 'turbine' rotors. Also, unless a mechanical 'lock-up' device is introduced, there will also be 'slip'-loss present in the unit even after the 'take-off' period due to the fluid connection between inut and output.

As with the friction clutch, the torque convertor only functions when the transmission input speed (RG) falls below the minimum speed for the i.c. engine used (RMIN). Above RMIN, a fixed slip speed loss of 10% is assumed, unless the torque convertor is locked up when no fixed loss results. Below RMIN, the torque convertor speed ratio is:

$$\frac{RG}{RMIN}$$

Using data given for various current torque convertor designs, the relationship between torque ratio and speed ratio can be found (Mangan et al.,1974) (Samuel, 1974) (Ratcliff 1976). The empirical data approximates to a straight line relationship between torque ratio and speed ratio - Figure 2.31. The model assumes a line that gives a typical 'stalled' (zero gearbox input speed) torque ratio, as higher torque ratios result in higher slip losses due to increased stator vane angles - unless variable stator blading is used (Samuel 1974):

$$\text{Torque ratio} = 2.5 - 1.724 \times \text{speed ratio} \quad - \quad (15)$$

$$T_G/T_E = 2.5 - 1.724 \times RG/R_E \quad - \quad (16)$$

When the torque ratio reaches a value of 1.0, the model maintains its constant at this value.

Efficiency of the torque convertor is then expressed as:

$$\eta_{TC} = \frac{TG}{TE} \times \frac{RG}{RE} \times 100 \quad - \quad (17)$$

A comparison between the torque ratio/speed ratio model and the empirical data from which it was derived is shown in Figure 2.31 - and shows the model curve lying in between the two current units (Mangan et al.,1974)(Samuel,1974).

2.3.2.4 Vehicle Braking Model

A model of vehicle braking is important, particularly in the simulation of electric and hybrid electric vehicles where a proportion of the total available deceleration energy can be recovered regeneratively and stored in the traction battery. This proportion will depend upon the rate of deceleration (severity of the driving cycle) and the handling capacity of the vehicle's electrical system. Only under 'mild' decelerations with a suitably sized electrical system will all of the available energy after losses be transferred to the battery.

The braking model therefore accounts for the power handling capacity of the electrical system, and the available deceleration energy after losses that cannot be handled by the motor/controller/battery combination is assumed to be dissipated in friction braking.

When no regeneration facility is available (as user option) the model still requires an absorbing loss in the traction motor and it is the motor mechanical losses that are used. Here again the energy that cannot be absorbed by the motor mechanical losses (which is larger now) is dissipated in friction braking.

Similarly when a conventional i.c. engined vehicle is simulated deceleration energy is absorbed after losses in i.c. engine compression braking. Again, of the deceleration energy available after losses, any that cannot be absorbed in compression braking is dissipated in friction braking. An explanation of the i.c. engine compression baking model is given in section 2.3.2.5.

In all cases (electric,hybrid-electric and conventional i.c. engined vehicles) for a given amount of deceleration energy available at the wheels over a given time-step, the procedure to determine the split between prime-mover braking and friction braking is iterative and is explained in appendix II.

As far as the electric and hybrid-electric vehicles are concerned regenerative braking philosophies fall into two categories : 'ideal' braking and 'practical' braking (Kuzak et al 1982).

2.3.2.4.1 Ideal Braking

Ideal braking, which applies to the conventional i.c. engined drive-train also, simply dissipates the deceleration energy available that cannot be absorbed by the prime-mover (in compression braking for the i.c. engine, in mechanical losses for a traction motor with no regenerative capacity and in regenerative braking for a motor with regenerative capacity) into the friction brakes at the wheels. Figures 2.32 and 2.33 show for the electric and i.c. engine drive-trains how deceleration energy available at the road wheels is absorbed in the various components.

The simulation approach to braking is the opposite to what would occur in practice - as was described for acceleration in section 2.2. During simulation braking demand comes from the pre-defined deceleration profile, whereas in practice driver brake pedal demand will dictate the deceleration profile. The 'ideal' braking philosophy characterises the simulation approach, in that a smooth blend is always achieved between the prime-mover braking and friction braking whatever the deceleration profile since the split between friction and electrical braking is determined 'after' the cycle has been imposed upon the drive train rather than 'before' in the case of practical brakes.

2.3.2.4.2 Practical Braking

Because of the complexity required to achieve a smooth blend between electrical and friction braking for all driver demands (driving cycles), a practical system can only approximate to the ideal case.

Practical braking schemes can be further broken down into two types : parallel and split. (Kuzak,et al.,1982)

In a parallel braking scheme a fixed relationship between electrical braking and friction braking is maintained. In practice electrical braking torque may be a fixed proportion of master cylinder pressure, which is in effect driver demand. This is not possible for a simulation working from cycle demand so therefore the program allows the user to define the proportion of the total deceleration torque to be handled by the friction brakes (deceleration torque effectively represents deceleration rate). The relationship is:

$$T_{friction} = K_{brake}\, T_{deceleration} \quad - \quad (19);$$ where K_{brake} is the user input fixed relationship.

The split braking system is simply a refinement of the parallel system, in that an initial fixed relationship between friction and electrical braking is maintained to a predetermined braking torque after which a final fixed relationship between friction and electrical braking prevails. Braking torque can be represented as comprising of the deceleration torque (which will be constant for a linear deceleration profile) minus rolling and drag torque, the latter of which decreases with speed:

$$T_{brake} = T_{decel} - T_{drag} - T_{roll} \quad - \quad (20)$$

Because T_{drag} decreases as speed decreases, so T_{brake} increases. In the simulation the brake torque at which the change over from one pre-defined brake fraction to the other occurs, is represented as vehicle velocity as it is more easily grasped by the user. The predefined electrical to friction braking relationships are therefore:

$$T_{friction\ braking} = K_{initial}\ T_{dedel} \quad - \quad (21);\ \text{and}$$

$$T_{friction\ braking} = K_{final}\ T_{decel} \quad - \quad (22).$$

When the practical schemes are used for an electric drive-train and the regeneration limit of the motor is exceeded, or for a conventional i.c. engine drive-train where the i.c. engine cannot absorb all of the deceleration power in compression braking, then the ideal case will apply until a satisfactory split between prime-mover and friction brakes has been achieved for the particular operating point (cycle time-step) in question.

2.3.2.5 A Compression Braking Model for the I.C. Engine

The i.c. engine compression braking model was introduced in section 2.3.7.4 as forming part of the vehicle braking model operation, and although not contributing to the simulation program energy usage calculations, nevertheless adds to the general depth of modelling within the simulation program.

The model assumes that i.c. engine compression braking is achieved by the absolute difference between work done on the gas during the compression stroke, and work done by the gas during the expansion stroke. A four stroke cycle is assumed and for the two remaining strokes (induction and exhaust) it is assumed that gas pumping losses occur.

The difference in work done during expansion and compression can be translated into the difference in average cylinder pressure (means effective pressure) during compression and expansion. Thus, knowing engine geometry (engine capacity), the average pressure difference can be converted to an average torque due to the gas load above the piston.

Ignoring engine friction and pumping losses for the present, and assuming the same gas in the cylinder during compression and expansion (which is not the case), the piston has to do more work on the gas during compression than it receives back during expansion due to irreversibilities (heat transfer). As far as modelling is concerned this manifests itself as different indices for compression and expansion.

The indicator on pressure volume (p-v) diagram for the compression braking process, along with cylinder geometry is shown in Figure 2.34.

The indices of compression and expansion are modified further by the consideration of different in cylinder gases during compression and expansion.

It is assumed that although fuel may be burned during compression braking (not for the fuel off at idle and overrun control systems currently available by VW and B.L.) no power stroke occurs.

Engine friction and pumping losses are not included in the model, but a loss due to accessory load is included.

A full description of the model derivation is given in appendix III.

2.3.2.6 A Combined DC Motor Control Strategy using a CVT plus Battery Switching

Battery switching is the simplest, cheapest, most efficient and most reliable form of D.C. traction motor control. However, because of the small number of discrete voltage steps, moving from one voltage level to the next (higher) voltage level will tend to accelerate the vehicle at a

greater rate than was intended by the driver demand on the accelerator pedal, so making the ride 'jerky'. The implications for computer simulation are that during a voltage step, the driving cycle would have to be modified (iteratively) at every time-step where a mismatch between demanded voltage and delivered battery voltage occurred. Therefore as well as adding complication to the simulation program, assessment of results would be made difficult when comparing with say a vehicle with a controller giving smooth voltage control.

By the addition of a mechanical coupling device such as a CVT into the electric vehicle drive-line the jerks can be smoothed out. Not only would driveability be improved in practice but now simulation can be made easier because it is now possible to assume that the vehicle continues to drive the cycle after a voltage switch.

Considering the DC Shunt motor in Figure 2.35, below the break speed full field is applied (see section 2.3.2.1.1). Demand voltage is:

$$V_{DEM} = RaIa + K_2 If\ RSW \quad - \quad (23);$$ where K_2 is a constant.

If RaIa is small, which is usual for DC machine armature windings,

$$V_{DEM} = K_2\ If\ RSW \quad - \quad (24);$$

in other words the motor shaft speed step is in proportion to the voltage step, therefore:

$$RSW\ (1) = RSW(2) = RSW \simeq RB/_3; \quad if$$

if is assumed that the break speed line is near vertical which is true if IaRa is small.

During the simulation with the 1st voltage step applied, motor speed is at RSW(1) and the CVT ratio equal to RSW(1)/R.

When V_{DEM} becomes greater than VSW(1) then the next voltage switch is applied, VSW(2) and motor speed moves t RSW(2) with the CVT ratio altered to RSW(2)/R. This pattern continues until the motor break-speed is reached.

For operation above the break speed, 3 options are available:

(i) transmission lock-up in a fixed ratio;

(ii) constrain the motor to run at the break speed by altering the CVT ratio;

(iii) allow the motor to follow a pre-defined locus of optimum efficiency above the break speed by altering the CVT ratio.

All three alternatives apply to both motoring and generating regions of the motor map.

The optimum locus strategy must satisfy a number of requirements in order to be feasible.

(i) Operation must be above the break speed in order to be free of battery switching control and because maximum efficiency occurs in this region (Figure 2.36).

(ii) High motor speeds at low torque should be avoided as this implies a high motor shaft speeds at low vehicle speeds, necessitating high and perhaps impractical transmission ratios for long periods.

(iii) Finally maximum motor power/torque must be made available to give adequate vehicle performance.

The resulting optimum efficiency loci (motoring and generating) may look as in Figure 2.36, and it is interesting to note that the constant break speed control option gives a reasonable approximation.

The model offers the user a maximum of 5 battery switches (2-3 being a typical number, particularly for the shunt motor where field voltage must be less than, or equal to, the smallest voltage step). For a given field power requirement and a large number of voltage steps, therefore, field currents (and hence controller electronics) will tend to become impractically large.

It is assumed during simulation that the motor accelerates instantaneously to its next switching speed, so ignoring rotor inertia penalties, which although may be significant for a given switch, because only 1-2 switches would generally occur per acceleration, would in effect form a small proportion of total cycle time.

2.3.2.7 I.C. Engine Cold Starting Model

Fuel consumption penalties incurred by i.c. engine cold starting can be modelled in one of two ways: the percentage increase in fuel consumption over the fully warmed up value at a particular loading condition can be described in terms of time elapsed; or alternatively the same percentage increase can be related to vehicle distance covered. The former method may be more representative of vehicle driving conditions as the i.c. engine could still be warming up whilst the vehicle is stationary (not covering any distance) at, say, traffic lights. However, if the philosophy of cutting i.c. engine fuel at idle is assumed, then there is no difference between the two methods.

Additionally in order to realistically model any cold start penalty associated with the hybrid-electric vehicle when the i.c. engine is stopped for a significant period and then restarted, it would be necessary to have some thermal model of the i.c. engine and its cooling system in order to predict temperature drop and rise with time or distance travelled.

The model included at present relates the percentage increase in fuel consumption over the fully warmed up fuel consumption, at a particular operating point, with distance travelled and ambient temperature, and uses experimentally obtained results (Shell Research).

The curves in Figure 2.37 show for two ambient temperatures (0°C and 20°C) empirical cumulative fuel consumption in mpg with distance travelled (Shell Research).

The model uses exponential curves to represent the data at the two temperature extremes, and linearly interpolates to find fuel consumption penalties corresponding to ambient temperatures in between and beyond these values.

For a given temperature T_a and distance travelled x, the fuel consumption penalty fraction y_{T_a} is:

$$y_{hot} = 0.48\ e^{\left(\frac{13.7}{13.7+x}\right)} \qquad \text{(at 20°C)} \qquad - \qquad (25);$$

$$y_{cold} = 0.88\ e^{\left(\frac{1.42}{1.42+x}\right)} \qquad \text{(at 0°C)} \qquad - \qquad (26).$$

At T_a:

$$y_{Ta} = y_{cold} - \frac{Ta}{20}\,(y_{cold} - y_{hot}) \qquad - \qquad (27)$$

At temperatures below 0°C the model simply extrapolates below the y_{cold} curve, so giving greater penalties.

It must be pointed out that the fuel consumption penalties y_{Ta}, y_{hot} and y_{cold} are the 'instantaneous' penalties whereas the empirical data is represented in terms of the 'cumulative' penalty. The values of the constants used in the exponential curve fits, however, were derived

penalty values at the extremes of the empirical curves. At x = 0, y_{hot} = 1.3, y_{cold} = 2.4; and at the points where the curves begin to level - at x = 5, y_{hot} = 1.0 and at x = 10, y_{cold} = 1.0. Therefore the maximum cold start penalty with no cumulative effect at x = 0 and the fully warmed up distance travelled at y_{cold} and y_{hot} = 1.0 are used, so enabling the 'cumulative' data to be converted into 'instantaneous' relationships. As the curves show, y_{hot} and y_{cold} never actually reach 1.0 for the cumulative empirical data because the initial penalty is always present, if in an ever decreasing percentage, but this discrepancy is small.

2.3.2.8 Vehicle and Component Weight Modelling

As was described in section 2.2, the simulation program will give the user three options as to how the vehicle weight is to be assembled. In the first of these options the user can choose a 'standard vehicle', in which case vehicle weight is 'picked up' , along with other characteristics, from default values depending upon vehicle class. Secondly, the weight can be added by the user 'manually', component by component (if known), starting with the 'basic bodyshell weight' (i.e. the kerb weight minus the power train and its associated structural weight). Finally, the third option is to allow the program to determine vehicle weight 'automatically'. component by component - starting with the basic bodyshell weight, again, which is input by the user. Typical values of bodyshell weight for various classes of European vehicle have been derived from various published sources (Autocar,1981) (Ford Motor Co.-UK).

The basic weight addition features of the simulation are described in the flow chart of Figure 2.38.

For both manual and automatic weight addition, the user must also input along with each component weight a 'weight progagation factor'. This factor increases the component weight to represent the amount of extra structural weight in the vehicle required to hold the component. Typical values of component weight increase are 30-40% and the program will default to a weight propagation factor of 1.35 at each component.

The automatic weight build up feature is particularly useful when altering component ratings (and hence their weights), and/or when comparing different drive-trains for a common vehicle class, where the basic bodyshell will form a common base onto which component weights are added. In this way completely differing drive-trains can be realistically compared in terms of weight.

2.3.2.8.1 Power to Weight Correlations

The power to weight correlations used for hardware building blocks in the simulation program are derived from the empirical data available in each case.

For mechanical transmission components, including prime-movers, a torque/weight relationship is more correct as it is the torque transmitted that dictates component sizes. Although, in the majority of cases power/weight relationships were only available, these relationships are modified according to the prime-mover speed range relative to a reference speed range. Because most of the empirical data was for components applicable to passenger cars, the reference speed range used was 0-5000 rpm.

The weight calculation equations used in each mechanical hardware building block can be written:

$$WT_{component} = WPR \times Prated \times \frac{5000}{max\ speed} (Kg) \quad - \quad (28)$$

For the i.c. engine, the empirical data for both gasoline and diesel engines suggests that the weight to power ratio, WPR, also varies with rated power (B.L. cars) and using straight line fits to the data obtained the resulting relationships derived were:

$$WPR = 3.0 - 0.0125 \times Prated \text{ (gasoline)} \quad - \quad (29)$$

$$WPR = 4.0 - 0.188 \times Prated \text{ (diesel)} \quad - \quad (30)$$

The D.C. series and shunt machines were also well supported as far as empirical power/weight data was concerned, although a single source for a current D.C. shunt machine was used (Wilson et al.,1982). The weight calculation equation of both 'series' and shunt machines is:

$$WT_{component} = 3.3 \times Prated \times \frac{5000}{max\ speed} \ (Kg) \quad - \quad (31)$$

As far as other hardware building blocks were concerned empirical data was limited in published sources and in some cases only available from the manufacturers directly. This is partly due to the the embryonic nature of certain components, such as the AC induction and DC switched reluctance machines, and partly because in certain cases there has not been a need to measure or publish certain component weights because of their small contribution to total vehicle weight.

The AC induction and D.C. switched relutance machines, because they both adopt such features as simple rotor construction but having complex and heavy control electronics - and since they are modelled as motor/controller units, are treated in exactly the same way.

Using data for an induction motor/controller available from a manufacturer (Ford Motor Co.U.K.) , the weight calculation equation for both induction and switched reluctance machines is

$$WT_{component} = 3.0 \times Prated \quad (Kg) \quad - \quad (32)$$

Data for mechanical transmission components such as fixed and variable ratio transmissions has also only been available through a manufacturer (Ford Motor Co.UK).

The weight calculation equations using data from the source:

$$WT_{component} = 0.5 \times Prated \times \frac{5000}{max\ speed} \quad \text{- manual transmission} \quad - (33)$$

$$WT_{component} = 0.5 \times Prated \times \frac{5000}{max\ speed} \quad \text{- spur gear final drive} \quad - (34)$$

$$WT_{component} = 0.7 \times Prated \times \frac{5000}{max\ speed} \quad \text{- bevel gear final drive} \quad - (35)$$

$$WT_{component} = 1.25 \times Prated \times \frac{5000}{max\ speed} \quad \text{- automatic transmission} \quad - (36)$$

The difference between the spur and bevel gear final drive types accounts for the spur-gear case being inherently a front-engine/front-wheel drive application and the bevel gear case being a front-engine/rear-wheel drive application. The bevel gear case having a long drive-shaft and a separate, remotely mounted unit.

Finally, the separate DC series and shunt motor controller building blocks are modelled in terms of weight by a simple weight to power constant and obviously have no speed modification. Two sources are shown, giving data for both field and armature controllers combined:

$$WT_{component} = 1.36 \text{ Prated (Wilson et al.,1982)} \quad - \quad (37)$$

$$WT_{component} = 0.75 \text{ Prated (Lucas Chloride)} \quad - \quad (38)$$

2.3.2.9 Tyre and Rolling Loss Models

Tyre rolling losses have only recently become the focus of attention in recent years as far as passenger cars are concerned, but have always been of significance in the larger commercial vehicle market. The model included in the simulation program uses empirical data from sources related to both markets (Slusser et al.,1981) (Cummins,1984).

Vehicle rolling resistance is the extra tractive effort needed to overcome tyre losses and is simply related to the vehicle weight by a non-dimensional coefficient:

$$T_{rol} = CR1 \text{ Wvg. (N)} \quad - \quad (39)$$

Because it is related to vehicle weight other rolling losses, such as wheel bearing friction will also be included.

From the published data the coefficient of rolling resistance shows a variation with road speed. At low and medium road speeds (<90 Km/hr) the coefficient remains roughly constant (Appendix VIII), but as road speed rises higher the effects (due to tyre heating) become significant.

It is because high speeds are very seldom considered for both simulation and actual vehicle testing, that values assumed or measured values obtained for the coefficient of rolling resistance have been constants.

The simulation program here employs a flexible model that allows rolling resistance to vary as:

$$CR1 = CR_{static} + CR_{dyn} (Ve)^N \quad - \quad (40)$$

The constants CR_{static} and CR_{dyn} are user input constant termed the 'static' and 'dynamic' rolling resistance coefficients, respectively.

The polynomial index,N, is also user input and typically lies between 1.0 and 2.0.

A constant value for the rolling resistance coefficient CR1 can be input by simply inputting the desired value for CR_{static} and then setting CR_{dyn} to zero.

2.3.3 Hybrid-Electric Vehicle Control

Initial work on hybrid-electric vehicles using the simulation program at Durham involved merging the conventional i.c. engine and the pure electric drive-trains together using arbitrary control strategies. Development to begin with was on a fixed parallel configuration using a simple velocity control strategy, the building blocks of which were introduced in section 2.2. A series configuration developed later for the simulation package employed control strategy based on battery state of charge (Bullock,1983). The building blocks for this strategy were also described in section 2.2.

From the initial arbitrary base as regards control strategy one approach to development would be to devise new strategies to always improve upon the previous strategy without getting any measure of whether an optimum strategy had been attained.

Alternatively, another approach would be to devise a method of optimising a given drive-train over any given driving cycle. The power train behaviour could then be observed throughout the cycle to achieve this optimum, the criteria for which could be minimum energy consumption, minimum cost to the user or minimum emissions.

From the optimum control strategy derived from observations at power-train behaviour, it would now be possible to work 'backwards' and devise implementable control strategies but now, not only with a clear target to aim for but also some indication on how to achieve it.

2.3.3.1 Optimum Control

Whatever the method chosen to optimise control there must be a criteria for optimisation, and, as suggested in 2.33 this may be minimising cost, energy consumption or emissions.

With the European market in mind, minimisation of energy consumption and cost to the user is of prime importance since emissions regulations have not progressed to the extent that they have in other world markets.

This aim can be expressed in what is called an objective function, which simply reduces to a linear equation with two terms - one relating to each energy source for the hybrid electric vehicle:

$$F = E_1 + E_2 \quad \text{(Kwhr)} \qquad - \quad (41)$$

In the equation, E_1 is the energy taken from one on board energy source, and E_2 is the energy taken from the other.

Both on board energy consumption terms, E_1 and E_2 are separate functions of the hybrid vehicle control variables, and for both series and parallel configurations these variables are clearly defined. Therefore F must be minimised with respect to all variables:

$$\text{if,} \quad F = fn'(v_1 v_2 v_3 .. v_n) + fn(v_1 v_2 v_3 ... v_n) \text{ (Kwhr)} \quad - \quad (42)$$

$$d\left(\frac{dF}{v_1 v_2 v_3 .. v_n}\right) = 0 \quad \text{for a minimum}$$

The parallel configuration will have a maximum of 3 control variables : a variable defining the torque or power split between the two power sources, X and two variables defining the transmission ratios, GR and GR1, of each power source transmission.

Similarly, the series configuration will also have a maximum of 3 variables : again a variable defining the power split between the two power sources, X, a variable defining the transmission ratio of a single transmission for the traction motor and a variable defining the generator set speed.

Without knowing function fn and fn' it is not possible to solve for a minimum of F analytically, but using computer based optimisation techniques a minimum value of F can be readily found at each driving cycle time-step.

Computer based optimisation techniques will achieve a 'numerical' solution to the objective function minimisation as they look at values of the objective function for discrete values of each control variable in a given range.

The slowest but most accurate method of minimisation is to calculate F for every possible combination of control variable and then search for the combination that gives the minimum value of F.

Faster methods reduce the computational burden by studying the value of F over a smaller range of control variable values. A simple 'gradient' method (Fox,1971) studies the rate of change of F and deduces a minimum when the rate of change $dF/_d(\nu_1\nu_2\nu_3..\nu_n)$ is zero. Also, there is a quadratic approximation method (Fox,1971) that calculates F over a small range of control variable values and then fits a quadratic equation to the data, the minimum of which can be found when, again $dF/_d(\nu_1\nu_2\nu_3...\nu_n)$ is zero.

The danger with the faster methods is that they rely upon the objective function F, being a reasonably smooth and continuous function. If the function is neither smooth nor continuous then a faster method may locate 'local' rather than 'global' minimum values of F because of the small range of control variable values considered.

In selecting the minimisation method it was appropriate to study a typical example of objective function that would be obtained from a hybrid-vehicle simulation program. For simplicity, a single variable X in a parallel configuration was considered, and as Figure 2.39 shows, the function F is neither smooth nor continuous. The main discontinuities occur at extreme value of X and are characterised by the i.c. engine cutting in when X≒0.05and by the traction motor cutting out at X = 1.0.

It was therefore for this reason, plus the fact that faster minimum searches are usually only attempted where large numbers of variables are present (>> 3),that the method that simply calculates F for every combination of control variable was selected.

2.3.3.1.1 Optimum Control Algorithm

The optimum control algorithm developed for the simulation program modifies the basic objective function by introducing two new terms into (41):

$$F = \lambda_1 E_1 + \lambda_2 E_2 \qquad \text{(Kwhr)} \qquad - \qquad (43)$$

Again, in the equation, E_1 is the energy taken from one of the on-board energy storage devices and E_1, the energy taken from the other.

The two new terms introduced into the objective function, and are user input 'weighting factors', the values of which can be interpreted

in any one of several ways. Firstly, if values of 1.0 are assigned to both λ_1 and λ_2, then the objective function F defines the on-board energy consumption of the vehicle (the energy consumption as the user sees it). Secondly, because the on-board stored energy of the vehicle has come via two conversion routes with different efficiencies, so λ_1 and λ_2 can be given values to represent the inverse of the conversion efficiencies of the respective routes. Hence the 'total' or 'primary' energy consumption at the point of extraction is defined by the objective function. Finally, the two on-board energy sources may have different costs per unit of energy associated, as far as the user is concerned. By inputting appropriate values of λ_1 and λ_2 to represent the cost per unit energy of the tow on-board sources, the objective function will now define the running cost to the user.

Both on-board energy sources and hence their respective power sources can be 'weighted' or penalised relative to the other by inputting apropriate values of λ_1 and λ_2. For example, if energy source E_1 is to be penalised, a large value of λ_1 relative to λ_2 (in effect a large value of λ_1/λ_2) is input. Thus, if E_1 refers to the liquid fuel tank and E_2 to the traction battery, a hybrid-electric vehicle can be made to run from an all i.c. engine mode to an all-electric mode by increase relative to λ_2 (increasing λ_1/λ_2). Furthermore, the values and meanings of the weighting factors change for vehicle driving modes other than the motoring case described. When charging the battery using excess power from the i.c. engine the secondary source factor λ_2 must now be given a value of 1.0 as the conversion efficiences (chemical to mechanical to electrical to chemical) is included automatically since it is internal to the vehicle simulation. The reconversion efficiency, however, (i.e.

reconverting this energy back to mechanical energy at the road wheels) will depend upon the loading condition but lies in a range of 25% to 100% - implying weighting values of 1.0 - 4.0 for λ_2 .

The optimum control algorithm calculates the value of the objective function F for every combination of control variable value at a given driving cycle time step, and puts the values of objective function, F into an array, the 'dimensions' of which depend upon how many control variables are involved in the drive-train. This array is then searched for the minimum value of F and the corresonding control variable values are identified. The program then performs the actual 1st dynamic and 2nd dynamic (see section 2.2) simulation passes using the optimum control variable values for that time step, before moving on to the next cycle time-step and repeating. If any of the control variable value combinations put unrealistic demands or either one or both of the two power sources (performance limits are exceeded) then the objective function is given an arbitrarily high value to ensure that this particular combintion is ignored during the minimum search. For the case when all control variable value combinations exceed prime-mover performance limits then the driving cycle is modified in the manner described in section 2.2

For the primary energy source (liquid fuel tank) energy removed is:

E_1 = FCS. CAL (Kwhr) - (44); where FCS is the

instantaneous fuel consumption (volume or weight and CAL is the calorific value of the fuel (per unit volume or weight).

Energy removed from the secndary energy source (traction battery) is similarly:

E_2 = ΔSOC. ED5. WBATT (Kwhr) - (45); where SOC is the

instantaneous change in battery state of charge, EDS is the energy density of the battery (5hr rate) and WBATT is the total weight of the battery.

The control variable common to all hybrid-electric configurations is the torque or power split fraction X and is simply the fraction of the road load power met by the i.c. engine. At a value of zero, the vehicle will run on the traction motor only and at a value of 1.0 the i.c. engine will meet the road-load alone. For values greater than 1.0, however, the i.c. engine (if enough power is available) is not only meeting the road-load power, but also a fraction at this road-load power developed by the i.c. engine is being used to charge the traction battery. For example, if X = 1.05, the i.c. engine not only meets the road load but delivers power to the battery corresponding to 5% of the road-load power.

Although X will have an infinite number of values in reality, for the purposes of simulation, this mut be reduced to a discrete number, and to reduce the computational burden a value of $\Delta X=0.05$ is used throughout. Other control variables are similarly given discrete values over a fixed range with the exception of the discrete ratio transmission variable which inherently embodies discrete steps. The CVT ratio range was therefore divided into 10 steps for the hybrid and 20 for the electric and conventional i.c. engine configurations (having only one variable), and the generator set speed range into 5 steps.

The optimisation method here differs somewhat from that suggested by other sources (Mosbech)(Jamazadesh et al 1982) where a path of minimum energy consumption is determined in order to reach a pre-defined energy level in one of the on-board energy sources at the end of the driving cycle. Here the same can be achieved if the user manipulates the weighting factors iteratively until the desired energy level in the traction battery is achieved (effectively range to battery discharge as it is this that is presented to the user here).

In section 2.2 it was introduced that there are a suite of optimisation building blocks available to the user, and these cover

drive-trains having one control variable (one dimensional optimsation), two control variables (two dimensional optimisation) and three control variables (three dimensional optimisation). For the one-dimensional case, Figure 2.40 shows the program flow chart and Figures 2.41 and 2.42 and 2.43 shows the application to a parallel hybrid with no variable ratio transmission and to conventional i.c. engined and pure electric drive-trains. The flow chart is also shown for the two-dimensional case in Figures 2.44 and 2.45 when applied to a parallel hybrid, and the applications of the program to both series and parallel configurations is shown in Figures 2.46 and 2.48. Finally, the flow chart for three dimensional optimisation is shown in Figures 2.49 and 2.50 when applied to a parallel configuration and Figures 2.51 and 2.52 show how it is applied to both series and parallel configurations.

2.3.3.2 Sub-optimum control

The optimum control algorithm simulates an ideal control system, controlling energy consumption. As a result this system would be difficult, if not impossible to implement in practice. However, by studying the behaviour of control variables for the optimum control strategy, a sub-optimum or implementable control algorithm may be devised and developed.

From observation of the control variables using the optimum control algorithm (see chapters 5 and 7), several significant patterns emerged. Firstly, below a certain i.c. engine speed (usually the i.c. engine minimum operating speed) all-electric operation was favoured. Secondly, below a certain i.c. engine load level, all-electric operation, was again favoured. Finally, above a certain i.c engine load-level which was below the full throttle curve, hybrid operation was favoured. An overall picture emerged

in that operation on one or the other of the two power sources was favoured and a blend of the two only resorted to when demand load exceeded the limits of either one. Generally, the electric tractionmotor was favoured for low load conditions and the i.c. engine for high load conditions. This can be explained by the positions of maximum efficiency on the performance maps for each case: for the i.c. engine maximum efficiency occurs at high load, whereas for the traction motor maximum efficiency occurs at low load to medium load.

2.3.3.2.1 Sub-Optimum Control Algorithm

The sub-optimum control algorithm devised, based on the aforementioned observations of the optimum control algorithm, simply defines a region on the i.c. engine fuel map where i.c. engine operation is desirable. In its most simple form this region is simply a 'box' with straight sides at right angles to each other. The user is allowed to alter the size and proportions of the box, and in so doing change the emphasis on either of the two power sources. (Figure 2.53)

The algorithm (a block diagram of which is shown in Figures 2.54 and 2.55) for a given operating condition (cycle time step) selects which (if any) gear ratios put this operating condition inside the 'box'. If more than one ratio puts the point inside the box, the 'box' is shrunk towards the region of maximum efficiency on the map, and if more than one ratio still satisfies this second criteria, simply the lst ratio to do so is selected. If no ratios put the operating point inside the box, the algorithm will test to see where on the i.c. engine fuel map they occur. If points occur below and/or to the left of the operating box, then the all electric mode is selected and a transmission ratio that puts the operating point as close to the motor break speed is selected as it is here that the region of maximum efficiency occurs, at least forthe DC machines. If

points are above the box the hybrid mode is selected, the i.c. engine operating point is moved to the top edge of the box and the lowest possible transmission ratio is selected (highest gear) in order to maximise i.c. engine efficiency. During deceleration with the i.c. engine decoupled, a transmission ratio to achieve as high a motor speed as possible is selected as not only does high efficiency occur in this region but it also corresponds to the motor field control region, so resulting in high controller efficiency.

As far as the hybrid-electric vehicles are concerned, the algorithm has only been applied to the parallel configuration having only a single variable ratio transmission. However, the basic principle has also been adapted for an electric vehicle application when a variable ratio transmission is used. Figure 2.56 shows the 'box' region when superimposed onto the motor performance map. Again, the algorithm selects which (if any) transmission ratios put the operating point (at a given time step) inside the box, and if more than one gear ratio satisfies this, the box is, again, shrunk towards the region of maximum efficiency for the traction motor. If no ratios fall inside the region then a ratio is selected that will put the operating point as close to the break speed as possible (even if the point falls above the box) as it is here that maximum efficiency occurs for the DC machines. Figure 2.57 shows the algorithm flow chart.

If no starting device (such as a friction clutch or torque converter) is present in the drive-line then the lower speed line must be coincident with the y-axis. The lower torque bound need not be coincident with the x-axis as ratios may be selected to raise the operating point above. Similarly the upper torque bound need not be coincident with the maximum torque as ratios in the transmission may compensate for the loss of maximum motor torque.

2.4 Conclusions

With the historical background of previous hybrid-electric vehicle simulation work the road vehicle simulation program written at the University of Durham has been described, both in terms of basic program operation and in terms of the major software developments carried out.

Any simulation program will need to have the results obtained validated at some point, but a more general simulation program will in addition require some measure of its user friendliness to be made.

Several of the software developments described in this chapter are important in that they have been carried out as a result of discrepancies highlighted during program verification, after which the verification was repeated, and also because of the role they play in the subsequent pure-electric and hybrid-electric vehicle studies.

As far as future simulation program developments are concerned, because the building blocks available have been developed to a satisfactory standard and short of the inclusion of new building blocks, these are likely to concentrate on the user friendliness aspects. The user-friendliness of programs such as HEAVY (Hammond et al, 1981) with its advanced model generation features remains a goal to aim for.

Listing of file : JANUSIC.FTN

```
      $BATCH
      $INCLUDE 9,JANUSST.FTN/G
      C
      C I.C. ENGINE VEHICLE SIMULATION
      C
      C      ********** VEHICLE ROUTINE STRUCTURE **********
             CALL VEHICLE(IFLAG)
             CALL DCYCLE(V,AC,IOPM,EFFDT,IFLAG)
             CALL WHEELS(V,AC,TORQW,RW,PB,IFLAG)
             CALL AXLE(TORQW,RW,TORQD,RD,PEMAX,REMAX,EFFDT,IFLAG)
             CALL TRANS(TORQD,RD,TORQG,RG,GR,EFFGB,GEAR,PEMAX,TRATE,RSW,IERGB1,
            *EFFDT,RMIN,REMAX,CVTP1,CVTP2,CVTS1,CVTS2,NCVT,PLIM1,RLIM1,NL,
            *10,IFLAG)
             CALL COUPL(TORQG,RG,TORQE,RE,RMIN,REMAX,PB,EFFDT,IFLAG)
             CALL ICENG(TORQE,RE,PEMAX,TRATE,RMIN,REMAX,CVTP1,CVTS1,NCVT,
            *PLIM1,RLIM1,NL,CC,PB,EFFDT,IFLAG)
      C      ********** END OF VEHICLE ROUTINE **********
      C
      $INCLUDE 9,JANUSF.FTN/G
      $BEND
```

FIGURE 2.1 I.C.Engined Vehicle Master Program

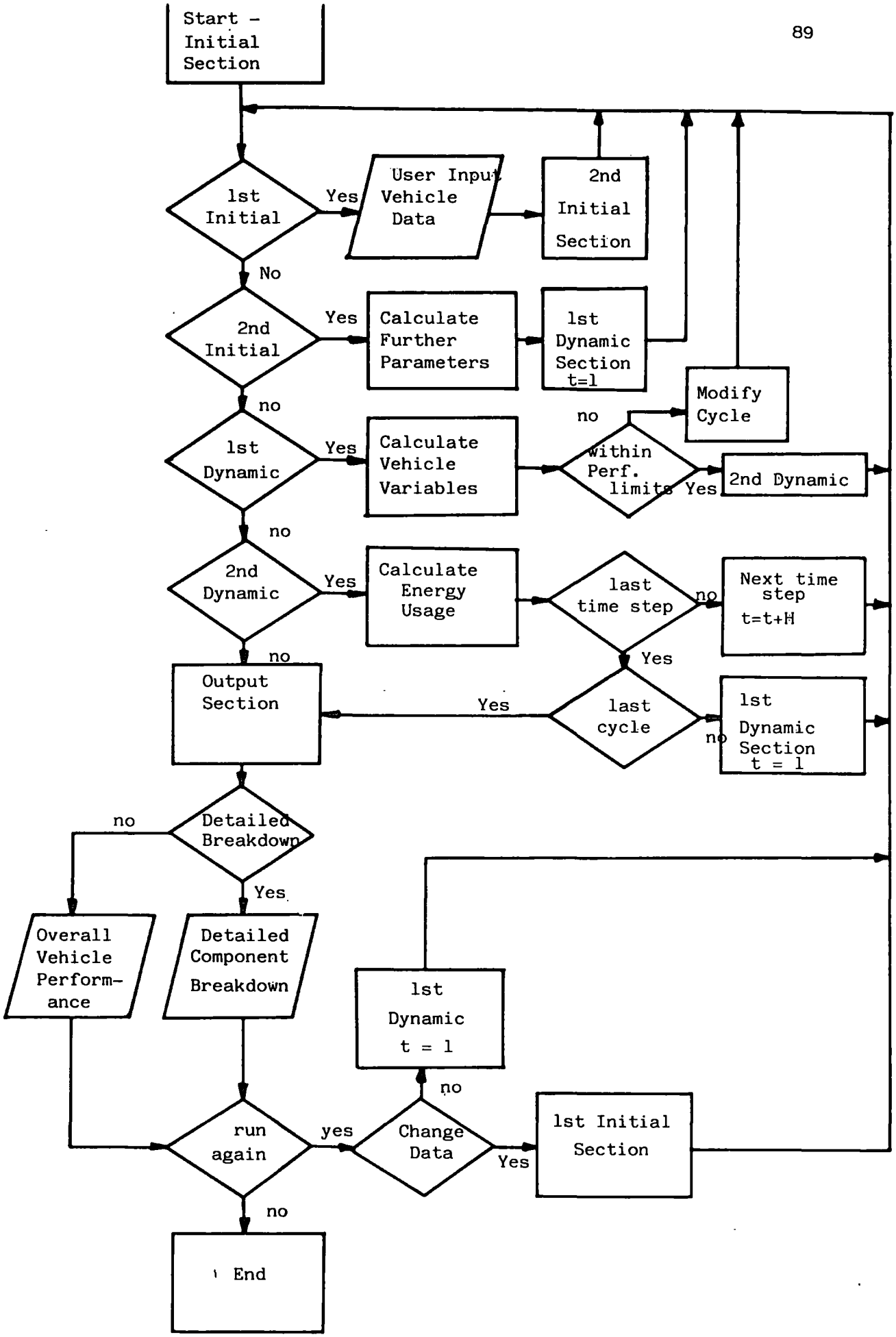

FIGURE 2.2: Basic Simulation Program Operation

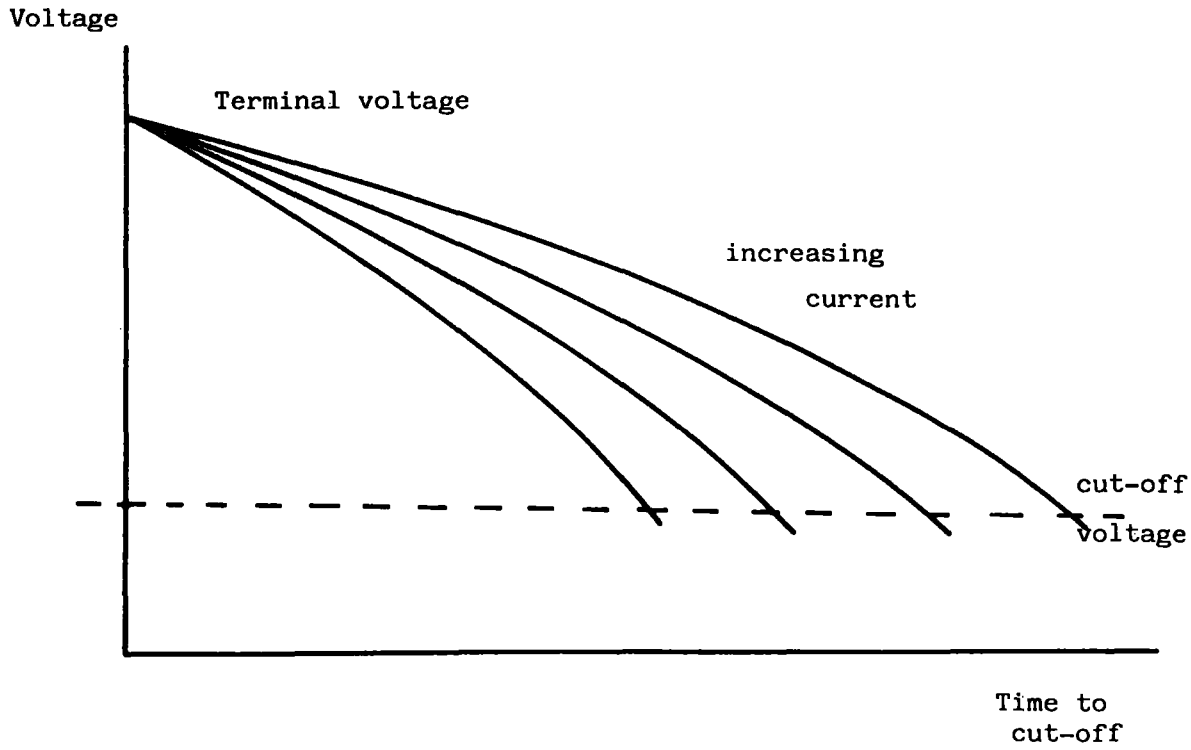

FIGURE 2.3: Battery Voltage/current/time Curves

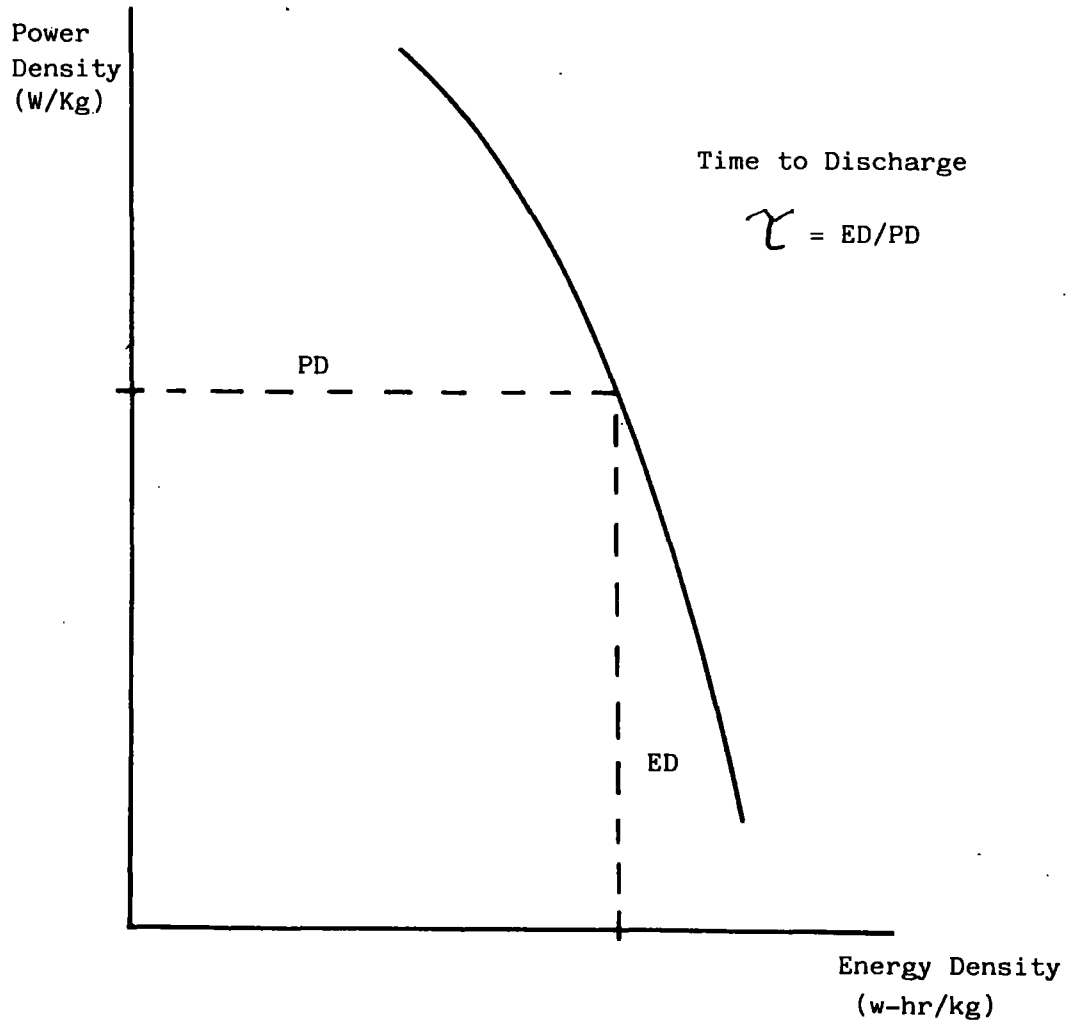

FIGURE 2.4: Battery Power density/energy density characteristic

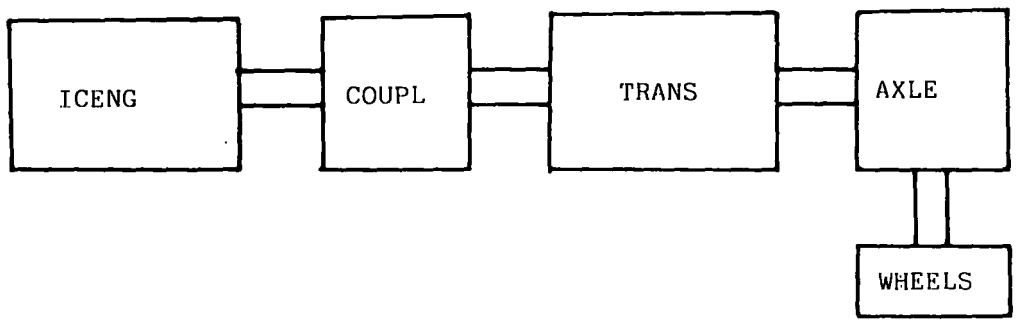

FIGURE 2.5: Conventional I.C.Engined Vehicle Drive-Train

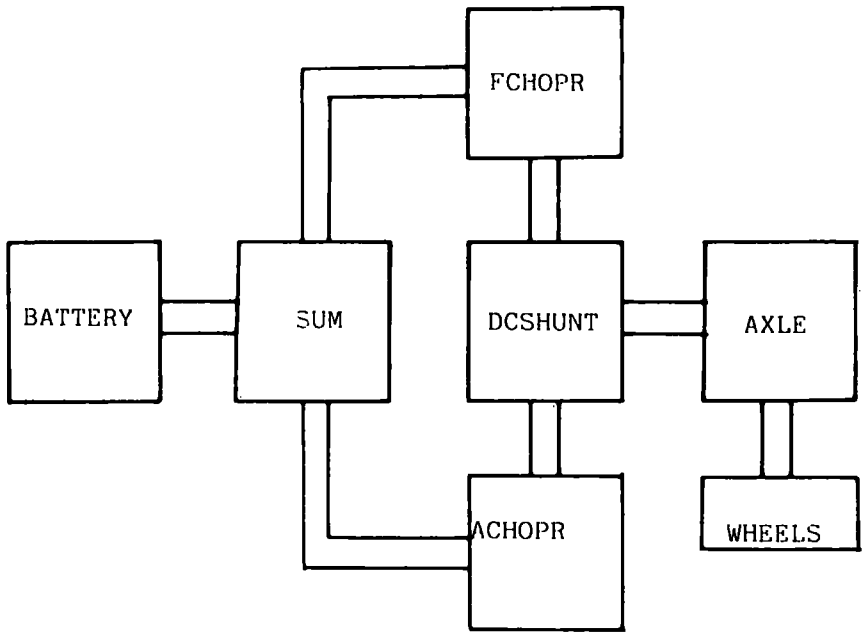

FIGURE 2.6: Electric Vehicle Drive-Train

Listing of file : JANUSEV1.FTN

```
      1   $BATCH
      2   $INCLUDE 9,JANUSST.FTN/G
      3   C
      4   C ELECTRIC VEHICLE SIMULATION
      5   C
      6   C      ********* VEHICLE ROUTINE STRUCTURE *********
      7          CALL VEHICLE(IFLAG)
      8          CALL DCYCLE(V,AC,IOPM,EFFDT,IFLAG)
      9          CALL WHEELS(V,AC,TORQW,RW,PB,IFLAG)
     10          CALL AXLE(TORQW,RW,TORQD,RD,PMAX,RMAX,EFFDT,IFLAG)
     11          CALL DCSHUNT(TORQD,RD,VA,CIA,VF,CIFL,PMAX,PAMAX,PFMAX,RB2,
     12         *VAM,VFB,CIAMAX,CIAMAXR,CIFMAX,CVTP1,CVTP2,CVTS1,CVTS2,NCVT,RMAX,
     13         *PB,EFFDT,IFLAG)
     14          CALL FCHOPR(VF,CIFL,CIA,VFB,CIBF,PFMAX,CIFMAX,IFLAG)
     15          CALL ACHOPR(VA,CIA,CIBA,VAM,PAMAX,CIAMAX,CIAMAXR,IFLAG)
     16          CALL SUM(CIBA,VB,VAM,CIBF,VFB,CIB,IFLAG)
     17          CALL BATTERY(VB,VAM,CIB,TNPP,1,SOC,IFLAG)
     18   C      ********* END OF VEHICLE ROUTINE ************
     19   C
     20   $INCLUDE 9,JANUSF.FTN/G
     21   $BEND
```

FIGURE 2.7: Electric Vehicle Master Program

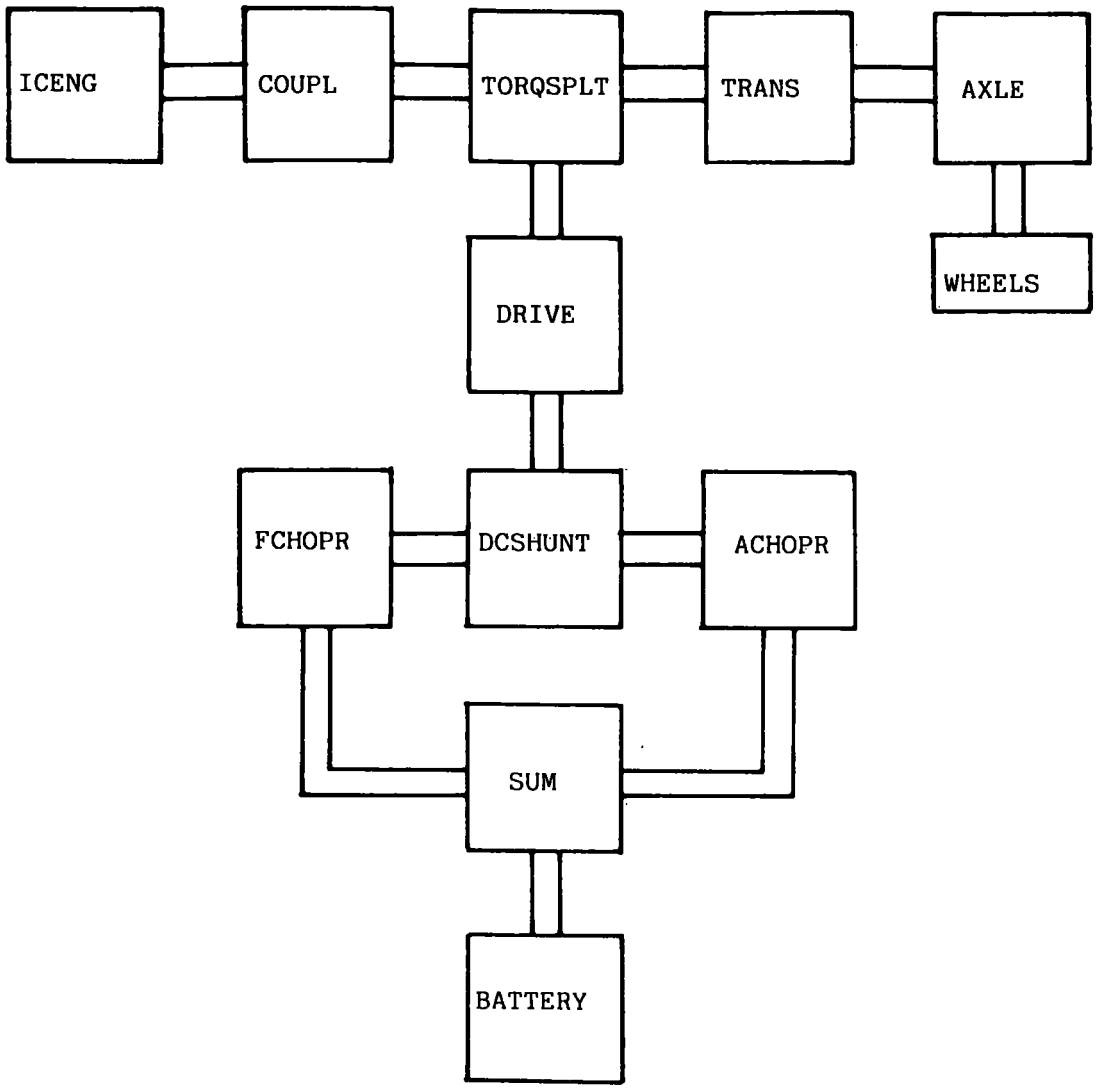

FIGURE 2.8: Parallel Hybrid-Electric Vehicle Drive-Train

Listing of file : JANUSHV.FTN

```
      C
      $BATCH
      $INCLUDE 9,JANUSST.FTN/G
      C
      C PARALLEL HYBRID SIMULATION
      C
      C     *********HYBRID VEHICLE SUBROUTINE STRUCTURE*********
      C
      C
      C     BLOCK 1
      C
            CALL VEHICLE(IFLAG)
            CALL DCYCLE(V,AC,IOPM,EFFDT,IFLAG)
            CALL CONTROLP(V,AC,SOC,MODE,IFLAG)
      C
      C     BLOCK 2
      C
            CALL WHEELS(V,AC,TORQW,RW,PB,IFLAG)
            CALL AXLE(TORQW,RW,TORQD,RD,PTOT,REMAX,EFFDT,IFLAG)
            CALL TRANS(TORQD,RD,TORQG,RG,GR,EFFGB,GEAR,PTOT,TRATE,RSW,0,EFFDT,
           *RMIN,REMAX,CVTP1,CVTP2,CVTS1,CVTS2,NCVT,PLIM1,RLIM1,NL,10,IFLAG)
            CALL TORQSPLT(TORQEIC,TORQG,TORQMGB,PEMAX,PMAX,PTOT,RG,RIC,
           *RMOT,RMIN,REMAX,MODE,PLIM1,RLIM1,NL,1.0,1.0,IFLAG)
            CALL COUPL(TORQEIC,RIC,TORQE,RE,RMIN,REMAX,0.0,0.0,IFLAG)
            CALL ICENG(TORQE,RE,PEMAX,TRATE,RMIN,REMAX,CVTP1,CVTS1,NCVT,
           *PLIM1,RLIM1,NL,CC,0.0,0.0,IFLAG)
      C
      C     BLOCK 3
      C
            CALL DRIVE(TORQMGB,RMOT,TORQM,REM,PMAX,RMAX,EFFDT,IFLAG)
            CALL DCSHUNT(TORQM,REM,VA,CIA,VF,CIFL,PMAX,PAMAX,PFMAX,RB2,VAM,
           *VFB,CIAMAX,CIAMAXR,CIFMAX,CVTP3,CVTP4,CVTS3,CVTS4,NCVT1,RMAX,
           *PB,EFFDT,IFLAG)
            CALL FCHOPR(VF,CIFL,CIA,VFB,CIBF,PFMAX,CIFMAX,IFLAG)
            CALL ACHOPR(VA,CIA,CIBA,VAM,PAMAX,CIAMAX,CIAMAXR,IFLAG)
            CALL SUM(CIBA,VB,VAM,CIBF,VFB,CIB,IFLAG)
            CALL BATTERY(VB,VAM,CIB,TNPP,1,SOC,IFLAG)
      C
      C     *********END OF SUBROUTINE STRUCTURE*********
      C
      $INCLUDE JANUSF.FTN/G
      $BEND
```

FIGURE 2.9: Parallel Hybrid-Electric Vehicle Master Program

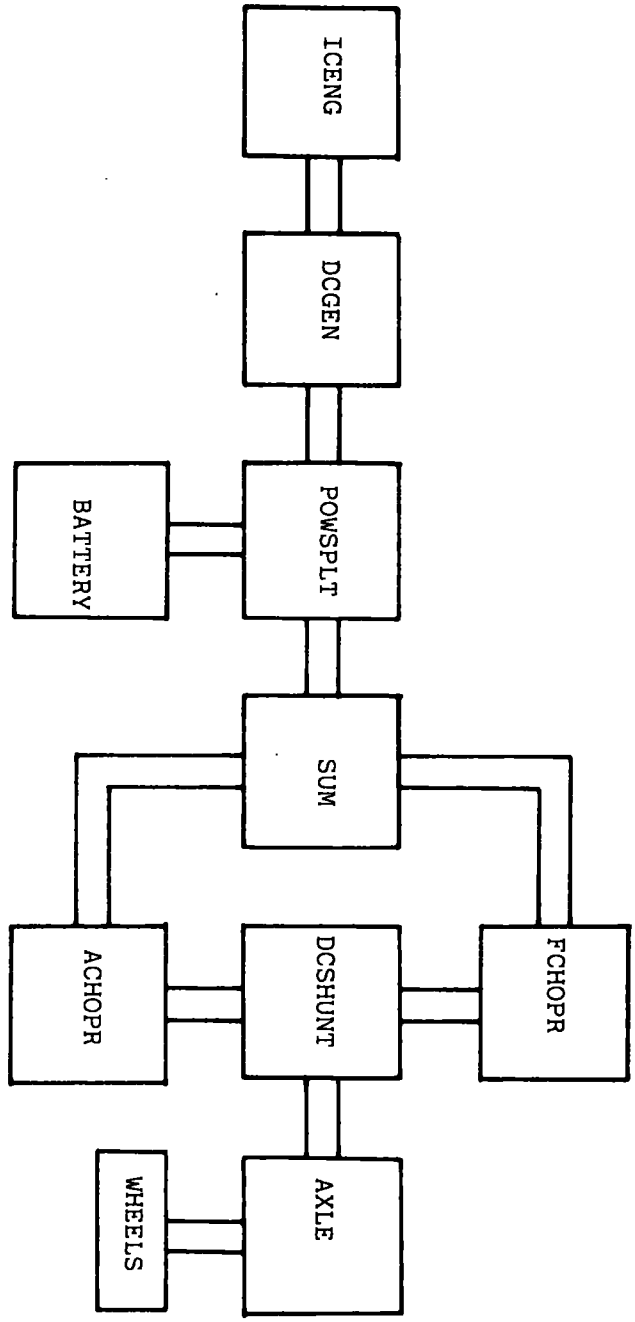

FIGURE 2.10: Series Hybrid Electric Vehicle Drive-Train

Listing of file : JANUSHV1.FTN

```
      C
      $BATCH
      $INCLUDE 9,JANUSST.FTN/G
      C
      C HYBRID VEHICLE SIMULATION
      C
      C     ********** VEHICLE SUBROUTINE STRUCTURE *********
      C
      C     ****** BLOCK 1 ******
      C
            CALL VEHICLE(IFLAG)
            CALL DCYCLE(V,AC,IOPM,EFFDT,IFLAG)
            CALL CONTROLS(SOC,V,AC,MODE,IFLAG)
      C
      C     ****** BLOCK 2 ******
      C
            CALL WHEELS(V,AC,TORQW,RW,PB,IFLAG)
            CALL AXLE(TORQW,RW,TORQD,RD,PMAX,RMAX,EFFDT,IFLAG)
            CALL DCSHUNT(TORQD,RD,VMOT,CIA,VF,CIFL,PMAX,PAMAX,PFMAX,RB2,VAM,
           *VFB,CIAM,CIAM1,CIFMAX,CVTP3,CVTP4,CVTS3,CVTS4,NCVT1,RMAX,PB,EFFDT,
           *IFLAG)
            CALL FCHOPR(VF,CIFL,CIA,VFB,CIBF,PFMAX,CIFMAX,IFLAG)
            CALL ACHOPR(VMOT,CIA,CIBA,VAM,PAMAX,CIAM,CIAM1,IFLAG)
            CALL SUM(CIBA,VA,VAM,CIBF,VFB,CIB,IFLAG)
         40 CALL POWSPLT(VB,VAM,CIB,MODE,CVTP1,CVTS1,NCVT,GEFF,TORQE,RE,
           *RMIN,PEMAX,REMAX,CC,CIBAT,IFLAG)
            CALL DCGEN(VAM,TORQE,RE,RMIN,ITGEN,GEFF,IFLAG)
            IF(ITGEN.EQ.1)GOTO 40
            CALL ICENG(TORQE,RE,PEMAX,TRATE,RMIN,REMAX,CVTP1,CVTS1,NCVT,
           *PLIM1,RLIM1,NL,CC,0.0,0.0,IFLAG)
      C
      C     ****** BLOCK 3 ******
      C
            CALL BATTERY(VB,VAM,CIBAT,TNPP,1,SOC,IFLAG)
      C     ********** END OF VEHICLE SUBROUTINE ENTERIES *********
      C
      $INCLUDE 9,JANUSF.FTN/G
      $BEND
```

FIGURE 2.11: Series Hybrid-Electric Vehicle Master Program

Listing of file : JANUSHV5.FTN

```
      C
      $BATCH
      $INCLUDE 9,JANUSST.FTN/G
      C
      C PARALLEL HYBRID SIMULATION
      C
      C     *********HYBRID VEHICLE SUBROUTINE STRUCTURE*********
      C
      C
      C     BLOCK 1
      C
            CALL VEHICLE(IFLAG)
            CALL DCYCLE(V,AC,IOPM,EFFDT,IFLAG)
      C
      C     BLOCK 2
      C
            CALL WHEELS(V,AC,TORQW,RW,PB,IFLAG)
            CALL OPTCONT(TORQW,IOPM,X,GR,ISTEP,IFLAG)
            CALL AXLE(TORQW,RW,TORQD,RD,PTOT,REMAX,EFFDT,IFLAG)
            CALL TRANS(TORQD,RD,TORQG,RG,GR,EFFGB,GEAR,PTOT,TRATE,RSW,0,
           *EFFDT,RMIN,REMAX,CVTP1,CVTP2,CVTS1,CVTS2,NCVT,PLIM1,RLIM1,NL,
           *ISTEP,IFLAG)
            CALL OPTQSPLT(TORQEIC,TORQMGB,TORQG,RIC,RMOT,RG,X,1.0,PEMAX,
           *PMAX,PTOT,ISTEP,IFLAG)
            CALL COUPL(TORQEIC,RIC,TORQE,RE,RMIN,REMAX,0.0,0.0,IFLAG)
            CALL ICENG(TORQE,RE,PEMAX,TRATE,RMIN,REMAX,CVTP1,CVTS1,NCVT,
           *PLIM1,RLIM1,NL,CC,0.0,0.0,IFLAG)
      C
      C     BLOCK 3
      C
            CALL DRIVE(TORQMGB,RMOT,TORQM,REM,PMAX,RMAX,EFFDT,IFLAG)
            CALL DCSHUNT(TORQM,REM,VA,CIA,VF,CIFL,PMAX,PAMAX,PFMAX,RB2,VAM,
           *VFB,CIAMAX,CIAMAXR,CIFMAX,CVTP3,CVTP4,CVTS3,CVTS4,NCVT1,RMAX,
           *PB,EFFDT,IFLAG)
            CALL FCHOPR(VF,CIFL,CIA,VFB,CIBF,PFMAX,CIFMAX,IFLAG)
            CALL ACHOPR(VA,CIA,CIBA,VAM,PAMAX,CIAMAX,CIAMAXR,IFLAG)
            CALL SUM(CIBA,VB,VAM,CIBF,VFB,CIB,IFLAG)
            CALL BATTERY(VB,VAM,CIB,TNPP,1,SOC,IFLAG)
      C
            CALL OPTIMISE(ISTEP,IOPM,X,GR,IFLAG)
            ETOTAL=W1*EFUEL+W2*EBATT
            WRITE(5,*)IOPM,X,GR,EFUEL,EBATT,ETOTAL,ISTEP,V,T
      C
      C     *********END OF SUBROUTINE STRUCTURE*********
      C
      $INCLUDE JANUSF.FTN/G
      $BEND
```

FIGURE 2.12: Parallel Configuration Master Program using Optimum Control

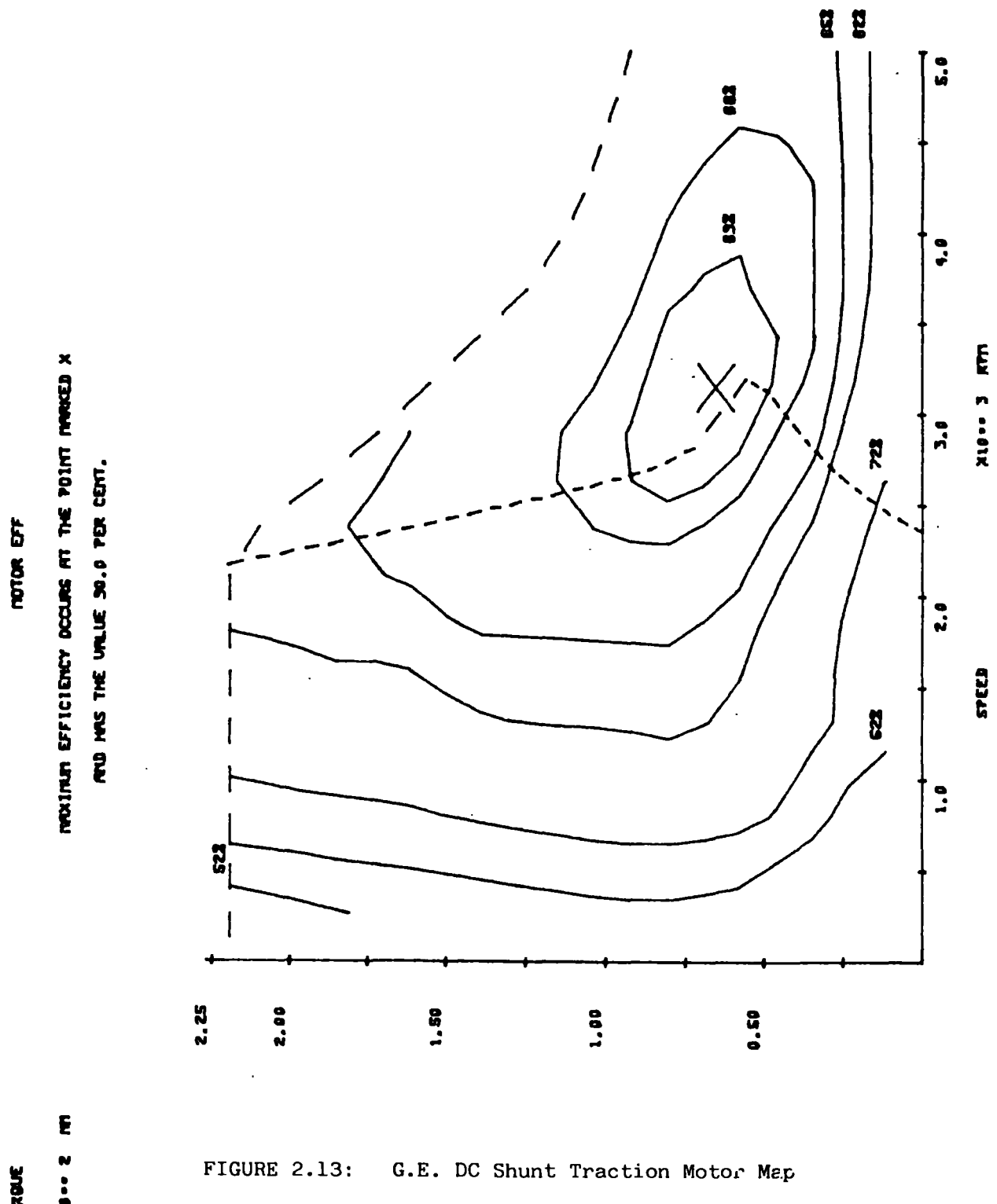

FIGURE 2.13: G.E. DC Shunt Traction Motor Map

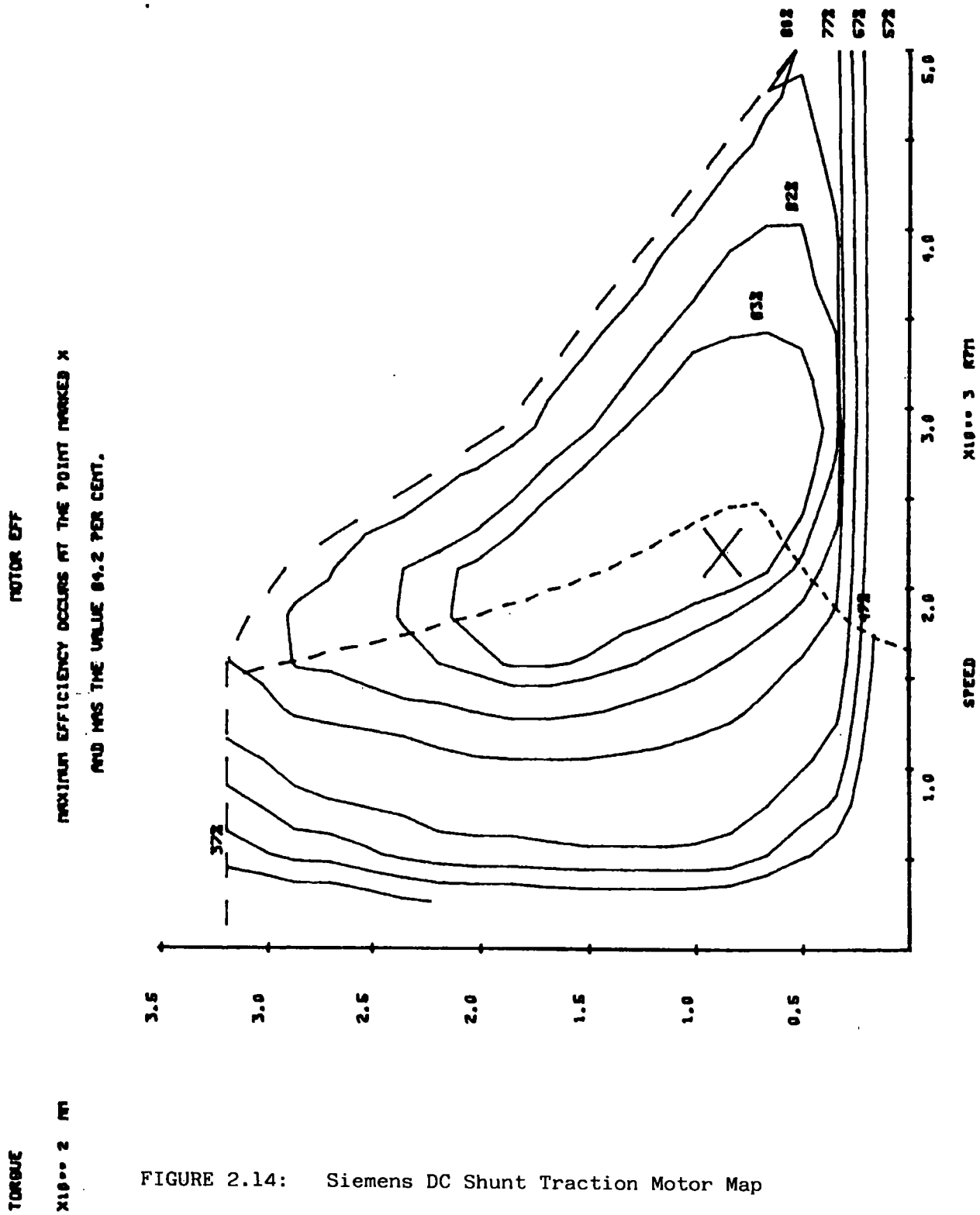

FIGURE 2.14: Siemens DC Shunt Traction Motor Map

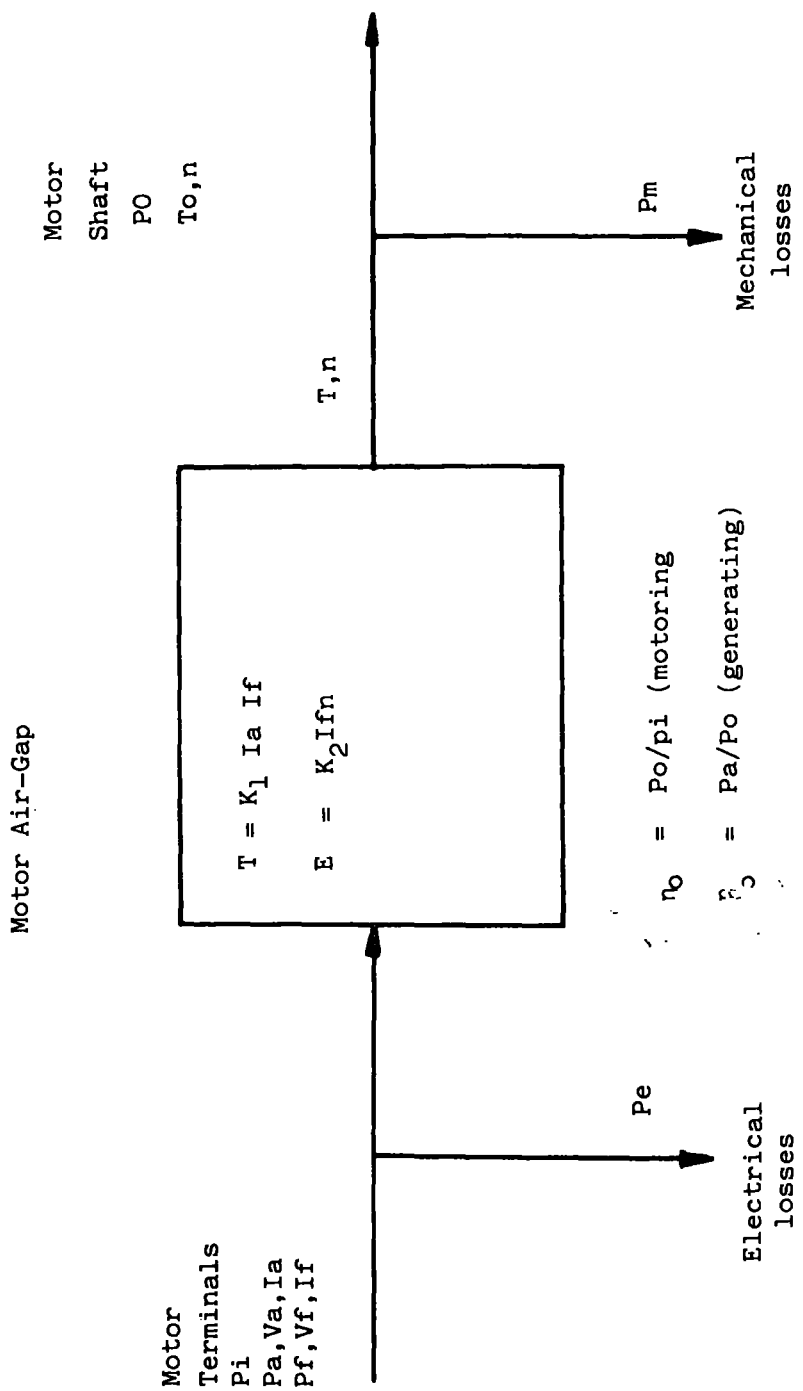

FIGURE 2.15: Loss Diagram for the DC Shunt Motor

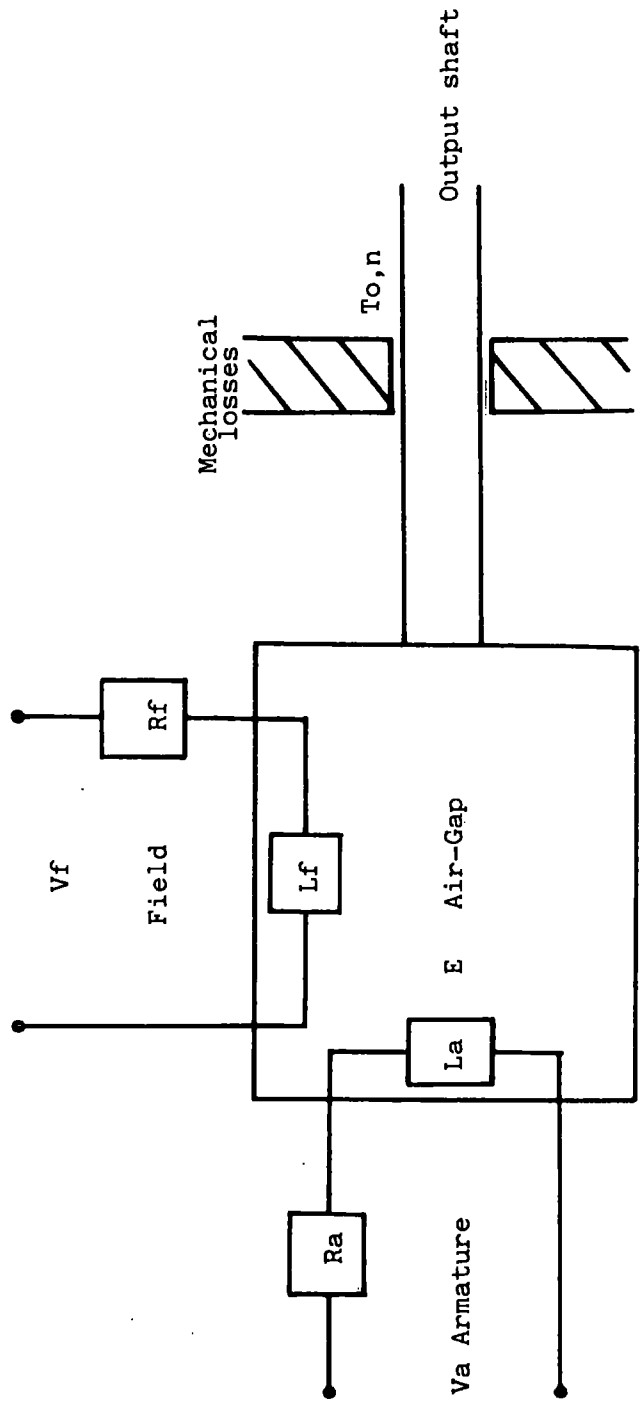

FIGURE 2.15: Electrical/Mechanical Interface in the DC Shunt Motor

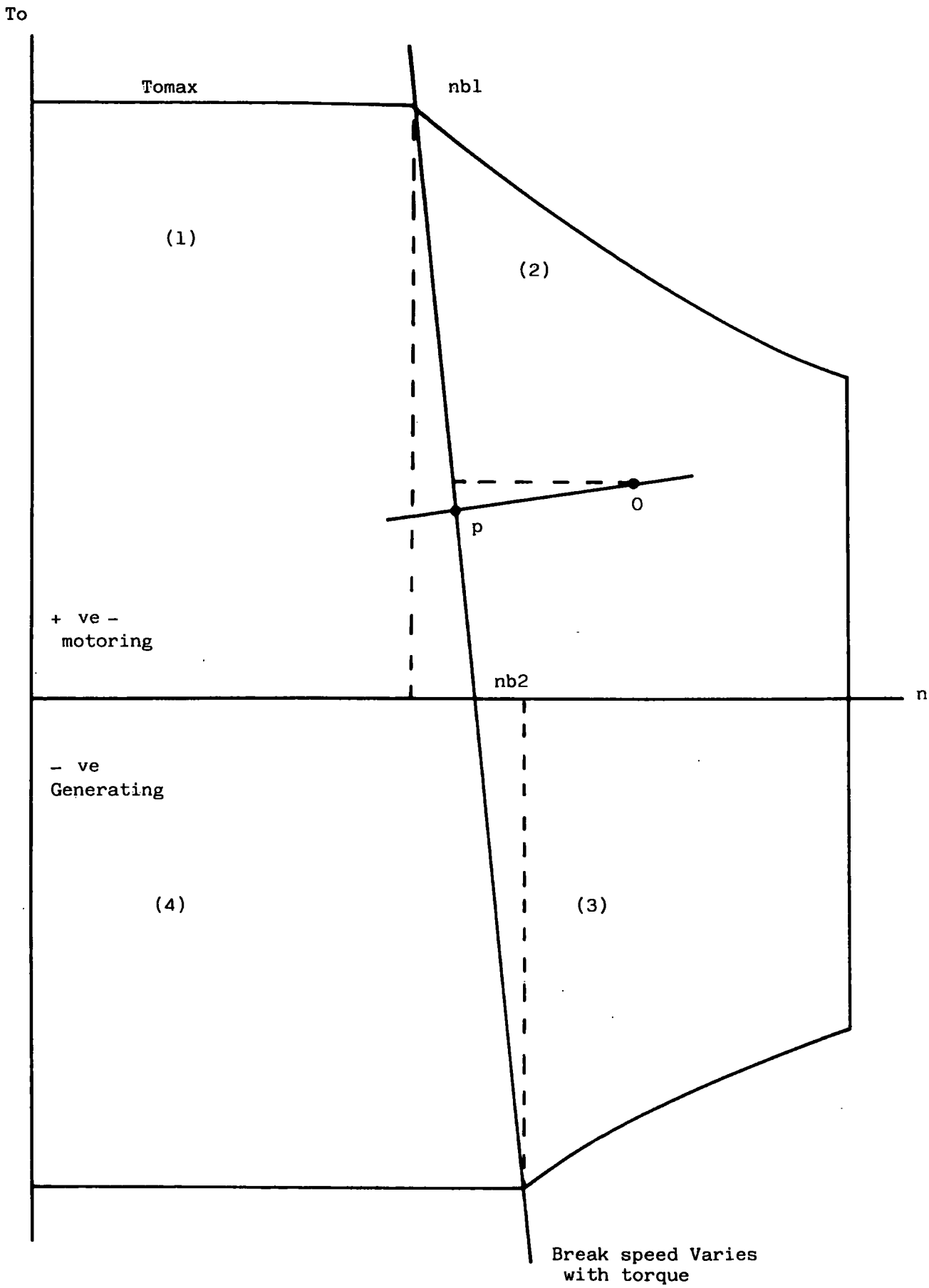

FIGURE 2.17: Operating Regions of the DC Shunt Motor

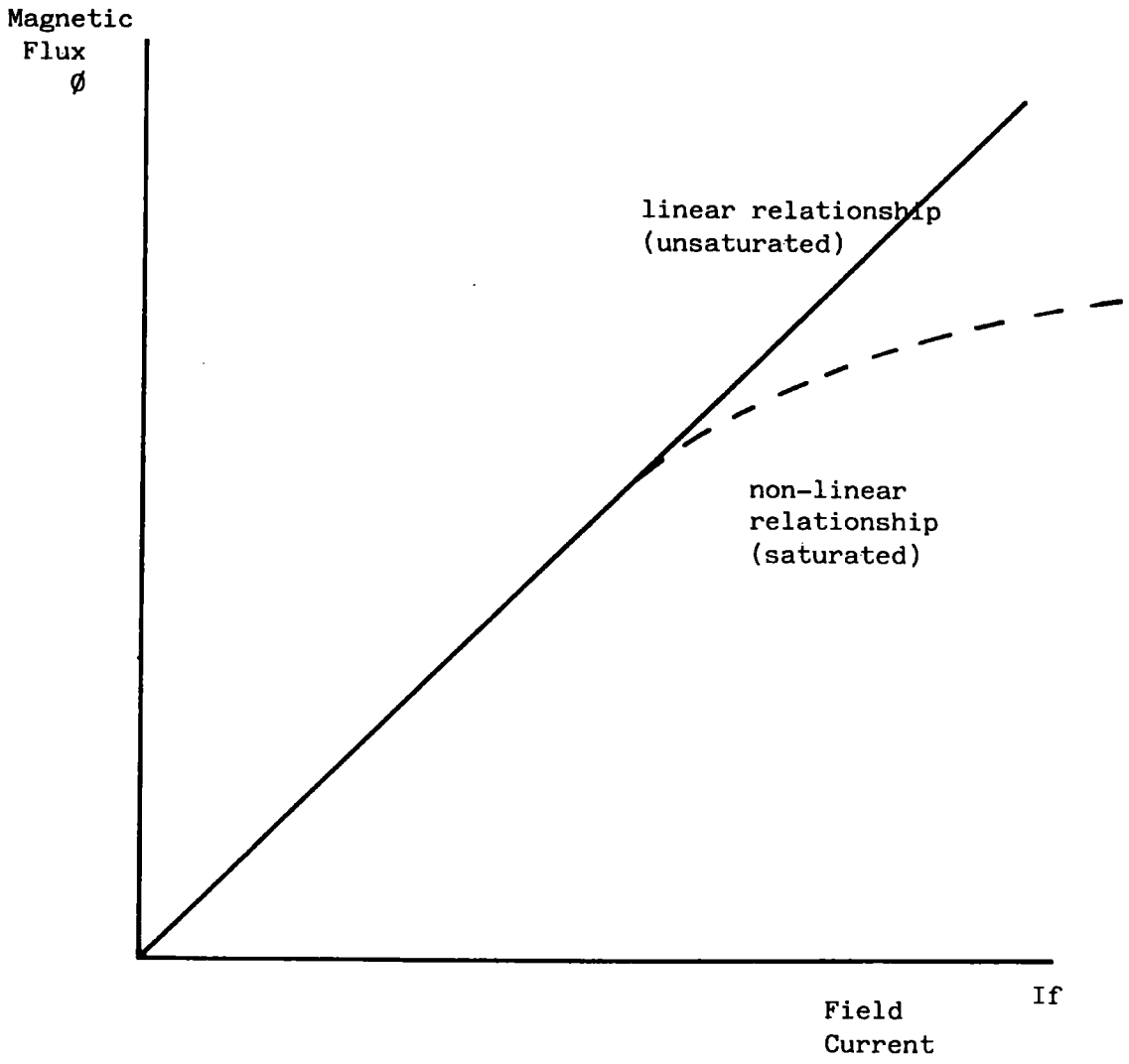

FIGURE 2.18: Field Current/Magnetic Flux Characteristic for Saturated and unsaturated Motors

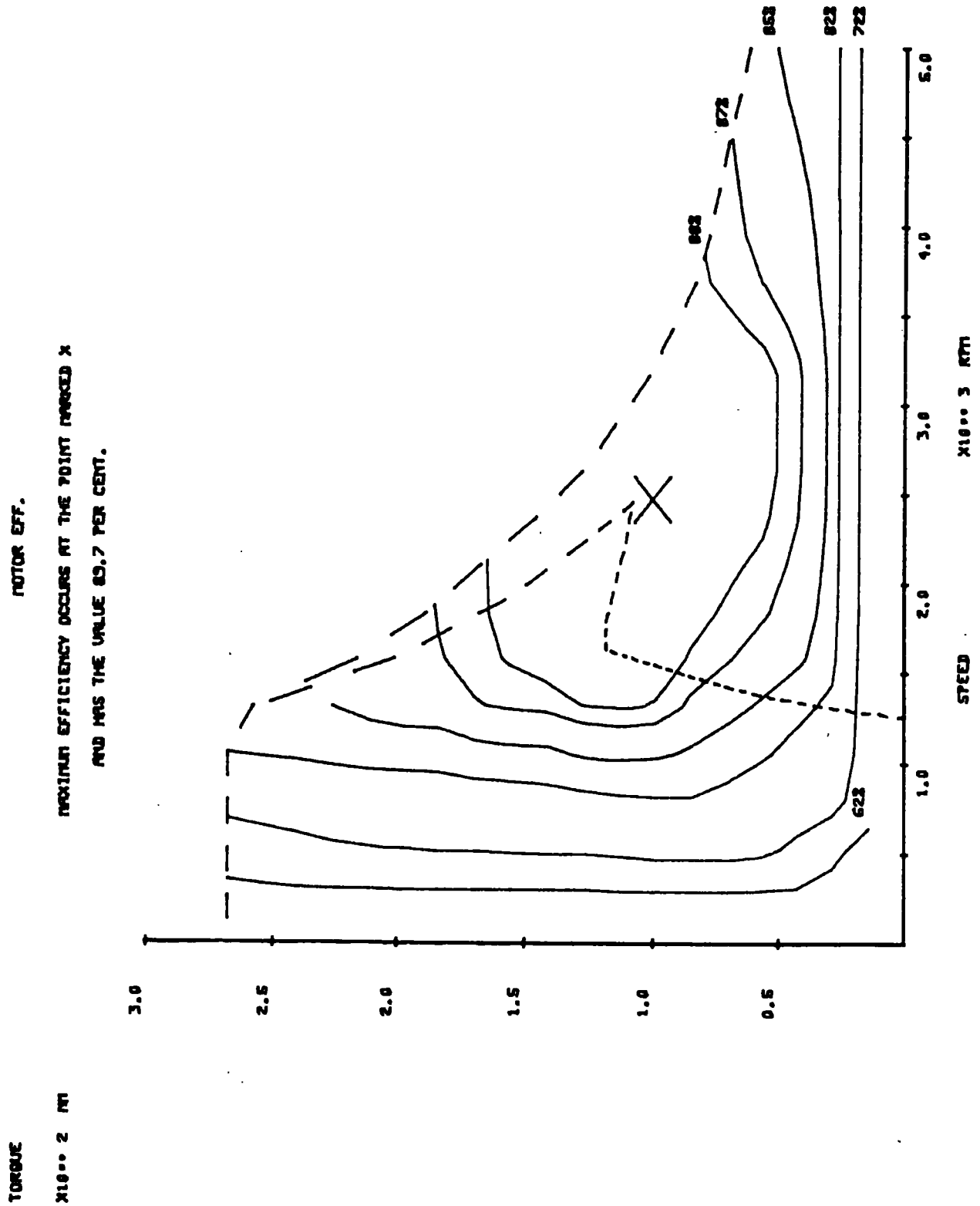

FIGURE 2.19: DC Switched Reluctance Motor Map

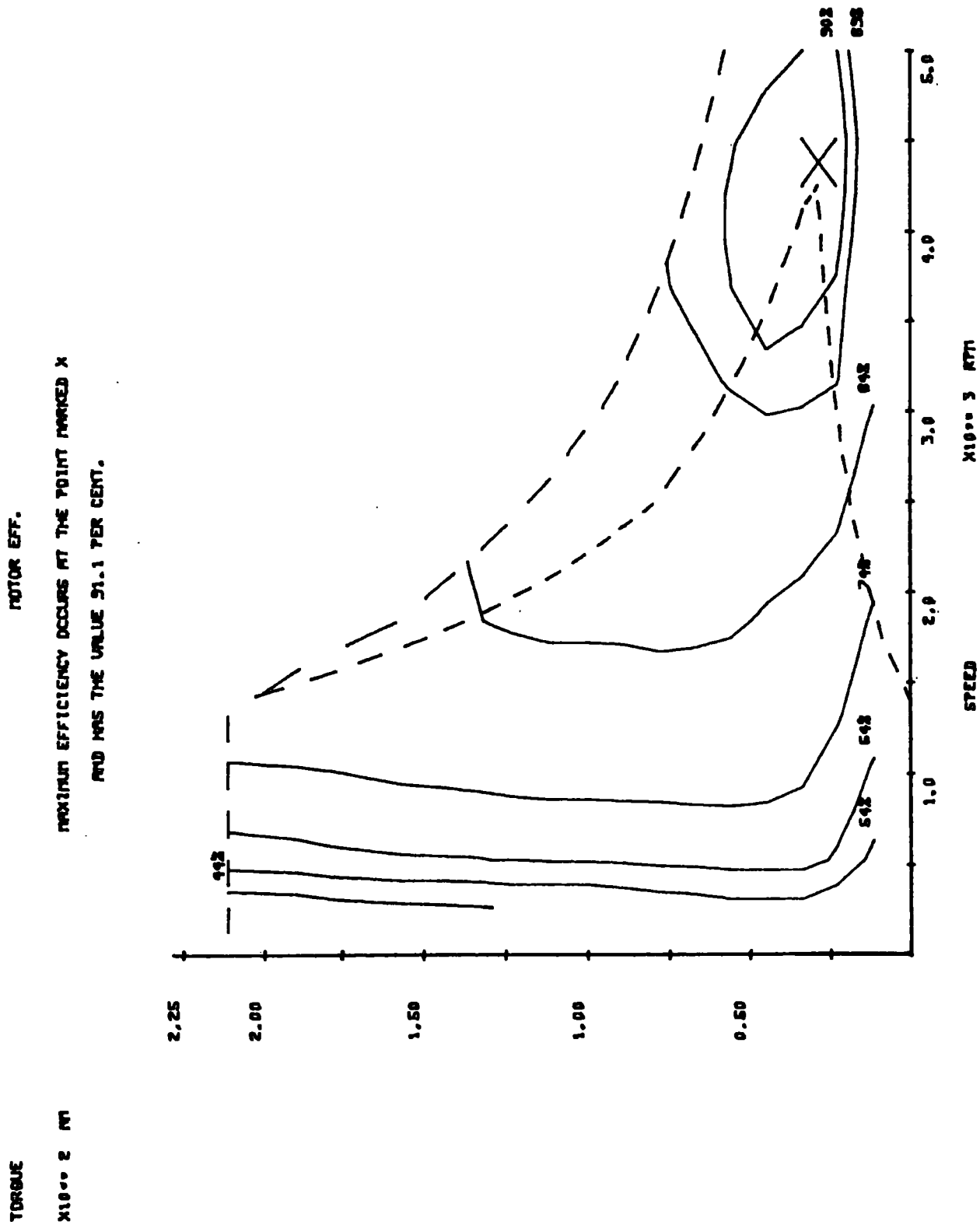

FIGURE 2.20: AC Induction Motor Map

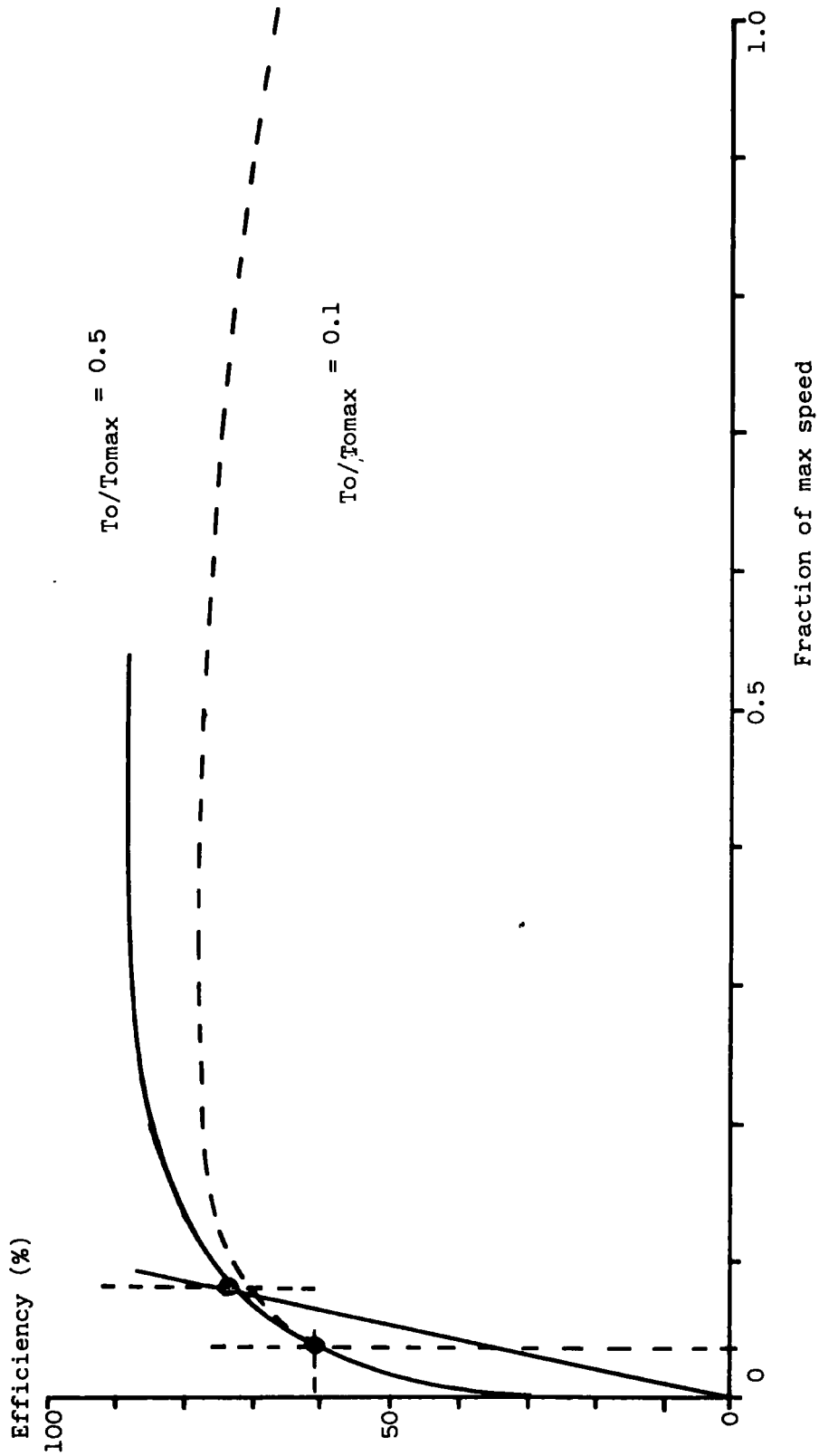

FIGURE 2.21: DC Switched Reluctance Efficiency Variation with Speed

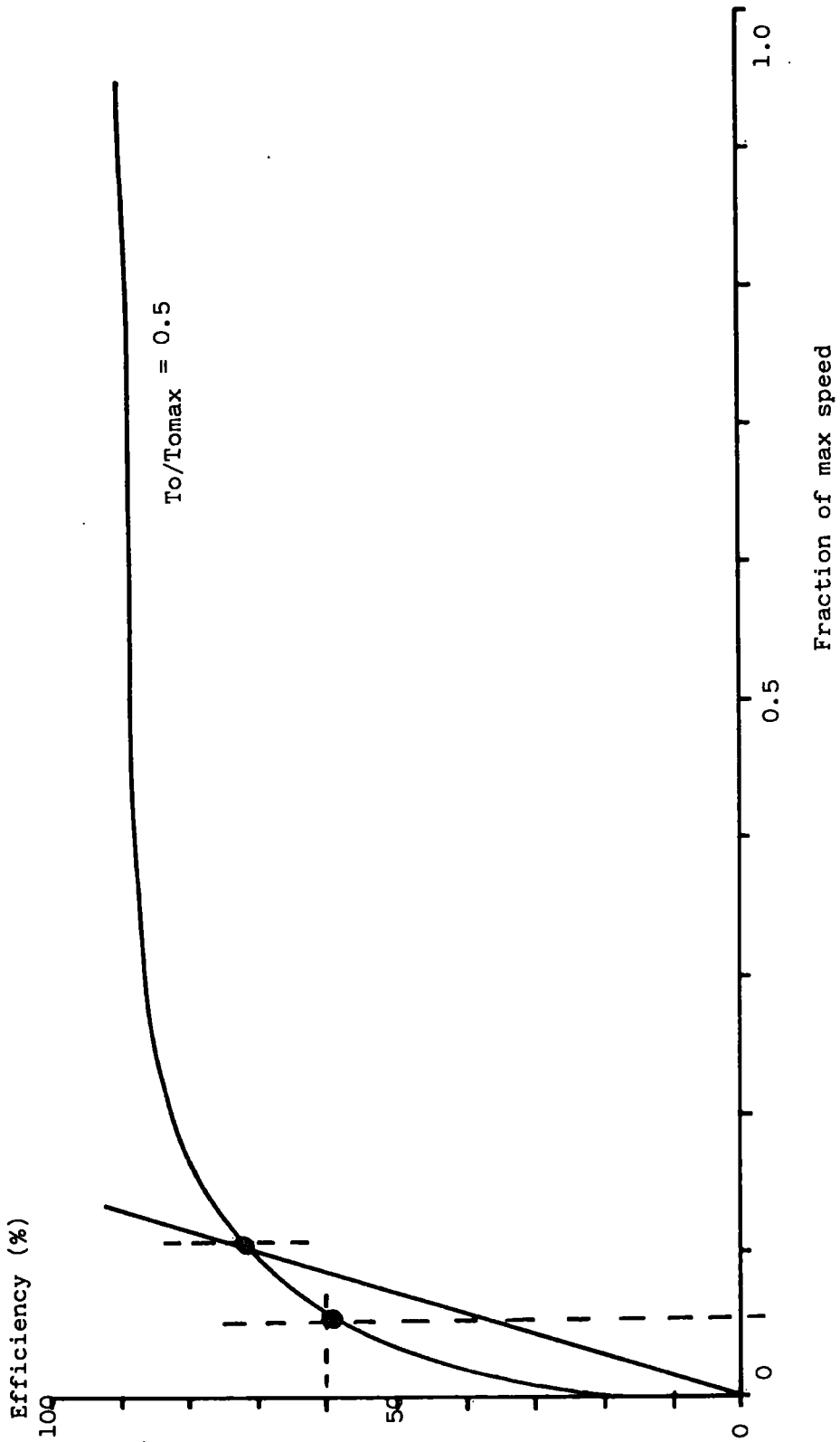

FIGURE 2.22: AC Induction Efficiency Variation with Speed

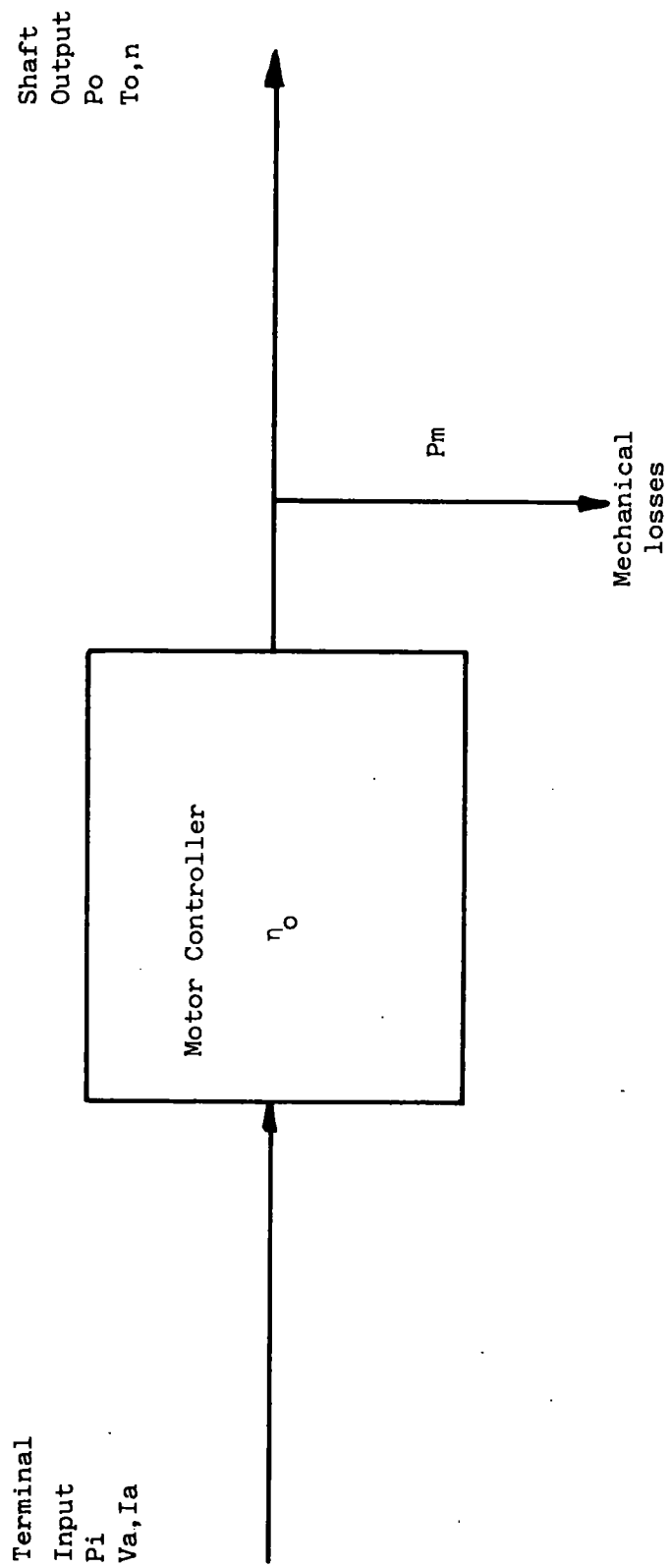

FIGURE 2.23: Loss Diagram for DC Switched Reluctance and AC Induction Motors

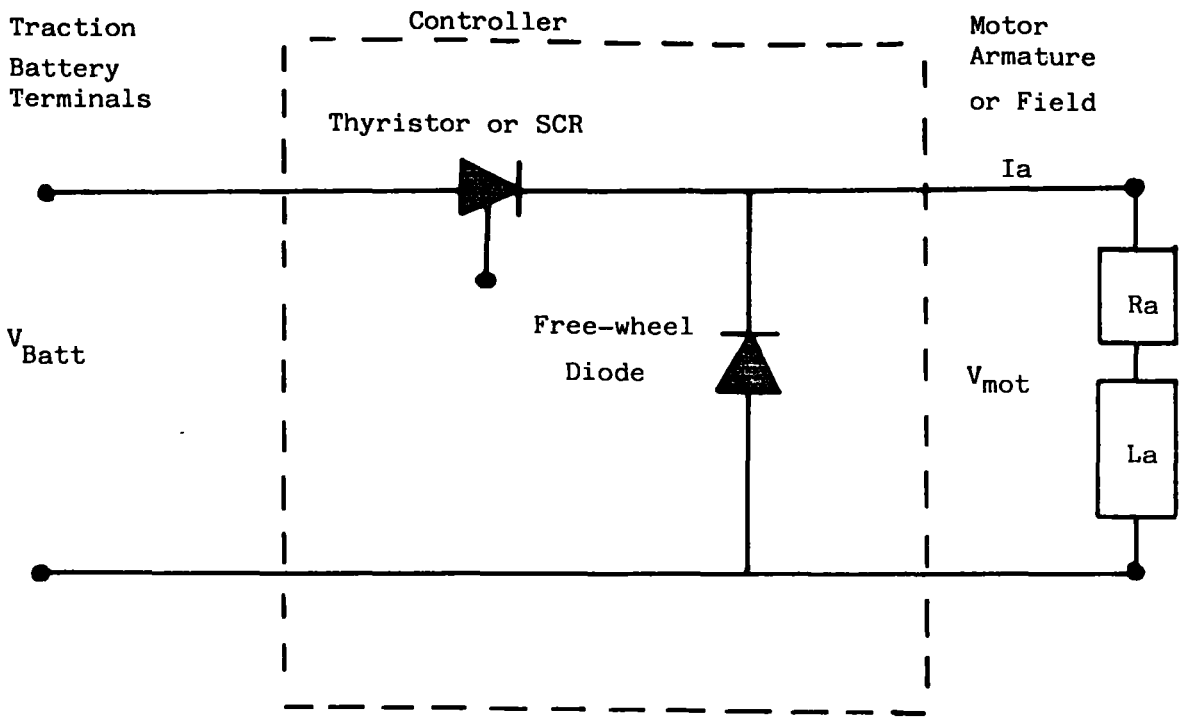

FIGURE 2.24: Diagrammatic DC Chopper Circuit for Motoring

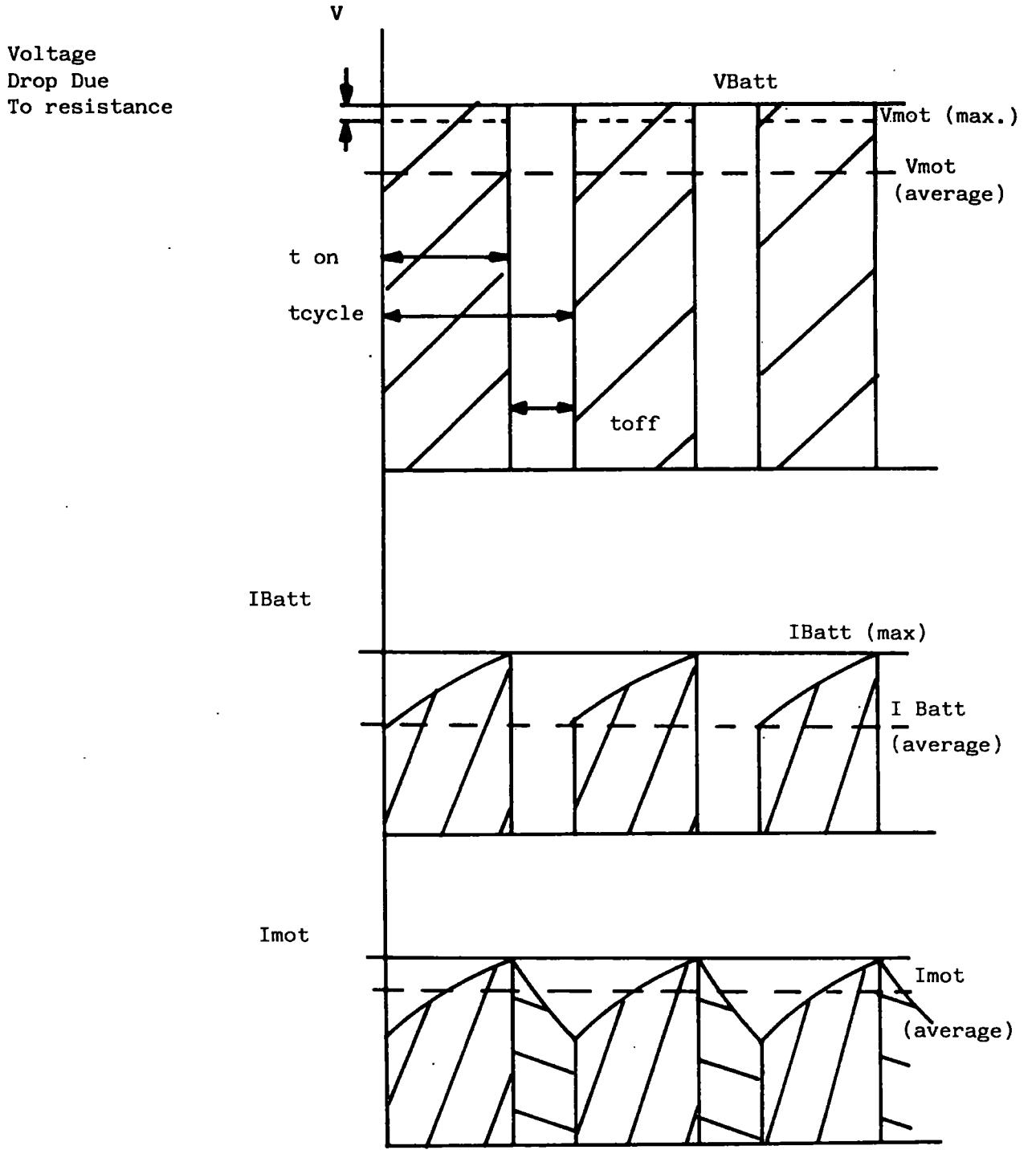

FIGURE 2.25: Switching Chracteristics of a DC Chopper Controller for Motoring

FIGURE 2.26: JANUS/JPL Chopper Controller Efficiency for Motoring

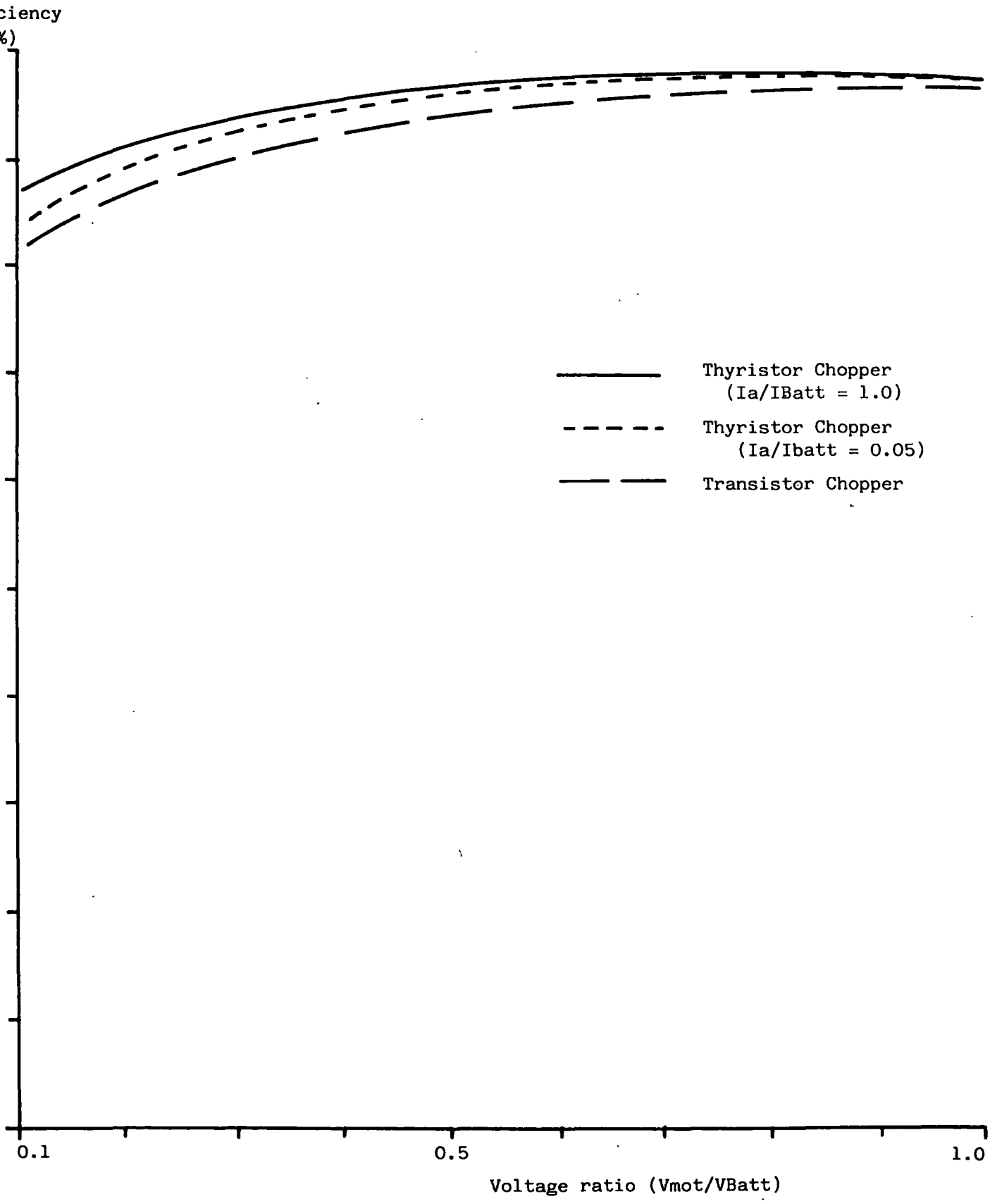

FIGURE 2.27: JANUS/JPL Chopper Controller Efficiency for Regeneration

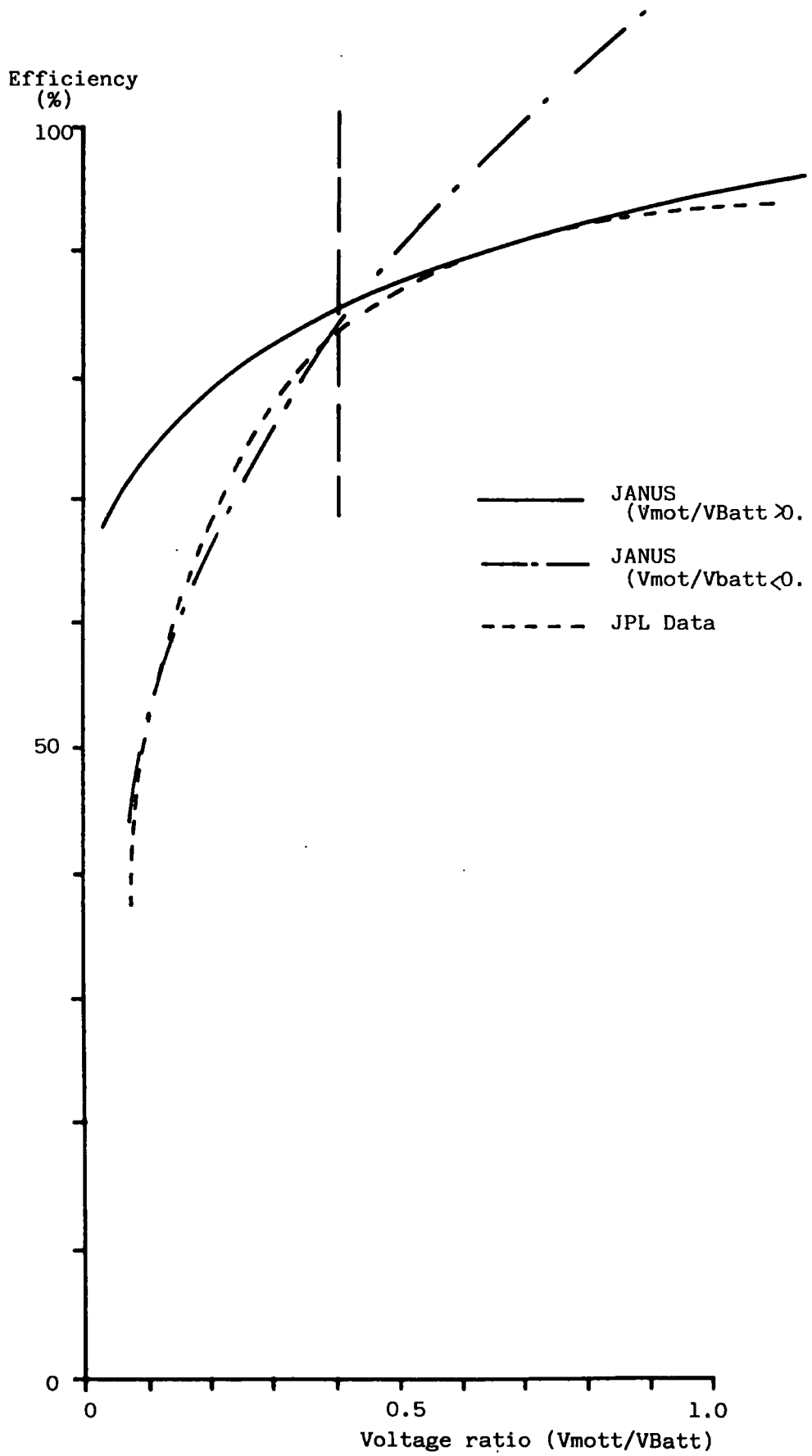

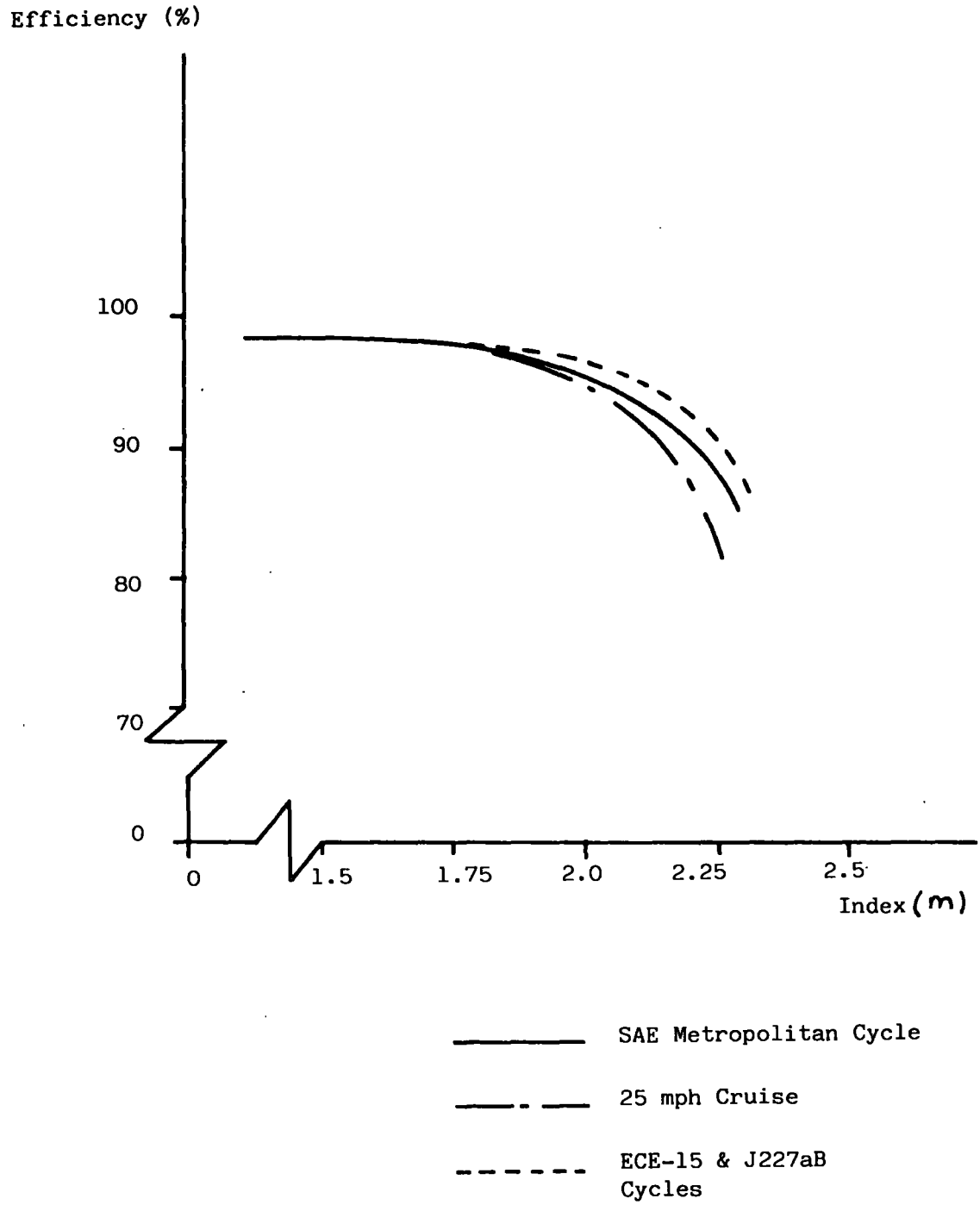

FIGURE 2.28: Effect of Transmission Efficiency Model Index on Efficiency over Varying Driving Conditions

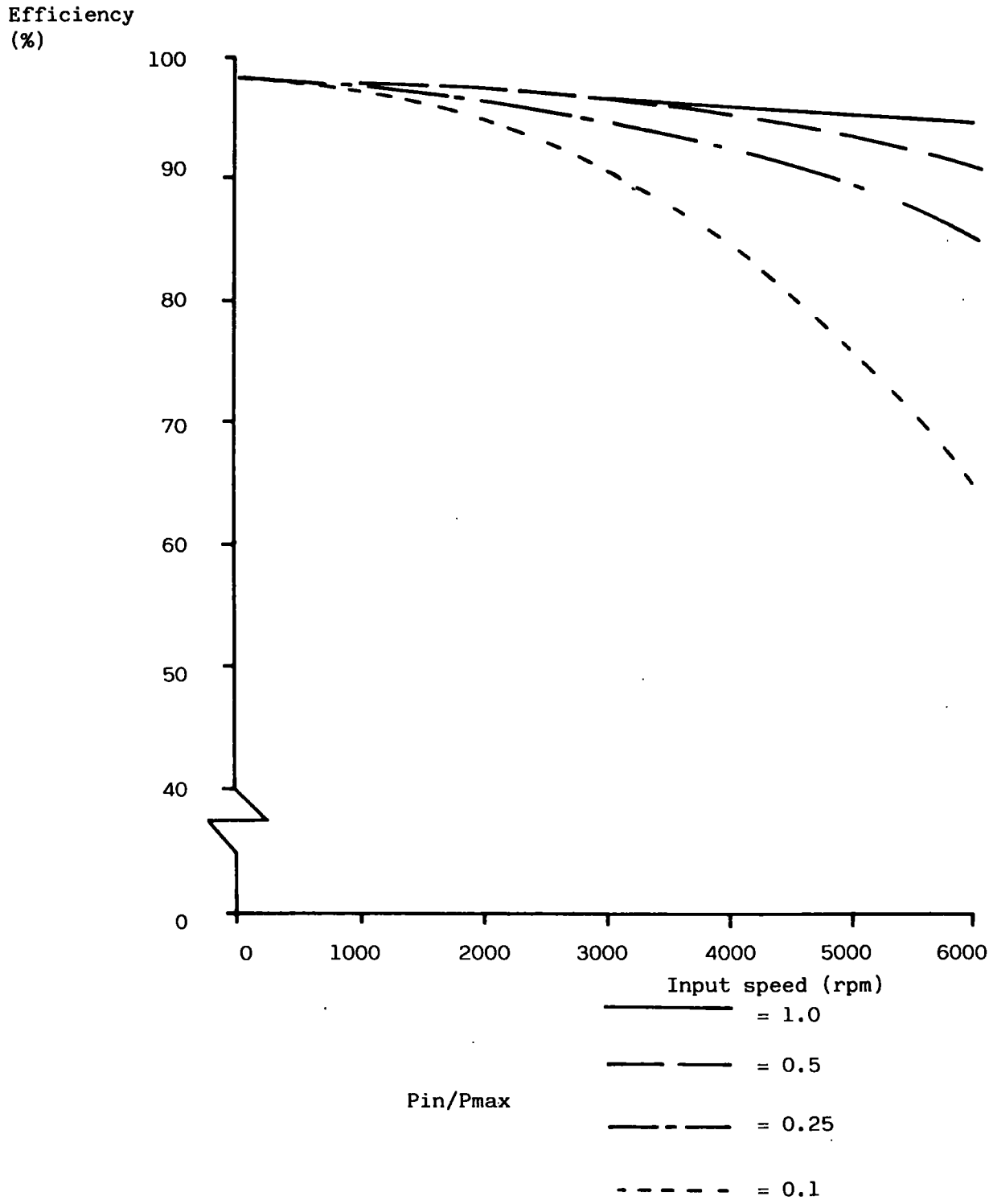

FIGURE 2.29: Gearbox Efficiency with Load and Speed

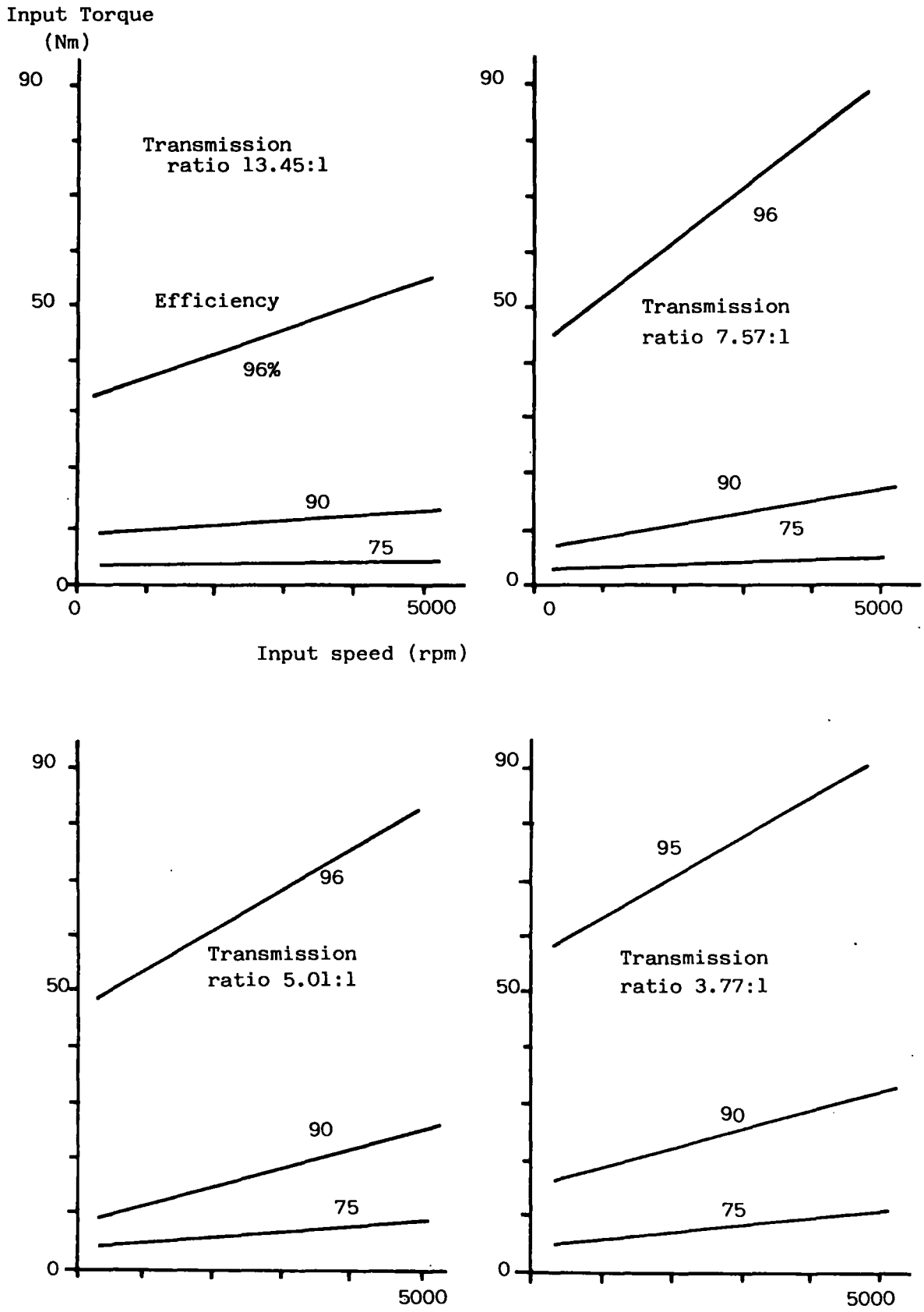

FIGURE 2.30: EUT Tranmission Efficiency Data with Load and Speed

FIGURE 2.31: Comparison of Simulation and Hardware Torque Converter Characterisics

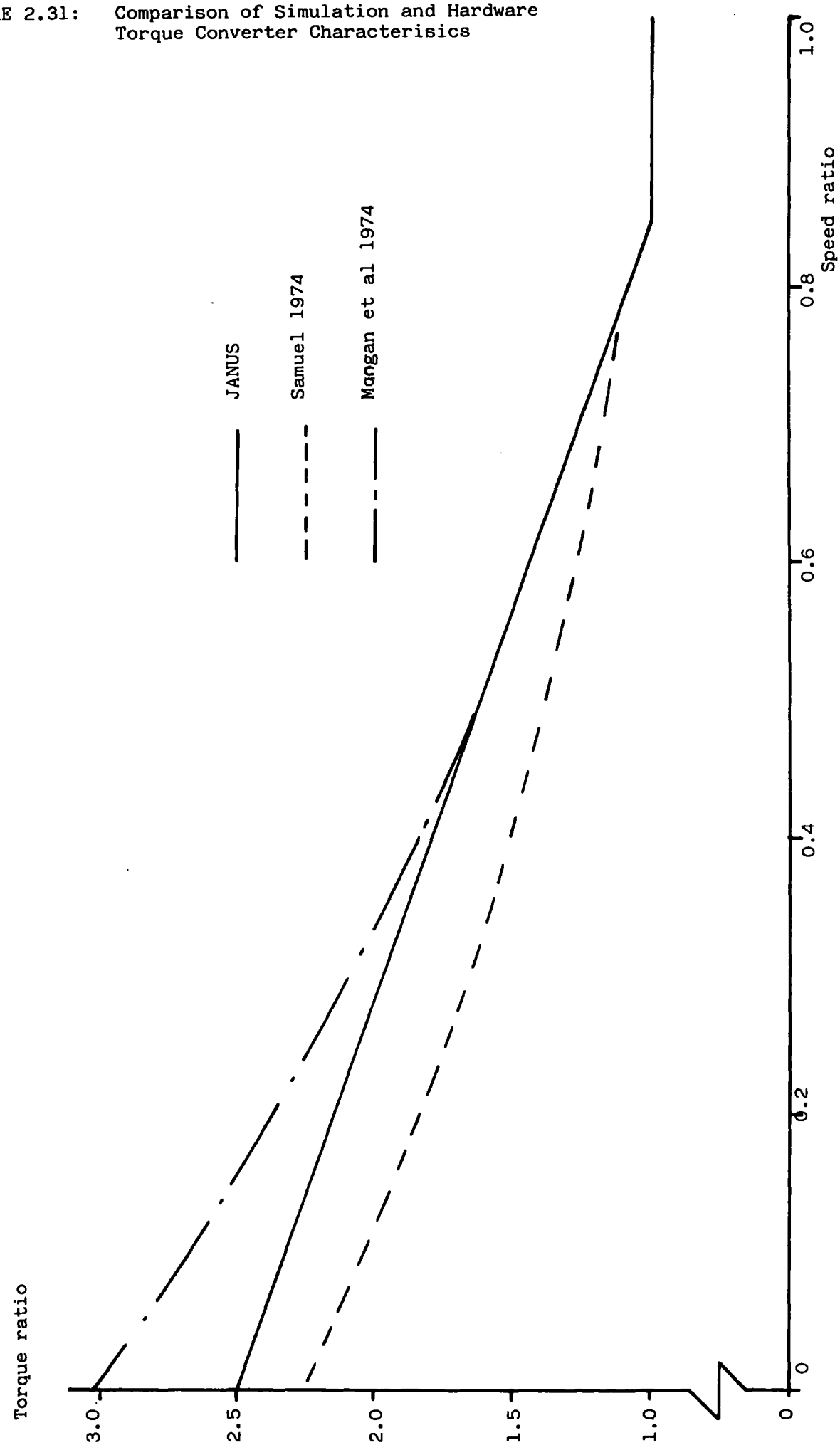

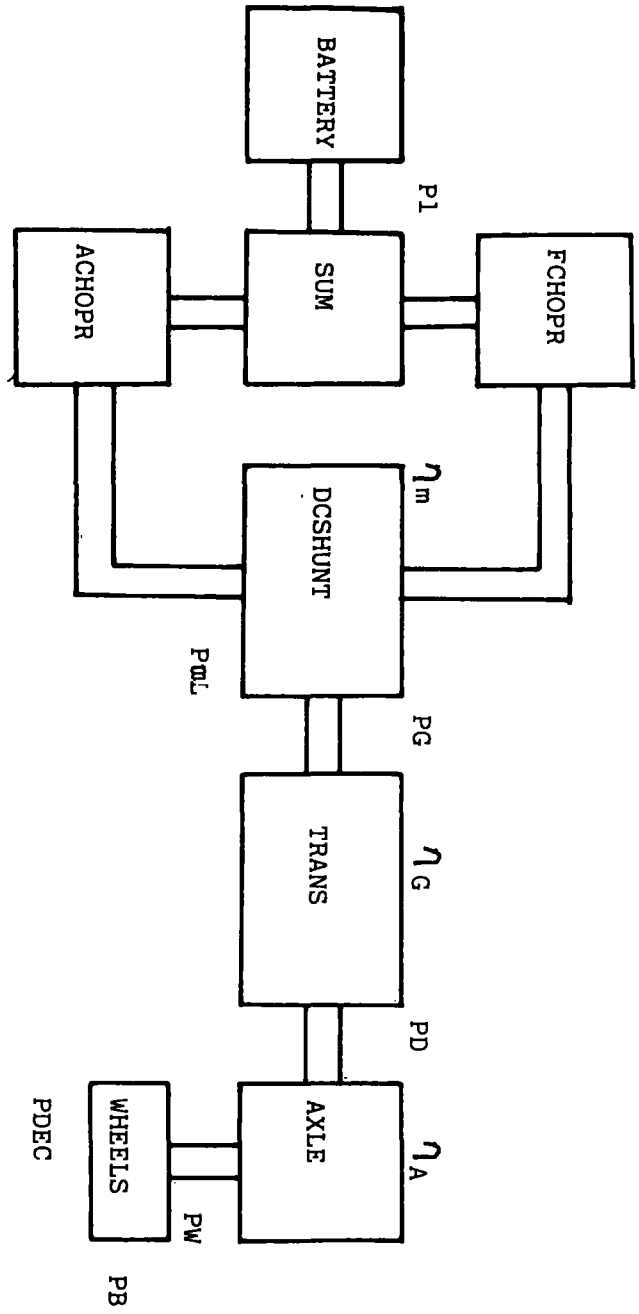

FIGURE 2.32: Electric Vehicle Ideal Braking

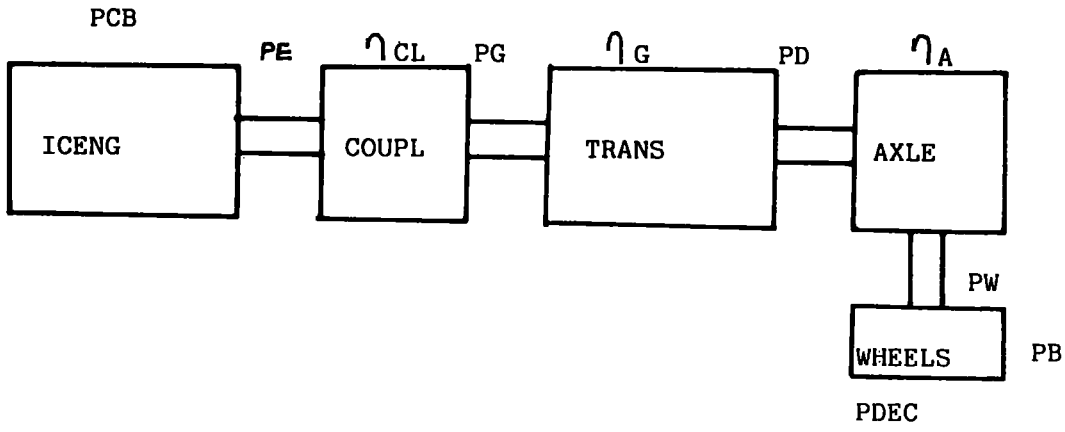

FIGURE 2.33: I.C. Engined Vehicle Ideal Braking

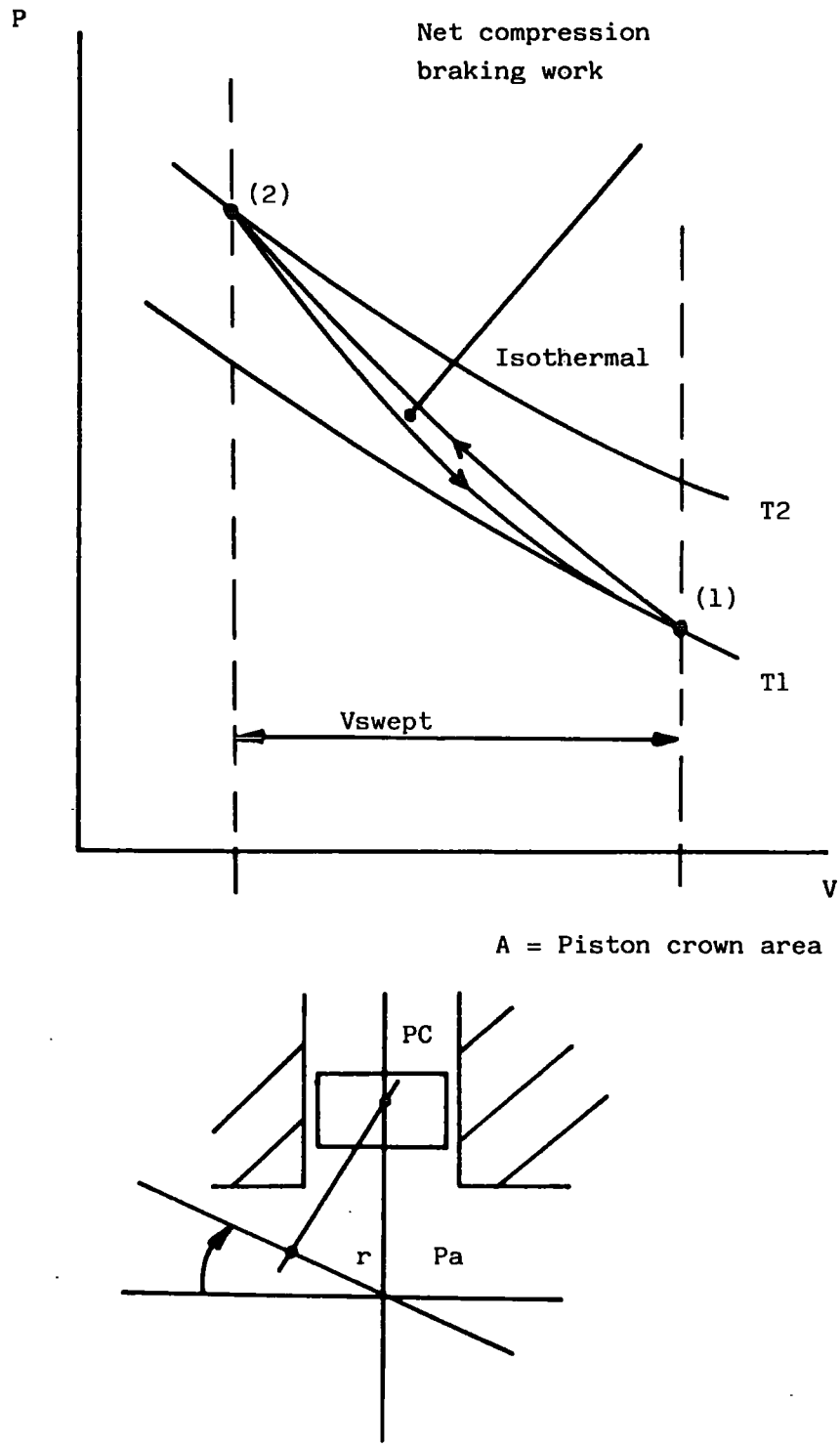

Figure 2.34: P-V Diagram for an I.C.Engine During Compression Braking

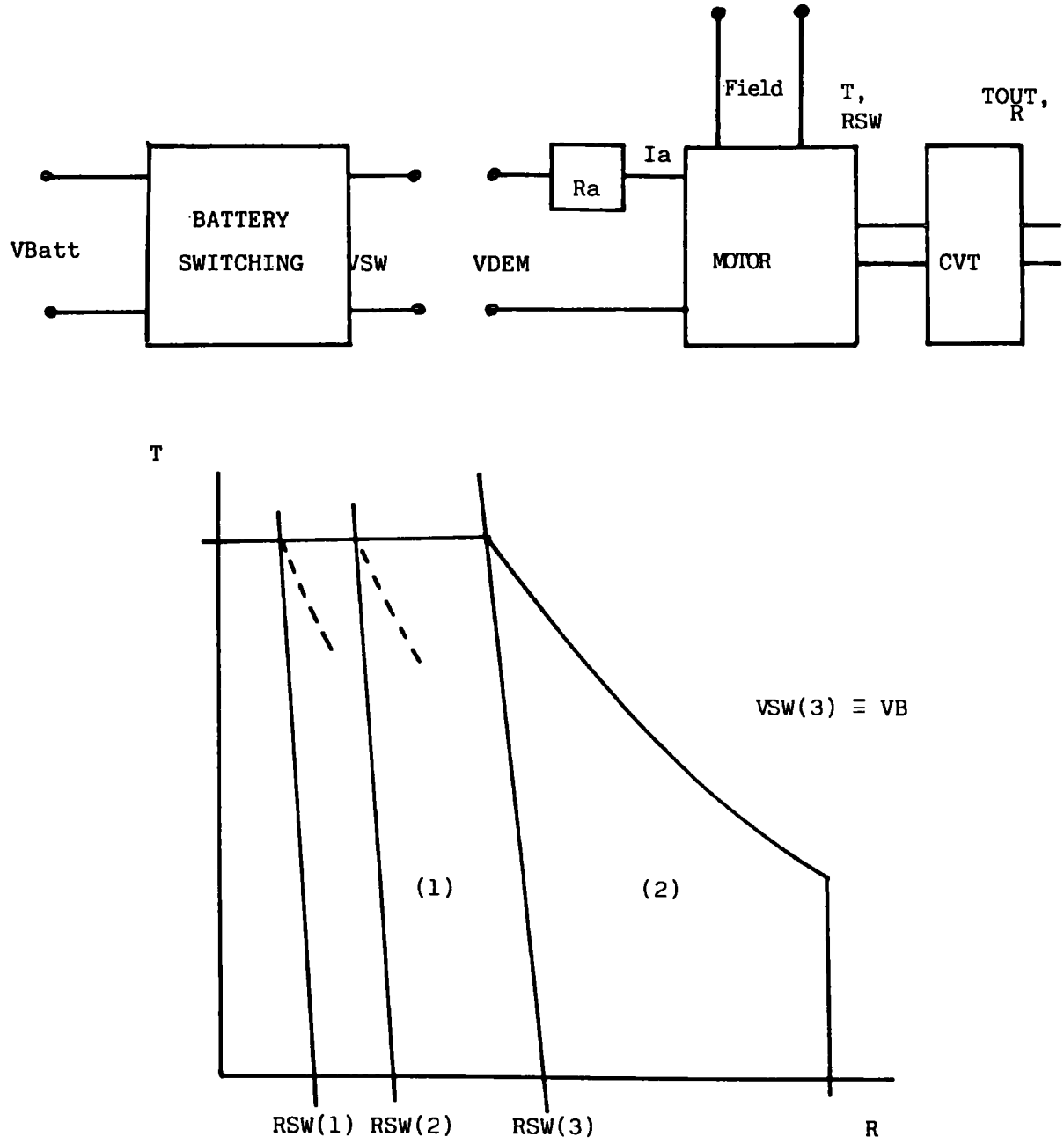

FIGURE 2.35: Motor Control By a Combination of a CVT Plus Battery Switching

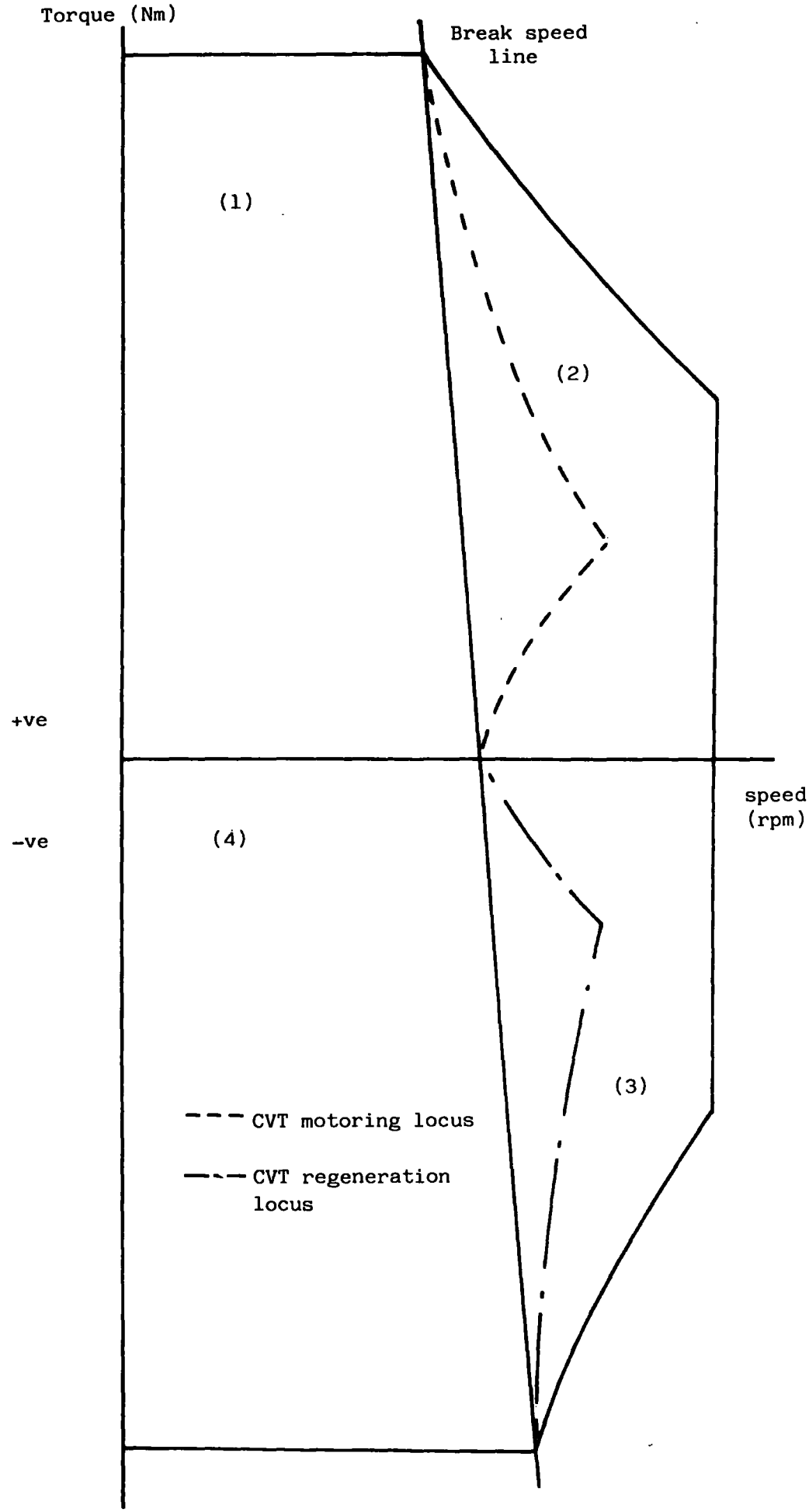

FIGURE 2.36: Traction Motor CVT lines for Motoring and Regeneration

FIGURE 2.37: Comparison of JANUS Cold Start Model with Measured Data with Ambient Temperature and Distance Travelled

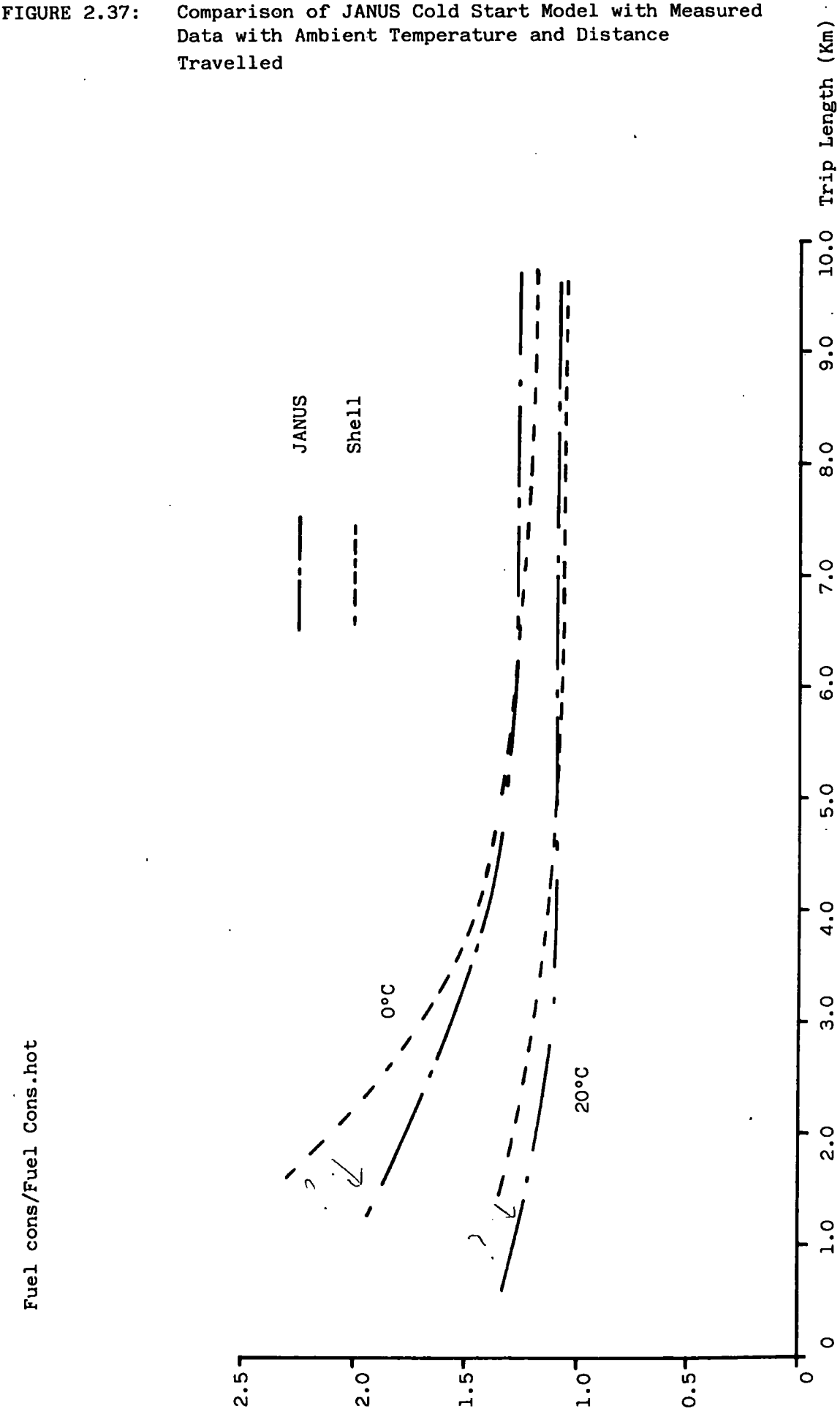

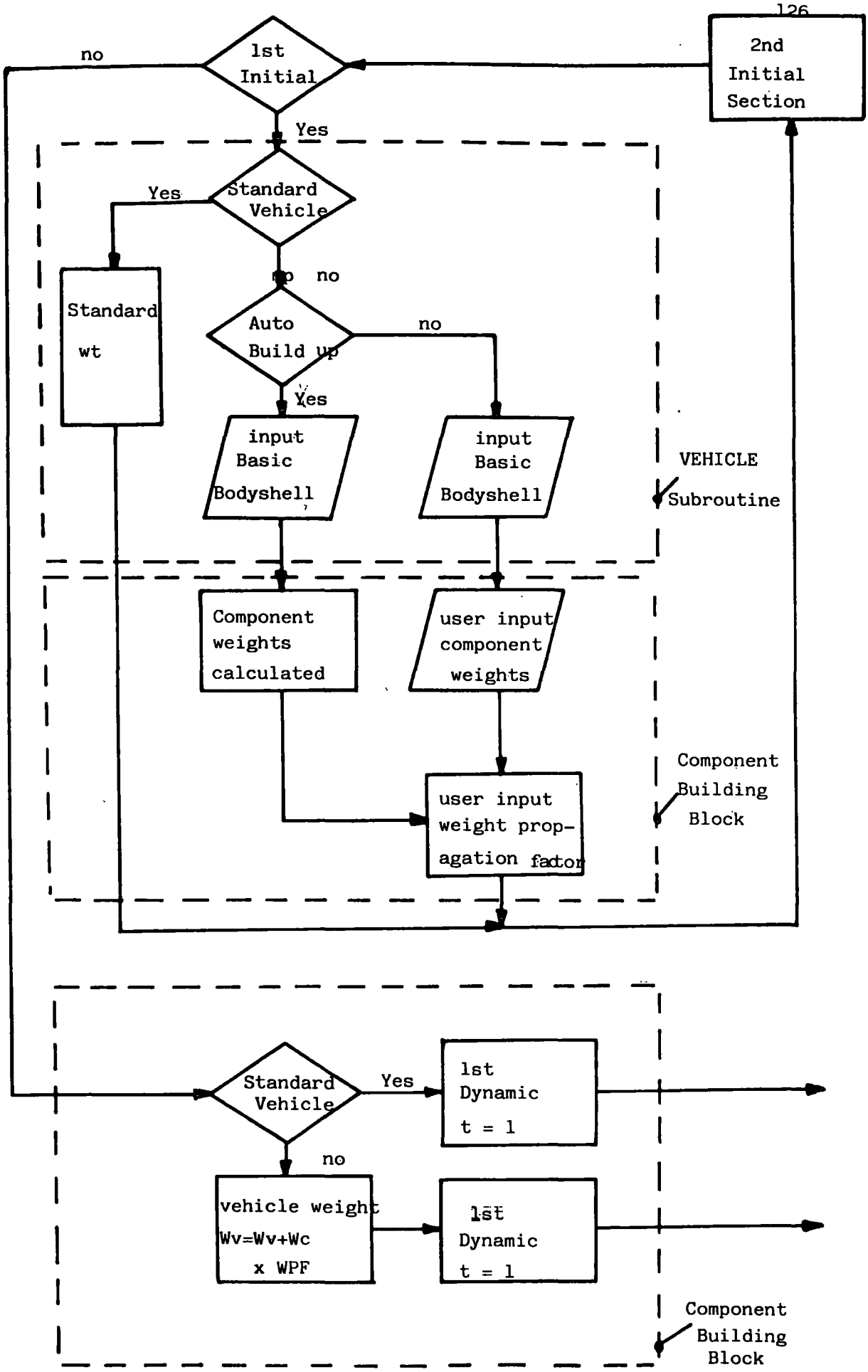

FIGURE 2.38: Flow Chart showing JANUS weight Build-up Algorithm

FIGURE 2.39: Variation of Objective Function F, with Torque Split X

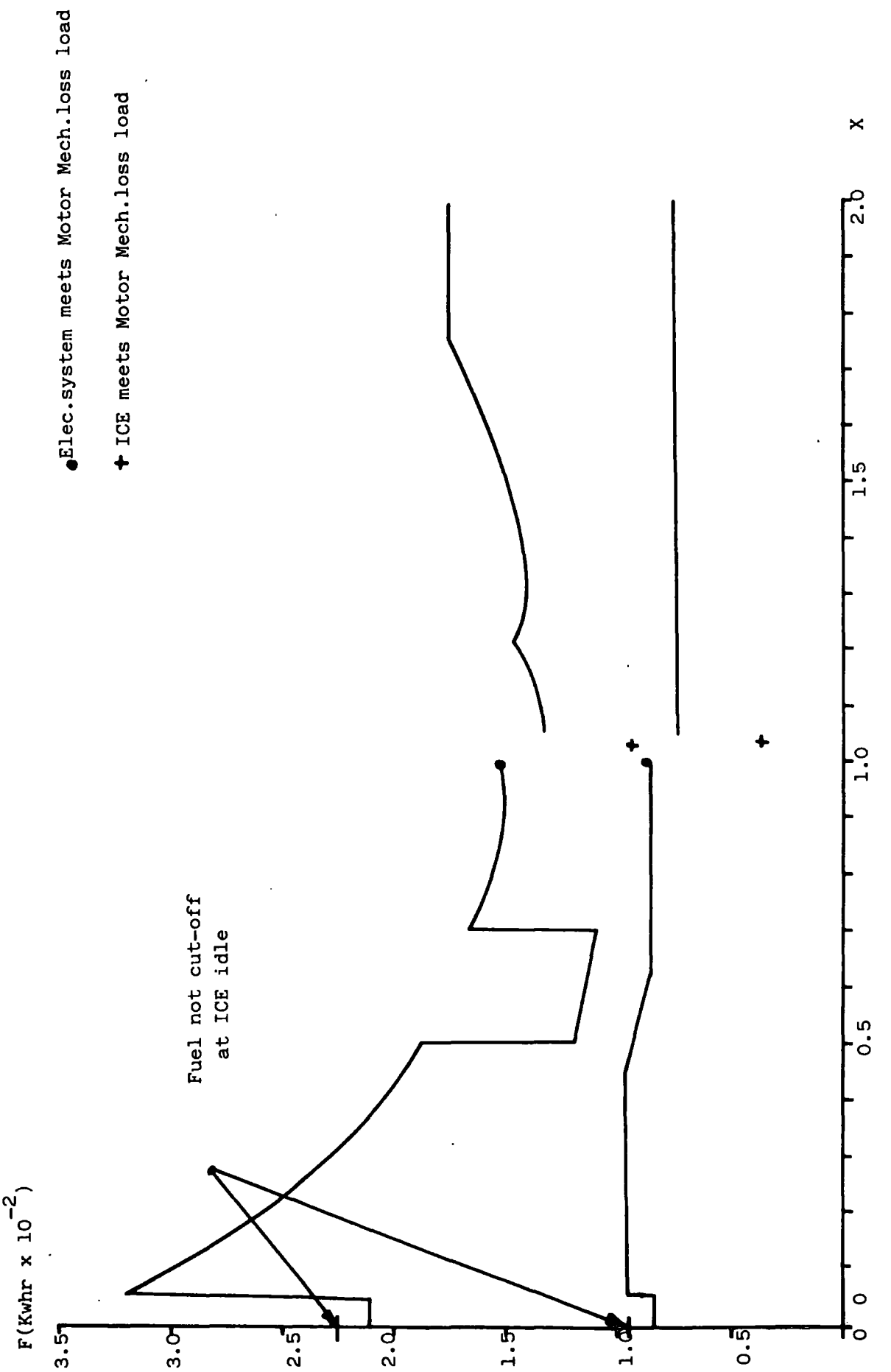

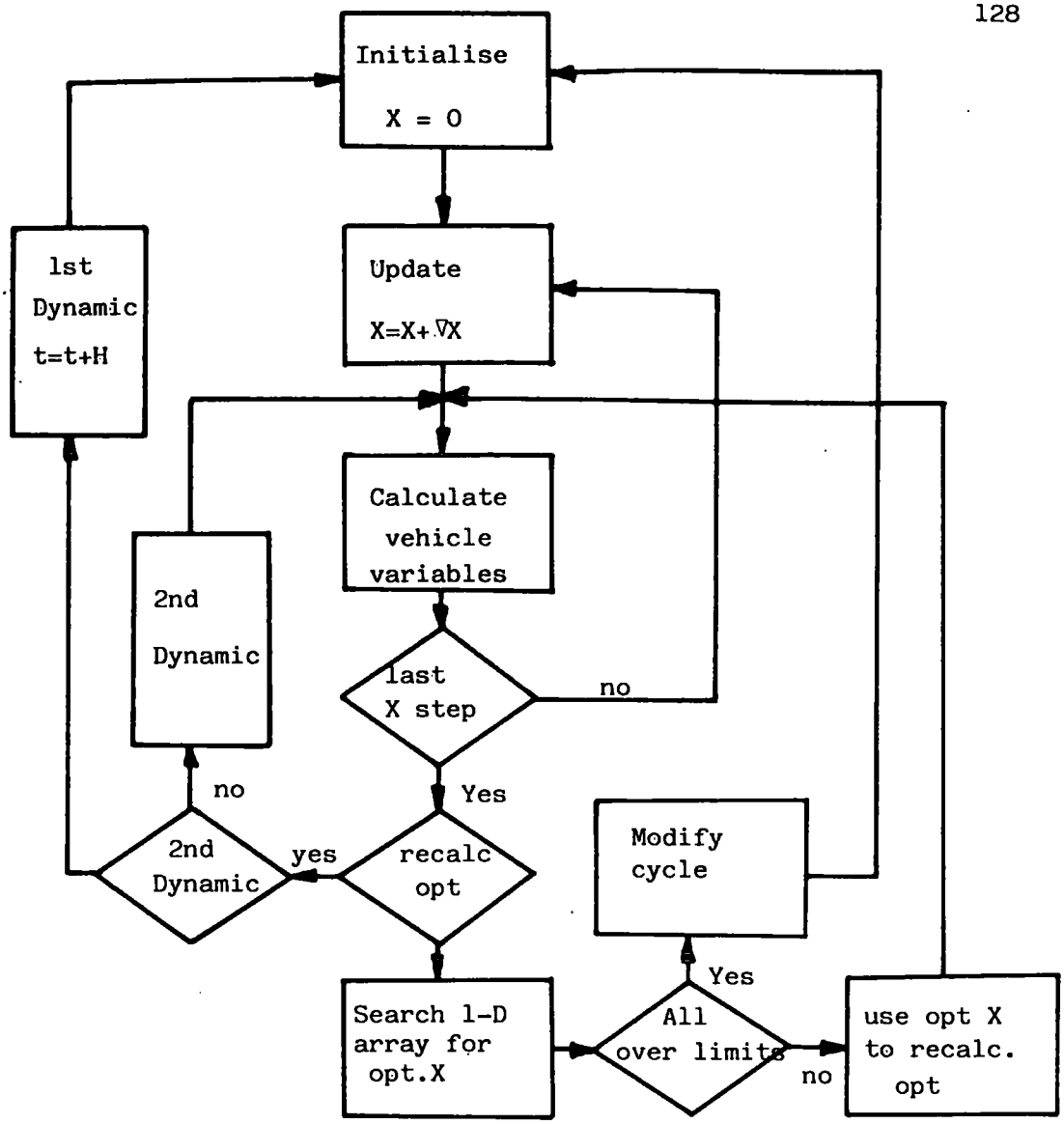

FIGURE 2.40: 1-Dimensional Optimisation Algorithm Flow Chart

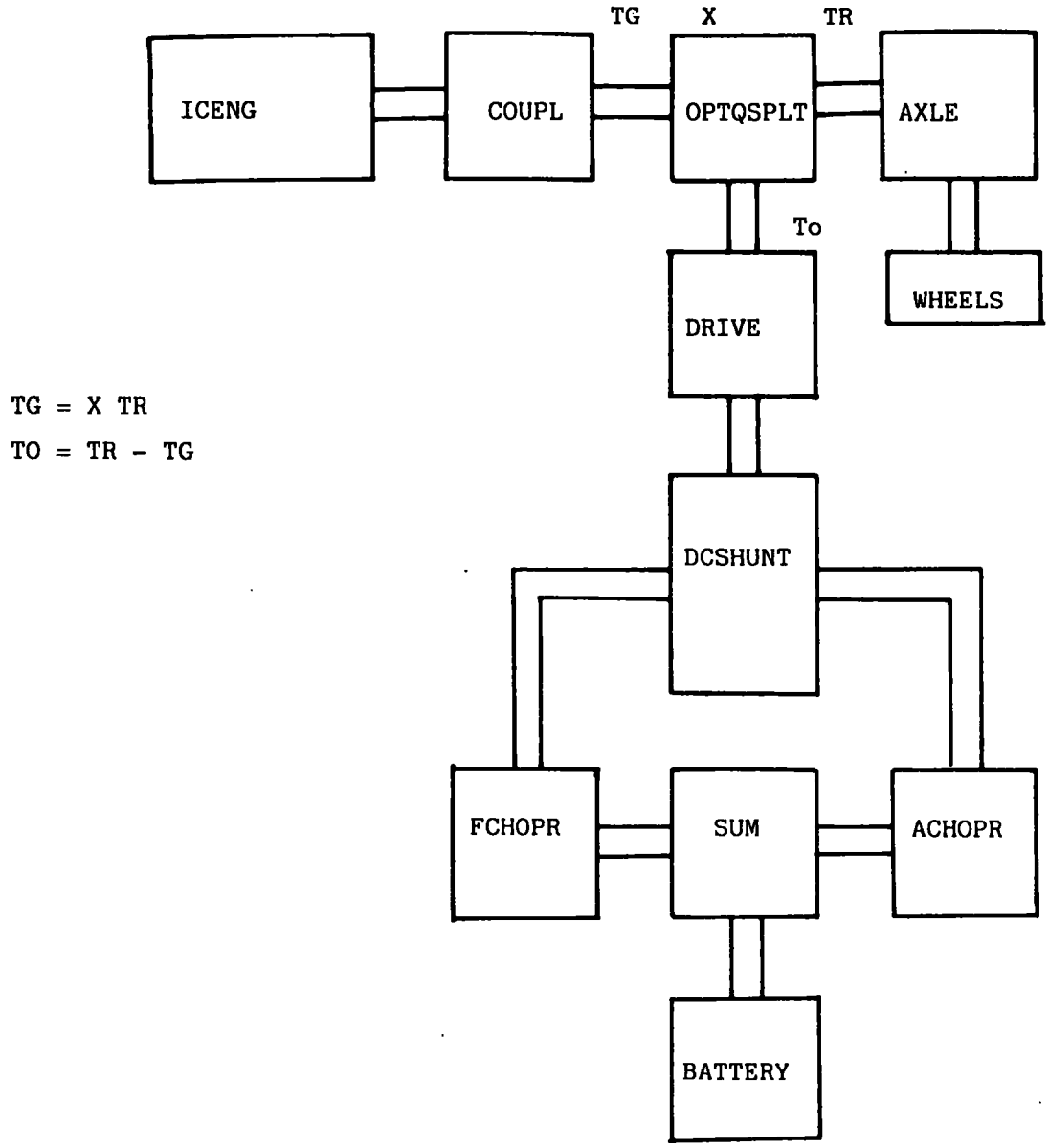

FIGURE 2.41: Parallel Configuration for 1-D Optimisation

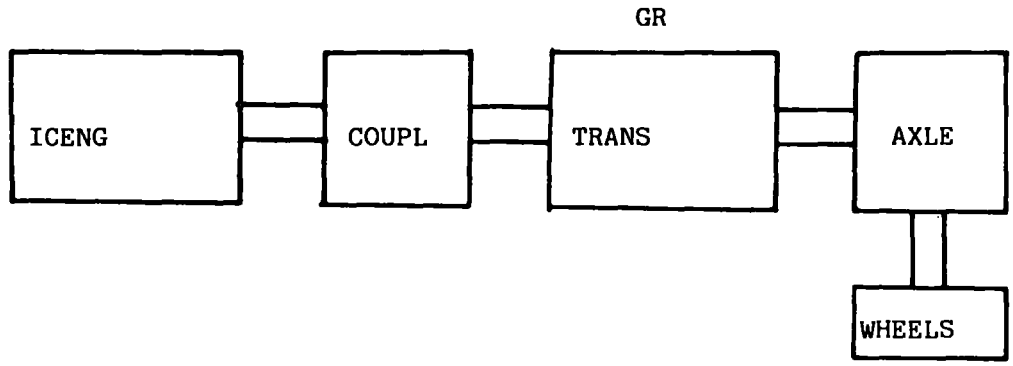

FIGURE 2.42: Conventional I.C.Engined Vehicle for 1-D Optimisation

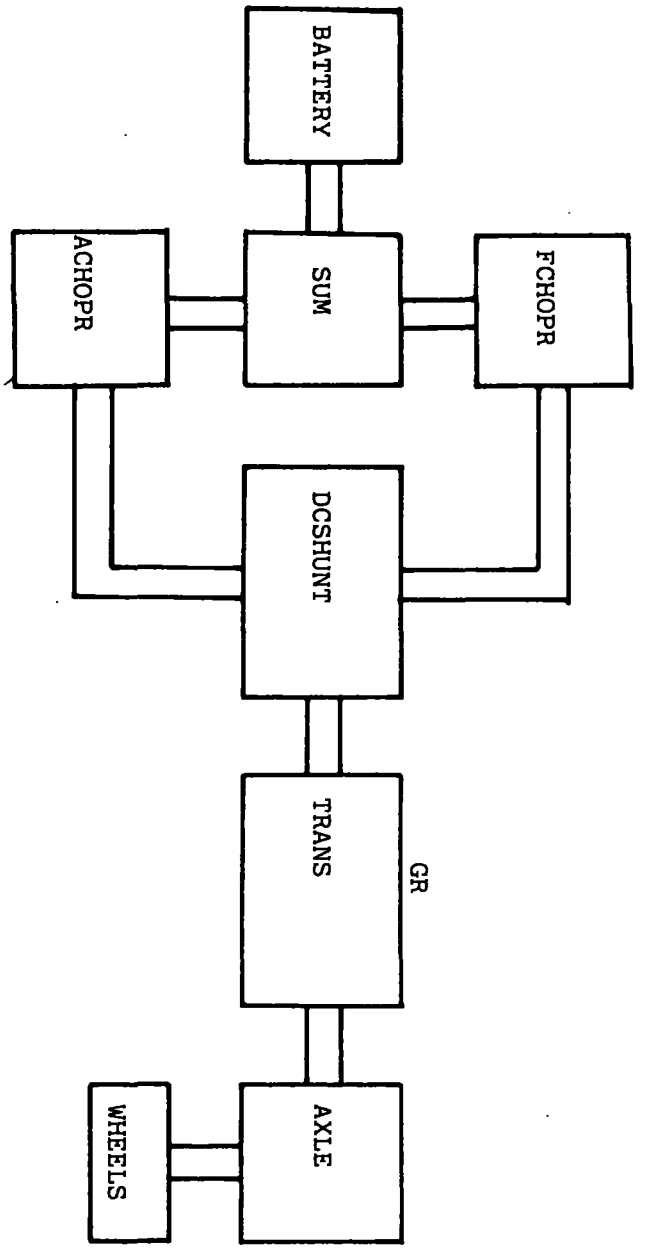

FIGURE 2.43: Electric Vehicle for 1-D Optimisation

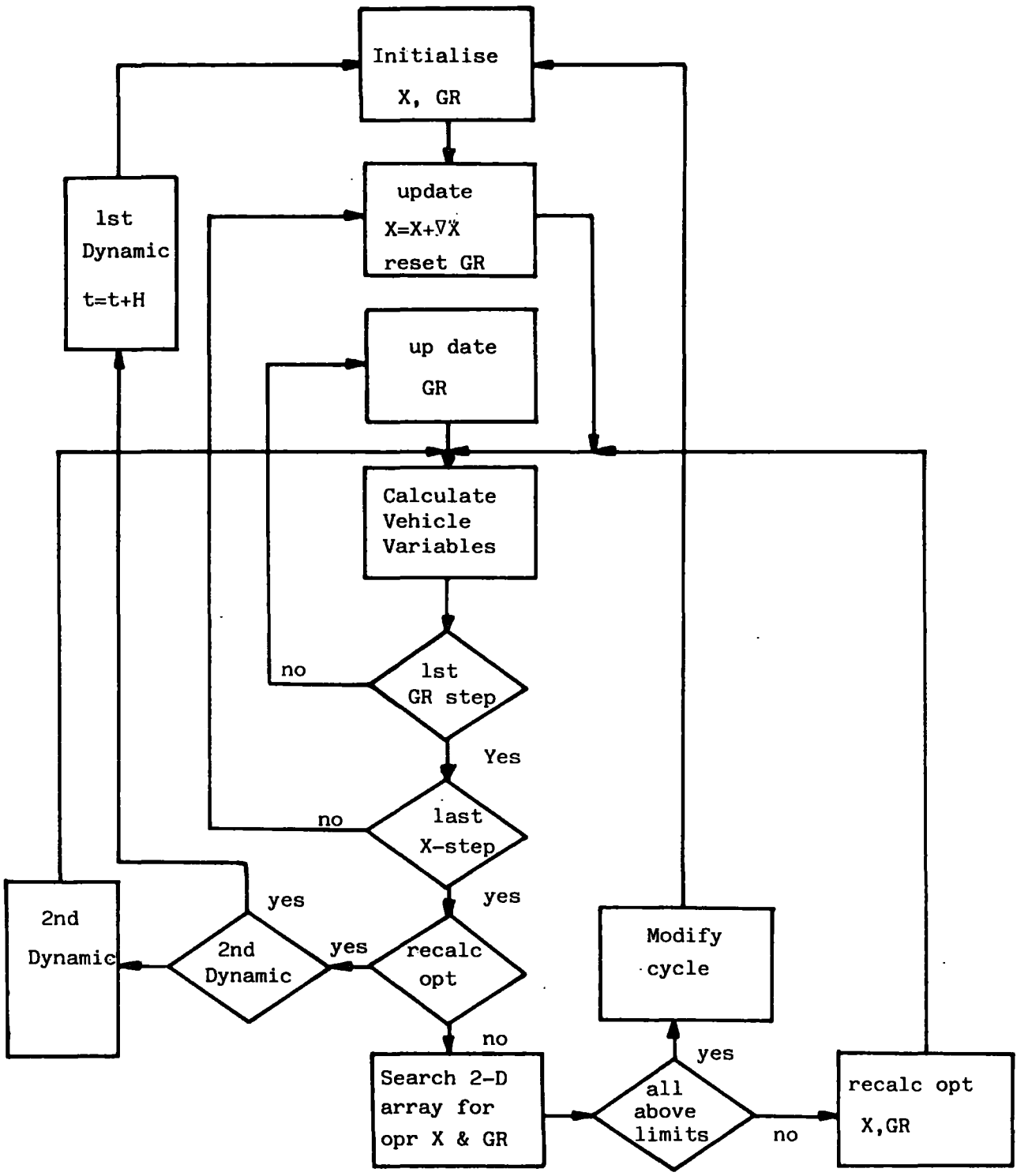

FIGURE 2.44: 2-Dimensional Optimisation Algorithm Flow Chart for Motoring

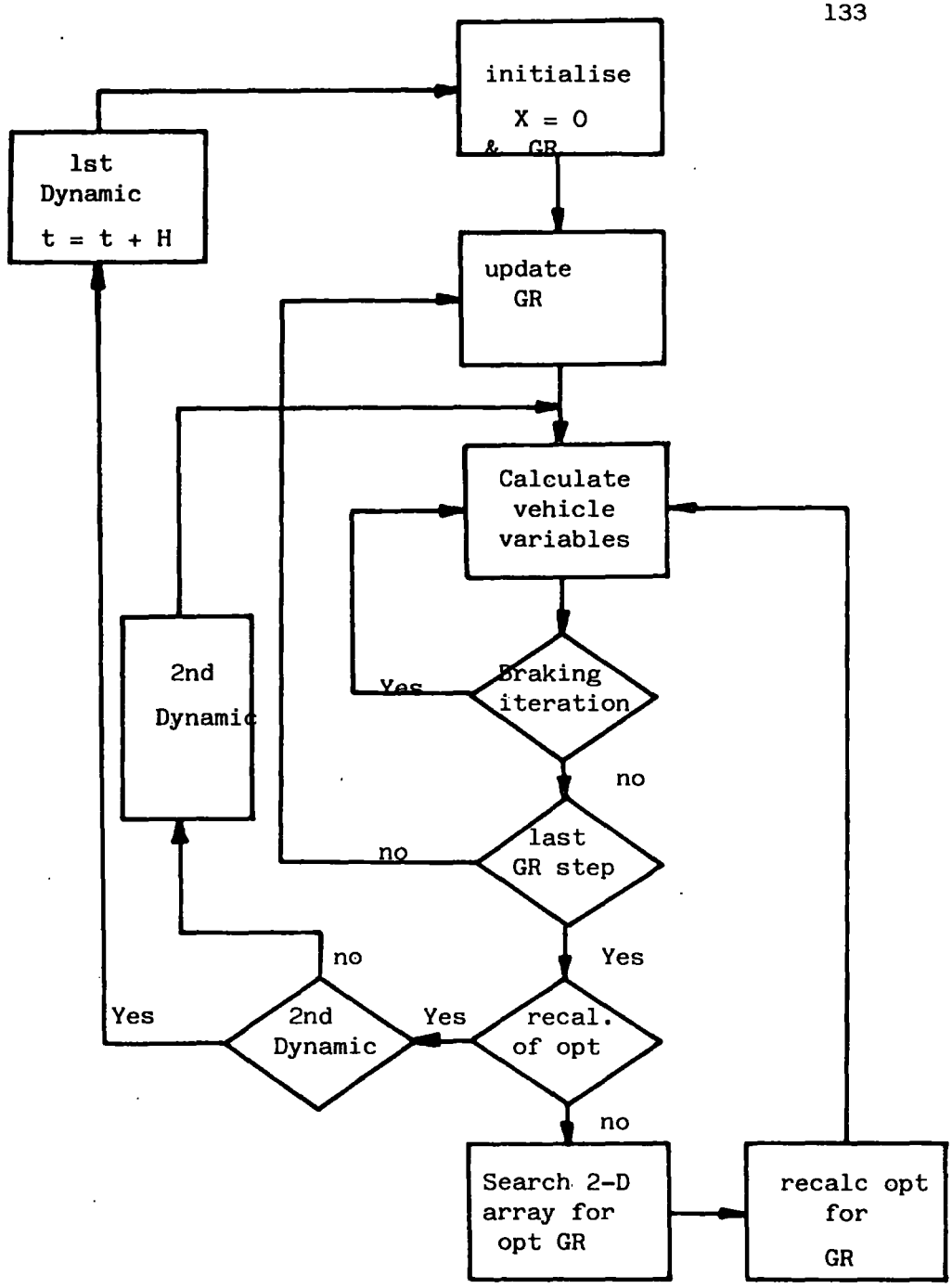

FIGURE 2.45: 2-D Optimisation Flow Chart for Regeneration

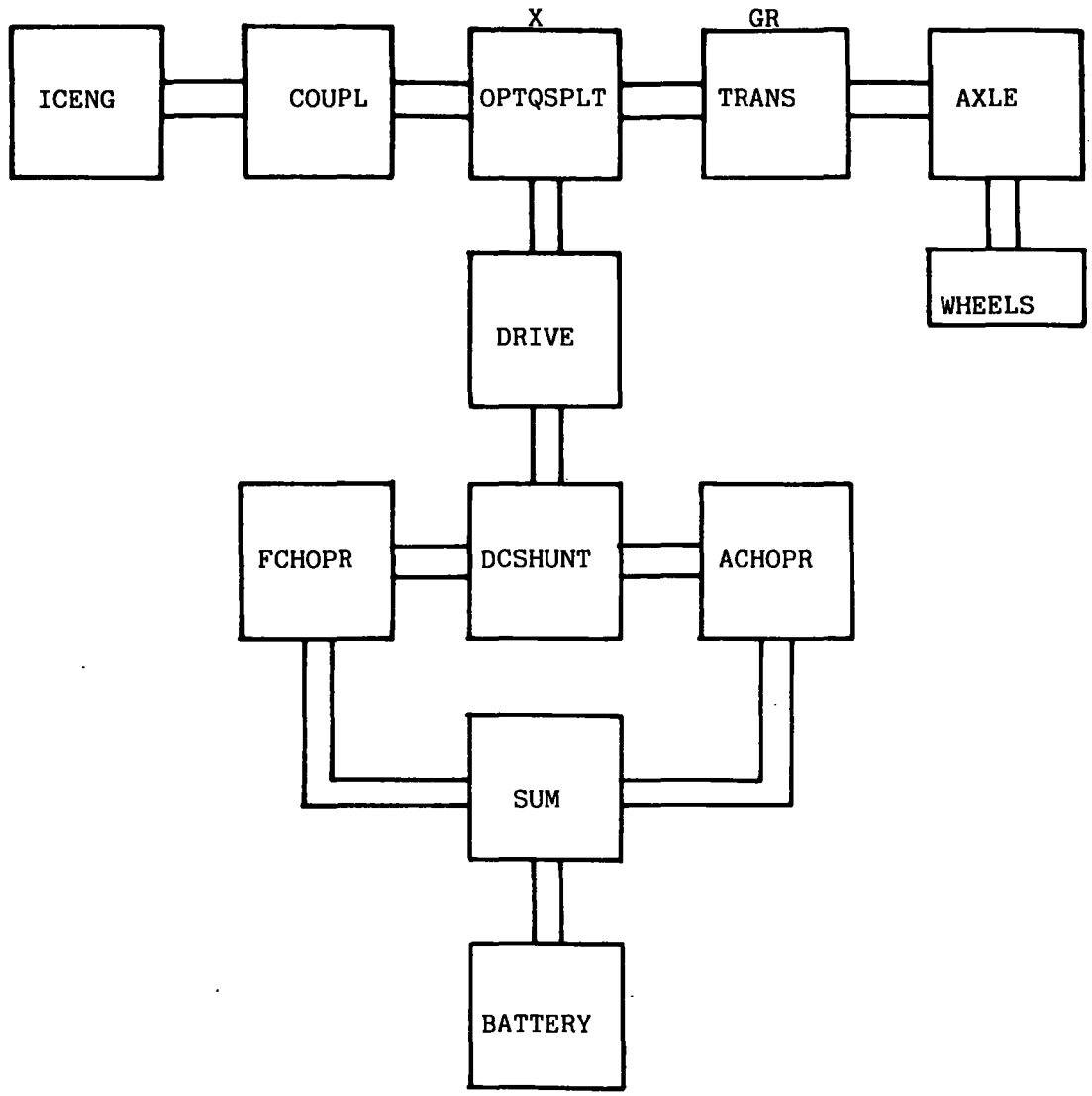

FIGURE 2.46: Parallel Hybrid Configuration using 2-D Optimisation

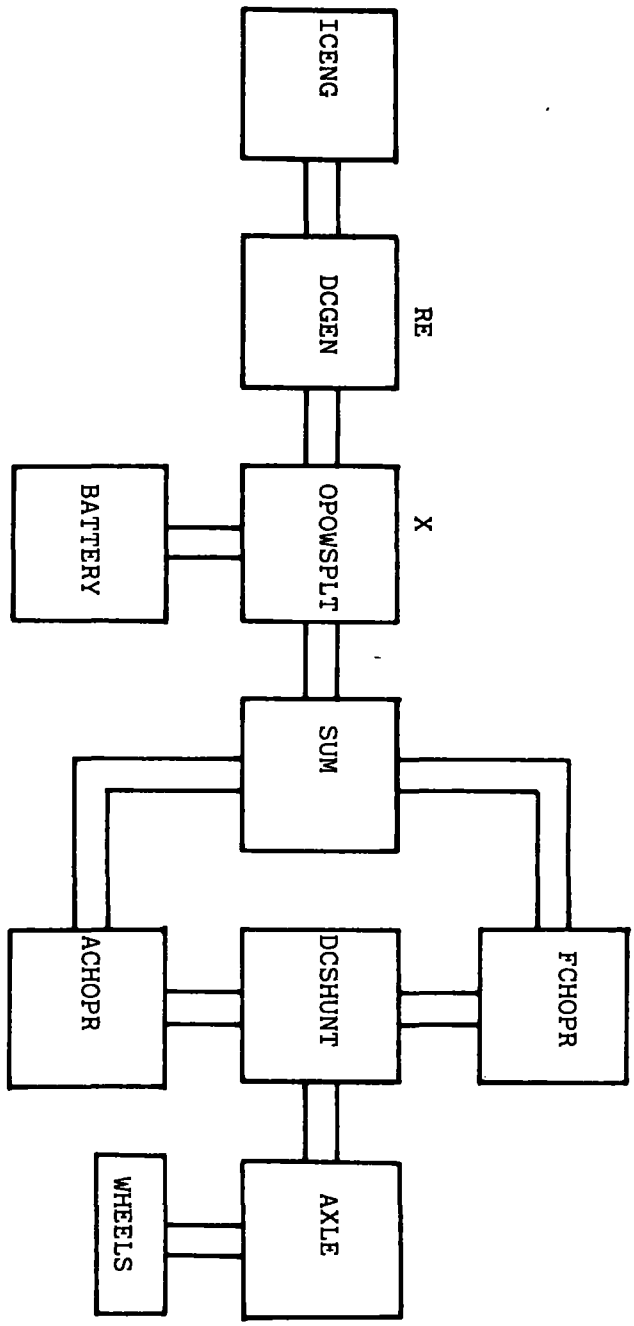

FIGURE 2.47: Series Hybrid Configuration using 2-D Optimisation

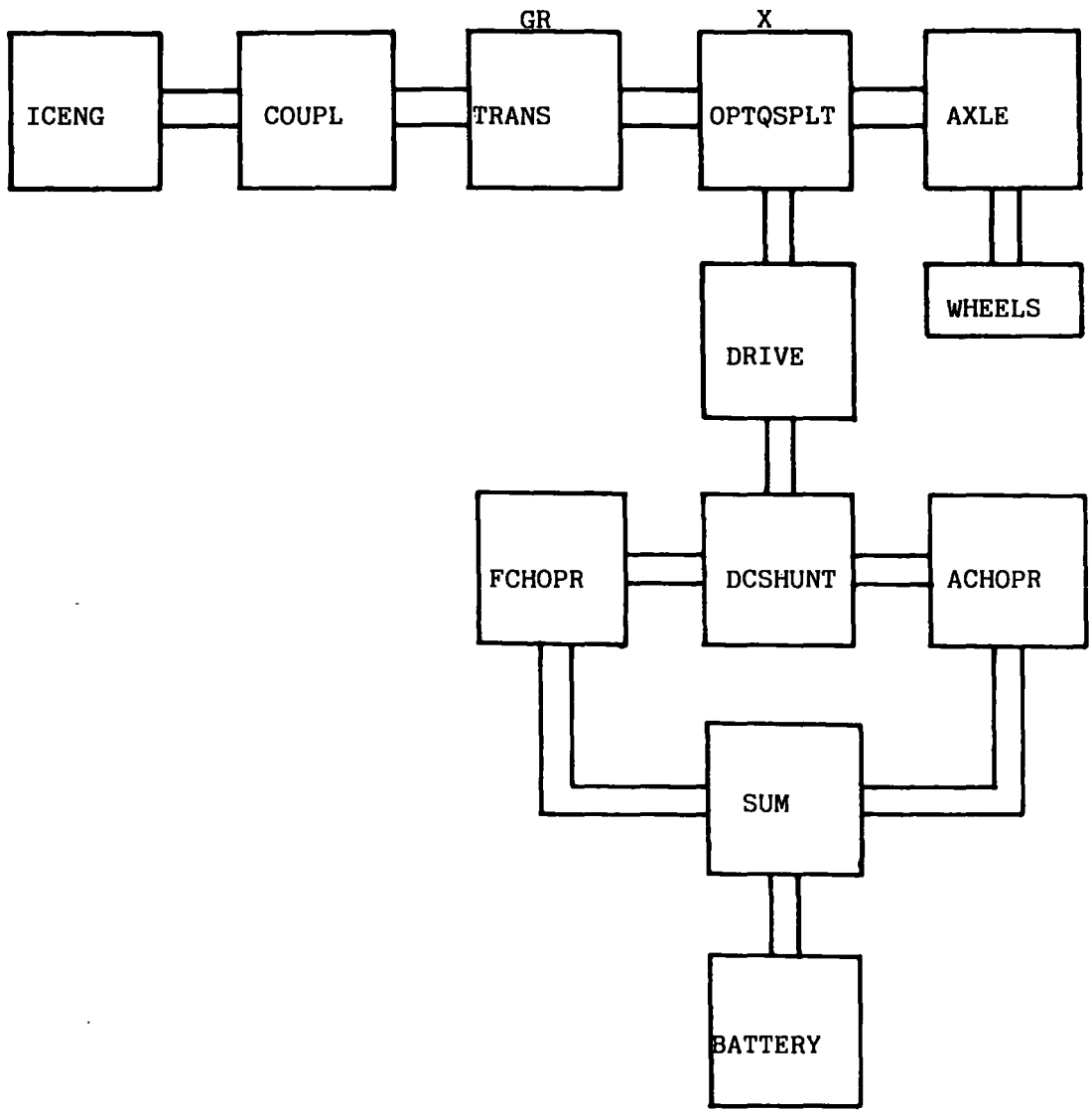

FIGURE 2.48: Alternative Parallel Hybrid Configuration using 2-D Optimisation

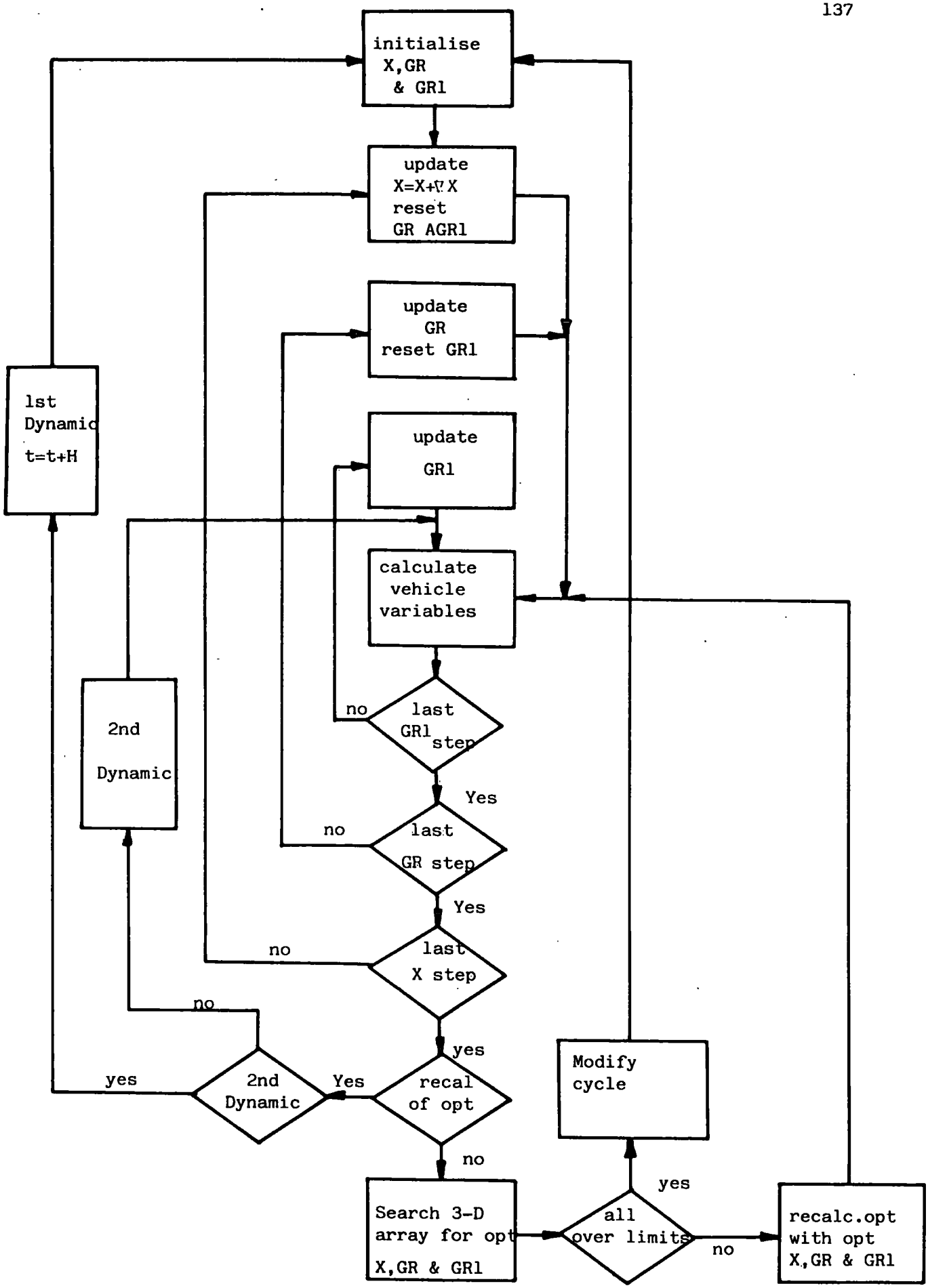

FIGURE 2.49: 3-Dimensional Optimisation Algorithm flow chart for motoring

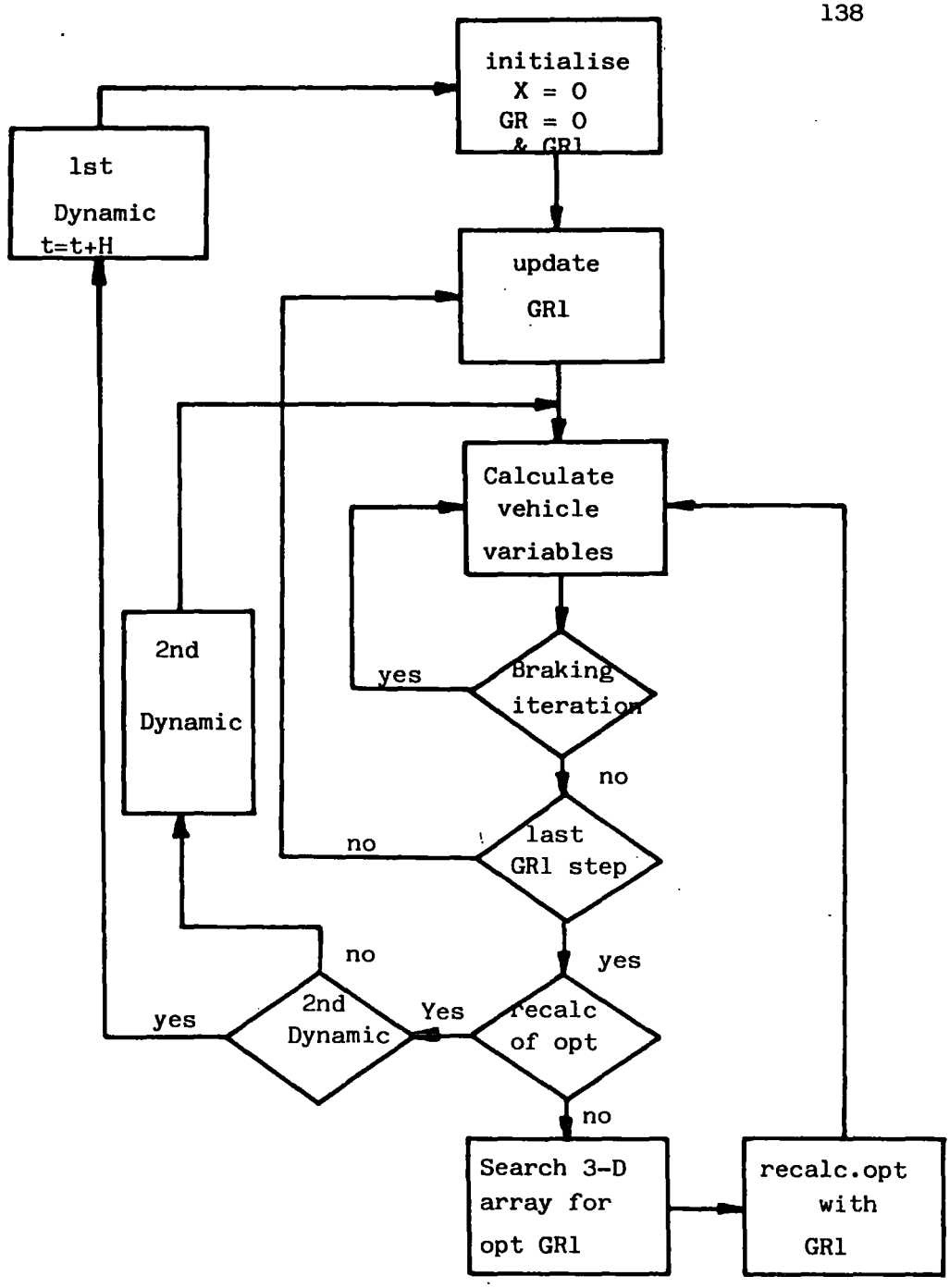

FIGURE 2.50: 3-D Optimisation Flow Chart for Regeneration

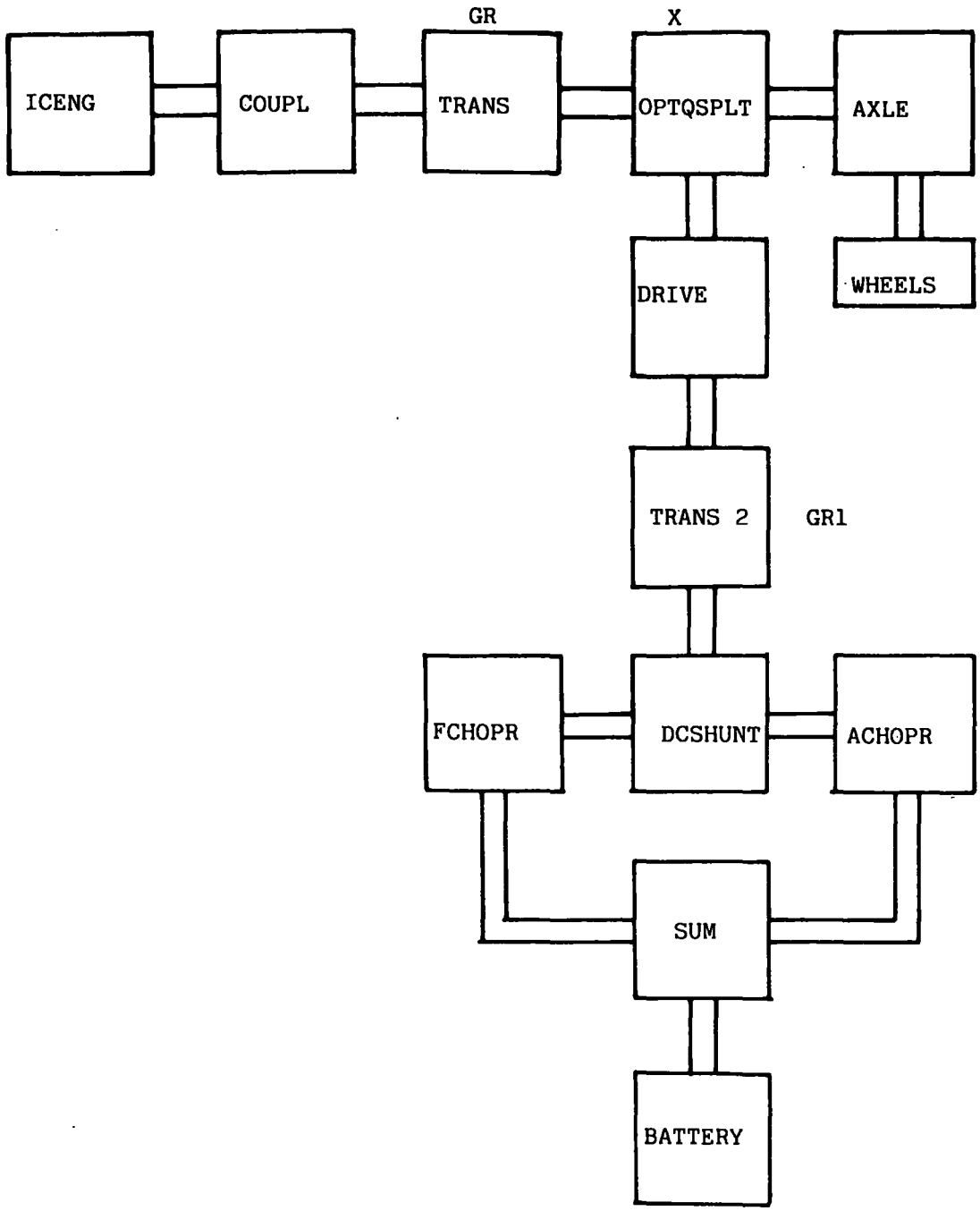

FIGURE 2.5L; Parallel Hybrid Configuration Using 3-D Optimisation

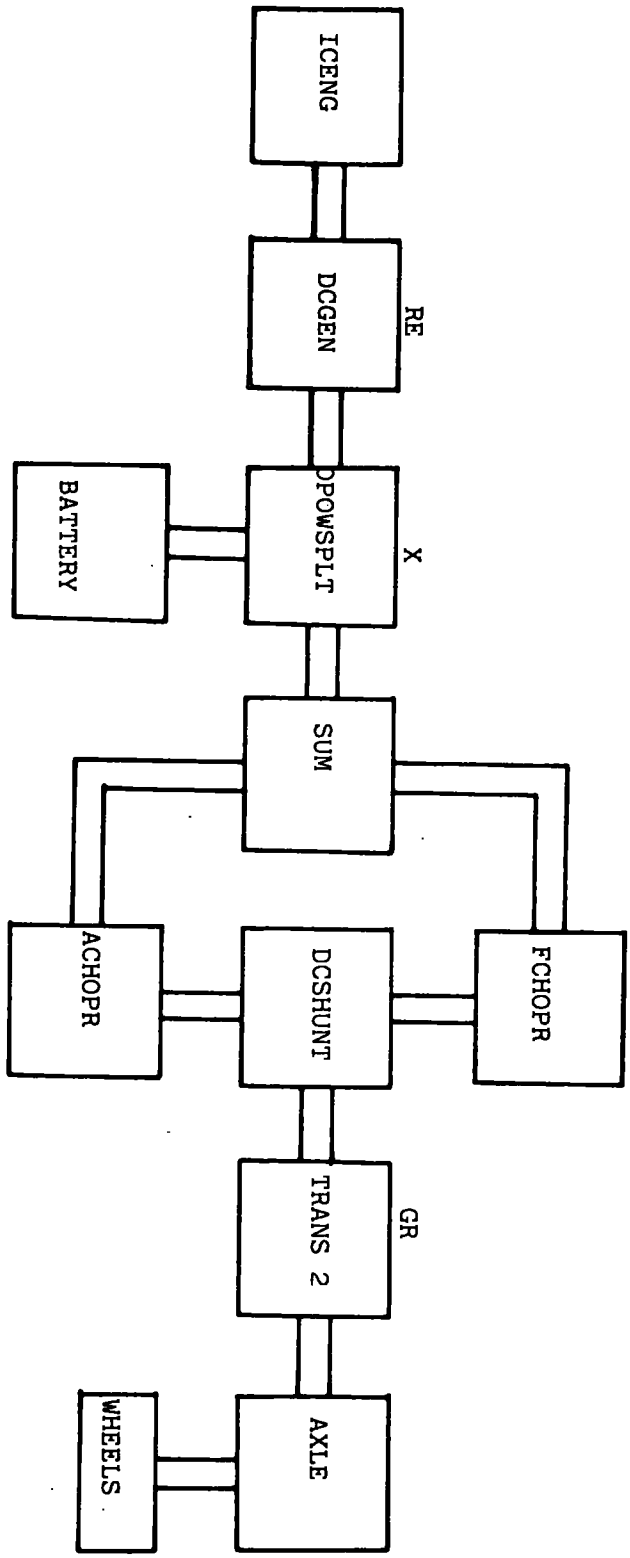

FIGURE 2.52: Series Hybrid Configuration using 3-D Optimisation

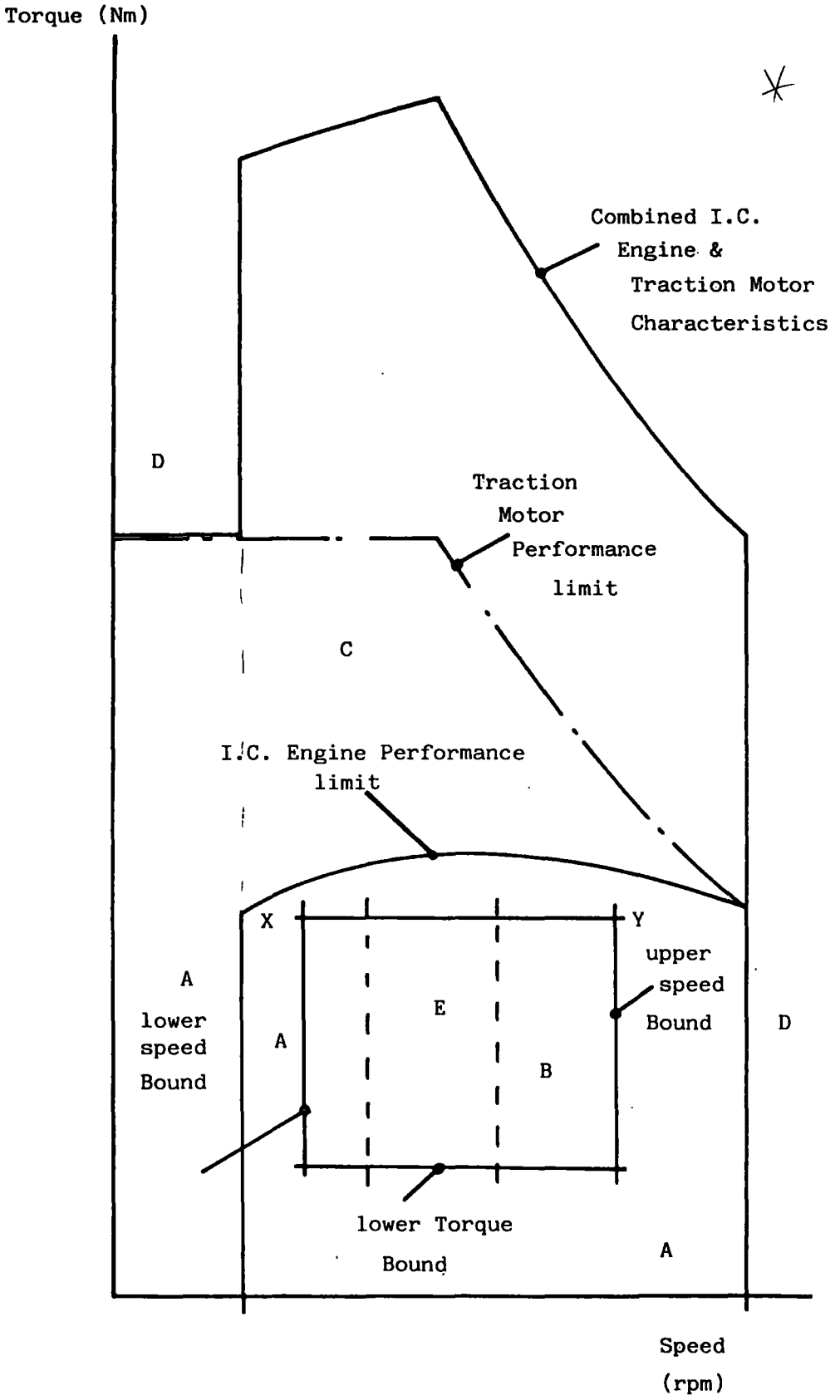

A - All Electric Operation
B - All I.C. Engine Operation
C - Hybrid Operation
D - Operation Not Allowed
E - Reduced Optimum Region Size

FIGURE 2.53: Sub-Optimum Control Strategy Operating Regions Superimposed upon power source maps for a Hybrid Vehicle

FIGURE 2.54: Sub-Optimum Control Strategy Flow Chart for a parallel Hybrid during Motoring

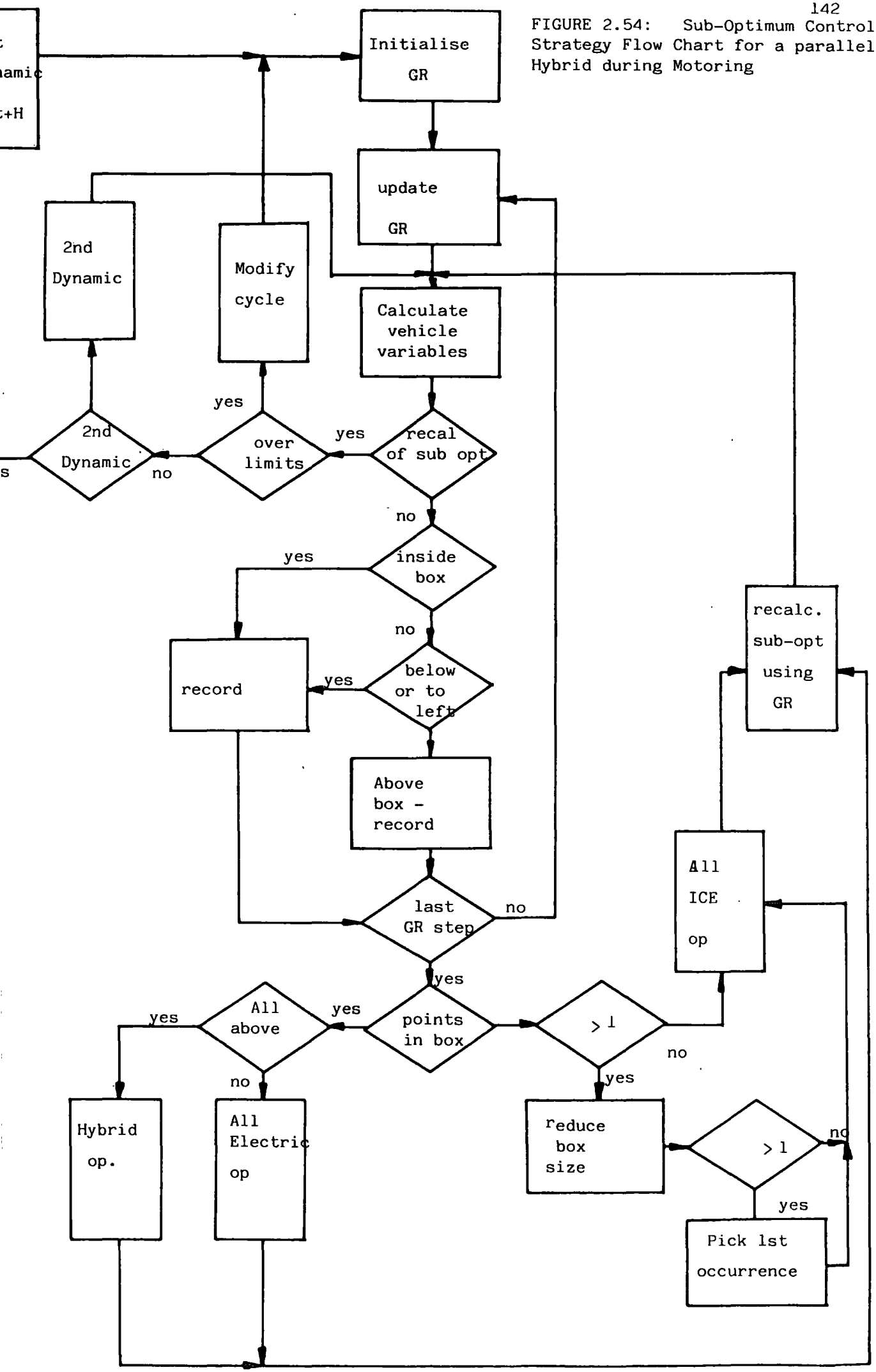

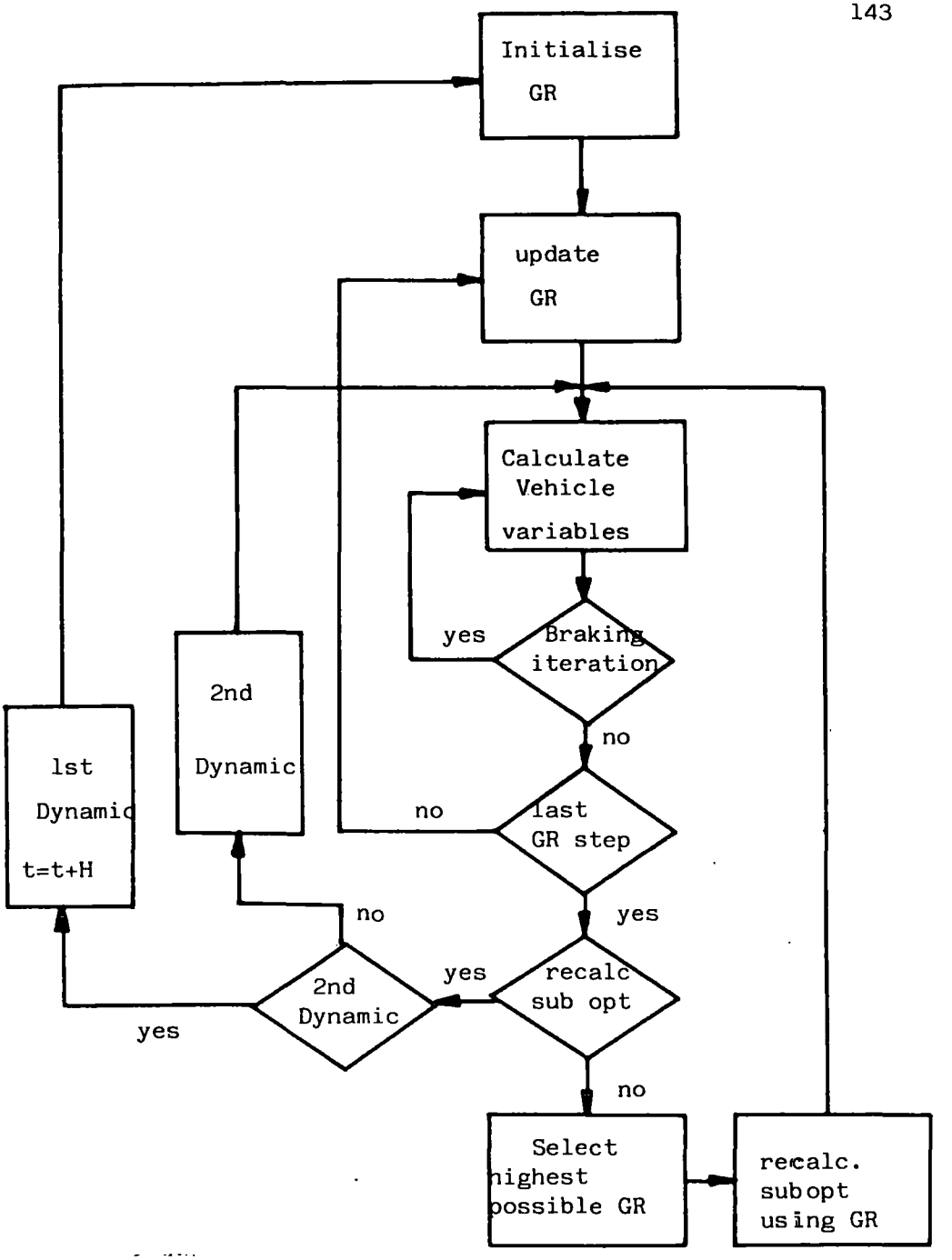

FIGURE 2.55: Sub-Optimum Control Strategy Flow Chart for a Parallel Hybrid During Regeneration

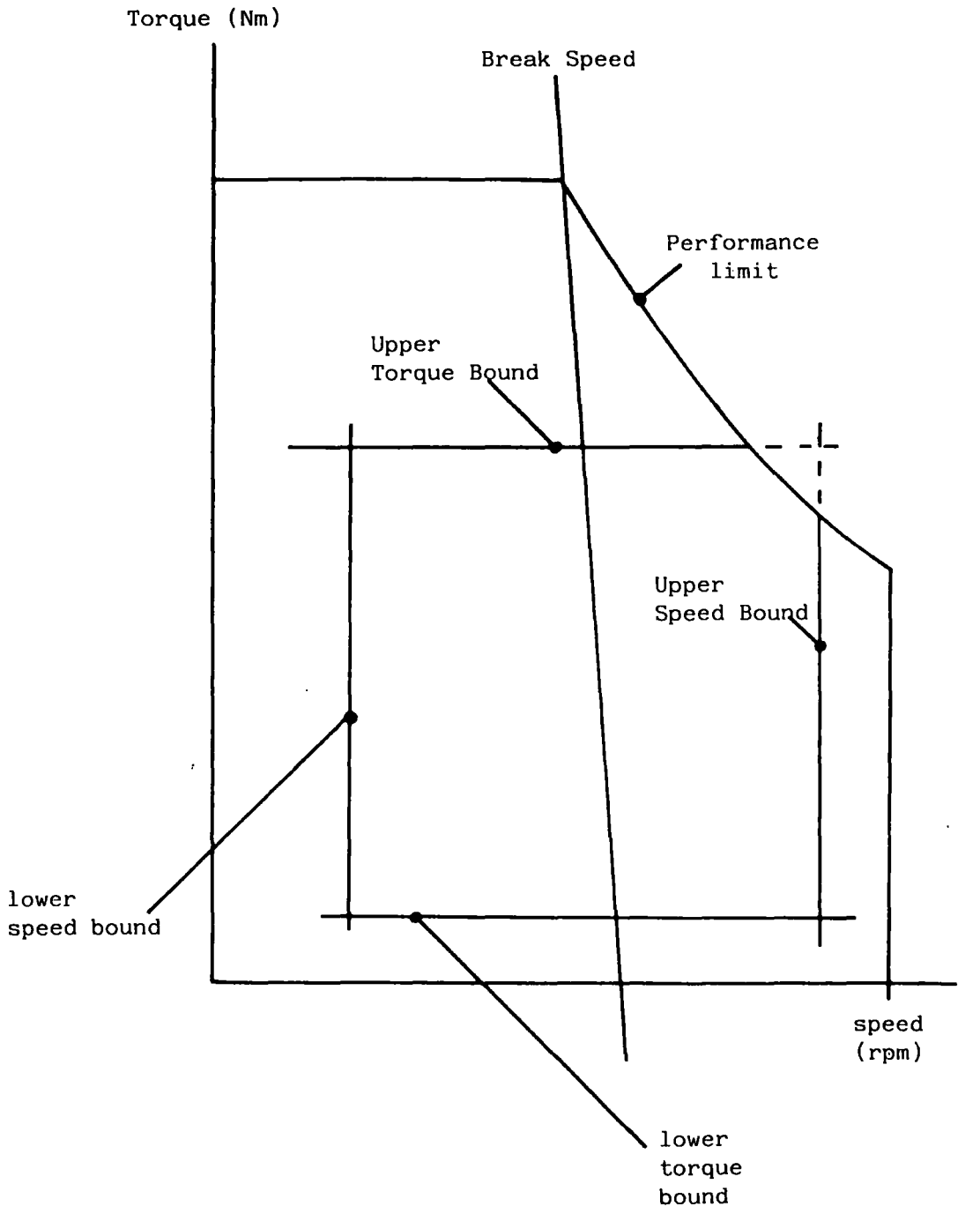

FIGURE 2.56: Sub-Optimum Control Strategy Operating Region for an Electric Vehicle

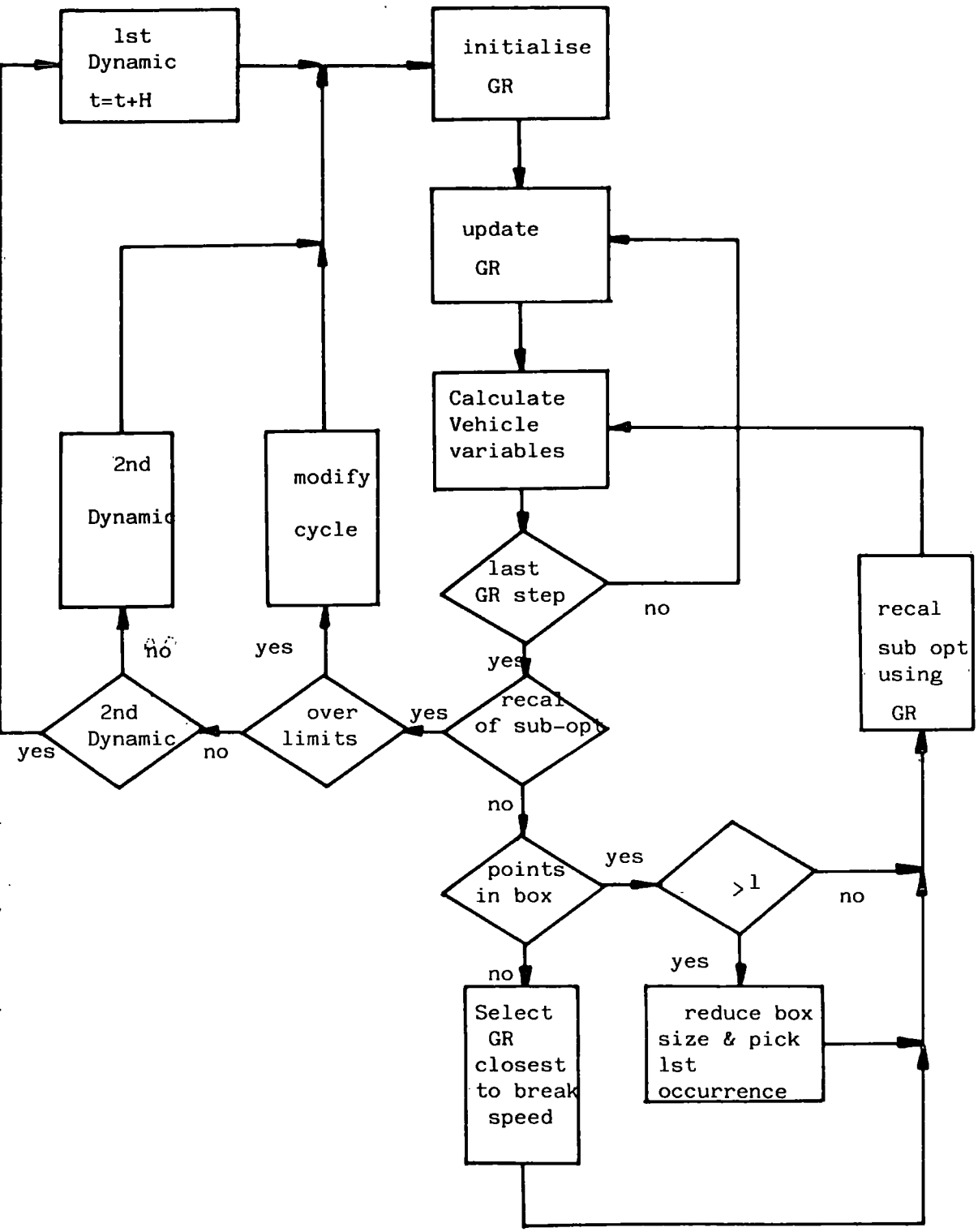

FIGURE 2.57: Sub-Optimum Control Strategy Flow Chart for an Electric Vehicle During Motoring

TABLE 2.1: JANUS Hardware Component Building Blocks

Component	Function
VEHICLE	Vehicle Characteristics
WHEELS	Road Wheel Characteristics
AXLE	Final Drive model
DRIVE	Utility Drive Model
TRANS) TRANS 2)	Variable Ratio Transmission models
COUPL	Mechanical Coupling Device Model
ICENG	I.C.Engine Model
DCSER	D.C. Series Motor Model
DCSHUNT	D.C.Shunt Motor Model
DCREL	D.C.Switched Reluctance Motor Model
ACINDUC	A.C. Induction Motor model
DCGEN	D.C.Generator Model
FCHOPR	Field Chopper Controller Model
ACHOPR	Armature Chopper Controller model
BATTERY	Battery Model
BATSWCH	Battery Switching Control model

TABLE 2.2: JANUS Software Component Building Blocks

Component	Function
DCYCLE	Driving Cycle & Environmental Conditions Definition
OPTCONT	Suite of Optimum Control Building Blocks for a variety of Drive Train Configurations
OPTQSPLT	
OPTIMISE	
OPCONT 2	
OPTIMS 2	
OPOWSPLT	
OPCONT 3	
OPTIMS 3	
OPCONT 4	
OPTIMS 4	
OPTCONT 5	
OPTIMS 5	
CONTROLP	Suite of Sub-Optimum Control Building Blocks for Hybrid Electric Configurations
CONTROLS	
TORQSPLT	
POWSPLT	
OPSPLIT	
CONTOPT	
CONTMOT	Sub-optimum Control Building Blocks for a pure Electric Drive Train
OPTMOT	
OPTGEAR	Sub-Optimum Control Building Block for an I.C. Engined Drive Train

TABLE 2.3: User Options Available in the Hardware Component Building Blocks

Building Block	Options
DCYCLE	- Choose 1 of 14 cycles
VEHICLE	- Choose a standard vehicle, weight addition manually or weight addition automatically
WHEELS	Choose ideal or one of two practical braking regimes
AXLE & DRIVE	Choose drive type
TRANS & TRANS 2	Choose discrete ratio (1-15 ratios) or continuously variable transmissions (4 designs available)
COUPL	Choose a friction clutch or torque converter with & without lockup
ICENG	Choose 1 of 20 maps
DCSER	Choose 1 of 3 maps
DCSHUNT	Choose 1 of 2 maps
DCREL & ACINDUC	1 map available at present
DCGEN	Choose 1 of 2 maps
ACHOPR	Choose transistor or thyristor chopper types
BATTERY	Choose 1 of 3 models, and for fractional and Shepherd models, also choose data for 1 of several types available

TABLE 2.4: JANUS - program operation features

Program Feature	Options
Multi-run Capability	1) Run again with no data changed 2) Run again but with data changed 3) End the simulation
Multi-cycle capabiltiy	Choose between 1 and 100 driving cyles (in DCYCLE) to be driven over consecutively.
Simulation Output Options	Both Numerical and graphical information can be directed to VDU or hard copy device covering a detailed vehicle breakdown or just overall vehicle energy consumption and/or performance

CHAPTER 3

Program Verification

3.1 The Purpose of Program Verification

The purpose of performing a detailed comparison between results obtained using a computer simulation program and results from other sources is to verify that the simulation program produces valid results both in terms of overall vehicle performance and also in terms of the individual component models.

Ideally, a comparison between simulation results and actual hardware test results is desirable, but as this is not always possible, such is the case here, a comparison between results from two or more completely independent simulation programs will still serve to highlight any shortfalls in the mathematical modelling.

Since the general simulation program at Durham is intended for the study of conventional i.c. engine, pure-electric and hybrid-electric drive-trains then it would be desirable to perform comparisons between simulation results and results from other sources for all of these vehicles. However, from the various published sources regarding hybrid-electric vehicle construction, a complete and accurate set of vehicle data was not available, so the verification was restricted to the conventional i.c. engined and pure-electric drive-trains with the knowledge that, because the hybrid comprises of components from both, at least the hardware models could be validated for this also.

3.2 Conventional i.c. engine Vehicle

Because fuel consumption data for i.c. engined vehicles is most readily available for the passenger car class of vehicles, the comparison has had to be restricted to this area (DOT 1984).

As a result, fuel consumption data has been obtained for several sizes of conventional i.c. engine passenger car, restricted by the fact that

complete, consistent and accurate vehicle data could only be obtained for a limited number of vehicles using information from various sources (B.L. cars)(Autocar,1981).

3.2.1 Description of Vehicle Data

Almost without exception, for British passenger cars, official test results on vehicle fuel consumption are presented in miles per gallon (mpg) over three different driving conditions: the ECE-15 simulated urban driving cycle (shown in Figure 3.10), at a steady 56 mph cruise and at a steady 75 mph cruise. The first two regimes are designed to represent typical passenger car driving conditions, whereas the third is intended to show the effect of higher speed driving on mpg figures (DOT,1984).

Although for two of the vehicles considered, a complete set of test data was available, data for the other vehicles was incomplete in that estimates of certain parameters such as frontal areas and drag coefficients, and/or an approximation as regards fuel map selection had to be made.

Two other items of vehicle input data which had to be estimated - but which would only affect vehicle results over the ECE-15 cycle - were i.c engine idle fuel consumption and i.c. engine rotational inertia - neither of which was specified in official tests or the published vehicle data.

Using empirical data obtained (B.L. cars) i.c. engine idle fuel consumption could be related to the engine power rating and the actual engine idling speed (Appendix IV). Thus, knowing an engine's rated power and picking a medium idling speed, the idle fuel consumption could be estimated.

For rotational inertias, such as i.c. engine and wheels, typical estimates had to be made. It was found from discussions with manufacturers that wheel inertia could be represented as a fraction of total vehicle weight (typically 5%), and that i.c. engine inertia, being almost entirely due to the i.c. engine flywheel, (Ford Motor Co. UK) could be related empirically to power rating.

However, as far as results are concerned, rotational inertia is not a significant vehicle parameter. Table 3.8 shows for simulated vehicles with and without rotational inertia included, the differences are a maximum of 5% over 3 different driving cycles.

Steady cruise results were not affected by estimates of idle fuel consumption or rotational inertia, so these regimes could be used as the first comparison between simulated and official results, but because the vehicle will spend almost 50% of the ECE-15 cycle at 'engine idle', the accuracy of the idle fuel consumption estimate may play a significant part in the validity of any comparison. (Appendix IV).

Where engine performance maps were approximated it was endeavoured to select a map with as close a capacity, compression ratio and speed range to the desired map, as due to the complex nature of the i.c. engine all 3 could have an important effect on SFC values, and hence the validity of any comparison. Finally, vehicle aerodynamic estimates were achieved by using empirical data, which in the case of drag coefficient meant scaling values from a chart (Appendix VI), and in the case of frontal area relating vehicle 'envelope' frontal area (height multilied by width) to 'actual' frontal area using vehicles with known frontal areas as a basis (Appendix VI).

The vehicle parameters used for both the simulated and actual vehicle test results are presented in tables 3.1 to 3.3.

3.2.2 Discussion of Results

Results from both simulation and from the officially published results for the vehicles considered are given in tables 3.4 to 3.8.

Using the cruise results as the most accurate comparison between test and simulation (having the minimum number of vehicle parameter unknowns associated), and looking at the vehicles with complete sets of aerodynamic and engine data available, the Metro 1275 and Princess 2227 in table 3.4, simulated results are within 3-6% of the official figures. The fact that all results are consistently lower than the official figures may indicate that the general rather than specific transmission model used is responsible.

Of the vehicles with aproximated engine fuel maps in table 3.5, results for the Princess 1700, Princess 2000 and Metro 1000 vehicles, still agree reasonably closely with the official results and are within 2-10%.

The vehicles with estimated aerodynamic data, but with the correct engine maps in table 3.6, simulated results are more adrift from the official figures, and vary between 1-13%.

Finally, the vehicles simulated with both estimated aerodynamic data and approximated fuel maps in table 3.7, the variation in results is even wider at 1-18% from the official figures.

It may be expected that as the quality of the vehicle input data diminishes, then the quality of the simulation results will accordingly drop. However this is not the case where several different vehicle parameters are being estimated, since the variable quality of one parameter may completely offset the variable quality of another. What does happen as the quality of the input data decreases, is that the reliability of the simulation results also decreases. From Table 3.4 to table 3.7 as the quality of data diminishes, so the results vary over a wider range.

Looking now at the ECE-15 results in tables 3.4 to 3.7, simulation results vary from 1-15% of the official figures.

Because it is not possible to separate the discrepancies due to engine map approximations and aeodynamic data estimates from the total discrepancies, it is therefore appropriate to look at the vehicles with the minimum of parametric estimates when looking for trends in the quality of the idle fuel consumption estimates. From table 3.4, therefore, for the Metro 1275 and Princess 2227 vehicles, large and small to medium engine sizes are represented. For the ECE-15 results the simulated Metro 1275 result is within 9% and the simulated Princess 2227 result is within 2% of the official figures. Although there are only two vehicles here from which to determine a trend, this suggests that the estimates for the small engine sizes (Appendix IV) may be at fault. However, as far as the official ECE-15 results are concerned there is no indication as to how the two engines in question were 'adjusted' for the test, so making the idle fuel consumption figure a complete unknown.

3.3 Electric Vehicle

As with the i.c. engined vehicle, complete and consistent data for individual electric vehicles was difficult to obtain from the published sources available. Furthermore, corresponding performance data was equally difficult to find.

Therefore the validation comparison has had to be restricted to a single electric vehicle, again a passenger car - the ETV-1 electric vehicle (Kurtz et al.,1981) (Slusser et al.,1981)(Hammond et al.,1981)(Hammond & McGehee,1981).

3.3.1 Description of Vehicle Data

Vehicle input data for the ETV-1 is given in table 3.9. The ETV-1 employs current electric vehicle drive-train technology in that a D.C. shunt wound (or separately excited), traction motor, controlled by a chopper controller and fed by a lead-acid traction battery, drives through a fixed ratio transmission.

As far as the ETV-1 was concerned, not only was there a complete set of vehicle parameters available, but there was also an equally comprehensive set of vehicle results available for comparison, in the form of JPL dynamometer tests (Kurtz et al.,1981) and simulation results using both the ELVEC program (Slusser et al.,1981) and the HEAVY program (Hammond et al.,1981).

Comparisons were possible at a series of cruising speeds, both with and without a headwind and gradient and over the J227aD urban driving cycle (Figure 3.11) for electrical systems with and without a regenerative capability.

In practice electric vehicles are run until a predetermined battery cut-off voltage is reached, at which point the battery is said to be discharged. For simulations using the 'fractional discharge' or the 'generic' battery models, vehicle range is determined when a predetermined battery depth of discharge (DOD) is reached. The problem of relating an experimental cut-off voltage to an equivalent DOD in order to make sensible range comparisons is now apparent.

As far as the ELVEC simulation results were concerned, the fractional discharge model was used to model the EV2-13 ETV-1 'prototype' battery, and range was determined at a battery DOD of 100%.

Because the JPL results were from practical dynamometer tests, the battery was discharged until predetermined cut-off voltages, depending upon

duty cycle (3.9 volts and 4.9 volts per cell for acceleration and cruise respectively). Furthermore, the JPL tests were also conducted using EV2-13 'production' standard batteries with a lower capacity than the 'prototype' batteries used by both the ELVEC and JANUS simulations.

Using the EV2-13 prototype battery characteristics as a rough guide, although cruise cut-off is at a higher voltage than the acceleration cut-off, it will be at a lower current and so the DOD at cruise cut-off will be less than the DOD for the acceleration cut-off (Appendix VII).

By determining the power density and discharge time for three ETV-1 cruising regimes an actual ETV-1 power density/discharge time curve for the production battery could be plotted and compared with the prototype curve used by JANUS (Appendix VII). The comparison shows the JANUS prototype battery to have 15-20% more capacity than the JPL production battery, depending upon the discharge rate. Therefore, for a sensible comparison to be made between JANUS and JPL results, the JANUS ETV-1 should be simulated at 80-85% DOD, depending upon the duty cycle.

3.3.2 Discussion of Results

Comparison was possible for the ETV-1 in terms of range to the predetermined battery discharge depths discussed, in terms of individual component energy usage and efficiency and over several power/time and current/time profiles.

Although a typical value of rotor inertia was used - as described by the motor models in chapter 2 and appendix I - an actual rotor inertia value was available for the ETV-1, so enabling an assessment of the JANUS rotor inertia calculation to be made.

As the battery depth of discharge for the JPL dynamometer test results was not explicit, the JANUS/JPL/HEAVY comparison is to be divided into

three areas. Firstly in the area of individual component energy usage and efficiency. Secondly as far as the power/time and current/time profiles are concerned. Finally, in terms of vehicle range to the implied battery depth of discharge.

To take the first area of comparison, component energy usage and efficiency presented in Figures 3.1 to 3.6, on the 'motoring' side, the JANUS simulation results agree well with the JPL results and are within 5%. The major sources for the discrepancy are the fact that JANUS does not account for accessory load (due to the unavailability of data) and because when the JANUS controller model is in the 'bypass' mode no account is taken of the contactor and parasitic loss.

On the regeneration side (for the J227aD cycle only) component energy usage and efficiency for JANUS and JPL differ by greater percentages and these differences can be explained by 3 assumptions used in the JANUS regenerative model. Firstly, JANUS assumes an ideal power split between friction and regenerative braking (i.e. it is assumed that the motor handles all braking until its limit is reached, whereupon the friction brakes are 'smoothly' blended in to make up the difference), whereas the ETV-1 has obviously a practical braking scheme that can only approach the ideal because of the limits of complexity that can be built in. Secondly, motor efficiency on the regneration side is assumed to be the 'mirror-image' of motor efficiency which may not be the case in practice. Finally, motor and transmission efficiency are combined for the JPL results, the latter of which for JANUS is assumed to be the same constant value used during motoring (which may be a reasonable assumption as chain drive efficiency does not vary significantly with load and speed in practice (Sargent et al., 1981)).

As far as the second area of comparison between the JANUS, JPL and HEAVY results, the power/time and current/time profiles, shown in Figures

3.11 to 3.17 along with driving cycle interpretations, agreement in general shape and magnitude is good. It must be pointed out that terminal power for the JANUS simulation refers to the armature power only (i.e., before the subtraction or addition of the field loss) whereas the JPL and HEAVY results refer to the 'net' terminal power.

There are two areas in the power/time and current/time profiles where discrepancies do occur. Firstly, there is a power/current peak during acceleration on the JPL/HEAVY results which does not appear on the JANUS results and can be explained by the different driving cycle interpretations for the J227aD cycle (an exponential profile is assumed for JANUS). The result is that maximum acceleration occurs at a slightly lower velocity for JANUS and consequently the peak power/current requirement is lower (Appendix IX). Secondly, the serrated appearance of both JPL and HEAVY profiles during the last portion of acceleration is due to the JPL test and the HEAVY simulation using discrete data points to define the driving cycle at this point, whereas JANUS assumes a smooth and continuous exponential relationship (Appendix IX). The difference is a function of how many points define the JPL and HEAVY curves rather than the size of cycle time-step used, and can be explained in detail by sharp changes in driving cycle acceleration between adjacent data points (falling acceleration) causing the initial drop in power/current (at a constant velocity). The following rise in power/current is due to the acceleration remaining constant up to the next data point with increasing velocity at which point the process is repeated.

Finally for the third area for comparisons between JPL and JANUS results, vehicle range, presented in Figures 3.1 to 3.6, if the 3 cruise regimes are considered for battery DOD's that vary between 80-85%, results from JANUS are within 5% of the JPL results. Despite the poorer energy

usage agreement between JPL and JANUS for regeneration, the contribution from regeneration to vehicle range is generally only 10%. However as the urban cycle battery depth of discharge was more difficult to estimate, no comparison on range is attempted.

The JANUS/ELVEC comparisons were made again, over the SAE J227aD cycle - but without regenerative braking - and at a steady 40 mph cruise with a 2% gradient and 23 mph headwind included. The results presented in tables 4.10 to 4.11 show that the JANUS results are consistently within 5% of the results of the ELVEC results.

Although the JANUS model does not include the effects of accessory load, the JPL results can be used to show how accessory load, as a percentage of battery output specific energy, varies with vehicle cruise speed (Appendix IV). The curve shows an approximate straight line relationship. This may be explained by the reduced component efficiencies (such as motor and controller) at low speed and the consequent need to remove unwanted heat (assuming that any cooling blowers are remote and were not included in the performance map compilation). The accessory load at 55 mph will be at the point of highest efficiency, hence minimum cooling requirement, so may be assumed to comprise of the continuous load such as lights and battery ventilation. However at the low cruising speeds component efficiency will be low and cooling requirement will be at a maximum and may now form the major portion at the total load. Although the curve shows accessory load as a percentage of battery output varies only between 1 and 10% its absolute vaue may still be large.

Finally, the results using the typical values of rotor inertia in the JANUS model just discussed could also be compared with the results if the exact value of ETV-1 motor inertia was included. The comparison, shown in Figures 3.1 and 3.5 shows a small discrepancy of less than 5%, and if zero

inertia is included in the JANUS model, shown in Figure 3.6, its contribution when compared with either Figure 3.5 or Figure 3.1 is still only of the order of 5%.

3.4 Conclusions

In the program verification described here results produced using the JANUS simulation have not only been compared with hardware dynamometer tests in the case of the i.c. engined vehicles and the ETV-1 electric vehicle but also simulation results from another source in the case of, again the ETV-1.

The simulation/dynamometer comparisons have given an assessment of the absolute accuracy of the simulation program in terms of component modelling and also the basic simulation approach of assuming discrete steady-state driving cycle time-steps instead of, say, a more complex differential equation solution - as discussed in chapter 2. However, in all cases (for the Metro 1275, the Princess 2227 and the ETV-1) all vehicle data with the exception of the general transmission model employed by JANUS was complete, so in effect all that was being assessed was essentially the basic simulation philosophy. The examples of the i.c. engined vehicle verification where vehicle input data was open to question showed quite clearly how the simulation results became more unreliable as the number of estimated parameters was increased.

The simulation/simulation comparison, although merely comparing one mathematical model with another cannot be discounted as having little value in determining the absolute accuracy of results, especially if different fundamental simulation approaches are being compared, which unfortunately in this case was not possible.

The JANUS/ELVEC and JANUS/HEAVY comparisons showed, how given consisent input data and a very similar simulation approach how close agreement would be achieved. In the case of the JANUS/ELVEC comparison, several aspects of the JANUS simulation program could be tested that was not possible in the JANUS/JPL comparison. These were, in the use of a more sophisticated rolling resistance model (appendix VIII), the addition of a headwind and gradient effects and the effects of no motor regeneration.

Two fundamental points can be concluded from this verification study as regards two very different uses of this simulation program. Firstly, when absolute accuracy is required from the results of a simulation, then the correct vehicle data must be input, which in the case of the i.c. engine model, requires the precise fuel map data also, since this component does not lend itself to generalisation easily - as was discussed in chapter 2. The applications of this requirement of a simulation are in the final design studies of a fixed power train where the i.c. engine may be altered in size within the constraints of the fuel map, gear ratios may be altered and vehicle characteristics may be altered. Secondly, when a more general study is being performed on vehicle power train concepts, no exact vehicle data may be available and typical values may be input for, say, vehicle characteristics and/or the engine fuel map. Although the power of simulation clearly allows any of these typical parameters to be varied at will within any realistic bounds imposed upon them, for certain studies possible with a general simulation program they may be held constant in order to study the effects of some other more fundamental parameters, namely altering the drive-train configuration from say, i.c. engined to pure-electric to hybrid electric.

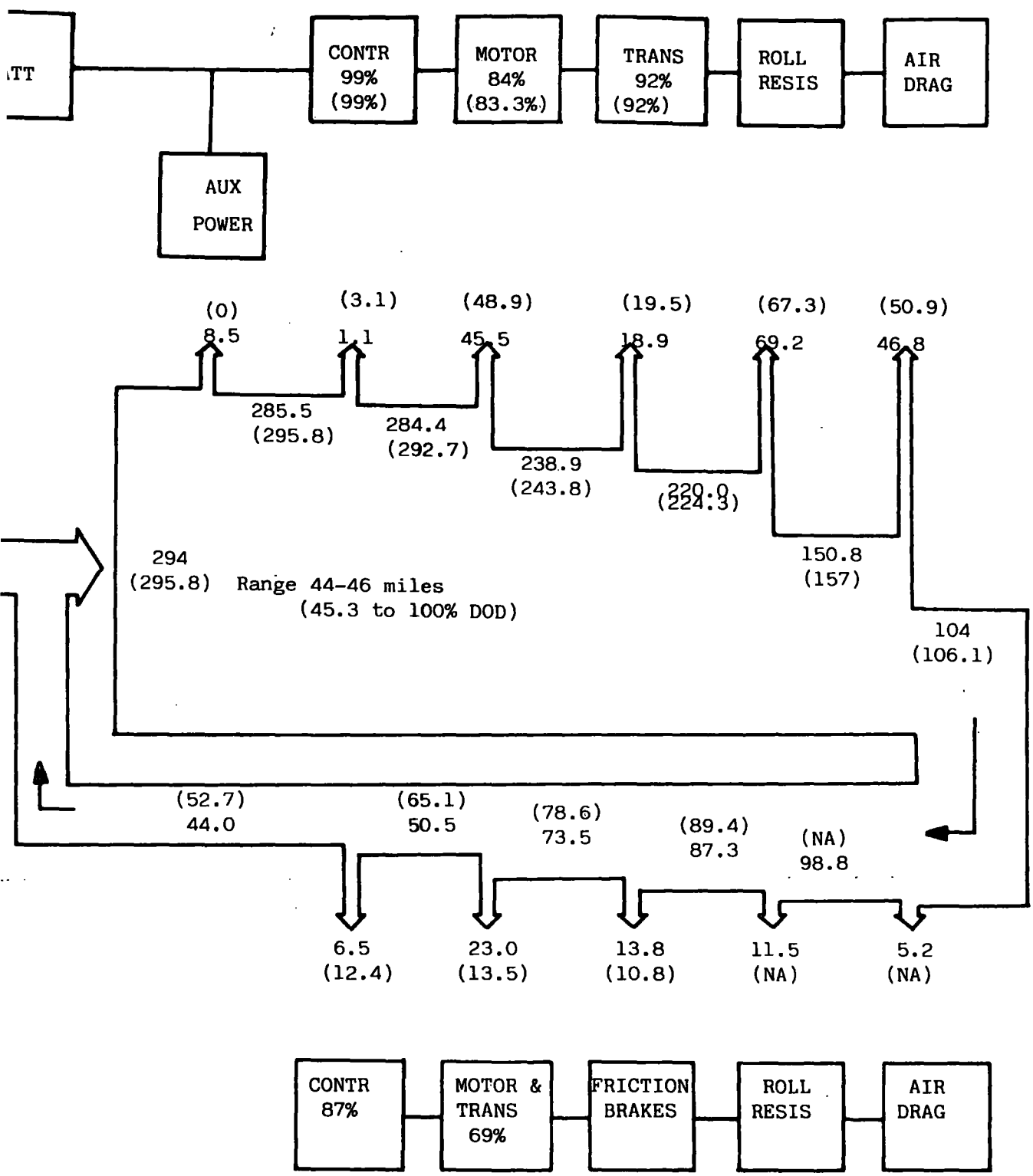

FIGURE 3.1: Energy Flow and Component Efficiency Diagram for the ETV-1 over the J227aD cycle

(All Energies in w-hr/mile and JANUS results in brackets)

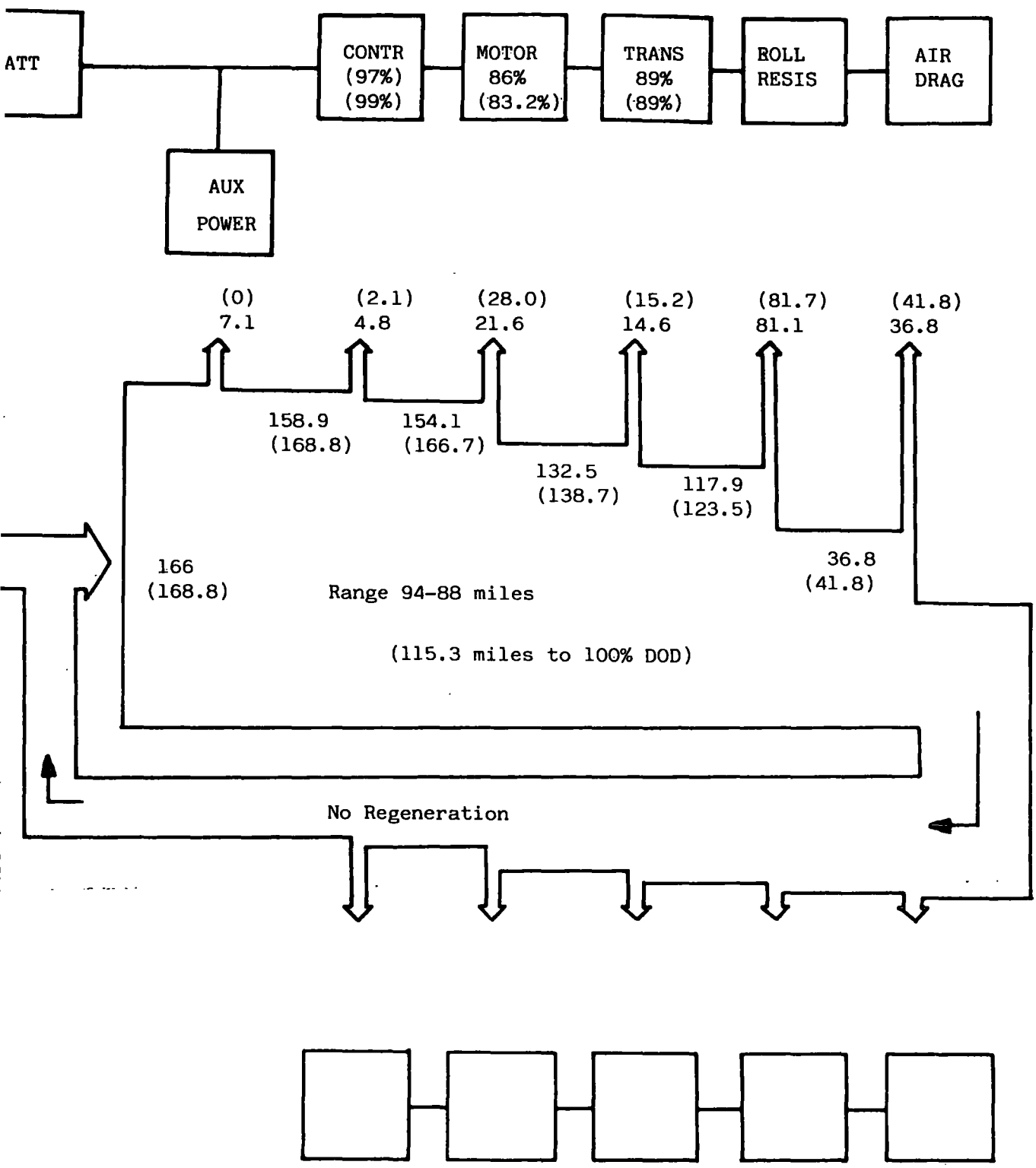

FIGURE 3.2: Energy Flow and Component Efficiency Diagram for the ETV-1 at 35 mph Cruise

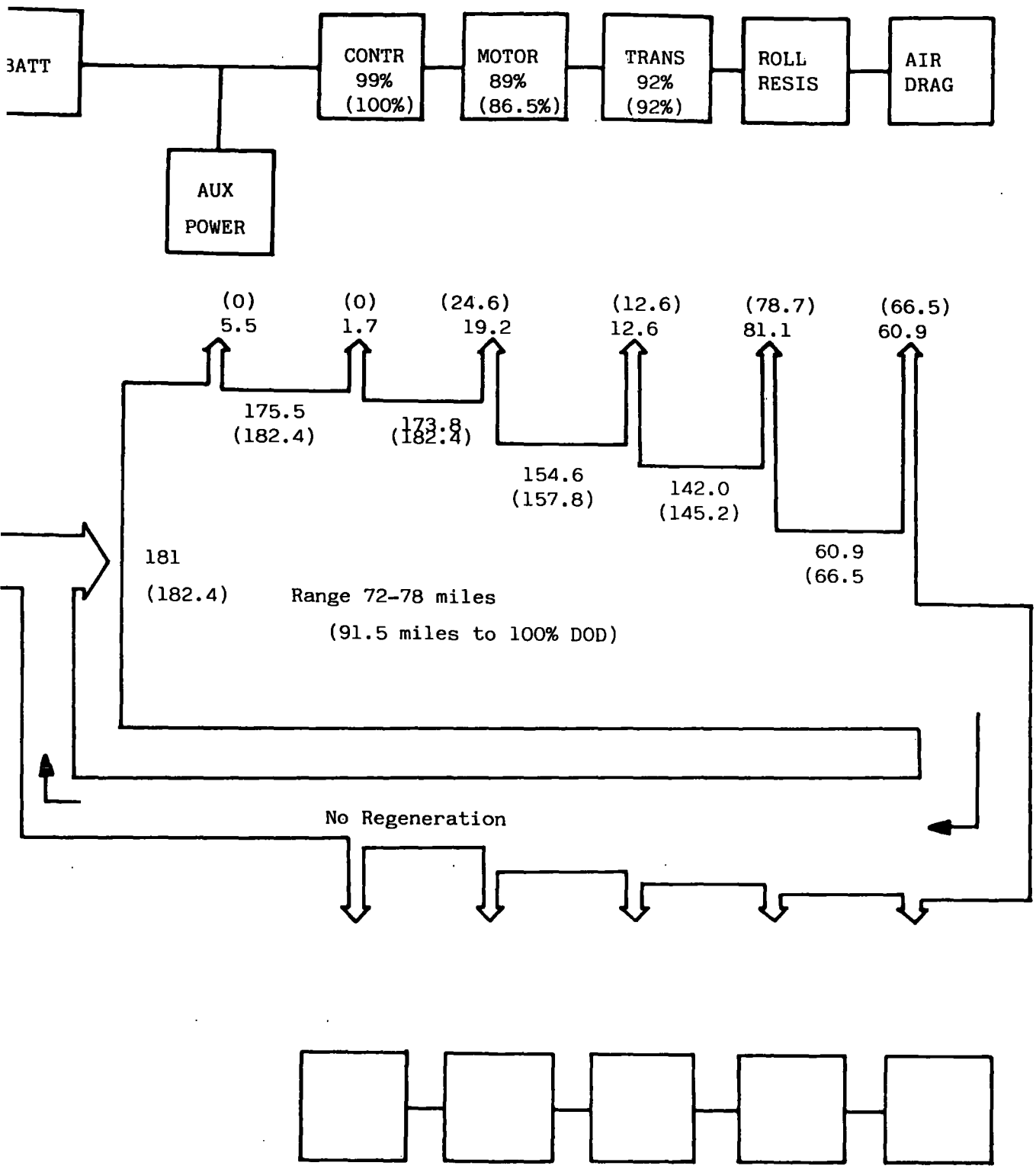

FIGURE 3.3: Energy Flow and Component Efficiency Diagram for the ETV-1 at 45 mph Cruise

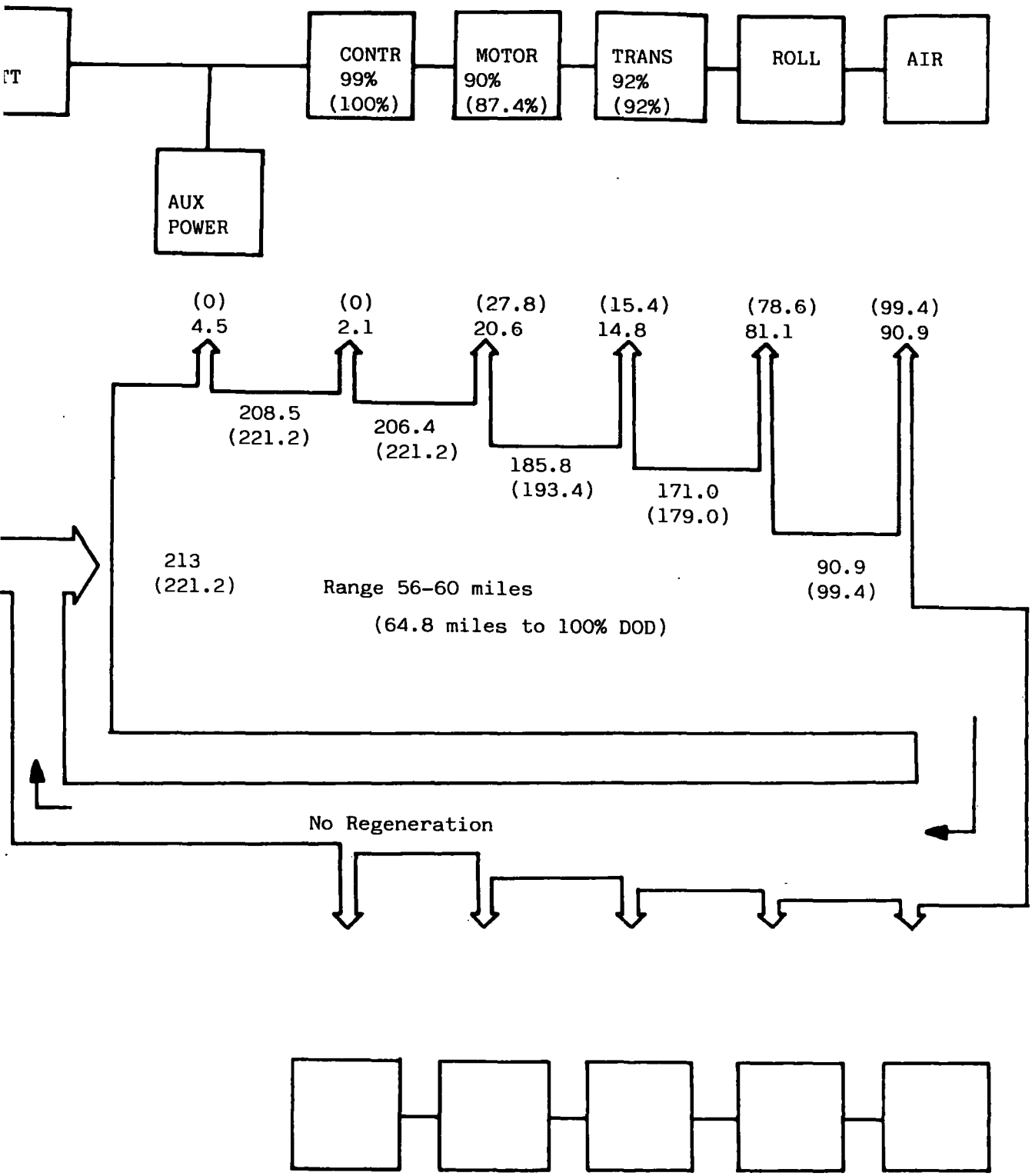

FIGURE 3.4: Energy Flow and Component Efficiency Diagram for the ETV-1 at 55 mph Cruise

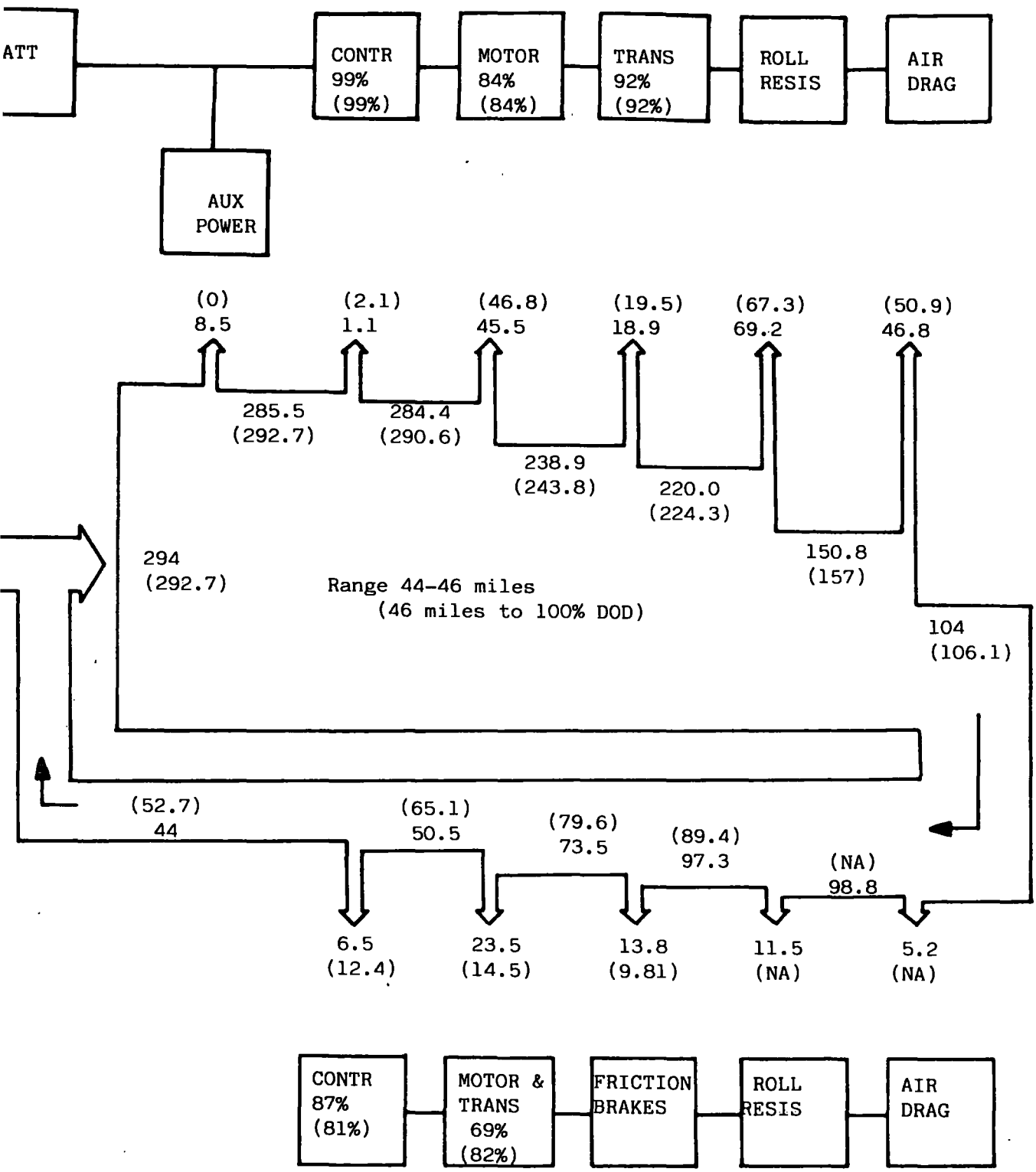

FIGURE 3.5: Energy Flow and Component Efficiency Diagram for the ETV-1 over the J227aD cycle with the exact value of Rotor Inertia included

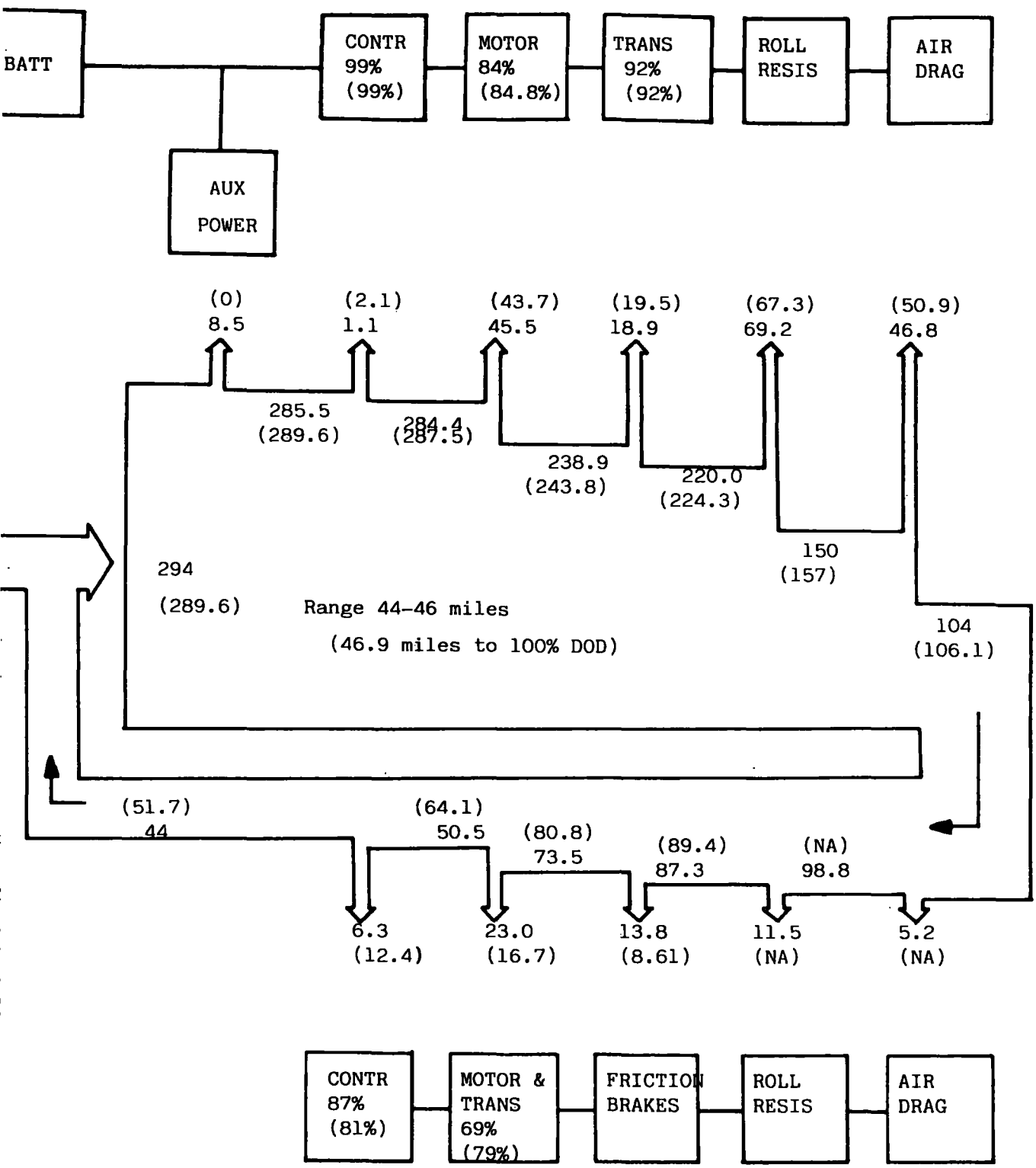

FIGURE 3.6: Energy Flow and Component Efficiency Diagram for the ETV-1 over the J227aD cycle with no Rotor Inertia Included

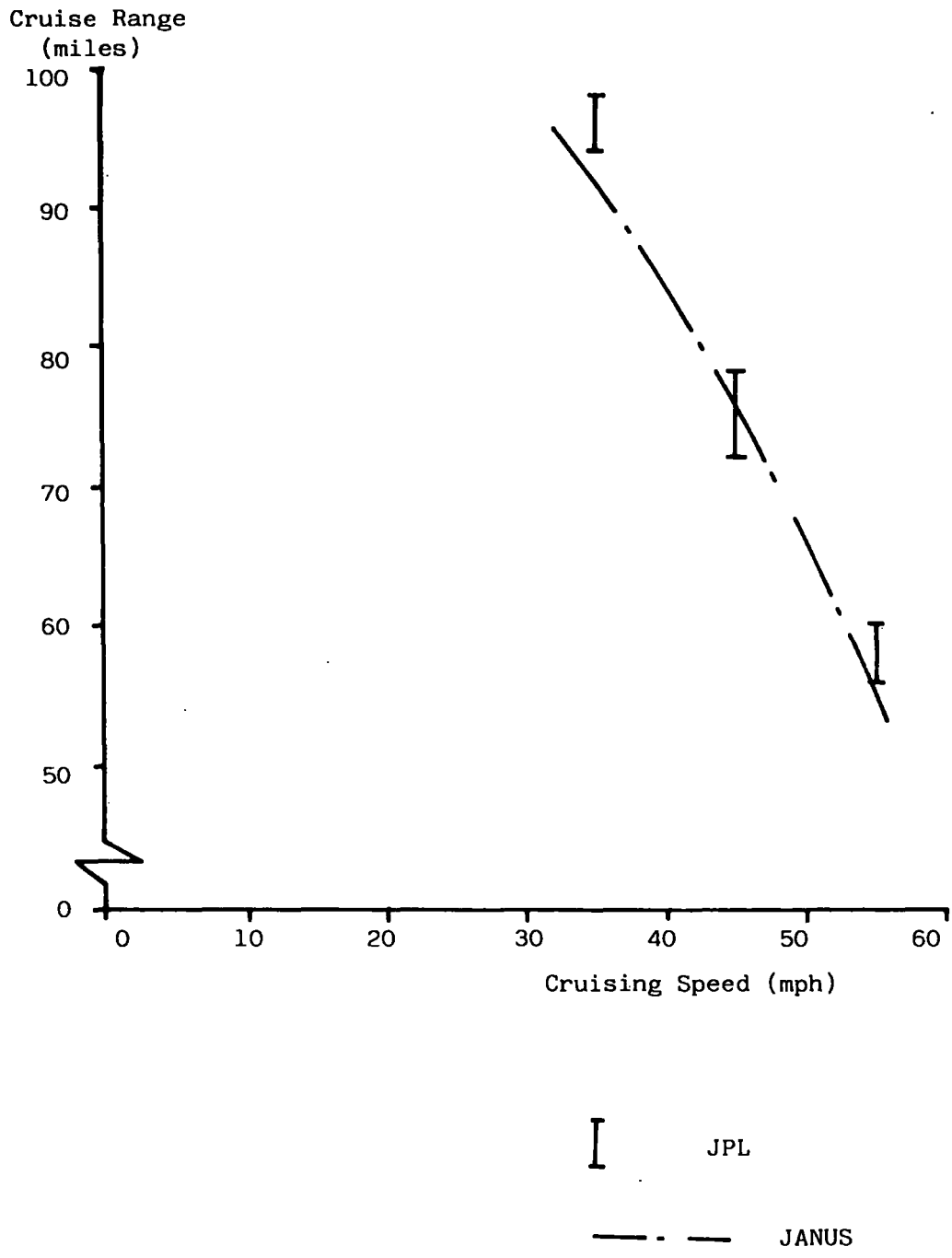

FIGURE 3.7: ETV-1 Range versus Cruising Speed Comparison Between JANUS and JPL

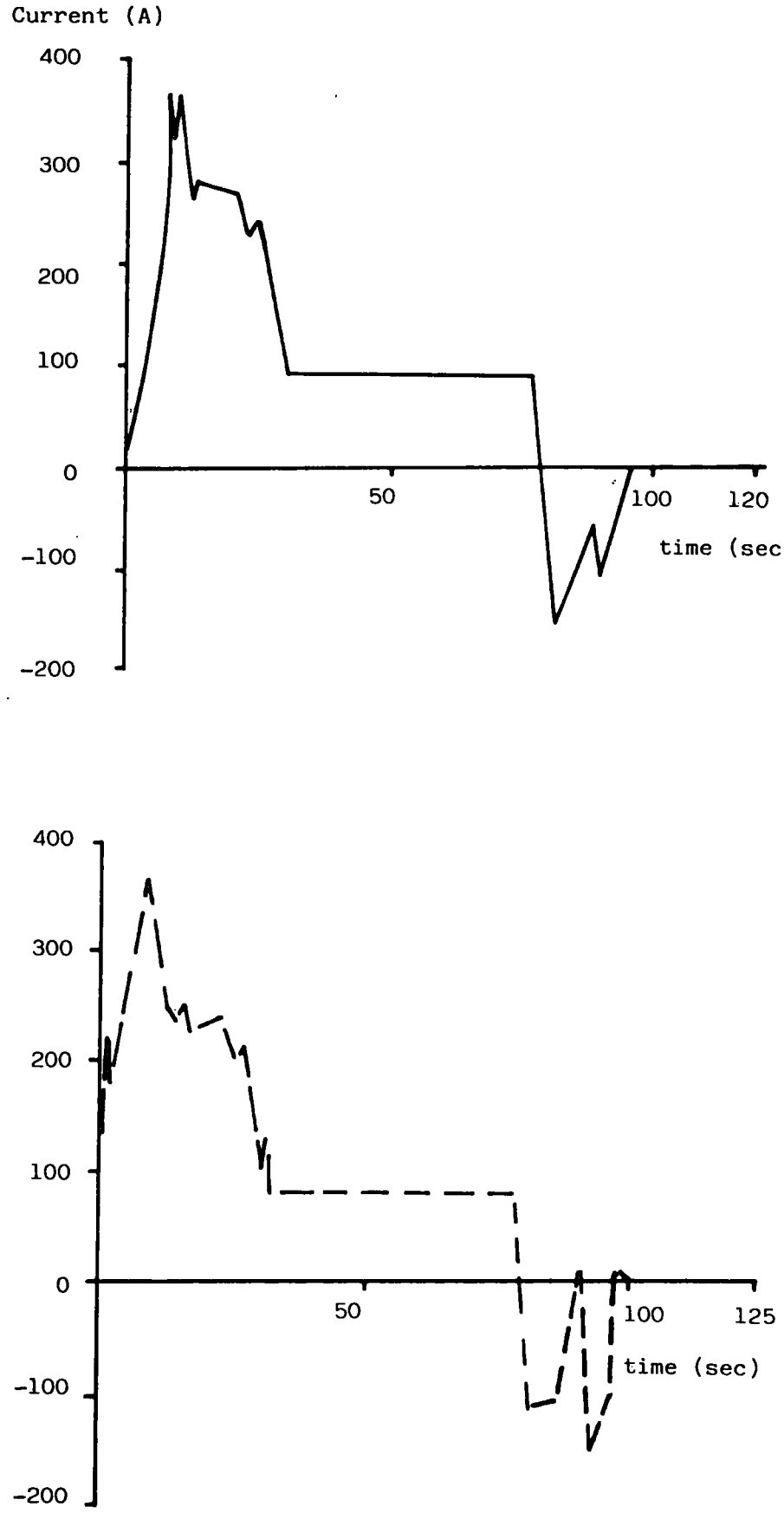

FIGURE 3.17: HEAVY and JPL graphical Representation of Battery Current/time profiles

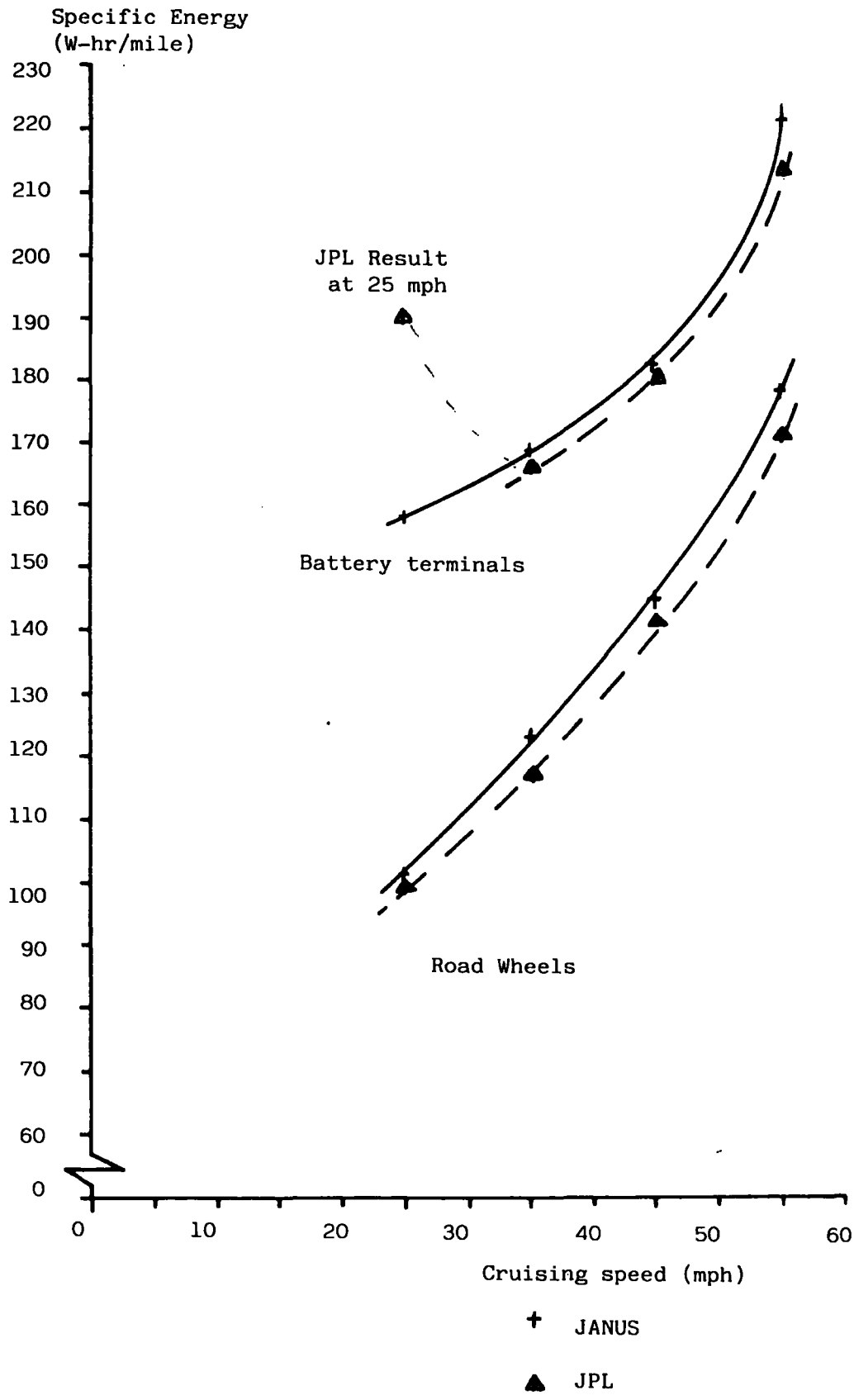

FIGURE 3.8: ETV-1 Specific Energy Usage versus Cruising Speed - JANUS/JPL

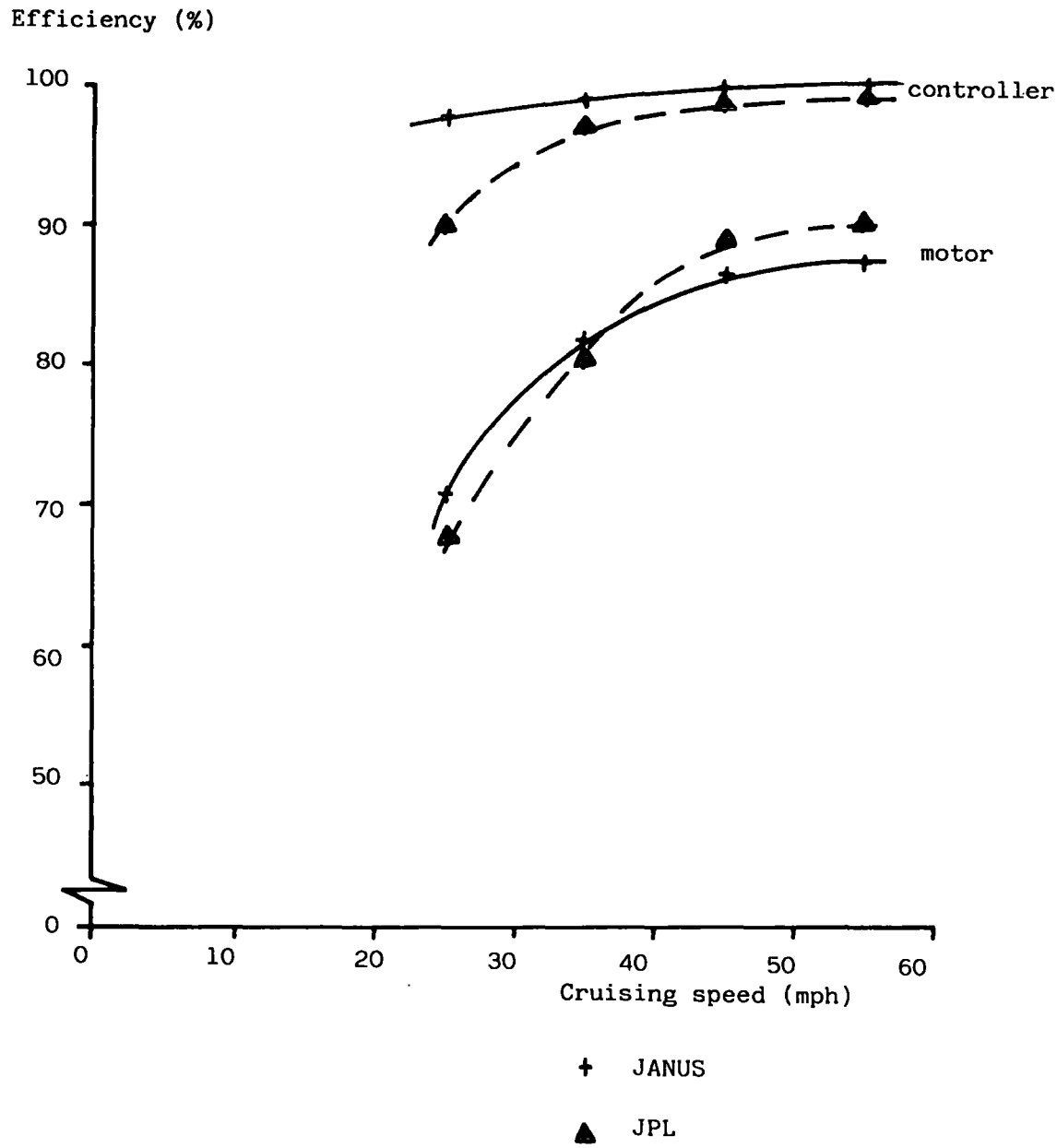

FIGURE 3.9: ETV-1 motor and controller efficiencies with cruising speed - JANUS/JPL

FIGURE 3.10: ECE-15 Urban Driving Cycle

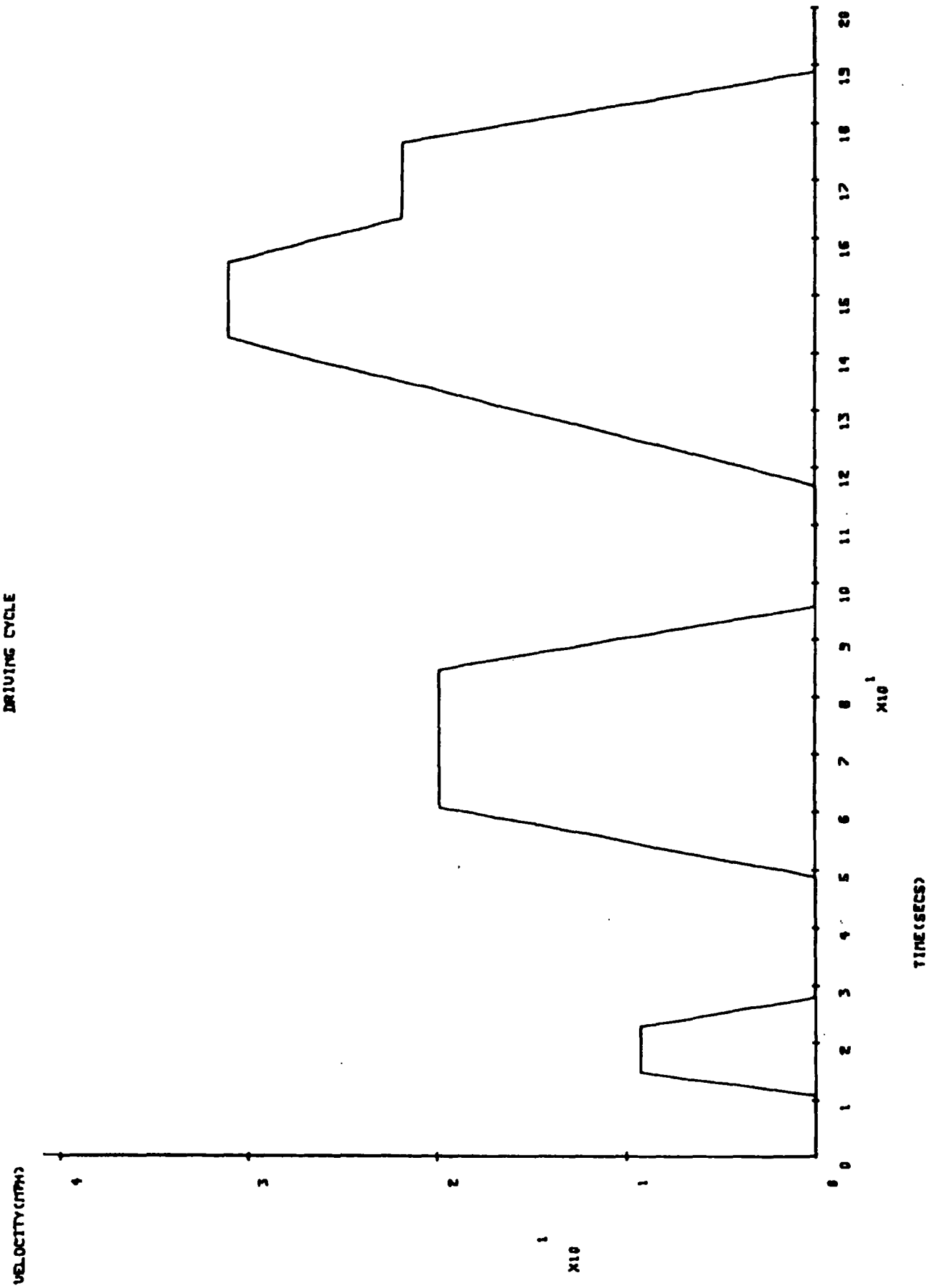

FIGURE 3.11: J227aD Urban Driving Cycle

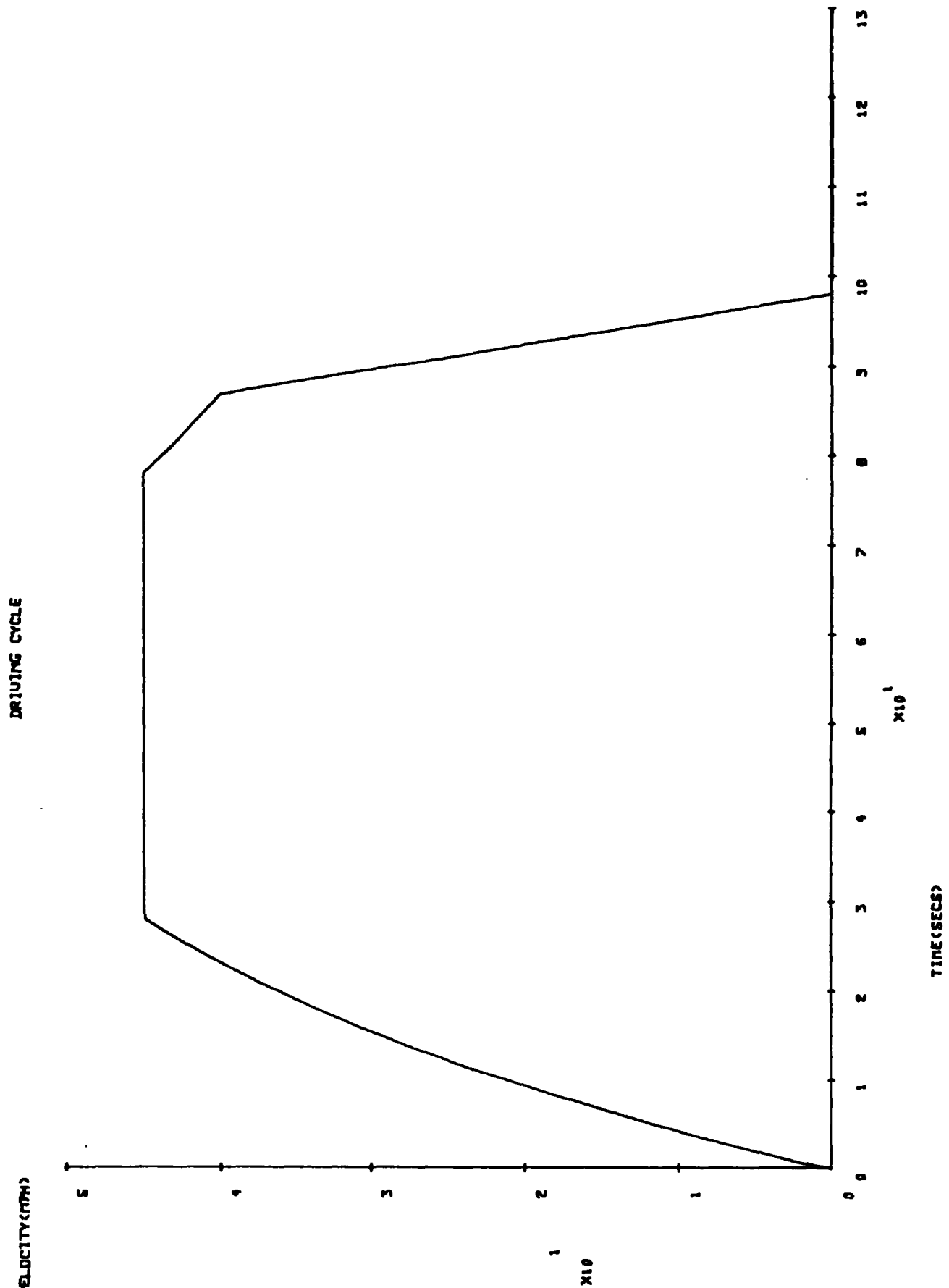

FIGURE 3.12: JANUS-Motor Shaft Power-time Profile for the ETV-1 over the J227aD cycle

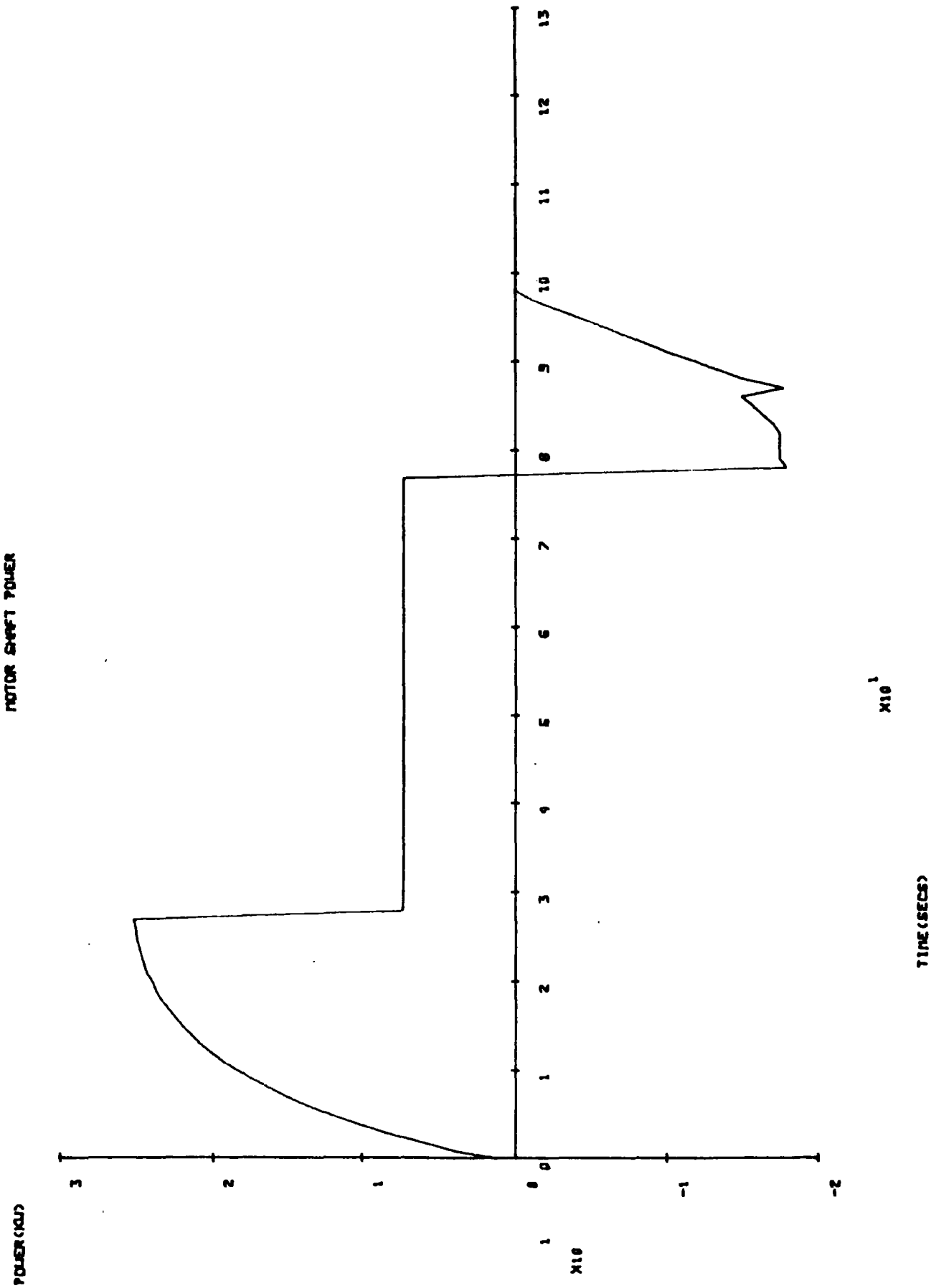

FIGURE 3.13: JANUS-Motor Armature Power/time Profile for the ETV-1 over the J227aD cycle

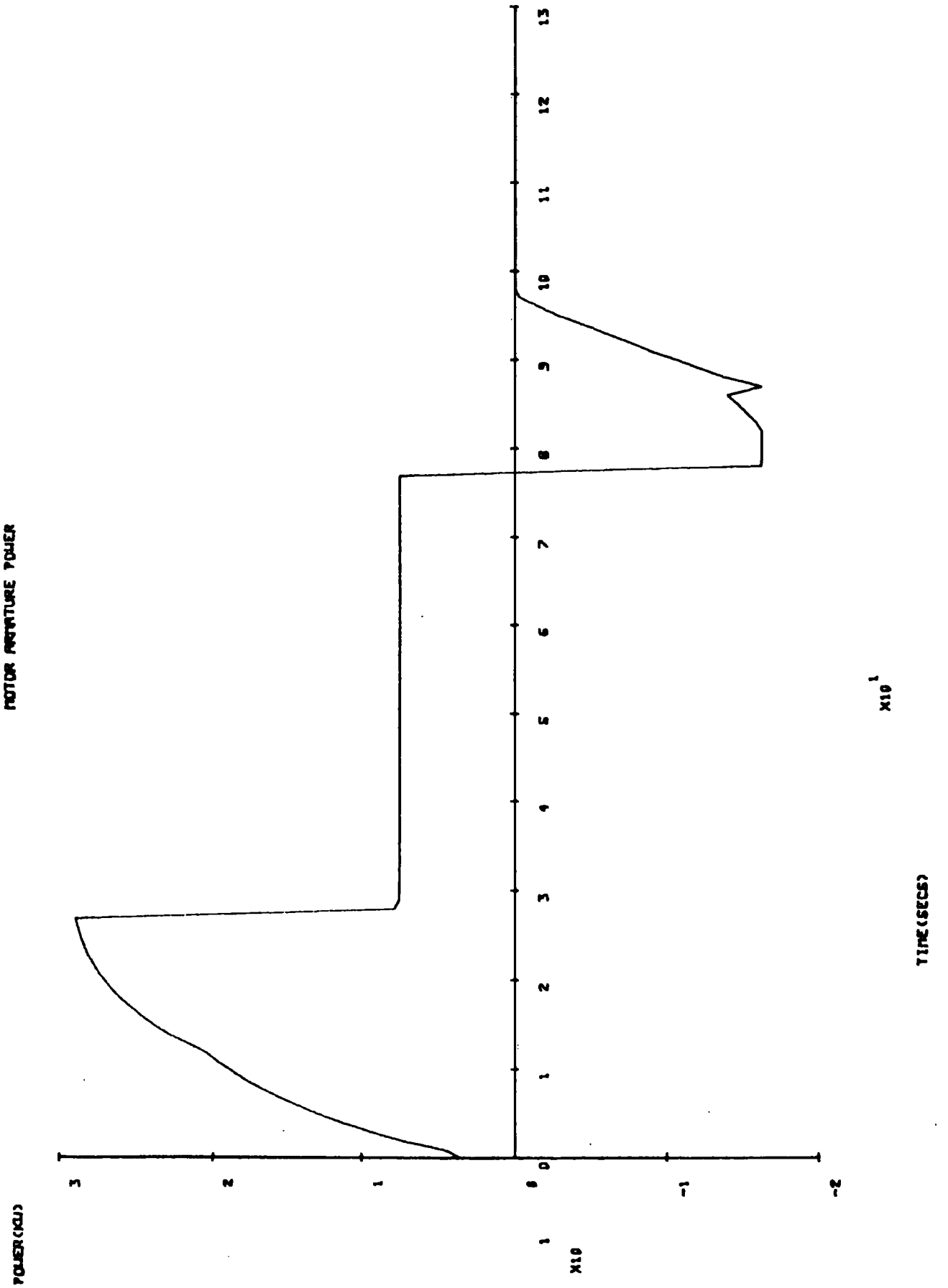

FIGURE 3.14: JANUS - Battery Current/time Profiles for the ETV-1 over the J227aD

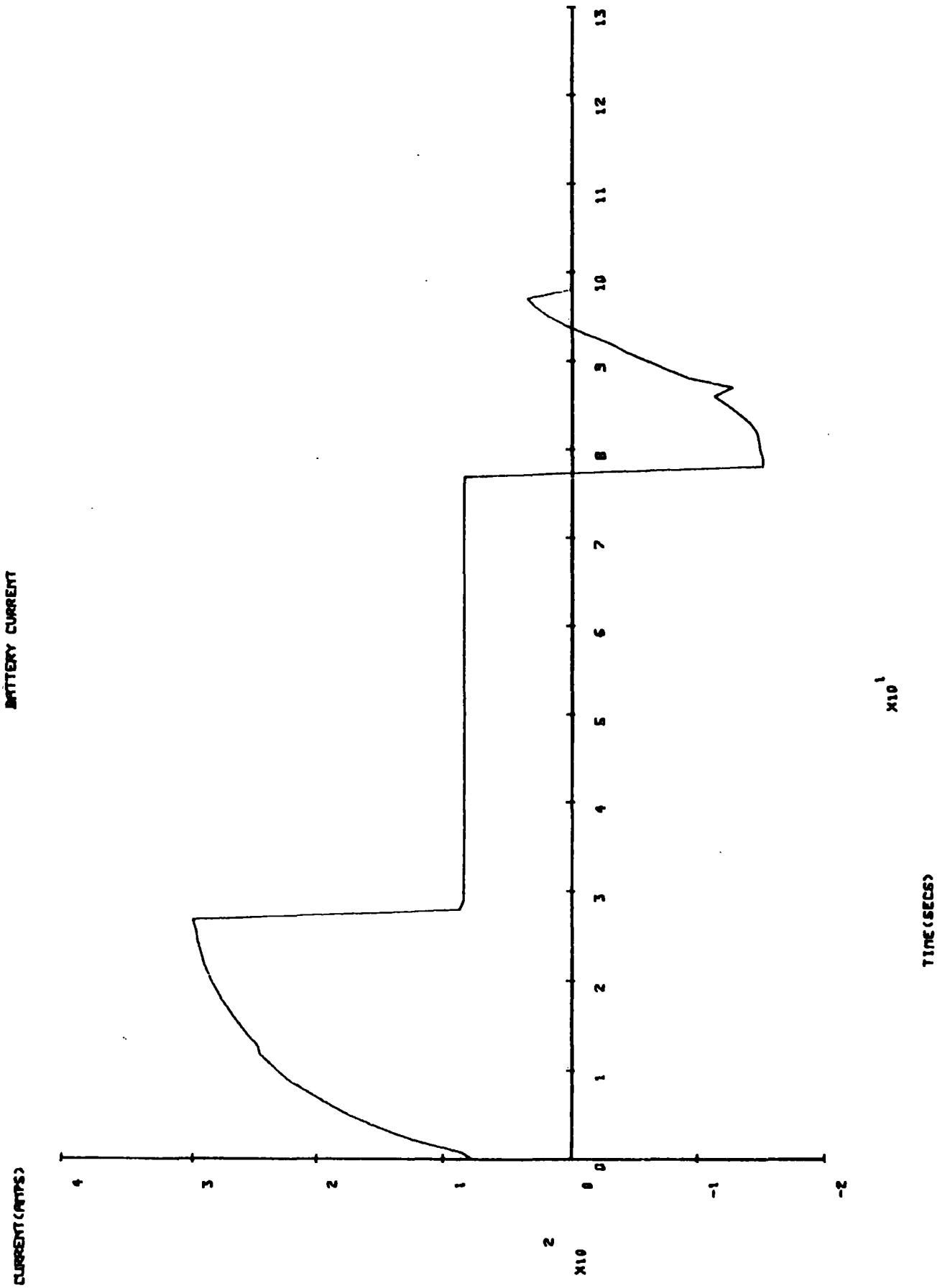

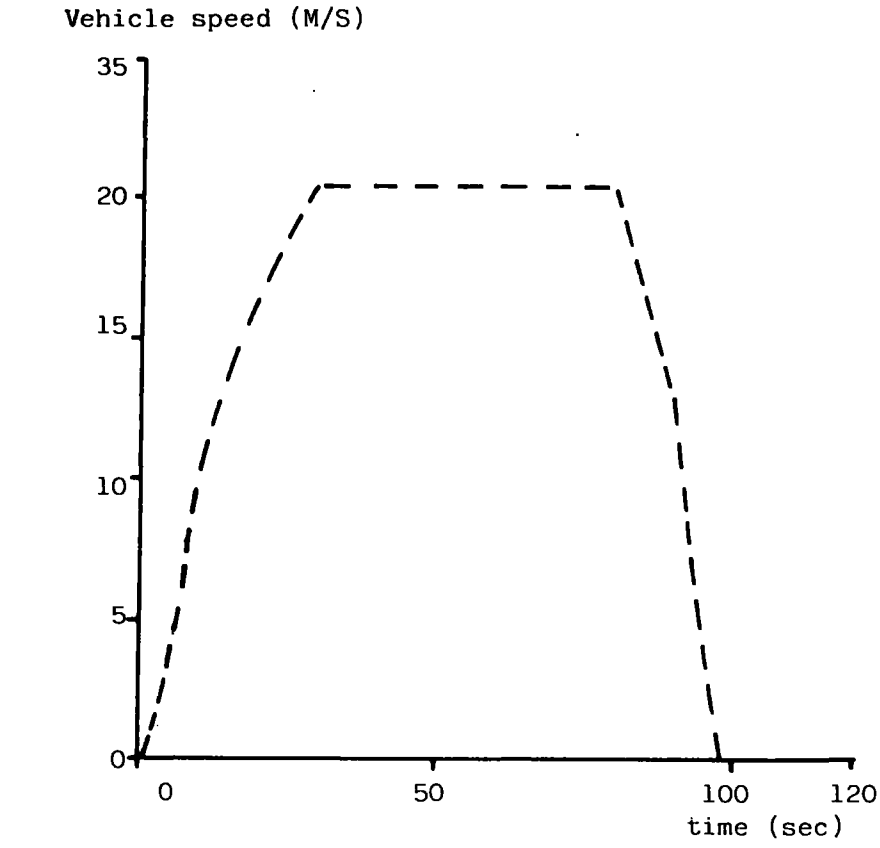

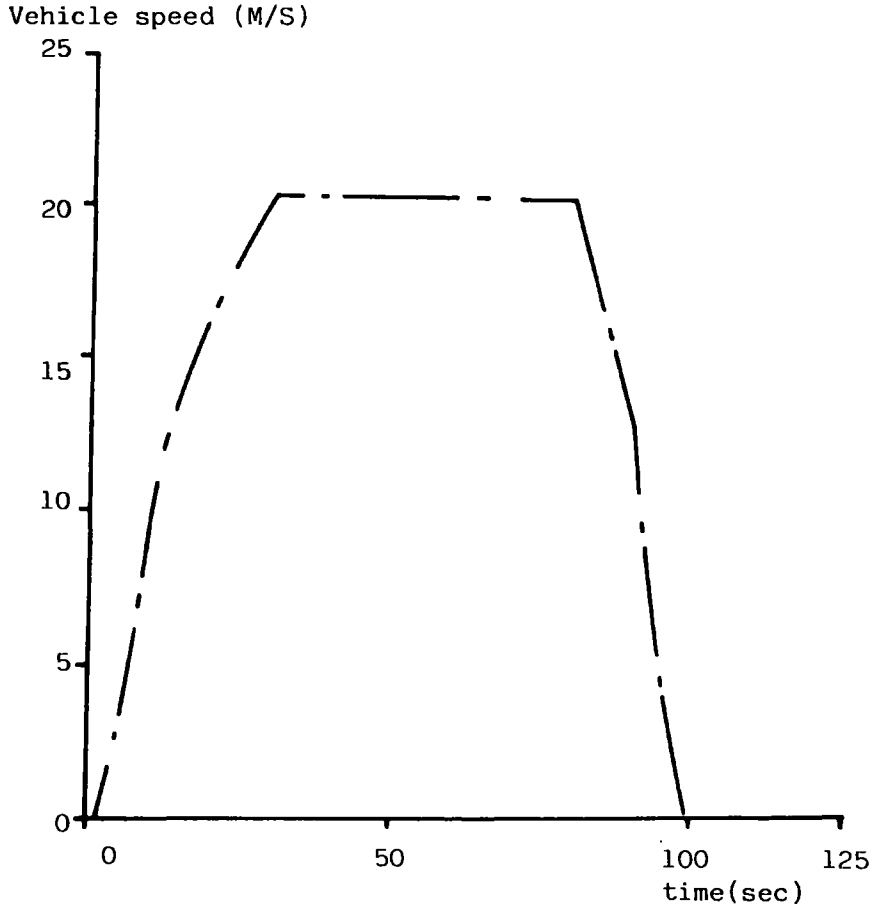

FIGURE 3.15: HEAVY and JPL graphical Representation of the J227aD cycle

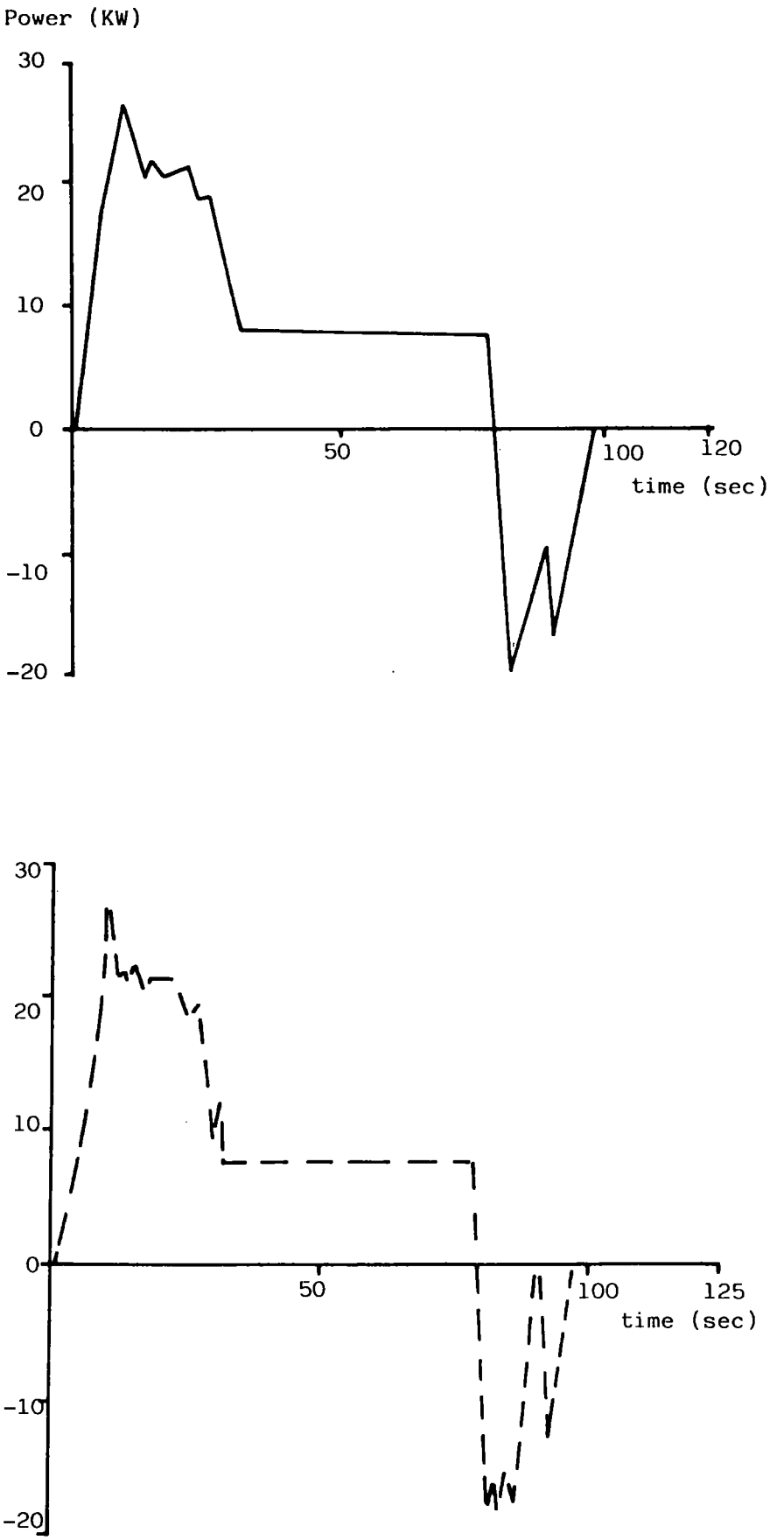

FIGURE 3.16: HEAVY and JPL graphical Representation of motor power/time profiles

TABLE 3.1: Metro' 1275 - Comparison of vehicle data

	Simulated	Official
Vehicle weight (Kg)	910	910
Drag coefficient	0.4	0.4
Frontal Area (m^2)	1.73	1.73
Coefficient of Rolling Resistance	0.010	NA
Wheel Radius (m)	0.25	0.25
Wheel Inertia as Effective Weight(Kg)	20	NA
Final Drive Type	Spur Gear	Spur Gear
Ratio	3.44:1	3.44:1
Gearbox Type	Manual	Manual
Ratios 1st	3.65:1	3.65:1
2nd	2.19:1	2.19:1
3rd	1.43:1	1.43:1
4th	1.00:1	1.00:1
5th	-	-
Engine Type	A-1275	A-1275
Engine Capacity (cc)	1275	1275
Compression Ratio	9.4:1	9.4.:1
Max Power (KW)	40	45
Max Speed (rpm)	5000	5650
Idle Fuel Cons (gm/s)	0.175	NA
Inertia (Kgm^2)	0.10	NA

TABLE 3.2: Princess 2227 - Comparaison of Vehicle Data

	Simulated	Official
Vehicle Weight (Kg)	1360	1360
Drag Coefficient	0.455	0.455
Frontal Area (m^2)	1.93	1.93
Coefficient of Rolling Resistance	0.010	NA
Wheel Radius (m)	0.32	0.32
Inertia as Effective Weight (Kg)	28	NA
Final Drive Type	Spur Gear	Spur Gear
Ratio	3.72:1	3.72:1
Gearbox Type	Manual	Manual
Ratios 1st	3.29:1	3.29:1
2nd	2.06:1	2.06:1
3rd	1.38:1	1.38:1
4th	1.00:1	1.00:1
5th	-	-
Engine Type	E-2227	E-2227
Engine Capacity (cc)	2227	2227
Compression Ratio	9.0:1	9.0:1
Max.Power (KW)	83(75)	83
Max.Speed (rem)	5250(5000)	5250
Idle Fuel cons. (gm/s)	0.25	NA
Inertia (Kgm^2)	0.20	NA

TABLE 3.3: Other ICE Vehicle Data

	Mini 1000	Metro 1000	Allegro 1000	Allegro 1275	Allegro 1748	Maxi 1748	Princess 1700	Princess 2000	Ital 1275	Ital 1700
Vehicle Weight (Kg)	680	910	910	910	910	1130	1360	1360	1130	1130
Drag Coefficient	0.54	0.4	0.45	0.45	0.45	0.48	0.4555	0.4555	0.46	0.46
Frontal Area (m^2)	1.55	1.73	1.8	1.8	1.8	1.93	1.93	1.93	1.98	1.98
Coefficient of Rolling Resistance	0.01	0.01	0.01	0.01	0.01	0.01	0.01	0.01	0.01	0.01
Wheel Radius (m)	0.23	0.25	0.27	0.27	0.27	0.32	0.32	0.32	0.27	0.27
Wheel Inertia (Kg)	15	20	20	20	20	25	28	28	25	25
Final Drive Type	Spur	Spur	Spur	Spur	Spur	Spur	Spur	Spur	Bevel	Bevel
Ratio	3.44:1	3.65:1	4.33:1	3.44:1	3.65:1	3.65:1	3.72:1	3.72:1	3.89:1	3.65:1
Gearbox Type	man.	man.	man.	man.	man.	man.	man.	man.	man.	man.
Ratios 1st	3.53:1	3.65:1	3.65:1	3.65:1	3.20:1	3.29:1	3.29:1	3.29:1	3.41:1	3.11:1
2nd	2.22:1	2.19:1	2.19:1	2.19:1	2.00:1	1.06:1	2.06:1	2.06:1	1.93:1	1.45:1
3rd	1.44:1	1.43:1	1.43:1	1.43:1	1.37:1	1.37:1	1.38:1	1.38:1	1.43:1	1.31:1
4th	1.00:1	1.00:1	1.00:1	1.00:1	1.00:1	1.00:1	1.00:1	1.00:1	1.00:1	1.00:1
5th	-	-	-	-	-	0.87:1	-	-	-	-
Engine Type	A1000	A1000	A1000	A1275	E1748	E1748	B1800	B1800	A1275	B1800
Capacity (cc)	1000	1000	1000	1275	1748	1748	1700	2000	1275	1700
Compression ratio	8.5:1	9.5:1	9.5:1	9.4:1	9.5:1	9.5:1	9.0:1	9.0:1	9.4:1	9.0:1
Max.power (KW)	30	33	33	45	67	67	65	70	45	58
Max.speed (rpm)	4750	5250	5250	5000	5500	5250	5800	4900	5300	5150
Idle Fuel Cons. (gm/s)	0.17	0.17	0.17	0.18	0.23	0.23	0.23	0.23	0.18	0.21
Inertia (Kg m^2)	0.1	0.1	0.1	0.1	0.15	0.15	0.15	0.2	0.1	0.15

TABLE 3.4: MPG Results for Vehicles with Complete Data

	Simulated				Official		
Vehicle	ECE-15	56 mph	75 mph		ECE-15	56 mph	75 mph
Metro 1275	35.6	52.2	38.4		32.8	51.2	37.9
Princess 2227	21.8	36.0	27.7		22.1	34.0	27.0

TABE 3.5: MPG Results for vehicles with Approximated Engine Maps

	Simulated				Official		
Vehicle	ECE-15	56 mph	75 mph		ECE-15	56 mph	75 mph
Metro 1000	36.4	52.0	36.8		38.4	53.1	38.5
Princess 1700	28.1	41.8	30.9		29.7	38.2	28.4
Princess 2000	25.6	35.5	26.7		27.2	37.7	27.7

TABLE 3.6: MPG Results for vehicles with Approximated Aerodynamic Data

	Simulated				Official		
Vehicle	ECE-15	56 mph	75 mph		ECE-15	56 mph	75 mph
Allegro 1275	34.7	48.7	35.4		31.6	46.3	33.7
Allegro 1748	29.4	40.2	30.9		26.1	43.6	33.3
Maxi 1748	29.0	44.9	29.0		25.6	40.0	29.3
Ital 1275	32.2	42.3	30.6		30.4	45.0	34.0

TABLE 3.7: MPG Results for vehicles with both approximated ICE and Aerodynamic Data

	Simulated				Official		
Vehicle	ECE-15	56 mph	75 mph		ECE-15	56 mph	75 mph
Mini 1000	37.6	46.9	27.8		38.3	48.5	33.0
Allegro 1000	34.6	45.2	32.1		34.5	45.7	33.2
Ital 1700	29.8	36.0	26.6		30.0	40.1	28.1

TABLE 3.8: The Effect of Rotational Inertia

	Driving Cycle with Inertia				Driving Cycle without Inertia		
Vehicle	ECE-15	SAE MET	SAE URB		ECE-15	SAE MET	SAE URB
Metro 1275	35.6	49.7	41.4		36.0	50.2	41.9
Princess 2227	21.8	31.9	24.0		22.0	32.2	24.3

TABLE 3.9: ETV-1-Comparison of Vehicle Data

	JPL	ELVEC	JANUS
Vehicle Weight (Kg)	1795	1795	1795
Drag Coefficient	0.32	0.32	0.32
Frontal Area (m^2)	1.875	1.875	1.875
Coeff. of Rolling Resistance	0.01	see note	0.01*
Wheel Radius (m)	0.28	0.28	0.28
Transmission Ratio	5.68:1	5.68:1	5.68:1
Max Motor Power (KW)	30	30	30
Max Motor Speed (rpm)	5000	5000	5000
Motor Voltage (v)	96	96	96
Controller Type	SCR	SCR	SCR
Battery Type	lead-acid	lead-acid	lead-acid
Battery Weight (Kg)	495	495	495

Note: The ELVEC Simulation uses a dynamic rolling resistance model that is a function of vehicle speed

* As well as enabling a constant value to be input, the JANUS model is also dynamic

TABLE 3.10: ELVEC/JANUS Comparison over the J227aD for the ETV-1

Source	Range (miles) 100% DOD	95% DOD	80% DOD	Sp. Road Energy (Whr/mile)	Trans Eff (%)	Motor Eff (%)	Contr Eff (%)	Sp. Energy at Battery (Whr/mile)	Road Energy (motoring Whr/mile) Drag	Roll	Accel.
JANUS	40.7	38.7	32.6	239.1	96.0	84.1	98.6	299.9	50.9	82.0	104.3
ELVEC	41.4	NA	NA	232.4	96.0	84.4	99.1	289.6	48.3	80.0	104.1

TABLE 3.11: ELVEC/JANUS comparison at 40 mph up a gradient and against a headwind for the ETV-1

Source	Range (miles)			Sp. Road Energy (Whr/mile)	Trans Eff (%)	Motor Eff (%)	Contr Eff (%)	Sp. Energy at Battery (Whr/mile)	Road Energy (motoring - Whr/mile)		
	100% DOD	95% DOD	80% DOD						Drag	Roll	Gradient
JANUS	25.3	24.0	20.2	399.7	96.0	89.5	94.5	465.8	130.3	112.2	157.2
ELVEC	26.2	NA	NA	380.3	96.0	89.1	100.0	444.8	127.3	96.0	157.0

CHAPTER 4

Electric Vehicle Study

4.1 Introduction

Present day electric vehicle technology is firmly based on experience with the D.C. Series field wound traction motor in a direct-drive arrangement and using the lead-acid traction battery as the energy storage medium. However, due to the potential for both improved controller efficiency and simplified regenerative braking, the near-term electric vehicle, such as the G.E. ETV-1 (Wilson,1981), employs the D.C.Shunt field wound (or separately excited) traction motor, but still favouring (with few exceptions) a direct-drive arrangement and a lead-acid battery as the energy storage device (Collie ,1979) (Gates et al.,1973).

Using the road-vehicle computer simulation program developed at the University of Durham (described in chapter 2), it is possible to study with comparative ease, the impact of different drive-train arrangements, different traction motor types, different battery types and also battery size on vehicle performance and range.

In making a valid and clear assessment of the aforementioned vehicle parameter variables, it was decided to select a single vehicle type or class that would realistically lend itself to an electric vehicle application, upon which to base the study.

Because of the inherent range limitation imposed on the electric vehicle by the nature of its energy storage medium (not easily or quickly replenished and having load dependent characteristics), a vehicle with a well defined daily usage (and hence range) was preferable.

This specification required the vehicle to have an urban duty cycle and a daily range requirement within the capabilities of current and near-term electric drive-trains. Three vehicle classes satisfy these requirements: the commuter car (or small passenger car), the small sized delivery vehicle, the medium sized delivery vehicle and the city bus.

The city bus can be dismissed as a possible electric vehicle application, since, despite having a well defined duty cycle it can cover ranges from 50-100 miles per day (Hagen,1974) (West Yorkshire P.T.E.1981) (Gurley,1977)- depending upon whether in rural, suburban or urban service. Thus, for an electric drive-train to meet these requirements would result in either a prohibitively large battery (necessitating a reduction in payload) or some means of battery exchange - as was discussed in chapter 1.

The small delivery vehicle (usually a van) does not lend itself to electric vehicle application easily either, as the 'bulk' associated with the traction battery will tend to be difficult to install, when compared with a large vehicle, and may result in a significant reduction in payload capacity.

Therefore the most likely applications of the electric vehicle at present appear to be the small or commuter car and the medium sized delivery vehicle or van. Both have very similar range requirements in that 95% of all journeys are under 50 miles (Bumby et al.,1982). However, despite considerable interest in the commuter car appliction, as with the small delivery van, battery displacement is not as easily achieved as in a larger vehicle. In addition the 5% of remaining journeys may be accounted for vary differently for both vehicles, in that for the passenger car they will cover journeys of greater than 50 miles, whereas for the medium sized delivery van, because an individual operator may have a fixed usage pattern, the 5% may refer to operators who daily travel greater than 50 miles. Therefore the delivery van may satisfy 95% of all users.

Thus, for the reasons just decribed plus the fact that the deterioration in acceleration performance inherent for the electric vehicle (due to the increased weight and the load-sensitive battery characteristics) will be probably be more acceptable (and may even be

unnoticed) in the delivery vehicle market, that it was decided to concentrate on this vehicle.

The medium sized delivery vehicle is of a size to make penetration by electric vehicle types a commercially viable proposition - to both manufacturers and purchasers - as is already being shown by manufacturers such as B.L. with the 'Sherpa' and General Motors (Bedford) with the 'C.F'. However, oil saving and displacement incentives in this area of the road-transport sector are modest - being about 11% of the total (House of Lords,1980). But in the U.K. and Europe most electric vehicle applications in the medium sized delivery vehicle market have offered significant benefits to the potential user of ease of driving, cheaper fuel costs (but with similar running costs overall), a longer vehicle life cycle and no emissions when compared to the i.c. engine powered alternatives. By demonstrating lower running costs to offset the higher capital costs the electric vehicle can make gradual inroads into other sectors of the road transport market (House of Lords,1980), as the buying public will come to accept it as an alternative should the need to move from the i.c. engined vehicle arise in the longer term as oil becomes scarce and more expensive.

Although it has been demonstrated that 'primary' energy savings will probably not be possible for an electric vehicle when compared with an i.c. engined vehicle if gasoline is derived from petroleum, should in the long-term gasoline be produced from coal with an inherently lower conversion efficiency (50-60% as opposed to 85-90%) then primary energy savings will be possible with an electric vehicle (House of Lords,1980) (IRD,1982).

4.2 Vehicle Parameters

The vehicle parameters chosen for the medium sized delivery vehicle are shown in table 4.1 and are thought to be fairly representative of present day designs.

Drag and rolling resistance coefficients were chosen to be typical of present day and near-term delivery vans. Frontal area and wheel radius are parameters that are esentially fixed for a vehicle type and size, so were chosen on the basis of present day designs. As was the basic bodyshell weight - the vehicle kerb weight minus the power train weight (Ford Motor Co.UK) (Bedford)(B.L.).

The aforementioned vehicle parametes from the common base from which the various electric vehicle alternatives to be studied here can be assembled, and any weight differences automatically accounted for.

As was mentioned in section 4.1, it is proposed to study the effects of drive-train configuration, motor type, battery type and battery weight. Except for the consideration of a possible method of motor control using a combination of battery switching and a CVT (see chapter 2) it is proposed to keep the motor controller type fixed and assume the D.C.Chopper type. Other possible alternatives such as battery switching alone and variable resitance have not found wide acceptance in the past because of inherent problems when compared to the chopper (i.e., the resistance type gives poor efficiency, and the battery switching method, because it does not provide a smooth voltage control, leads to driveability problems).

Throughout the study any changes to vehicle weight are to be accompanied by changes to the installed power (here the motor power rating) in order to maintain the traffic compatible acceleration and maximum speed acceptable for this class of vehicle (0-30 mph in 10-15 seconds and 50 mph maximum speed) under fully laden conditions.

Final drive ratio for the direct drive arrangements was selected to give the maximum vehicle speed required, whilst still giving acceptable acceleration performance. For the drive arrangements using variable ratio transmissions, however, final drive ratio need not be fixed. As it forms

one component of the overall transmission ratio, and because it is the overall ratio that is the important parameter, then by fixing the final drive ratio and wheel radius, the effects of overall transmission ratio can be studied using the variable ratio unit.

Unlike the i.c. engine, the traction motor does not require the same minimum ratio span from a variable ratio transmission as the motor operates down to zero speed - hence direct drive arrangements are possible using electric traction. But the effects of 2,3 and 4 speed discrete ratio transmissions and a continuously variable transmission can also be studied. For the discrete ratio cases the ratio spans (largest ratio divided by the smallest ratio) can be arranged to either increase or to decrease the overall transmission ratio using the direct drive arrangement as a datum. As far as the CVT is concerned, the unit considered here operates over a large ratio span already (10:1) so the latter consideration was thought unnecessary.

Variable ratio gear shifting for both discrete ratio and CVT cases was initially according to the optimum control algorithm described in chapter 2 when applied to a single control variable (here transmission ratio). The flow chart for the modified algorithm is shown in Figure 4.1.

Vehicle ranges are assessed over typical urban driving conditions for such a vehicle type as represented by the J227aC urban cycle - shown in Figure 4.2. - (Wilson et al.,1982) and for two cruising regimes - at 30 mph and 40 mph. The fractional discharge battery model is to be used and all vehicle ranges are quoted to 100% battery depth of discharge. Furthermore, except for a discussion of vehicle braking in section 4.7, full regenerative braking is assumed in all cases with an 'ideal' vehicle braking philosophy - as introduced and described in chapter 2.

4.3 Effect of Traction Motor Type

The effect of traction motor type must be viewed relative to the currently favoured traction motor units - namely the D.C. Series and the D.C.Shunt field wound motors.

Alternative traction motor types can be catagorised into D.C. types and A.C. types, all of which offer simplification of rotor construction with the removal of the mechanical commutator required for the series and shunt machines.

In several cases the removal of the armature windings is also possible, but with the requirement of more complex and costly control electronics. Of the D.C. alternatives, two types are evident from the published sources available: the electronically commutated versions of the series and shunt machines and the switched reluctance machine.

Both D.C. alternatives are not recent ideas but have only been considered as traction alternatives with the developments in microprocessor control and power electronics (La France et al.,1973) (Fulton,et al.,1984), and have in common the requirement of rotor position feedback. Of the two, the switched reluctance type appears to be in a much more advanced state of development for automotive applications.

The A.C. alternatives are the synchronous and the induction machines, both of which require roughly the same degree of complexity in terms of control electronics - namely the requirement of converting from D.C. to A.C. during motoring and from A.C. to D.C. during regeneration. The induction machine however has the advantage of employing the extremely simple 'squirrel cage' rotor construction and as a result has received the most attention (Wilson et al.,1982) (Murphy,1972)(Berman et al.,1972).

Therefore of the alternatives described it is proposed to consider the most attractive D.C. and A.C. types - the switched reluctance machine and the induction machine - using efficiency data for present day versions of these machines.

Although at present the D.C. Series and D.C. shunt machines are finding equal favour, because of the potential for both increased motor controller efficiency and simplification of regeneration, it seems likely that the D.C. shunt type will prevail in the near-term - as has been demonstrated with the G.E. ETV-1. Therefore it is also proposed to include these motor types in the study.

The base line for comparison will be the DC series machine, shown in Figure 4.3, and in all cases the drive-train configuration will be fixed as a direct drive arrangement with a lead-acid traction battery.

The three motor maps to be compared with the base-line (DC shunt, AC induction and DC switched reluctance) were given in Figures 2.13, 2.19 and 2.20 and the fixed drive-train configuration is shown in Figure 4.4.

4.3.1 Discussion

The results for the four traction motor types considered are presented in table 4.2. When comparing a well developed version of the D.C. series motor - shown in Figure 4.3 (Lucas Chloride) - with a well developed version of the D.C. shunt motor - shown in Figure 2.13 (Wilson et al.,1982) - no significant benefit over the urban cycle is apparent for the shunt motor both in terms of motor efficiency and vehicle range. Furthermore for a direct drive shunt motor arrangement the benefits of simplified regenerative field control cannot be realised as the majority of regeneration occurs over a motor speed range corresponding to armature chopper control. Deceleration from 30 mph to rest corresponds to a motor speed range of 3000 rpm to zero, and since the armature control region extends from zero to 2400 rpm (as shown in Figure 2.13), therefore 80% of regenerative braking will be through armature control. Thus armature control electronics will be required to the same extent as for the series machine.

Table 4.2 does show the shunt machine to give an improvement over the series machine for both cruise regimes. This can be explained by the fact that the efficiency contours between 3000 and 4000 rpm at part load (corresponding to the two cruising speeds) are wider apart for the shunt machine when compared to the series machine (Figures 4.3 and 2.13), so making motor efficiency less load-sensitive. Table 4.2 shows the shunt motor to have only slightly higher motor efficiency at cruise, but there will also be a knock-on effect in the traction battery due to the corresponding smaller currents being drawn.

There is a practical benefit from moving from the D.C. series to the D.C. shunt machine in that for the shunt machine there is no requirement for heavy duty switching contactors in order to reverse the field to achieve reverse rotation as the field is independent of the armature and generally only draws a current that is an order of magnitude lower than the armature current.

Results for both advanced or alternative motor types given in table 4.2. show significant improvements for the urban cycle over the series and shunt machines. The corresponding maps shown in Figures 2.19 and 2.20 are for motor and controller combined and give efficiency values comparable to the series and shunt machines without the inclusion of their controllers. Therefore the benefit of the A.C. induction and D.C. switched reluctance machines is due to higher motor/controller efficiency at the moderately high loads experienced over this urban cycle.

Of particular interest is the map for the typical A.C. induction motor, given in Figure 2.20 which shows the maximum efficiency occurring over a much higher speed range than for the D.C. machines (>4000 rpm compared to 2000-3000 rpm) and also in that the efficiency contours remain comparatively 'flat' over a wide speed and load range. The switched reluctance motor map, however, shows a very similar pattern to that of the

D.C. series machine - having load-sensitive (closely spaced and horizontal) efficiency contours between 2000 and 4000 rpm - but with the aforementioned higher efficiency values.

The results for the two advanced motor types at cruise, therefore show only the A.C. induction type to have any significant benefit due to the aforementioned map characteristics, and the D.C.switched reluctance giving similar ranges to that of the series machine.

4.4 Alternative Drive Train Configurations

As far as an electric vehicle drive-train is concerned drive-train configuration options are very limited in that there is only one alternative to the 'traditional' direct drive in that the traction motor can also drive through a variable ratio transmission - Figure 4.5.

The variable ratio transmission can be of the discrete ratio type or the CVT type. Other mechanical motor control devices such as slipping friction clutches and torque converters - as suggested by other sources (Altendorf 1979)(Samuel 1974)(Ratclif 1976)(Bader 1977)(Klink,1984) - are all similar to the discrete ratio and CVT transmissions in that they are intended to remove (to varying degrees) the need for electronic motor control, but because of their smooth characteristics can be discussed under the broader heading of the CVT.

Section 4.2 discussed how for 2,3 and 4 speed discrete ratio transmission, comparison can be made by adjusting the variable ratio transmission ratio span to increase or reduce the overall transmission ratio from the direct drive datum, but for the CVT, because the unit considered here (the Perbury type (Stubbs,1981)) has inherently a wide ratio span - ranging from a large starting ratio to a 'deep' overdrive ratio - there is no need for this consideration.

A single traction motor type is to be considered throughout this section of the study - the D.C. shunt type and the basis for comparison will be the D.C. shunt motor in a direct drive arrangement - as shown in Figure 4.4, and results in table 4.2.

4.4.1 Discussion of Results Using Optimum Control

Using the optimum control strategy when applied to the electric vehicle with a variable ratio transmission, introduced in section 4.2, results for both the discrete ratio transmission options and the continuously variable transmission can be compared with the direct-drive base configuration.

4.4.1.1 Discrete Ratio Transmission

Table 4.3. shows the urban and cruise results for the 2,3 and 4 speed discrete ratio transmissions for ratio spans increasing and decreasing the overall transmission ratio relative to the direct drive datum (cases i) and ii) respectively - the ratios of which are given in table 4.1). Over the urban cycle for 2, 3 and 4 speed cases the ratio spans that increase the overall transmission ratio give improved ranges because transmission ratios that enable the motor to operate at a high speed (hence high efficiency) for a greater proportion of the cycle are now available. The ratio spans that decrease the overall transmission ratio show lower ranges compared to the base line because although motor efficiency does not change, transmission efficiency is lower.

At cruise for 2, 3 and 4 speed cases there is no difference in motor efficiency for the two ratio span options because the datum overall transmission ratio is giving the best overall result. But again, due to the reduced transmission efficiency, ranges compared to the baseline (datum) are reduced.

Overall, for the urban cycle case, the 3 and 4 speed units show the highest ranges due to the larger transmission ratios being made available as the number of ratios increases. Since, however, the 4-speed case shows no noticeable improvement over the 3-speed case, indicates that an optimum at the 3-speed case, or corresponding to a maximum ratio in between the 2.0:1 maximum for the 3-speed and the 2.5:1 maximum for the 4-speed case, has occurred. The coarse steps between ratios (0.5:1) are purely intended to indicate any trends and although it is quite possible to determine the optimum number of ratios and ratio span, this would be a final design exercise and is not the purpose of this study.

Despite yielding reduced range relative to the baseline vehicle over urban and at cruise conditions, the ratio span that decreases the overall transmission ratio relative to the datum does, however, have the advantage over, not only the baseline case, but also the ratio spans that increase the overall transmission ratio, in that maximum vehicle speed may be increased - having been limited in the base configuration by the final drive ratio. However, for an urban delivery vehicle the 50 mph limit already imposed by the final drive ratio in the baseline case may be quite adequate.

As well as improving motor efficiency, which, as table 4.3 shows is clearly not being erroded by the reduced transmission efficiency and increased vehicle weight, the discrete ratio transmission with the ratio span arranged to increase the overall ratio has a further advantage. For a given motor power, initial vehicle acceleration will be increased (Gates et al.,1973). Therefore, as table 4.4 shows, the motor power rating can be reduced to enable the constant performance constraint to be met. Table 4.5 now shows, again for the 2, 3 and 4-speed transmissions, how by reducing motor size in this manner, motor efficiency rises due to the increased load factor, resulting in range increases - particularly at cruise where the load-factor is inherently low.

4.4.1.2 CVT

Table 4.5 shows for the single CVT considered here - having a large ratio span that both increases and decreases the overall transmission ratio relative to the baseline datum - results for the urban cycle and for the two cruise regimes. The urban cycle result shows no improvement over the baseline case for the CVT because the gain in motor efficiency achieved by the wide and infinite spread of ratios, is erroded by poor transmission efficiency inherent in current CVT designs. For the two cruise cases, the same picture is echoed.

As with the discrete ratio transmission, because of the improvements in initial vehicle acceleration due to the increased overall transmission ratios available, motor size can also be reduced relative to the baseline case to achieve the constant performance constraint, and, as table 4.7 shows, so enabling improvements to be made over the baseline case for the urban cycle, but still showing a range shortfall at cruise.

4.4.1.3 CVT Allied to Battery Switching Motor Control

If a CVT is used in conjunction with battery switching as a means of control, one important benefit is apparent for a vehicle powered by either a D.C. series or D.C. shunt motor. The power electronics required for motor armature control can be eliminated (Mangan et al.,1974) so making the drive-train cheaper, more reliable and more efficient.

The familiar 'jerks' associated with battery switching can be 'smoothed' by suitable control of the transmission, possibly to the point of requiring only one switch (i.e., full battery voltage applied).

For a vehicle powered by a series motor, the armature electronics could be eliminated for 'motoring' but for regeneration, in order to

achieve a comparable urban range, electronic control would still be required. In the case of the shunt motor, the armature electronics could be eliminated for both motoring and regenerating as, by suitable control of the transmission ratio regenerative braking can be achieved by using field control only.

In the case of the shunt motor, the number of battery switches will be limited in practice as the lowest armature voltage step must be equal to or greater than the maximum field voltage. Thus, for a small first voltage step resulting from a large number of switches, maximum field voltage may be small, and for a given field power requirement, maximum field current may then be large - so requiring the need for power electronics in the field controller now. A maximum of about three switching steps appears to be the limit before the field current starts to become prohibitively large.

4.4.1.3.1 Optimum Control Plus Battery Switching

When the optimum control algorithm is used in conjunction with battery switching, the optimum CVT ratio is only searched for in the motor operating region above the break speed. In other words when all of the allotted battery switching steps have been completed. The CVT ratio below the break speed is fixed at each battery switch, due to the motor speed corresponding to that switch voltage and the road speed, if no 'jerking' is to occur.

The results for this particular case of motor control are shown in table 4.8 for 1, 2 and 3 battery switches, again over the urban and the two cruise regimes. Because the switching process occurs in a region on the motor map of comparatively low efficiency, the control strategies with the least number of switches will move the operating point quickly through this region and into the region of high efficiency above the break speed and yield the highest average motor efficiences.

Table 4.8 shows that the best results are achieved with 1 and 2 switching steps and case having 3 switches gives no improveent over the CVT employing armature control electronics. The fact that the 2 switch case gives the same result as the 1 switch case will yield a practical benefit in that because the 1 switch case may result in large and impractical CVT ratios being demanded for long periods during urban duty, the 2 switch case can be adopted wth no penalty noticeable as far as vehicle range is concerned.

4.4.2 Discussion of Results Using Implementable Control

The comparisons of section 4.4.1 were performed using the optimum control for transmission ratio selection. In practice the optimum control algorithm would be difficult to implement, so therefore for both discrete ratio and CVT transmissions an implementable or sub-optimum strategy was required to represent what would likely be achieved in practice.

4.4.2.1 Discrete Ratio Transmission

By looking at the motor performance map usage data when the optimum control strategy was used - shown in Figures 4.9 and 4.10 - it is apparent that the majority of usage points congregate in a region close to the maximum efficiency during motoring and regeneration.

For the discrete ratio transmission, therefore a sub-optimum control strategy may take the form of a predefined operating region on the motor map-as dictated by high motor efficiency - into which a selected gear ratio must put the vehicle operating condition (at the transmission output). If more than one ratio satisfies this criteria, then the region may be shrunk towards the point of maximum efficiency and the process repeated. For the case when no ratios place the operating point inside the box then a ratio

that places the operating point closest to the break speed is selected. Figure 2.57 shows the algorithm flow chart and Figure 2.56, a schematic of the operating box. Figure 4.6 shows the box selected for the study. A full description of the sub-optimum control algorithm applied to an electric vehicle was given in chapter 2.

The results for this control strategy when applied to the 3-speed transmission are shown in table 4.9 and the corresponding motor map usage points for the urban cycle in Figures 4.15 and 4.16. As table 4.9 indicates, the strategy gives a reasonable approximation to the optimum results over the urban cycle (giving a discrepancy on range of less than 10%) and for the cruise cases sub-optimum results are identical optimum results since to select the correct ratio from 3 for one operation point in each case is relatively straight forward to achieve. The usage data in Figures 4.15 and 4.16 also shows close agreement to the optimum usage data of Figures 4.9 and 4.10.

4.4.2.2 CVT

In a similar fashion to the discrete ratio tansmission, by looking at the urban cycle usage data produced by the optimum control strategy when using a CVT it will be possible to devise a sub-optimum control regime. Figures 4.7 and 4.8 show that usage points congregate in the region of high efficiency with very few points occurring below the break speed for both motoring and regenerating. This implies that it would be possible to use the CVT plus battery switching control combination, as the armature control region seems to be virtually unused. Also, using a CVT, because of the infinite number of ratios, control above the break speed can be achieved more precisely by using a trajectory of optimum efficiency rather than a region of optimum efficiency that was necessary for the discrete ratio transmission.

The control devised for the combination of a CVT plus battery switching was described in chapter 2, but a brief resume will be covered here.

Above the break point there are 3 control options available:

i) following a locus of optimum efficiency;

ii) following the break speed line;

iii) lock up in a fixed ratio.

For the case of i), the operating locus would have to meet several requirements:

a) the locus must pass through the region of maximum efficiency;

b) maximum motor power/torque must be made available;

c) and avoiding the maximum motor speed region for low power demands to prevent high motor speeds and hence high transmission ratios for long periods.

When the optimum efficiency locii are superimposed upon the motor map - as has been shown for all of the motor maps presented so far - it is interesting to note that break-speed control strategy gives a reasonable approximation to the optimum efficiency locus whereas the option of locking the CVT into a fixed ratio gives no control over motor efficiency at all. The break-speed control alternative also has the added benefit of removing the need for field control electronics also as now full field and full armature voltage can be applied continuously.

The results forthe combination of CVT and battery switching are shown in table 4.10 and the corresponding urban cycle usage points in Figures 4.11 to 4.14. As with the optimum control case the effects of 1 and 3 voltage switches shows the latter case to give slightly lower range due to a proportion of time spent below the break point. Also, as would be expected, locus control shows a higher range than break-speed control, although not significantly higher. This is explained by the usage maps -showing the usage points for locus control to approximately follow the break speed.

When compared to the results using optimum control, agreement is of the same order as that obtained for the discrete ratio transmission over the urban cycle. Over the cruise cycles, the results although in quite close agreement are not identical to the optimum results because of constraints imposed by the sub-optimum break-speed line and optimum locus.

In practice the CVT transmission may be of the traction type described here (with a suitable mechanical starting device/clutch) (Stubbs, 1981) or may be a hydrodynamic device, such as a torque converter with variable stator vanes to extend the ratio range (Samuel 1974). If such a large ratio span was not required then a conventional torque coverter may suffice but careful matching of the converter and motor would be required (Ratcliff 1976) (Bader 1977)(Mangan, 1974)(Klink,1984).

4.5 The Effect of Battery Type

In considering the effect of battery type what is in fact being studied is the effect of changing the characteristics of currently used battery types.

In the area of automotive traction the most widely favoured battery type has been, and will also be in the near-term, the lead acid type. Despite its popularity, the lead-acid battery has load-dependent characteristics that limit the performance of current electric vehicles, in that the rate of extraction of the energy stored (power demand) affects the energy stored. This characteristic is shown in Figure 4.17 in terms of the power demanded per unit battery mass (power density) and the energy stored per unit battery mass (energy density). As well as the load-dependency of the lead-acid battery, there is also a restriction on the maximum energy storable per unit mass (maximum energy density) which is several orders of magnitude less ($\simeq$300) than for a liquid fuel such as gasoline or diesel.

Therefore in studying different battery types, the slope of the curves in Figure 4.17 plus the intercept with the x-axis are of equal importance.

Of the types currently under development that show improvements over the lead-acid battery in the areas discussed the sodium-sulphur, the lithium-iron the nickel-zinc and the nickel-iron types are consistently the focus of the most attention. The sodium-sulphur type, despite having received a considerable amount of development both in Europe and the USA, still has the problem of safely containing its electrolite (Collie,1979). The introduction of the Lithium-iron battery, on the other hand, depends upon the cost and availability of lithium in the future (Collie,1979).

Because the nickel-zinc and nickel-iron battery types do not at their present state of development face such fundamental stumbling blocks as do the sodium-sulphur and lithium-iron types, it is the purposes of this section to consider these two types only when comparing the lead-acid battery with advanced batteries.

The power density/energy density characteristics for both nickel-zinc (Ni/Zn) and nickel-iron (Ni/Fe) batteries are shown in Figure 4.17 along with the lead-acid battery. Not only do they exhibit a higher maximum energy density, but also have curves that show the energy density to have a reduced dependence on power density (more vertical slopes).

However, although the Ni/Fe battery offers greater cyclic life than the lead-acid battery (1500 cycles compared with 750-1000 for the lead-acid), the Ni/Zn battery has yet to be developed to exhibit an adequate cyclic life (currently 200-500 cycles)(Burris et al.,1978) (Kurtz et al.,1979)(Mietbrink et al.,1983).

In studying the effects of battery type here, the same baseline configuration used in sections 4.3 and 4.4 - namely the lead-acid battery/D.C. shunt motor/direct drive arrangement - is to be used here to form the basis of comparison.

The study can be divided into two parts: to study the effects of battery type on vehicle range for a fixed battery size and also to consider the effects of battery type on battery size for a fixed urban range.

4.5.1 Fixed Battery Weight-Discussion

For a fixed battery size/weight, table 4.11 shows for the urban and cruise cycles, the effect on battery type on vehicle range when compared to the lead-acid case. Because of the more favourable characteristics of the advanced batteries in terms of increased energy stored per unit mass plus reduced load dependency, range to battery discharge is significantly greater than the lead-acid case.

4.5.2 Fixed Vehicle Urban Range-Discussion

For an urban delivery vehicle such as is being considered here, it may be that the 50-60 miles range offered by the lead acid battery is all that is required by an operator, in which case it would be desirable to fix this range and consider the effect on battery size for the two advanced battery cases. Table 4.12 shows the effect of battery type on battery size, vehicle weight and the knock-on effect in to motor size (to achieve a constant peformance) for a fixed urban range, dictated by the lead-acid baseline, of about 50 miles.

With this range constraint battery and hence vehicle costs may be kept down.

It is interesting to note that the cruise range for the vehicles with the reduced size advanced batteries - shown in table 4.12 - is lower than for the lead-acid case because of the reduced amount of energy stored. This is because at cruise vehicle weight plays a much smaller part in the total vehicle's energy requirement than over an urban cycle. Thus, over

the urban cycle the reduction in stored energy is balanced by the reduced vehicle energy requirement due to weight reduction.

A vehicle could be designed to accommodate a variable battery size depending upon the duty cycle to be undertaken. For a long journey mostly at constant speed, a large battery would be included, whereas for urban duty the battery pack could be reduced. However, in order to match the voltage requirements of the traction motor, the battery would have to be assembled, in total, in 2 or more sections in parallel.

4.6 The Effect of Battery Weight

Although changing the battery weight in an electric vehicle will change the amount of energy stored within the vehicle, as has been indicated in section 4.5, the effects on vehicle range are more complex. As has been discussed in 4.5, the instantaneous energy stored per unit mass (energy density) is dependent upon the rate at which energy is withdrawn per unit mass (power density) and this will serve to not only complicate the picture for a given battery type, but because these characteristics vary from type to type (Figure 4.17), the picture may become more complex when considering the more advanced types of 4.5.

Throughout this section, as battery, and hence, vehicle weight is altered motor rating is also changed accordingly in order to maintain the constant performance base.

4.6.1 The Lead-Acid Battery-Discussion of Results

Because, as battery weight is increased, the effect is to always increase vehicle range, Figure 4.18 for the lead acid battery shows a plot of the range per unit battery weight (specific range) versus the battery weight as a fraction of the total vehicle weight (battery fraction). The curves for both the J227aC urban cycle and the 40 mph cruise show a maximum at 25-30% battery weight as a percentage of total vehicle weight.

The curves are essentially a measure of the 'effectiveness' of the battery (the range achieveable for a given battery mass) and in shape can be explained by considering the curves on both sides of the maximum. On the portion of the curves to the left of maximum the combination of reducing battery weight and moderate power demands results in increasing power density - as shown in Figure 4.18. The resulting decreasing energy density from Figure 4.17 is effectively decreasing range per battery mass. However, on the portion of the curves to the right of maximum Figure 4.18 shows the power density in each case to be decreasing due to increasing battery mass and still moderate power demands, so the battery characteristic is not an influencing factor. But as the battery weight becomes a larger proportion of total vehicle weight, more of the stored energy increment is being used to propel the battery weight increment - meaning that the increased energy stored is being gradually offset by increased weight - although zero range increase for a given battery weight increase will never result because a vehicle made up of 100% battery weight cannot be achieved, plus cycle energy demand does not depend totally on vehicle weight (implying vehicle drag and rolling losses of zero).

The optimum value of battery weight fraction shown in Figure 4.18 (0.25-0.30, for both urban and cruise conditions) corresponds with the values chosen by current electric vehicle manufacturers when using the lead-acid battery (Collie, 1979)(Lucas-Chloride).

4.6.2 Nickel-Zinc and Nickel-Iron Battery Types - Discussion of Results

In a similar fashion to the lead-acid battery just discussed, specific range/battery fraction curves for urban duty and at cruise can also be produced for different battery types, and those are shown in Figure 4.19 for the Ni/Zn battery and in 4.20 for the Ni/Fe battery.

Due to the steeper slopes of the power density/energy density curves in each case - shown in Figure 4.17 - the effect of increasing power density for decreasing battery weight (effectively battery weight fraction) occurs for much lower values of battery weight fraction in each case. The result is that although a maximum specific range still results, it is now shifted to the left, and is much further to the left for the Ni/Fe case because it has a more vertical slope on its characteristic. The maximum values now correspond to battery weight fractions of 0.1 - 0.15 for the Ni/Zn battery and 0.05-0.1 for the Ni/Fe case.

4.6.3 The Effect of Different Driving Cycles

The effect of driving cycle will also play an important role in shape of the specific range/battery fraction curves - depending upon to what extent vehicle energy demand is dependent upon vehicle weight, and indirectly, battery weight. The urban and cruise cycles for each battery type shown in Figures 4.18 - 4.20 represent the opposite extremes as far as driving cycle is concerned, in that the energy requirements over the urban cycle are heavily dependent on vehicle weight, whereas at cruise they are not. In each case for cruise a maximum value is implied at a higher battery fraction than for the urban cycle because extra battery energy is not being used to propel extra battery weight until larger vehicle weights are reached. To the left at maximum the effects of battery power density on specific range will still apply, and Figure 4.18 shows for the lead-acid battery that power density at a 40 mph cruise is higher than for the J227aC cycle overall.

4.7 The Effect of Electric Vehicle Braking Regime

The braking regime in an electric vehicle is of considerable importance as this will determine what proportion of the total deceleration

energy at the road wheels is recovered by the vehicle's electrical system regeneratively and what proportion is simply dissipated in the vehicle's friction brakes as wasted heat.

So far throughout this study the braking philosophy used has assumed that the electrical system performs all braking until its limits are reached after which the friction brakes are blended in smoothly to meet the deficit.

This system is called 'ideal' braking and typifies the simulation approach to braking in that given a deceleration rate the split between electrical and friction braking is then determined depending upon how much of the energy the electrical system can handle. In practice vehicle braking begins with a driver demand which then determines the proportion at deceleration energy carried out by the electrical system according to a pre-determined relationship.

It is the purposes of this section to study the effects of the practical braking regimes that were described in chapter 2 - the 'parallel' and 'split' systems - when compared with the 'ideal' braking regime.

Again, as has been the case throughout, the baseline electric vehicle configuration - lead-acid battery, D.C.Shunt motor and a direct-drive arrangement - will be used here.

The driving cycle deceleration profile was altered to be steeper in order to emphasise the differences between the three braking strategies - and this is shown in Figure 4.2.

In order to determine the predefined relationships between electrical and friction brakes it was first necessary to study the wheel power time profile for the ideal case - shown in Figure 4.21. From this profile the portion of the deceleration profile that can be braked electrically extends from 23 mph to rest whereas above 23 mph there must be a proprtion of the

total deceleration power (20%) handled by the friction brakes. Thus for the crude parallel system the brake torque fraction is 0.20 - and covers the entire deceleration profile - whereas for the more sophisticated split system a brake torque fraction of 0.20 down to 23 mph is followed by a brake torque fraction of zero from 23 mph to rest.

4.7.1 Discussion

The results, showing the energy split at the road wheels between friction and electrical braking, are shown in table 4.13 for the 'ideal', 'split' and 'parallel' braking alternatives.

As would be expected, the two practical regimes can only approach the ideal case in terms of the proportion of the total energy available being recovered regeneratively. Of the two practical systems, table 4.13 shows the split system to be the better of the two as it allows the electrical system braking profile to follow the deceleration profile more closely. This is made clearer if one looks at the wheel power/time profiles for the 3 regimes - shown in Figures 4.21 - 4.23. In each case the inner curve represents the power recovered electrically, the outer curve the total deceleration power available and the difference being the power dissipated in the friction brakes.

Table 4.13 also shows how the energy split at the wheels between friction and electrical brakes is affected if firstly the armature regenerative capability is removed (field weakening control only), and secondly if no regenerative capability at all is possible for the motor. The corresponding wheel power/time profiles are shown in Figures 4.24 and 4.25 and emphasise for the direct drive shunt motor the large proportion of regeneration performed in the armature control region of the motor map - as was discussed in 4.3.

Instead

4.8 Conclusions

It has not been the purpose of this study to develop a best design for a medium sized delivery vehicle - electric vehicle application. Although this can be relatively easily achieved, [illegible] what has been intended, is to show by the use of a flexible computer simulation program how sensitive vehicle performance (range to battery discharge, 0-30 mph acceleration time and vehicle maximum speed) is to sensible changes in vehicle parameters.

It is possible using a flexible computer simulation program to study the effects of all vehicle parameters changes, but since the electric drive-train for this vehicle class will have parameters that are common to other drive-train configurations - such as the conventional i.c. engined and hybrid-electric types - this study has concentrated on the parameters that are peculiar to the pure-electric drive-train. Nevertheless, since the hybrid-electric vehicle includes a pure electric drive-train, several of the conclusions reached here will also have a bearing on the hybrid-electric vehicle.

From this study it is possible to conclude that the vehicle parameter that has the single most significant effect on electric vehicle performance (and hence due to its present state of development, also limits it) is the traction battery type - or more fundamentally the traction battery power density/energy density characteristics. Of the variations to other vehicle parameters considered here - such as transmission type and ratio span, motor type and the vehicle braking regime adopted - it may be possible to improve vehicle range by as much as 10-20% in each case over current electric vehicle technology. But with the development of an advanced battery having a more favourable power density/energy density characteristic, range improvements could easily be an order of magnitude higher than this.

Nevertheless, even with the advent of battery types more advanced than those considered here, such as the sodium-sulphur type, maximum energy density will still be more than an order of magnitude less than that for liquid fuel. Therefore over the time-scale that this will involve (probably to the turn of the next century) a range and/or payload restriction will always be the handicap of the electric vehicle.

However with the impending oil shortages and resulting price increases predicted at the turn of the next century, the main motivation for the introduction of the electric vehicle may well be of necessity rather than user preference if no suitable alternative to oil as an energy source can be found.

The electric vehicle user today enjoys the benefits of cheap overnight electricity made possible by the daily usage patterns most road-vehicle users perform. For a given battery size, although a more advanced battery will be attractive to the user in terms of range, in terms of charging time it may not because of the greater amount of stored energy. A typical 1000 Kg lead acid battery, having a 5 hr energy density of 40 w-hr/Kg, requires 6-10 hrs to charge, whereas a 1000 Kg Ni/Zn battery, having a 5 hr energy density of 70 w-hr/Kg would now need 10-15 hrs for charging - so making vehicle utilization difficult. However, the problem would be overcome by the use of a smaller battery size if a fixed urban range was all that was required of the vehicle - as discussed in section 4.5.2.

In general conclusion, therefore, although the electric vehicle may find a wide application in road-vehicles where a fairly well defined urban range is apparent, unless an expensive infrastructure of recharging or battery exchange stations is introduced, it will not satisfy the requirement of the occasional long trip currently enjoyed by other users - even with the advantage of more advanced battery types.

One solution to the problem is for these other users to have two vehicles - an electric vehicle for urban duty where emissions and noise regulations may be tight in the future, and one (perhaps an i.c. engined vehicle) to undertake the occasional long trip. Although the second car market in the USA is significant and forms the basis of the argument for constructing electric passenger cars (commuter cars), it is not so well established in the UK or Europe and is the main reason why electric vehicle construction at present has focused on urban delivery vehicles.

The second alternative to the range restriction of the electric vehicle is to merge the pure-electric drive-train and, say, the i.c. engined drive-train into one vehicle to allow urban electric operation and long distance travel using the i.c. engine - so overcoming the problems associated with the user requirement of two vehicles.

For European market conditions at the present at least, the second solution appears to be more applicable and is the hybrid-electric vehicle solution - discussed in chapter 1.

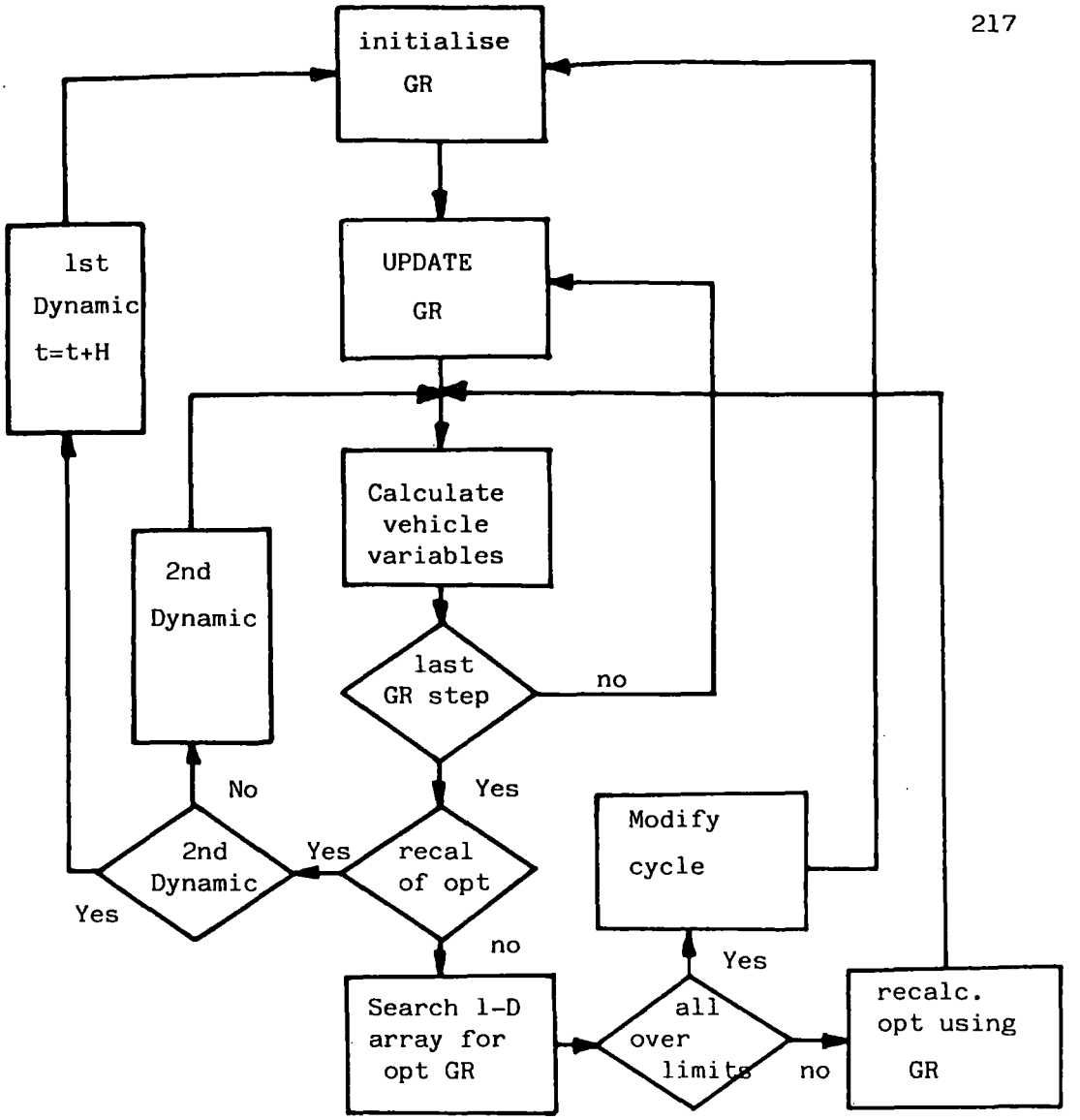

FIGURE 4.1: Optimum Control Flow Chart for the Electric Vehicle using a CVT or Discrete Ratio Transmission

FIGURE 4.2: J227aC Cycle

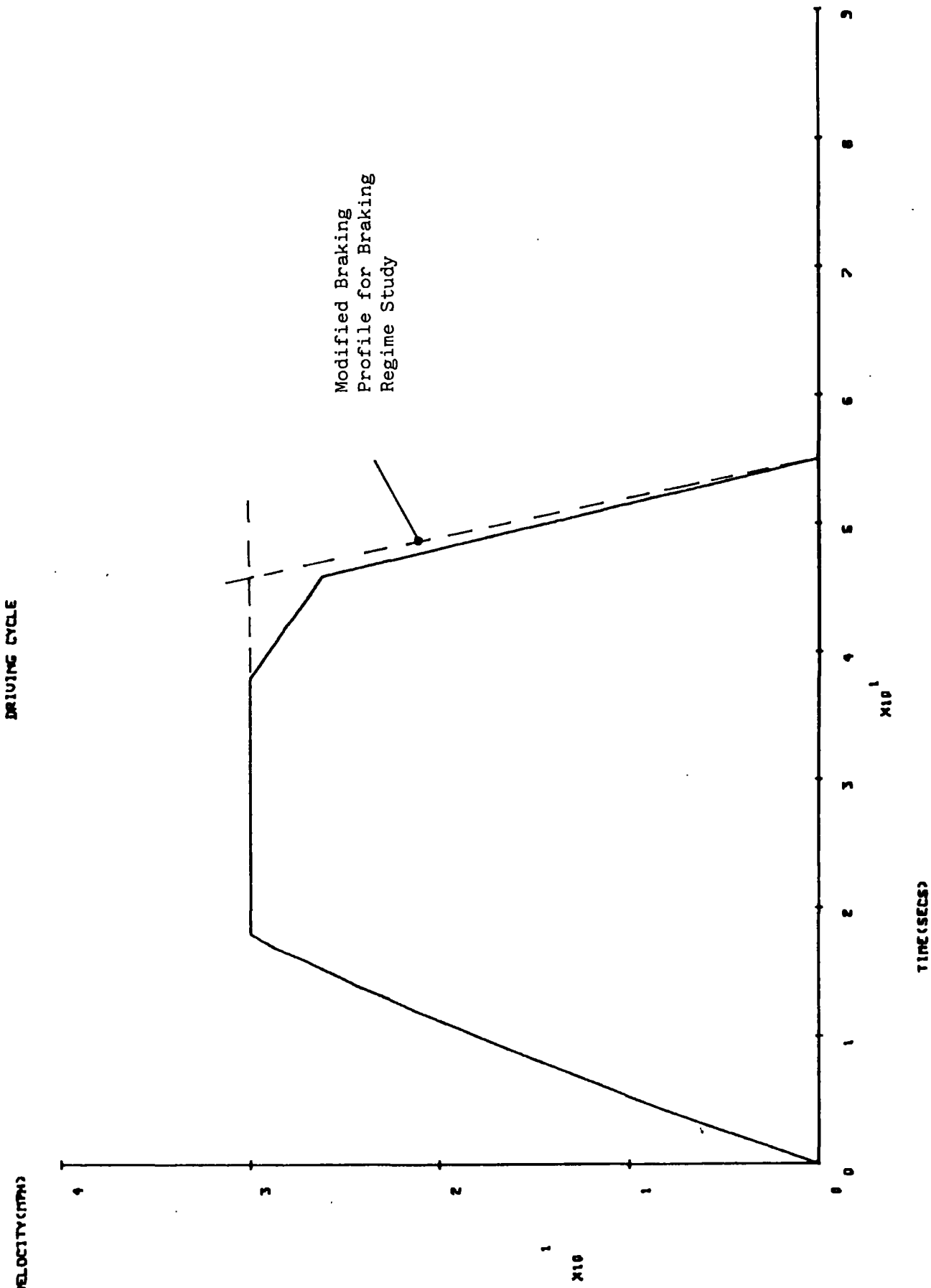

FIGURE 4.3 Lucas DC Series Traction Motor Map

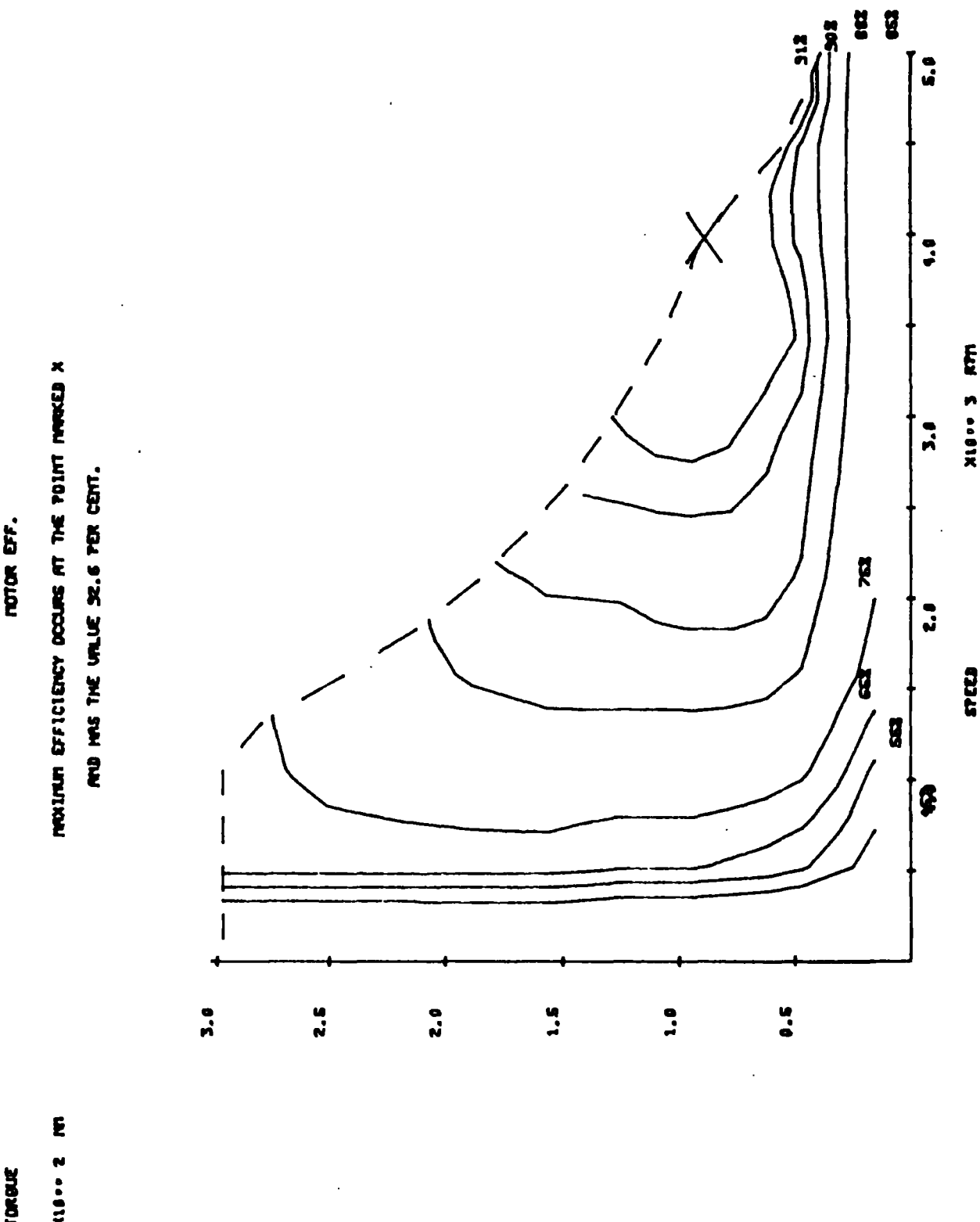

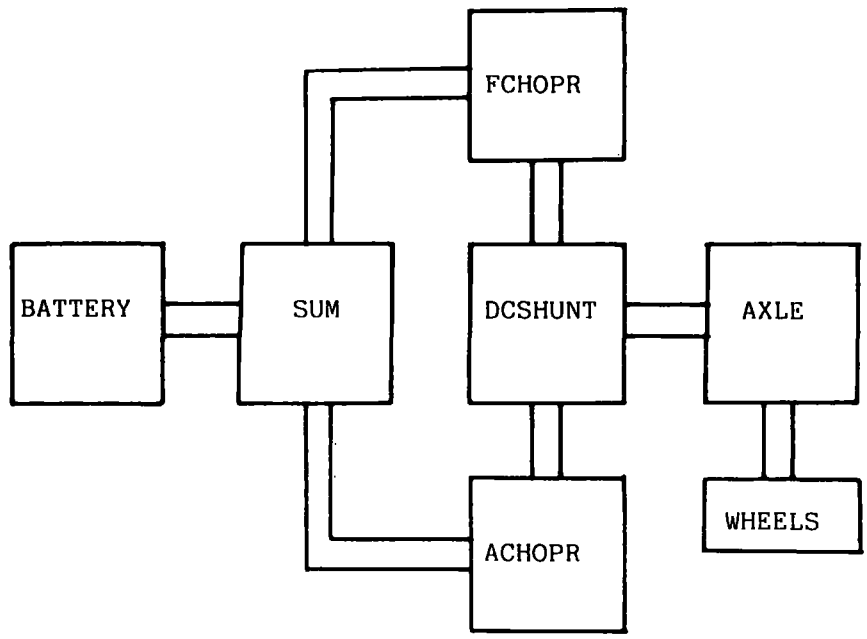

FIGURE 4.4: Direct Drive Electric Vehicle Configuration

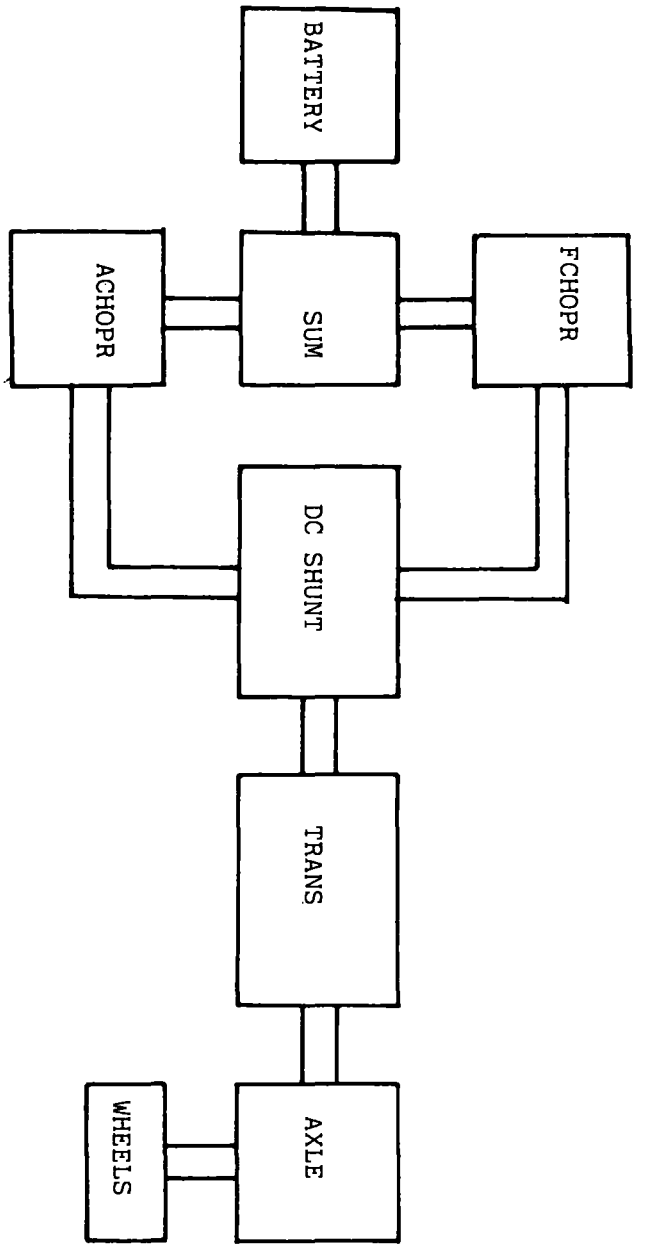

FIGURE 4.5: Electric Vehicle Configuration with a variable Ratio Transmission

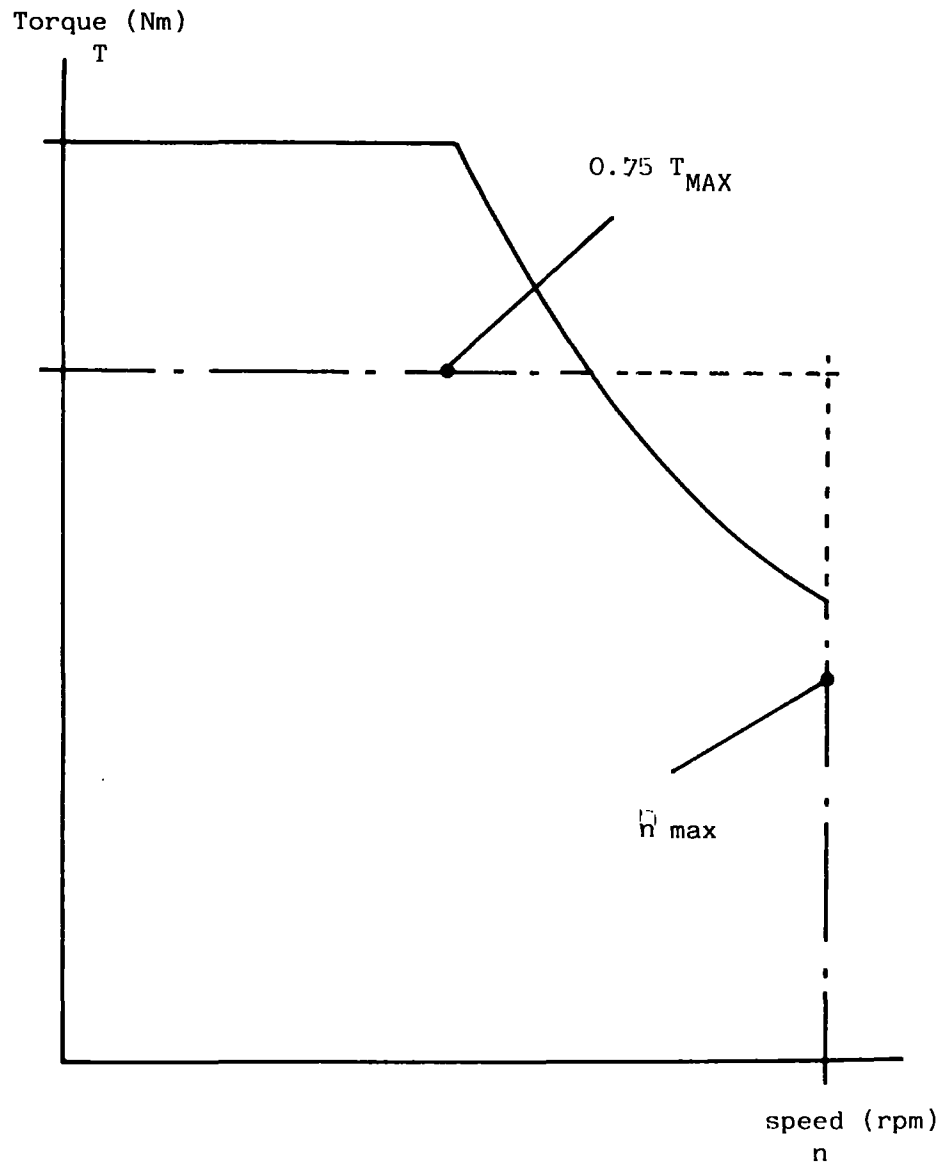

FIGURE 4.6: Sub-Optimum Control Region Dimensions for a Discrete Ratio Transmission

FIGURE 4.7: Usage Data for a CVT under Optimum Control when motoring

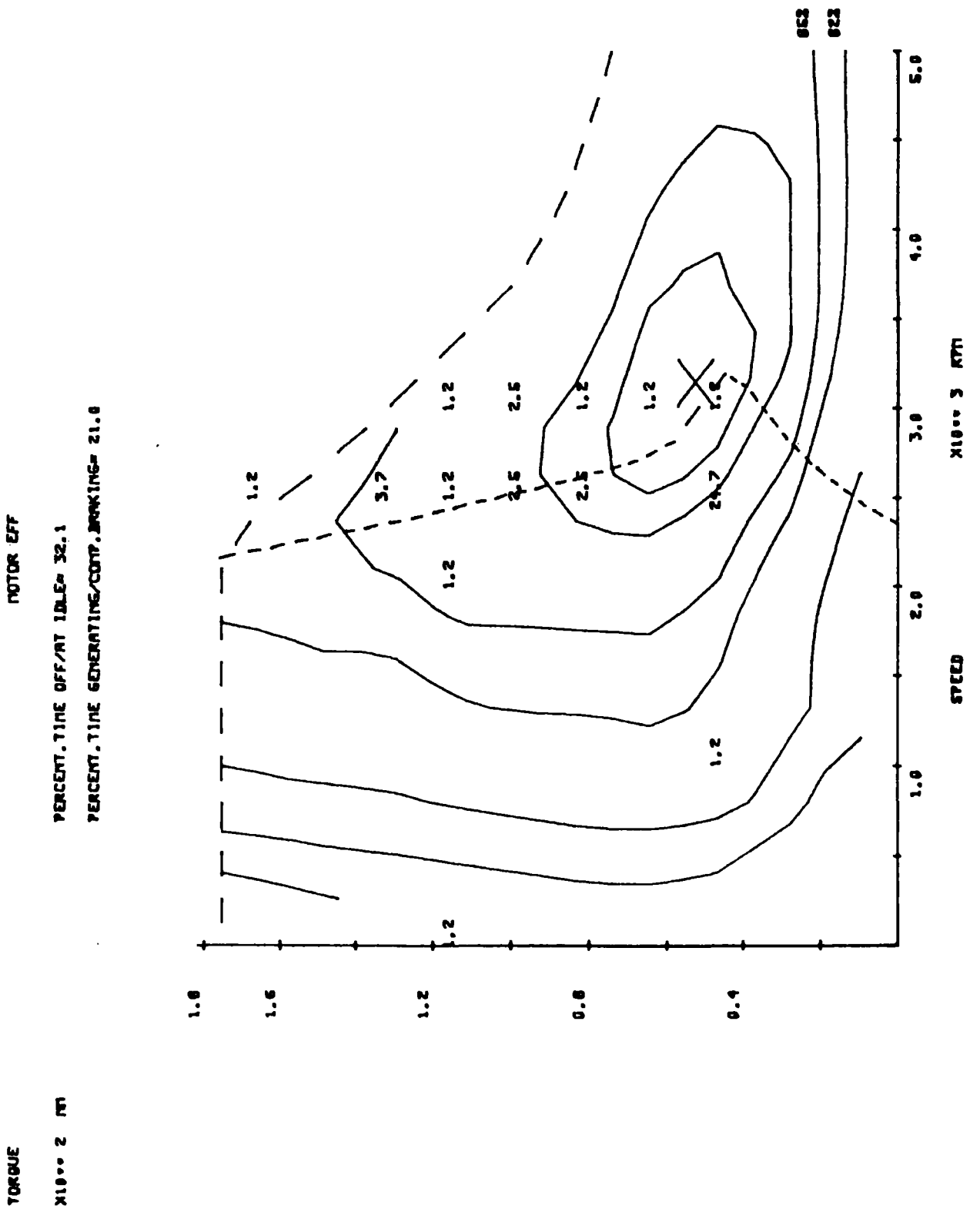

FIGURE 4.8 : Usage Data for a CVT under Optimum Control when Regenerating

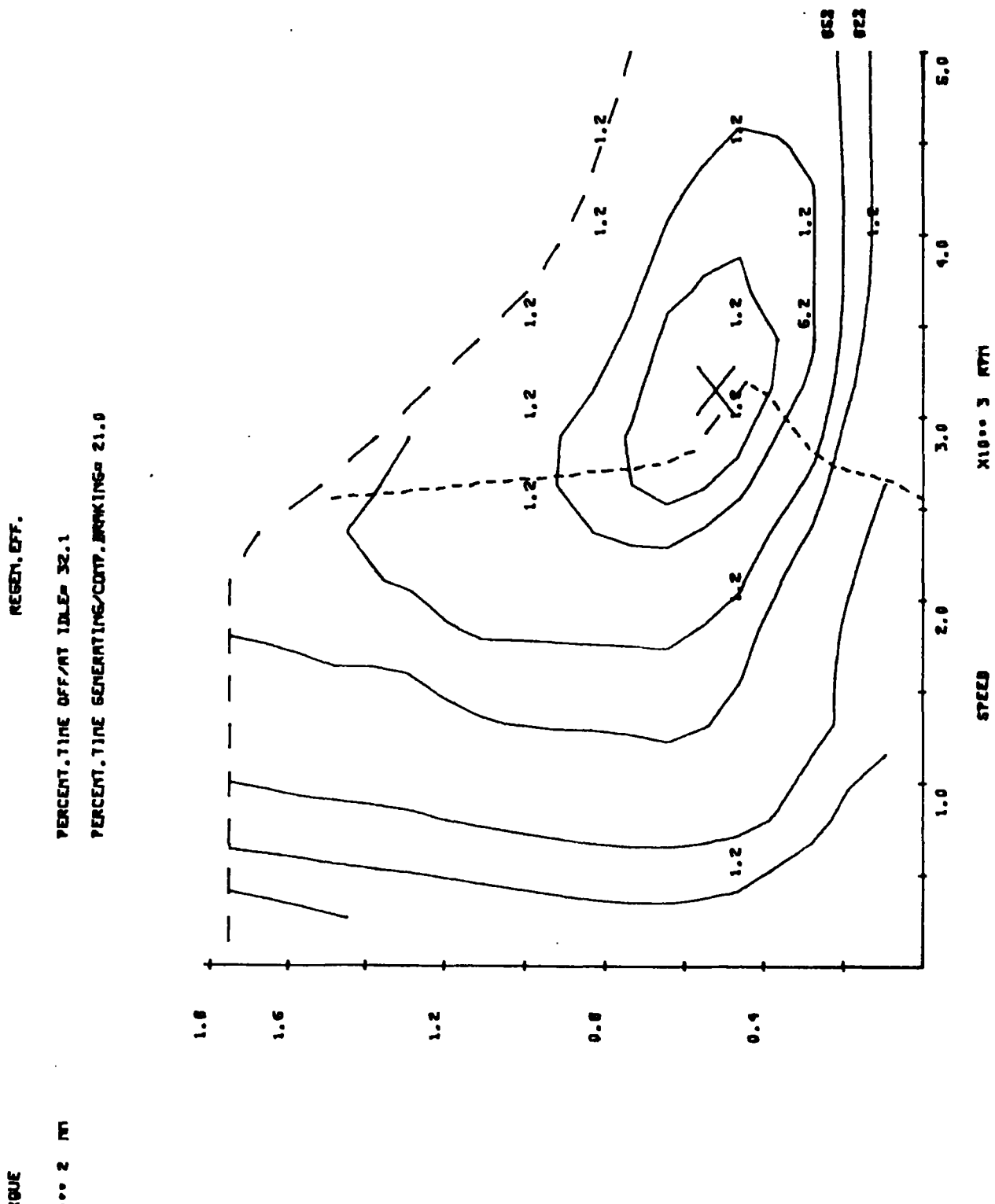

FIGURE 4.9: Usage Data for a Discrete Ratio Unit under optimum control when motoring

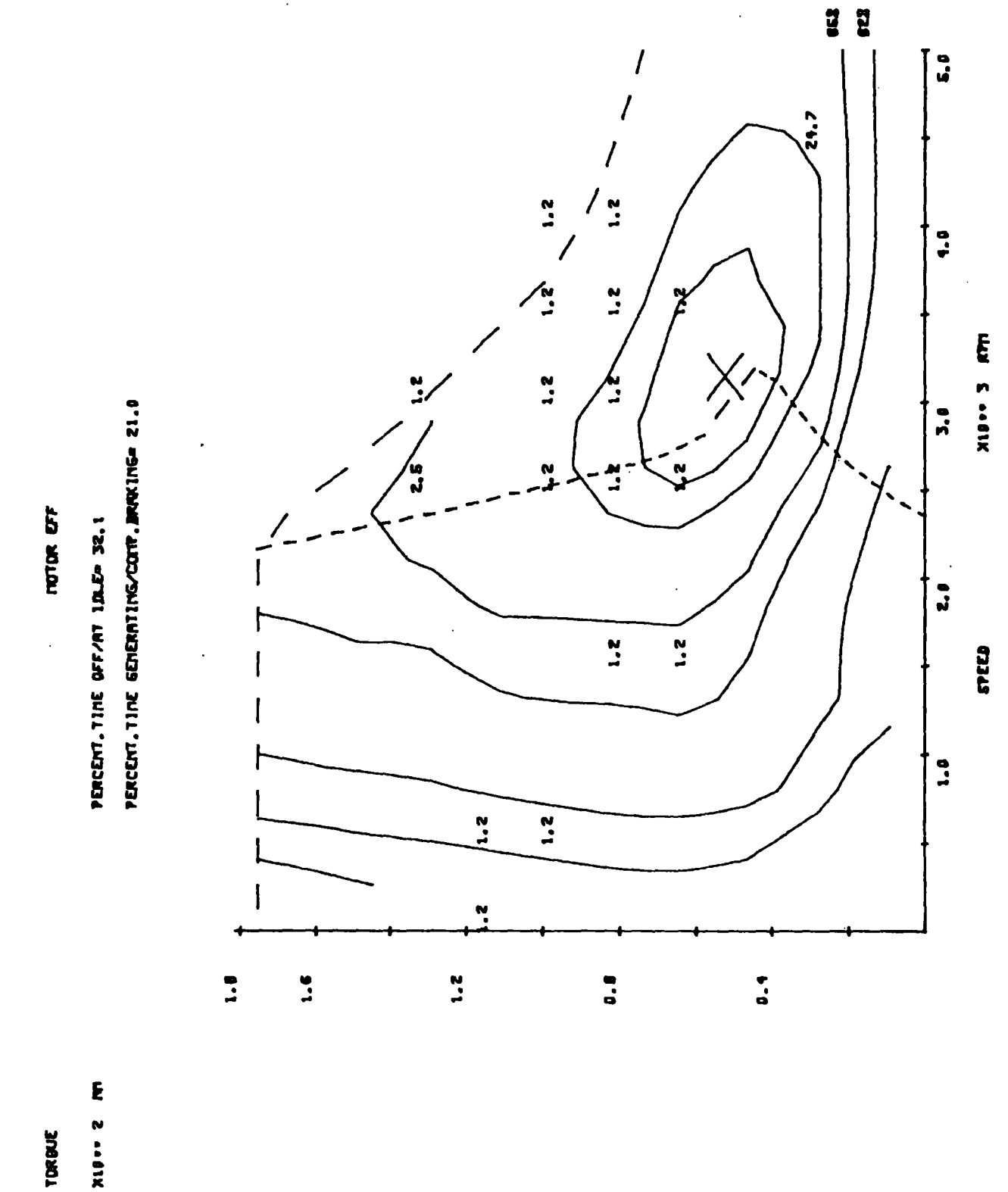

FIGURE 4.10: Usage Data for a Discrete Ratio Unit under Optimum Control when Regenerating

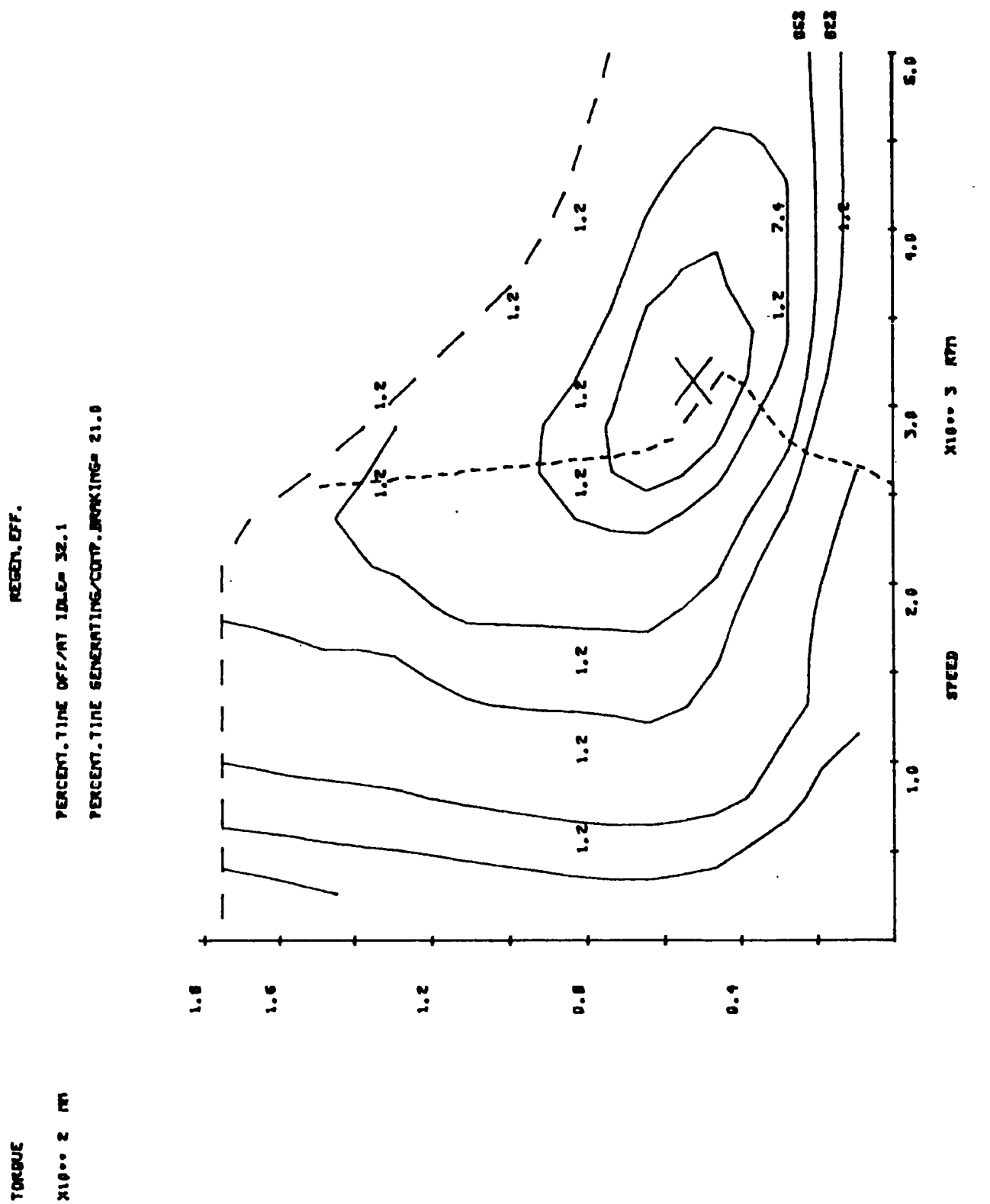

FIGURE 4.11: Usage Data for a CVT under Sub-Optimum Locus Control plus 1 Battery Switch when motoring

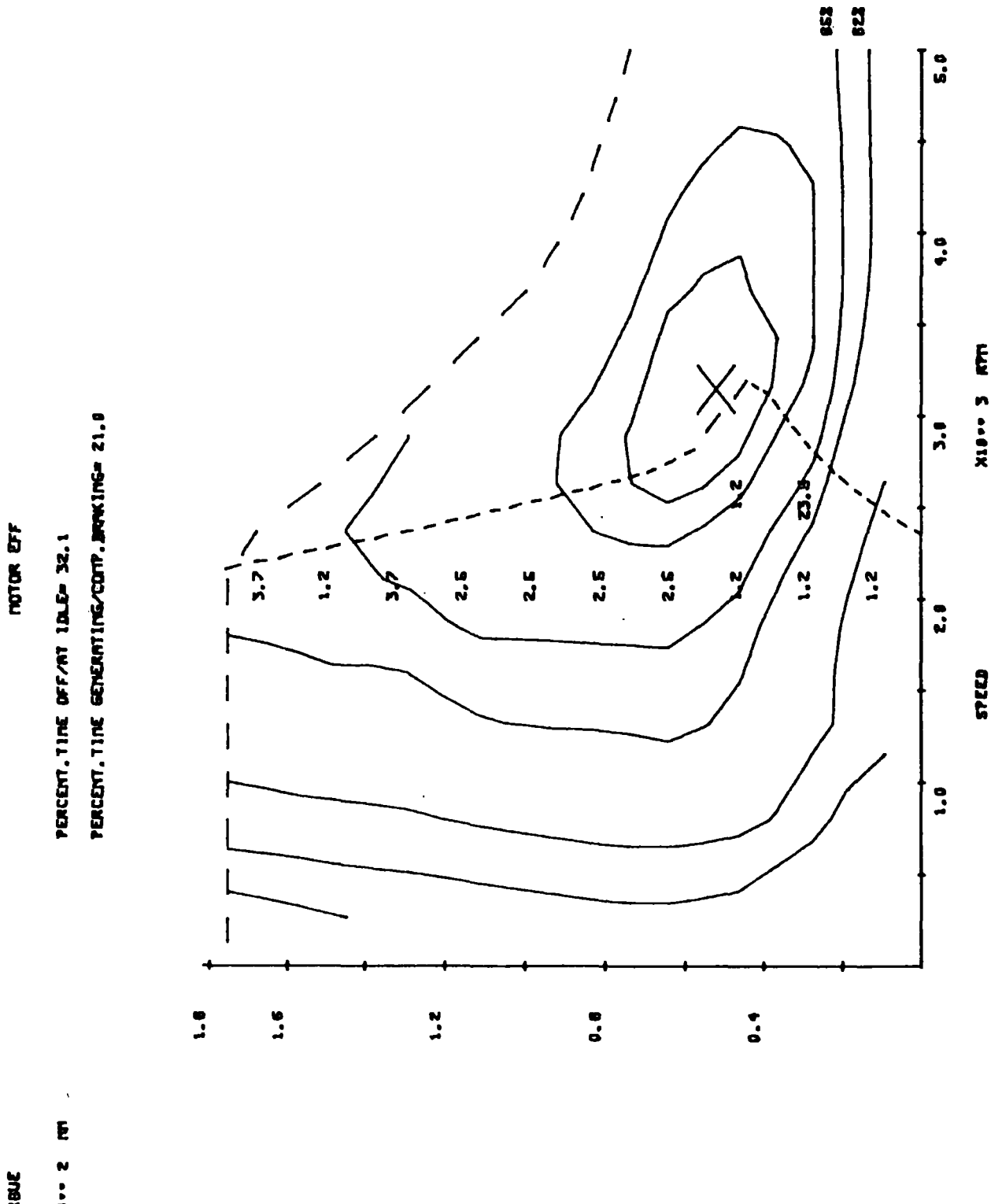

FIGURE 4.12: Usage Data for a CVT Under Sub-optimum Locus control plus 3 Battery Switches - motoring

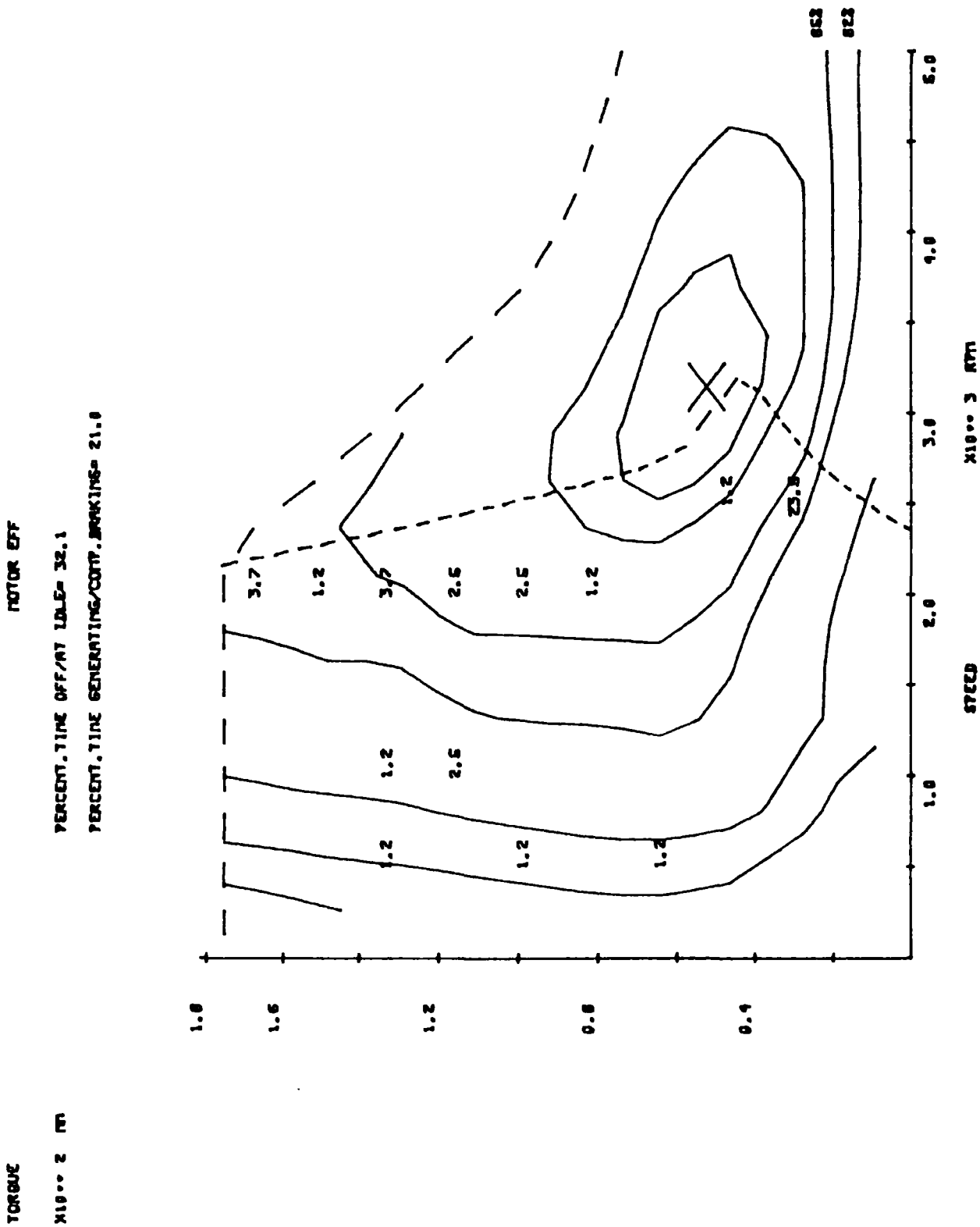

FIGURE 4.13: Usage Data for a CVT under Sub-Optimum Locus Control plus 1 Battery Switch-Regeneration

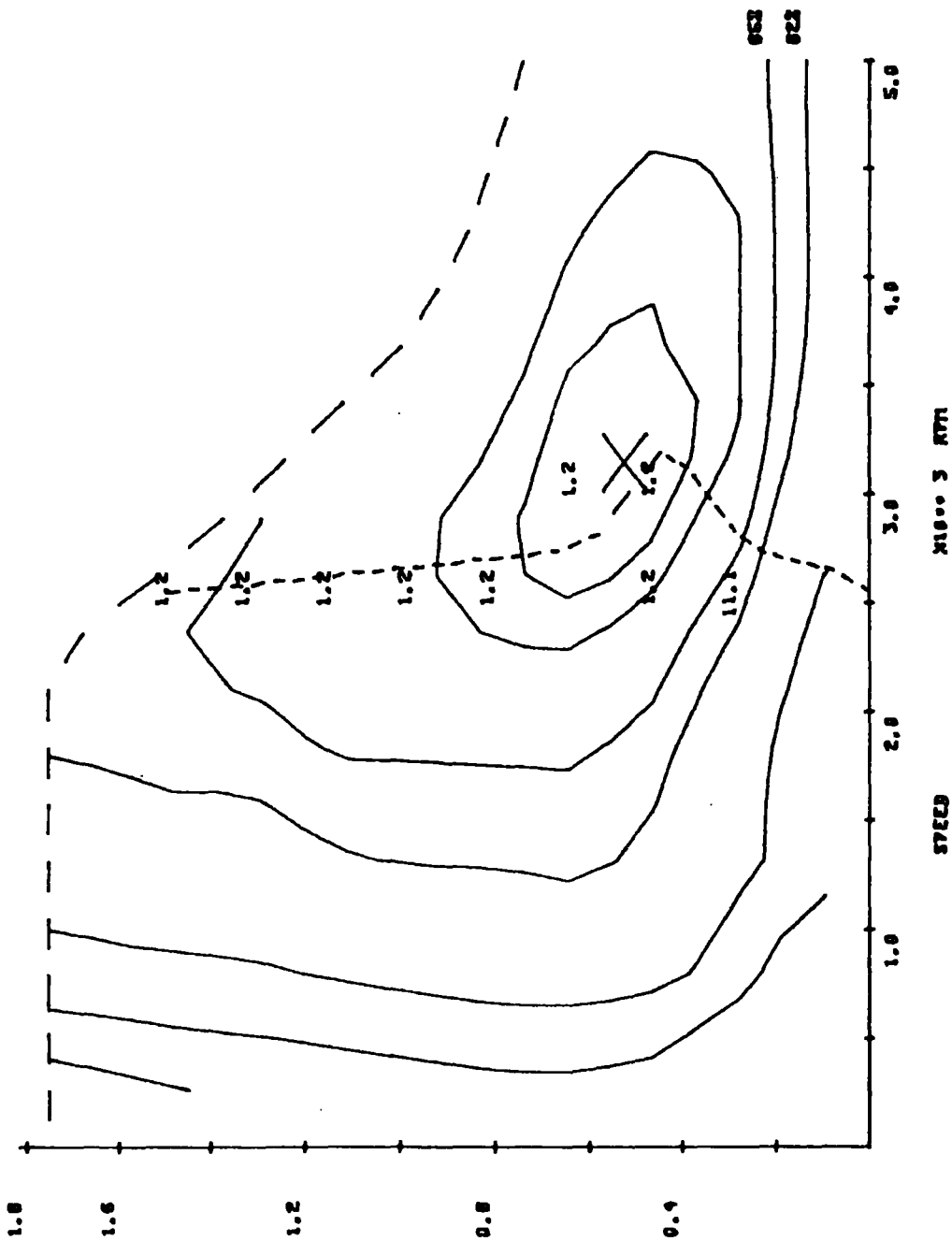

FIGURE 4.14a: Usage Data for a CVT under Sub-Optimum Break Speed control - motoring

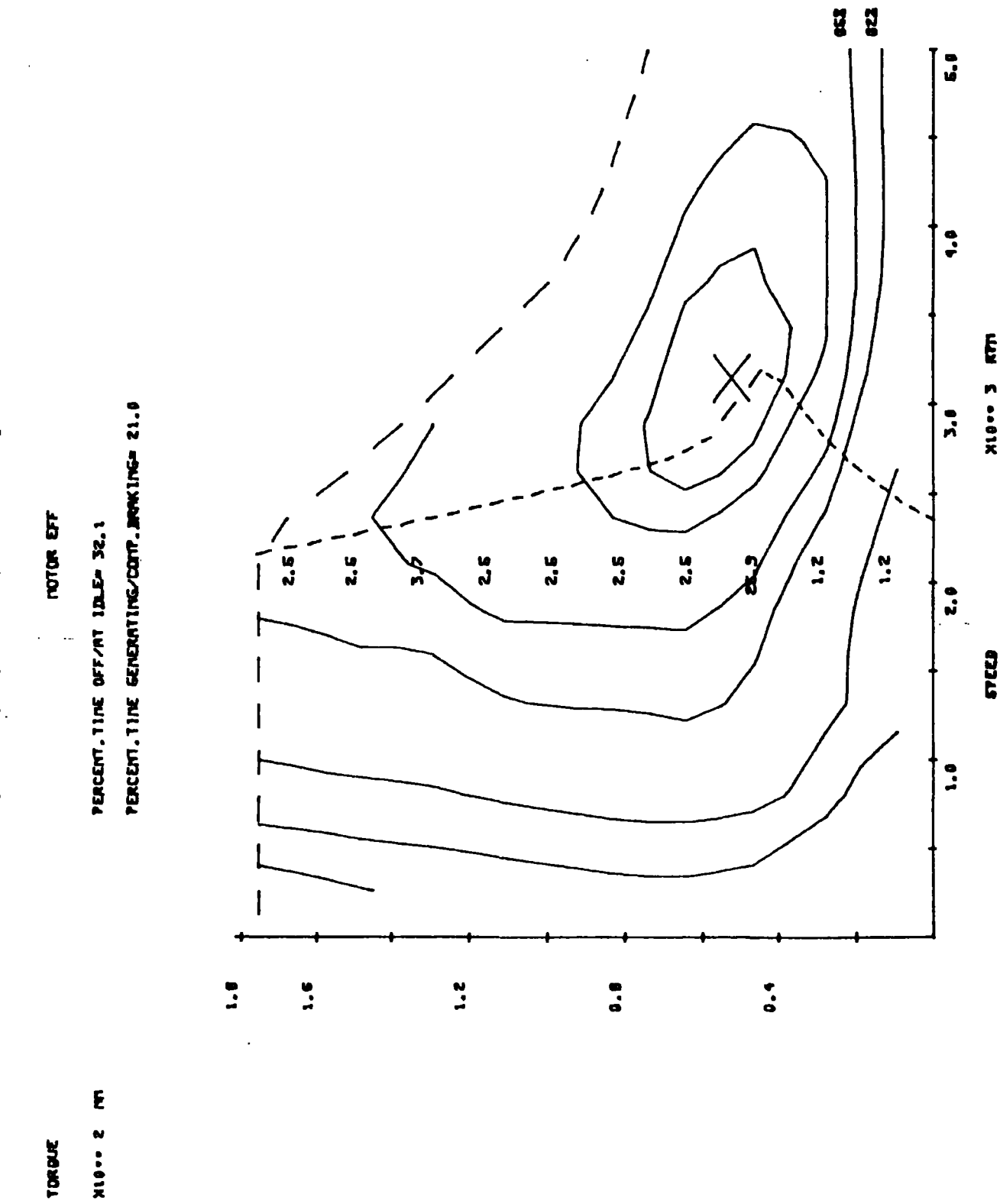

FIGURE 4.14b: Usage Data for a CVT under Sub-Optimum Break Speed Control - Regeneration

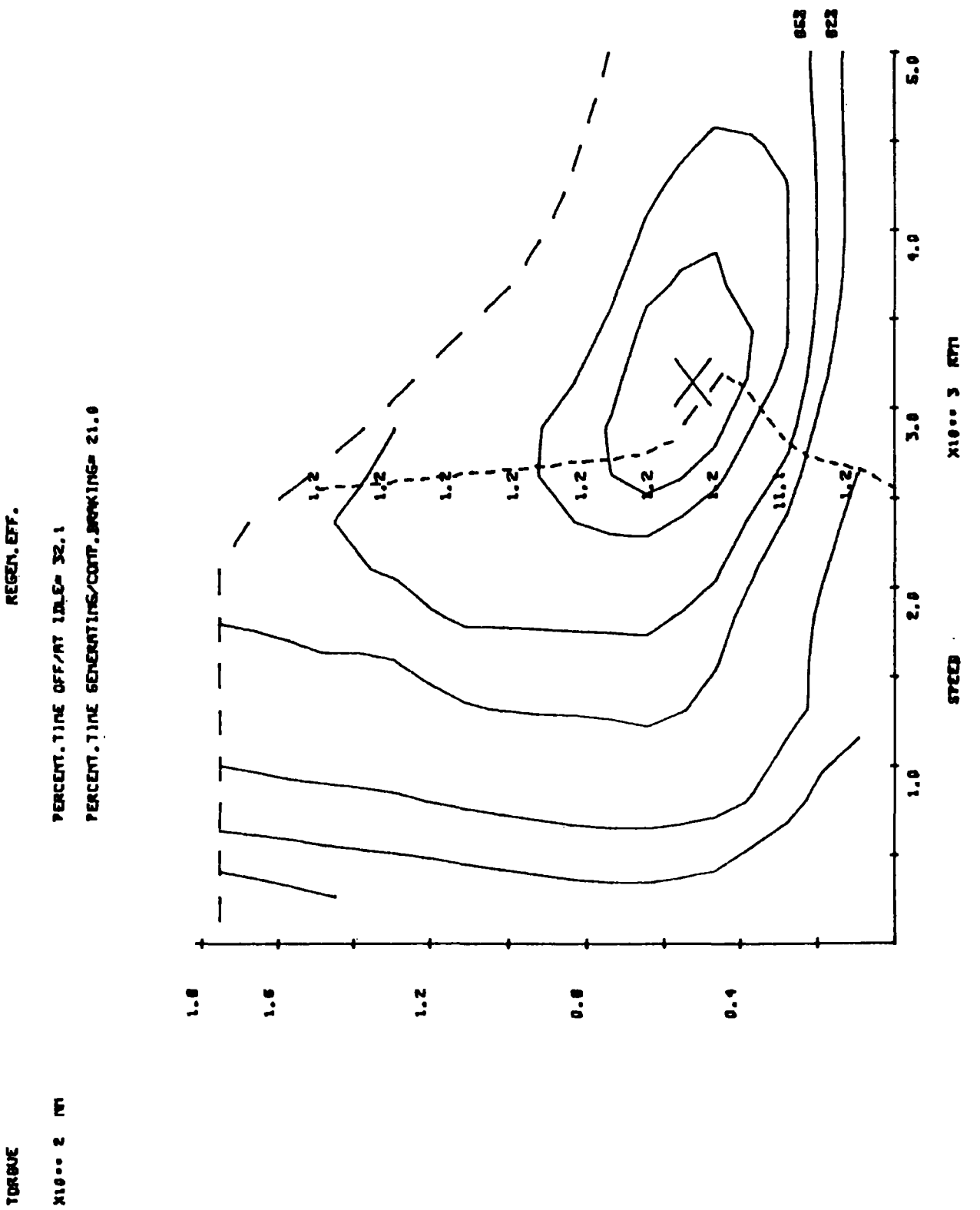

FIGURE 4.15: Usage Data for a Discrete Ratio Unit under Sub-Optimum control when motoring

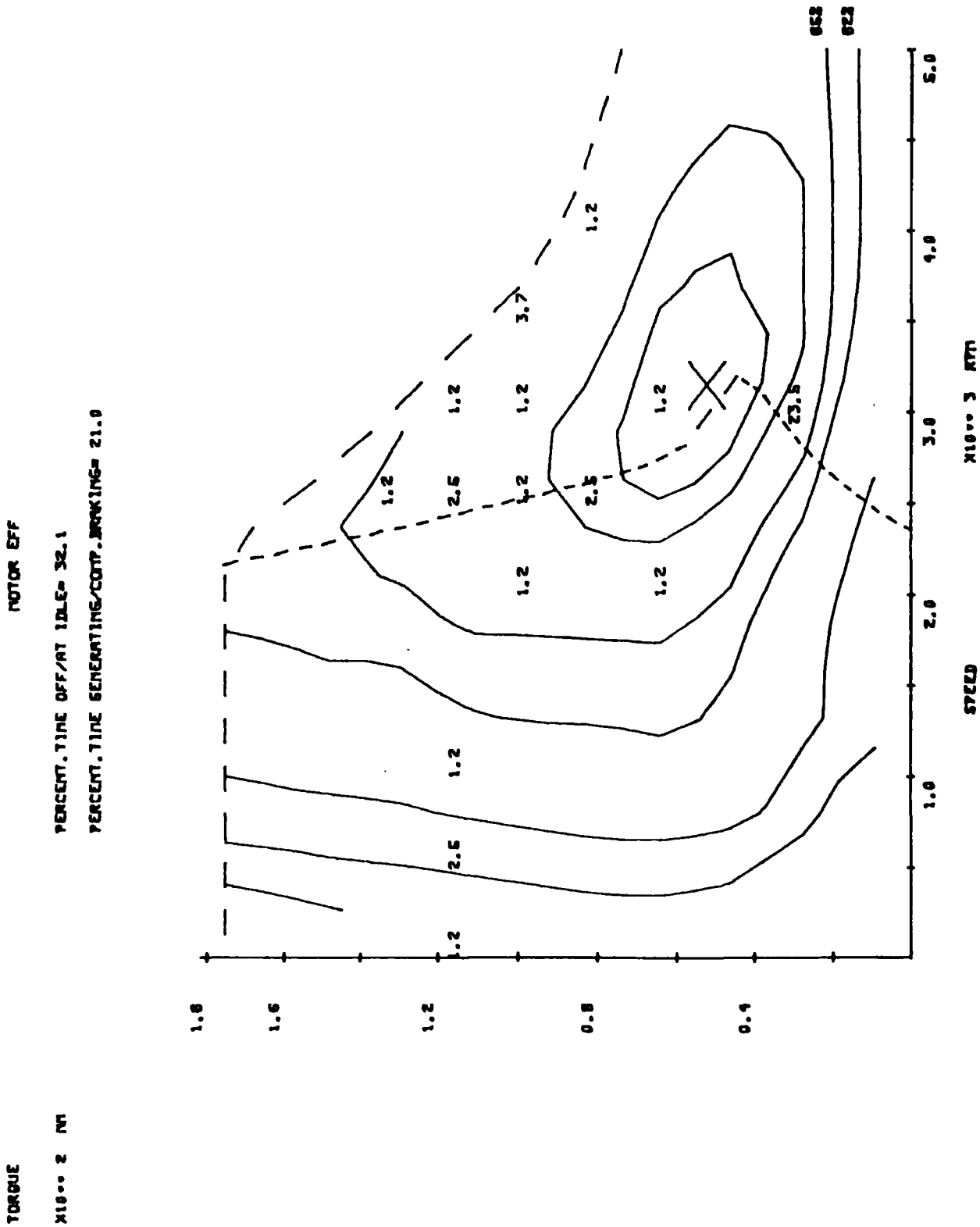

FIGURE 4.16 : Usage Data for a Discrete Ratio Unit under Sub-Optimum control when Regenerating

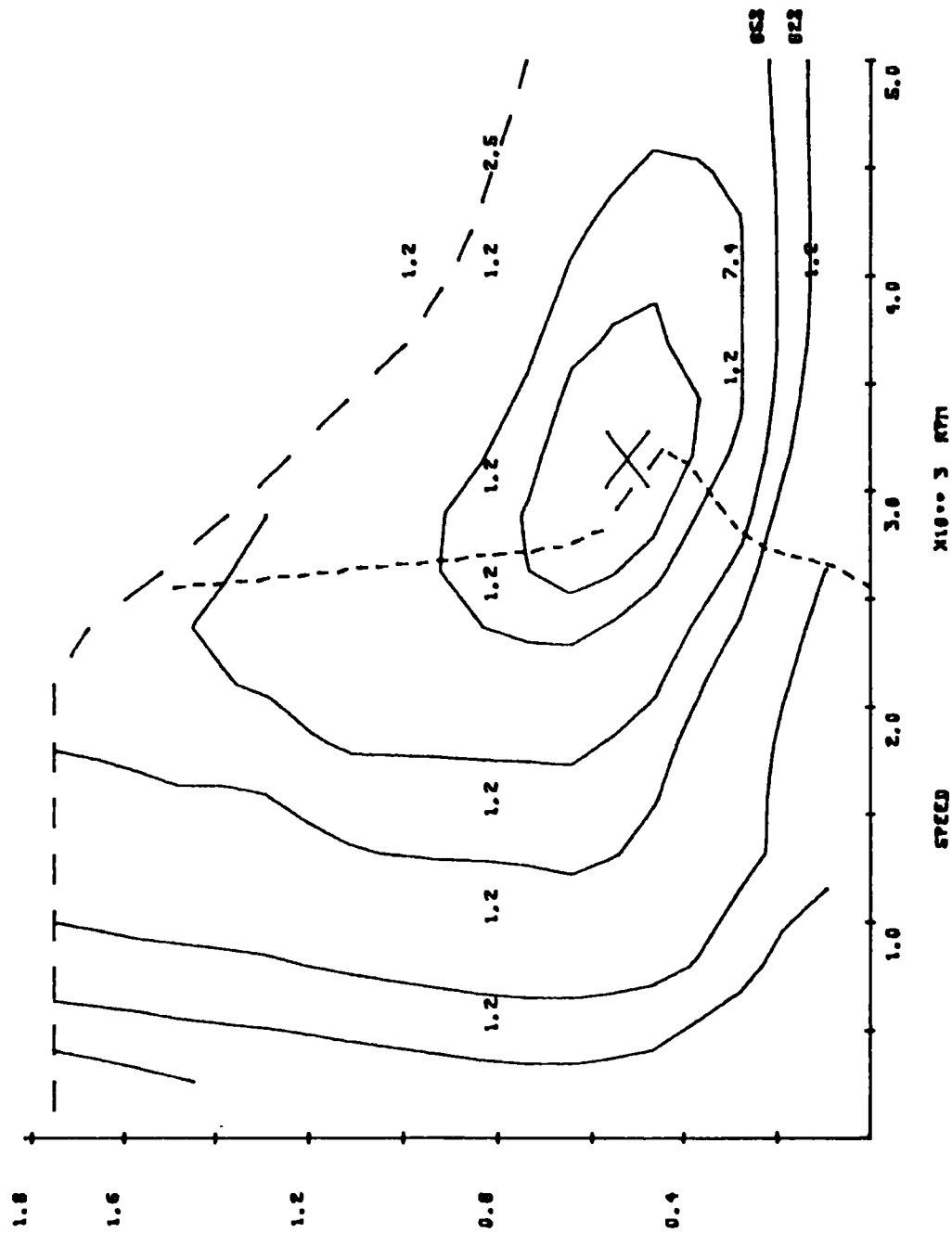

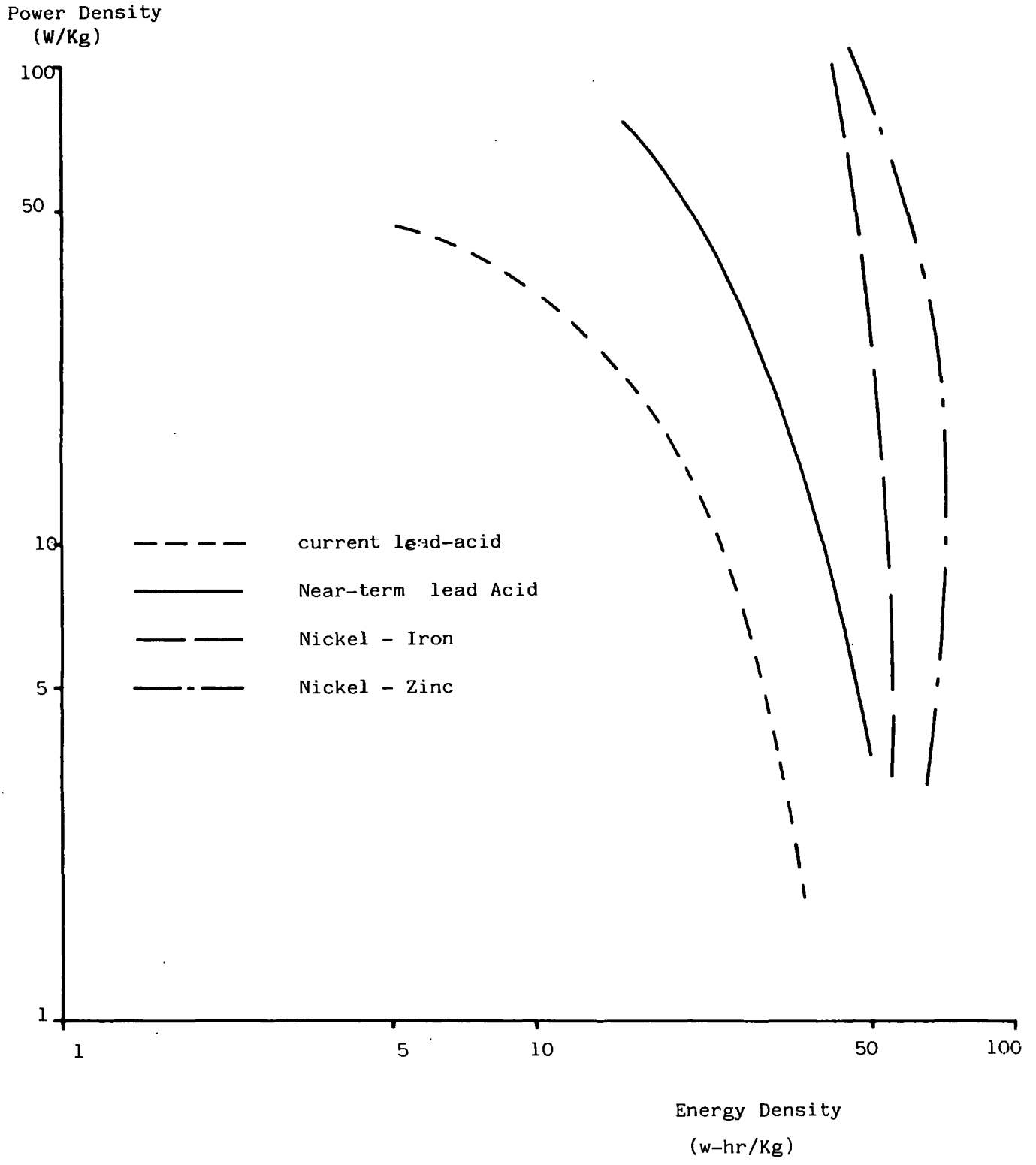

FIGURE 4.17: Power Density/Energy Density Characteristics for different Battery types

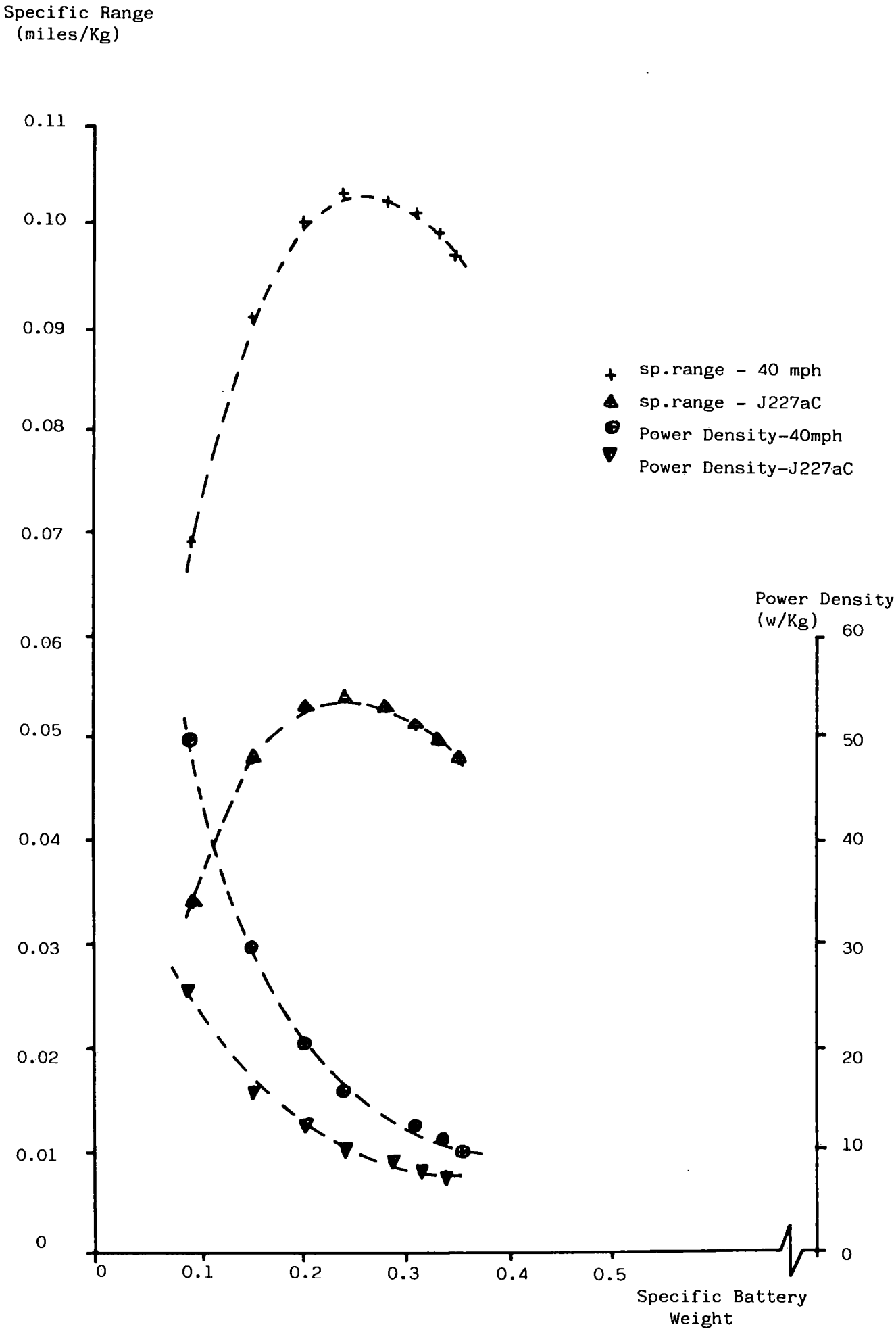

FIGURE 4.18: Specific Range/Battery Fraction Curves for a lead-acid

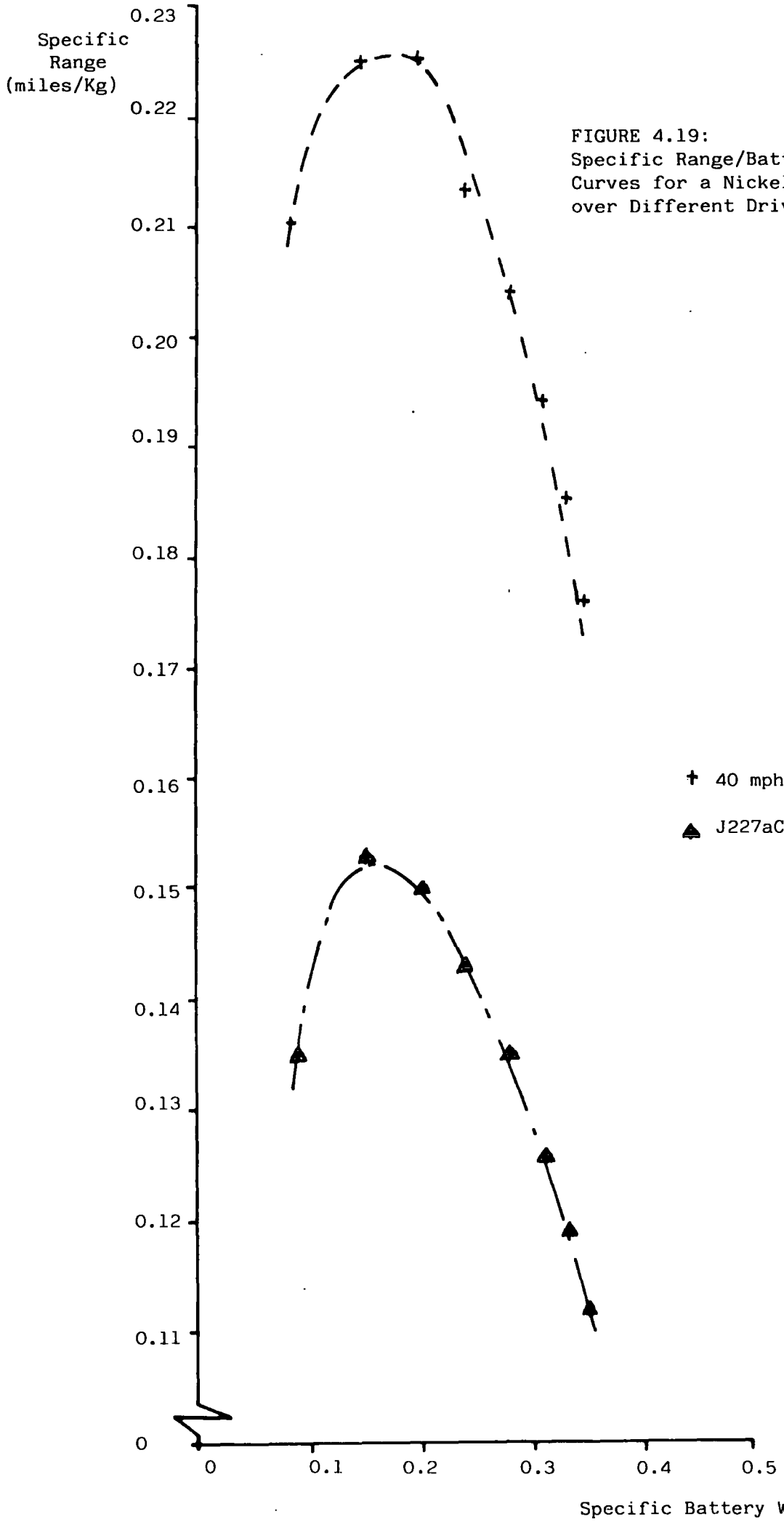

FIGURE 4.19:
Specific Range/Battery Fraction Curves for a Nickel-zinc Battery over Different Driving cycles.

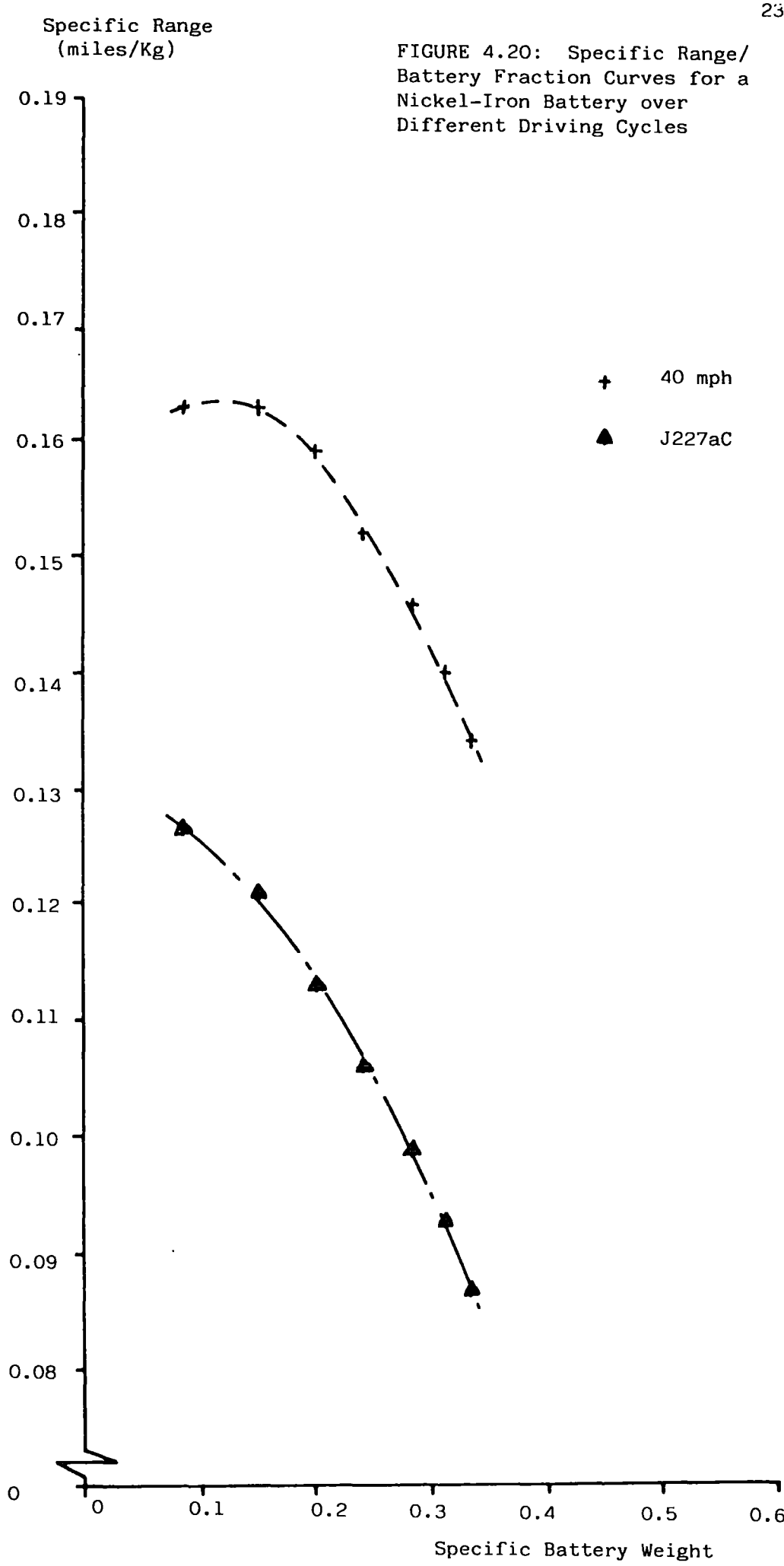

FIGURE 4.20: Specific Range/ Battery Fraction Curves for a Nickel-Iron Battery over Different Driving Cycles

FIGURE 4.21: Wheel Power/time profile over the J227aC cycle under Ideal Braking

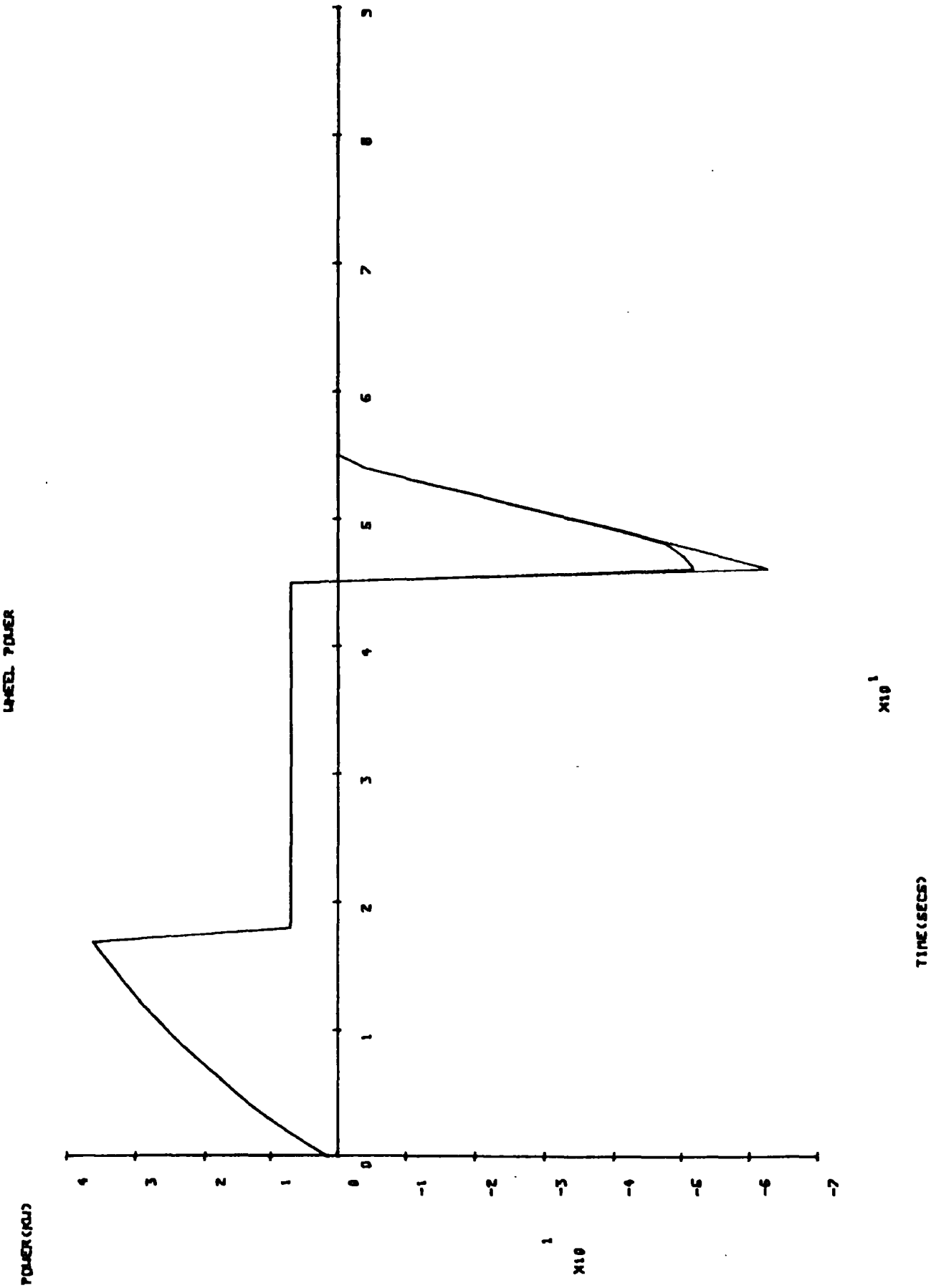

Figure 4.22: Wheel Power/time Profile over the J227aC Cycle under Split Braking

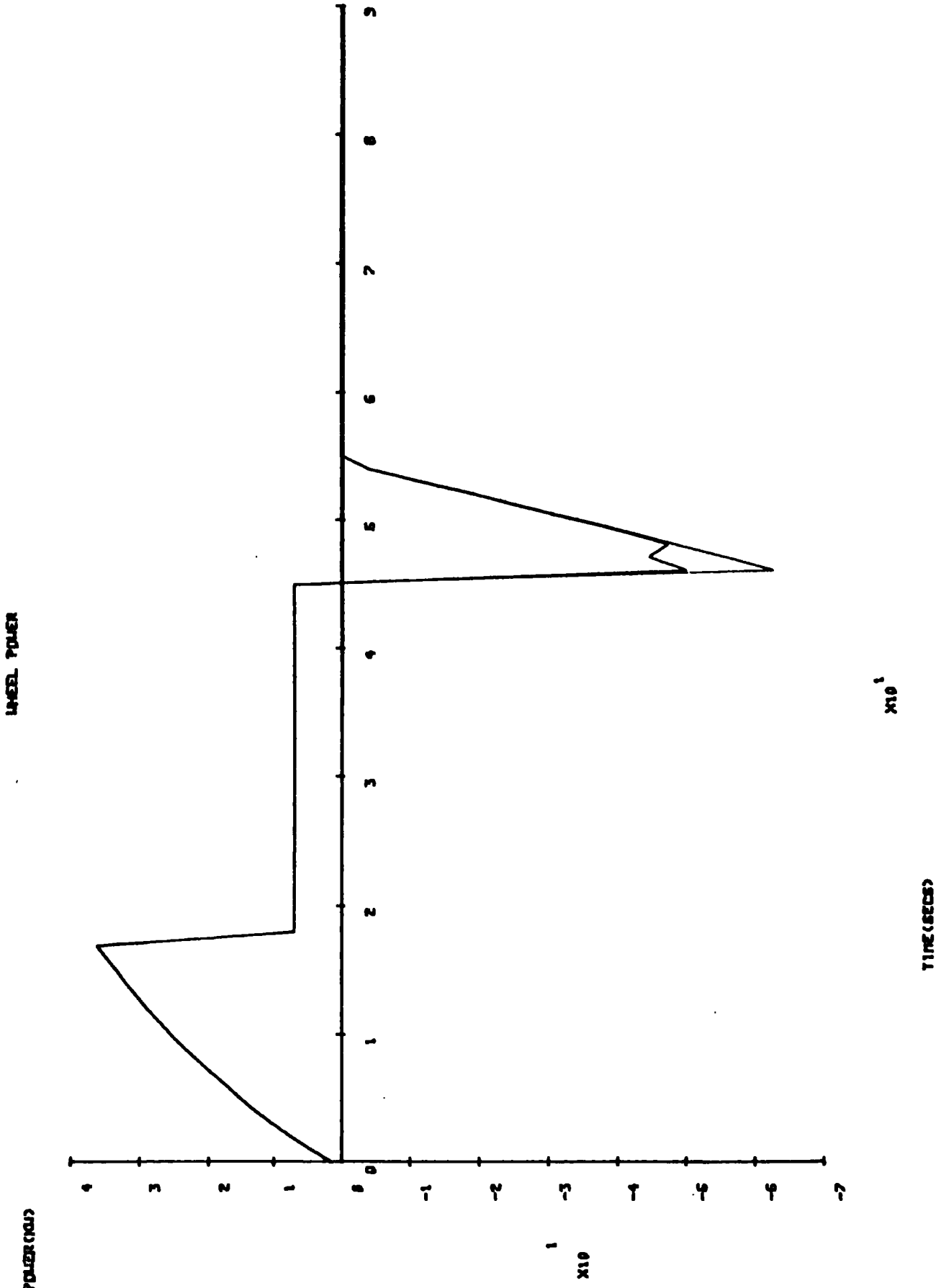

FIGURE 4.23: Wheel Power/time Profile over the J227aC cycle under Parallel Braking

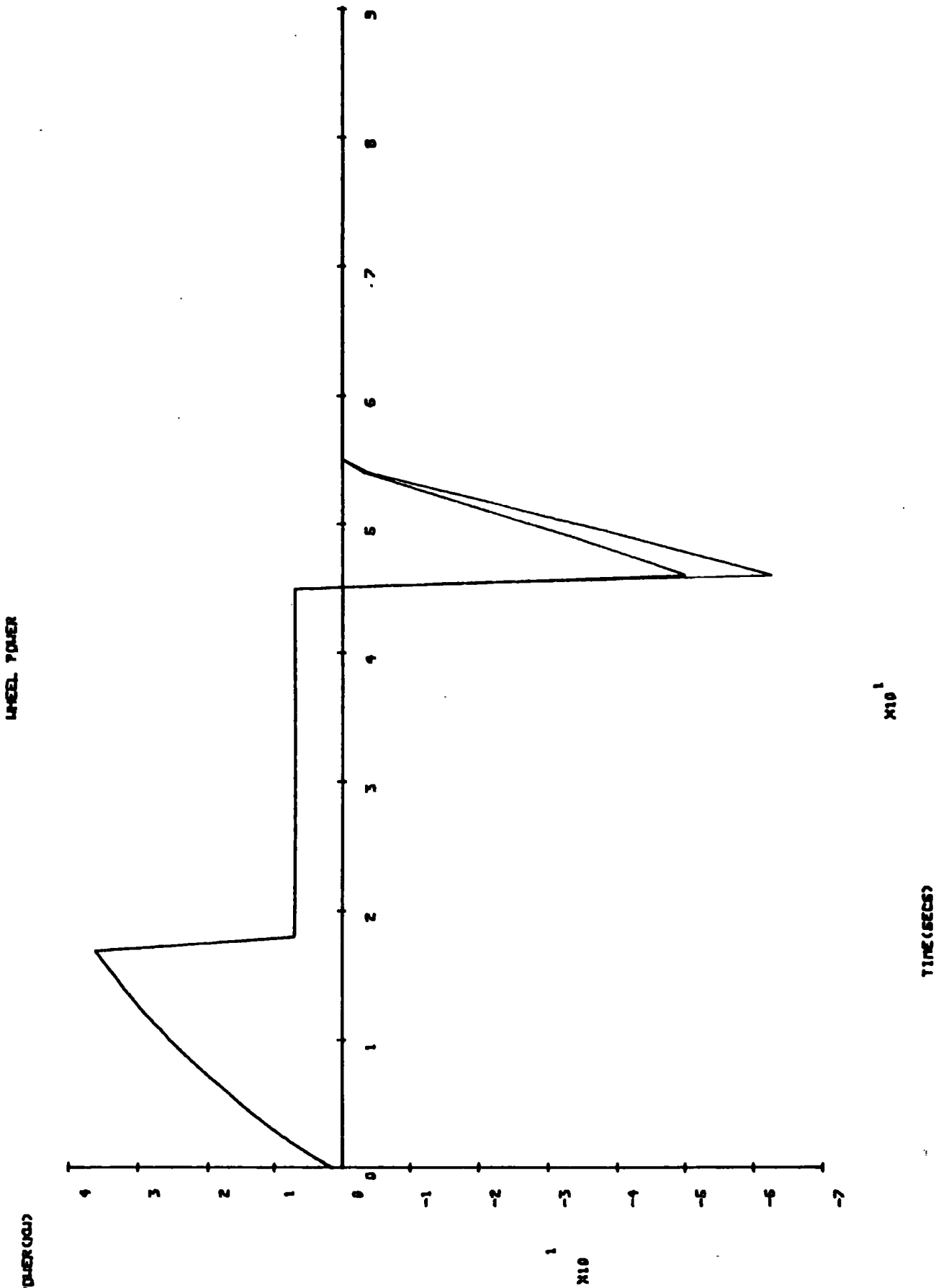

FIGURE 4.24: Wheel Power/time Profile over the J227aC cycle with no Armature Regeneration

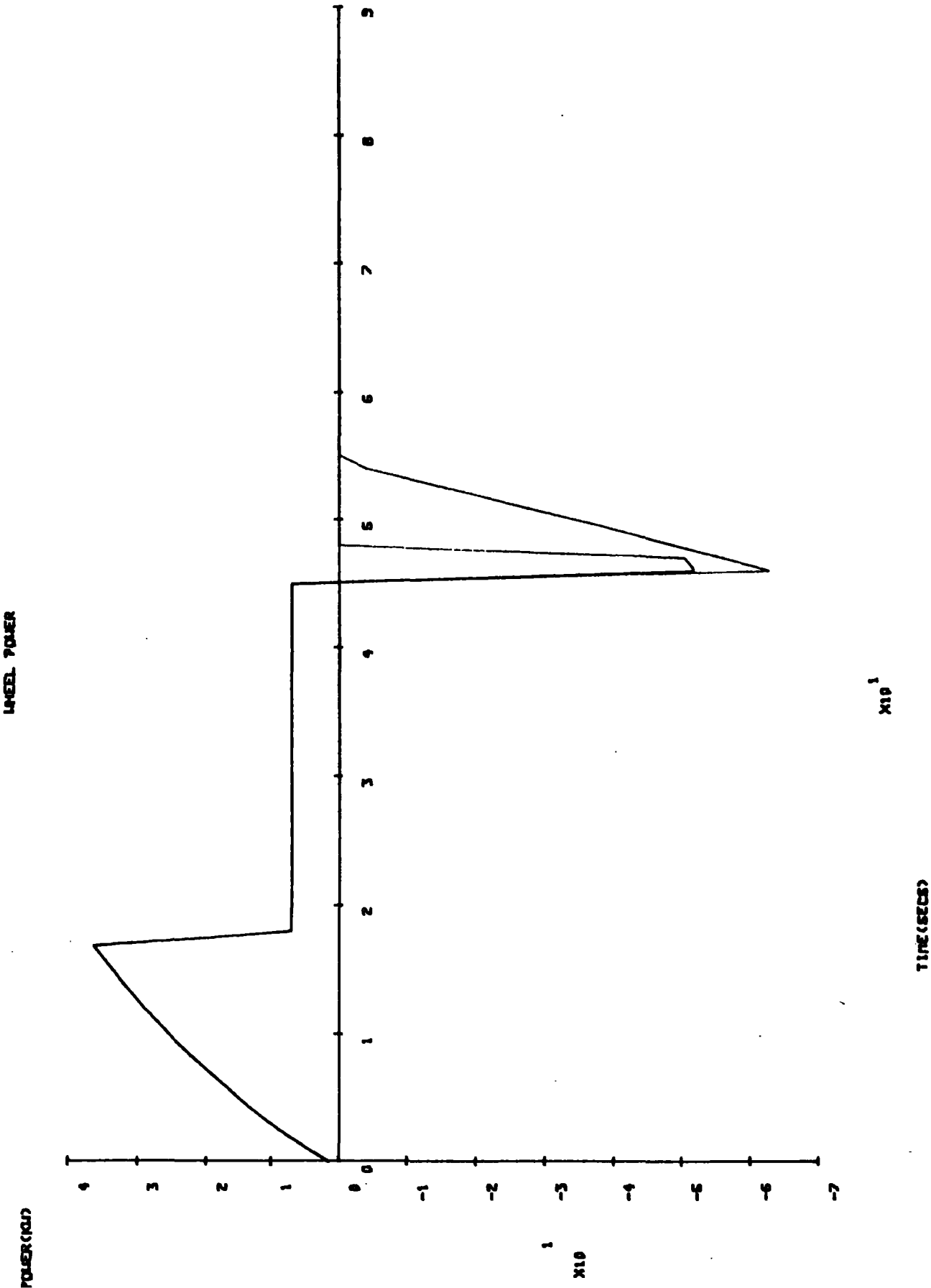

FIGURE 4.25: Wheel Power/time Profile over the J227aC cycle with no Armature or Field Regeneration

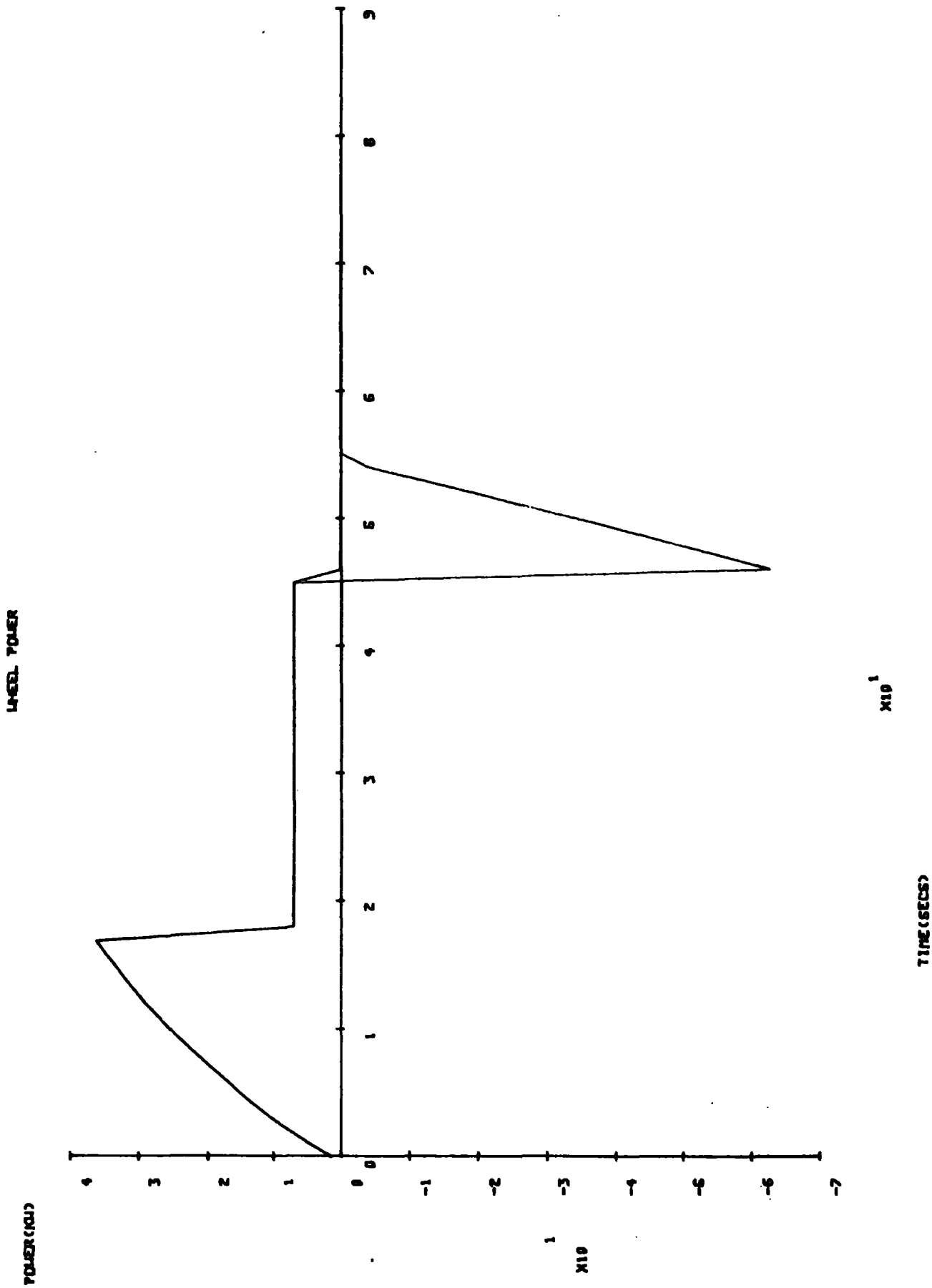

TABLE 4.1 Vehicle Parameters Selected for the Medium Sized Delivery vehicle/van

1. Base Vehicle Parameters

Drag Coefficient - 0.42
Frontal Area (m^2) - 3.5

Coefficient of Rolling Resistance - 0.01

Bodyshell Weight (Kg) - 1000
No. of passengers - 2 (70 Kg each)
Payload (kg) - 750

Wheel Radius (m) - 0.32
Wheel Inertia (Kg) - 60

Final Drive Ratio - 7.47:1
Final Drive Type - Chain
Final Drive efficiency - 95% (constant)

Motor Rating (Kw) - 50
Maximum speed (rpm) - 5000
Motor voltage - 100

Motor Controller type - Transistor

Battery Type - lead-acid
EV2-13 - 42 W-hr/Kg at the 5 hr rate

Battery Weight (Kg) - 1000

2. Basic Performance Constraints

Acceleration - 0.30 mph in 10-15 seconds

Maximum speed on a level road - 50 mph

TABLE 4.1 cont'd

3) Variable Ratio Transmission Alternatives

a) Discrete ratio - transmission ratios

	2 speed		3 speed		4 speed	
Case	i)	ii)	i)	ii)	i)	ii)
					2.5	
			2.0		2.0	
	1.5		1.5		1.5	
Datum	1.0	1.0	1.0	1.0	1.0	1.0
		0.5		0.5		0.5
				0.25		0.25
						0.1

Case i) Ratio span increasing the overall ratio

Case ii) Ratio span decreasing the overall ratio

(b) CVT - transmission ratios in the range 5.0 - 0.5 - Perbury traction drive

TABLE 4.2 Effect of Motor Type

Motor type	Cycle	T	m	range (miles)	range (miles) no regen.	Accel. 0-30 mph
D.C.Series	J227aC	95	82/72	53	45	8.8
	30 mph	95	80	121		sec
	40 mph	95	82	89		
D.C.Shunt	J227aC	95	81/61	51	44	12.3
	30mph	95	81	135		sec
	40 mph	95	86	102		
D.C. Switched Reluctance	J227aC	95	81/74	61	49	9.0
	30 mph	95	69	114		sec
	40 mph	95	74	85		
A.C. Induction	J227aC	95	82/71	59	48	9.5
	30 mph	95	84	146		sec
	40 mph	95	88	108		

TABLE 4.3: Effect of Discrete Ratio Transmission using Optimum control

Transmission	Cycle	T	m	range (miles)	range no regen (miles)	Accel. 0-30 mph
2 speed case (i)	J227aC	90	83/70	54	46	11
	30 mph	89	82	124		sec
	40 mph	89	87	93		
2 speed case ii)	J227aC	91	80/60	46	42	No
	30 mph	89	82	124		Adv.
	40 mph	88	87	93		
3 speed case i)	J227aC	90	84/72	57	48	10.3
	30 mph	89	82	124		sec
	40 mph	88	87	93		
3 speed case ii)	J227aC	91	80/60	46	42	No
	30 mph	89	82	124		Adv.
	40 mph	88	87	93		
4 speed case i)	J228aC	90	84/72	57	48	9.8
	30 mph	89	82	124		sec
	40 mph	88	87	93		
4 speed case ii)	J227aC	91	80/60	46	42	No
	30 mph	89	82	124		Adv.
	40 mph	88	87	92		

TABLE 4.4: Effect of Motor Size and Transmission type on Acceleration Performance

	Motor Size (Kw)			
Transmission	50	45	40	35
2 speed case i)	11.0	11.8	13.0	
3 speed case i)	10.3	11.0	12.3	
4 speed case i)	9.8	10.8	11.8	13.5

Baseline - DC Shunt/direct drive - 0.30 mph in 12.3 seconds

TABLE 4.5: Effect of Reduced Motor Size and Transmission type on range - optimum control

Transmission & motor size	cycle	T	m	range (miles)	range no regen (miles)	Accel. 0-30 mph
2 speed case i) 45 KW	J227aC	90	83/70	54	47	11.8
	30 mph	89	83	128		sec
	40 mph	88	88	95		
3 speed case i) 40 KW	J227aC	90	84/72	57	49	12.3
	30 mph	89	85	132		sec
	40 mph	88	88	96		
4 speed case i) 40 KW	J227aC	90	84/73	57	49	11.8
	30 mph	89	83	132		sec
	40 mph	88	88	96		

TABLE 4.6: Effect of CVT on range - optimum control

cycle	T	m	range (miles)	range no regen (miles)
J227aC	84	85/72	53	45
30 mph	85	83	120	
40 mph	85	88	90	

TABLE 4.7: Effect of CVT and Reduced motor size on range - optimum control

cycle	T	m	range (miles)	range No regen (miles)
J227aC	84	86/74	55	47
30 mph	85	85	127	
40 mph	86	88	93	

TABLE 4.8: Effect of CVT plus battery switching on range using optimum control

Combination	cycle	T	m	range (miles)	range no regen (miles)
CVT + 3 switches	J227aC	85	84/76	55	47
	30 mph	85	85	129	
	40 mph	86	88	94	
CVT + 2 switches	J227aC	85	85/76	56	48
	30 mph	85	85	129	
	40 mph	86	88	94	
CVT + 1 switch	J227aC	84	86/76	56	48
	30 mph	85	85	129	
	40 mph	86	88	94	

TABLE 4.9: Effect of Sub-Optimum control on Range using a 3-speed unit

cycle	T	m	range (miles)	range no regen (miles)
J227aC	90	84/73	54	44
30 mph	89	85	132	
40 mph	88	88	96	

TABLE 4.10: Effect of sub-optimum control on Range using a CVT plus battery switching

control	cycle	T	m	range (miles)	range no regen (miles)
locus control + 3 switches	J227aC	84	84/65	51	47
	30 mph	85	85	129	
	40 mph	85	89	95	
locus control + 1 switch	J227aC	85	84/67	52	47
	30 mph	85	85	128	
	40 mph	85	89	95	
Brake speed control + 1 switch	J227aC	85	84/65	51	46
	30 mph	85	83	124	
	40 mph	84	87	91	

TABLE 4.11: Effect of Battery Type on Range for a fixed Battery size

cycle	lead/acid	Ni/Zn	Ni/Fe
J227aC	51	127	93
30 mph	135	237	175
40 mph	102	203	144

TABLE 4.12: Effect of Battery Type on Vehicle Size for a Fixed Urban Range

Battery type	Vehicle Wt(Kg)	Motor (Kw)	Battery Wt(Kg)	Range (miles)		
				J227aC	30 mph	40 mph
Lead-Acid	3600	50	1000	51	135	102
Ni/Zn	2670	40	370	52	105	81
Ni/Fe	2800	40	450	50	89	71

TABLE 4.13: Effect of braking Regime on Energy usage at the wheels

Braking Regime	Energy (Kwhr)			Range (miles)
	Total	Diss in Brakes	Net after Brakes	
Ideal + Arm+Field	0.08404	0.00564	0.07840	51
Ideal-Field only	"	0.05574	0.02830	45
Parallel	"	0.01681	0.06723	50
Split	"	0.00763	0.07640	51

CHAPTER 5

Hybrid Electric Vehicle Drive-Train Configurations

5.1 Introduction

Of the two fundamental hybrid-electric vehicle drive-train configurations introduced in chapter 1, it was seen that they differed only by the way in which the traction motor and heat-engine power sources were connected in each case. When the traction motor and heat-engine were connected in series a hybrid-electric vehicle was said to be of a 'series' configuration, whereas when they were connected in parallel the hybrid-electric vehicle would then be of a 'parallel' configuration.

The fundamental parallel configuration is shown in Figure 5.1 and consists of the i.c. engine and traction motor connected by fixed transmission ratios. The i.c. engine would have a coupling device (COUPL) between it and the rest of the drive-train, since the inability of this power source to operate below a minimum set speed would mean that it would either have to be disconnected under these circumstances, or 'soft'-coupled by means of a slipping clutch or torque converter. The characteristics of this drive-train configuration are that the fixed transmission ratio selected for one power source will tend to compromise, or limit, operation of the other, and also because neither power source can be matched to all road conditions.

Similarly,the fundamental series configuration is shown in Figure 5.2 and consists of the i.c. engine power source in series, via a generator, with the traction motor which, in turn is connected to the road-wheels via fixed transmission ratio. As was discussed in chapter 1, the characteristics of this drive-train configuration are that it is inefficient because of the larger number of energy conversions than for the parallel case and also because the traction motor must be rated to meet full vehicle power requirement - making it operate inefficiently over mild cycles. Because of the electrical connection, the i.c. engine may be

matched to all road conditions, but because of the fixed transmission ratio, this is not possible for the traction motor.

Within the confines of each fundamental configuration there are several configurations made possible by the inclusion of components into the vehicle drive-line in order to overcome the shortcomings just discussed. For the parallel configuration it is possible to include a variable ratio transmission for either or both power sources and so improve operation for all vehicle operating conditions. However, in the case of the series configuration it is only possible to include a variable ratio transmission for the traction motor power source, as the i.c. engine power source is connected to the road wheels via a motor/generator set - in effect an electrical CVT.

The various parallel drive-train configuration alternatives are shown in Figures 5.3 to 5.6, and the single series drive-train configuration alternative shown in Figure 5.7. An additional transmission alteration is possible for the parallel configuration, in that a clutch may be added to the traction motor to enable this power source to be disconnected when running on the i.c. engine alone, with the result that the traction motor mechanical loss-load may be removed from the total transmission load.

A further hybrid-electric configuration is apparent for the series configuration if the i.c. engine is connected to the wheels via differential gearing, thus forming a power path between the i.c. engine and the road wheels that may be split in varying proportions between the direct mechanical path and the less efficient but 'soft' electrical CVT path (Figure 5.8). This transmission arrangement will combine the efficiency benefits of the parallel configuration with the advantage of decoupling the i.c. engine from the road wheels made possible with the series configuration, and has been the subject of several studies in the past (Beachley et al.,1973) (Dorey et al.,1984) - both in hybrid-electric and mechanical hybrid forms.

Despite the obvious advantages of this transmission because it is the subject of a separate study in the Department of Engineering at the University of Durham it will therefore not be included in the study presented here.

So far only configuration changes have been discussed for the mechanical power transmission paths of the series and parallel drive-trains, but any changes to their respective electrical systems would amount to changes in component type - such as alternative traction motors, motor controllers and battery types - with the drive-train configuration remaining constant. Since it is the purposes of this chapter to consider the inclusion or removal of drive-train components relative to the fundamental series and parallel configurations of Figures 5.1 and 5.2, such changes will not be studied.

Finally, as with the electric vehicle study of chapter 4, it will be appropriate to study the effects of hybrid-electric drive-train configuration for a vehicle class that would be the most likely applications.

In chapter 1, the discussion on the road-transport sector energy usage highlighted the 'medium sized' passenger car as having the largest single market and having the greatest potential for petroleum displacement. Furthermore in chapter 4, it was also concluded that the occasional long range requirement of certain road-vehicles - in particular the passenger car - may not prevent the penetration of the electric vehicle concept, if, for European market conditions, the hybrid-electric solution was adopted.

Therefore, for the European market conditions and energy usage trends considered so far, the vehicle class that is the most likely application of the hybrid-electric concept is the medium-sized passenger car, and it is this class of vehicle that will form the basis of the study here.

5.2 Vehicle Parameters

As was the case with the electric vehicle study in chapter 4, a true comparison of drive-train configuration can only be made if the vehicle configuration has the same aerodynamic drag, rolling loss characteristics - assumed achievable, whatever the drive-train configuration. The parameters chosen to represent these characteristics were done so to be fairly representative of what will be readily achieved for this vehicle class in the near-term on the basis of present day values and current trends (Autocar,1981)(B.L. cars)(Ford Motor Co.U.K.)

When comparing hybrid-electric drive-train configurations an important effect to consider when components are added to or subtracted from a drive-train is that of vehicle weight changes. As with the electric vehicle study of chapter 4, the automatic weight algorithm, described in chapter 2, is used to assemble the relevant vehicles from a common base or bodyshell weight which is simply the vehicle kerb weight minus the powertrain weight. The value of the common body-shell weight was derived using current medium sized passenger cars as the basis, and projected forward to the near-term (Autocar,1981)(B.L. cars)(Ford Motor Co.UK).

A full list of all vehicle parameters that are assumed to form a common base -whatever the drive-train configuration - are shown in table 5.1.

Other vehicle parameters such as transmission ratios, power source ratings and traction battery size are therefore vehicle parameters that do vary between certain drive-train configurations and have their values selected on the basis that a given vehicle configuration has to meet a set of performance requirements thought to be typical of the medium sized passenger car. The performance requirements are also shown in table 5.1 and consist of a 0-60 mph acceleration time of 10-15 seconds and a vehicle maximum speed, achievable using the i.c. engine power source only, in

excess of 80 mph, to represent long distance travel on motorways. Figure 9 shows typical torque-speed characteristics for both i.c. engine and traction motor with the parallel configuration in mind - both separately and superimposed. An i.c. engine power rating of 30-35 KW will satisfy a 'steady' maximum cruise speed of >80 mph. The traction motor rating - also 30-35 KW - is therefore what is required over and above the i.c. engine rating to meet the acceleration requirement.

In the case of the series configuration, given that any incurred weight penalty will not significantly affect the power requirement at cruise, the same i.c. engine power rating to meet the steady maximum cruise speed will apply, but the traction motor power rating will be that necessary to meet the maximum speed requirement and/or the vehicle accleration requirement alone - and is also shown in table 5.1.

With the wheels radius fixed at a value typical of this vehicle class, the overall transmission ratio will consist of either the final drive alone or the combination of final drive and variable ratio transmission. The fundamental series and parallel configurations have no variable ratio transmission and therefore the final drive ratio must be selected on the basis of the vehicle performance requirements. For both series and parallel configurations, the ratio selected will be a compromise of the high ratio requirement of vehicle acceleration and the low ratio requirement of vehicle maximum speed.

With the exceptions of the parallel configurations where a variable ratio transmission is included for one power source only - Figures 5.4 and 5.5 - the final drive ratio in a transmission incorporating a variable ratio unit can be fixed at a typical value along with the wheel radius, discussed previously, and any changes to the overall transmission ratio, along with the ratio span, made using the variable ratio unit. For the

parallel case where the variable ratio unit only operates for the traction motor, the final drive ratio will be as for the fundamental parallel configuration in that it will be a compromise of acceleration performance and vehicle maximum all ICE speed. However the parallel case where the variable ratio unit only operates for the i.c. engine, the final drive ratio can be given the fixed typical value of above, but the traction motor drive ratio (DRIVE) would have to be modified from the 1.0:1 ratio used for all other cases, to a value that will enable satisfactory all electric operation with the fixed typical final drive ratio used. This ratio will compromise all-electric acceleration performance and all-electric maximum speed.

Three variable ratio transmissions are to be considered for the appropriate configurations of this study to represent different ratio spans. A 4-speed unit is used with a 3.5:1 ratio span - though to be a minimum for all i.c. engine operation over the entire vehicle operating speed range, as this is the limiting factor since the traction motor will typically have a 25% greater speed range than the i.c. engine (0-5000 rpm compared with 1000-5000 rpm). (Thring, 1982). The 6-speed unit increases the ratio span by simply including 2 over-drive ratios onto the 4-speed unit as increasing the maximum ratio (1st gear ratio) simply serves to improve vehicle starting from rest. (Morello,1977). Finally the CVT unit considered here is the Perbury traction drive (Stubbs, 1981) and incorporates both a high starting ratio and a 'deep' overdrive ratio, with the added advantage of an infinite number of ratios in between these extremes.

The individual ratios for both 4 and 6-speed cases are fixed at typical values for the ratio spans considered, as a more detailed discussion of transmission parameters is given in chapter 6. The ratios selected are also shown in table 5.1.

Finally, the traction battery sizes in each case were chosen to give the same all-electric urban range to battery discharge. This range was chosen at 20-25 miles and was thought to give the useful all-electric operation that is fundamental to the hybrid-electric vehicle when used in sensitive urban areas. A lighter battery resulted for the parallel configuration because the series configuration requires the increased storage capacity to compensate for the increased vehicle weight (due to the presence of the generator and the requirement of the large traction motor) and the poorer drive-train efficiency. Nevertheless, the fundamental series configuration still does not meet the basic performance requirements for this class of vehicle. Increasing battery weight further to improve all-electric range would increase the 0-60 mph acceleration time and increasing motor size to improve the 0-60 mph acceleration time would reduce motor efficiency and all-electric range. Furthermore because the final drive ratio, for both the fundamental parallel configuration and the parallel configuration with a variable ratio transmission for the traction motor only, was a compromise of acceleration performance and vehicle maximum speed, it follows that these two configurations do not meet the basic performance requirements either.

In section 5.1 it was stated that variations in component type would not be considered in this chapter, so therefore each configuration will have a fixed set of component types. These types are typical of present day and near-term technology and comprise of a gasoline i.c. engine, a D.C. shunt traction motor, a transistor chopper motor controller and a lead-acid traction battery. It is assumed throughout the study that regenerative braking is possible with an 'ideal' braking regime - as discussed in chapters 2 and 4.

As is typical of European passenger car testing conditions, comparison will be made for each configuration over the ECE-15 urban cycle (shown in Figure 5.10), at a steady 56 mph cruise and at a steady 75 mph cruise, and throughout the comparison the optimum control algorithm, described in chapter 2, will be used in order to determine transmission ratios, torque and power-splits and generator-set speed - where appropriate. Furthermore, it is assumed that for the near-term timescale considered for hybrid introduction that the concept of shutting off the i.c. engine during vehicle stationary and deceleration periods (idle and overrun respectively) will be feasible as it is already being introduced by several manufactuers to varying extents at present (B.L. cars)(VW).

Therefore for all configurations to be considered in this study, fuel-cut off at idle and overrun will be assumed.

5.3 Description of Parallel Configurations

Using the optimum control algorithm, described in chapter 2, the three control variables for the parallel configuration will be the torque or power split, the primary (i.c. engine) power source transmission ratio (where applicable) and the secondary (traction motor) power source transmission ratio (also where applicable). The common control variable to all parallel configurations will be the torque or power split between the two power sources.

In chapter 2, the functions of the energy source (and hence power source) weighting factors, λ_1 and λ_2, were described - where subscript 1 refers to the primary source and subscript 2, to the secondary source. One of the functions was to penalise one on-board energy source relative to the other - so enabling the vehicle over a given driving cycle, to depend less upon the penalised source - and is achieved by choosing a suitable value of λ_1 relative to λ_2 (in effect λ_1/λ_2). Thus at a value of

equal to zero, the hybrid-electric configuration will run on the i.c. engine only as the traction motor has been heavily penalised for the optimisation procedure. Similarly for an increasing value of λ_1/λ_2 , the penalty on the traction motor will decrease and hence the vehicle dependency on this power source will increase, up to the point when all-electric operation occurs.

By plotting the ratio of the weighting factors, λ_1/λ_2 , against the energy consumptions of the two power surces (mpg in the case of the i.c. engine and effectively range to battery discharge in the case of the traction motor), for values of λ_1/λ_2 ranging from zero until the vehicle runs in an all-electric mode, an overall picture of the energy consumption of any given hybrid-electric configuration can be obtained.

5.3.1 Fundamental Parallel Hybrid-Electric Con figuration

The results of range and mpg versus the weighting factors ratio λ_1/λ_2 are shown in Figure 5.11 for the fundamental parallel configuration described by the block diagram of Figure 5.1. Because no variable ratio transmissions are present in the drive-line, the control variable to be optimised is the torque or power split fraction X. The final drive ratio selected does not permit urban (ECE-15) operation on the i.c. engine alone and also limits the maximum speed to 70 mph. Increasing the ratio to permit all i.c. engine urban operation will simply reduce the maximum speed permissible even further.

5.3.2 Including a variable Ratio Transmission for the I.C.Engine only

The configuration resulting from the inclusion of a variable ratio transmission for the i.c.engine power source only is shown in Figure 5.4 and the corresponding results, in terms of mpg and range versus λ_1/λ_2 ,

are shown for the 3 transmission options in Figure 5.12. The control variables for this configuration are the torque split fraction, X, and transmission ratio, GR.

5.3.3 Including a Variable Ratio Transmission for the Traction Motor Only

Figure 5.5 shows the drive train configuration of a single variable ratio transmission for the traction motor alone, and the corresponding graph of mpg and range versus λ_1/λ_2 for the 3 possible transmission options is shown in Figure 5.13. It is interesting to note that because there is no variable ratio transmission acting for the i.c. engine, operation on this power source alone is therefore resticted by the final drive ratio selected - as was the case for the fundamental configuration the ratio selected is a compromise between acceleration performance and vehicle maximum speed.

Again, control variables for this configuration are the torque split fraction, X, and the transmission ratio, GR.

5.3.4 Including Variable ratio Transmission for each On-Board Power Source

The drive-train configuration having 2 variable ratio transmissions - one for each power source - is shown in Figure 5.6 and the results in terms of mpg and range versus λ_1/λ_2 are shown in Figure 5.14.

With this drive-train configuration, not only is it possible to have 2 discrete ratio units (both 4 and 6 speeds) or CVT units, but also a combination of discrete ratio and CVT units for both power sources.

The control variables for this configuration are now the torque split fraction, X, the primary (i.e. engine) power source transmission ratio, GR, and the secondary (traction motor) power source transmission ratio, GR1.

This configuration has the obvious advantage over the configurations just described of being able to select a transmission ratio appropriate to each power source simultaneously for a given driving condition (road-load). Additionally, as with the configuration having a transmission acting for the traction motor only, this configuration has the ability to reduce the motor mechanical loss-load when in the i.c. engine only mode. This can be achieved, providing suitable overdrive ratios are available, by selecting the lowest ratio in the traction motor transmission and hence reducing motor shaft speed compared to the cases with no secondary transmission present.

5.3.5 Including a Variable Ratio Transmission down-stream of the Torque-split point

The drive-train configuration resulting from the inclusion of a single variable ratio transmission downstream of the torque split point is shown in Figure 5.3 and the results in terms of range and mpg versus λ_1/λ_2, shown in Figure 5.15.

This configuration offers a compromise solution between the relative simplicity of the single transmission cases and the operating flexibility (all i.c. engine, all-electric and hybrid modes) of the 2 transmission case. However this transmission arrangement does not allow the motor mechanical loss-load on the i.c. engine to be reduced as the i.c. engine is coupled to the traction motor via a fixed ratio.

5.3.6 The Effect of Decoupling the Traction Motor from the Drive-line During the I.C. engine only Mode

Decoupling the traction motor from the drive-train during the i.c. engine only mode serves to completely remove the motor mechanical

loss-load from the i.c. engine and as such forms an alternative to selecting a transmission ratio in the secondary variable ratio transmission for those configurations where this is included.

Therefore, the effect of such a clutch can only be sensibly studied in a drive-train configuration that has no secondary transmission, and so it is proposed to study this effect on the configuration having the single variable ratio unit downstream of the torque-split in section 5.3.5 - the results of which are shown in Figure 5.16.

5.4 Description of Series Configurations

Again, as with the parallel configuration, results for the series configuration can be presented in terms of mpg and range versus λ_1/λ_2 , but unlike the parallel configuration, there is only one drive-train alternative to the fundamental series configuration - that of introducing a variable ratio transmission between the traction motor and final drive.

The control variables common to both configurations are therefore the power split fraction, X, and the generator set speed, RE.

5.4.1 Fundamental Series Configuration

The block diagram of the fundamental series configurations shown in Figure 5.2 and the energy consumption results, in terms of mpg and range versus λ_1/λ_2 , shown in Figure 5.17. As was described in 5.2, the final drive ratio selected is a compromise between vehicle acceleration performance and maximum permissible speed, so therefore even with an acceleration performance that does not meet the basic requirements, vehicle speed is limited to 70 mph.

The control variables for this configuration are the power-split fraction,X, and the generator set speed, RE.

5.4.2 Including a Variable Ratio Transmission between the Traction Motor and Final Drive

The drive-train configuration with a variable ratio transmission included between the traction motor and final drive is shown in Figure 5.7 and the corresponding results in Figure 5.18.

With this configuration it is possible to reduce the final drive ratio, from that of the fundamental configuration to some arbitrary value, in order to achieve a greater vehicle maximum speed without compromising the vehicle acceleration performance, as the ratio span in the variable ratio unit (being a minimum of 3.5:1) will cover ratios from the acceleration extreme to the cruising extreme.

The control variables for this configuration are now power split fraction, generator set speed and variable ratio transmission ratio. The transmission ratio selected using the optimum control algorithm will enable better matching between the traction motor and road load characteristics, the extent of which will depend upon the number and spread (span) of ratios.

5.5 Discussion of Results

It seems logical when considering the drive-trains just described in 5.3 and 5.4, because of the fundamental differences between series and parallel configurations, to consider the drive-train alternatives within these categories before embarking upon a comparison between the two.

5.5.1 Parallel Configurations

Moving away from the fundamental parallel configuration and considering the configuration with a single variable ratio transmission acting on the i.c. engine only - shown in Figures 5.4 and 5.12 - several

differences are now apparent. Firstly the variable ratio transmission enables all i.c. engine operation over the ECE-15 cycle. Secondly maximum cruising speed is raised, using the i.c. engine only, from 70 mph to >80 mph and fuel consumption at 56 mph is reduced due to the availability of lower transmission ratios - so enabling i.c. engine speed to be reduced and i.c. engine load-factor (torque loading) and hence efficiency to be increased. Finally, in the hybrid mode mpg for a given range, and vice-versa, is increased due to the above increases in i.c. engine efficiency, which, incidentally offset any shortfall in transmission efficiency by the inclusion of the additional component. However, all-electric range shows no improvement due to the fact that the traction motor drives through a similar transmission ratio. Furthermore, the mechanical loss-load on the i.c. engine is increased due to the necessity of the 1.5:1 traction motor drive ratio, necessary for all electric operation - so undercutting the cruise gains.

Of the 3 transmissions considered, the 4 and 6 speed units show no differences over the urban cycle, although at 56 mph the 6-speed unit shows reduced fuel consumption due to the overdrive ratios enabling i.c. engine load-factor to be increased. At 75 mph the overdrive ratios cannot be used because there is insufficient power available from the i.c. engine, so 4 and 6 speed results are identical. The CVT transmission shows increased fuel consumption relative to the 4 and 6 speed units at 75 mph and 56 mph due to the inherently poorer transmission efficiency offsetting any increases in i.c. engine efficiency. However over the urban cycle, both in the all i.c. engine mode and the hybrid mode, results relative to the 4 and 6 speed units are improved - both in terms of mpg for the former case and mpg for a given range for the latter.

Next to consider is the configuration, again, with a single transmission, but acting upon the traction motor only - shown in Figures 5.5 and 5.13. Because, as with the fundamental configuration, the i.c. engine drives through a fixed ratio, all i.c. engine operation is not possible over the urban cycle, and also cruise performance is similar in that maximum speed is restricted. All electric operation over the urban cycle is increased in terms of range due to the availability of high transmission ratios in the variable ratio unit enabling motor speed to be kept high and in an operating region of high efficiency. Hybrid performance is improved relative to the fundamental configuration due to the variable ratio unit generally improving motor efficiency, but over a limited portion of the hybrid operating range - defined by λ_1/λ_2 - shows greater mpg for a given range than the configuration with the transmission acting on the i.c. engine.

Of the 3 transmissions the CVT shows lower fuel consumption at cruise and generally higher mpg for a given range over the urban cycle relative to the 4 and 6 speed units. The cruise results may be explained by the low overdrive ratios available in the CVT enabling the mechanical loss-load on the i.c. engine to be reduced, for both 75 mph and 56 mph cases. Over the urban cycle, the higher transmission ratios available in the CVT enables motor efficiency to be higher and offsetting the poorer efficiency of the CVT unit.

Moving now to the configuration with a variable ratio transmission acting on each power source - shown in Figures 5.6 and 5.14 - the benefits of the variable ratio transmissions acting upon the two power sources in turn are now combined. All i.c. engine operation is now possible over the urban cycle. Vehicle maximum speed is raised above 80 mph when using the i.c. engine only. Cruise fuel consumption is reduced due to the lower transmission ratios available enabling i.c. engine load-factors and

efficiency to be raised. Finally hybrid performance is generally improved to all 3 configurations previously discussed in terms of mpg for a given range due to the high transmission ratios in the secondary transmission raising motor efficiency and the low transmission ratios in the primary transmission raising i.c. engine load-factors and efficiency. In each case, the increases in prime-mover efficiency offset the reductions in overall transmission efficiency due to the inclusion of the additional components.

Results for the 5 transmission combinations considered here are also shown in Figure 5.14. For the urban cycle there is no noticeable difference between the 2 x 4 speed and 2 x 6 speed combinations as the overdrive ratios for the i.c.engine/6-speed unit cannot be used at such low load and hence i.c. engine speeds due to the limits to available power from the unit. At the 56 mph cruise, however, the overdrive ratios in the 6-speed unit can be used and so due to the increased i.c. engine load factor and efficiency fuel consumption is reduced. Additionally the overdrive ratios in the traction motor transmission enables the motor mechanical loss-load on the i.c. engine to be reduced, thus making a contribution to the fuel consumption reduction. At 75 mph, due to the limits of i.c. engine power not allowing the primary transmission overdrive ratios to be used, the small gain the 2 x 6 speed combination has over the 2 x 4 speed combination is due solely to the reduction of the motor mechanical loss-load.

The 2 x CVT combination shows improvements over the 2 x 4 and 2 x 6 speed combinations for the urban cycle in terms of mpg for a given range because the increases in i.c. engine efficiency due to its transmission's overdrive ratios and the increases in motor efficiency due to its transmission's maximum ratios are not offset by reduced transmission efficiency. At cruise, however, the poorer efficiency inherent for the

CVT relative to the discrete ratio units means that the gains in i.c. engine efficiency due to the overdrive ratios of both transmissions (increased i.c. engine load factor and reduced motor mechanical loss load) are being offset and no improvement is apparent relative to the 2 x 4 speed combination.

Of the CVT/discrete ratio combinations, the CVT/motor - 4 speed/i.c. engine case shows improved hybrid performance in terms of mpg for a given range over the 2 x 4 and 2 x 6 speed combinations due to the improved motor efficiency offsetting the reduction in secondary transmission efficiency over the urban cycle. However, the CVT/i.c. engine - 4 speed/motor combination shows no improvement in mpg for a given range compared to the 2 x 4 and 2 x 6 speed combinations due to the improvements in i.c. engine efficiency being offset by the reductions in primary transmission efficiency. This indicates that in the case of the 2 x CVT combination, the CVT acting on the traction motor is yielding the largest contribution to the overall gain over the 2 x 4 and 2 x 6 speed combinations. At both 56 mph and 75 mph cruises, due to reduction in the mechanical loss-load on the i.c. engine, the CVT/motor - 4 speed/i.c. engine gives a reduction in fuel consumption over the 2 x 4 speed case but not over the 2 x 6 speed case as no overdrive ratios are available to the i.c. engine in the 4 speed unit considered here. The CVT/ i.c engine - 4 speed motor combination at cruise shows an increase in fuel consumption relative to the 2 x 4 speed combination because the gains in i.c. engine efficiency are being offset by reduced transmission efficiency and also because no overdrive ratios are available in the secondary transmission considered here in order to reduce the mechanical loss-load on the i.c. engine.

Finally, moving to the drive-train configuration having a single variable ratio transmission downstream of the torque-split point - shown in Figures 5.3 and 5.15 - a compromise solution to the 2 transmission

configuration is offered in terms of reducing general complexity but increasing energy consumption. Over the urban cycle both all i.c. engine and hybrid energy consumptions are of the order of 10% higher than for the 2 transmission case, although all-electric performance remains unchanged. When in the all i.c. engine mode, this configuration does not have the facility of reducing the motor mechanical loss-load, and when in the hybrid mode, the transmission ratio selected does not match both prime movers to the road load conditions to the same extent as is possible for the ratios selected in the 2 transmission case. At cruise, again, fuel consumption is generally higher because of inability to reduce the motor mechanical loss-load.

Of the 3 transmissions considered, over the urban cycle, the 4 speed and 6 speed units show no noticeable difference due to the limits to i.c. engine power under these conditions not allowing the overdrive ratios of the 6 speed unit to be used. The CVT does show a small improvement in terms of mpg for a given range, but over a narrow hybrid operating range, as defined by λ_1/λ_2 due to improvements in motor efficiency not being offset by reduced transmission efficiency. At the two cruise regimes, the picture is very much the same as for several of the other configurations in that the 6-speed unit only shows a benefit over the 4 speed unit at 56 mph because the limits to i.c. engine power at 75 mph prevent the overdrive ratios of the 6 speed unit being used. The CVT shows increased fuel consumption both at 56 mph and at 75 mph relative to the 4 speed case because the significant reduction in transmission efficiency inherent for this unit is tending to more than offset any increases in i.c. engine efficiency.

This drive-train configuration can also be used to study another aspect of the hybrid-electric power train - that of decoupling the traction motor from the drive-line when in the i.c. engine only mode in order to

remove the mechanical loss-load on the i.c. engine. The results for the drive-trains with and without motor clutches are shown in Figures 5.16 for the 4 speed transmissions case only. Over the urban cycle energy consumption is only reduced in the all i.c. engine mode whereas during hybrid-electric operation, although the mpg and range curves diverge, mpg for a given range remains unchanged. At cruise in the all i.c. engine mode, because of the removal of the motor mechanical loss-load on the i.c. engine, results for both 56 mph and 75 mph show reductions in fuel consumption relative to the drive-line with no motor clutch.

5.5.2 Series Configurations

Results, again, in terms of mpg and range with the weighting factors ratio λ_1/λ_2 are shown for the fundamental series configuration (described by the block diagram of Figure 5.2) in Figure 5.17. In common with the fundamental parallel configuration this configuration is unable to operate over the ECE-15 urban cycle on the i.c. engine alone and the final drive ratio selected - being a compromise between acceleration and maximum cruise speed performance - limits vehicle maximum speed to 70 mph.

By including a variable ratio transmission into the fundamental series configuration -shown in Figures 5.7 and 5.18 - ratios may be selected to improve the match between the traction motor and road-load characteristics of the vehicle in that there will be a minimum ratio available to achieve cruise speeds of > 70 mph, a maximum ratio available to maintain acceleration peformance requirements and a spread of ratios in between to enable motor efficiency to be maintained higher over a range of road-load conditions compared to a fixed ratio transmission. The result is that because of the improvements made to traction motor efficiency, all i.c. engine operation is now possible over the urban cycle (since the traction motor is a part of the all i.c. engine drive-train), all electric urban

range is increased and hybrid performance - in terms of range for a given mpg - is improved. In all urban cases the improvements in traction motor efficiency are not offset by reduced mechanical transmission efficiency due to the inclusion of the additional component. However, at cruise the reduction in transmission efficiency is more than offsetting any gains in motor efficiency and so all i.c. engine cruise fuel consumption is increased relative to the fundamental series configuration.

Of the 3 transmission types considered, over the urban cycle there is no difference between the 4 and 6 speed units as the over-drive ratios in the latter case are not used to increase motor efficiency, since generally increasing motor speed will tend to place an operating point in a region of high motor efficiency. The CVT case, however, does show urban improvements over the 4 and 6 speed units as the larger maximum ratio for this unit does make a contribution to increasing motor efficiency, despite the reduced transmission efficiency relative to the discrete ratio cases. At cruise, the picture is reversed with the poorer transmission efficiency inherent for the CVT more than offsetting any gains in motor efficiency, and therefore increasing fuel consumption relative to the 4 and 6 speed discrete ratio units.

5.5.3 Series Versus Parallel Configurations

Having discussed the various drive-train configuration possibilities within the series and parallel general alternatives, in sections 5.51 and 5.52, it is now possible to take the most promising series and parallel configurations and compare their results.

The most promising parallel configuration relative to the fundamental configuration is clearly the 2 tansmission case of Figures 5.6 and 5.14, but with the alternative to this in terms of simplicity being the configuration with the single transmission down-stream of the torque-split point of

Figures 5.3 and 5.15. Similarly, for the series configuration the most promising configuration, which, incidentally forms the only alternative to the fundamental configuration, is the configuration with the inclusion of a variable ratio transmission in between the traction motor and final drive - shown in Figures 5.7 and 5.18.

When a comparison between the single series and two parallel configurations in terms of all i.c. engine urban fuel consumption, urban hybrid mode energy consumption in terms of mpg for a given range, all i.c. engine cruise fuel consumption and all electic urban range, the well reported shortcomings of the series configuration compared to the parallel configuration are apparent. Firstly, all i.c. engine urban fuel consumption for the series case is twice that for the parallel case, partly because of the inefficient chemical-mechanical-electrical-mechanical energy conversion route for the former compared to the chemical-mechanical route for the latter, and partly because of the inherent weight increase of the series configuration over the parallel configuration due to the large traction motor and traction battery requirements. The large traction motor required is also inefficient under part-load urban duty compared with the much smaller unit in the parallel configuration. Secondly urban hybrid energy consumption in terms of mpg for a given range for the best series case with a CVT is still 20-30% above that for the best parallel configuration with 2 transmissions, again due to the relatively inefficient power transmission path and weight increase. Thirdly all i.c. engine cruise fuel consumption is of the order of 20% greater for the series configuration, but on this occasion only due to the inefficient power train since vehicle weight plays a much smaller role in the vehicle energy requirements at cruise than for ubran duty. Finally the all electic range for the series case is comparable to that of the parallel cases for the simple reason that as all-electric range is thought to be a fundamental

hybrid-electric vehicle performance requirement, the traction battery was sized to meet this - with the aforementioned knock-on effects in terms of vehicle weight and traction motor size.

5.6 Optimum Control of the Hybrid Electic Vehicle

Although in section 5.5 a comparison was made between the various hybrid-electric options available using the optimum control algorithm to select the best values of control variable in each case - so forming a common control base for comparison - the behaviour of the control strategy was not considered.

In this section, therefore, it is proposed to consider the optimum control strategy in more detail and to do this it is approriate to consider the results from one drive-train configuration.

Because the parallel configuration, from the results of 5.5 appears to have greater importance than the series configuration, and also because the configuration with the single transmission downstream of the torque-split point offers a good compromise of complexity and energy consumption, it is therefore proposed to study this case only.

From the results presented for this configuration in Figure 5.14 it is apparent that below a given λ_1 / λ_2 value of 0.36, no battery discharge (effectively infinite range) is experienced over the ECE-15 urban cycle. The corresponding mpg figure is also higher than that for all i.c. engine urban operation. At this value of $\lambda_1/\lambda_2 \equiv 0.36$, the energy taken from the battery during acceleration - for all-electric and/or hybrid operation - is being replaced by the energy recovered using regenerative braking during vehicle deceleration. The electrical system is therefore simply being used as a 'load-leveller', and as a result when in this mode, the control strategy will seek to save energy (the 'energy saving' aim) over the conventional i.c. engined vehicle as liquid fuel is the only on-board energy that is consumed.

For values of $\lambda_1/\lambda_2 > 0.36$ energy that would otherwise come from the liquid fuel tank is now being displaced or substituted, in an increasing proportion as increases, by energy taken from the traction battery. Over this range of λ_1/λ_2 values, the control strategy will seek to substitute liquid fuel using on-board electrical energy and has been previously described as the 'petroleum substitution' aim.

For a value of $\lambda_1/\lambda_2 = 0.36$, the objective function, described in chapter 2, can be plotted for values of torque split fraction, X, if the gear ratio, GR, is held constant at 1.0:1. Figure 2.39 showed the variation of objective function, F, with torque split fraction, X, for time intervals in the ECE-15 cycle at 56 and 65 seconds - to represent typical acceleration and cruise conditions respectively (Figure 5.10). The value of X ranges from zero to 2.0. For values of X >1.0, the i.c. engine is being used to both meet the road-load and to charge the battery if power is available, and shows a constant value of F at cruise but an upward trend in F during acceleration. At cruise, i.c. engine load factor is low due to the road load alone and with increasing generating requirements (increasing X > 1.0) the gains in i.c. engine efficiency are compensating for the increased power requirement. During acceleration, however, i.c. engine load-factor is already high due to the road-load, so increasing the load factor further may serve (and does so in this case) to reduce i.c. engine efficiency - resulting in a rising value of F with X.

The two other points of interest on the objective function curves of Figure 5.19 occur when the i.c. engine is turned on (X = 0 - 0.05) and when the traction motor is turned off (X = 0.95 - 1.0). When the i.c. engine is turned on, the objective function takes a step increase, which for the acceleration point is greater because of the increased absolute value of load on 'load-pickup' - being the same fraction of road load in each case. Figure 2.39 also shows how the value of F is increased at X = 0

when the i.c. engine fuel is not cut at idle, and indicates that under certain 'mild' cruising conditions, the penalty imposed upon all electric operation at X = 0 may favour the use of the i.c. engine alone rather than the traction motor alone.

Now at the value of X where the traction motor is turned off, the alternatives of decoupling the motor or allowing the i.c. engine to meet the mechanical loss-load have already been discussed. However there is a third alternative in that the electrical system can be used to supply power to the motor to meet its own mechanical losses. Figure 2.39 shows the effect on F of both the i.c. engine and the electrical system meeting the motor mechanical losses, indicating that the former case is to be favoured, besides which, the latter case will result in battery discharge - so range limiting all i.c. engine cruising operation. The reason why the function F takes a step decrease when the i.c. engine meets the mechanical losses of the motor, is because of the discontinuinity in moving from the motor efficiency map at X = 0.95 to the JANUS assumptions of motor mechanical losses at X = 1.0.

It is also possible using this same drive-train configuration to study gear-shifts and the torque/power splits between the two power sources in order to determine any emerging patterns. Figure 5.19 is a usage plot on the i.c. engine performance map for the energy saving aim ($\lambda_1/\lambda_2 = 0.36$), and shows where gear shifting (using a 4 speed unit in this case) is placing the operating points over the ECE-15 cycle. It is apparent that the usage points (in %) congregate around the region of maximum i.c. engine efficiency. In Figure 5.20 a plot of i.c. engine torque versus time for the ECE-15 cycle is shown at $\lambda_1/\lambda_2 = 0.36$, and indicates that engine torque lies in the region of 80-90% of maximum during acceleration. Now Figure 5.21 shows the variation in transmission

ratio with time over the cycle (which is also shown) and shows, apart from occasional erratic shifting, that shifting is generally smooth. Finally Figure 5.22 shows the variation of X with time over the cycle and quite clearly shows that almost without exception that a torque split of 1.0 or 0 is being favoured and any fraction in between, a result of the i.c. engine not being able to meet the road-load alone - as is shown between 135 and 145 seconds.

A similar set of graphical results can also be produced for a typical petroleum substitution aim at a λ_1/λ_2 value of 0.5 - shown in Figure 5.15. Again Figure 5.23 shows the i.c. engine usage data, and although the usage points still congregate around the region of maximum efficiency, the grouping has now contracted. The i.c. engine torque/time variation of Figure 5.24 that although, the i.c. engine on-time has decreased to just for the heavy load conditions during acceleration - with the exception of the 1st cruise which is performed using the i.c. engine in high gear with a slipping clutch - the i.c. engine load is still being maintained between 80-90% of maximum. Figure 5.25 shows the plot of X versus time and, again, indicates that with the exception of the heavy load condition at the end of the 3rd acceleration, torque split fractions of 1.0 or 0 are being favoured. Finally, the variation in gear ratio with time on Figure 5.26 shows that the majority of gear-shifting is performed smoothly over the cycle.

When the i.c. engine fuel flow is not cut during idle periods - as was discussed previously - for the energy saving case when $\lambda_1/\lambda_2 = 0.36$ a very similar set of graphical output is obtained to that of the case when the fuel is cut, and these are shown in Figures 5.27 to 5.30. During an ECE-15 cycle an energy saving hybrid returns a fuel consumption of 38 mpg when the fuel is not cut at idle, compared with a fuel consumption of 50 mpg when it is cut at idle - ably demonstrating the importance of the fuel-cut-off at idle concept for hybrids or conventional i.c. engined vehicles over urban cycles with substantial idle and deceleration periods.

5.7 Conclusions

Using fundamental series and parallel configurations as a basis from which to study drive-train configurations, two parallel configurations and a single series configuration have emerged from the discussion as giving significant improvements in terms of energy consumption and operational flexibility. The series configuration incorporates a variable ratio transmission in between the traction motor and final drive, whereas for the parallel configurations, one includes a variable ratio transmission for each power source and the other, a single transmission downstream of the torque-split point.

When comparing the series configuration with either of the two parallel configurations, the weight and efficiency penalties inherent for the series case, at least for the class of vehicle being considered here, make this configuration significantly poorer in terms of energy consumption.

Of the two parallel configurations considered, although the 2 transmission case yields an overall urban energy saving of up to 10% over the single transmission case, the drive-train configuration and control system required would be significantly more complex. Furthermore in the simulation study it has been assumed that no weight penalty will result for the 2 transmission case relative to the single transmission case since the weight algorithm in JANUS (see chapter 2) assumes that a transmission element handling half the power requirement of another will be half of the weight - which may or may not be the case in practice.

Additional energy saving features of the parallel hybrid drive-train, such as decoupling the traction motor when not in use, are again subject to the degree of complexity one wishes to building into vehicle whilst at the same time considering the likely gains to be achieved.

Because the gains suggested by the studies of the 2 transmission and/or the decoupled motor drive trains do not seem to justify the added complexity, unreliability and cost to the user, it is therefore proposed to concentrate the studies of the remaining chapters on the parallel drive-train with a single transmission downstream of the torque split point - as shown in Figure 5.3.

By using the parallel configuration chosen here as a basis from which to make comparison, the effects of variations in the vehicle parameters, that were chosen to be fixed here, can be studied, but again because of the requirement of a common control base the optimum control strategy should be used. As any control strategy developed using the optimum may well be parameter dependent, a study of such a control strategy would best be performed using as few vehicle parameter variations as possible.

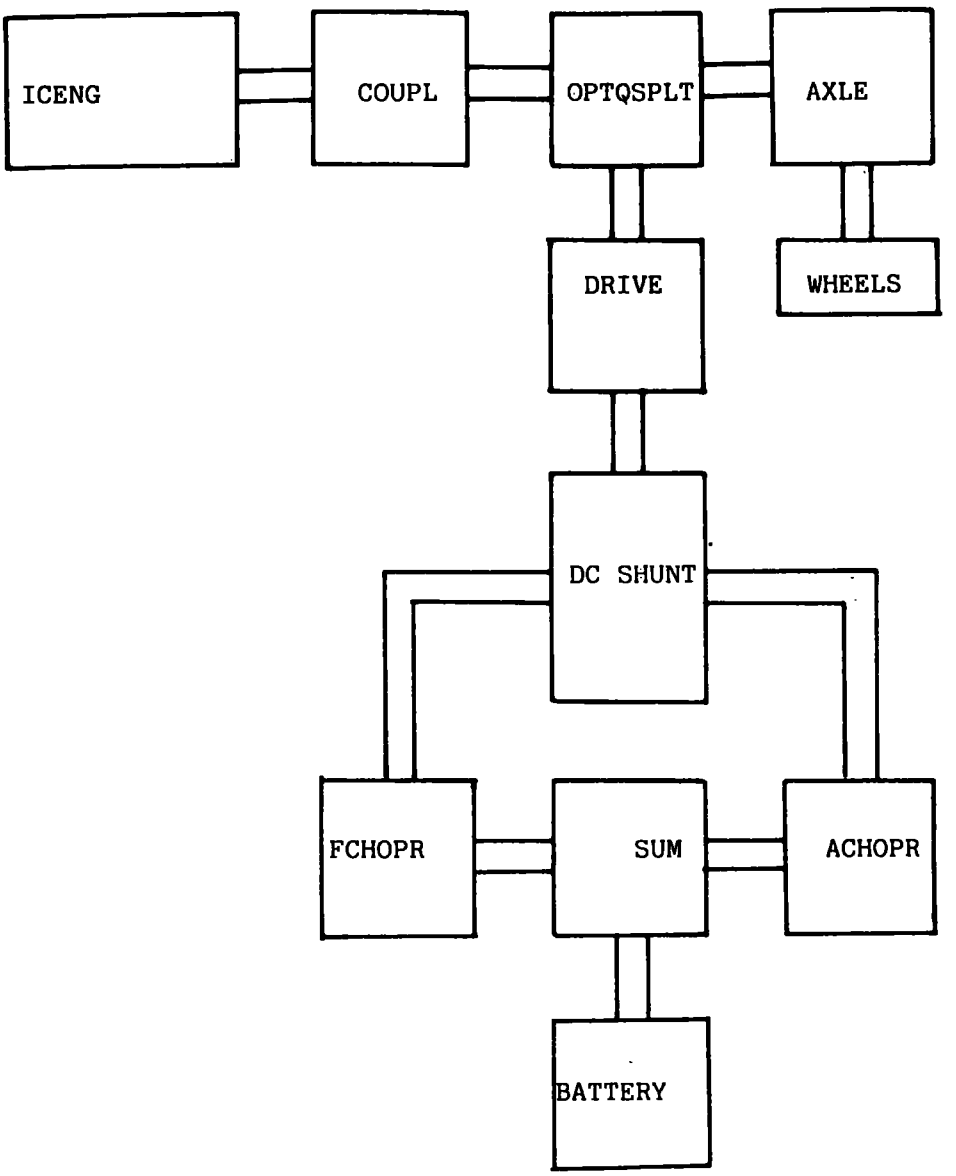

FIGURE 5.1: Fundamental Parallel Configuration

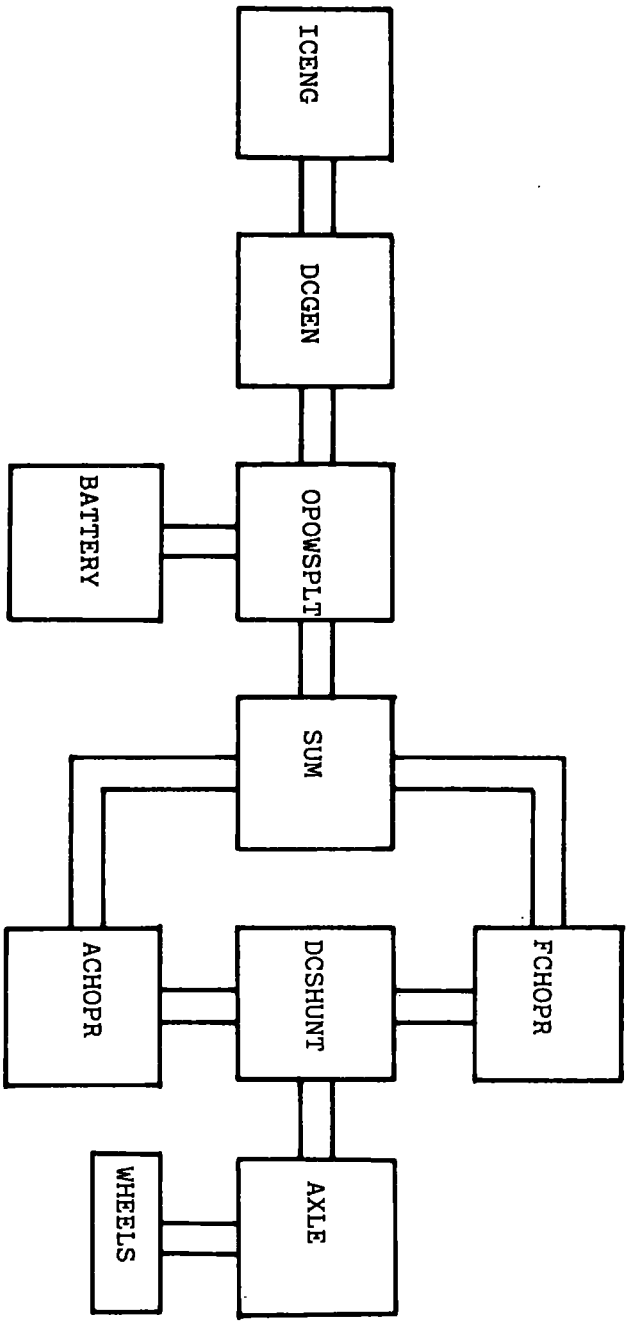

FIGURE 5.2: Fundamental Series Configuration

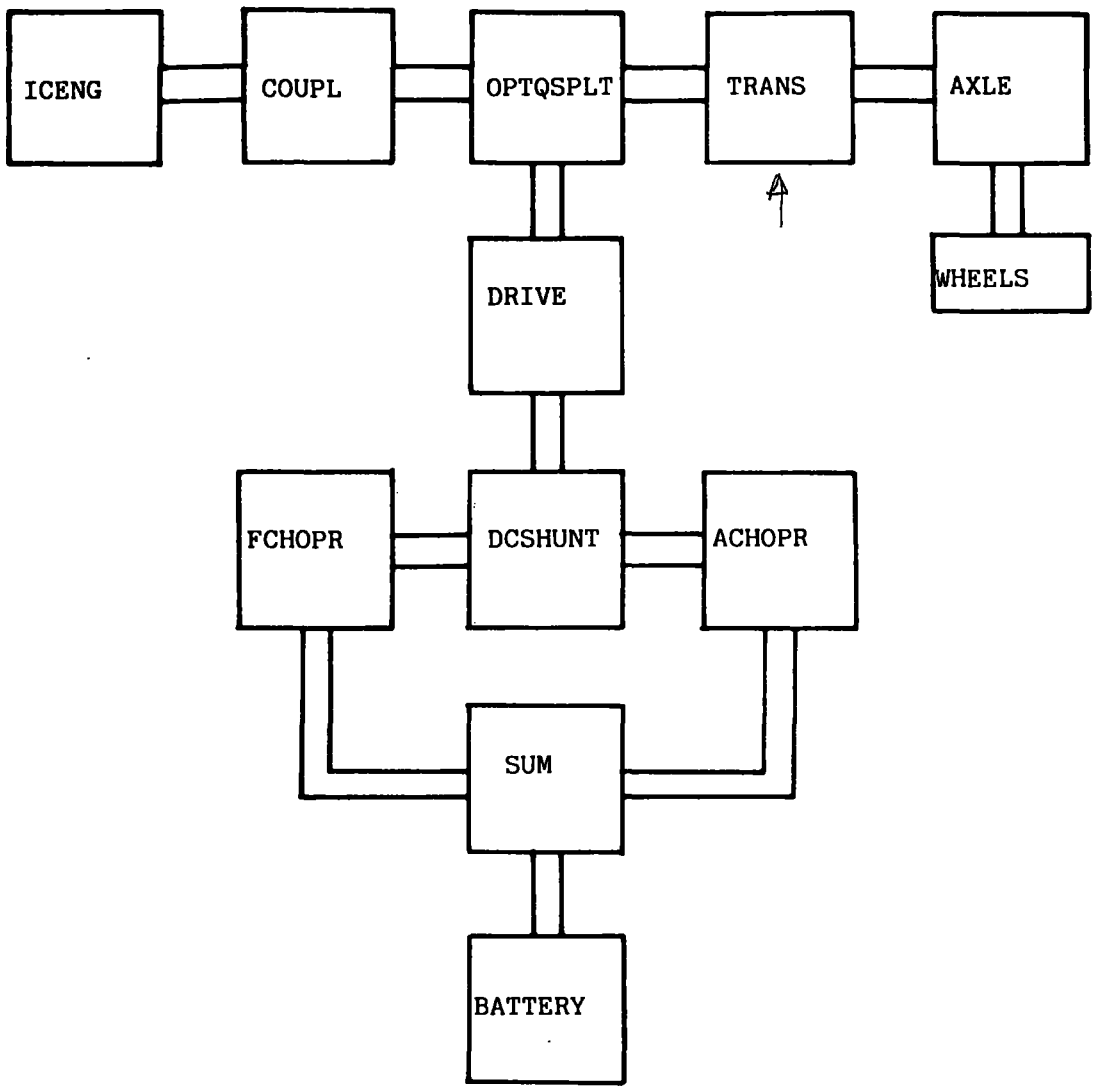

FIGURE 5.3: Including a Single Variable Ratio Transmission Downstream of the Torque Split Point in the Fundamental Parallel Configuration.

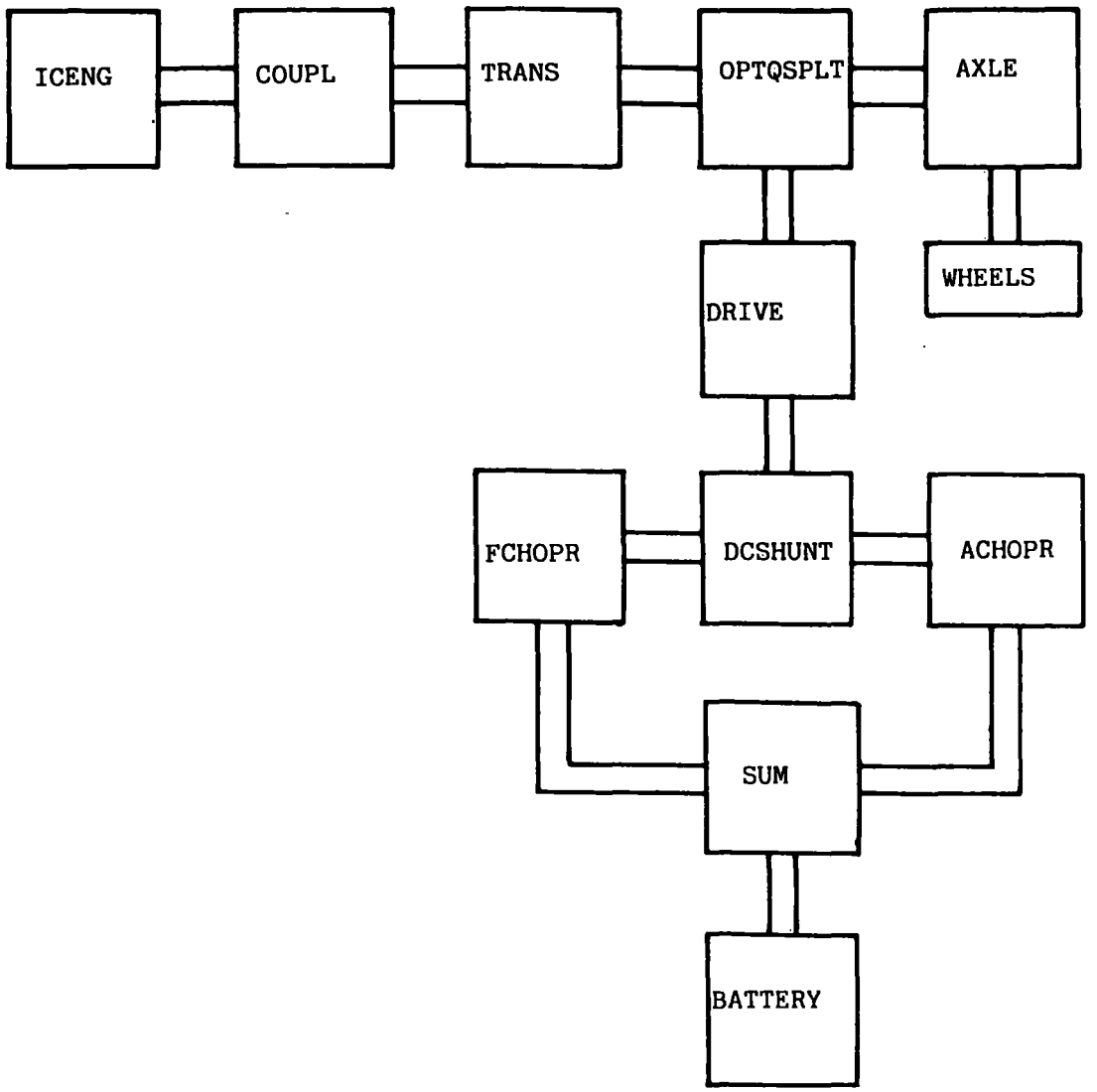

FIGURE 5.4: Including a Variable Ratio Unit on the I.C.Engine only in the Fundamental Parallel Configuration.

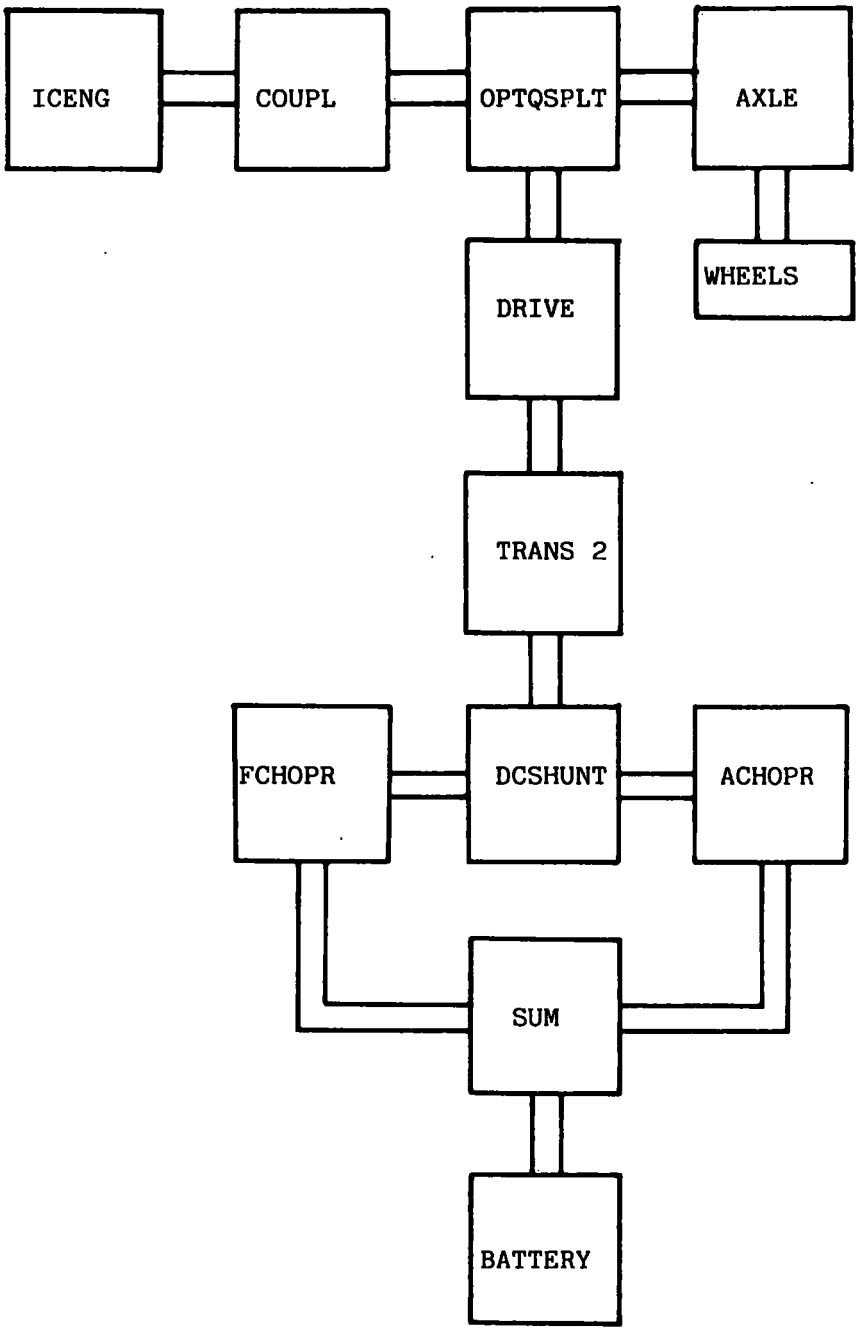

FIGURE 5.5: Including a Variable Ratio Unit on the Traction Motor only in the Fundamental Parallel Configuration.

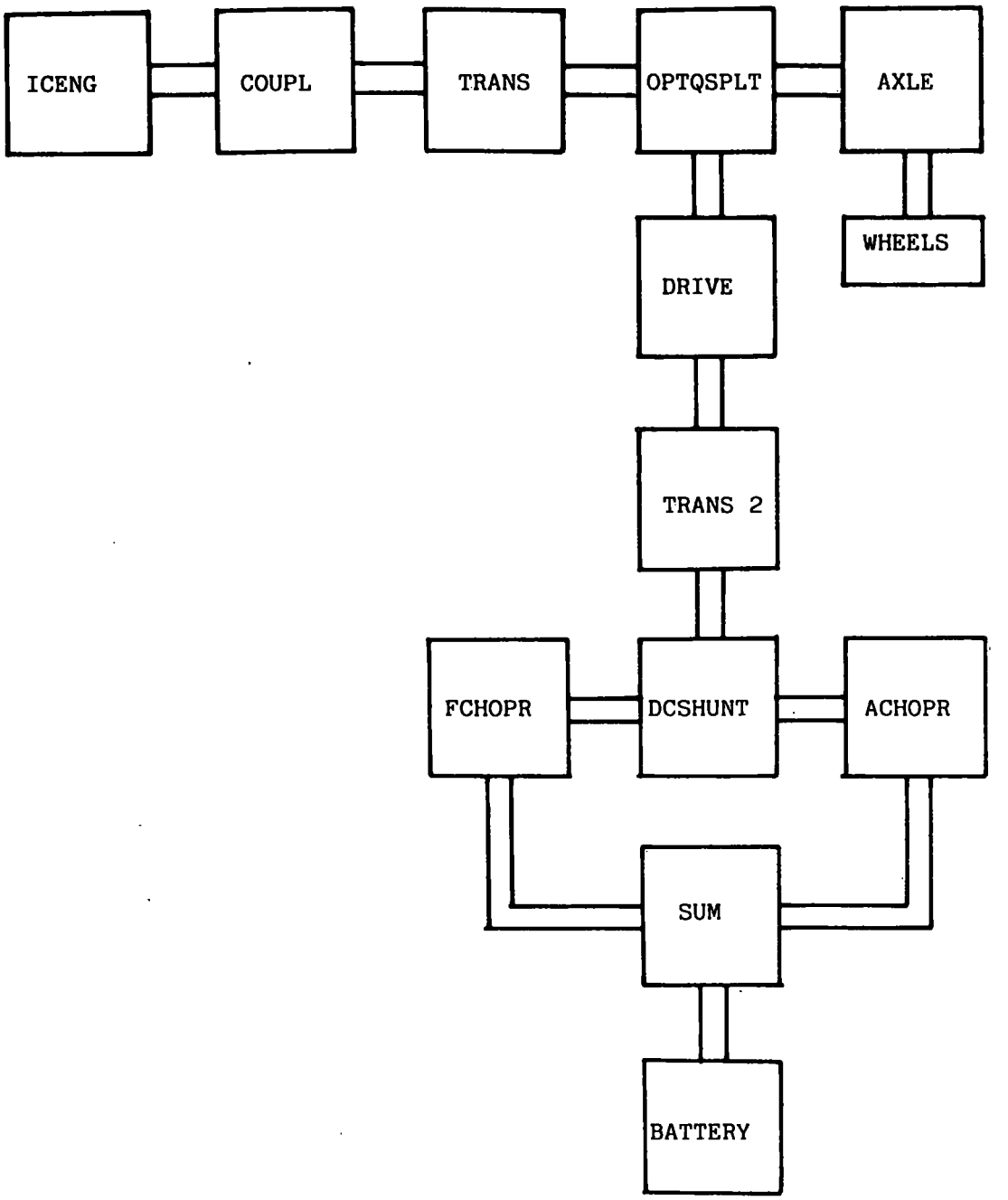

FIGURE 5.6: Including a Variable Ratio Unit for Each Power Source in the Fundamental Parallel Configuration.

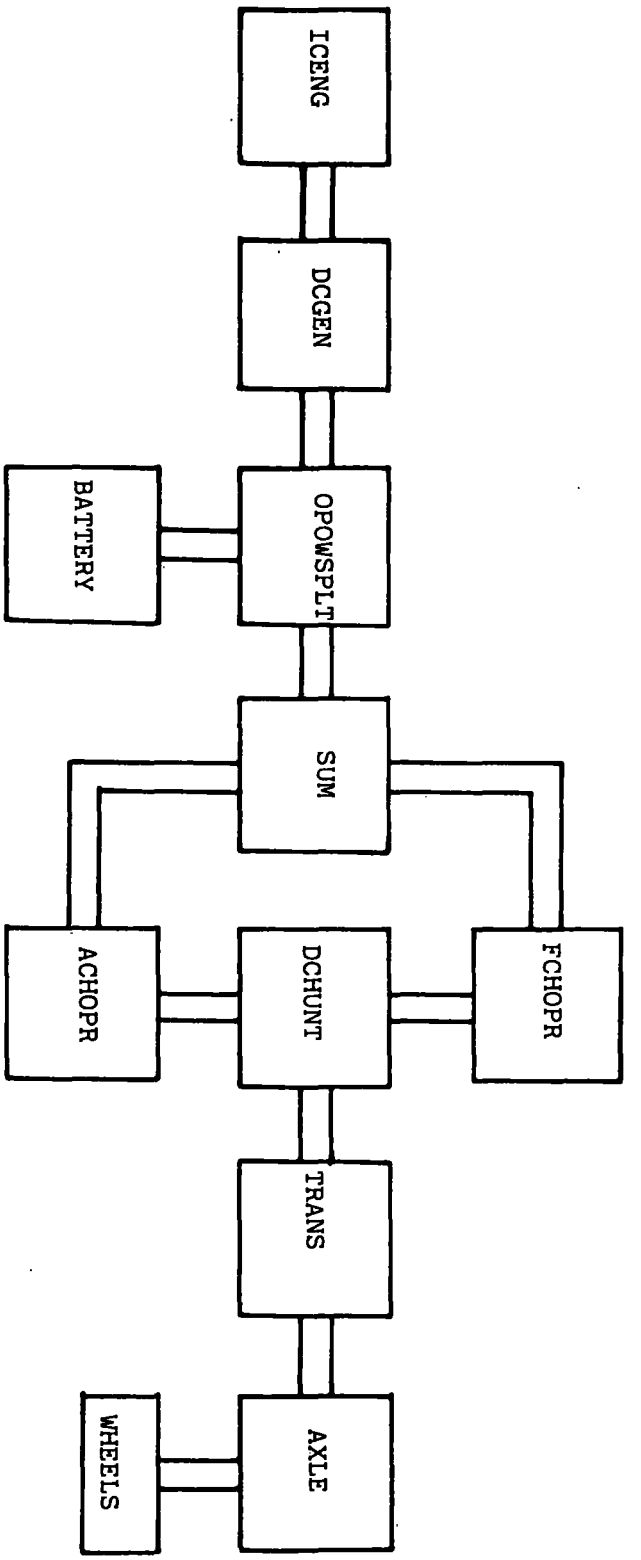

FIGURE 5.7: Including a Variable Ratio Transmission for the Traction Motor in the Fundamental Series Configuration

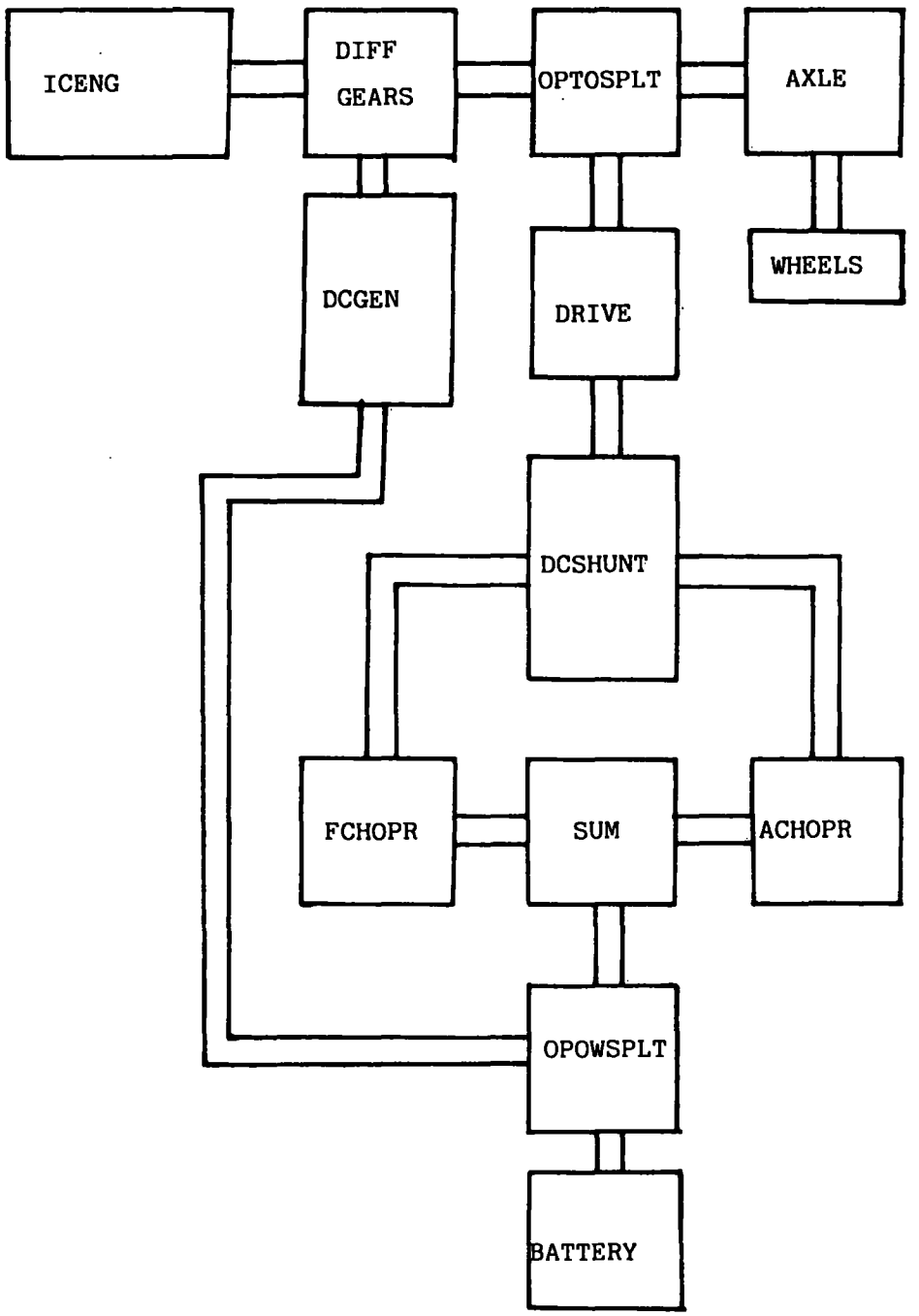

FIGURE 5.8: An Alternative Hybrid Electric Power Split Drive Train Configuration

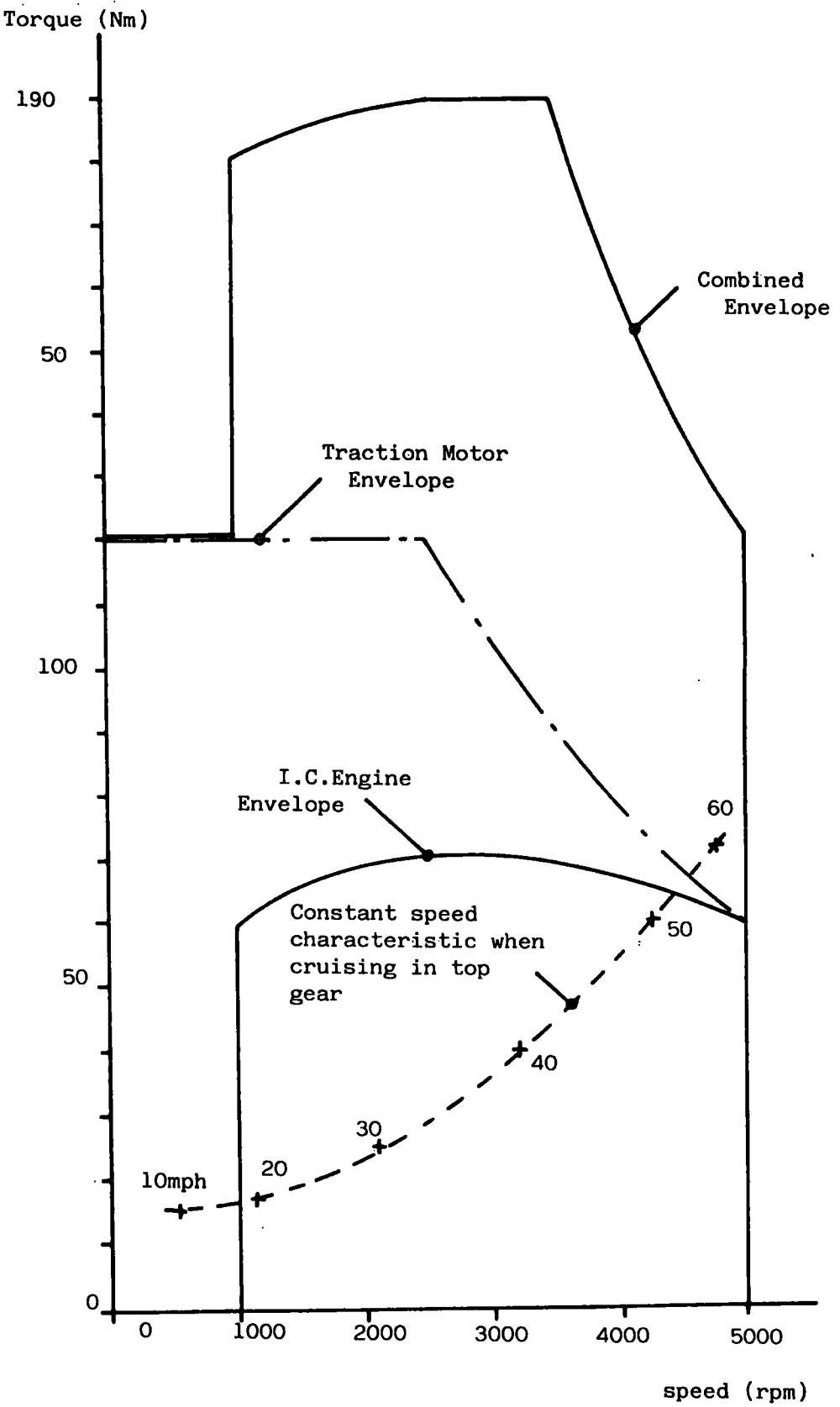

FIGURE 5.9: Combined Traction Motor and I.C. Engine Characteristics for the Hybrid Electric Vehicle

FIGURE 5.10: ECE-15 Urban Cycle

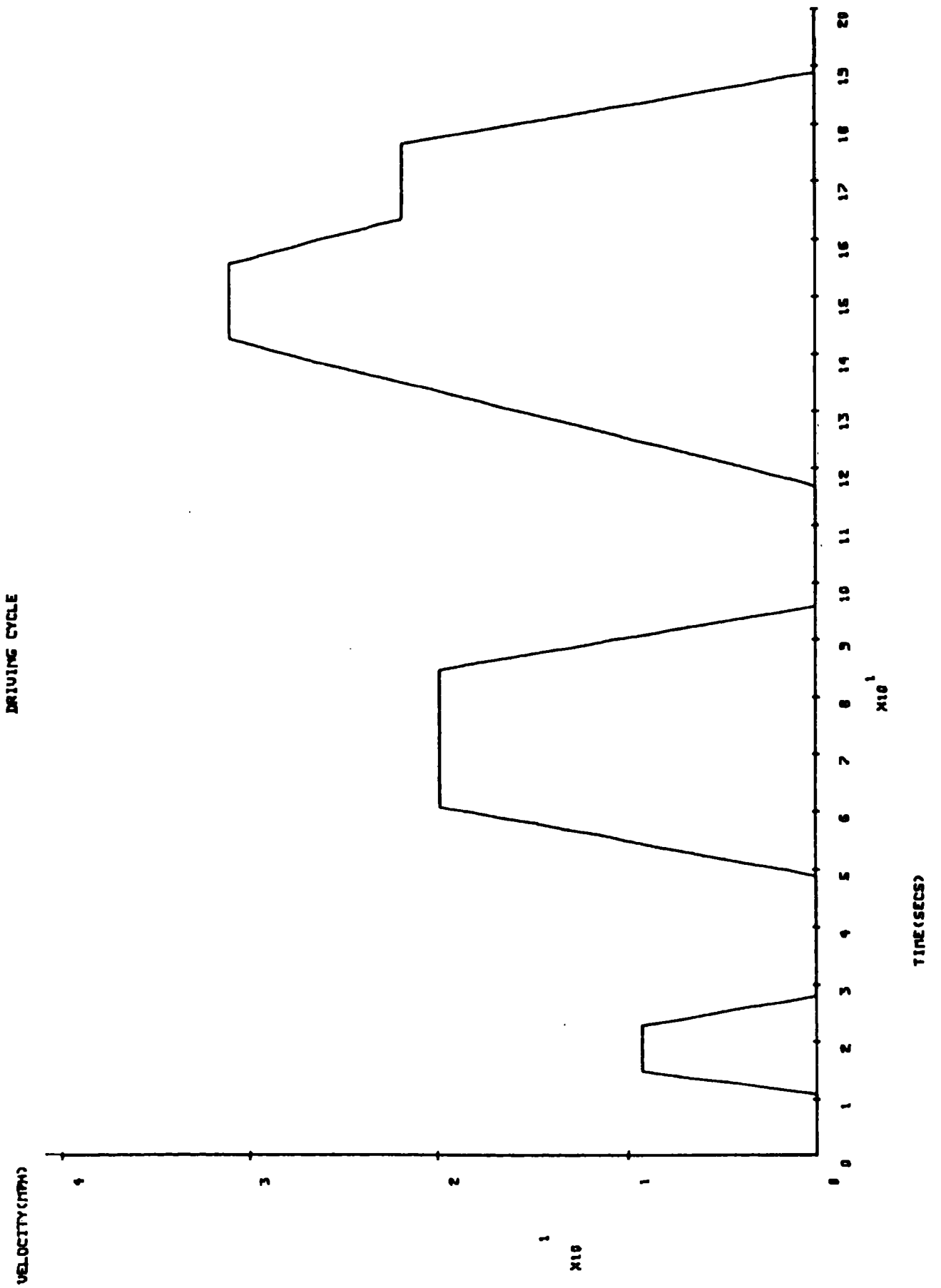

FIGURE 5.11: Range/mpg versus λ_1 / λ_2 for the Fundamental Parallel Configuration

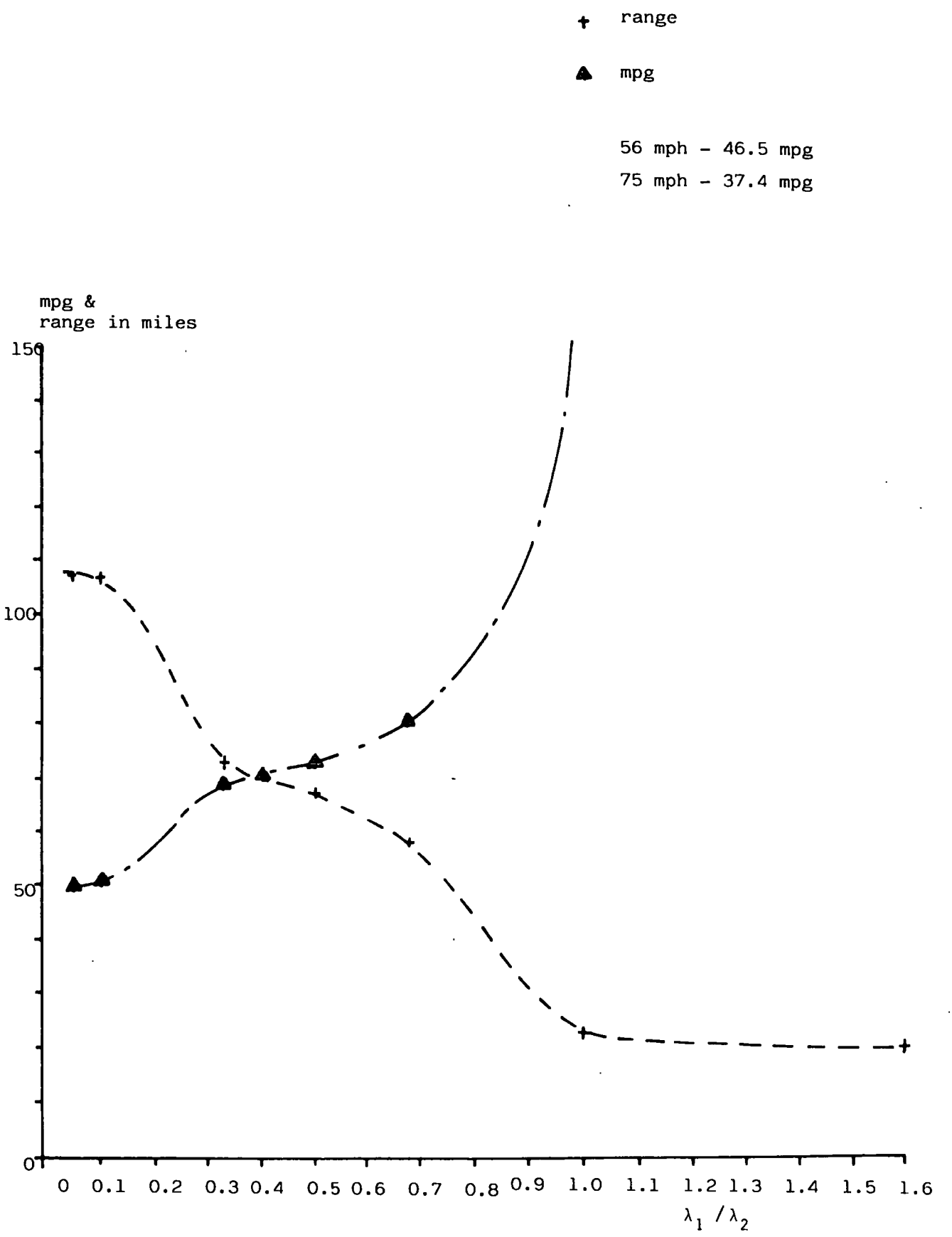

FIGURE 5.12: Range/mpg versus λ_1/λ_2 for the Fundamental Parallel Configuration with a variable ratio unit included for the i.c. engine only

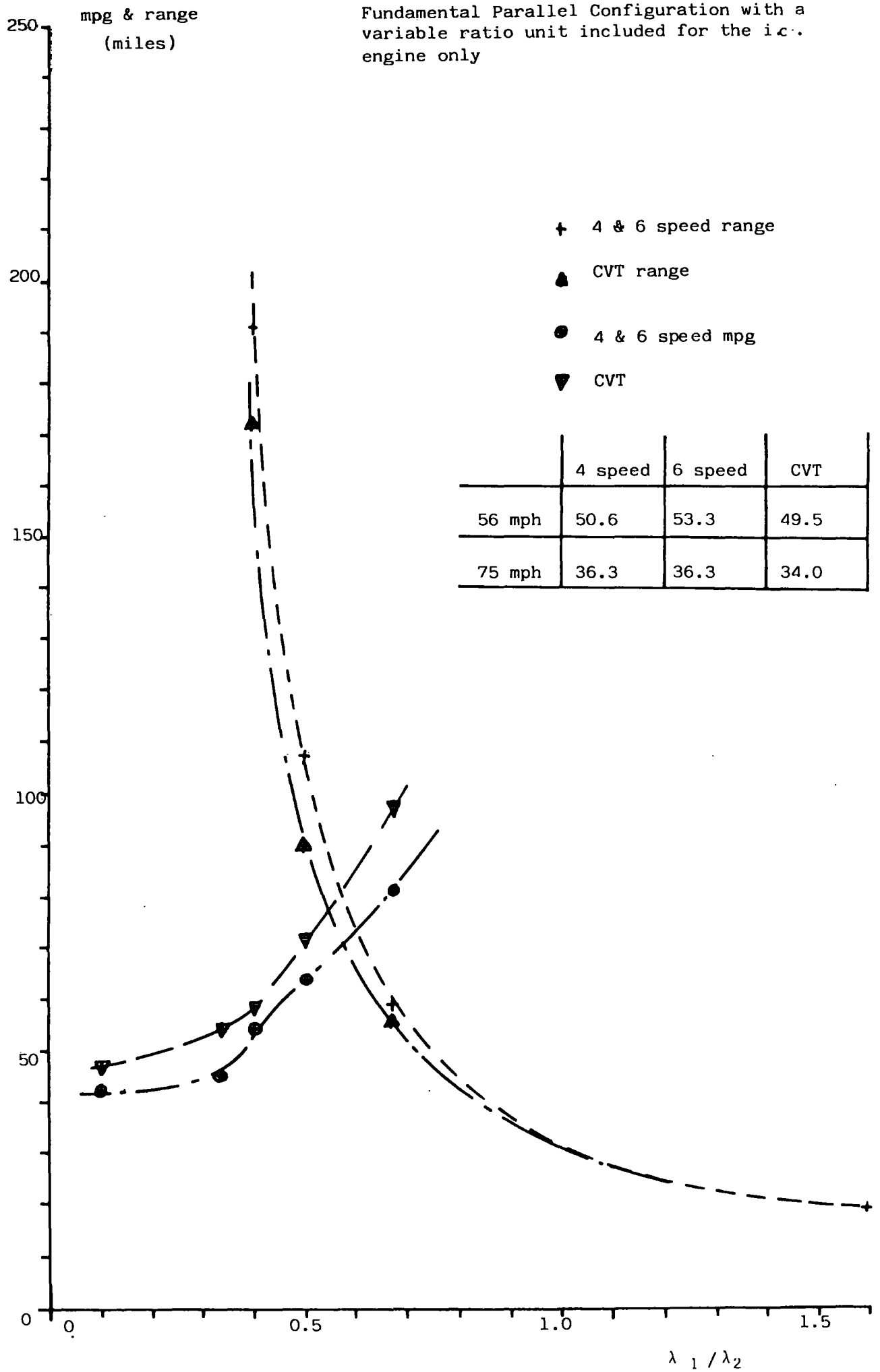

	4 speed	6 speed	CVT
56 mph	50.6	53.3	49.5
75 mph	36.3	36.3	34.0

FIGURE 5.13: Range/mpg versus λ_1 / λ_2 for the Fundalmental Parallel Configuration with a Variable Ratio Unit included for the Traction Motor only.

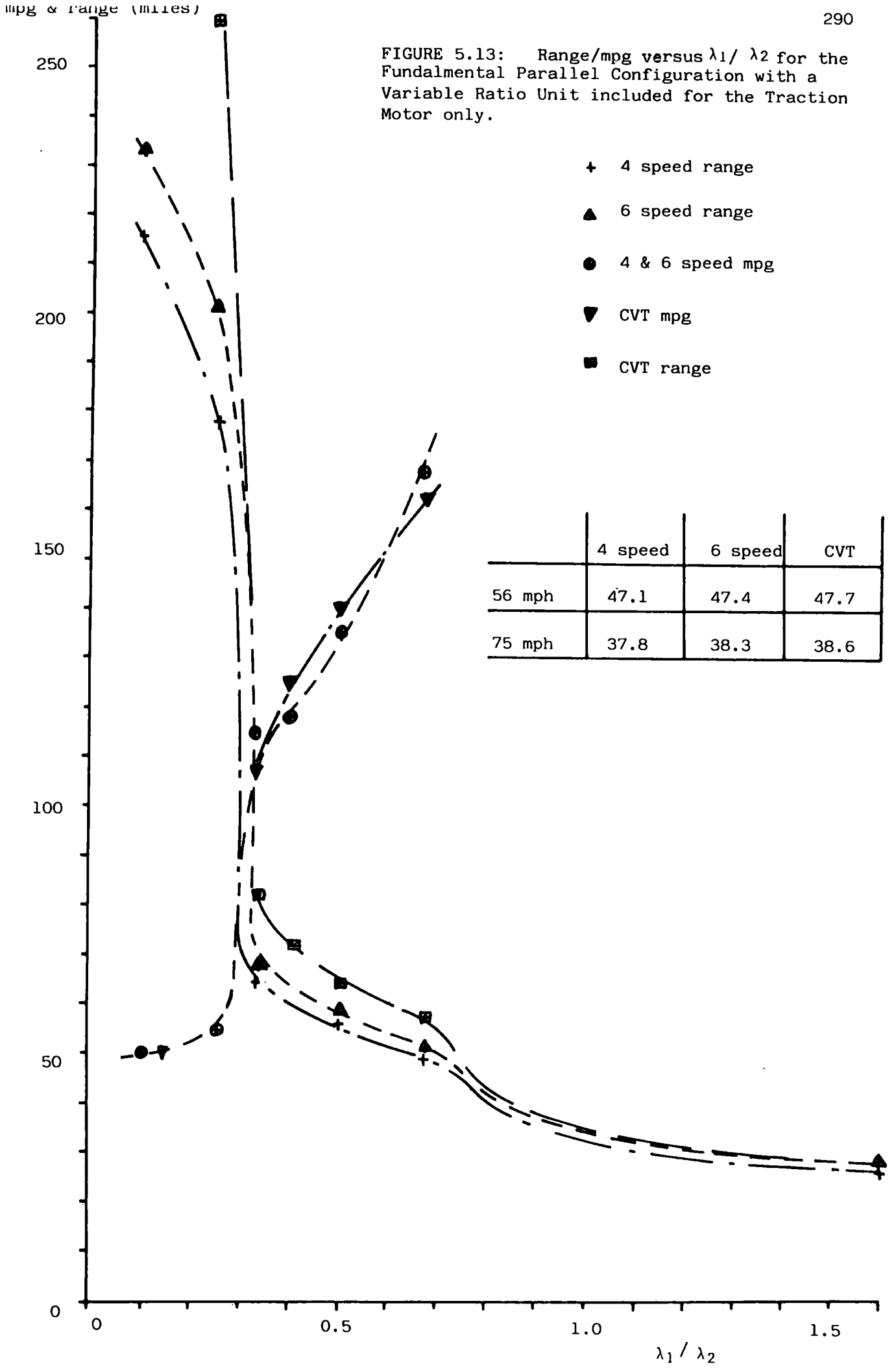

	4 speed	6 speed	CVT
56 mph	47.1	47.4	47.7
75 mph	37.8	38.3	38.6

	4 speed x 2	6 speed x 2	CVT x2	A	B
56 mph	52.2	56.2	52.6	50.9	53.8
75 mph	36.3	36.9	36.1	35.0	37.2

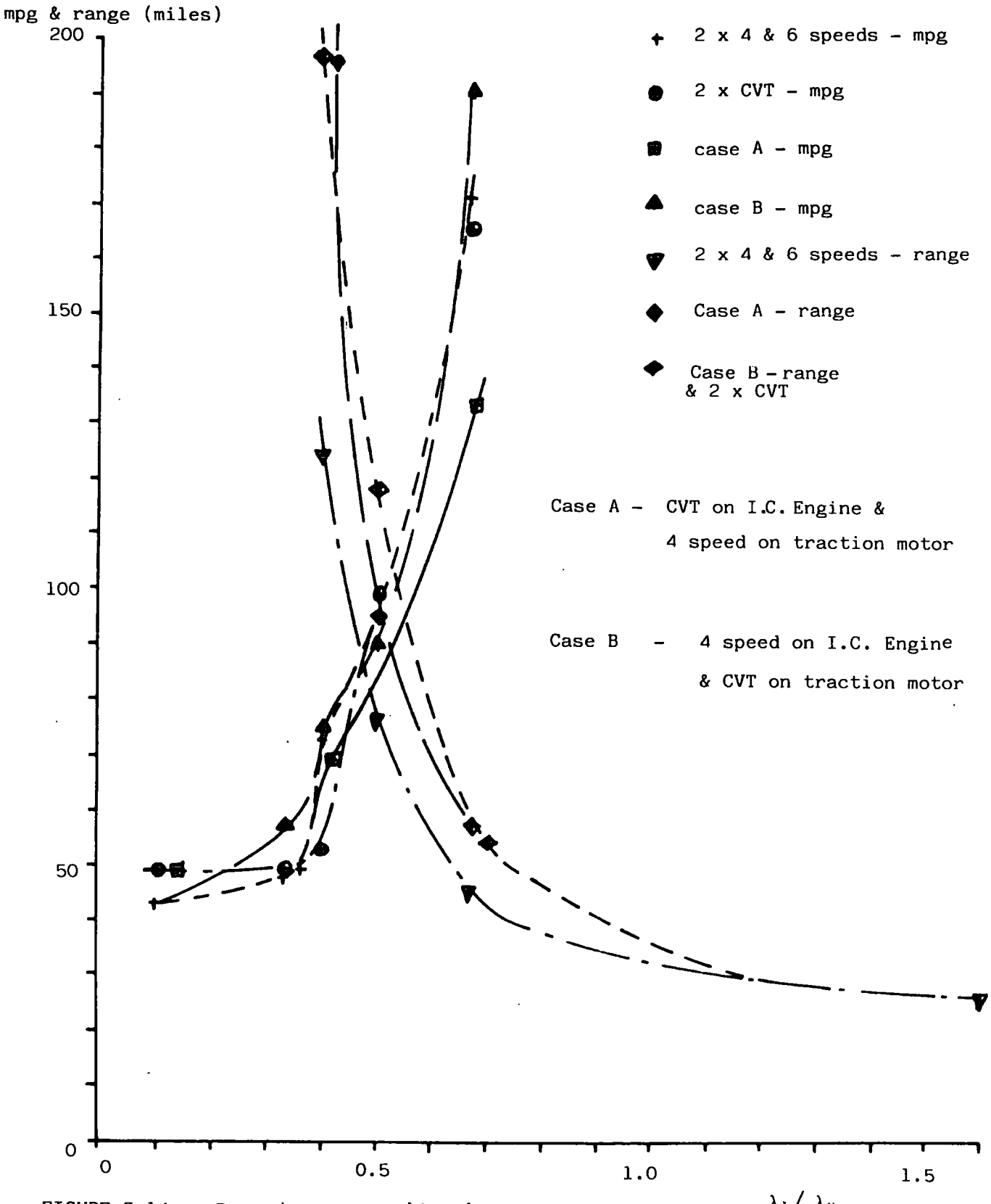

FIGURE 5.14: Range/mpg versus λ_1 / λ_2 for the Fundamental Parallel Configuration with a Variable

FIGURE 5.15 Range/mpg versus λ_1/λ_2 for the Fundamental Parallel Configuration with a Single Variable Ratio Unit included Downstream of the Torque Split Point.

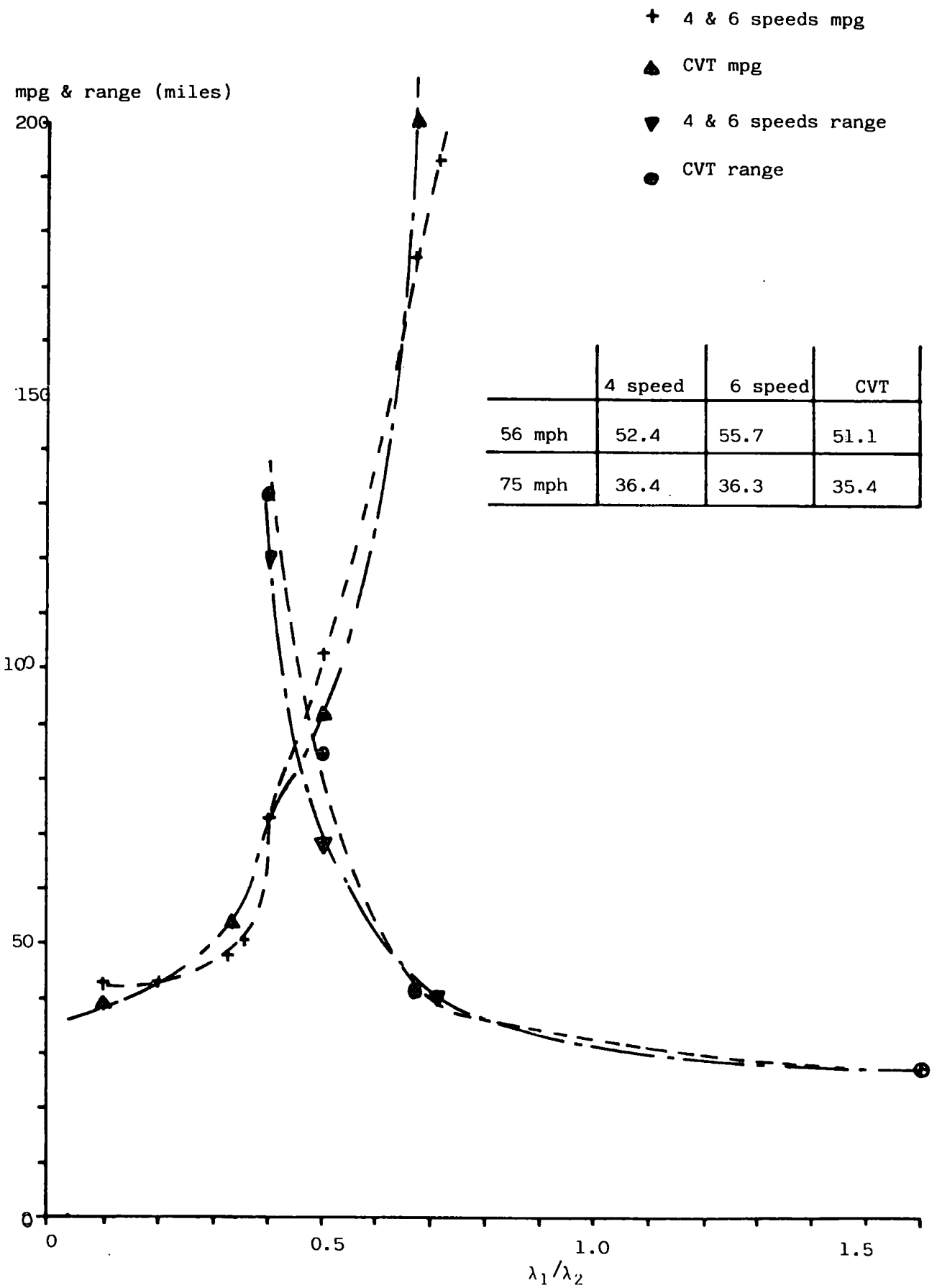

	4 speed	6 speed	CVT
56 mph	52.4	55.7	51.1
75 mph	36.4	36.3	35.4

FIGURE 5.16: Range/mpg versus λ_1 / λ_2 for the configuration of 5.15 but with the Traction Motor Decoupled during i.c. Engine only Periods.

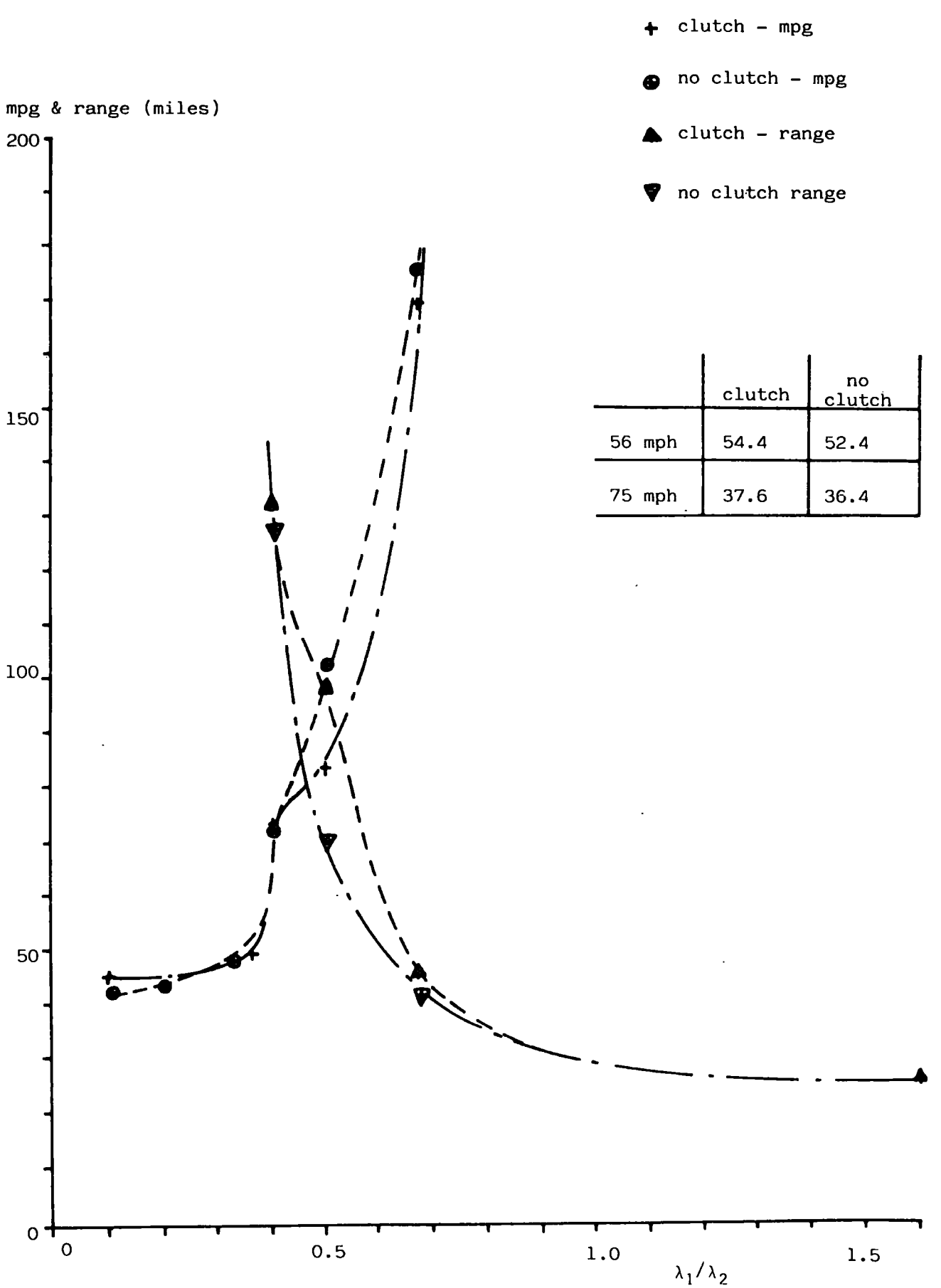

	clutch	no clutch
56 mph	54.4	52.4
75 mph	37.6	36.4

FIGURE 5.17: Range/mpg versus λ_1 / λ_2 for the Fundamental Series Configuration

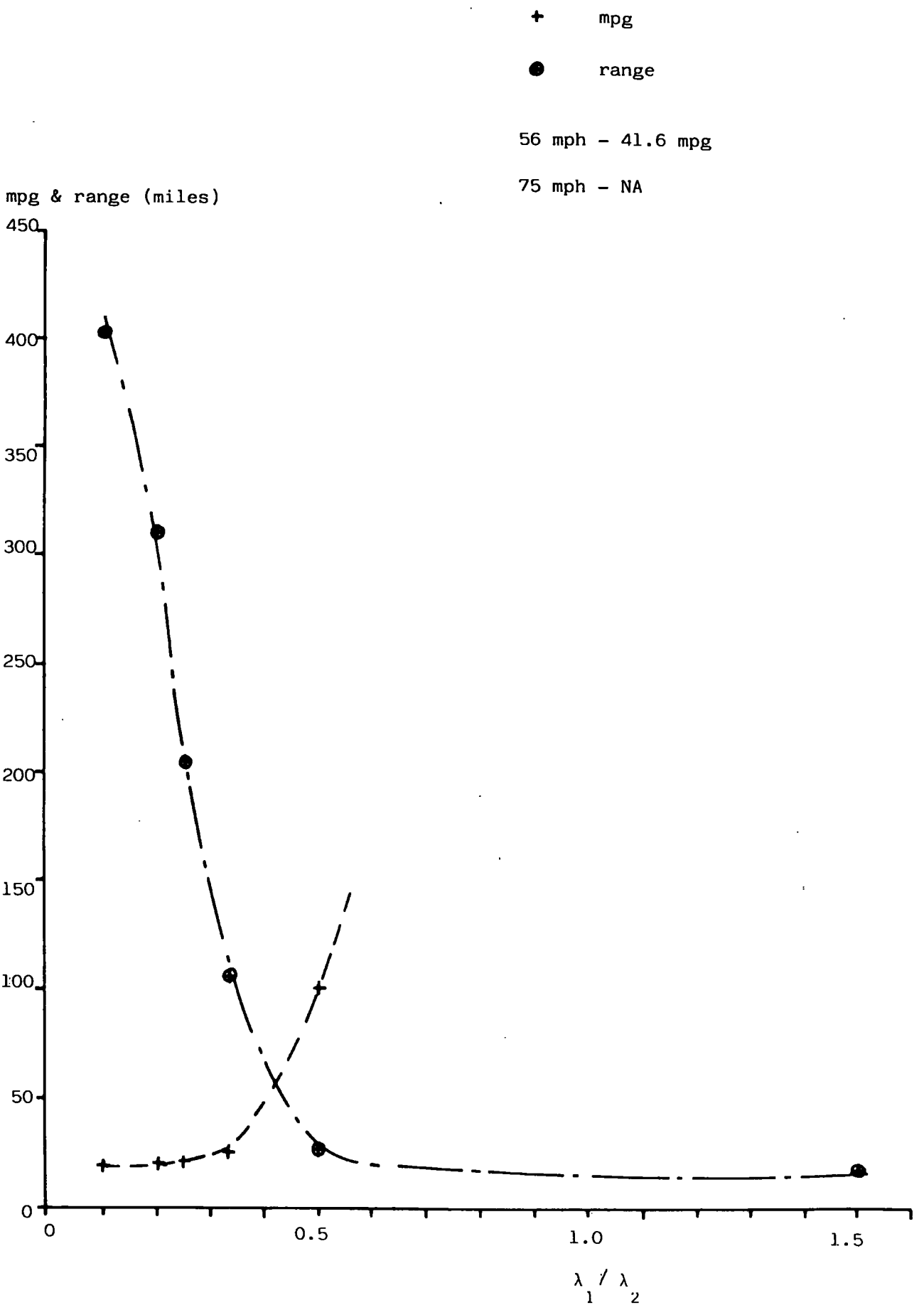

FIGURE 5.18: Range/mpg versus λ_1/λ_2 for the Fundamental Series Configuration with a Variable Ratio Unit Included for the Traction Motor.

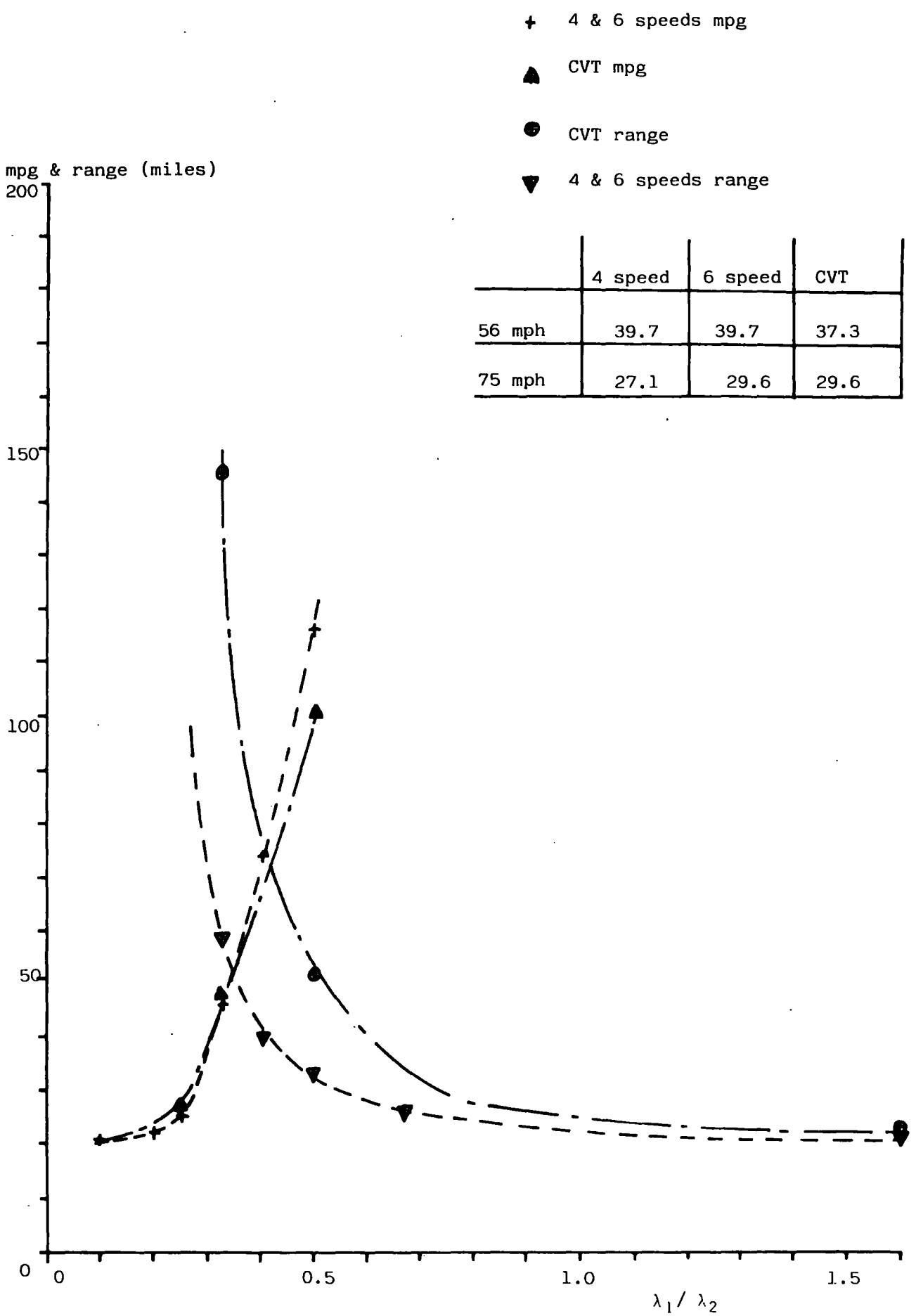

	4 speed	6 speed	CVT
56 mph	39.7	39.7	37.3
75 mph	27.1	29.6	29.6

FIGURE 5.19: Usage Data for the Energy Saving Aim over the ECE-15

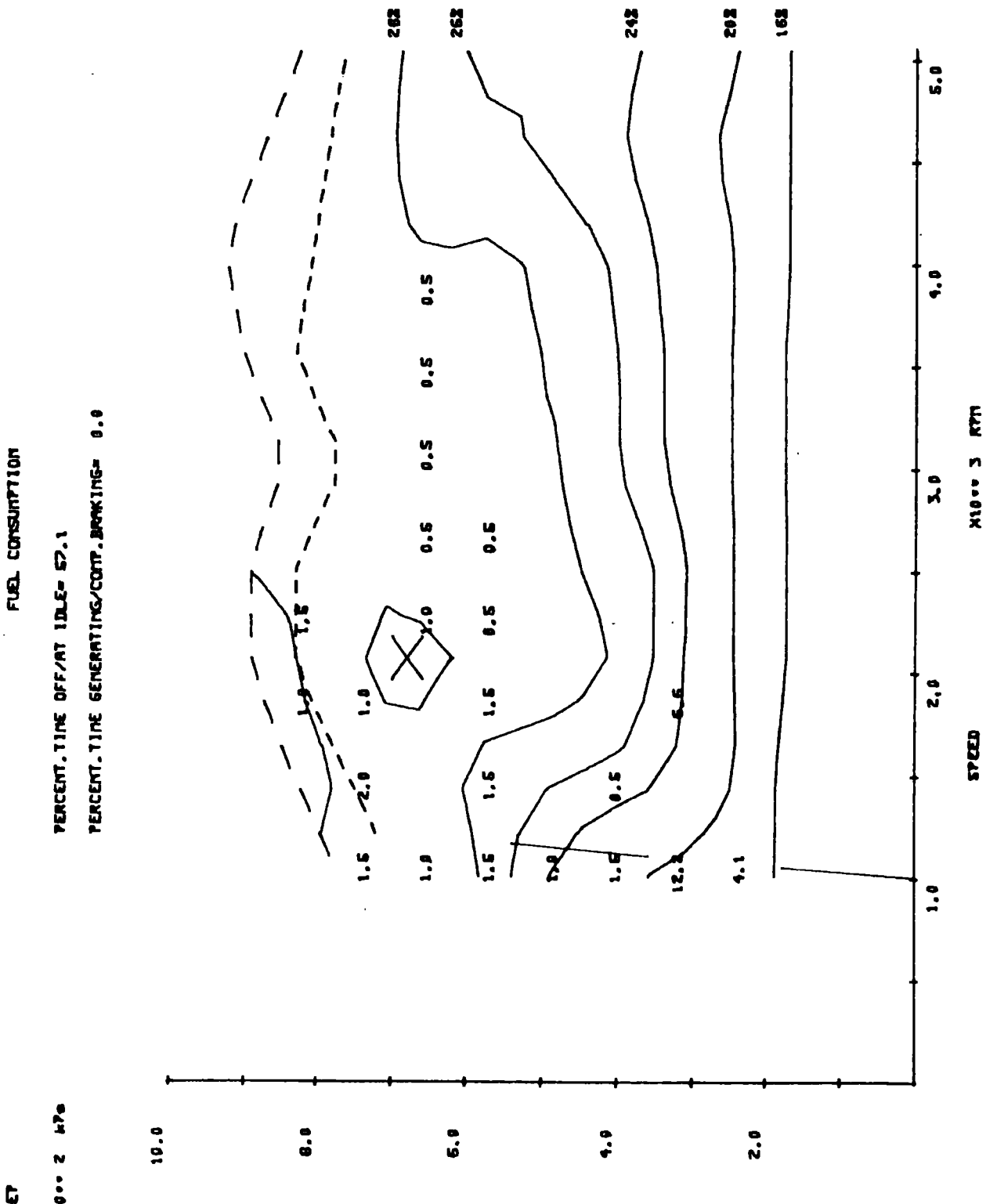

FIGURE 5.20: I.C. Engine Torque/time Profile for the Energy Saving Aim over the ECE-15

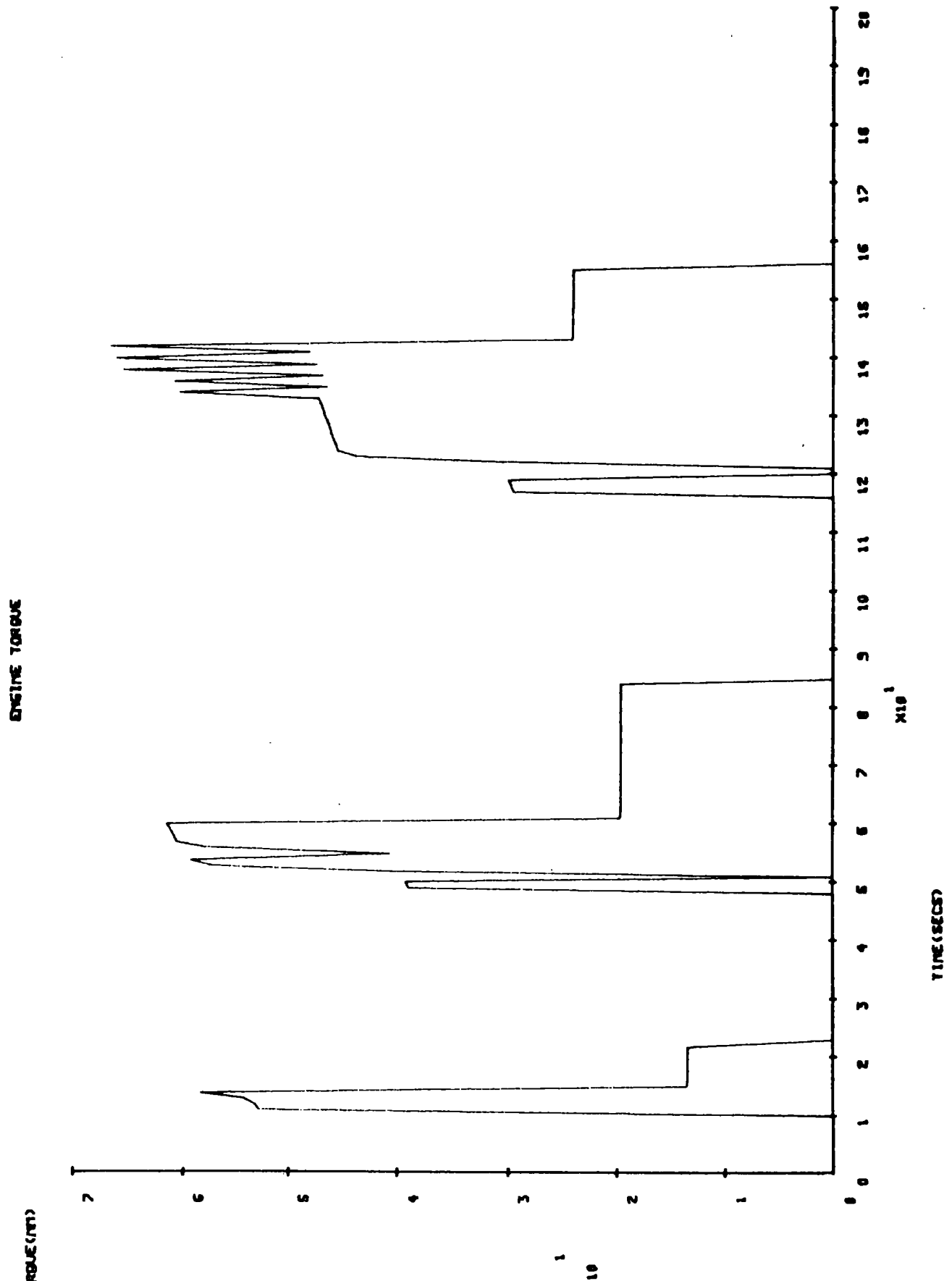

FIGURE 5.21: Transmission Ratio/time Profile for the Energy Saving Aim over the ECE-15

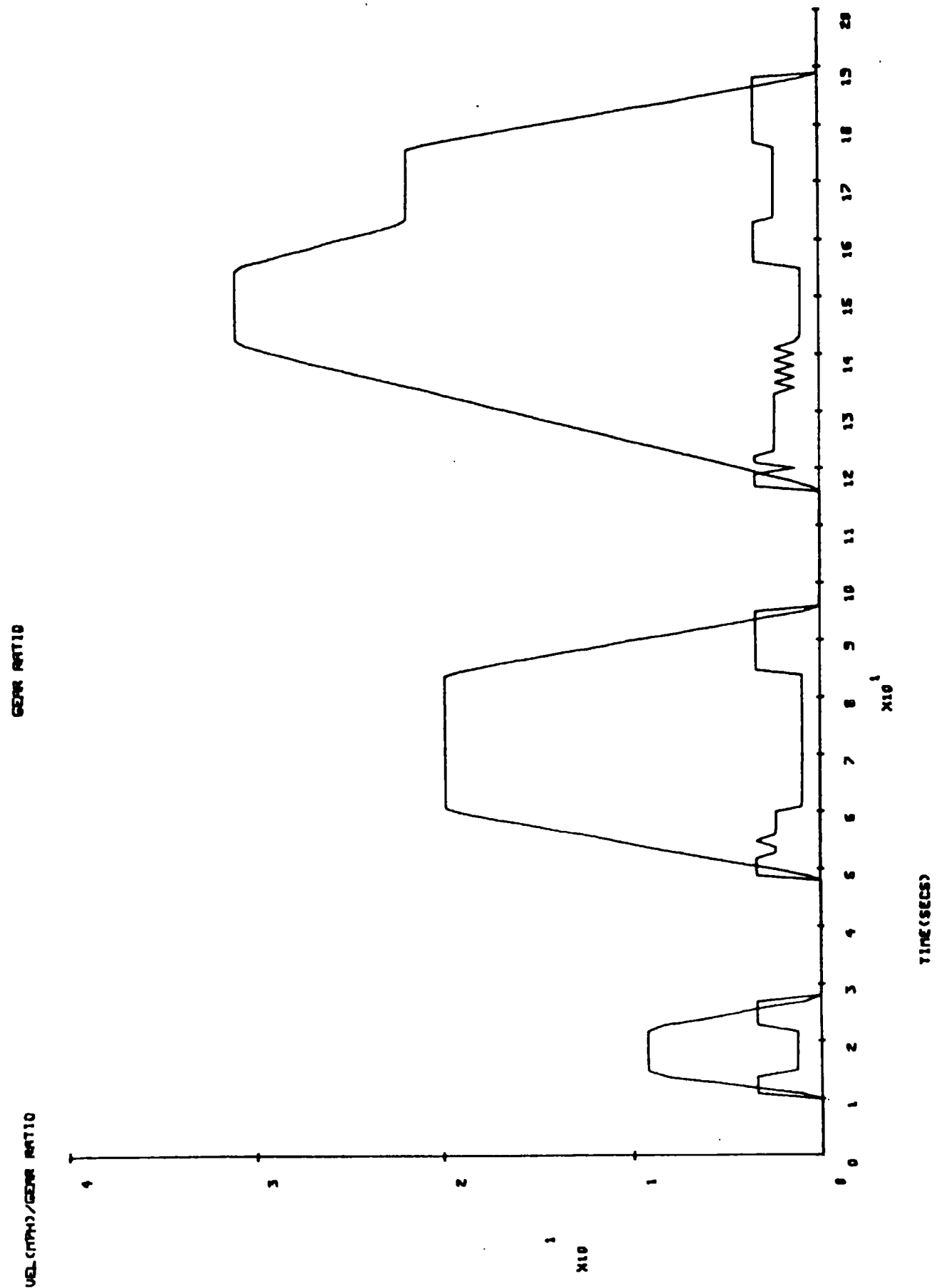

FIGURE 5.22: Torque Split/time Profile for the Energy Saving Aim over the ECE-15

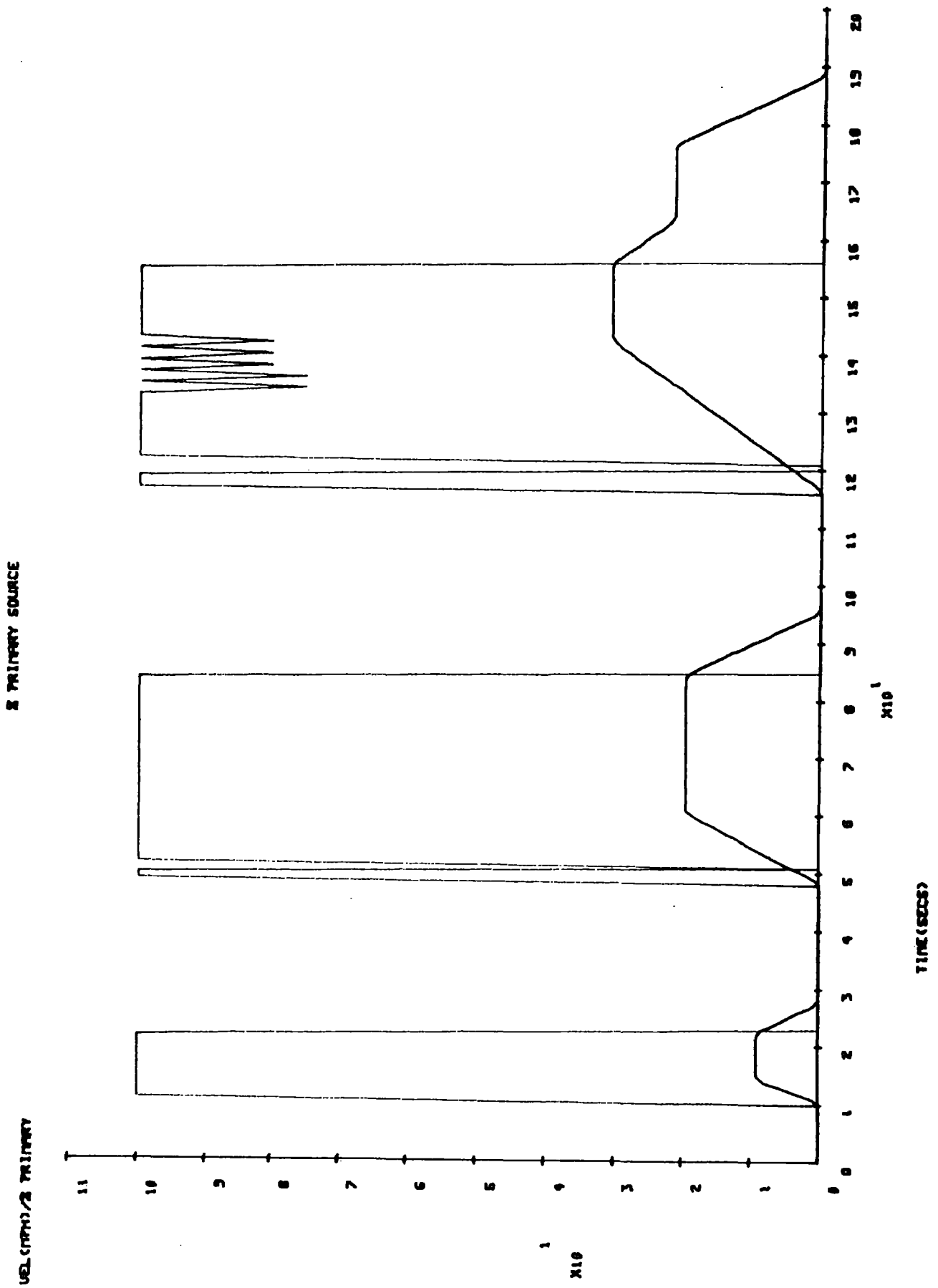

FIGURE 5.23: Usage Data for the Petroleum Substitution Aim over the ECE-15

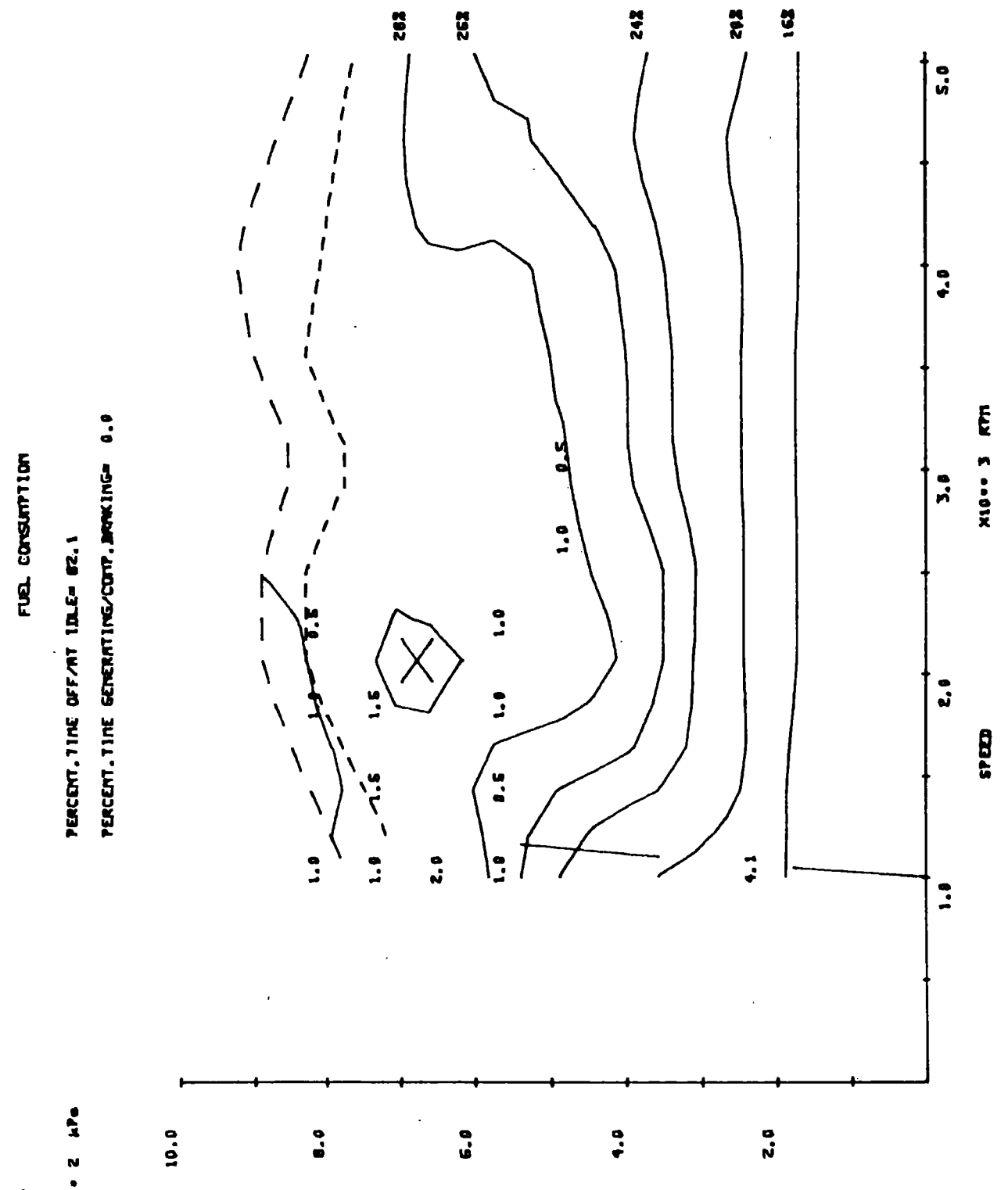

FIGURE 5.24: I.C. Engine Torque/time Profile for the Petroleum Substitution Aim over the ECE-15

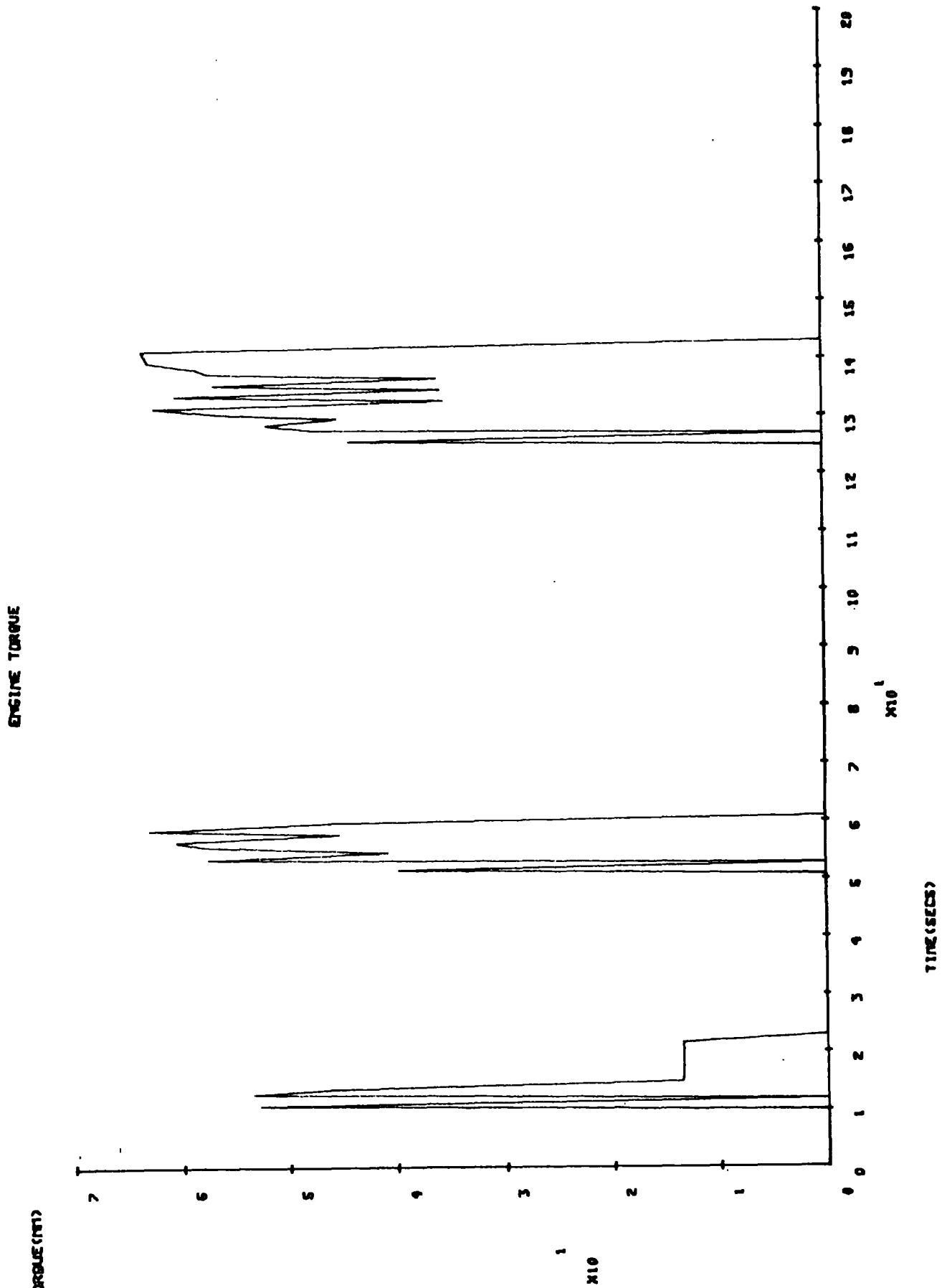

FIGURE 5.25: Torque Split/time Profile for the Petroleum Substitution Aim over the ECE-15

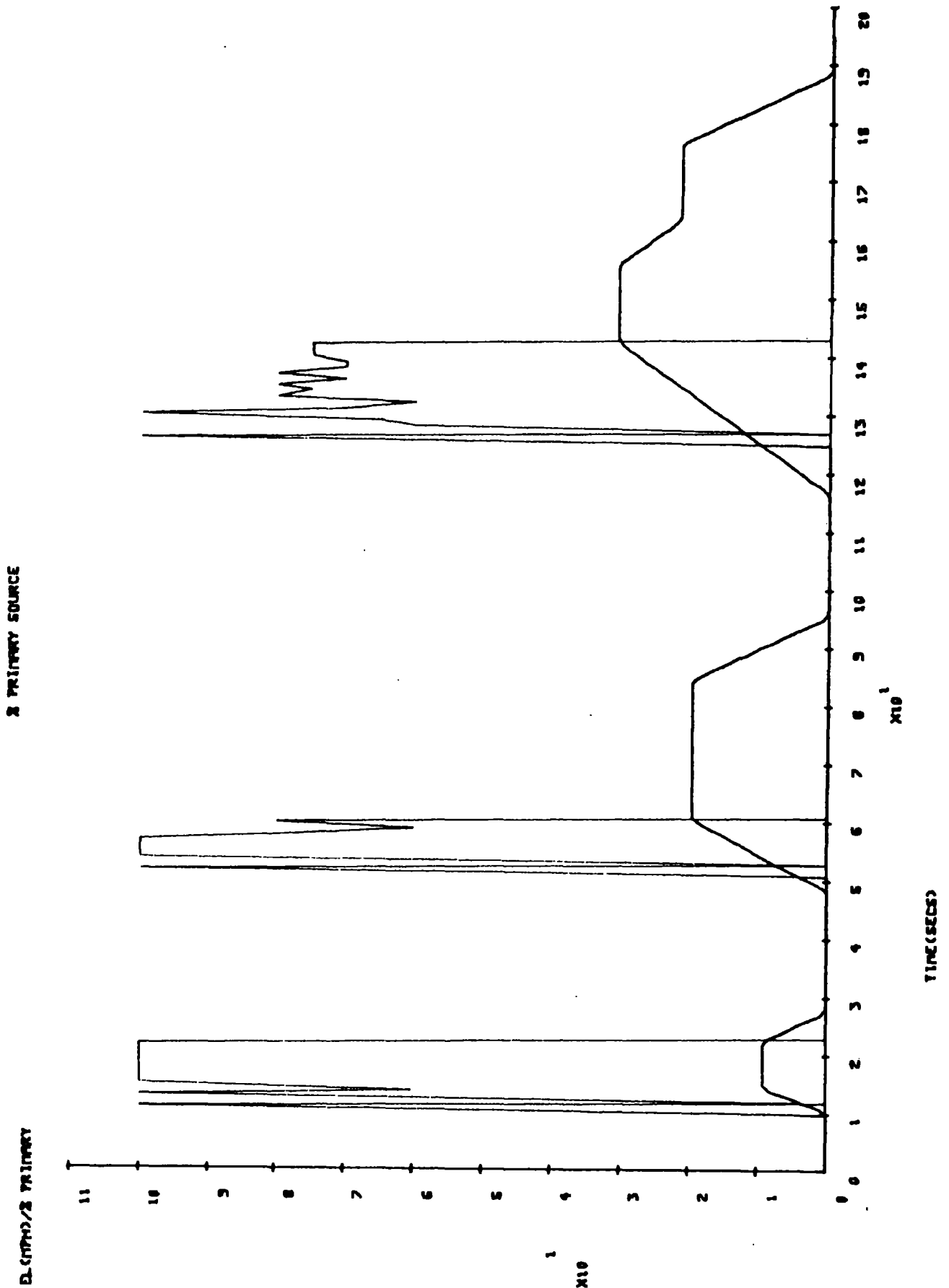

FIGURE 5.26: Transmission Ratio/time Profile for the Petroleum Substitution Aim over the ECE-15

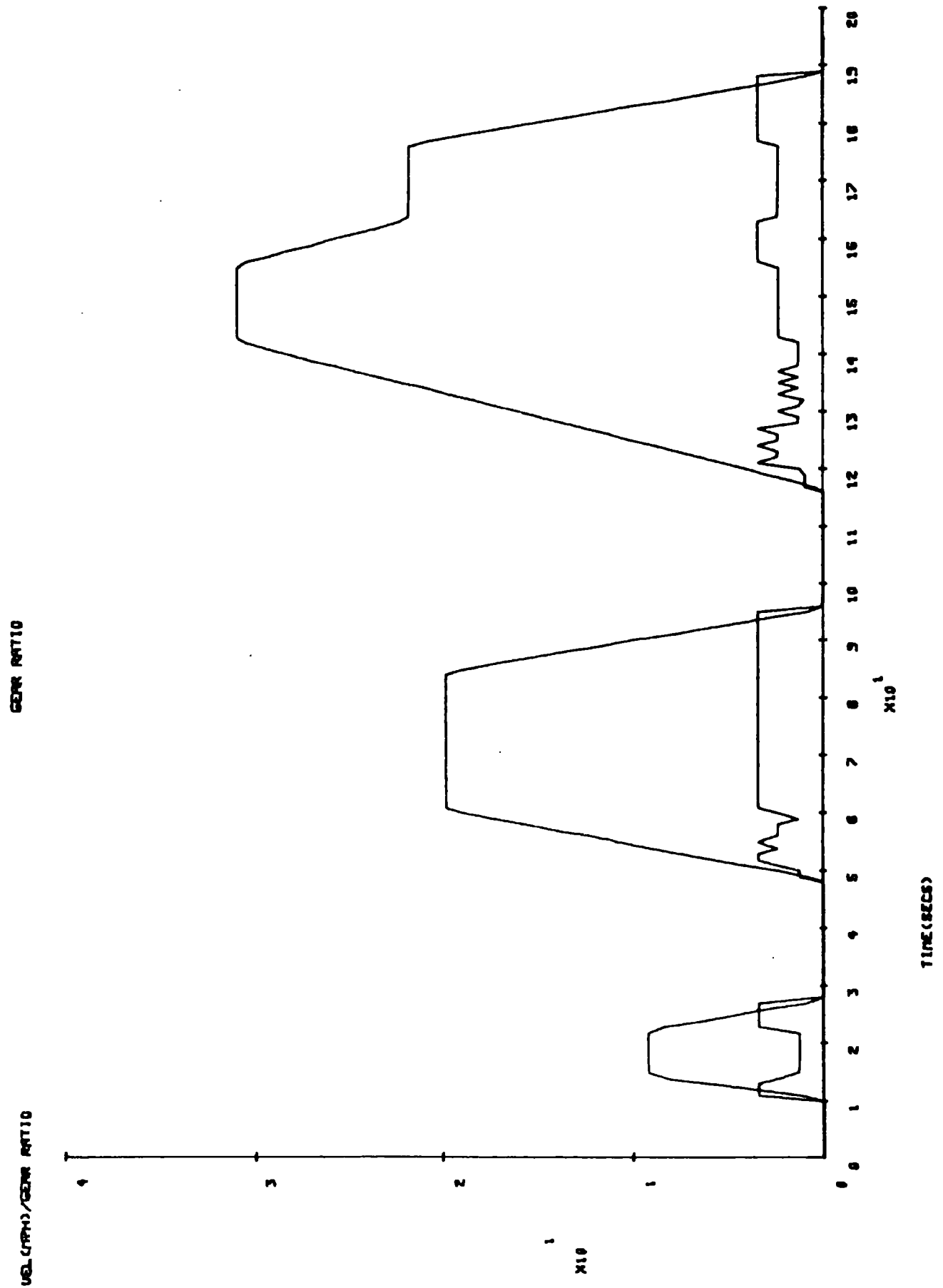

FIGURE 5.27: Usage Data as for Figure 5.19 but with no Fuel cut-off at Idle and Overrun

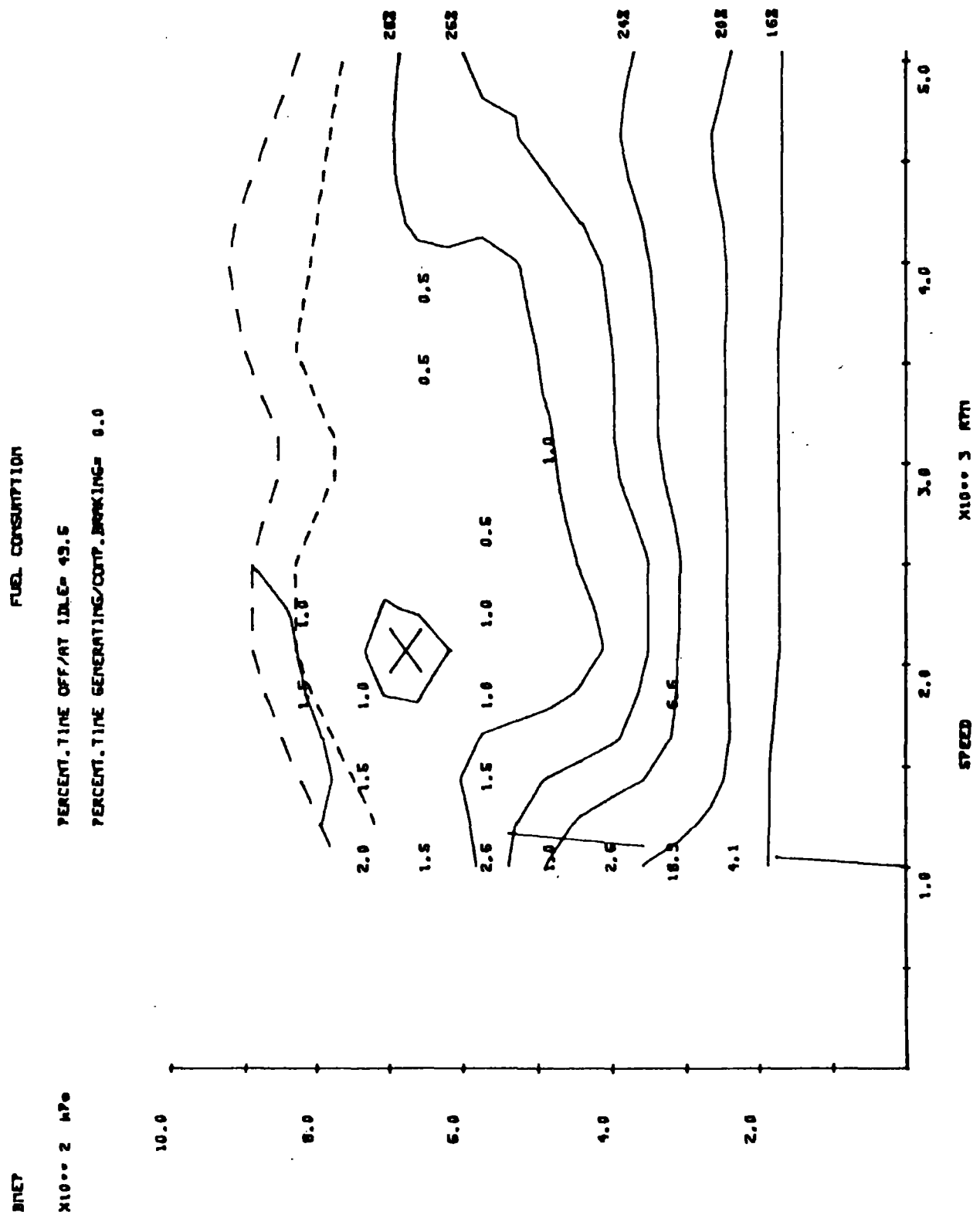

FIGURE 5.28: Torque Split/time Profile as Figure 5.22 but with no fuel cut-off at Idle and Overrun

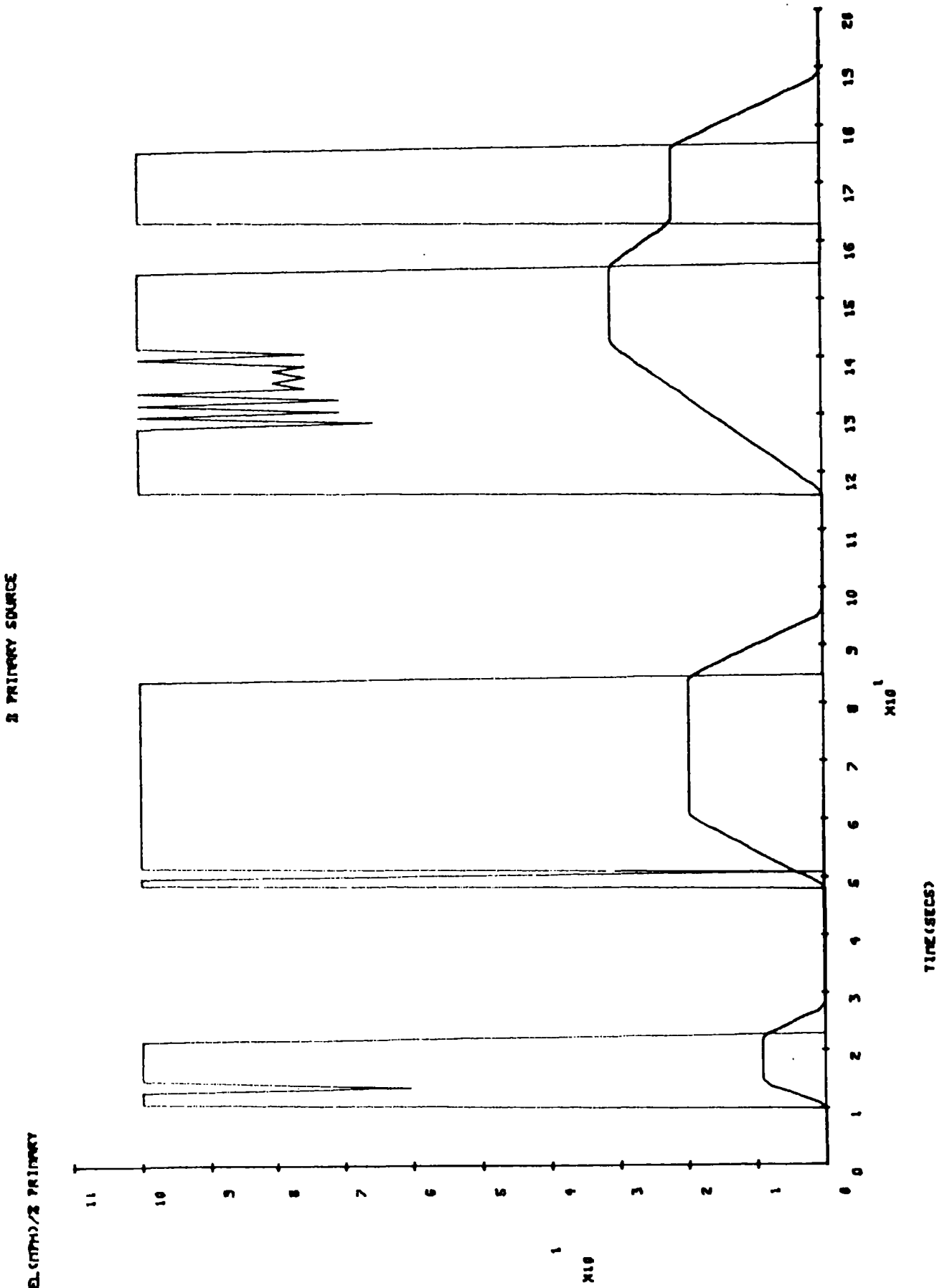

FIGURE 5.29: Transmission Ratio/time Profile as Figure 5.20 but with no fuel cut-off at idle and overrun

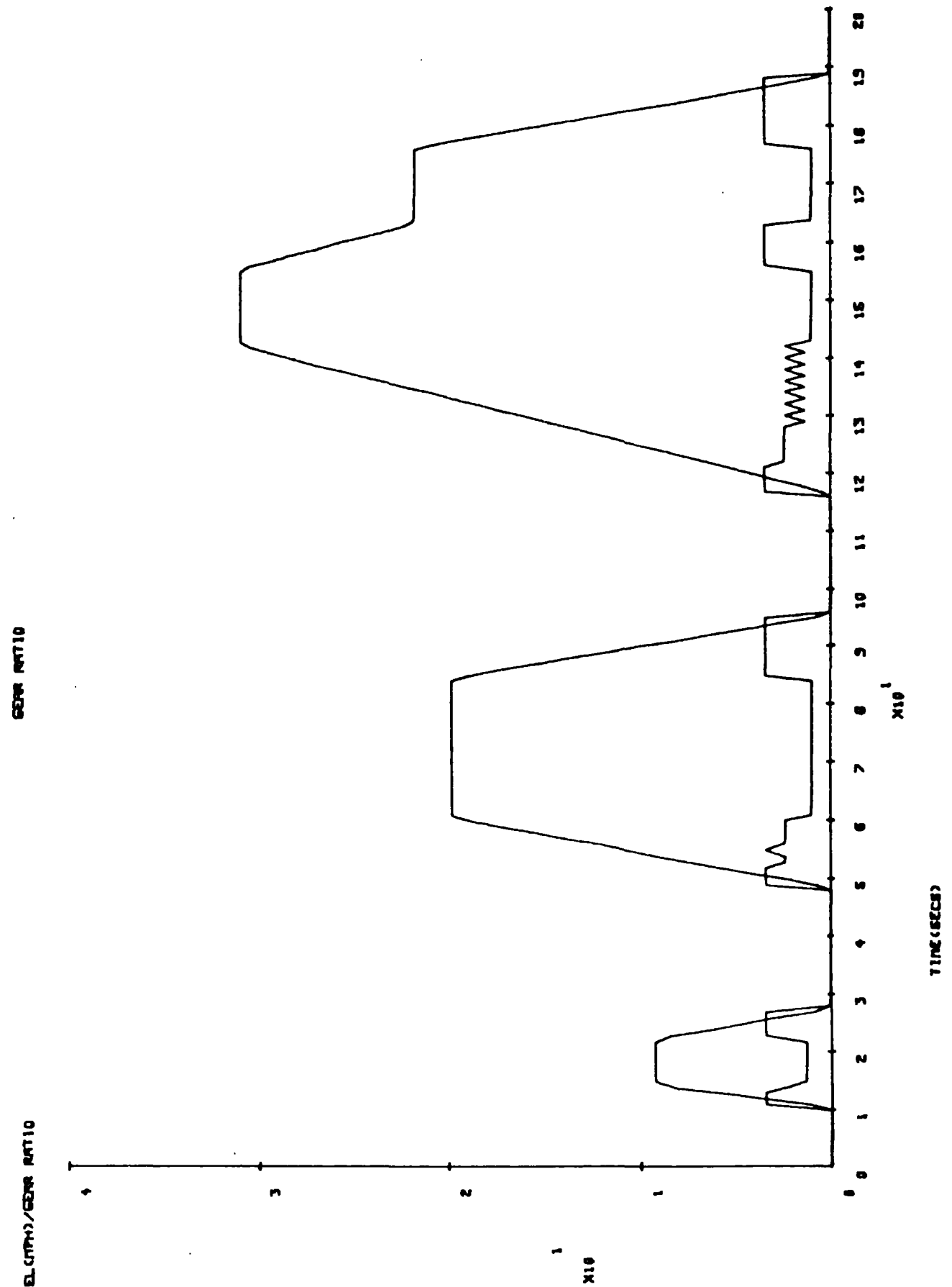

FIGURE 5.30: I.C. Engine Torque/time Profile as Figure 5.20 but with no fuel cut-off at idle and overrun

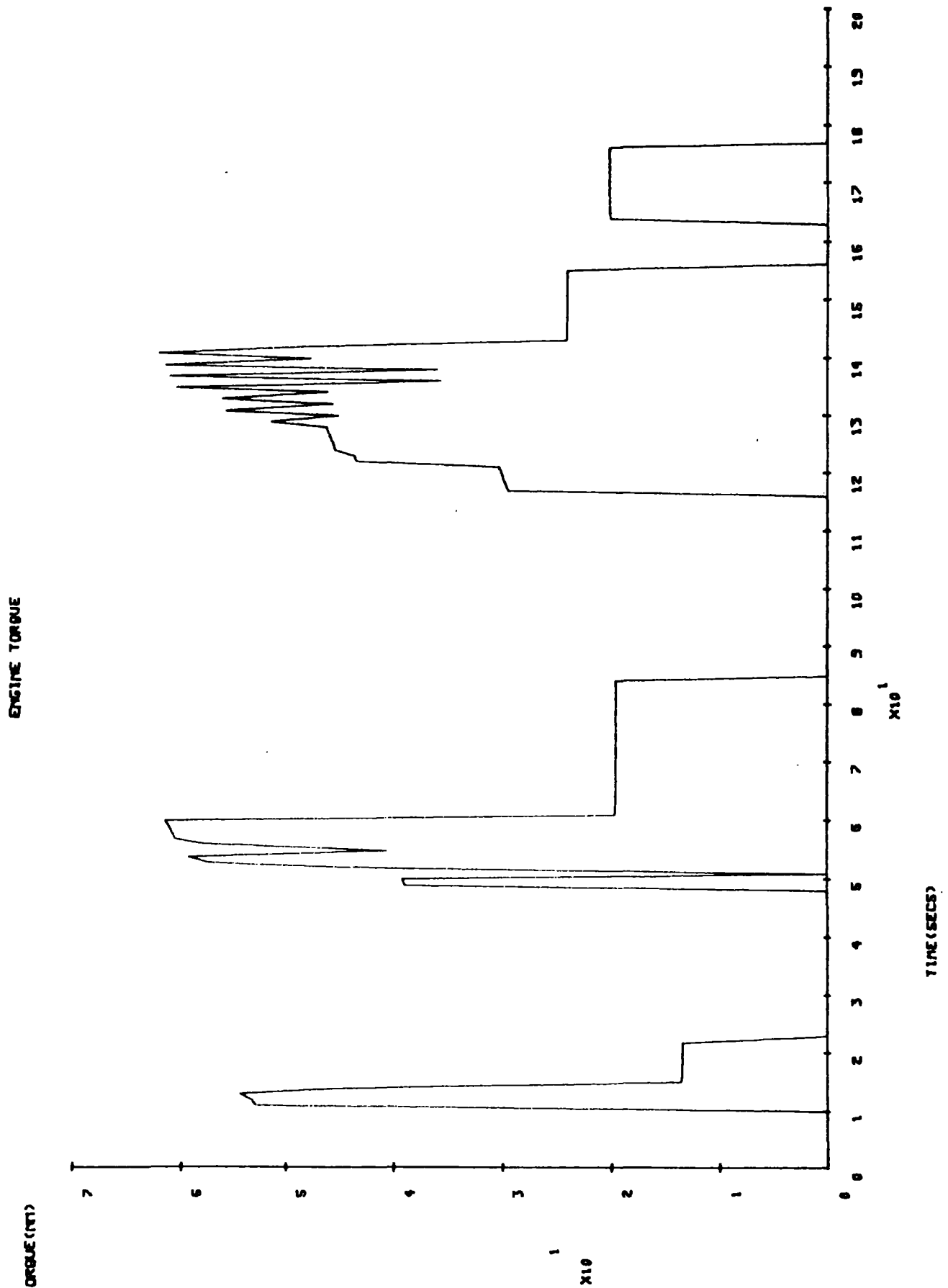

Table 5.1 Hybrid-Electric Vehicle Parameters

Common Base Parameters

Drag Coefficient, CD = 0.35
Frontal Area, FA = 1.95m²
Coefficient of Rolling Resistance, CR1 = 0.01
Wheel radius = 0.28m
wheel inertia = 35 Kg

Bodyshell weight = 700 Kg
No. of passengers = 2 (70 Kg each)
Payload = 100 Kg

Common Performance Requirements

0-60 mph in 10-15 sec
maximum cruise speed
achievable on the i.c. engine only - > 80 mph

All Electric Urban range - 20-25 miles

Variable Ratio Transmission Ratios

4-speed	6-speed	CVT (Perbury)
3.5:1	3.5:1	5.0:1
2.4:1	2.4:1	
1.3:1	1.3:1	
1.0:1	1.0:1	
	0.8:1	
	0.6:1	
		0.5:1

Series Configuration Parameters

Generator set size:

I.c.engine - 35 KW at 500 rpm (gasoline)
" inertia - 0.1 Kgm²
idle cons - 0.1 gm/s
generator - 35 Kw at 5000 rpm

Traction motor - 60 Kw at 5000 rpm (DC Shunt)
Voltage - 100 volts

Transistor chopper type controller

Table 5.1 - continued

Final drive ratio - 4.68:1 (fundamental series config.)
Final drive type - chain
- 3.5:1 (with a transmission included)

Battery - lead-acid - EV2-13 type (42 Wh/Kg)
Battery weight - 400 Kg

Performance achieved using the fundamental config.

0-60 mph - 15-20 seconds

max speed (no trans) - 70 mph
" (trans) - 80 mph

Parallel Configuration Parameters

i.c. engine - 35KW at 5000 rpm (gasoline)
i.c. engine inertia - 0.1 Kgm^2
i.c. engine idle cons - 0.1 gm/s

Traction motor - 35 Kw at 5000 rpm (DC Shunt)
Traction motor voltage - 100 volts

Transistor chopper type controller

Final drive ratio - 3.5:1 (with a variable ration transmission for the ICE)

- 4.6 3:1 (no variable ratio trans.)

Final drive type - train

Electric motor drive - 1.0:1 (for variable ratio trans. on motor)

- 1.5:1 (for no variable ratio trans. on motor)

Battery type - lead acid - EV2-13 - 42 Wh/Kg

Battery weight - 300 Kg

Performance Achieved Using Fundamental Configuration

0-60 mph - 15-20 seconds
max all ICE speed - 70 mph

CHAPTER 6

Parameter Study of a Hybrid Electric Vehicle Drive Train Configuration

6.1 Introduction

In chapter 5 it was shown that, for a fixed set of vehicle parameters and using an optimum control strategy, the effects of drive-train configuration on vehicle performance could be studied. However, in a hybrid-electric or any other vehicle type, not only can the drive-train configuration be varied but, given the same optimum control strategy, the vehicle parameters of any given drive-train can also be varied.

Although it is possible to take each configuration discussed in chapter 5 and consider the parametric variations, it was concluded that only 2 parallel configurations should be realistically considered for the hybrid-electric application to the medium-sized passenger car. Of these two, the configuration with the single variable ratio transmission was favoured as its relative simplicity was thought to justify the shortfall in energy consumption compared to the configuration with 2 transmissions.

It is therefore the purposes of this chapter to consider the effects on vehicle performance of changes to vehicle parameters for the single drive-train configuration just described.

Furthermore, because the two basic hybrid aims introduced in chapter 1 and expanded upon in chapter 5 - the "energy-saving" aim and the "petroleum sustitution" aim - have such different impacts on vehicle parameters, it is proposed to consider them separately. This is illustrated by the fact that the "energy saving" vehicle places greater emphasis on the i.c. engine power source relative to the electrical system, whereas for the "petroleum substitution" vehicle because all electric operation is increasingly important, the reverse is true.

6.2 Vehicle Parameters to be Varied

In a hybrid-electric vehicle, the vehicle parameter that determines the degree of "petroleum displacement" that will be achieved is the

traction battery size or weight. This will equally apply to the "energy saving" aim as even here, substitution is still possible although not to the same extent as the "petroleum substitution" aim because of the reduced emphasis on the electrical system.

As battery weight is changed in a hybrid-electric vehicle the vehicle weight will also change, but in order to maintain the constant performance constraints described in chapter 5 (0-60 mph acceleration time and/or maximum all i.c. engine cruise speed), so adjustments must be made to the "total installed power" of the vehicle. The total installed power is comprised of the i.c. engine power source rating plus the traction motor power source rating and adjustments to these will have a knock-on effect on vehicle weight. Furthermore, for a given "total installed power" requirement, the size of one power source - say the i.c. engine - relative to the other can also be varied - the "relative power source fraction" - which is defined here as the ratio of the i.c. engine power rating to the total installed power rating (PICE/PTOT).

Therefore the battery weight, because of its implications as regards other parameters, is perhaps the principle vehicle parameter to consider.

As was discussed in the configuration study of chapter 5, a vehicle may be assembled from a common base of parameters (common to i.c. engined, electric and hybrid-electric drive-trains within the medium sized passenger car class). This is also the case here and for the single drive-train being considered, the base parameter values will be the same as those chosen for the medium sized passenger car parallel hybrid of table 5.1 in chapter 5.

Transmission type was considered in chapter 5 but only as a component to be added or subtracted from a drive-train configuration, and even then with the intention of considering the ratio span. In a more detailed study here, not only can the ratio span be considered (in effect looking at

the different transmission types) but also, in the discrete ratio case, the individual ratios and number of ratios within a given span. The transmission types to be considered here are as table 5.1 of chapter 5, as are the ratio values and ratio span with the exception of the more detailed study of ratio values.

In chapter 5 it was argued that the final drive ratio can be fixed at a typical value since it forms only one component of the overall transmission ratio. This is the case here since a variable ratio transmission is being considered throughout and the value chosen is also given in table 5.1.

As well as the transmission type, other vehicle parameters to consider here that were fixed as typical in the study of chapter 5, are the battery type and the prime-mover types (both i.c. engine and traction motor). In the electric vehicle study of chapter 4, advanced battery and traction motor types were considered, but although the conclusions reached regarding the pure-electric drive-train will have definite implications as regards the hybrid-electric drive-train, because of the addition of the i.c. engine power source it is as well to consider them here also.

Although regenerative braking was assumed as being a typical vehicle parameter in chapter 5 its use must be argued in this chapter. For the energy saving aim, regenerative braking is fundamental, in that without it no deceleration energy recovery is possible. But for the petroleum substitution aim, although not crucial, will have a significant effect- indeed the electric vehicle study of chapter 4 has shown that it can improve range by up to 10-20%. Because regenerative braking is a state-of-the-art concept in that it is being readily implemented on current electric vehicles, it will be considered throughout this chapter.

In chapter 4 it was also shown how the practical alternatives could give a close approximation to the ideal braking philosophy, so, as for the study of chapter 5, the ideal philosophy will be considered here also.

Similarly, because it was argued in chapter 5 that fuel shut-off from the i.c. engine during idle and overrun periods is fast becoming a state-of-the-art concept, and because it is crucial to the degree of petroleum displacement and/or energy saving achievable in the hybrid-electric vehicle, it will also be considered throughout.

Finally, the effects of the aforementioned parametric variations on vehicle performance - in terms of energy consumption, acceleration performance and maximum speed (on a level road and up a gradient) - can be assessed by simulation over not only the ECE-15 mild urban cycle of chapter 5 (shown in Figure 5.10), but also over the more severe SAE J227aD urban cycle (shown in Figure 6.1) and at the two steady-state cruises - at 56 mph and 75 mph of chapter 5.

6.3 The Energy Saving Aim

For the energy saving hybrid philosophy, because the electrical system is used mainly for load-levelling with the traction battery experiencing little or no discharge at the end of a duty cycle, and also with the consideration that a certain 'useful' all-electric range must be available (see chapter 5), then the traction battery is sized to cope with the power density demands of acceleration and decleration more than to meet a stored energy requirement. Furthermore, in chapter 5 it was shown that for the 300Kg battery size chosen for the parallel hybrid that the energy saving (constant SOC) aim was easily achievable.

It is appropriate, therefore, to consider battery size variations above and below this value as there will be benefits and penalties for both. Below 300 Kg, although vehicle weight savings will improve fuel consumption, all electric range will fall below the figure chosen in chapter 5 of 25 miles. Whereas above 300 Kg, the fuel economy decreases due to the vehicle weight increase must be considered alongside the increase in all-electric range.

A battery size range of 100 Kg to 500 Kg is to be considered here as the 300 Kg size of chapter 5 falls at the mid-point.

The basis for comparing the various parametric variations will be a vehicle having a lead-acid battery, a D.C. shunt traction motor with a chopper controller and a state-of-the-art gasoline i.c. engine.

6.3.1 Effect of Battery Weight

Figure 6.2a shows how for each battery weight over the range 100 Kg to 500 Kg in steps of 100 Kg, the relative power source fraction/size (PICE/PTOT) affects the fuel consumption in mpg for a constant SOC over the ECE-15 cycle. It is important to note that values of PICE/PTOT are only considered over the range 0.35 - 0.75 as moving below will restrict all i.c. engine operation and moving above will restrict all electric operation. Ideally, a value of 0.5 will achieve the best compromise in terms of acceleration and maximum speed performance when operating on either of the two on-board power sources alone.

It is clear from Figure 6.2a that as PICE/PTOT is increased for a given battery weight, the general trend is for mpg to increase also. This is largely due to vehicle weight decreasing over this range as the i.c. engine becomes the more dominant power source (attributed to a reduction in motor controller weight and because the weight-to-power ratio for the i.c. engine is less than for the traction motor).

Figure 6.2b shows as far as component efficiencies are concerned for the 200 Kg and 400 Kg battery sizes, i.c. engine efficiency remains roughly constant at between 20-25%, traction motor efficiency during motoring rises sharply then levels as PICE/PTOT increases and during regeneration rises steadily as PICE/PTOT increases. Clearly, as the electrical system becomes smaller as PICE/PTOT increases, so it becomes more efficient and can be used more often during motoring periods and more braking energy can be recovered during decleration. The result is that the i.c. engine can now be used less and only for the high loading conditions (yielding a high i.c. engine efficiency) and so mpg rises.

However, as 6.2a shows, the curves for the individual battery weights do not show smooth trends and this can be explained by the nature of the driving cycle (ECE-15). Because of the 'mild' nature of the ECE-15 cycle, the electrical system is seldom called upon during acceleration to supplement the i.c. engine with the result that the difference between 'under using' the electrical system (more or less all i.c. engine operation) and 'over using' the electrical system (returning wth a significant battery discharge at the end of the cycle) is in the optimum control system choosing to run all i.c. engine on all-electric on one or more of the 4 cruise modes respectively. This accounts for sudden drops in mpg in the otherwise upward trends - depending upon battery size, i.c. engine size and motor size - where the control algorithm has chosen to run all i.c. engine in order to return with a constant SOC for one or more of the cruise modes.

This argument is born out if one looks at similar results but over the more severe J227aD cycle, shown in Figure 6.3a. Because of its relative severity, the electrical system is called upon to supplement the i.c. engine for a significant period during acceleration, with the result that the difference between constant SOC and range-limited operation is in a few individual acceleration points (rather than a large number of cruise points for the ECE-15 cycle) - hence no 'ripples' occur in the curves.

Unlike the ECE-15 cycle, here the trend is for an optimum PICE/PTOT to occur at each battery weight. Looking at component efficiencies in Figure 6.3b, to the left of optimum, reductions in vehicle weight are more than compensating for reductions in the i.c. engine efficiency as PICE/PTOT rises (due to its decreasing load factor), whereas to the right of optimum, further reductions in i.c. engine efficiency are now dominating over the weight reductions as PICE/PTOT rises.

Because of the aforementioned ECE-15 cycle effects, it is unclear how battery affects vehicle fuel consumption. Indeed, there appears to be no significant change overall over the range of battery sizes shown in Figure 6.2a. Over the J227aD cycle, however, the picture is clearer (Figure 6.3a), and, as battery is increased, the increase in vehicle weight (due to the battery and the knock-on effect of increased total installed power) has the effect of increasing fuel consumption (decreasing mpg).

Although this suggests that as small a battery as possible should be installed in a hybrid vehicle with the energy saving aim in mind, there are several factors that will impose a minimum size restriction on the battery. Firstly, as the battery becomes smaller (for 100 Kg and below) the all-electric range becomes unacceptable and does not permit significant all-electric urban or even a 'get-you-home' mode. Secondly, the size of the battery puts a maximum achievable voltage restriction on the electrical system with the result that for a given power requirement currents in the motor and controller will be large. Component size and weight will tend to increase and reliability will tend to decrease.

In Figures 6.4a and 6.4b the effects of the aforementioned changes to the relative power source fraction and battery weight are presented for the 56 mph cruise and the 75 mph cruise respectively. Figure 6.4c shows the i.c. engine efficiency for the two cruise cases for the 200 Kg battery size alone as PICE/PTOT varies. At 56 mph, as the i.c. engine load factor decreases with increasing PICE/PTOT, Figure 6.4c shows i.c. engine efficiency decreasing from 28% to 25% with a corresponding reduction in mpg from 55 mpg to 50 mpg - shown in Figue 6.4a.

Generally, at 56mph, as battery weight increases from 100 Kg to 500 Kg, due to the increase in vehicle weight and knock-on effect in the total installed power, mpg decreases from 53-56 mpg down to 43-48 mpg.

At 75mph, Figure 6.4c shows i.c. engine efficiency not to change with PICE/PTOT due to the fact that the load factor is high even for the larger PICE/PTOT case. As a result, as Figure 6.4b shows, the mpg for a given battery weight over a range of PICE/PTOT remains approximately constant. Again, however, due to the increase in vehicle weight and knock-on effect in total installed power as battery weight rises, mpg falls from 38-39 mpg at 100 Kg to 33-34 mpg at 500 Kg.

An additional effect of both the relative power source fraction, PICE/PTOT, and the battery/vehicle weight, relates to the "gradeability" of the vehicle, or the maximum speed achievable on a given gradient. A 2% gradient was selected as being fairly typical of what is encountered during long-distance motorway driving when the i.c. engine only mode would be used.

As Figure 6.5 shows for the base vehicle, as the value of PICE/PTOT rises for each battery weight, so does the maximum speed on a 2% gradient. Furthermore, the trend, as the battery/vehicle weight rises, is for the maximum speed on a 2% gradient to decrease at a given value of PICE/PTOT.

6.3.2 Influence of Battery Type

In the electric vehicle study of chapter 4 an inherent disadvantage of the lead-acid traction battery was highlighted as being the strong dependence of the available energy density on the power density - as illustrated in the curves of Figure 4.22. Other, more advanced battery types such as the Nickel-zinc and Nickel-iron types do not show such a strong dependence and could be suited to the hybrid-electric vehicle -particularly for the energy saving aim where power densities may be high due to relatively small battery sizes.

Of the two advanced cell types highlighted in chapter 4, although the nickel-iron type is very robust and has a long cyclic life, its recharge

efficiency is low compared with both the lead-acid and nickel-zinc types (Collie, 1979). Since regeneration during vehicle braking is of fundamental importance for the energy saving aim, this cell type is at a disadvantage. It is therefore the purposes of this study to concentrate on the nickel-zinc type, which despite the fact it requires development in terms of cyclic life, by far exhibits the more favourable performance characteristics.

If the results of Figure 6.2 are repeated but with the lead-acid battery now replaced by a nickel-zinc battery then generally a higher mpg is achieved over the range of battery sizes and relative power source fractions - as shown in Figure 6.6a. This improvement is a result of the fact that at high power density demands, available energy density does not reduce as much as with the lead-acid type - allowing greater emphasis to be put on the electrial system during the driving cycle. This leads to improved mpg of up to 20%. For the results using the Ni/Zn cell, only (see chapter 5) was different at each combination of battery weight and PICE/PTOT, compared to the lead-acid case. This adjustment was made to achieve the requirement of the same battery state of charge at the beginning and end of the cycle, and also to compensate for the altered (improved) electrical system efficiency.

An additional benefit of the Ni/Zn cell is that with, say, a 200 Kg battery size, not only is a greater fuel economy possible than with the same weight of lead-acid cells, but also the all-electric range would now increase due to the more favourable power density/energy density characteristic and due to the higher maximum energy density.

The main disadvantage of the Ni/Zn cell is its low cyclic life which is typically 400-500 cycles (Kurtz et al.,1979)(Bucci et al.,1981) compared with 750-1000 cycles for the lead-acid case (Kurtz et al.,1979)(Burris et al.,1978). This value, however, is quoted to 'total' battery discharge,

and since the energy saving hybrid may only be subjected to partial discharges with perhaps the occasional full discharge, the cyclic life may not be such a limiting factor.

Figure 6.6a also repeats the ripples in the battery weight - PICE/PTOT curves that were present for the lead-acid battery over the ECE-15 cycle, only here they are more pronounced. This is because, although the electrical system may be called upon more often using the nickel-zinc battery, the battery may still experience discharges generally, with the result that the difference between under or over using the electrical system may be a longer period of cruising than for the lead-acid case. Nevertheless, the upward trend in mpg as PICE/PTOT is increased generally for the reasons described in section 6.3.1. Furthermore if one looks at the component efficiencies, shown in Fgure 6.6b, it is seen that they follow the same trends and values as for the lead-acid case of Figure 6.2b, indicating the battery alone (i.e., no knock-on effects into the other electrical system components) is responsible for the gains.

6.3.3 The Influence of Transmission Type

Because of the frequent use of the i.c. engine over a large proportion of the vehicle operating speed range, a minimum transmission ratio range/span of about 3.5:1 is required for this type of hybrid -consistent with the conventional i.c. engined vehicle. Despite the fact that this span can be achieved with less than 3 steps (4 ratios) for the discrete ratio case, it is unlikely to be acceptable for both driveability and reduced efficiency reasons. Although a study by Ricardo (Thring,1981) concluded that the span or ratio range was the important factor on driveability and fuel economy and that the number of steps in a span played no part, the minimum number of ratios studied was 4 to cover the minimum span of about 3.5:1.

As a consequence of this, only a 6-speed discrete ratio transmission and a continuously variable transmission (CVT) are to be considered in the comparison with the base 4-speed transmission used in the results of section 6.3.1.

Returning to the base 4-speed case, the extreme (highest and lowest) ratios are chosen for the vehicle starting and cruising requirments respectively, whilst the intermediate ratios are a compromise between vehicle acceleration peformance and fuel consumption over urban cycle conditions. Figure 6.7 shows that for the intermediate ratios chosen, how, if one is fixed at its base (or datum) value and the other is varied, vehicle urban fuel consumption, all-electric range and hybrid acceleration performance are affected. For each of the two ratios, they are varied over such a range that at the extremes they are equal to their adjacent ratios - so making the transmission effectively a 3-speed unit. Maximum all-electric range and mpg occur for ratios in between the respective adjacent ratios -showing that the intermediate ratios selected are reasonably close to this optimum. Acceleration time is at a minimum also midway between adjacent ratios, for each of the two ratios being varied. Consequently a 4-speed transmission will give better acceleration performance than a 3-speed unit over the same ratio range (in effect 'closer' ratios), through being able to make maximum i.c.engine and traction motor power available for a greater proportion of a given vehicle speed range (say, 0-60 mph).

The 6-speed transmission can be designed to have either a close ratio range or a wide ratio range. With the close ratio transmission, the same ratio range as the 4-speed case is maintained but with reduced steps. Although this gives improved acceleration times and driveability, no fuel economy or all electric range improvements were observed. A similar conclusion was also reached by Ricardo (Thring,1981) in a similar study on a conventional i.c. engined passenger car.

Alternatively, the wide ratio transmission allows the base 4-speed transmission ratio range/span to be extended at either or both ends of the 3.5:1 basic range. If used solely to increase the maximum gear ratio, then vehicle starting ability, particularly on a gradient, is improved but with little improvement on fuel economy (Morello,1977). In contrast, if the ratio range is extended by including two overdrive ratios of 0.8:1 and 0.6:1 then within the limits of power available lower i.c. engine speeds and higher torque loadings may be achieved both over the urban and cruise conditions relative to the base 4-speed case. I.C. engine maximum efficiency occurs at just such operating conditions and so mpg may be increased under these circumstances.

Figure 6.8a repeats the results for the base vehicle of section 6.3.1, but with a 6-speed transmission included over the urban cycle and shows generally higher mpg due to the aforementioned improvements in i.c. engine efficiency. The component efficencies of Figure 6.8b only show a small improvement in i.c. engine efficiency generally due to the small proportion of cycle where it is possible to use the overdrive ratios within the limits of power available.

At cruise, results are only presented in Figure 6.9a for the 56 mph cruise since at 75 mph because of the limits to i.c. engine power available at this speed, the overdrive ratios cannot be selected and as a consquence of this results are identical to the base 4-speed results of Figure 6.4b and Figure 6.4c.

Returning to the results at 56 mph, because the overdrive ratios can be used because of the lower power demanded at this speed, an improvement in mpg over the 4-speed case of up to 20% is observed in Figure 6.9a. This is due to the overdrive ratios raising i.c. engine load factor at a given road speed, with the result that i.c. engine efficiency rises from 25% in the 4-speed case to 29% as shown in Figure 6.9b.

Additionally, the battery weight - PICE/PTOT curves of Figure 6.9a show at 56 mph for the 6-speed unit, an optimum PICE/PTOT occurring. To the left of optimum there is insufficient i.c. engine power available for the overdrive ratios to be used, so results are identical to the 4 speed case. But to the right of optimum, the reducing i.c. engine load factor (and hence efficiency) result in the reductions in mpg despite the overdrive ratios. For the 4-speed case, it was shown that the reduction in mpg wth PICE/PTOT increasing occurs with no optimum (Figure 6.4a).

Much publicity has been recently focussed on the advantages of the continuously variable transmission (CVT). There are many ways of achieving an infinite number of ratios in a given span, but the two most well developed and therefore at present, feasible designs are the Perbury traction drive (Stubbs,1981) and the vee-belt drive (Scrinvansan et al,1982)(Steig et al.,1982)(Ludolph,1964).

The advantage the CVT has over the discrete ratio transmission lies in the continuous or infinitely variable nature of the transmission - being able to operate an i.c. engine at its most efficient point of any given speed over a wide ratio span. Mapping this locus onto an engine fuel map produces the so-called CVT line (the dashed line in Figure 6.10). This leads to an improvement in the average i.c. engine efficiency, and, providing CVT efficiency can be maintained sufficiently high, an improvement in fuel economy. Unfortunately, however, CVT efficiency, particularly at part-load can be significantly lower than a discrete ratio unit (80-90% compared to >90%) respectively).

When used in the hybrid-electric vehicle appliction, not only is the CVT ratio selected to optimise i.c. engine efficiency, but also electrical system efficiency. Thus, the optimistion algorithm creates a CVT line unique to the hybrid - although for the energy saving aim, because the i.c. engine dominates, the resulting usage points on the fuel map of Figure 6.10 (shown for both discrete ratio and CVT cases) resemble the dashed CVT line.

The results obtained by substituting the base 4-speed unit with a typical CVT design - the Perbury traction drive, similar to the one described by Stubbs (Stubbs,1981) - are shown for the ECE-15 cycle in Figure 6.11a. The CVT shows no improvement over either the 4 or the 6-speed units over the range of battery sizes from 500 Kg to 300 Kg. However, for the vehicles with the very small battery sizes (100 Kg and 200 Kg), the CVT does show a significant improvement - as illustrated more clearly in Figure 6.11c for the 3 transmission types over a range of battery sizes but using the PICE/PTOT value corresponding to the best result in each case. This is reflected in the i.c. engine efficiency shown in Figure 6.11b which was previously shown to be 23-26% for the 2 discrete ratio units, but now is 27-28% for the CVT. This improvement in i.c. engine efficiency for the CVT occurs because, as the battery size (and hence electrical system) is reduced, so the i.c. engine must play a larger role throughout the driving cycle. Without a significant 'load-levelling' contribution from the electrical system to maintain i.c. engine efficiency high, the transmission must now perform this task - at which the CVT is superior than the discrete ratio transmission.

For the two cruise cases - shown for 56 mph in Figue 6.12a and 75 mph in Figure 6.12b - the CVT gives no benefit over the 4 speed discrete ratio unit. This is because the small i.c. engine (compared to the conventional vehicle) inherent in the hybrid returns efficiencies at cruise of typically 24-28% for the 4-speed case,and so does not offer the same scope for improvements experienced for conventional vehicles. The CVT does improve i.c. engine efficiency relative to the base 4-speed case - raising it to 27-29% as Figure 6.12c shows - but these benefits are eroded by signficantly poorer transmission efficiency for the CVT of typically 80-90% compared to >90% for the discrete ratio unit.

The battery weight - PICE/PTOT curves shown for the CVT at cruise in Figures 6.12a and 6.12b also show no significant fall-off in mpg as PICE/PTOT rises - indicating that the CVT, because of its infinite number of ratios available in a given span is superior at matching the i.c. engine to the road-load to achieve a high i.c. engine efficiency.

6.3.4 Effect of Changing Power Source Type/Map

The effect of different and more advanced power source types are studied using computer simulation by using a different efficiency map (see chapter 2) relative to the base-line units described in section 6.2 (i.e., the spark-ignition or gasoline i.c. engine and the DC shunt field wound traction motor).

Highly advanced power source types, such as gas-turbine, rankine or stirling heat engines and synchronons traction motors will not be considered here, partly because of the timescale involved in their development and partly due to the unavailability of adequate data in map form.

In the case of the heat-engine the obvious alternative to the spark-ignition engine is the compression ignition or diesel engine. However, due to, again the lack of data for an advanced (probably high-speed direct injection) diesel engine type, it is proposed to study the effect of an advanced i.c. engine by using an advanced spark-ignition i.c. engine map. The map in question is for a 3 cyclinder unit currently under development by several manufacturers and with significantly higher efficiency (lower SFC) than current units.

Despite the unavailability of a suitable diesel engine map, the trend in results for the hybrid-electric vehicle will be the same whatever the map used providing it does not exhibit any radical shift in the position of the maximum efficiency with load and speed and also providing it exhibits an improvement in efficiency relative to the base-line unit.

In the case of the traction motor, the two most attractive near-term alternatives to the series and shunt machines were highlighted in chapter 4 as being the D.C. switched reluctance machine and the A.C. induction machine. Of these two it is proposed in this section to consider only the A.C. induction motor as it has already been considered as an alternative traction drive for several applications - not least of which was the Stirlec hybrid-electric car (Agarwal et al., 1967)

6.3.4.1 Effect of I.C. engine Type

The results for the base vehicle with the advanced 3 cylinder i.c. engine over the ECE-15 are given in Figure 6.13a. Because of the lower SFC (higher efficiency) inherent in the 3 cylinder map mpg over the range of battery sizes and values of PICE/PTOT is 10-20% higher than for the base vehicle of section 6.3.1. Figure 6.13b gives corresponding component efficiencies and although motor efficiency (both motoring and regenerating) remains roughly unchanged, i.c. engine efficiency is now ranging from 25-30%.

The 56 mph and 75 mph cruise results for the 3 cylinder map are shown in Figure 6.14a and exhibit the same trends discussed in section 6.3.1 for the base vehicle, but with higher mpg values due to the reductions in SFC over the range of battery sizes and relative power source fractions. The i.c. engine efficiency variations at 56 mph and 75 mph for the 200 Kg battery size is presented in Figure 6.14b and shows efficiency to now vary over the range 25-35%. At the 75 mph cruise condtion an interesting trend is observed in terms of i.c. engine efficiency and correspondig mpg - in that an optimum PICE/PTOT is consistently indicated - Figures 6.14a and b. This is due to an extremely symmetrical contour layout for the 3 cylinder map - as shown in Figure 6.15. At the engine speed corresponding to the

75 mph cruise (4000 rpm) as the load factor (torque or BMEP) is reduced with increasing PICE/PTOT the operating point will move vertically downwards. Efficiency will initially rise and then fall off.

An important point to make in this section is that the 3 cylinder map has been used to span the required power range of 25 KW to 55 KW for the study in this chapter, whereas for the state-of-the-art units in the base vehicle, 3 maps were used. For the current maps there is recommended range either side of the nominal over which scaling can be realistically achieved (see chapter 2), as a result of which typical 1.0 litre, 1.1 litre and 1.6 litre maps (shown in Figures 6.16 to 6.18) were used to span the required range. Wider ranges are theoretically possible with the advanced 3 cylinder engine, however, because the cylinder size used (300-400cc) is thought to enable capacity/rating changes to be made by increasing the number of cyclinders - rather than a combination of cylinder capacity and cylinder number changes - so linearising the scaling process in practice and justifying the use of a single map for simulation (B.L.).

With the differing SFC values due to mechanical differences between the 3 current maps there will be a 'clouding' effect on results in terms of the discontinuity of moving from one map to the next. Figure 6.19 repeats the results for the base vehicle at section 6.3:1 using the 300 Kg battery size when using the 3 maps and also the single 1.1 litre map to span the require power range. Although, as Figures 6.16 - 6.18 show, the 3 maps have different SFC values and contour layouts (i.e. maximum efficiency occurring at different loads and speeds), Figure 6.19 shows that overall results are not significantly clouded. The fact that the 1.1 litre map is more efficient than the 1.0 litre map, and the 1.6 litre map is more efficient than the 1.1 litre map (Figures 6.16 - 6.18) is borne out by these results.

6.3.4.2 Effect of Traction Motor Type

Results for the A.C. induction motor in place of the D.C. shunt motor over the ECE-15 cycle are shown in Figure 6.20a. Due to the significantly higher motor/controller efficiency for the induction machine compared to the shunt machine, (Figures 2.20 and 2.13 respectively) plus the knock-on effect in the traction battery (reduced average power density leads to greater average energy density), electrical system efficiency as a whole is increased. The result is that the electrical system can be used to a greater extent than for the base vehicle, meaning that the i.c. engine is used less and generally only for the heavier loading conditions - so returning a higher mpg. The improvement in mpg of up to 40-50%, in Figure 6.20a, is shown to be largely due to traction motor efficiency by the component efficency curves of Figure 6.20b - with the i.c. engine efficiency only slightly improved relative to the base vehicle. The absolute value of the improvement will clearly be due to the accuracy of the data obtained for the advanced machine.

At both 56 mph and 75 mph cruise conditions, although there is a small weight advantage for the induction motor/controller, (see chapter 2) results are not affected as vehicle power requirements at cruise depend more upon vehicle drag than weight.

Unlike the heat engine, scaling of the traction motor maps for the traction motors has been achieved using a single map within a given motor type over the range required of 20 KW to 55 KW. This assumption is valid since due to the inherent mechanical simplicity, mechanical changes do not accompany power rating changes, with the result that efficiency does not change.

6.4 Petroleum Substitution Aim

As was introduced in chapter 1 and expanded upon in chapter 5, the petroleum substitution aim seeks to reduce petroleum dependence by the substitution of petroleum by the more abundant broader energy base associated with wall-plug electricity. For this hybrid philosophy to be viable, the vehicle must return, when in the hybrid mode, a petroleum fuel economy greater than the equivalent i.c. engined vehicle whilst being capable of a greater range to battery discharge than the equivalent pure electric vehicle.

Because substitution is the principle aim, the battery size required will be larger than for the energy saving aim of section 6.3, and to demonstrate an increasing degree of substitution will therefore be considered over the range of 400 Kg to 700 Kg.

6.4.1 Effect of Relative Power Source Fraction

In chapter 5 for a fixed battery size and relative power source fraction, results for the petroleum substitution hybrid were presented in terms of range for a given mpg and vice-versa. However in this chapter to show the effects of the variations in battery weight and PICE/PTOT on both range and mpg, results are presented for each battery weight - from 400 Kg to 700 Kg in steps of 100 Kg - and show the range versus the mpg for a discrete set of PICE/PTOT values. Figure 6.21a shows how these results are presented for the 400 Kg battery size. For each PICE/PTOT curve results are produced in exactly the same way as was done in chapter 5 - by varying the ratio of to force the optimum control algorithm to change the empahsis between the two on-board energy sources.

The results in Figure 6.21a over the ECE-15 cycle show that, as the value of PICE/PTOT increases over the range previously described, vehicle range for a given mpg increases. The reason for this trend is apparent if

one considers moving over the relative power source fraction range 0.53 to 0.6. Over this range i.c. engine 'off-time' increases from 83.7% to 84.7%, and, as the component efficiency curves of Figure 6.21b show, although i.c. engine efficiency remains roughly constant at 27%, motor efficiency increases from 75% to 76% on motoring and from 61% to 63% on regeneration. Therefore although experiencing greater use as PICE/PTOT increases, the electrical system is also becoming more efficient as it decreases in size over this range. The electrical system increased use is therefore compensated for by the increased efficiency and mpg for a given range increases. Figures 6.22a and 6.22b show the variation of primary source fraction X over the ECE-15 for PICE/PTOT values of 0.53 and 0.6 respectively and illustrate the decrease in i.c. engine use.

When the same vehicle is simulated over the more severe J227aD cycle - the results of which are presented in Figure 6.23a - there is no such clear trend in the variation of the mpg/range curves with PICE/PTOT. Indeed the points are sufficiently close together to suggest little or no variation. The reason for this is apparent if one looks at the component efficiency curves over this range of PICE/PTOT, which are shown in Figure 6.23. Because of the severity of the cycle, i.c. engine load factors remain high with increasing PICE/PTOT, resulting in a high constant efficiency of about 30%. Similarly, for the traction motor as PICE/PTOT increases, due to the relative severity of the cycle average load factors on the motor remain high for both motoring and regenerating with the result that efficiency stays approximately constant. Although vehicle weight decreases as PICE/PTOT rises, for the reasons explained in section 6.3, the change is small and so as PICE/PTOT rises the suggestion is that mpg for a given range does not significantly change.

It is also interesting to note that the value of PICE/PTOT is limited over the J227aD cycle in that above a value of 0.67 all electric operation

is restricted due to the small size of the traction motor. This is a lower value than the figure of 0.75 obtained when the vehicle was simulated over the comparatively mild ECE-15 cycle.

The trend highlighted for the 400 Kg battery size over the ECE-15 cycle in Figure 6.21a is repeated consistently over the range of battery sizes considered here - from 400 Kg to 700 Kg - and the results for the 500 Kg, 600 Kg and 700 Kg battery sizes are presented in Figures 6.24, 6.25 and 6.26 respectively. Generally, as battery weight increases then range for a given fuel consumption also increases due to the increasing on board electrical stored energy. As with the energy saving aim of section 6.3 total installed power is adjusted as vehicle weight increases to maintain a constant performance with the result that generally, prime mover load-factors, and hence efficiency, remain constant over the range of battery sizes. Thus the increase in range for a given mpg is largely due to the difference between the stored energy increment and the vehicle propulsive energy increment.

In a similar fashion to the energy saving vehicle of section 6.3, the petroleum substitution fuel consumption at 56 mph and 75 mph cruise over the range of battery sizes and values of PICE/PTOT, and using the base 4-speed transmission, can also be presented, and are shown in Figure 6.27. The results show the same trends as for the energy saving aim for a given battery weight, with increasing PICE/PTOT in that as i.c. engine load factor decreases, so does its efficiency and hence mpg decreases. The trend is less pronounced for the 75 mph case as i.c. engine load factors at this speed remain relatively high, even at the high values of PICE/PTOT. Similarly as battery size increases, due to the increase in vehicle weight offsetting any gains in i.c. engine load-factor, mpg falls. At 75 mph, again the trend is less pronounced due to the fact that as vehicle speed increases, propulsive energy requirements are more dependent on vehicle drag

than weight. The result is that at 56 mph over the range of battery sizes from 400 Kg to 700 Kg mpg falls from 43-50 down to 40-45, whereas at 75 mph over the same range, mpg falls from 33-35 down to 32.

Again, as with the energy saving aim, the effects of the relative power source fraction on vehicle gradeability can be studied. Figure 6.28 shows how the value of PICE/PTOT affects vehicle maximum speed on a 2% gradient for the 400 Kg battery size only, and gives the same trend obtained for the energy saving case. If different battery sizes were to be studied it is fairly clear that the trends would, again, follow those presented for the energy saving case.

6.4.2 Effect of Battery Weignt

Although the effects of battery weight were briefly discussed in the previous section, this section seeks to study the effects of battery size on the hybrid-electric vehicle in terms of its all-electric performance.

Although all-electric performance was highlighted in section 6.3 for the energy saving aim as being important in terms of increasing the vehicle operating flexibility in sensitive urban areas or after i.c. engine breakdown as a get-you-home mode, this aspect is more important for the petroleum substitution aim since the vehicle is intended to displace petroleum as much as is possible without unduly restricting all i.c. engine operation for, say, long distance operation.

All electric urban operation is desirable for two reasons. Firstly, to minimise noise and pollution in sensitive urban areas, and secondly to remove the cold-start penalty associated with such journeys undertaken by i.c. engined vehicles, or indeed by a hybrid vehicle when running in a hybrid or all i.c. engine mode.

In a similar fashion to the pure electric vehicle study of chapter 4 the all-electric range of the hybrid, per unit battery weight (the specific range) versus the battery weight, per unit vehicle weight (specific battery weight), can be plotted for several driving cycles and using different battery types. The hybrid, however, differs from the electric vehicle in that several all-electric ranges are possible for a given battery weight, depending upon the value of PICE/PTOT. The value of PICE/PTOT to give the maximum range without restricting all-electric performance was therefore selected, and the results are presented in Figure 6.29.

Essentially, the specific range is a measure of the "effectiveness" of the battery, and for the lead-acid case over the ECE-15 cycle, shows a maximum at a specific battery weight of 0.2 - 0.25.. To the left of this optimum, because of the small battery sizes relative to the size of the vehicle, (hence its propulsive power requirements) power density demand on the battery is high, so reducing the energy available - as shown in the power density/energy density curves of Figure 4.17. But to the right of optimum, as the battery is an increasing fraction of total vehicle weight, the result is that an increasing proportion of the stored energy increment is being used to propel the corresponding battery weight increment rather than useful payload.

The battery fraction corresponding to the optimum is lower than the fraction suggested for the lead-acid battery in the electric vehicle study of chapter 4 (0.2 - 0.25 compared with 0.25), and suggests a battery weight for the base hybrid of about 400-500 Kg. The lower optimum battery weight fraction for the hybrid when compared with the pure electric vehicle can be explained by the fact that the ECE-15 cycle used here is 'milder' than the J227aC cycle used in chapter 4. Although both cycles specify the same maximum speed (30 mph), the latter demands a greater acceleration to reach this velocity with the result that in order to achieve the same power

density demands on the traction battery, a larger battery size in relation to vehicle power requirements (battery fraction) must result.

As Figure 6.29 shows the aforementioned curve is repeated for the lead-acid battery at a steady 56 mph cruise and over the more severe J227aD cycle; and for two advanced batteries (the nickel-zinc and nickel-iron types) again, over the ECE-15 and also at a steady 56 mph cruise.

Over the J227aD cycle the optimum occurs at a higher battery weight fraction than for the ECE-15 cycle (0.25), implying that, because of its relative severity, a larger battery must be used in order to minimise power density demands. However, at a steady 56 mph cruise, the optimum is implied at a higher battery weight fraction still, suggesting that, since vehicle power demand is not so dependent upon vehicle weight, extra battery energy is mainly going towards propelling payload over this range.

When considering the two advanced cell types in Figure 6.29 over the ECE-15 cycle, because of the slopes of the power density/energy density curves relative to the lead-acid battery of Figure 4.17 (steeper) for small battery sizes relative to vehicle power requirements energy stored does not reduce to the same extent as for the lead-acid battery and so the optimum occurs at a lower battery fraction in each case. In a similar fashion to the lead-acid battery at 56 mph, the two advanced cell types show the same trends relative to their respective urban cycle results, in that because of smaller dependence vehicle power requirements have on vehicle weight at cruise, a higher optimum battery fraction is implied.

It is important to note that for each of the 56 mph cruise results of Figure 6.29 the curve still has to rise to an optimum, even though power density demands on the smaller battery sizes are comparatively low, because now the amount of on-board stored energy is limited by battery size rather than battery size in relation to the vehicle power requirements (power density).

6.4.3. Effect of Battery Type

Section 6.4.2 has already discussed how battery type will affect vehicle performance in the all-electric mode, but with the emphasis on studying battery size.

In this section, for a fixed battery size - again the 400 Kg case - seeks to assess the effect of the same advanced cell type used in the energy saving study of section 6.3 (the nickel-zinc type) over the ECE-15 urban cycle.

Figure 6.30 repeats the results of Figure 6.21a with the lead-acid battery now replaced by the advanced nickel-zinc type.

The mpg/range curves at each value of PICE/PTOT show an identical trend to that of the lead-acid case in Figure 6.21a - in that mpg for a given range consistently rises as PICE/PTOT increases. However, due to the more favourable power density/energy density characteristic of the nickel-zinc cell compared to the lead-acid cell both in terms of slope and maximum energy density, at each value of PICE/PTOT range for a given mpg is higher - the extent of which is more than 100%.

The more advanced battery has the added advantage of increasing all electric range by the same order of magnitude as for the hybrid mode.

6.4.4 Effect of Transmission Type

In a similar fashion to the energy saving aim of section 6.3, the petroleum substitution hybrid with a 400 Kg battery of the lead-acid type and a 4 speed tansmission can be used to discuss the effects of a wide-ratio 6-speed discrete ratio transmission (chosen for the reasons discussed in section 6.3) and a state-of-the-art CVT (again, as for section 6.3 - the Perbury type). Figure 6.31a repeats the results of Figure 6.21a for the 400 Kg battery size over the ECE-15 cycle but with the 4-speed transmission replaced by a 6-speed unit. No significant improvement in

terms of mpg for a given range is observed since the overdrive ratios in the 6-speed unit cannot be used to any significant extent due to the limits of power available under these driving conditions.

In the results presented in Figure 6.31b, the 4-speed unit is replaced by a Perbury CVT, and shows slightly poorer results compared to the 4-speed unit. Again, as was discussed in section 6.3, although the CVT has the benefit of an infinite number of ratios over a wide span, any gains in prime-mover efficiency are erroded by the pooor transmission efficiency inherent compared to the discrete ratio units.

Although when in the all-electric mode, (which is important for this hybrid) fewer ratios and a reduced span could be used in the variable ratio unit with satisfactory results, because the vehicle needs the i.c. engine only mode to maintain vehicle flexibility a minimum ratio span of 3.5:1 is required - which if met by less than 4 ratios, would lead to driveability problems and increased energy consumption.

The results for the 400 Kg battery size at 56 mph and 75 mph steady-state cruises are shown in Figure 6.32a for both 4-speed, 6-speed and CVT units over a range of PICE/PTOT values.

Results for the 4-speed unit display results previously discussed in section 6.4.1, but for the 6-speed unit at 56 mph mpg remains roughly constant with PICE/PTOT as the overdrive ratios raise i.c. engine load-factor sufficiently high to maintain a roughly constant efficiency - as shown in Figure 6.32b. At 75 mph the 6-speed unit is still able to use the 0.8:1 overdrive ratio at low values of PICE/PTOT - so raising mpg relative to the 4 speed unit - but as PICE/PTOT increases, the deeper (0.6:1) overdrive ratio is available, with the result that mpg, in Figure 6.32, and i.c. engine efficiency, in Figure 6.32c experience a sudden step change.

Results for the CVT at 56 mph at low values of PICE/PTOT are similar to the 4-speed unit since there is insufficient power for the deep overdrive ratios to be used and any gains in i.c. engine efficiency - shown in Figure 6.32b - are erroded by poorer transmission efficiency. At higher values of PICE/PTOT, however, the deep overdrive ratios can be used, and as with the 6-speed unit at 75 mph, i.c. engine efficiency and mpg take a step change. Because at 75 mph over the whole range of PICE/PTOT values the overdrive ratios in the CVT cannot be used as the i.c. engine power available at the higher PICE/PTOT values is lost due to poor CVT efficiency. As a result, mpg is only slightly improved on the 4-speed unit, despite there being a substantial gain in i.c. engine efficiency - shown in Figure 6.32c - due to, again, poor CVT efficiency.

6.4.5 Effect of Changing Power Source Type

In a similar manner to that for the energy saving aim of section 6.3, the effect of advanced power source types can be studied by the use of the appropriae performance map in the simulation program. As with the energy saving aim it is proposed here to use the advanced 3 cylinder engine map and the A.C. induction motor map.

6.4.5.1 Effect of I.C. Engine Type

Figure 6.33a repeats the results of Figure 6.22a but with the state-of-the-art i.c. engine now replaced by the advanced 3 cylinder engine. As results show, because of higher overall i.c. engine efficiency (Figure 6.33b), mpg for a given range is raised over the range of PICE/PTOT values.

A similar pattern is repeated for the 56 mph and 75 mph cruise results - shown in Figure 6.34a - in that due to higher i.c. engine efficiency (Figure 6.34b) mpg values are raised relative to the base hybrid.

The point raised during the energy saving hybrid study of replacing several maps by a single map to span a given power range can also be studied here. Figure 6.35 shows for the base petroleum substitution case of section 6.4.1 how a single map compares with 2 maps to span the required power range of 45-55 KW. Although there are noticeable differences due to the discontinuity of moving from one map to another, the trends discussed in section 6.4.1 remain unchanged.

6.4.5.2 Effect of Traction Motor Type

Again, the effects of replacing the base-line D.C. shunt machine by an advaned A.C. induction machine can be studied and these are shown in Figure 6.36a.

Due to significantly improved motor/controller efficiency over a wide load and speed range, mpg for a given range is increased. The component efficiency curves - shown in Figure 6.36b show how, due to the improvement in electrical system efficiency (particularly during regeneration) the i.c. engine is used less and only during high load conditions, with the result that its efficiency is rasied also.

Although there is a small weight saving using the induction machine, cruise results are not affected to any noticeable extent and are therefore identical to those of section 6.4.1.

6.5 Conclusions

Of the vehicle parameters peculiar to the hybrid electric vehicle, that have been sensibly varied in this chapter, it has been assumed that as each has been considered in turn the others do not interact in any way - with the result that they have been held constant. This will probably not be the case for the majority of parameters considered here, but since an optimum combination of parameters is not suggested at any stage, as it is the purposes of this chapter to show trends as a parameter is varied (assuming that the remainder cannot) the approach can be justified.

To achieve an optimum combination of vehicle parameters would require to test all sensible combinations. In other words if there are NP parameters and NV1, NV2, NV3.....NV_{NP} values for each parameter, then there will be NV1 x NV2 x NV3....xNV_{NP} combinations to test in order to arrive at an optimum. However, simply finding an optimum combination will not indicate to what extent each parameter is contributing, so the approach here will enable the individual contributions to be sensibly predicted.

The general conclusions that are possible to make of the parametric study here can be directed at the energy saving aim and the petroleum substitution aim base vehicles in turn.

In this study of the energy saving hybrid the trend was for mpg to steadily increase as battery size was reduced. But the practical limitations in terms of battery voltage and useful all-electric urban range would limit the battery weight to 200 Kg for the lead-acid type.

For any given battery size, results for ECE-15 cycle suggested a relative power source fraction of up to 0.7 before all-electric performance was affected. Over the more severe J227aD cycle this fraction was lower at 0.5, and at the two cruise regimes - particularly at 56 mph where load factors are generally low - 0.5 - 0.6.

Results for the petroleum substitution aim on the other hand suggested a battery size as large as possible to maximise the amount of petroleum displacement achieved. Apart from the physical size of the vehicle there would be no definite constraint to the battery size to achieve substitution. But to make efficient use of the battery when in the all electric mode, a battery fraction of 0.2-0.25 was indicated - giving a battery size for this hybrid of about 400 Kg-500 Kg.

Again, for any given battery size the results suggested as large a relative power source fraction as possible before all-electric operation was restricted over the ECE-15 cycle - which was, again a value of 0.7.

Over the more severe J227aD urban cycle, results suggested that hybrid performance was independent of PICE/PTOT, however. But at the two cruise regimes, the trend was similar to that suggested by the energy saving results, again with values ranging from 0.5-0.6.

The inclusion of more advanced component types into the base vehicles, for both energy saving and petroleum substitution aims served to alter somewhat the values just described. Firstly, a more advanced battery type may suggest even smaller battery types in each case, although achievable voltage will still be a limiting factor in the energy saving case. Secondly, a wide ratio transmission serves to improve cruise performance only - and then only in the medium speed range (56 mph) due to the limits of available i.c. engine power at high speeds. Finally, more efficient prime mover types may serve to alter the previously suggested PICE/PTOT values in that a more advanced i.c. engine may suggest a larger values - given the limits at all-electric performance -, whereas a more advanced traction motor type may suggest a smaller value - so placing greater emphasis on the electrical system. Conversely the advanced prime mover types may simply allow greater emphasis to be placed upon one or the other power source - favouring the power source with the improved efficiency - within the previously suggested PICE/PTOT values - as has been shown here.

Finally, perhaps the most important vehicle parameter in the hybrid-electric vehicle, that has not been considered in this chapter is the control strategy that enables the two on-board power sources to be combined to achieve the energy saving and/or the petroleum substitution aim.

An optimum strategy has been considered throughout this parametric study so as not to 'cloud' the effects each parameter considered has on hybrid performance.

With a 'feel' for how each vehicle parameter will affect vehicle energy consumption, acceleration performance and maximum speed, the control strategy may now be studied in more detail.

FIGURE 6.1: J227aD Cycle

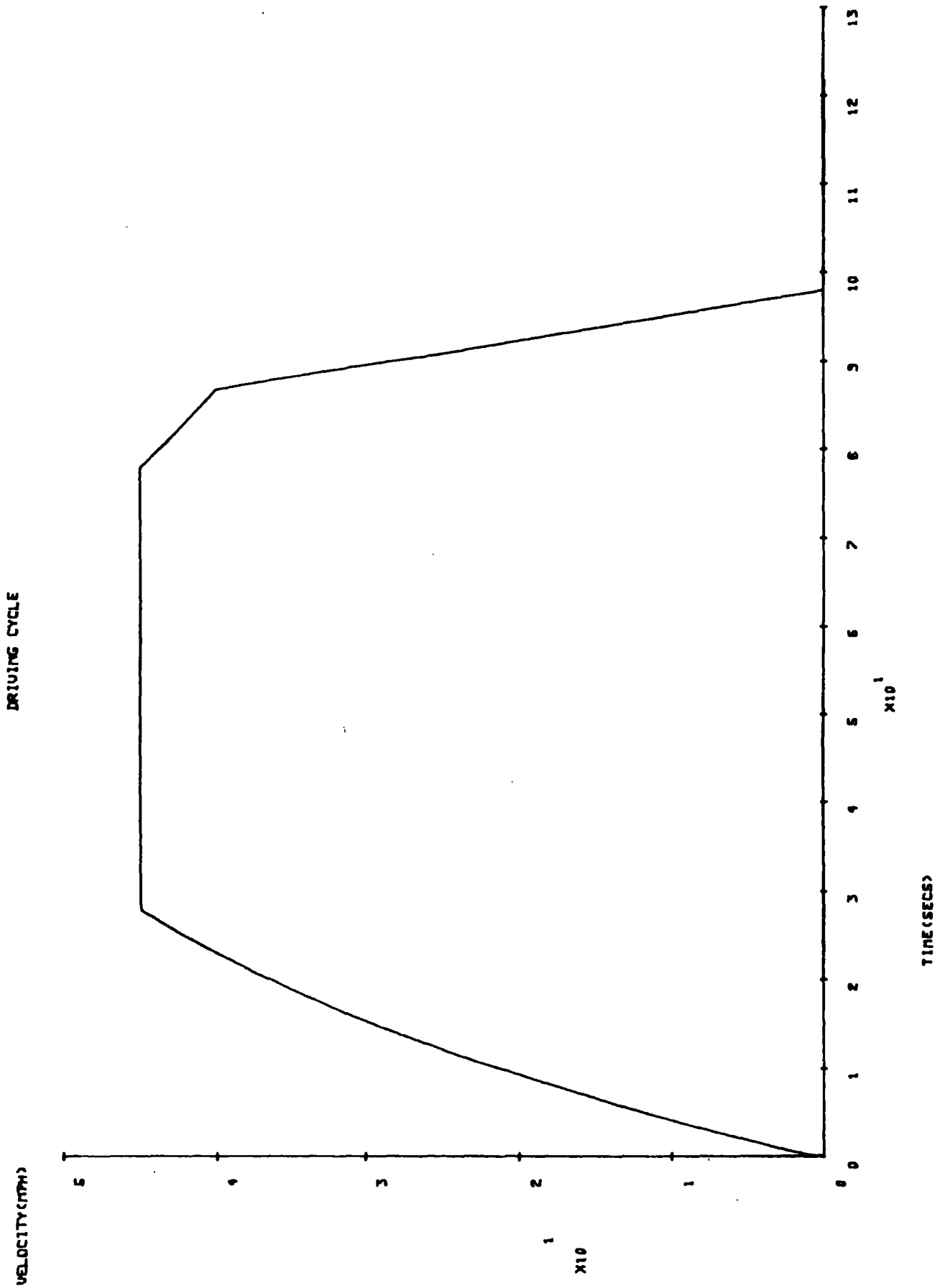

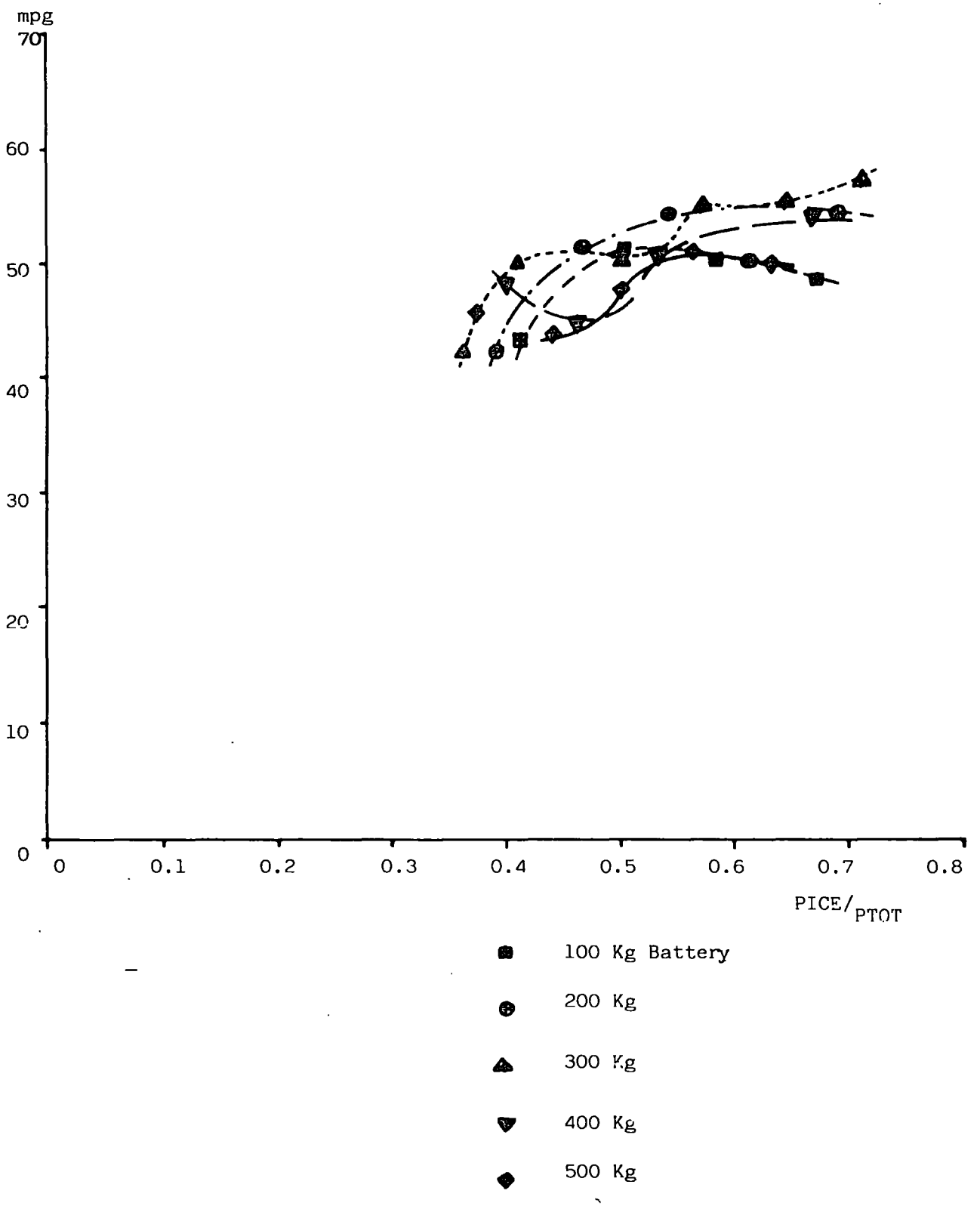

FIGURE 6.2a: Effect of Relative Power Source Size and Battery Weight on mpg for the Energy Saving Aim over the ECE-15 - base hybrid.

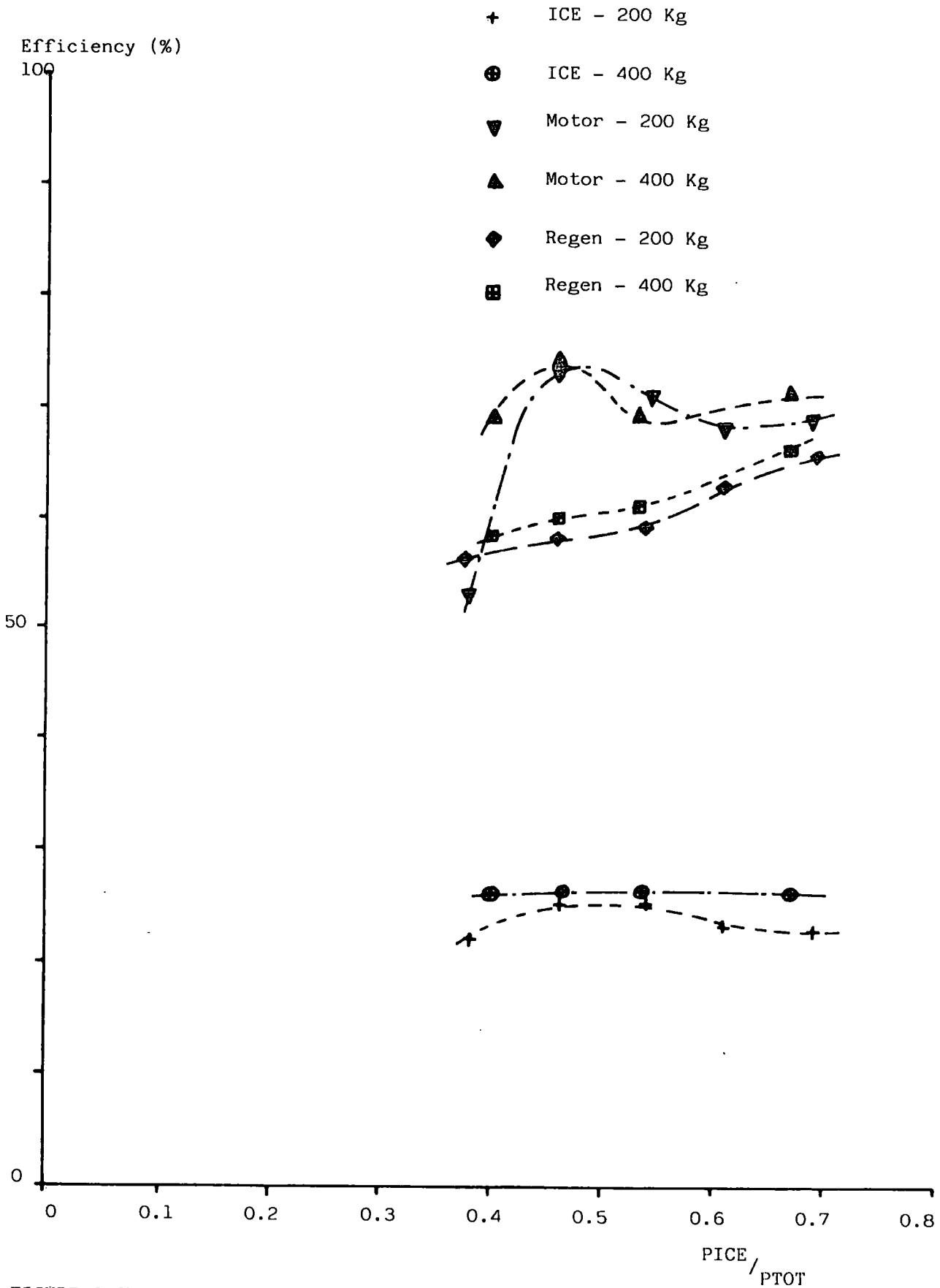

FIGURE 6.2b: Effect of Relative Power Source Size on Component Efficiency for the Energy Saving Aim over the ECE-15- 200 Kg and 400 Kg Battery Sizes - base hybrid.

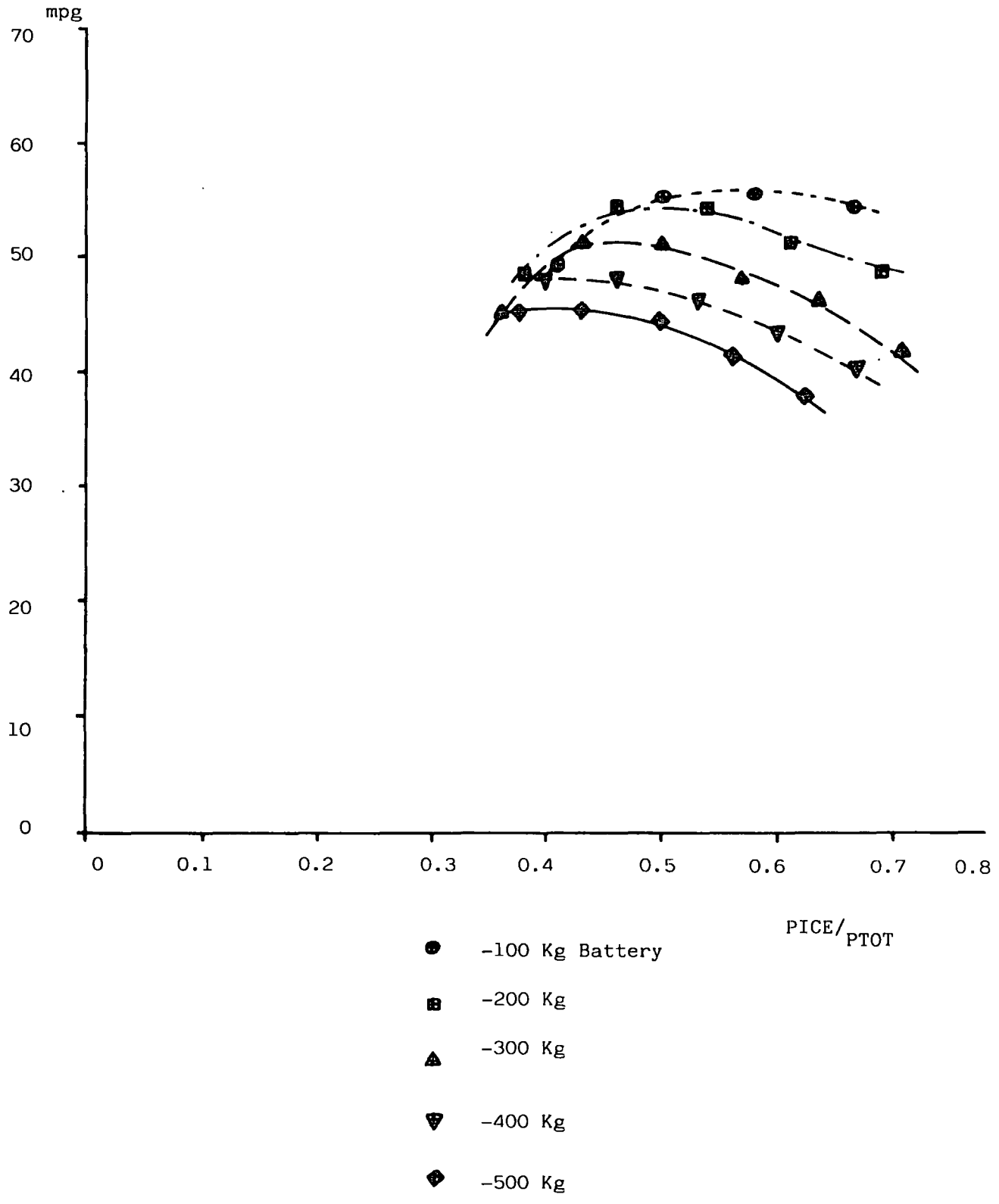

FIGURE 6.3a: Effective of Relative Power Source Size and Battery Weight on mpg for the Energy Saving aim over the J227aD - base hybrid.

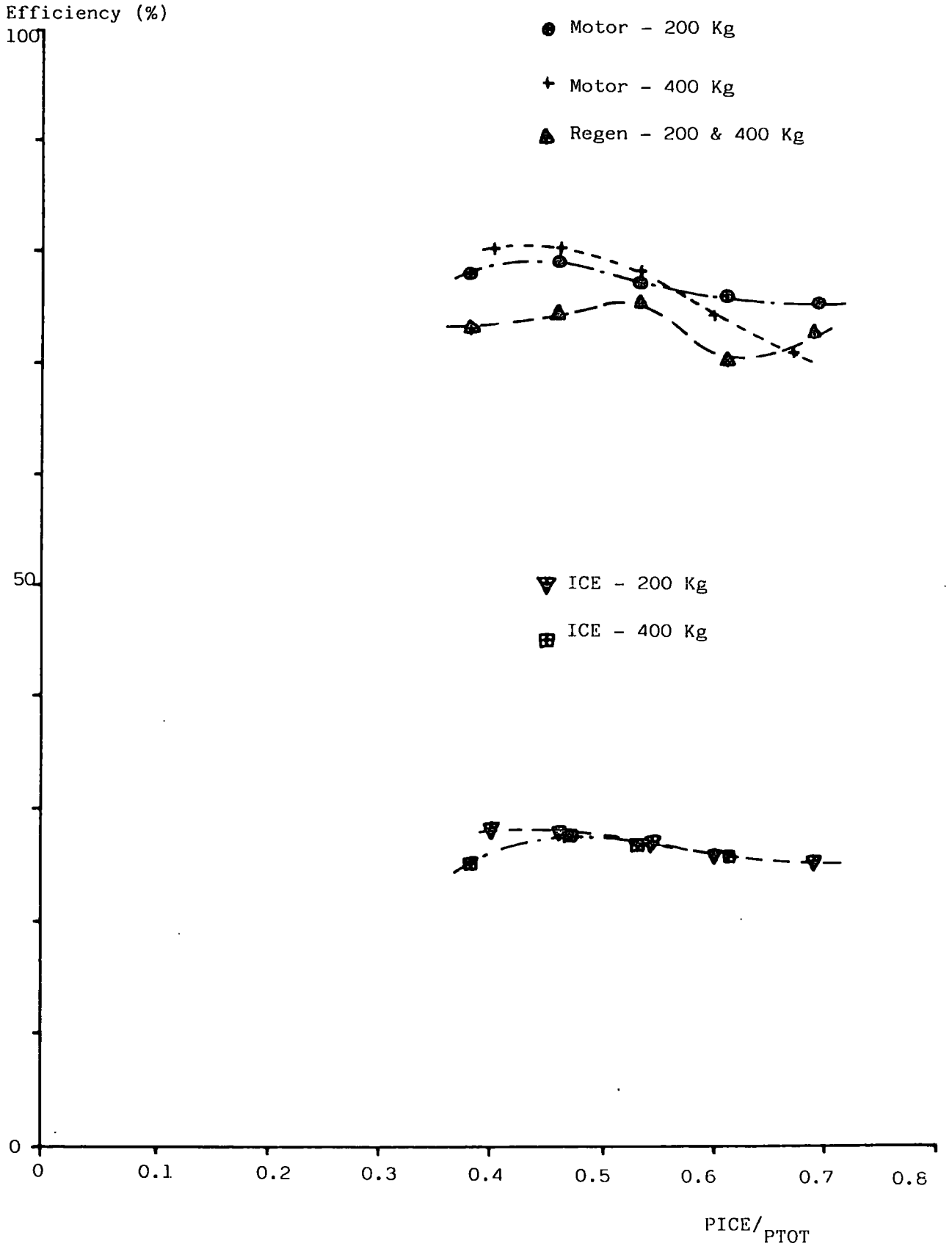

FIGURE 6.3b: Effect of Relative Power Source Size on Component efficiency for the Energy Saving Aim over the J227aD-200 Kg and 400 Kg Battery sizes - base hybrid.

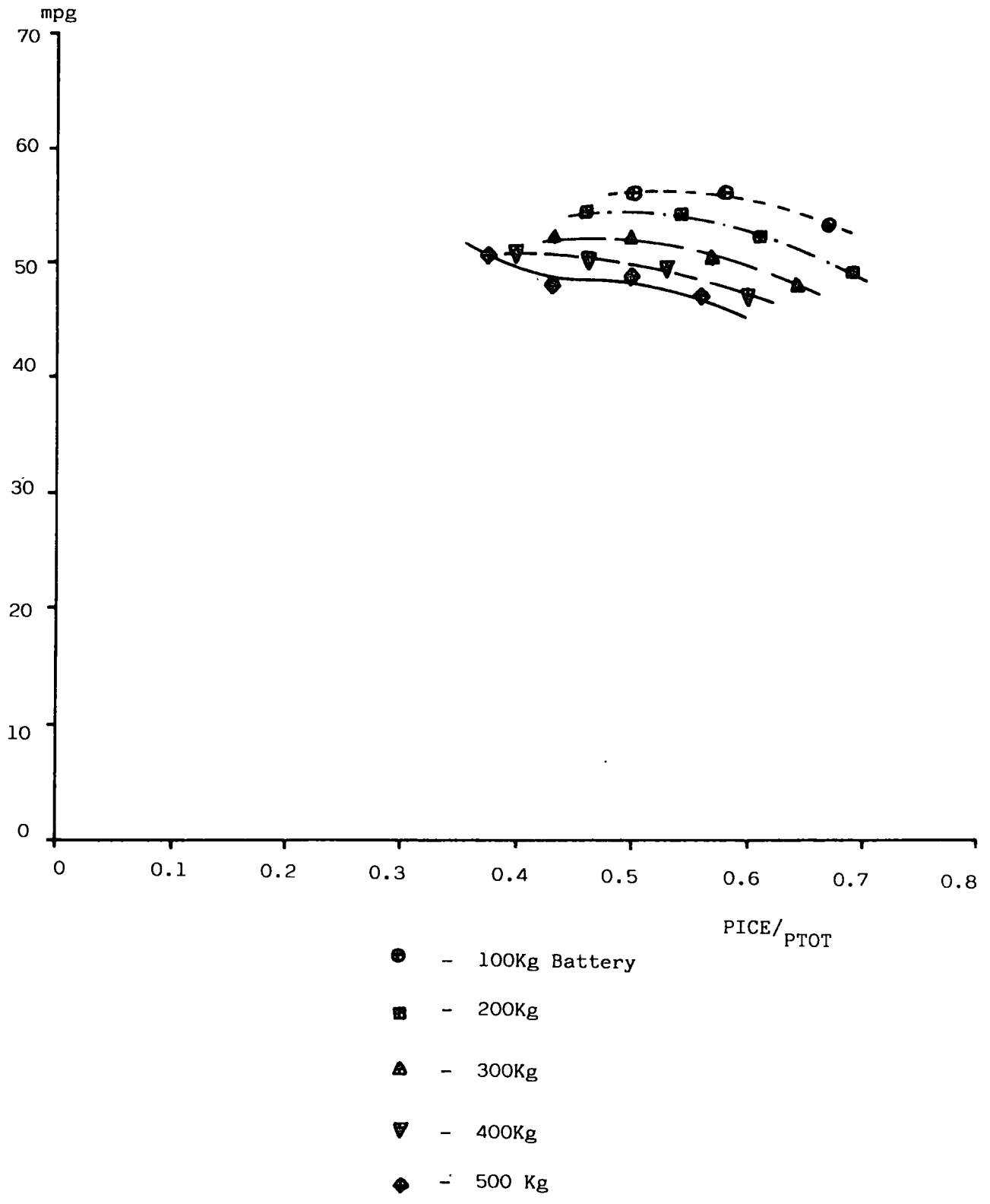

FIGURE 6.4a: Effective of Relative Power Source Size and Battery Weight on mpg for the Energy Saving Aim at 56mph cruise - base hybrid.

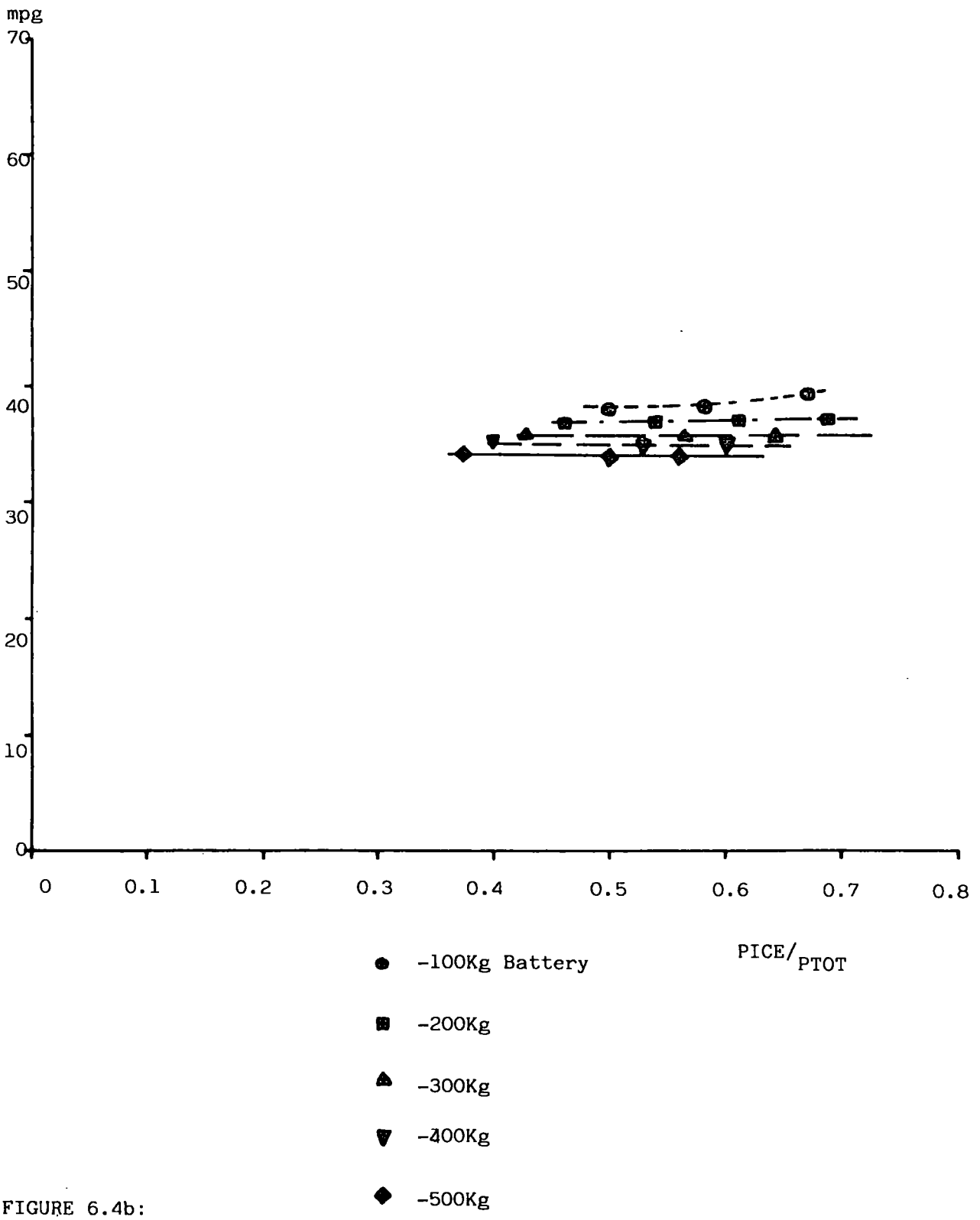

FIGURE 6.4b:

Effect of Relative Power Source Size and Battery Weight on mpg for the Energy Saving Aim at 75 mph cruise - base hybrid.

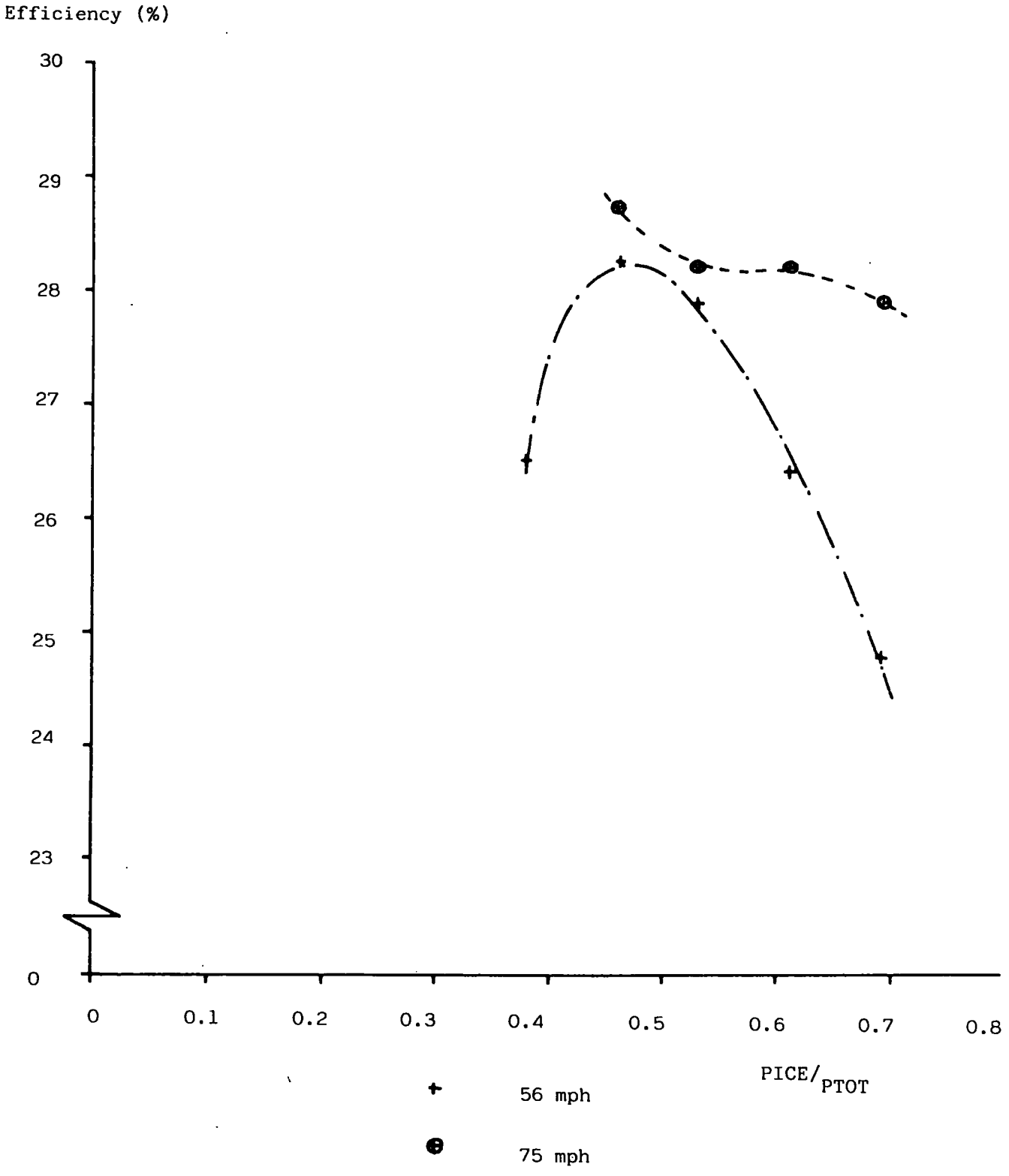

FIGURE 6.4c: Effect of Relative Power Source Size on Component Efficiency for the Energy Saving Aim at 56mph and 75mph cruise - base hybrid.

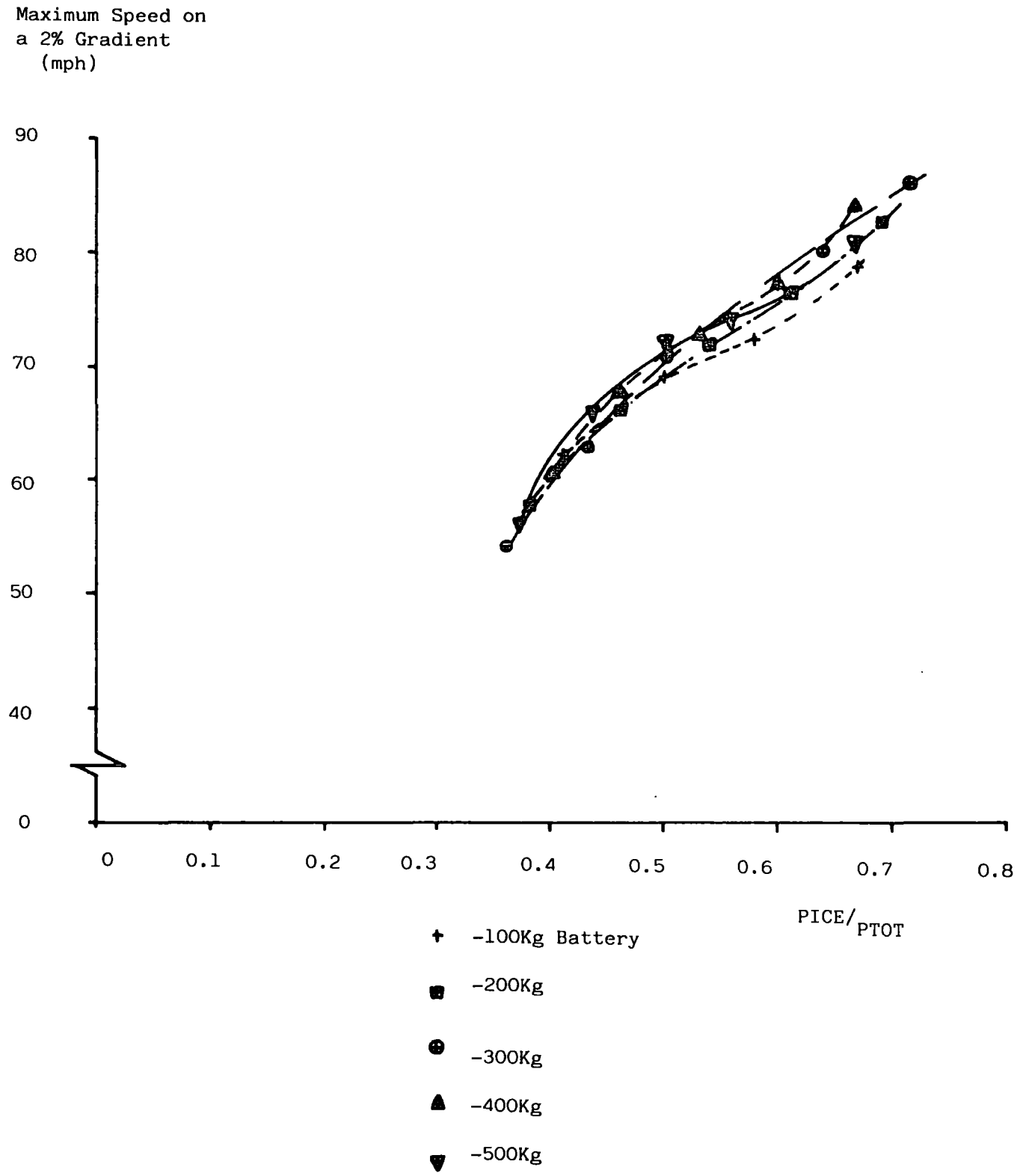

FIGURE 6.5: Effect of Relative Power Source Size and Battery weight on Gradeability for the Energy Saving Aim - base hybrid

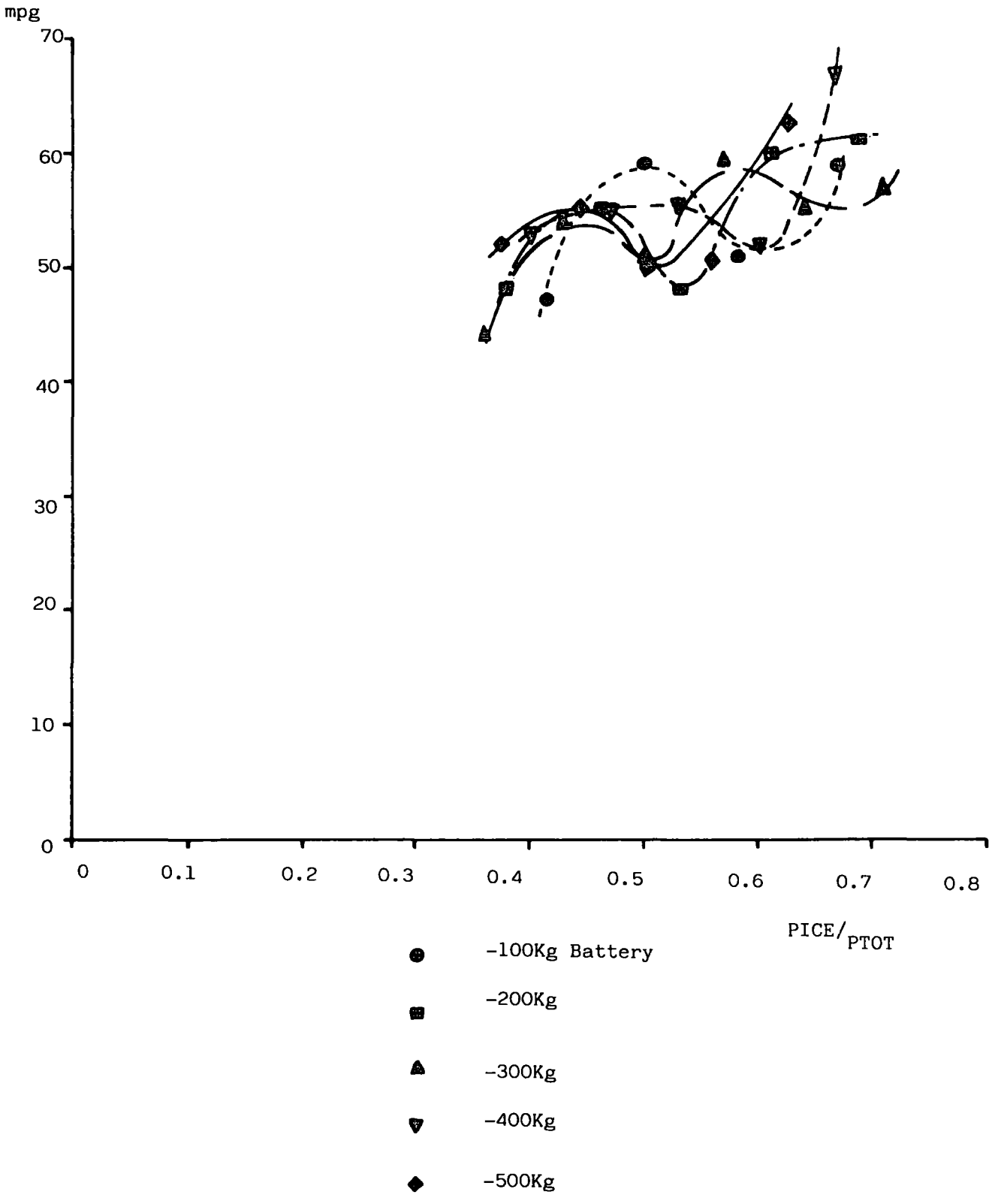

FIGURE 6.6a: The Base Hybrid of Figure 6.2a but with a Nickel-Zinc Battery type

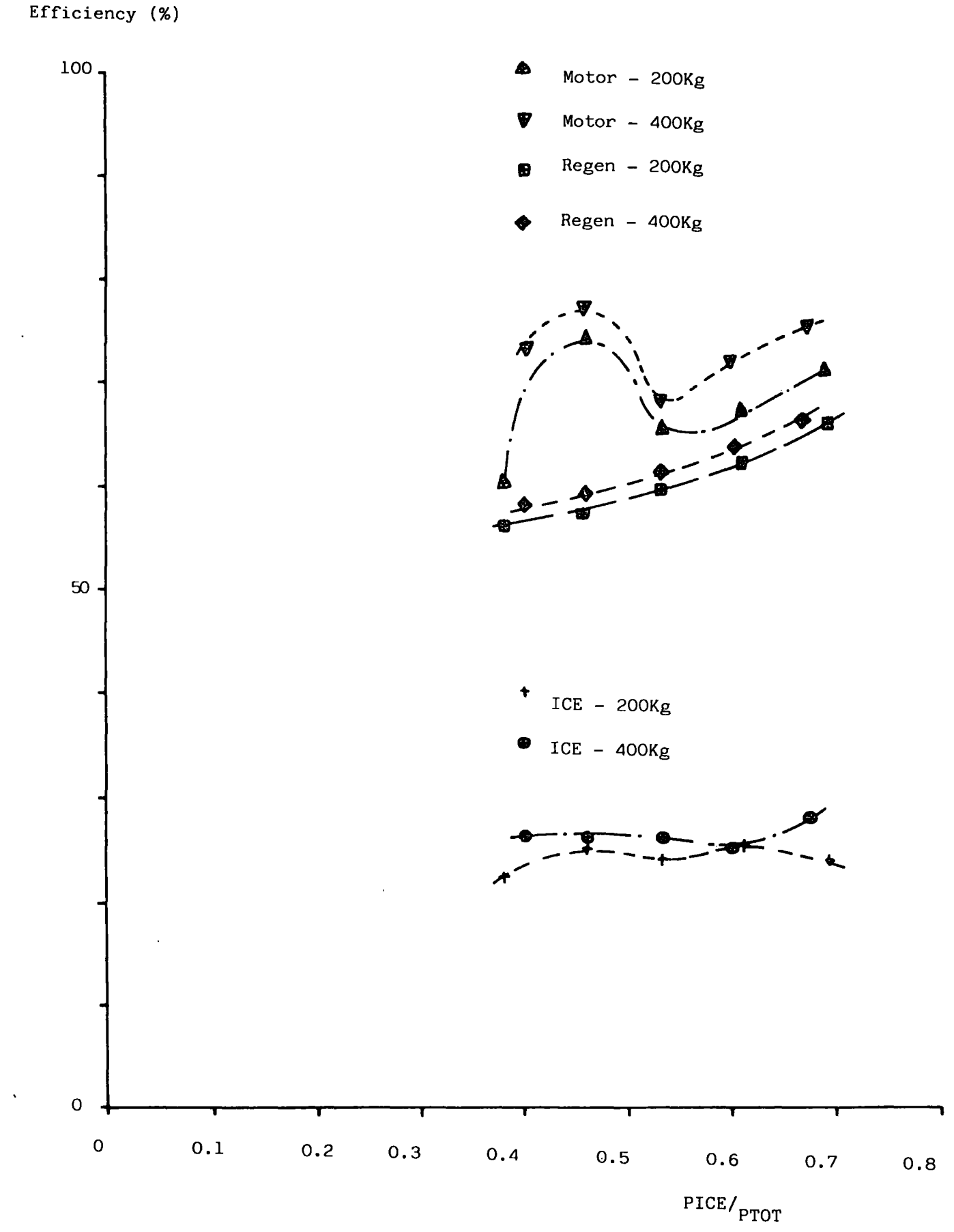

FIGURE 6.6b: The Base Hybrid of figure 6.2b but with a Nickel-Zinc Battery Type

FIGURE 6.7: Effect on mpg and Range of Altering the intermediate ratios in the base 4-speed variable ratio unit

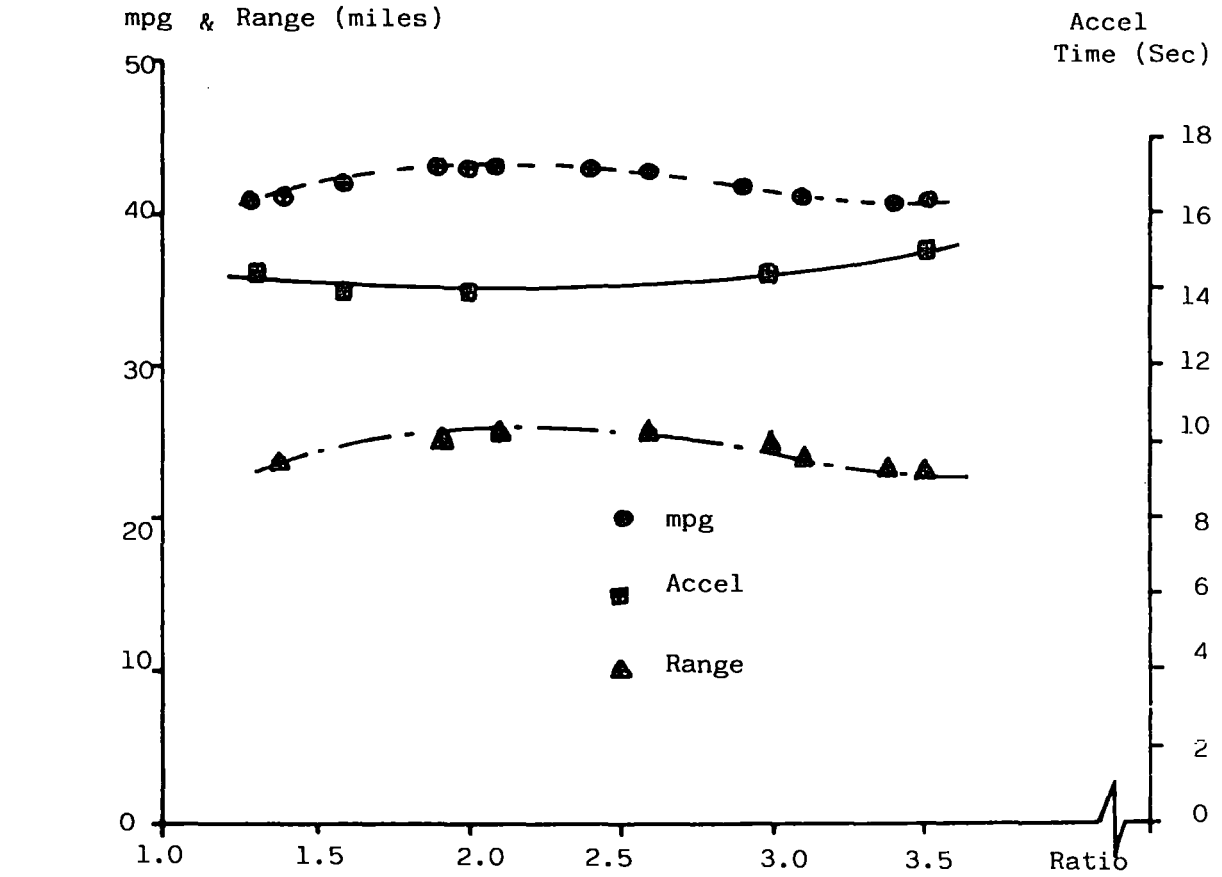

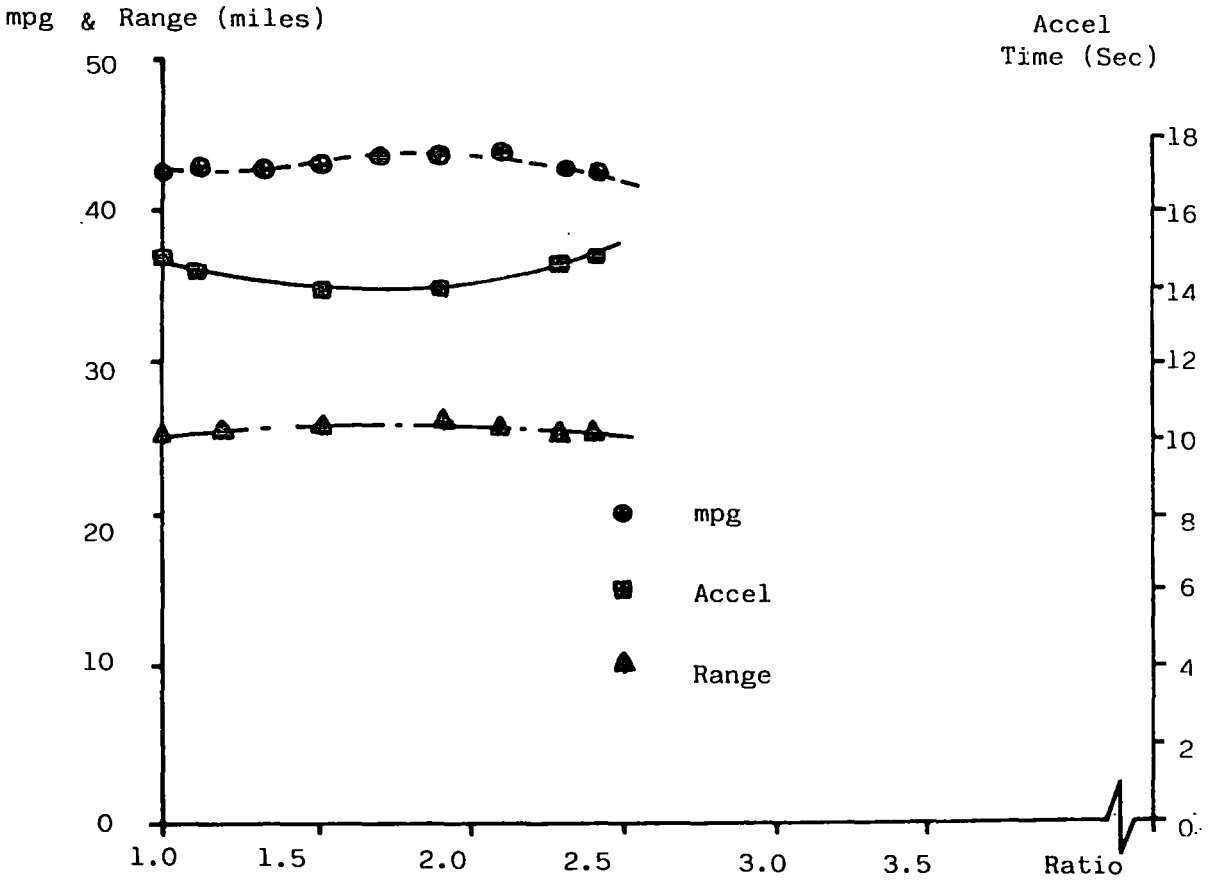

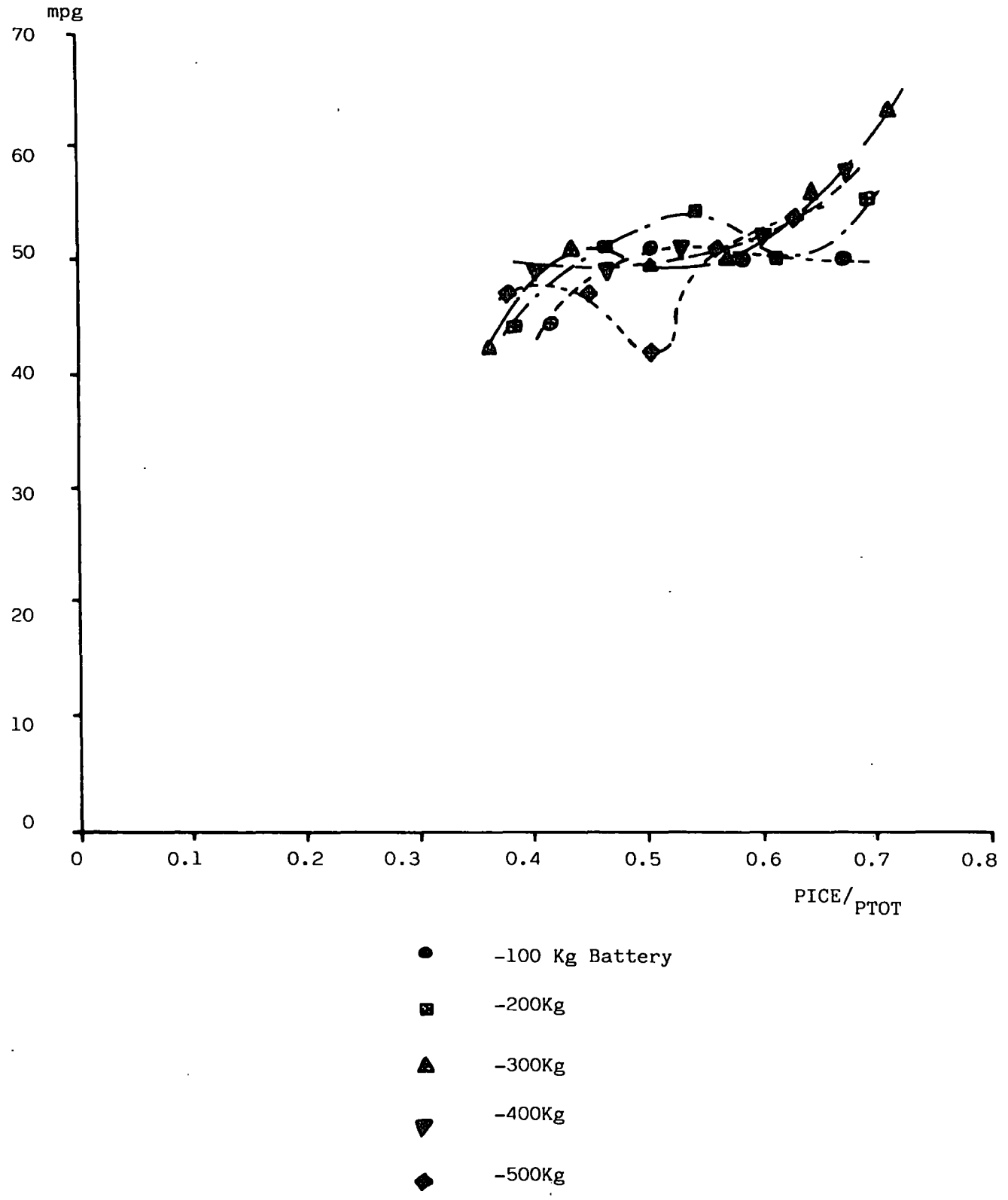

FIGURE 6.8a: The Base Hybrid of Figure 6.2a but with a 6-speed Variable ratio transmission.

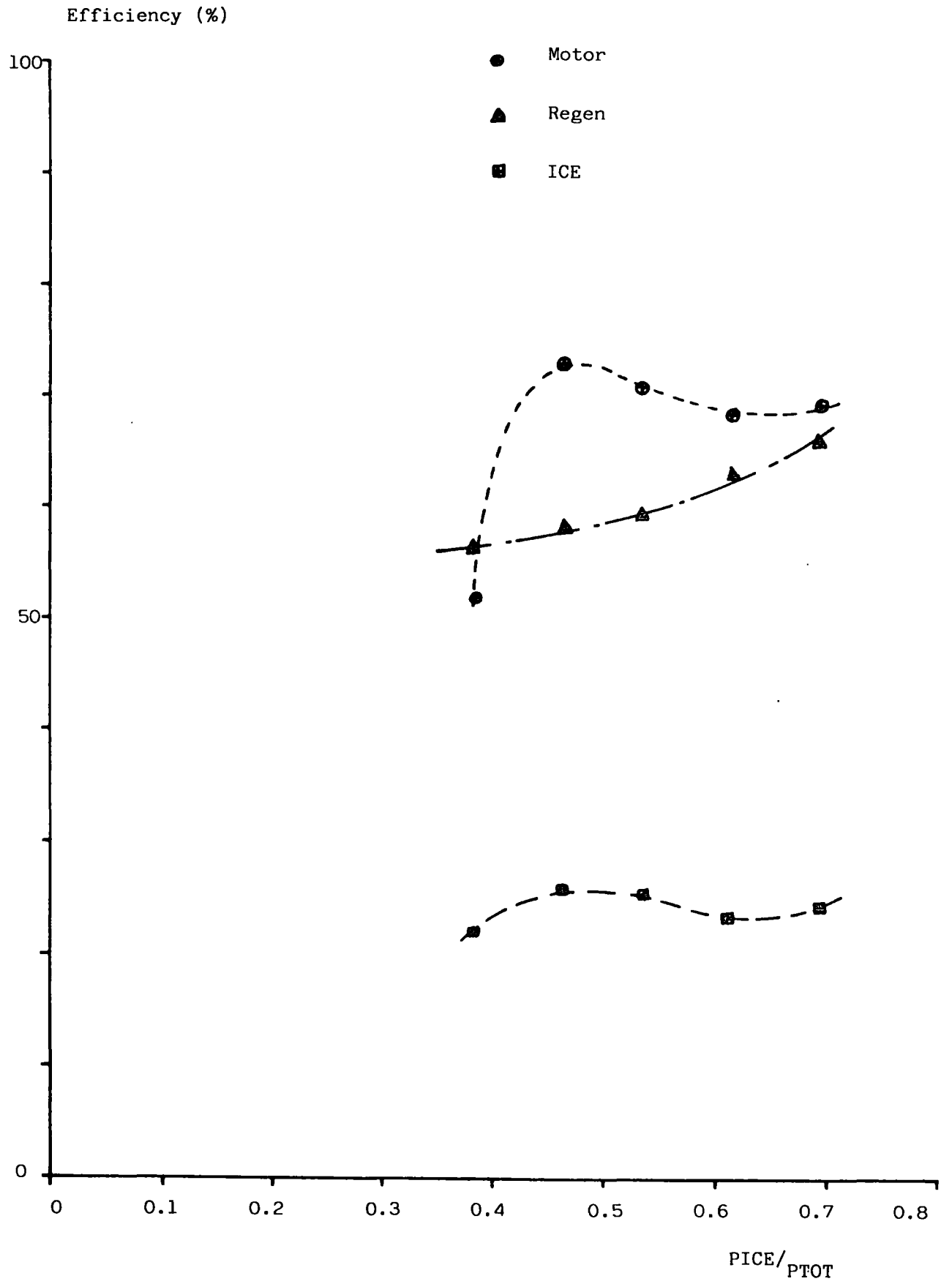

FIGURE 6.8b: The Base Hybrid of figure 6.2b but with a 6-speed variable ratio unit

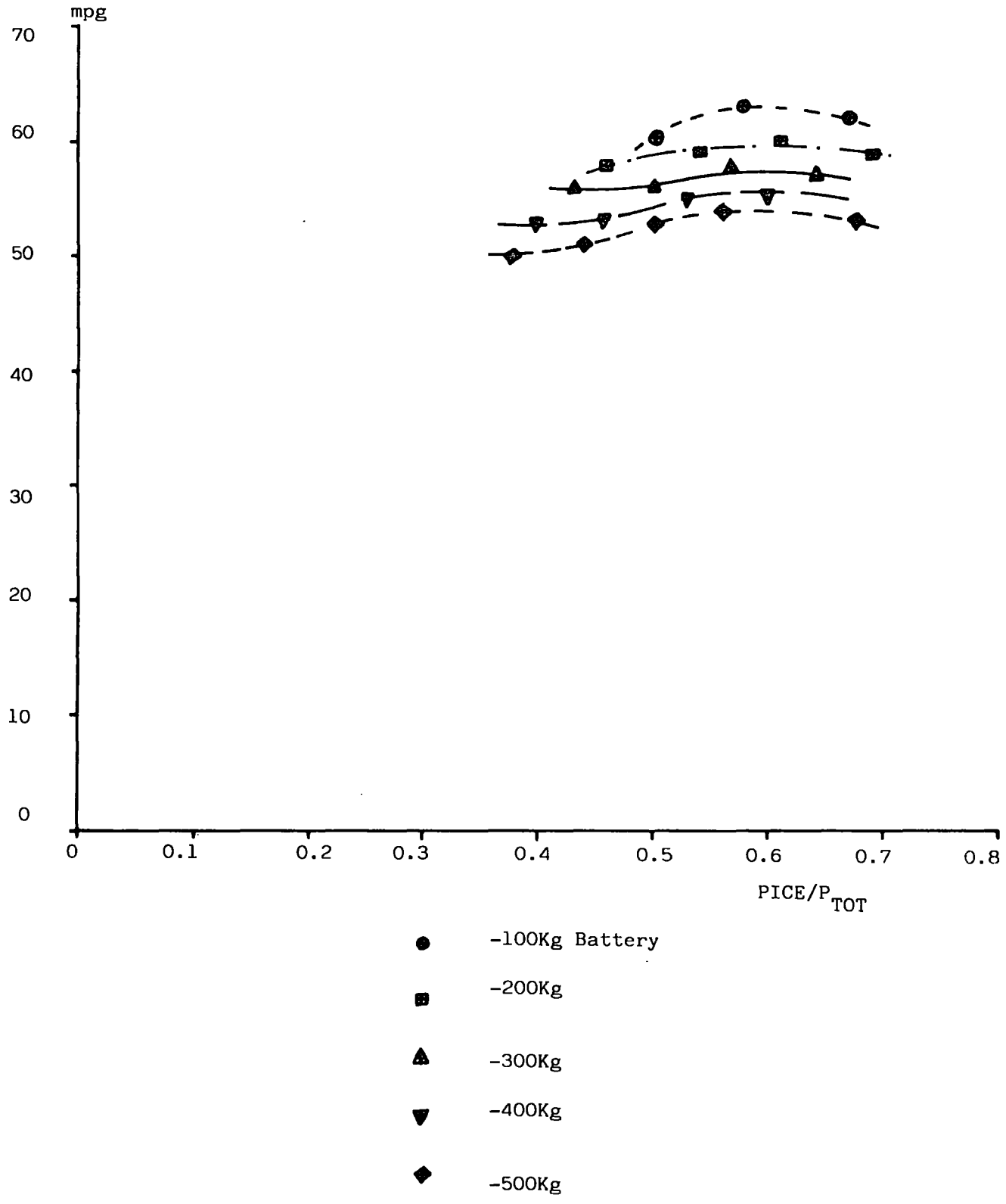

FIGURE 6.9a: The Base Hybrid of figure 6.4a but with a 6-speed variable ratio unit.

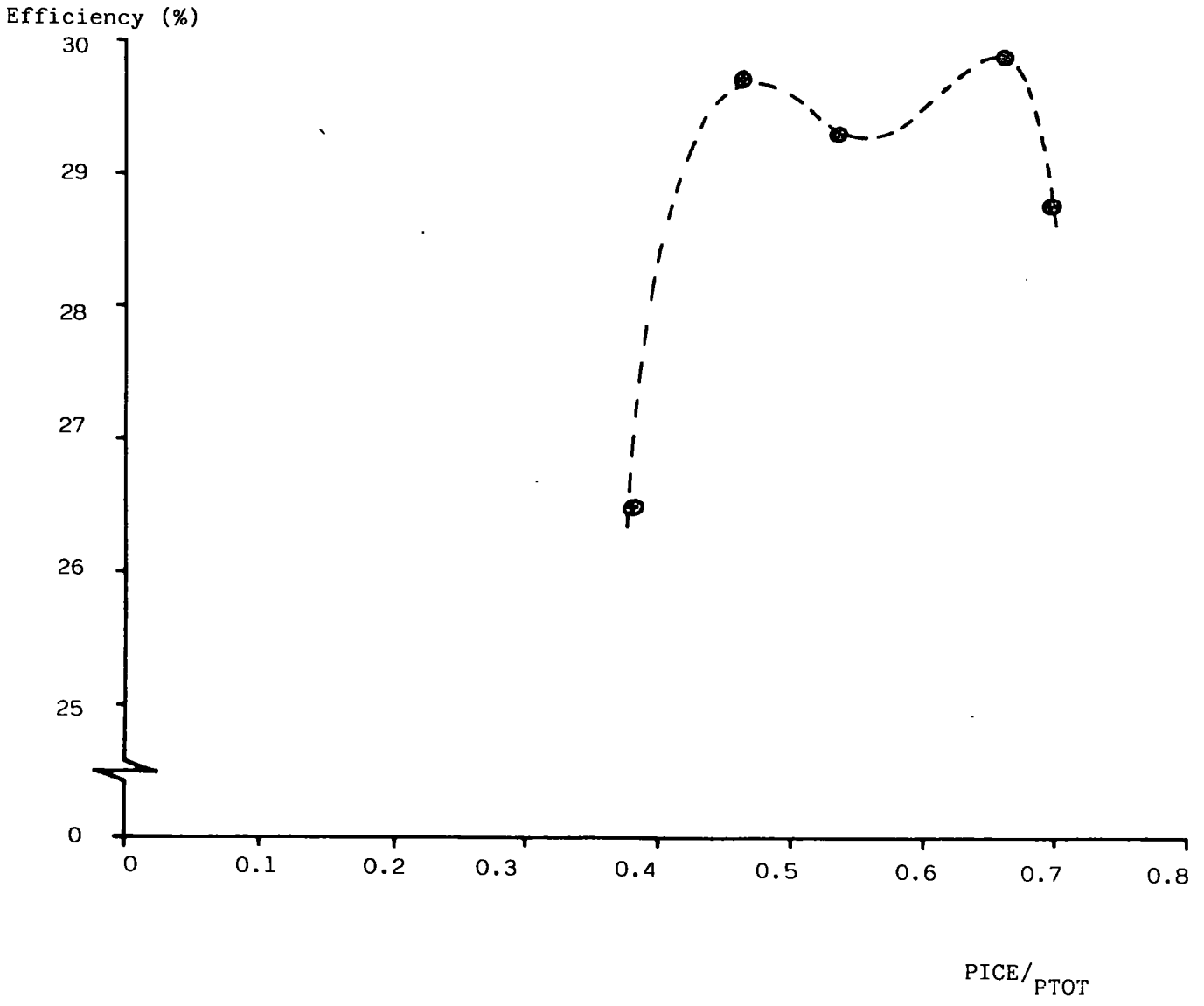

FIGURE 6.9b: The Base Hybrid of figure 6.4c but with a 6-speed variable ratio unit

FIGURE 6.10: I.C.Engine Usage Data for a 4-speed Discrete Ratio Unit using optimum control in a Hybrid

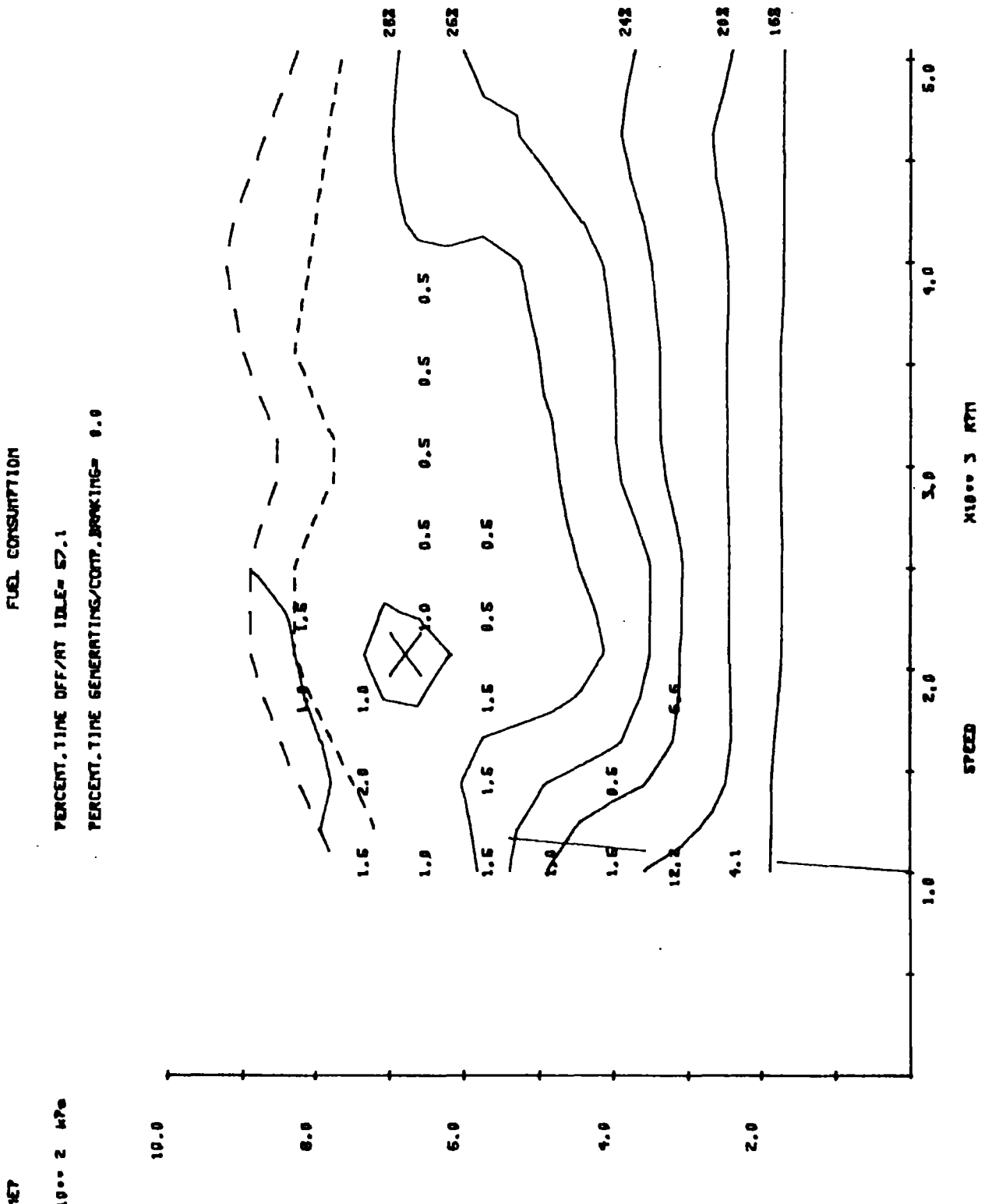

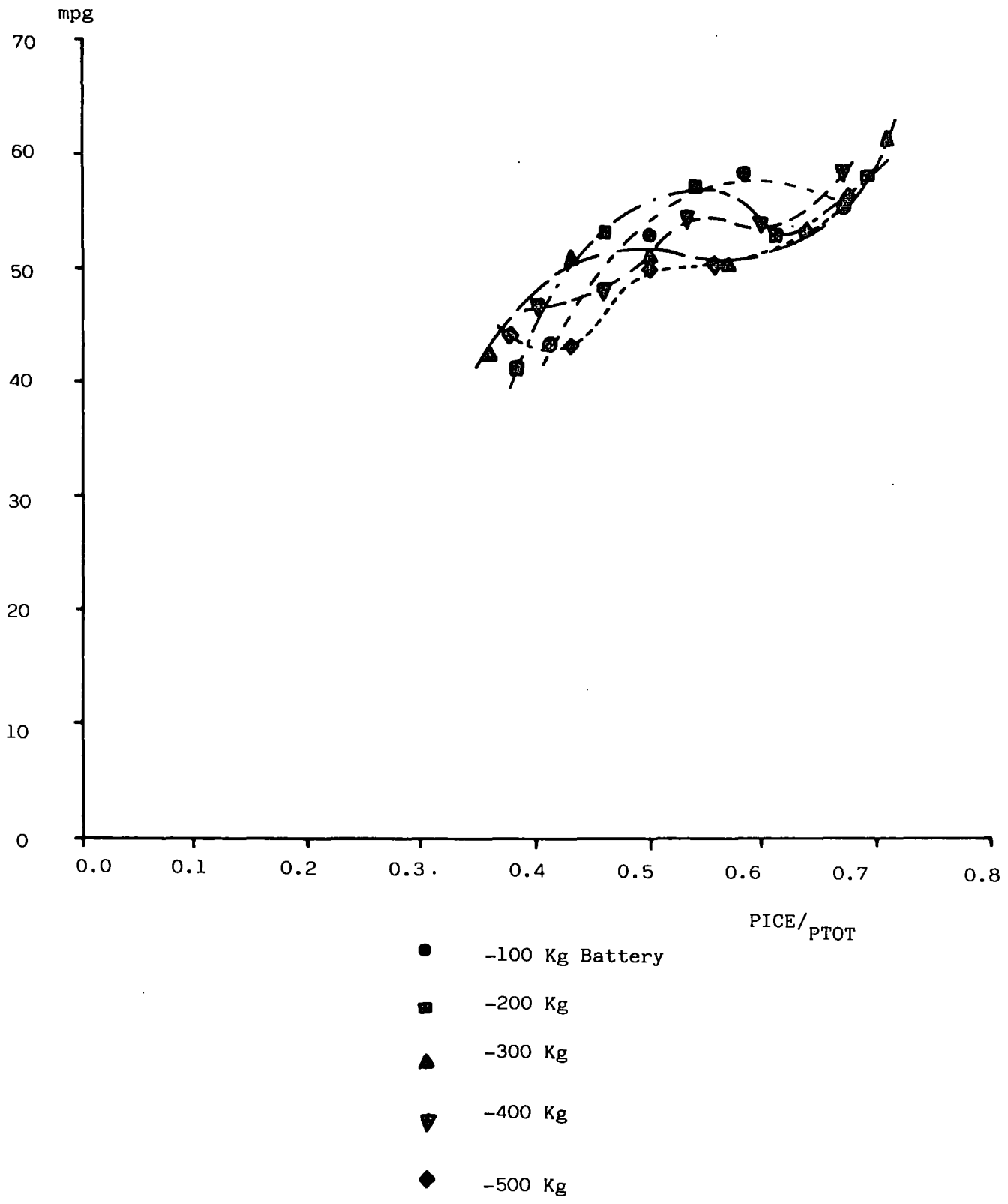

FIGURE 6.11a: The Base Hybrid of figure 6.2a but with a CVT

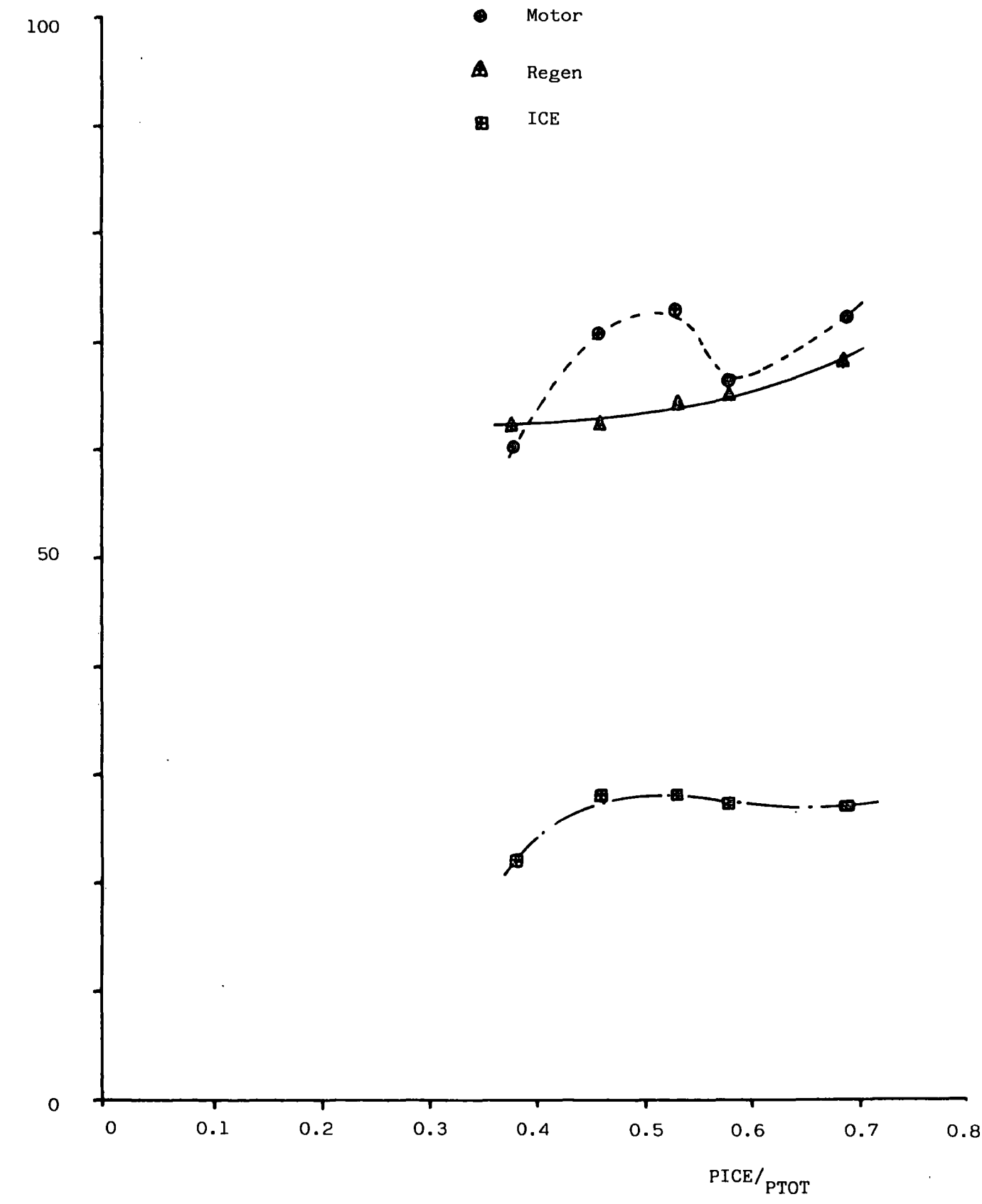

FIGURE 6.11b: The Base Hybrid of figure 6.2b but with a CVT

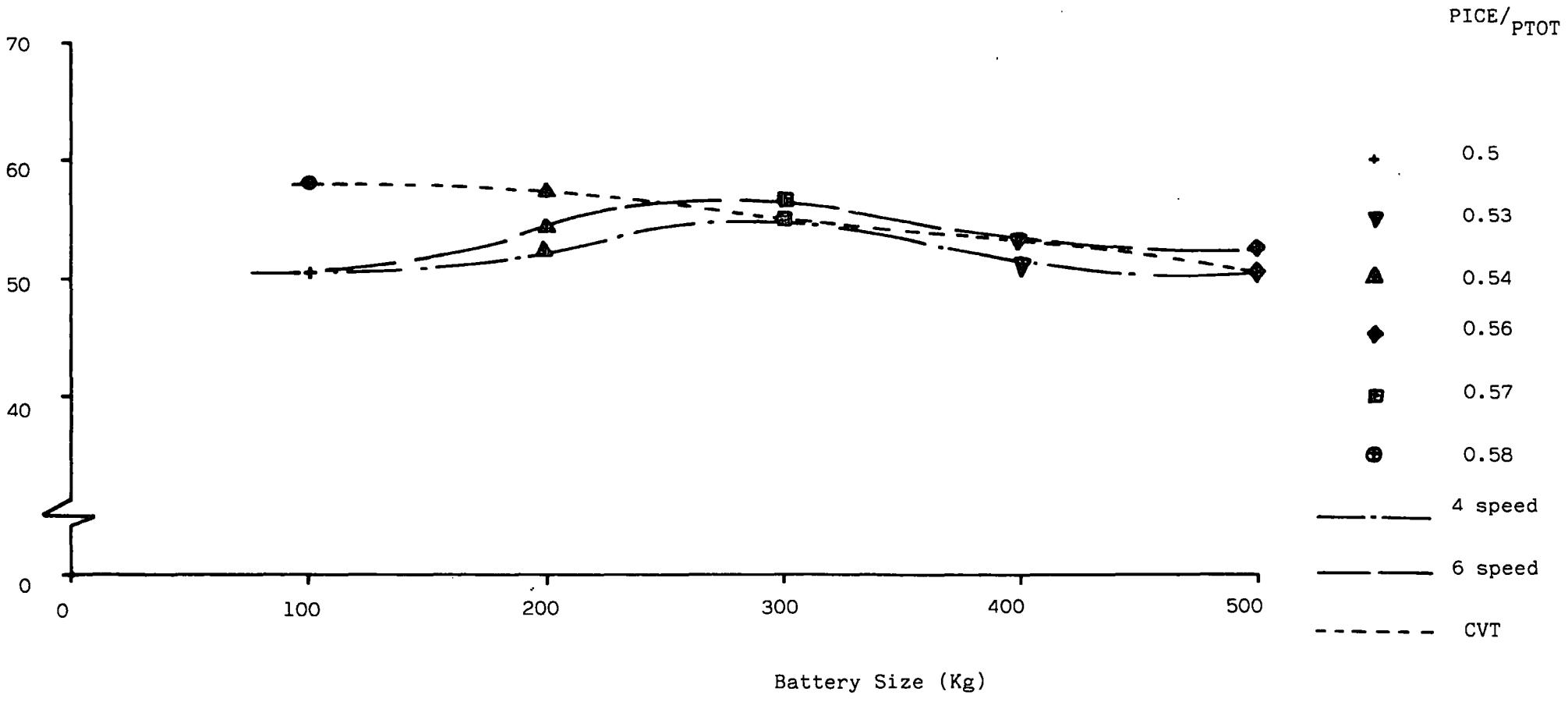

FIGURE 6.11c: Effect of Battery Weight and Transmission Type on mpg for the Energy Saving Aim with the Relative Power Source Sizes fixed over the ECE-15

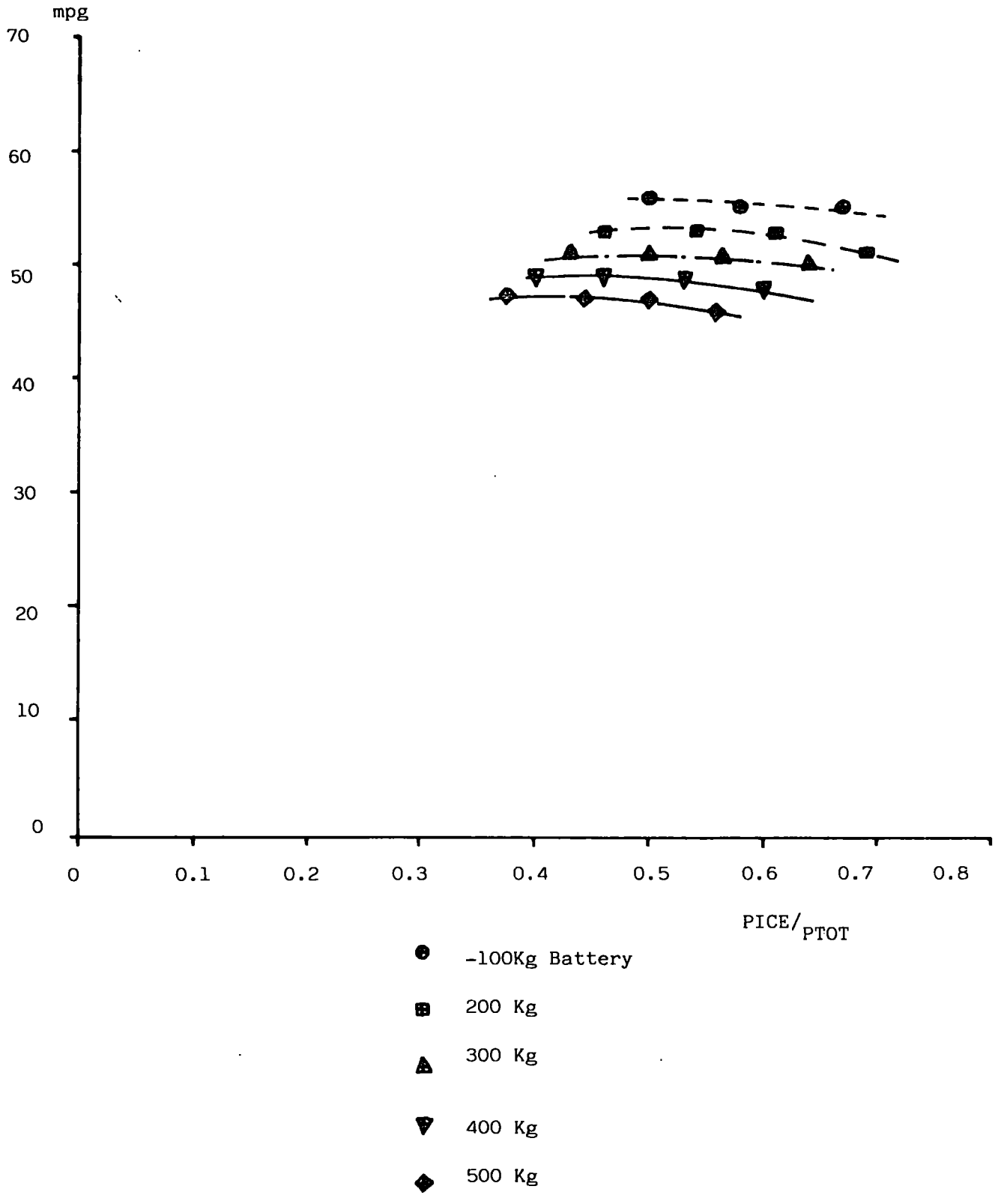

FIGURE 6.12a: The base Hybrid of figure 6.4a but with a CVT

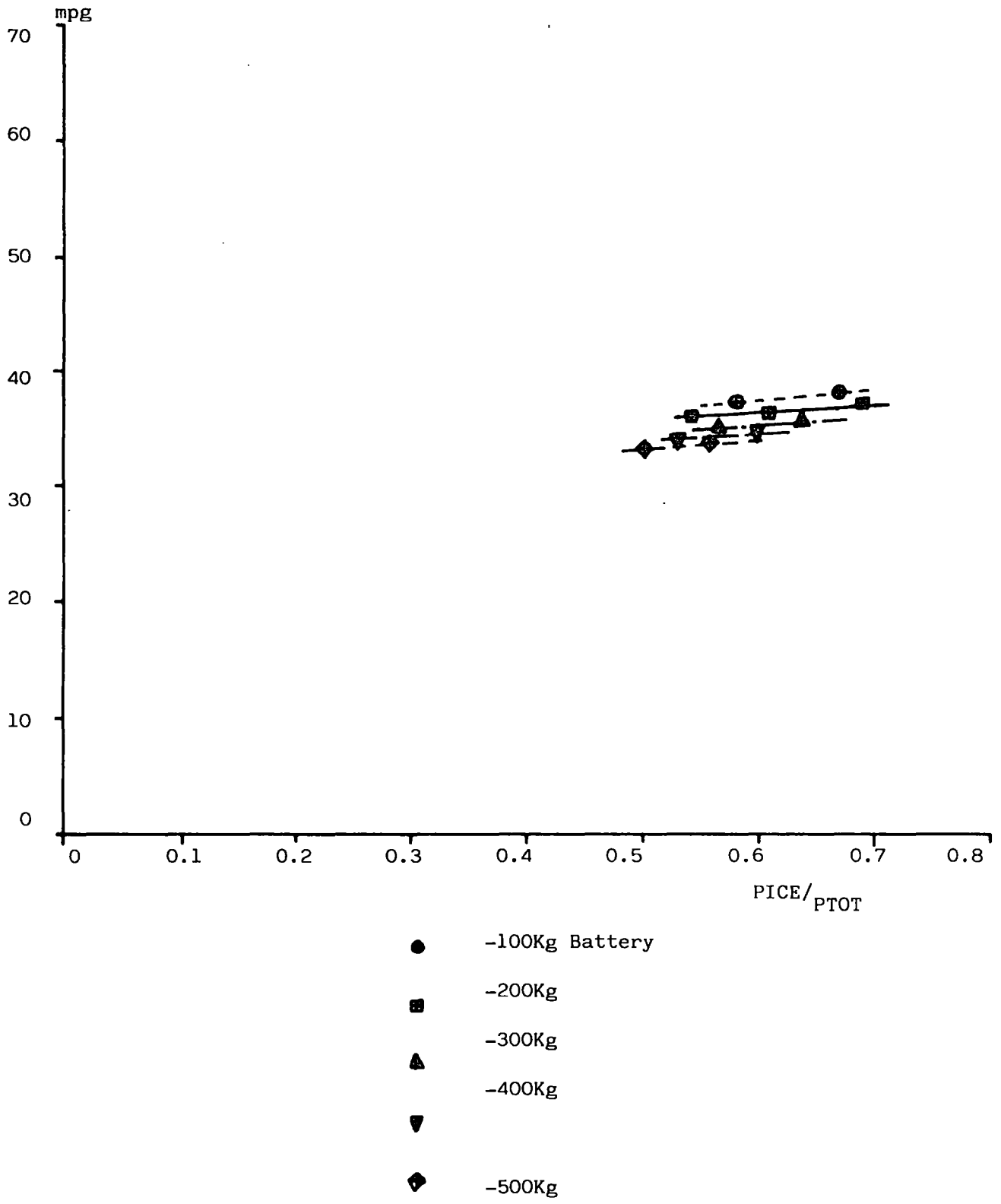

FIGURE 6.12b: The Base Hybrid at figure 6.4b but with a CVT

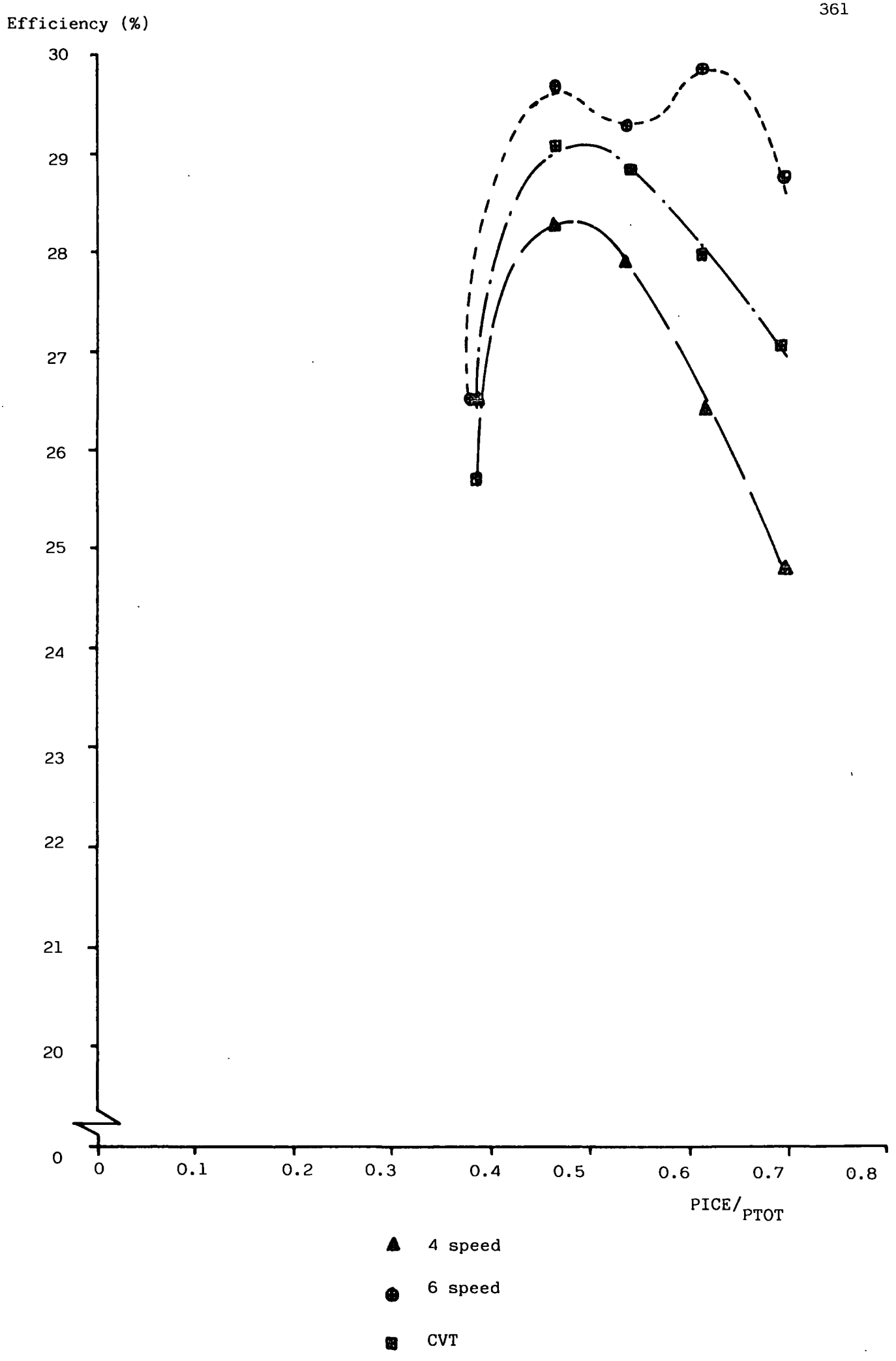

FIGURE 6.12c: The base Hybrid of figure 6.4c but with a CVT at 56 mph.

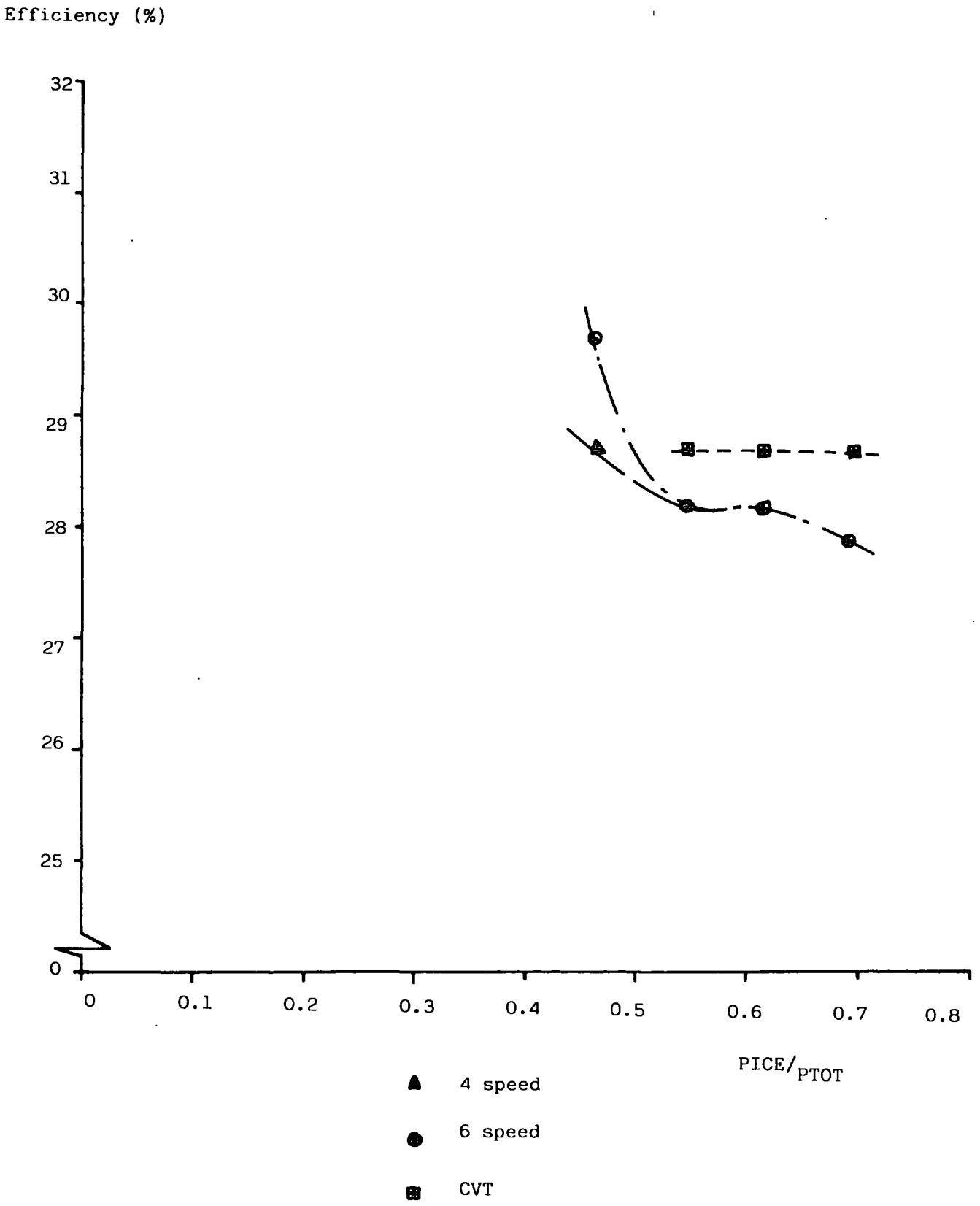

FIGURE 6.12d: The Base Hybrid of figure 6.4c but with a CVT

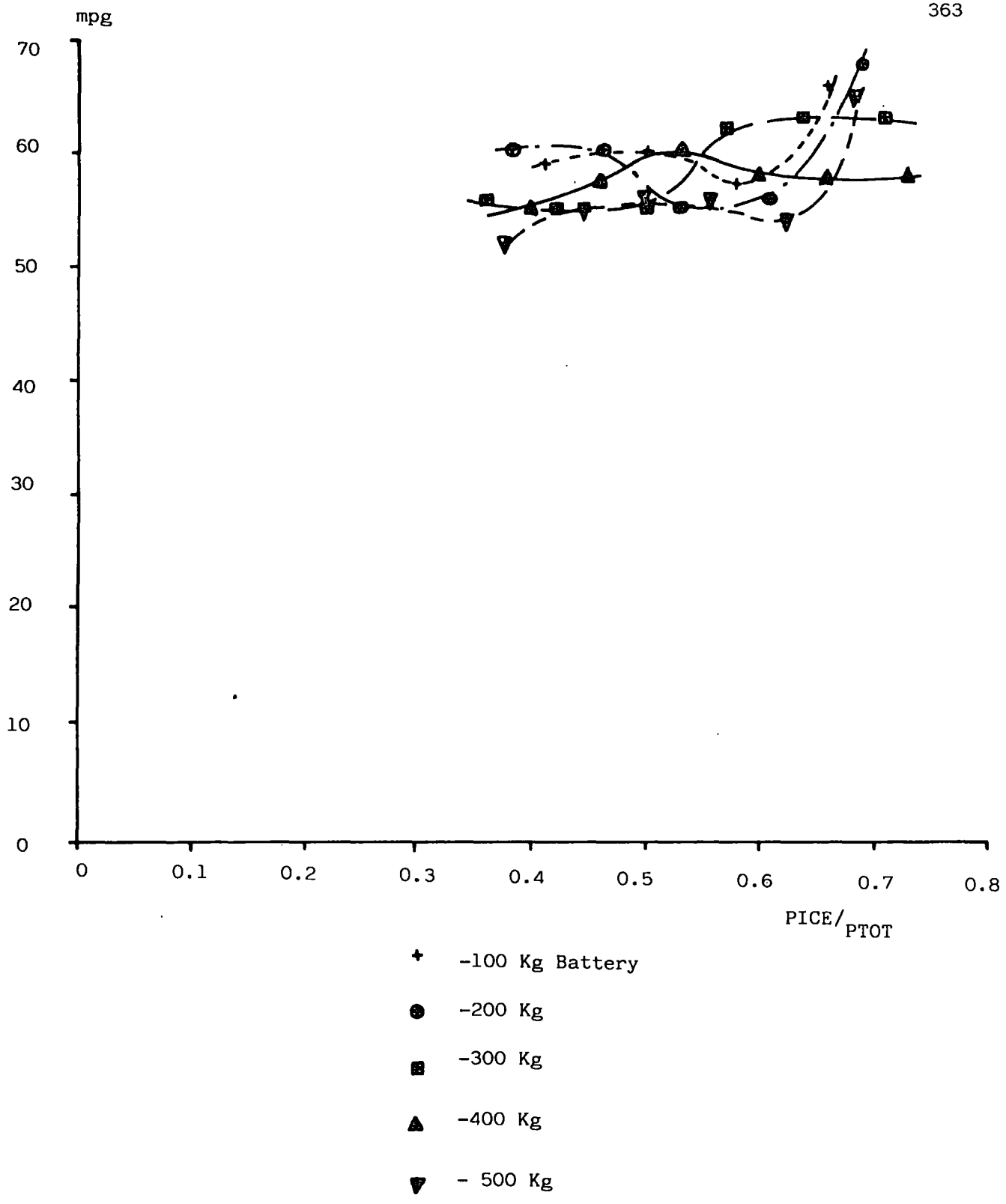

FIGURE 6.13a: The Base Hybrid of figure 6.2a but with an Advanced I.C.Engine

FIGURE 6.13b: The Base Hybrid of figure 6.2b but with an Advanced I.C.Engine

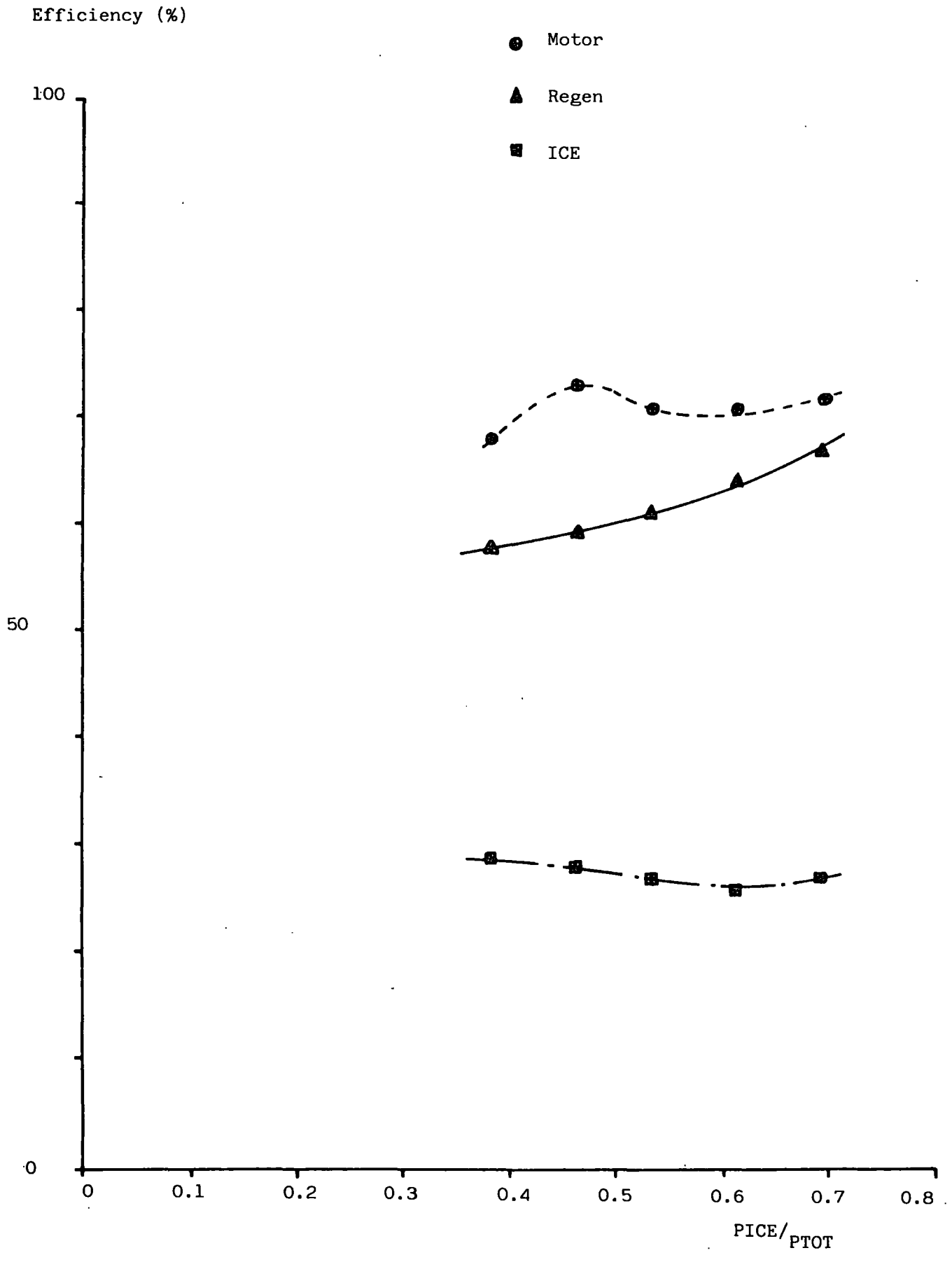

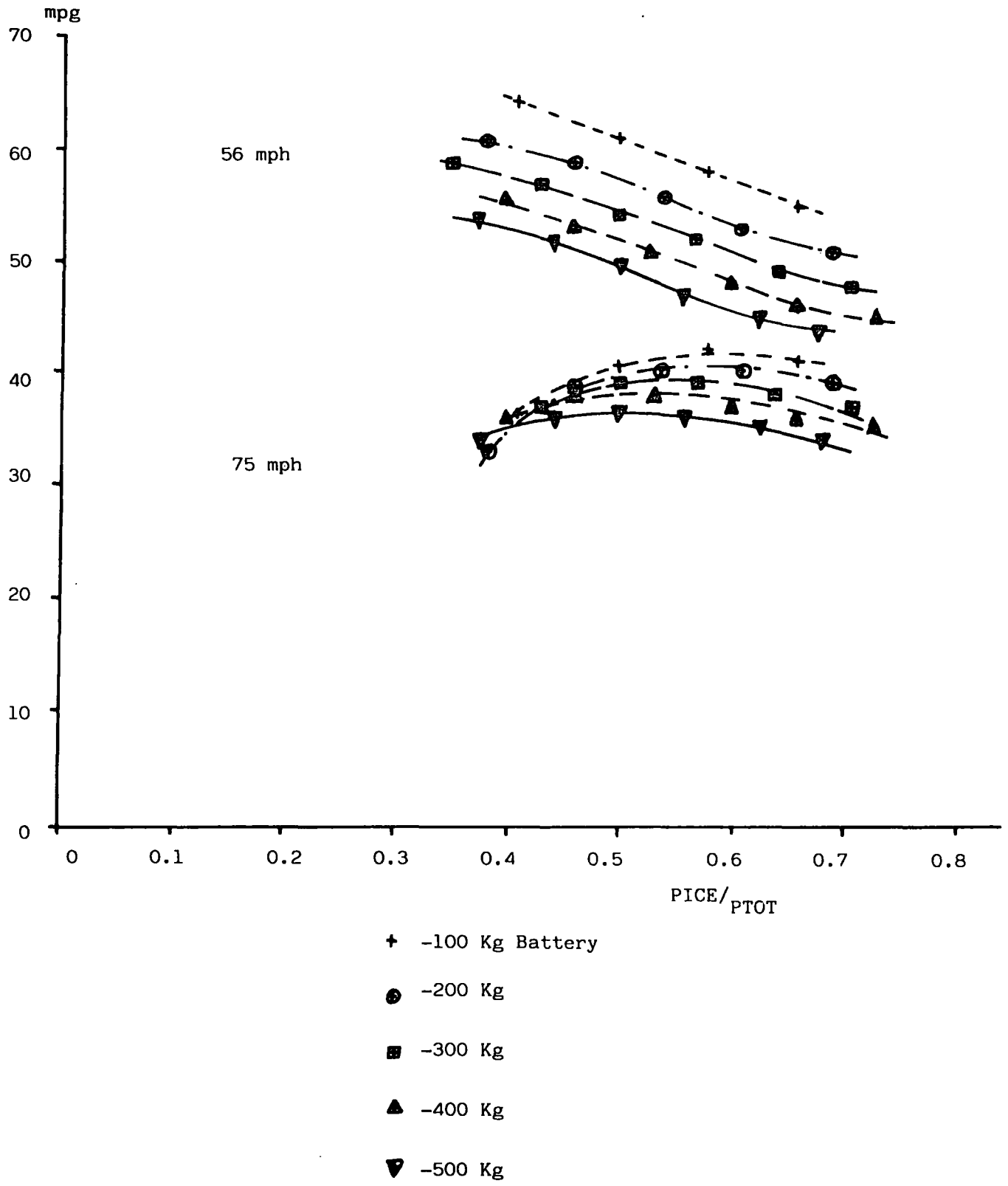

IGURE 6.14a: The Base Hybrid of figures 6.4a and 6.4b but with an Advanced I.C Engine

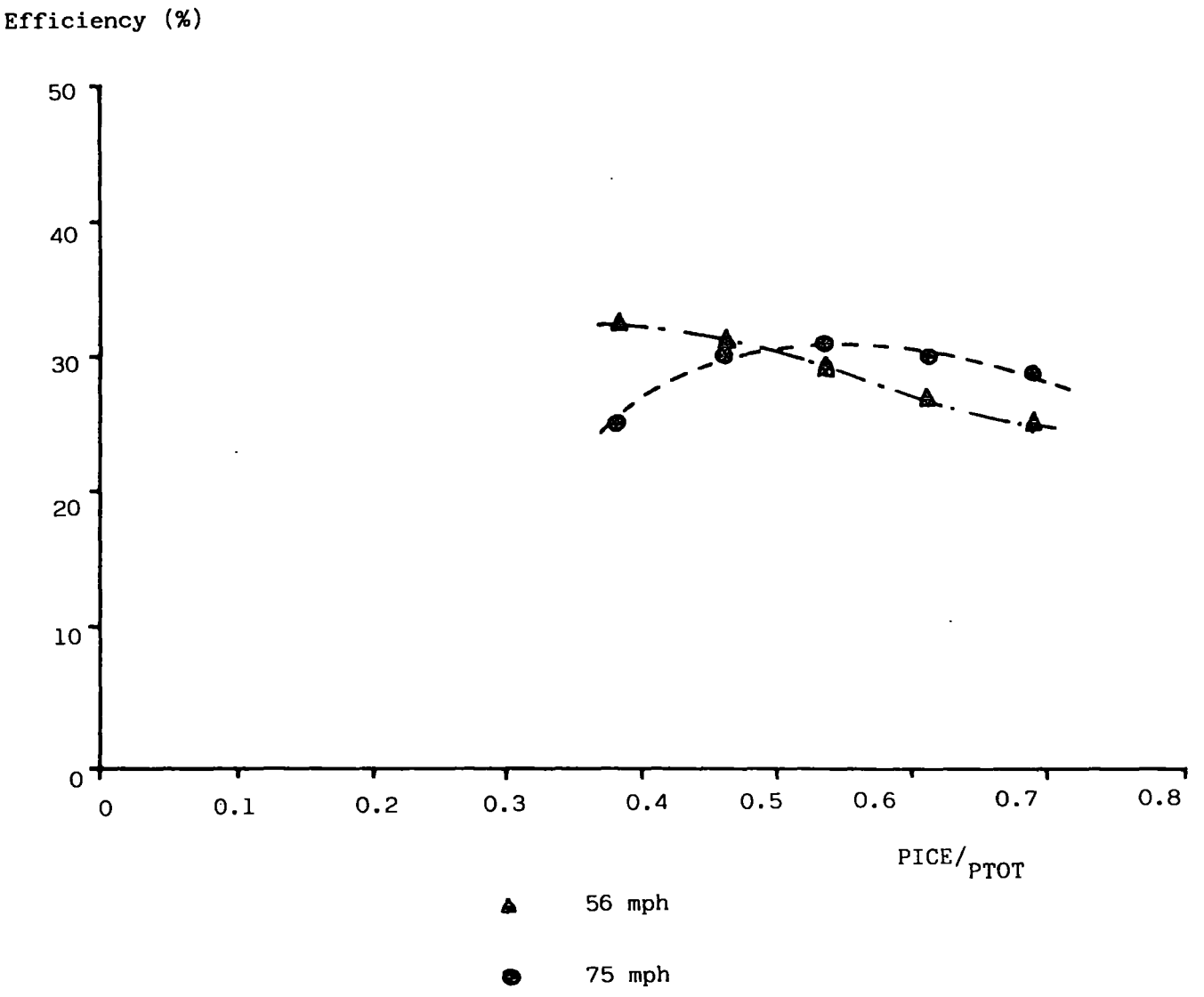

FIGURE 6.14b: The Base Hybrid of figure 6.4c but with an Advanced i.c.Engine

FIGURE 6.15 Advanced 3 cylinder i.c. engine map

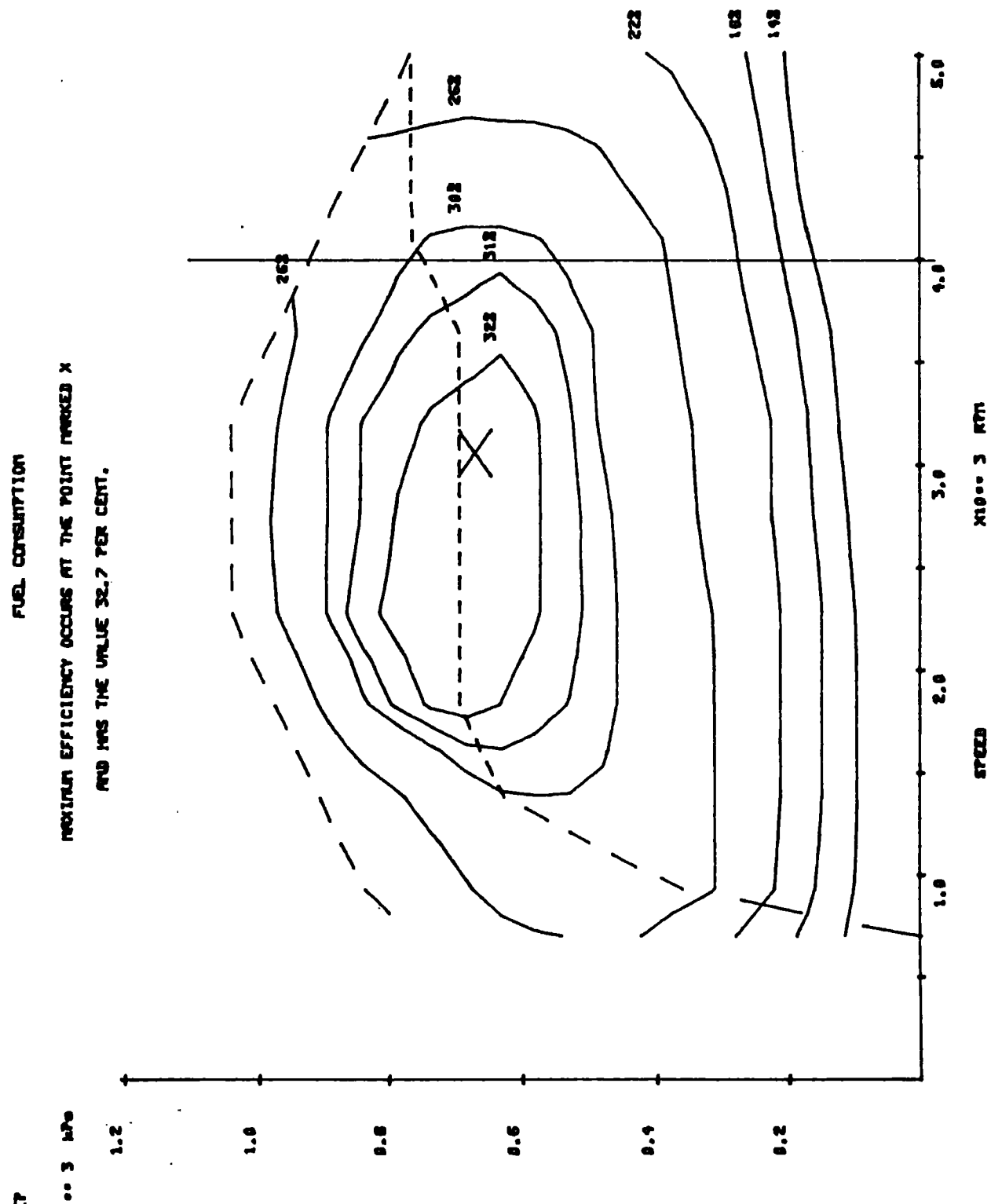

FIGURE 6.16: Current 1.0 litre i.c. Engine Map

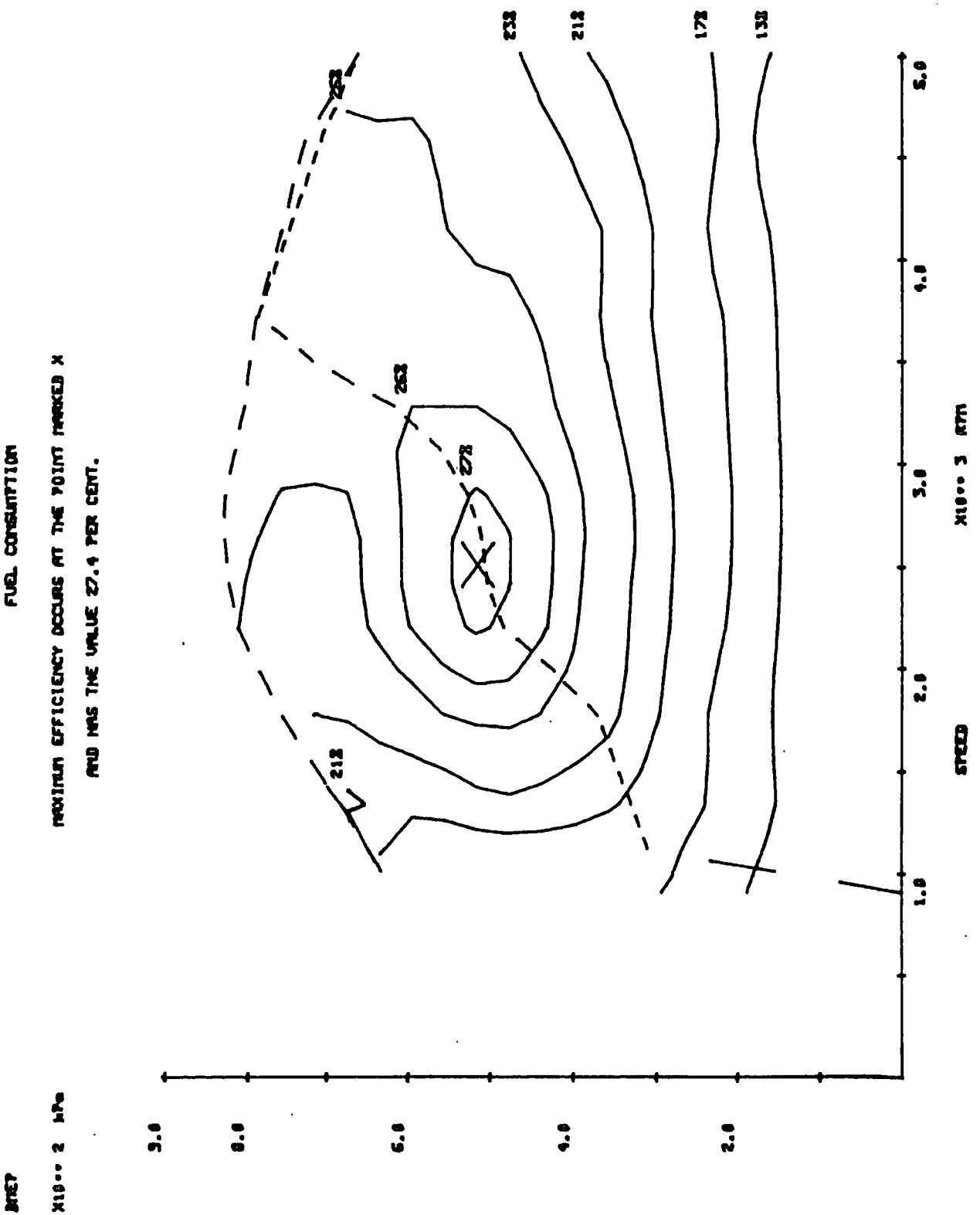

FIGURE 6.17 Current 1.1 litre I.C. Engine map

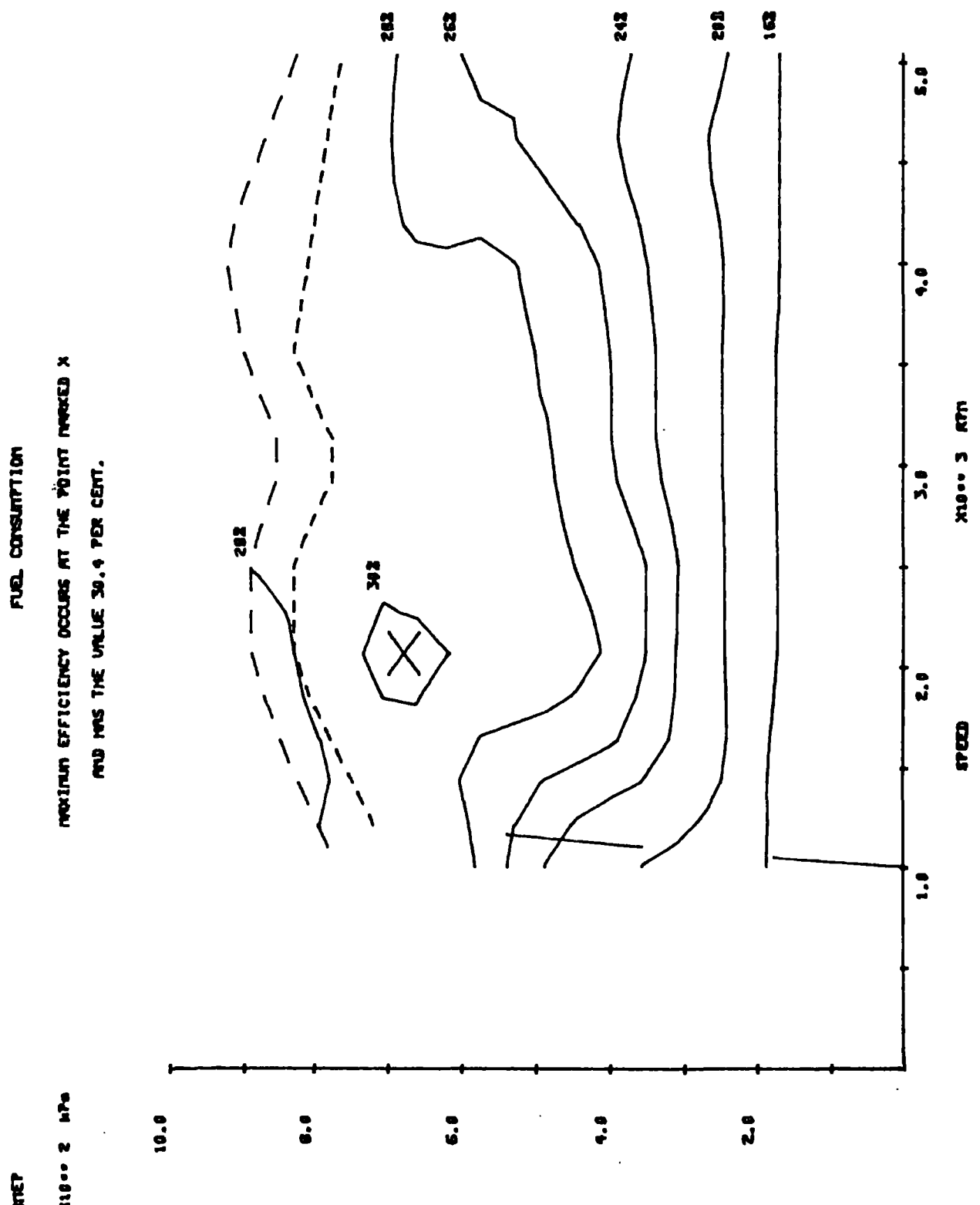

FIGURE 6.18 Current 1.6 litre I.C. Engine Map

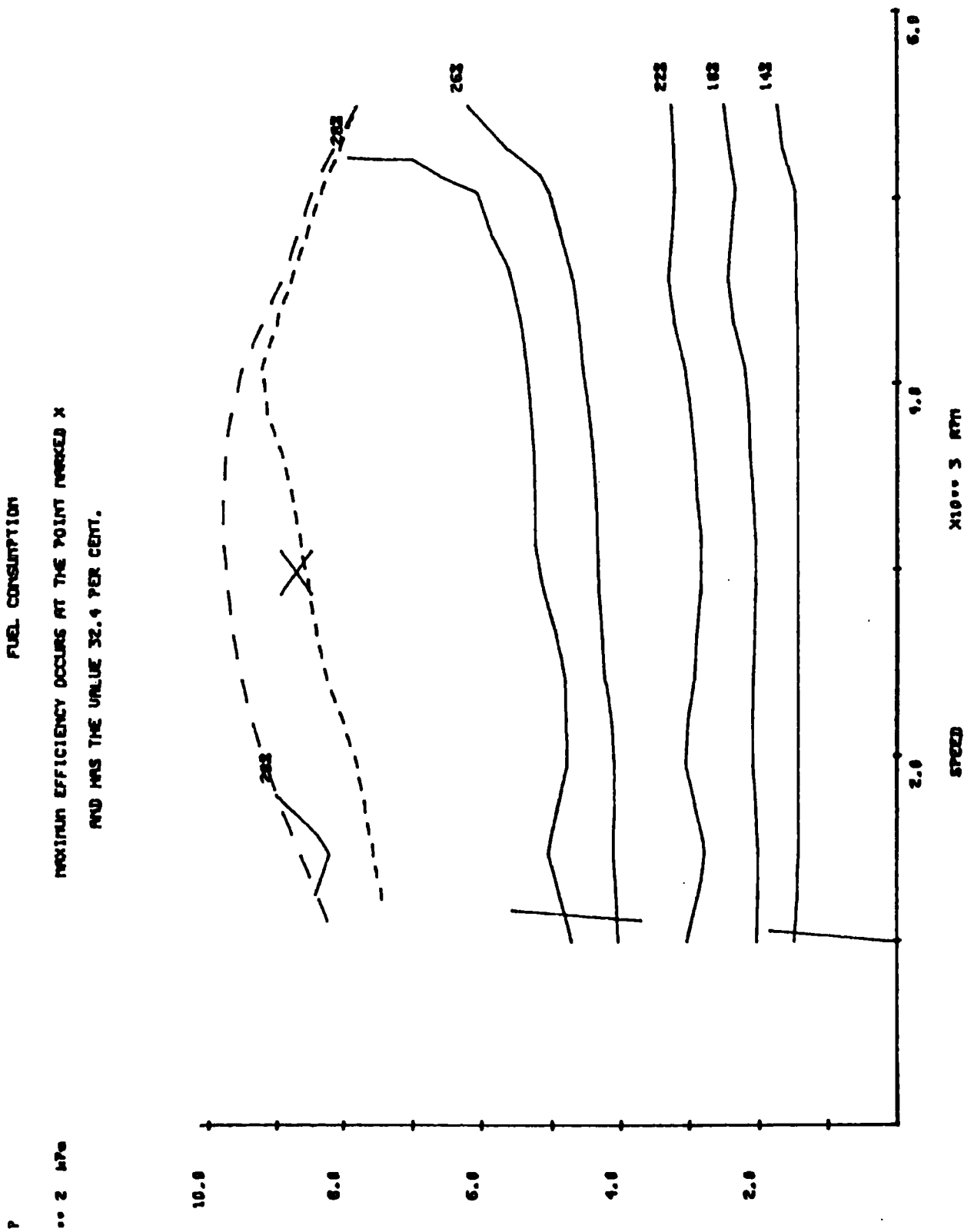

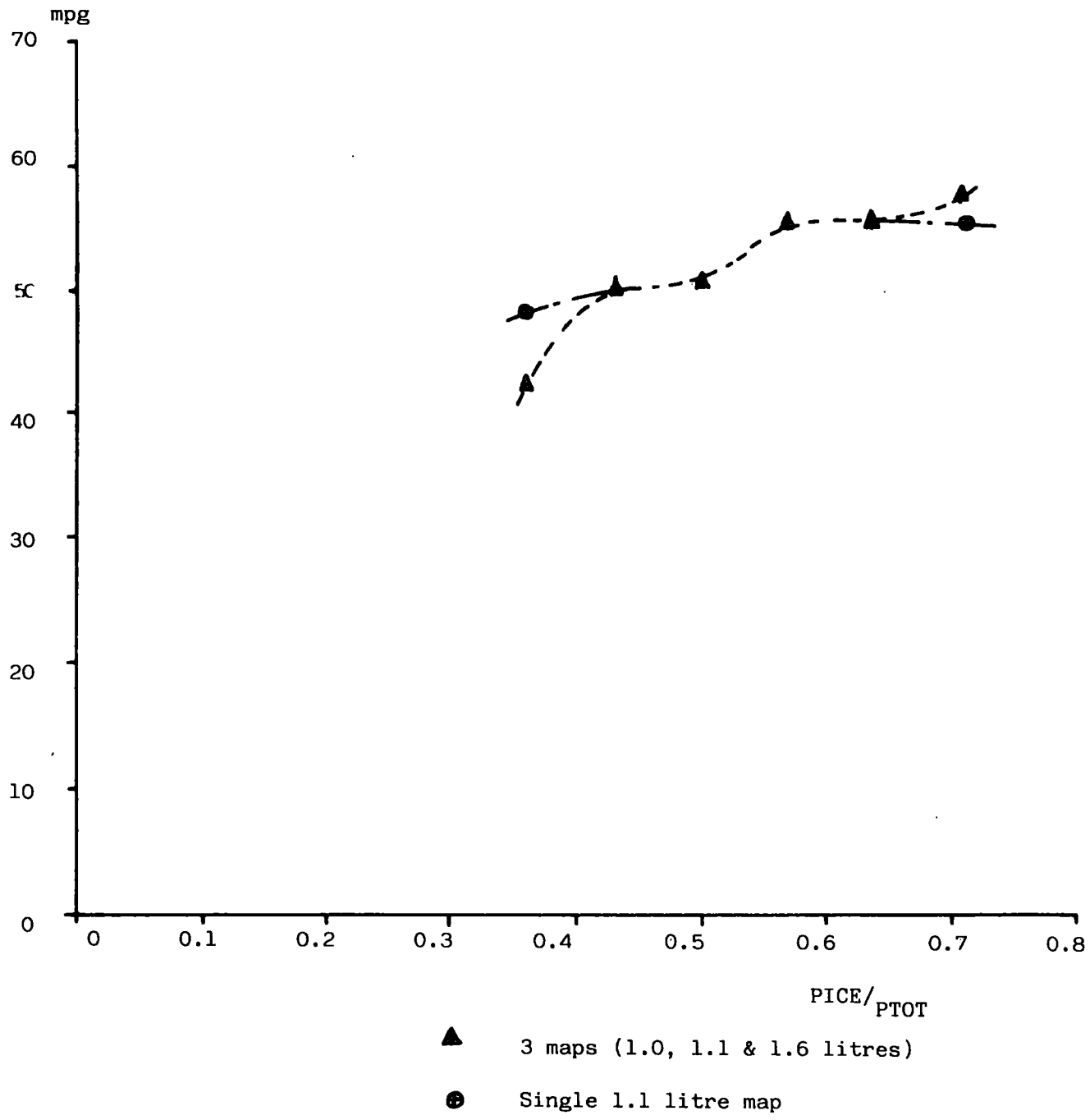

FIGURE 6.19 Effect of using 3 maps compared with 1 map to span a given power range

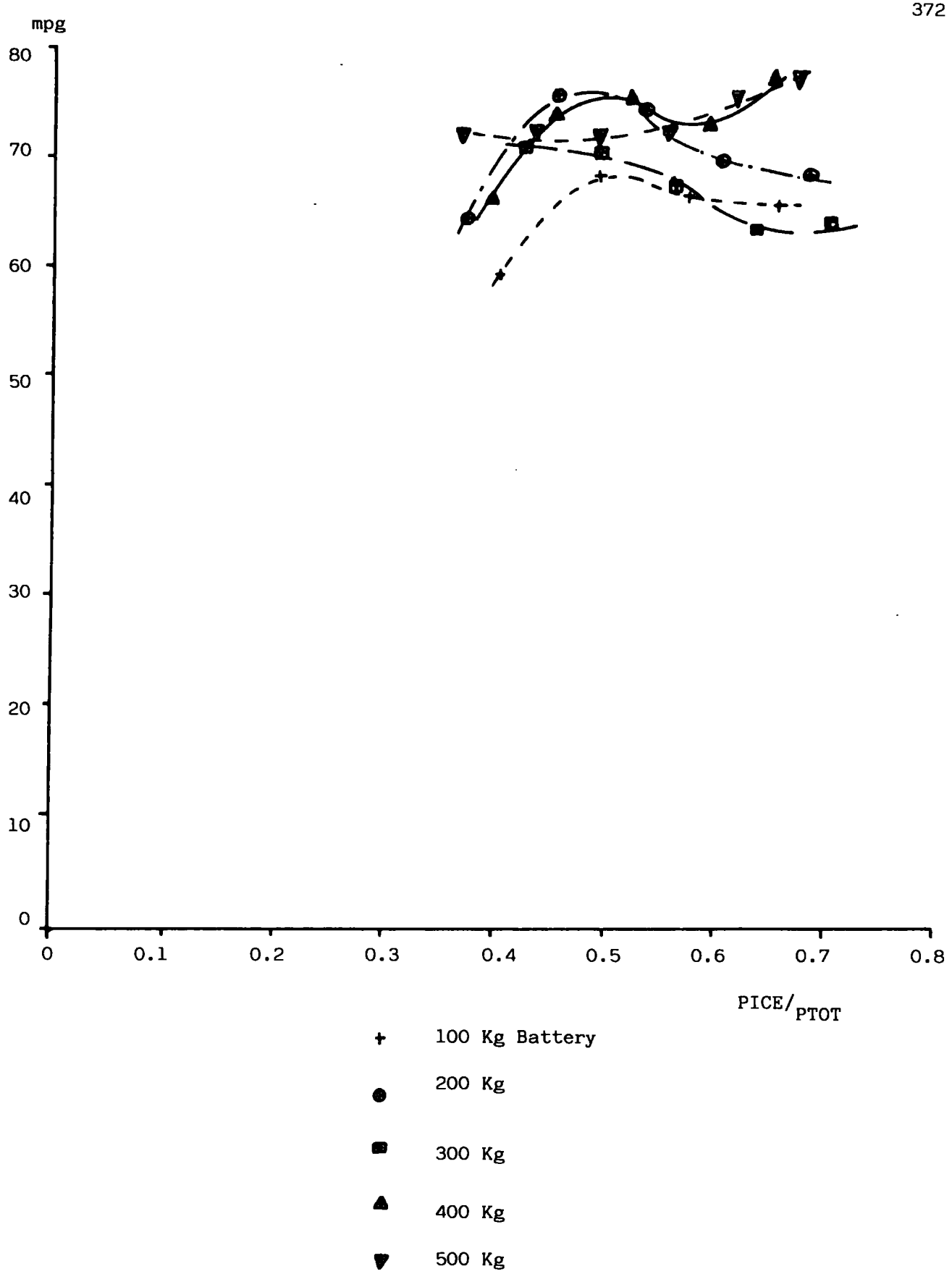

FIGURE 6.20a: The Base Hybrid of figure 6.2a but with an Advanced Traction Motor

FIGURE 6.20b The Base Hybrid of figure 6.2b but with an Advanced Traction Motor

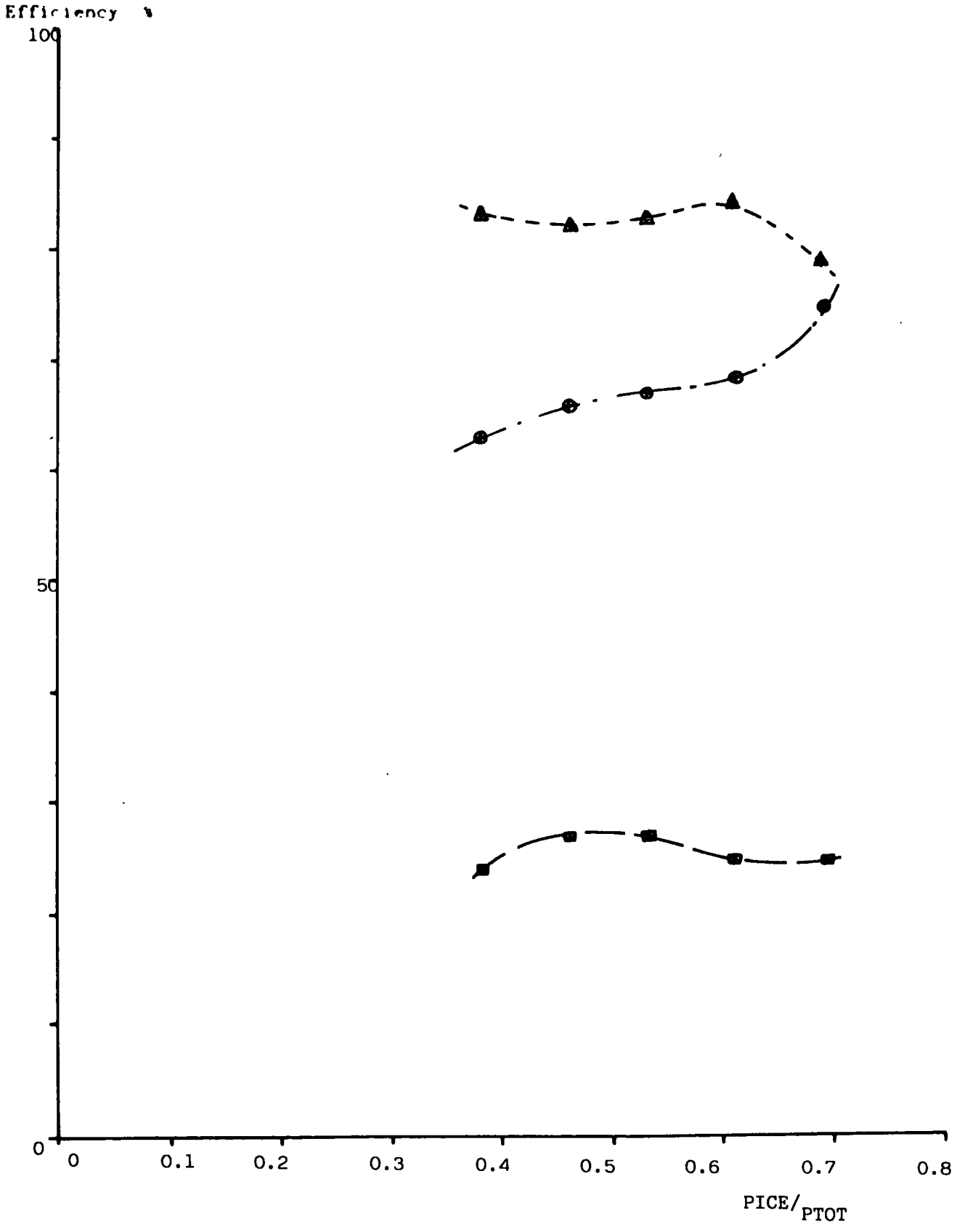

FIGURE 6.21a: Effect of Relative Power Source Size on mpg/range curves for the base hybrid with a 400 Kg Battery size over the ECE-15 for the Petroleum Substitution Aim

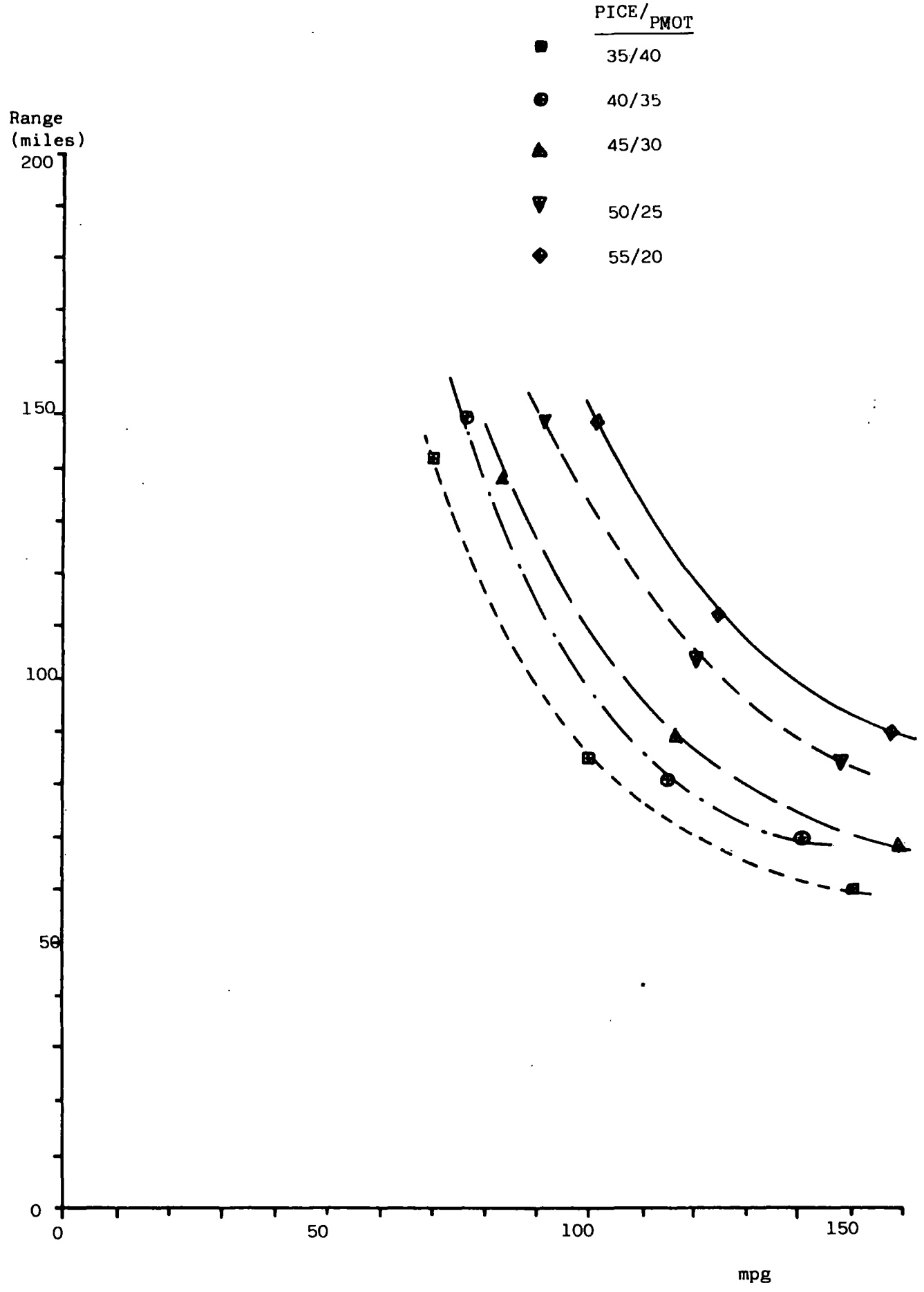

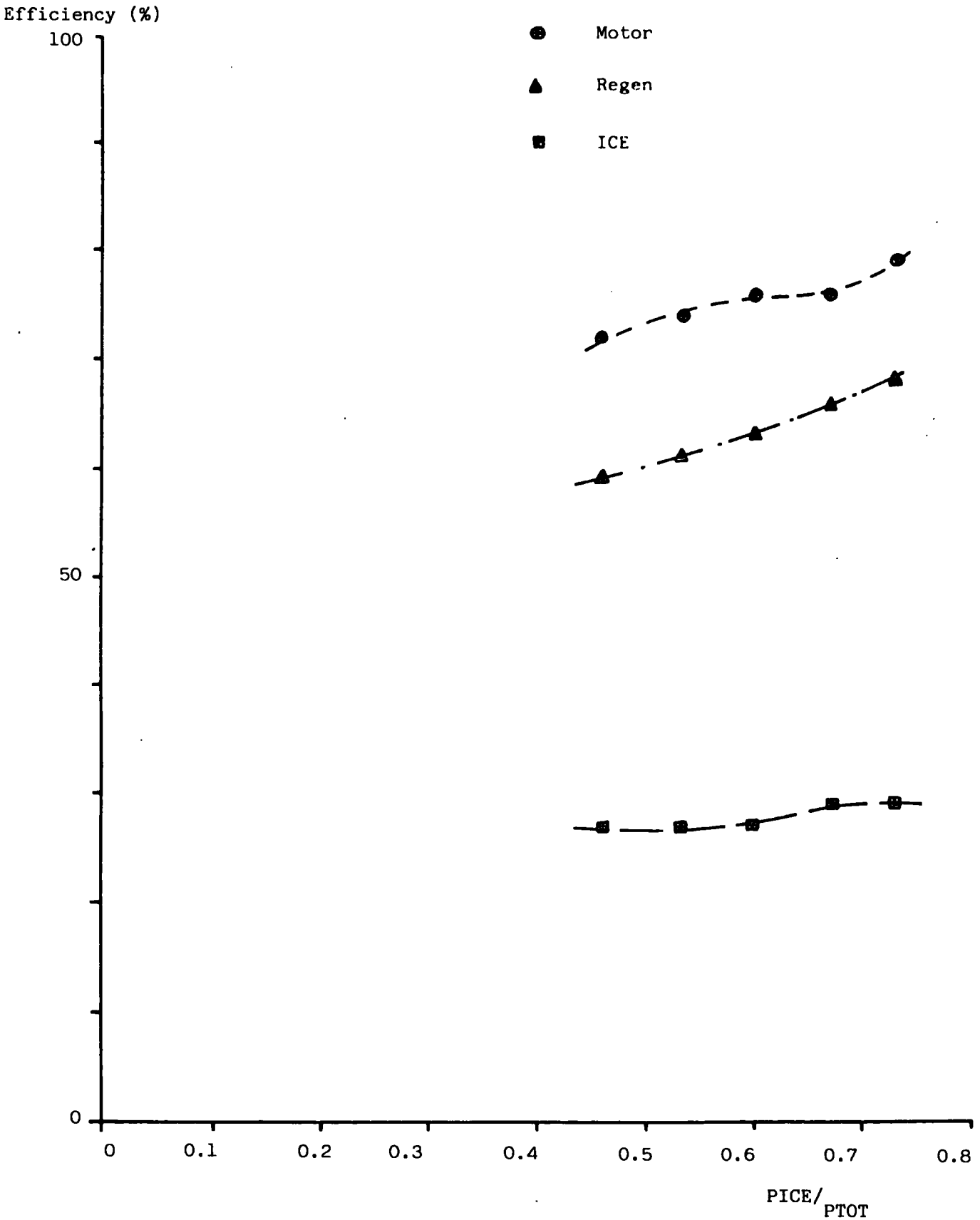

FIGURE 6.21b: Effect of Relative Power Source size on Component Efficiency for the 400 Kg battery size over the ECE-15 cycle for the Petroleum Substitution Aim.

FIGURE 6.22a: Torque split/time Profile for the Base Hybrid with a 400 Kg Battery size and a relative power source fraction of 0.533 over the ECE-15 for the Petroleum Substitution Aim.

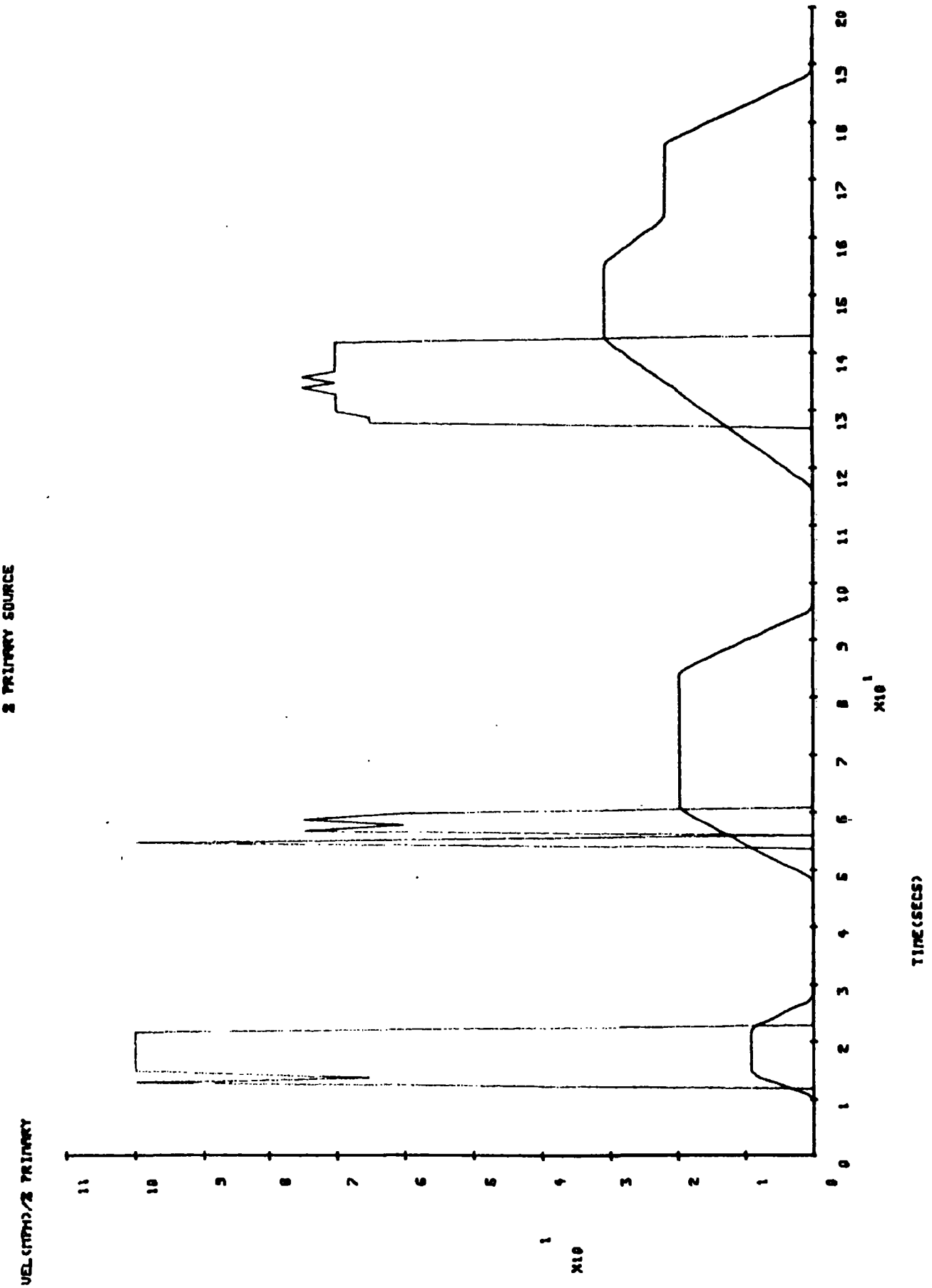

FIGURE 6.22b: As for Figure 6.22a but with a Relative power source fraction of 0.6

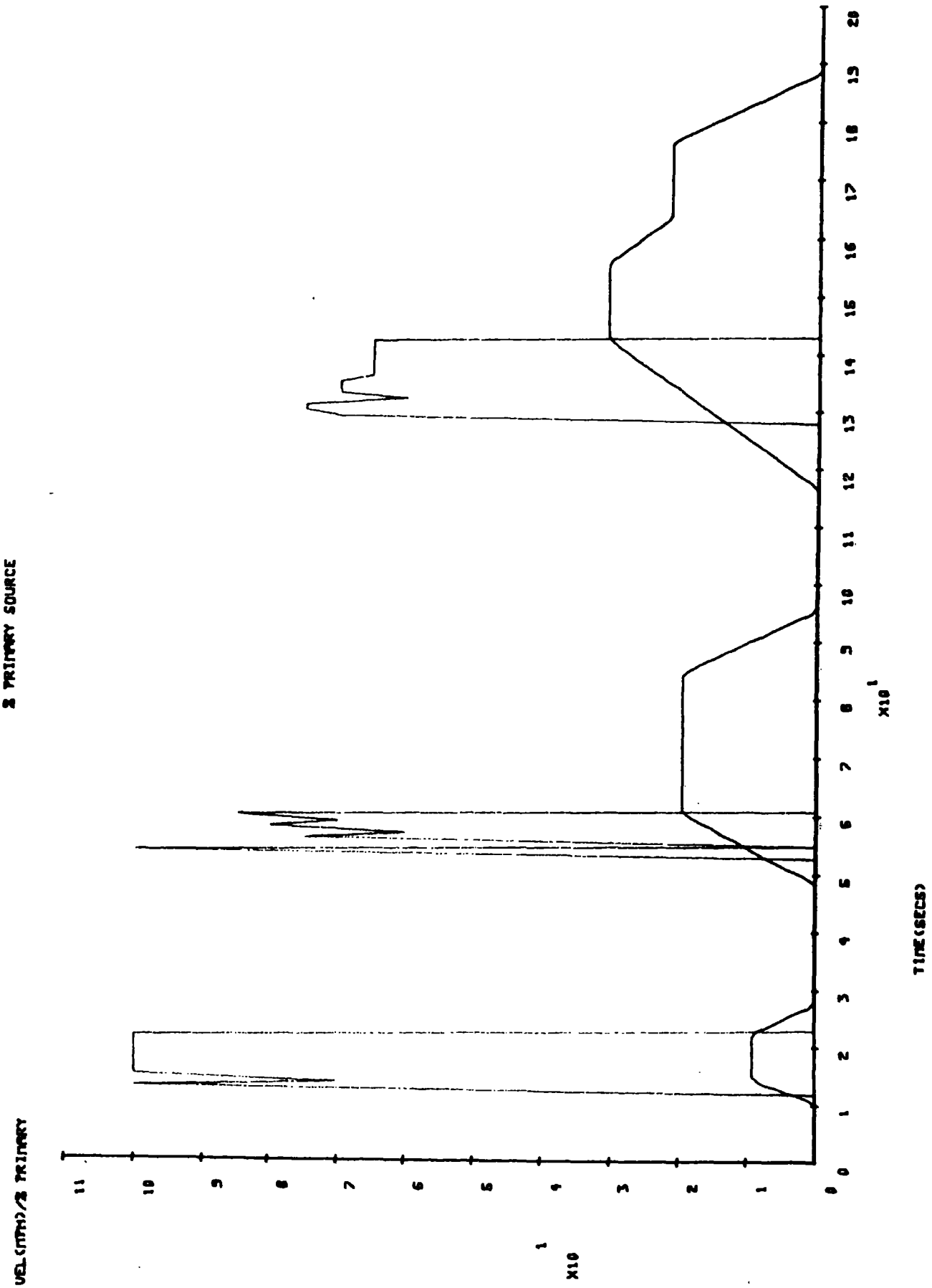

FIGURE 6.23a: The Base Hybrid of Figure 6.21a but over the J227aD

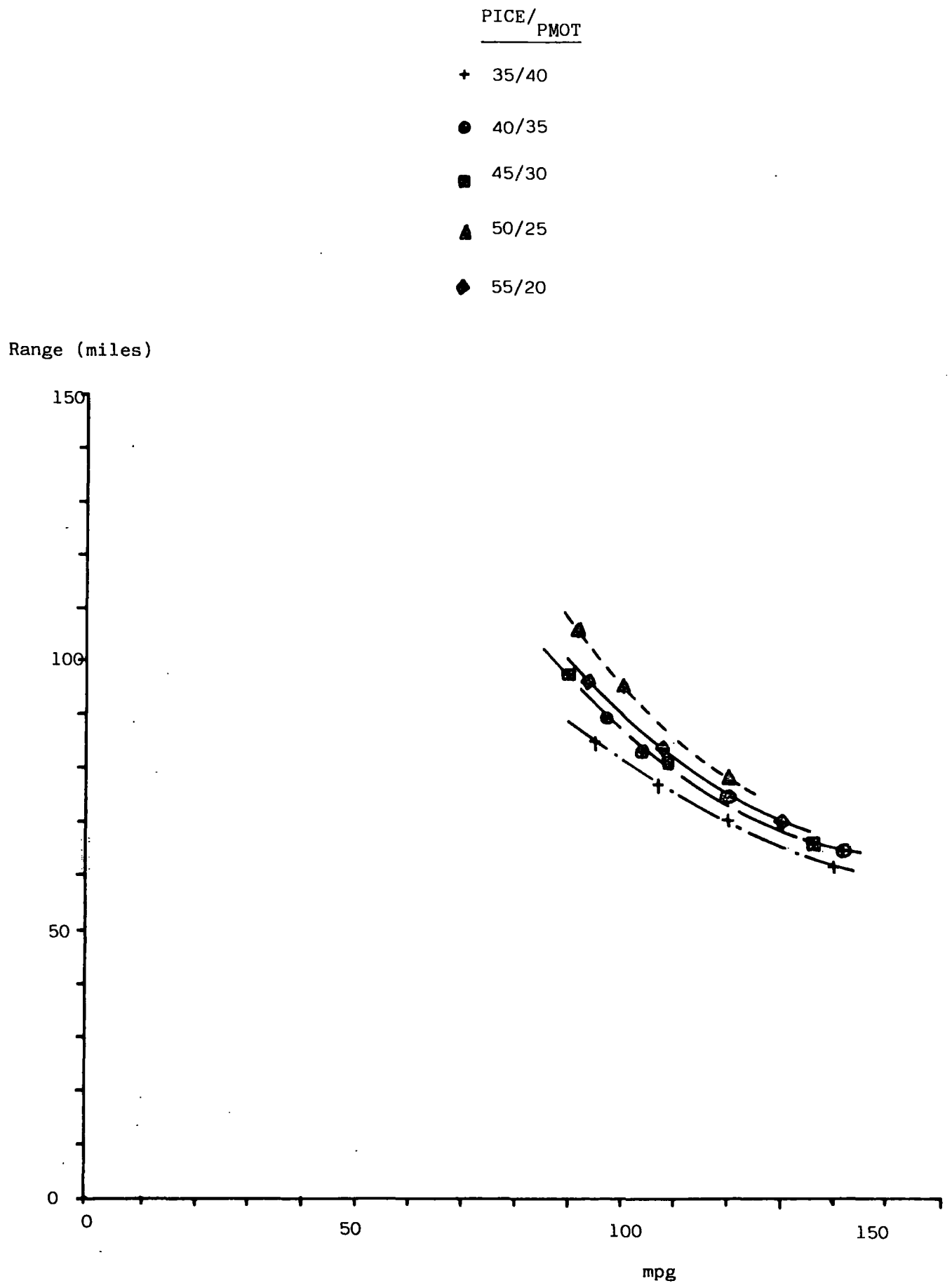

FIGURE 6.23b: The Base Hybrid of figure 6.21b but over the J227aD

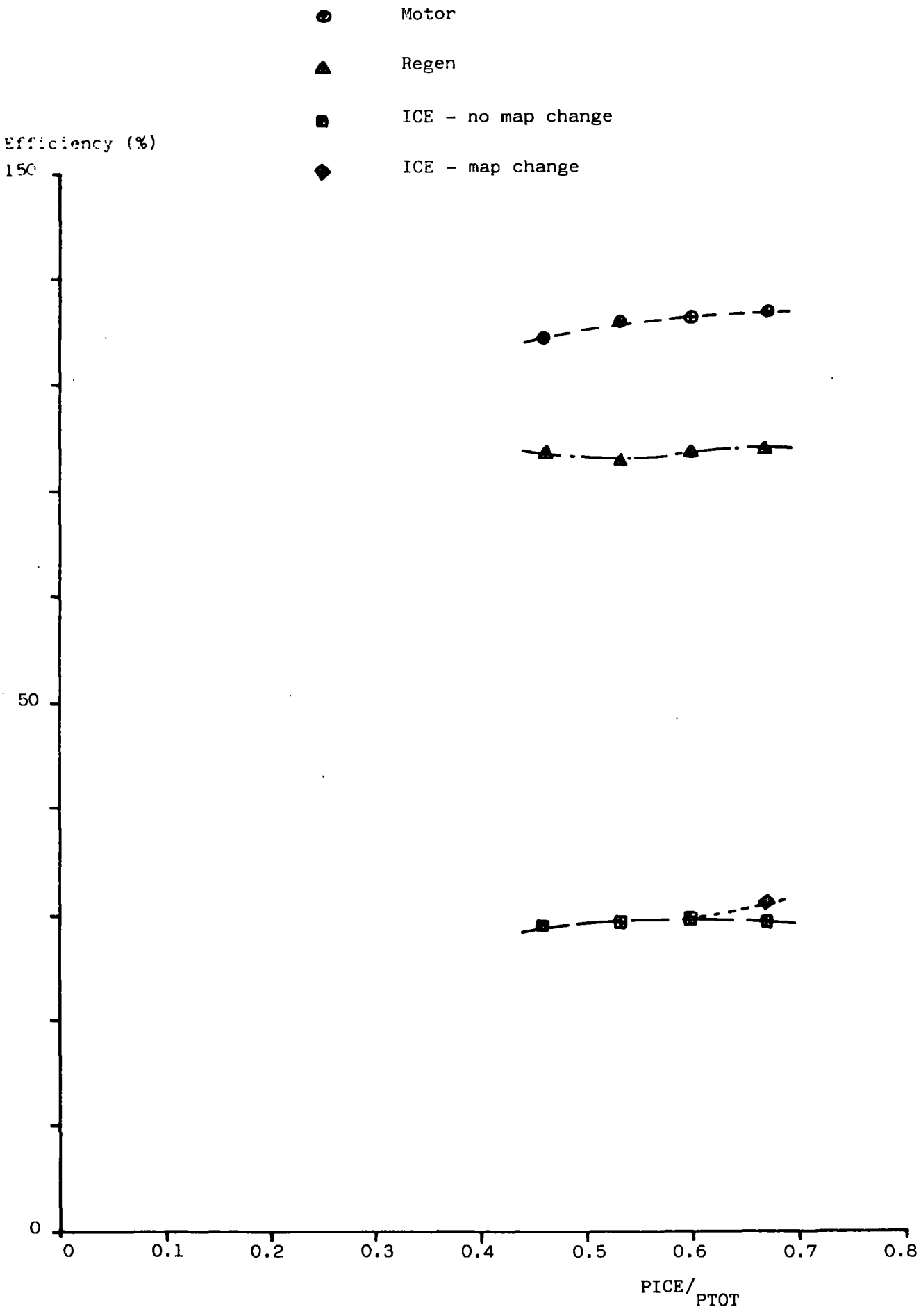

FIGURE 6.24: The Base Hybrid of Figure 6.21a but with a 500 Kg Battery size

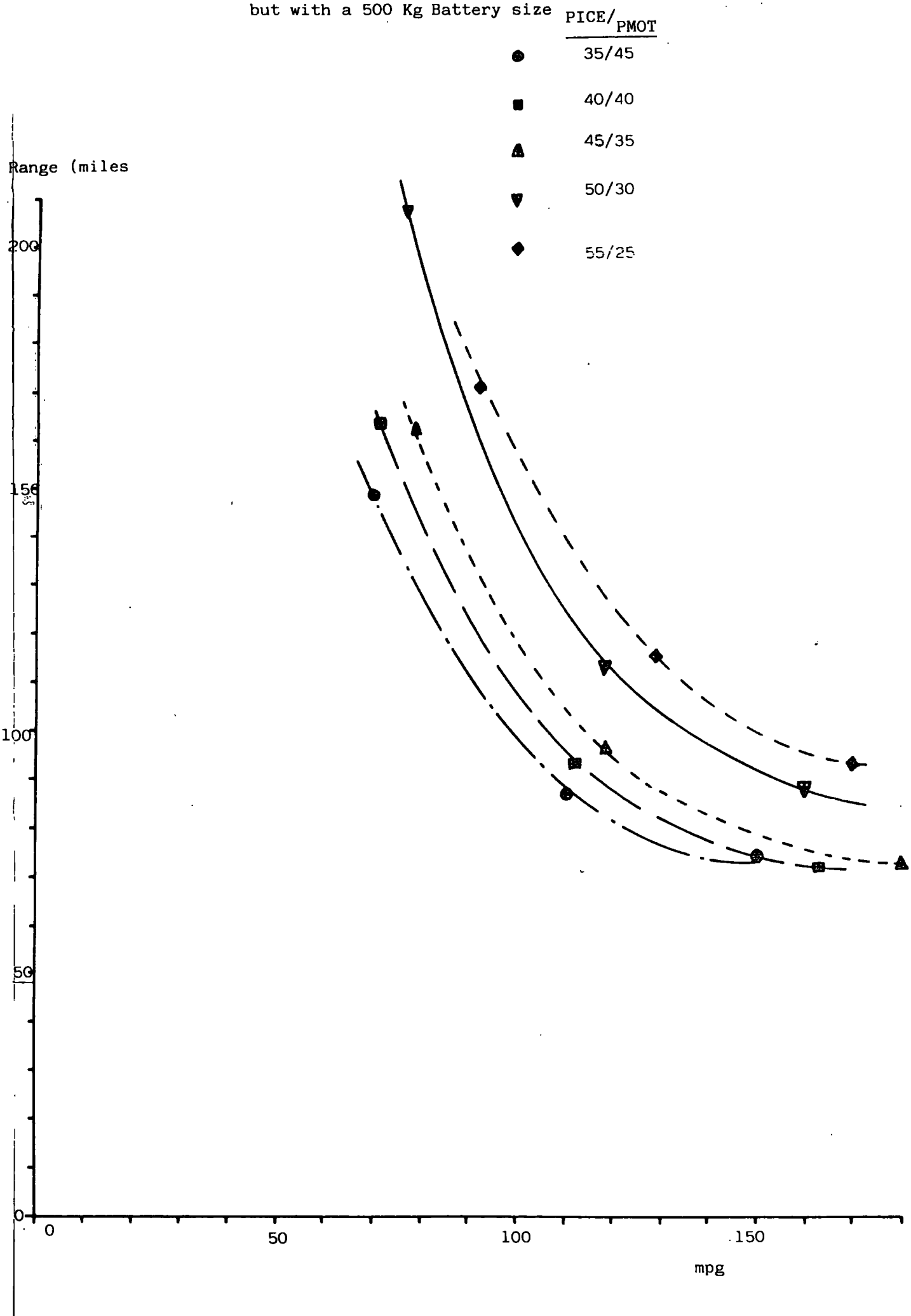

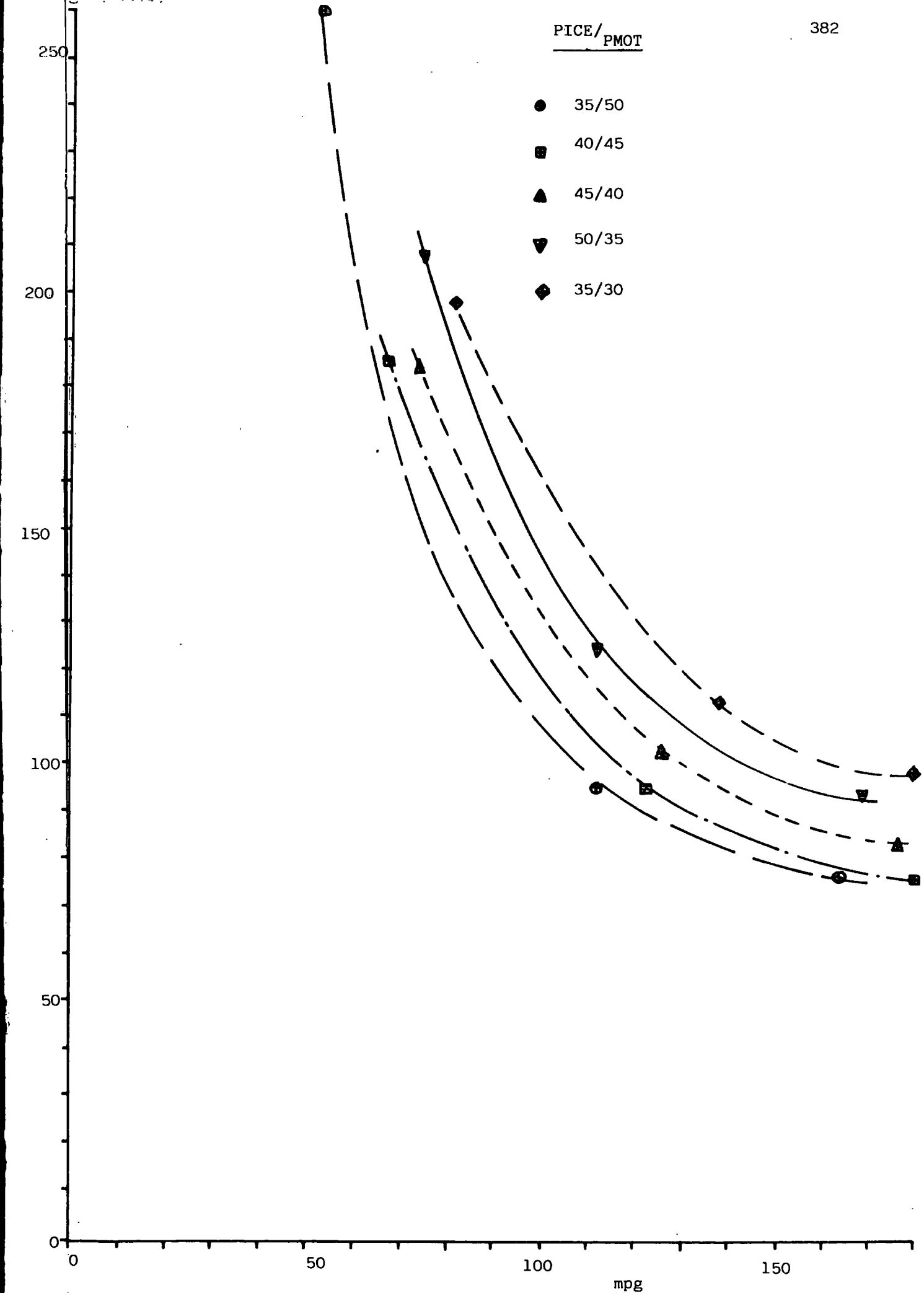

FIGURE 6.25 The Base Hybrid of figure 6.21a but with a 600 Kg Battery size

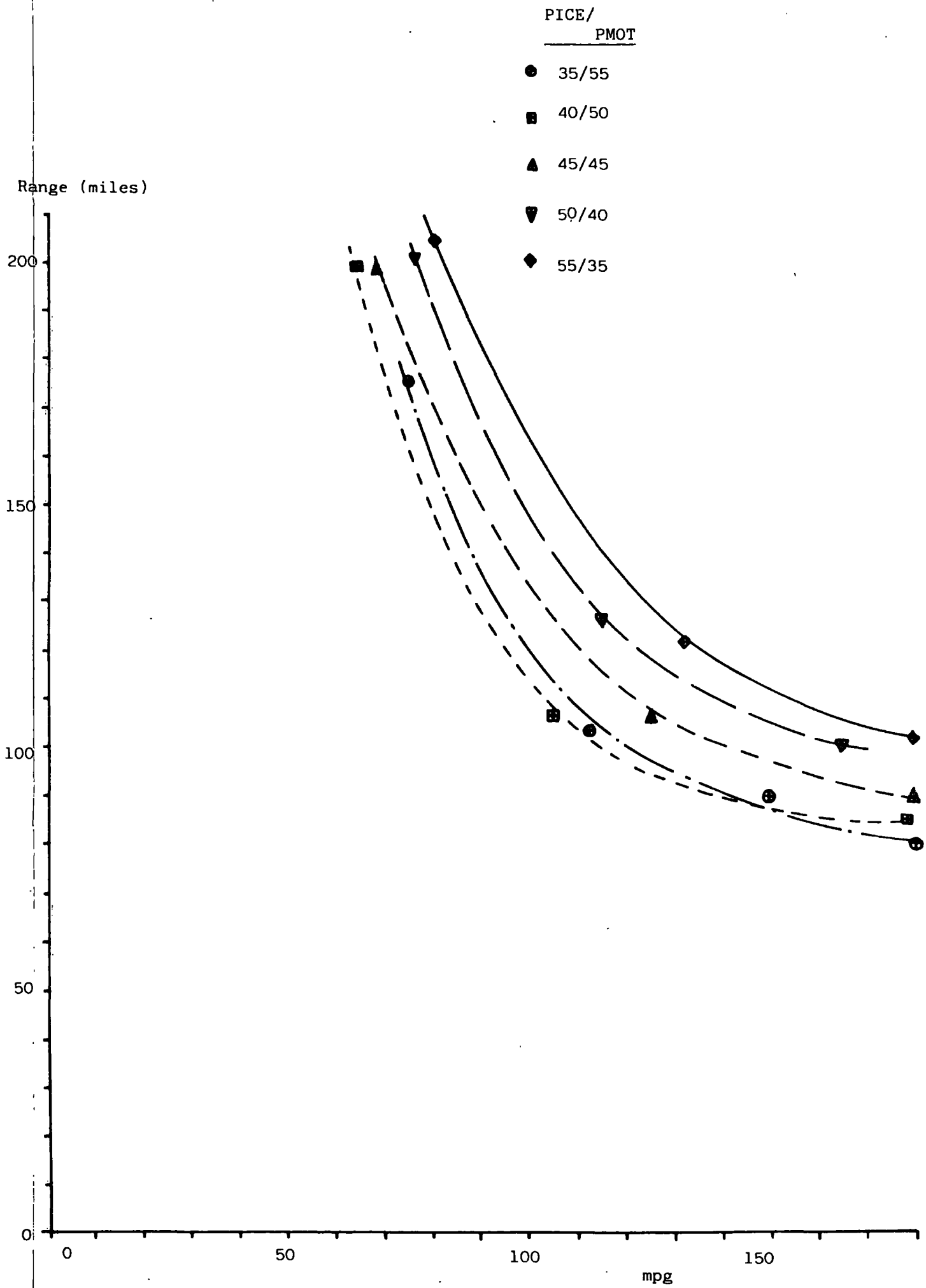

FIGURE:6.26 The Base Hybrid of figure 6.21a but with a 700Kg battery size

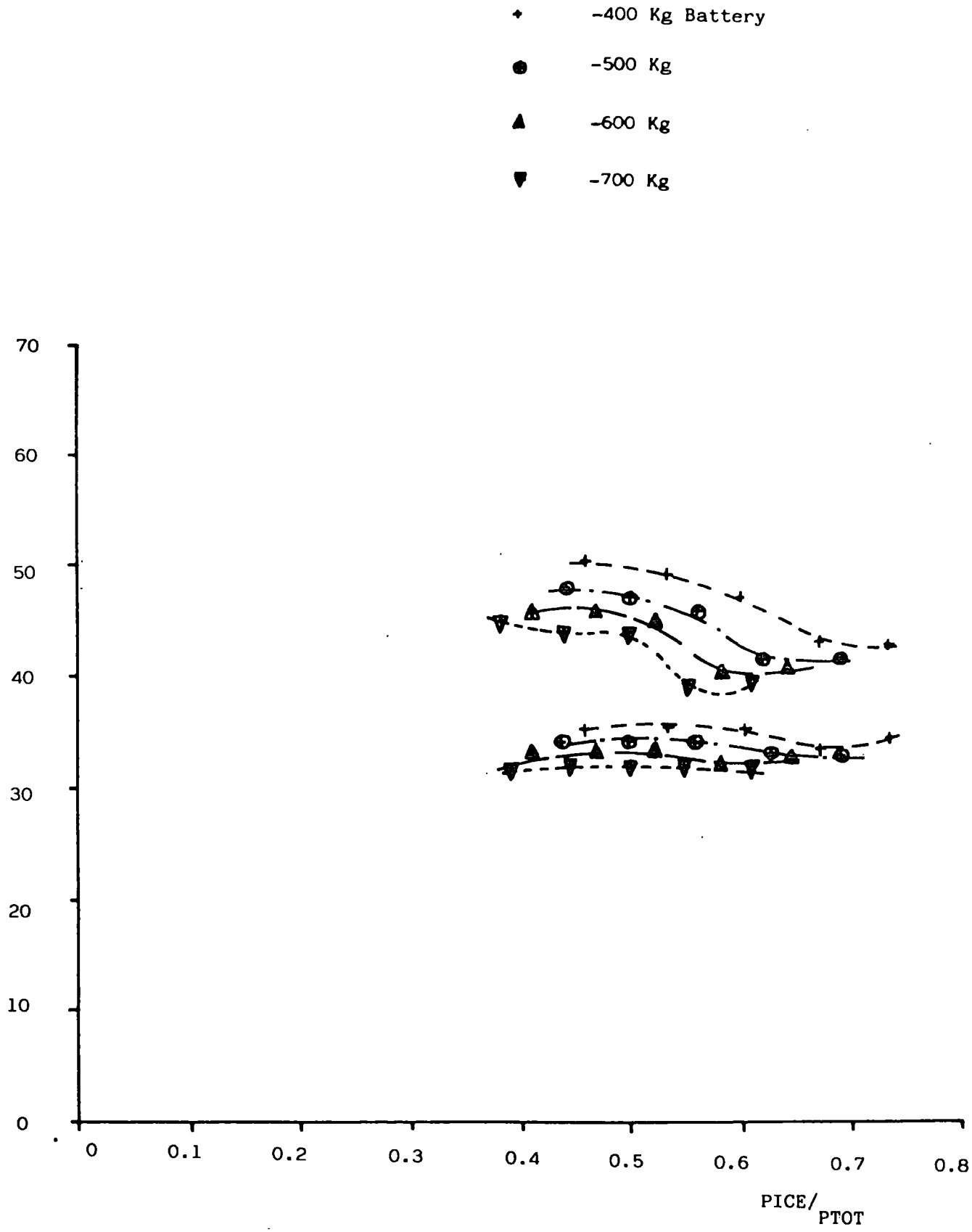

FIGURE 6.27: The Effect of Battery Size and Relative Power Source size on mpg at 56mph and 75 mph cruises for the Petroleum Substitution Aim with the Base Hybrid

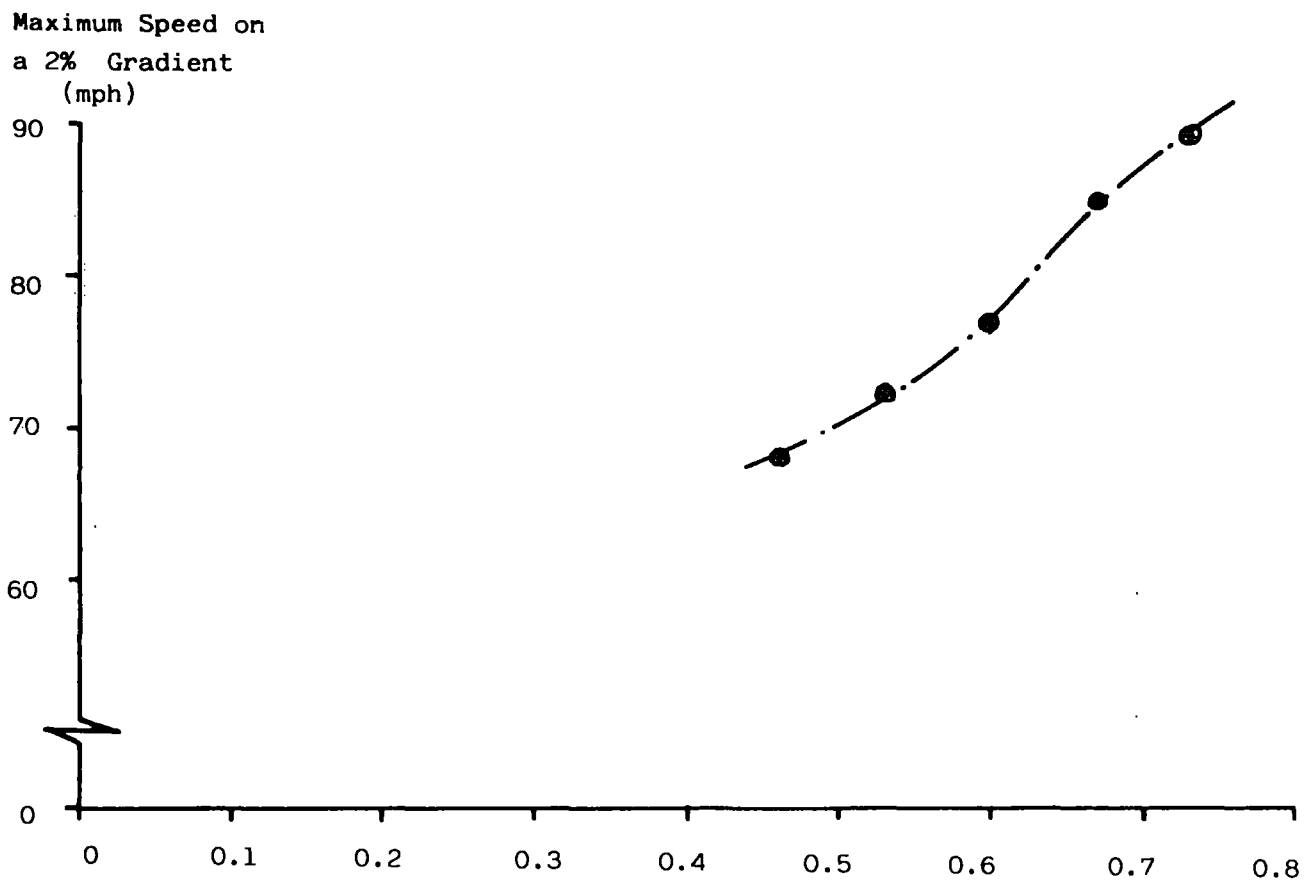

FIGURE 6.28: The Effect of Relative Power Source Size on Gradeability for the Petroleum Substitution Aim base Hybrid with a 400 Kg Battery size.

FIGURE 6.29: Effect of Battery Type and Driving Cycle on Specific Range/Battery Fraction curves for the Petroleum Substitution Aim.

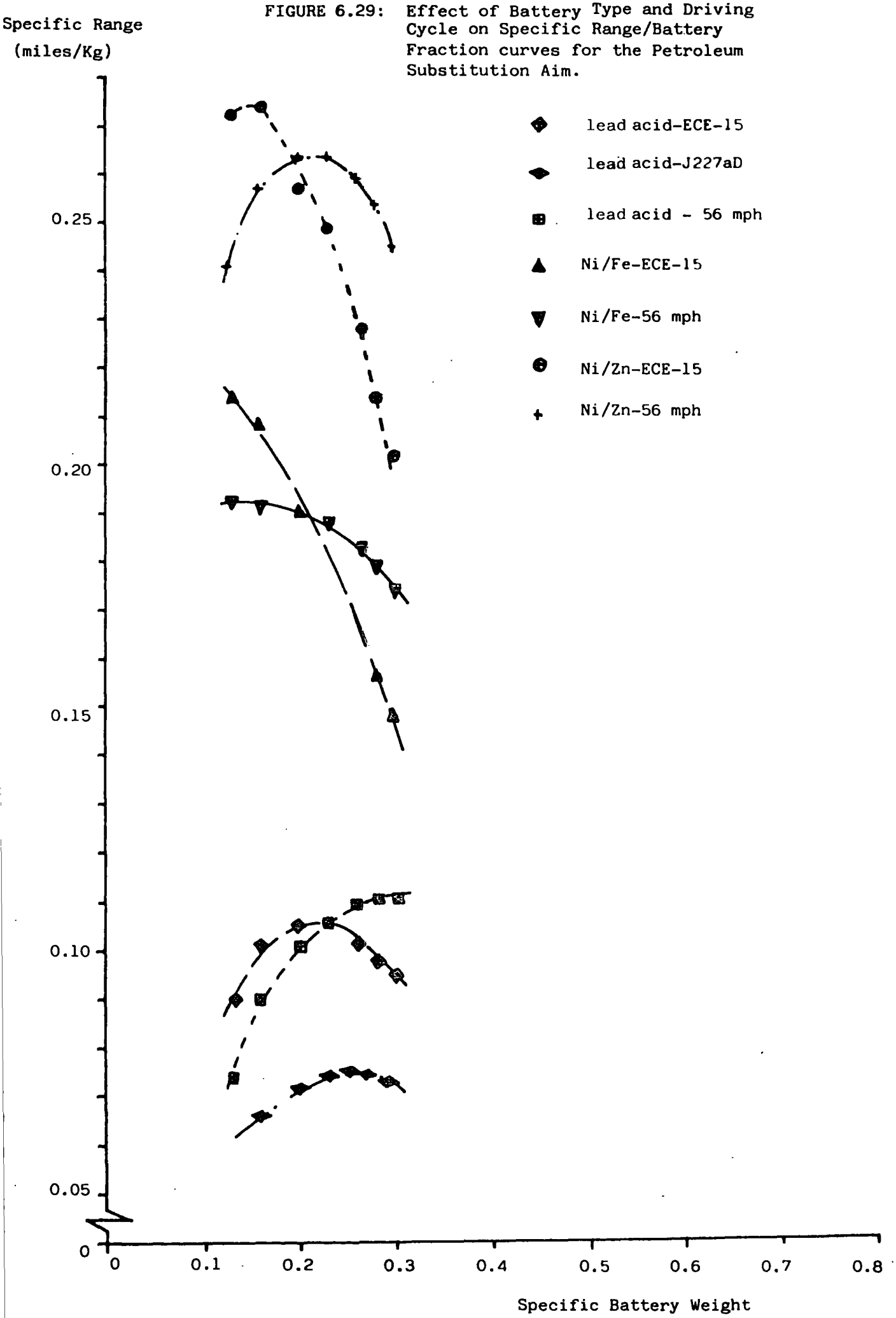

FIGURE 6.30: The Base Hybrid of figure 6.21a but with a Nickel-Zinc Battery Type

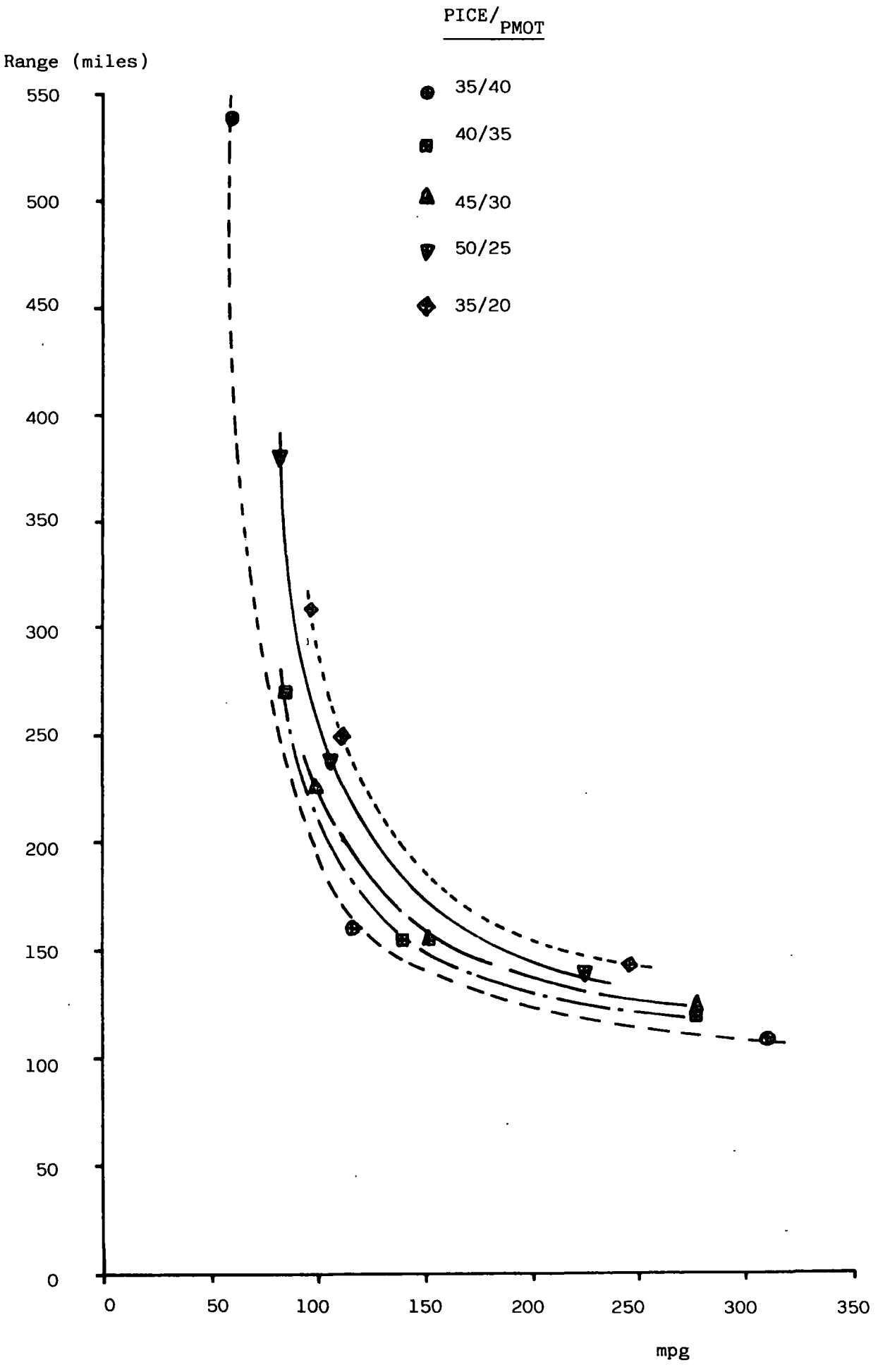

FIGURE 6.31a: The Base Hybrid of Figure 6.21a but with a 6-speed Discrete ratio unit

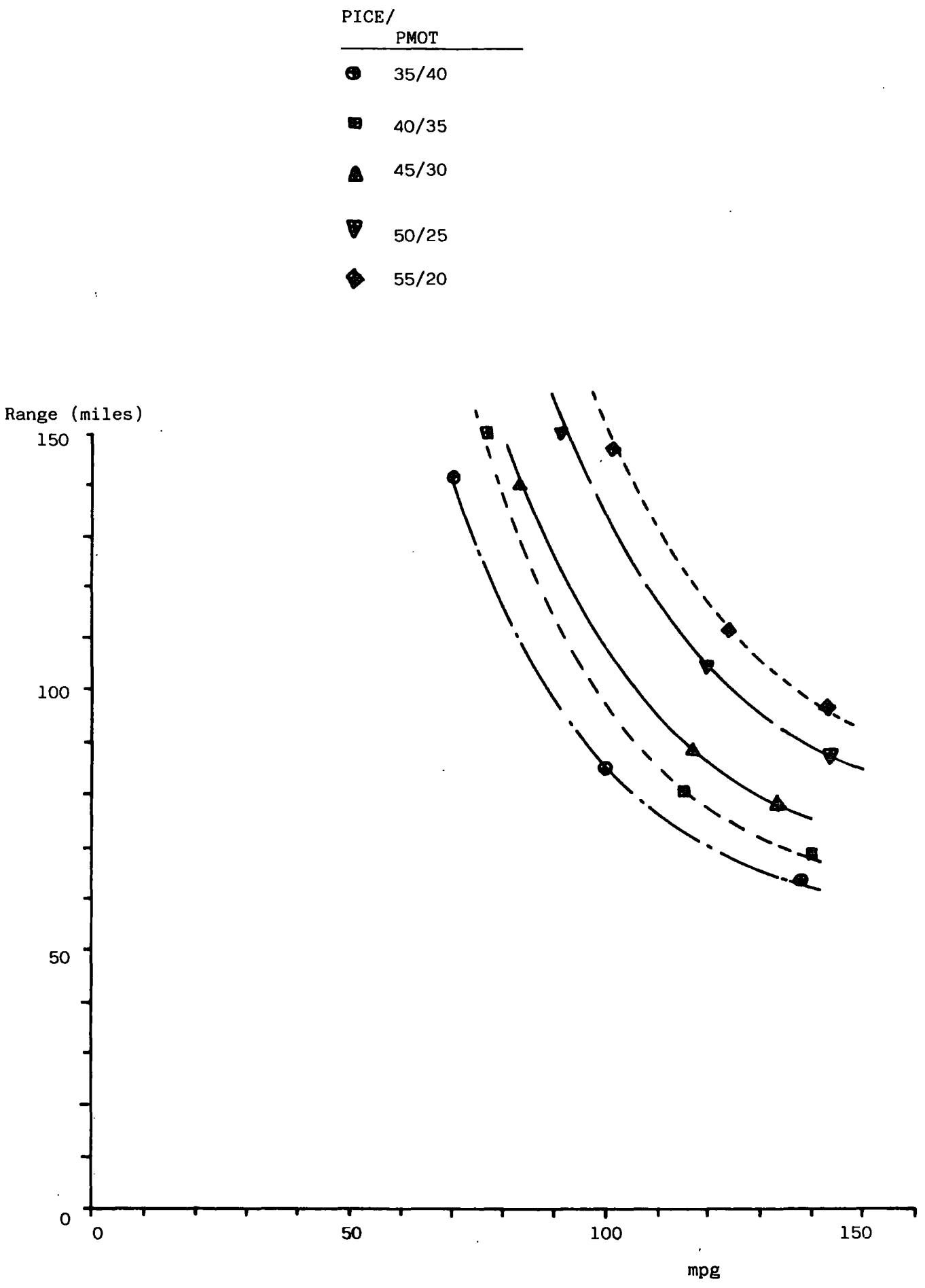

FIGURE 6.31b: The Base Hybrid of figure 6.21a but with a CVT

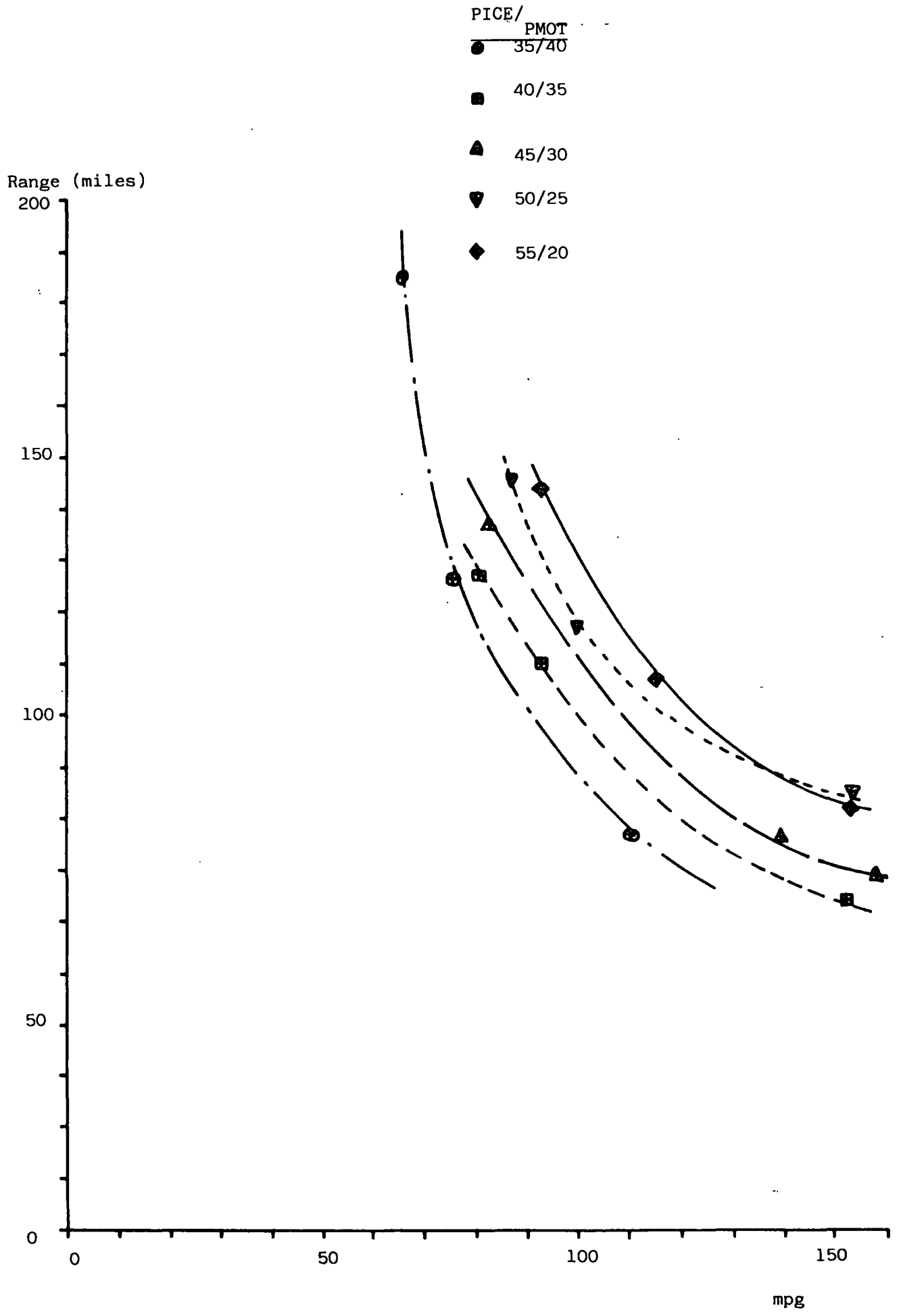

FIGURE 6.32a: Effect of Transmission Type on 56 mph and 75 mph cruise mpg for the petroleum substitution Aim with changing relative Power Source size for the 400 Kg Battery Size.

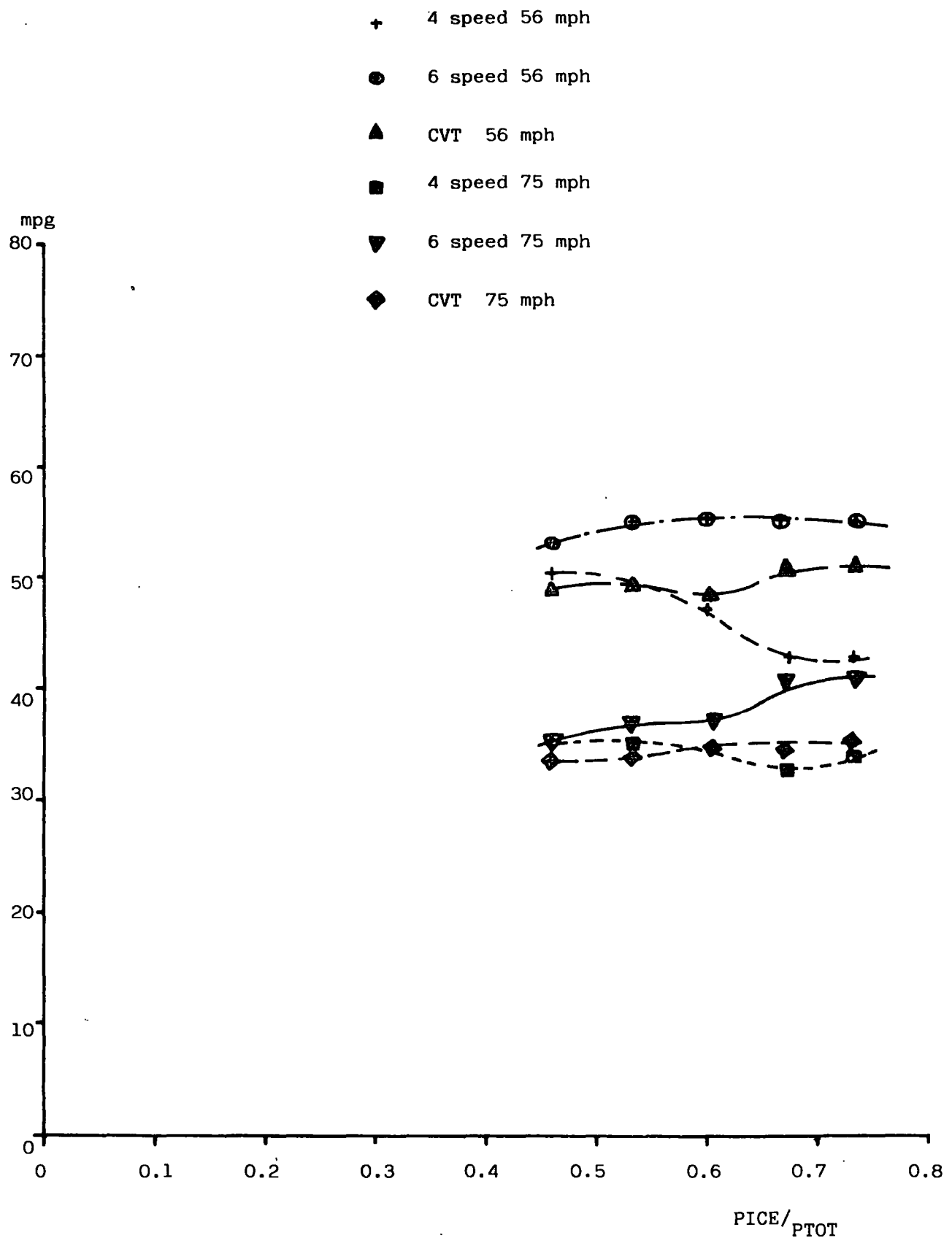

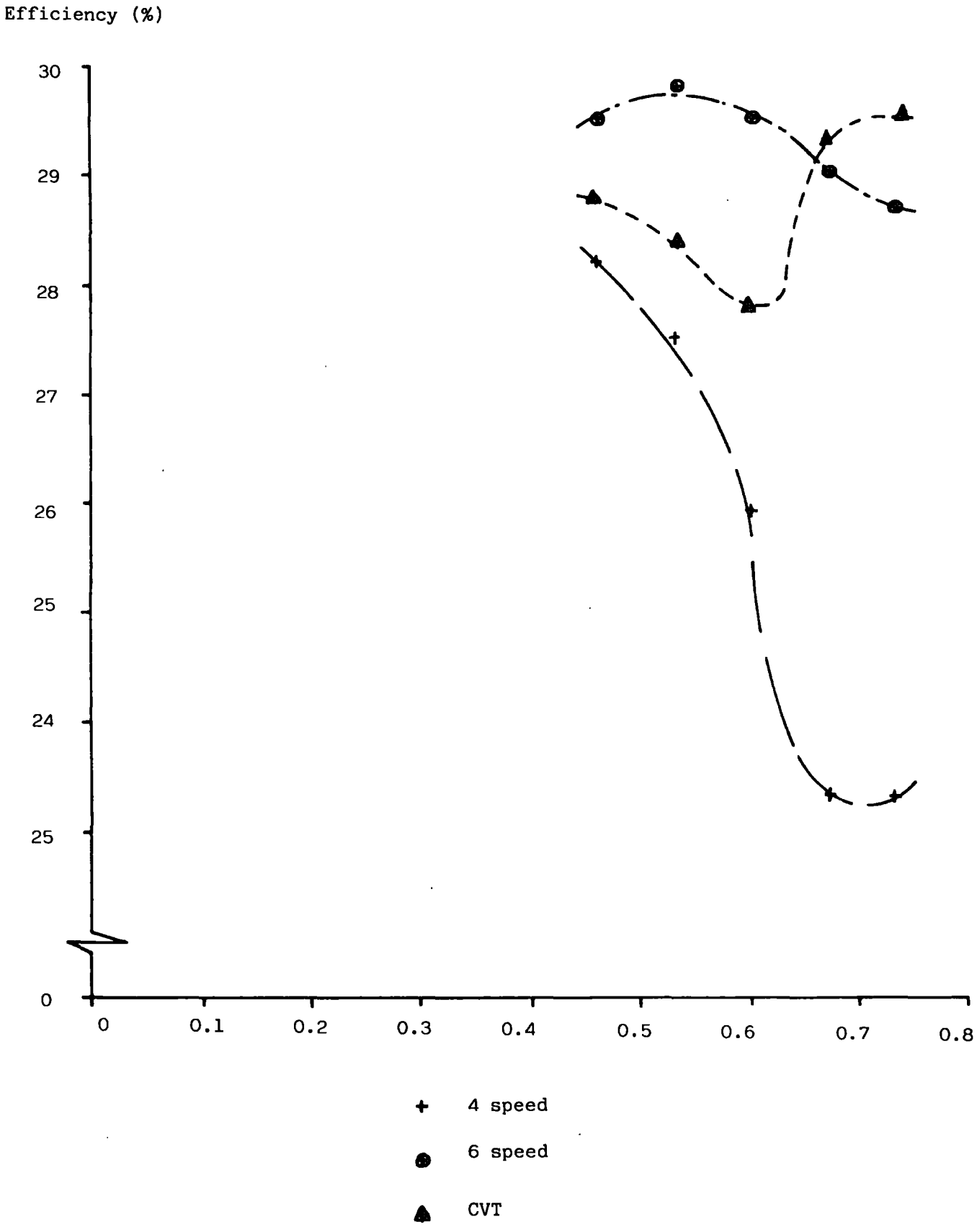

FIGURE 6.32b: Effect of Transmission Type and Relative Power Source Size on Component Efficiency at 56 mph cruise for the Petroleum Substitution Aim

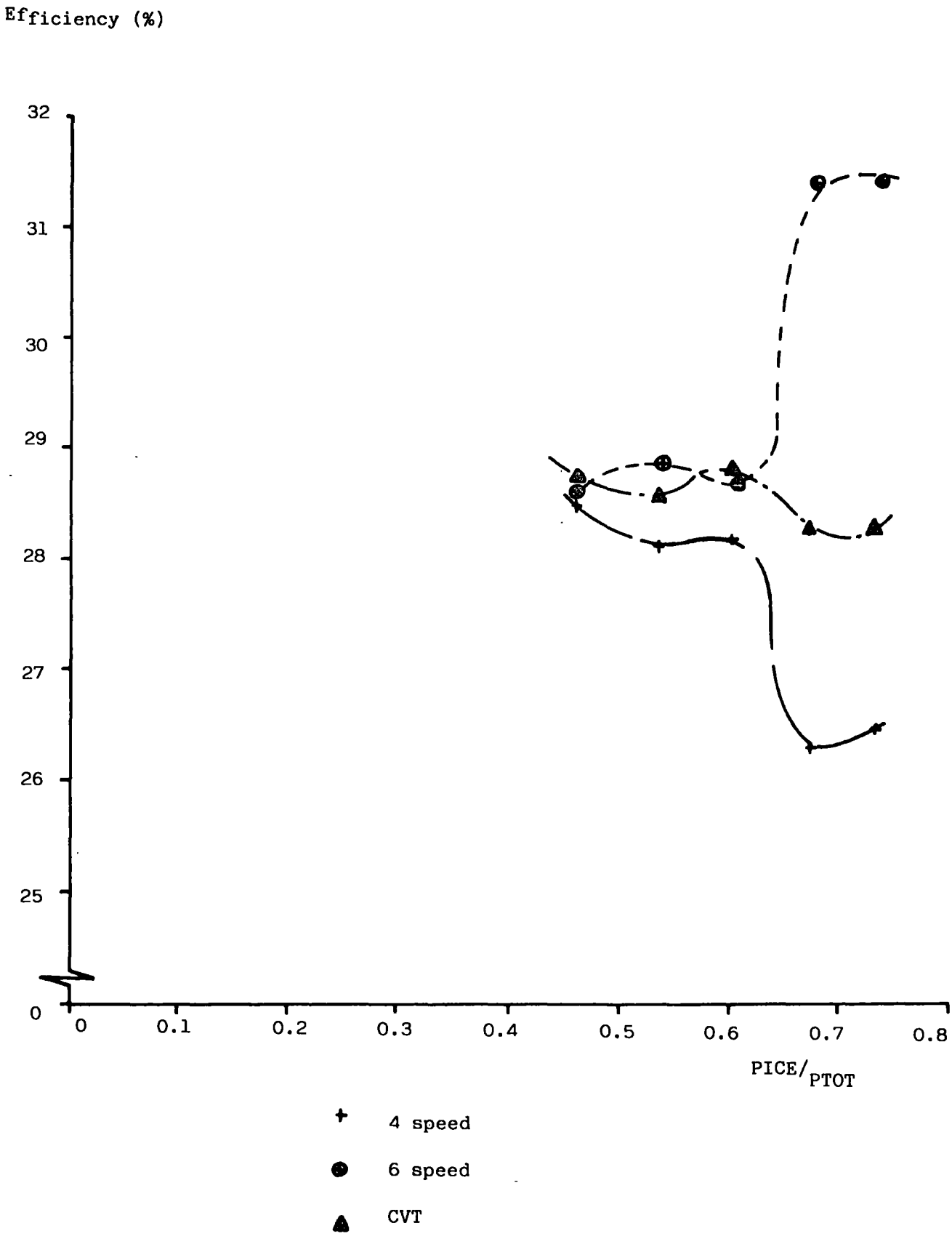

FIGURE 6.32c: As for figure 6.32b but at 75mph cruise

FIGURE 6.33a: The Base Hybrid of figure 6.21a but with an advanced i.c. Engine

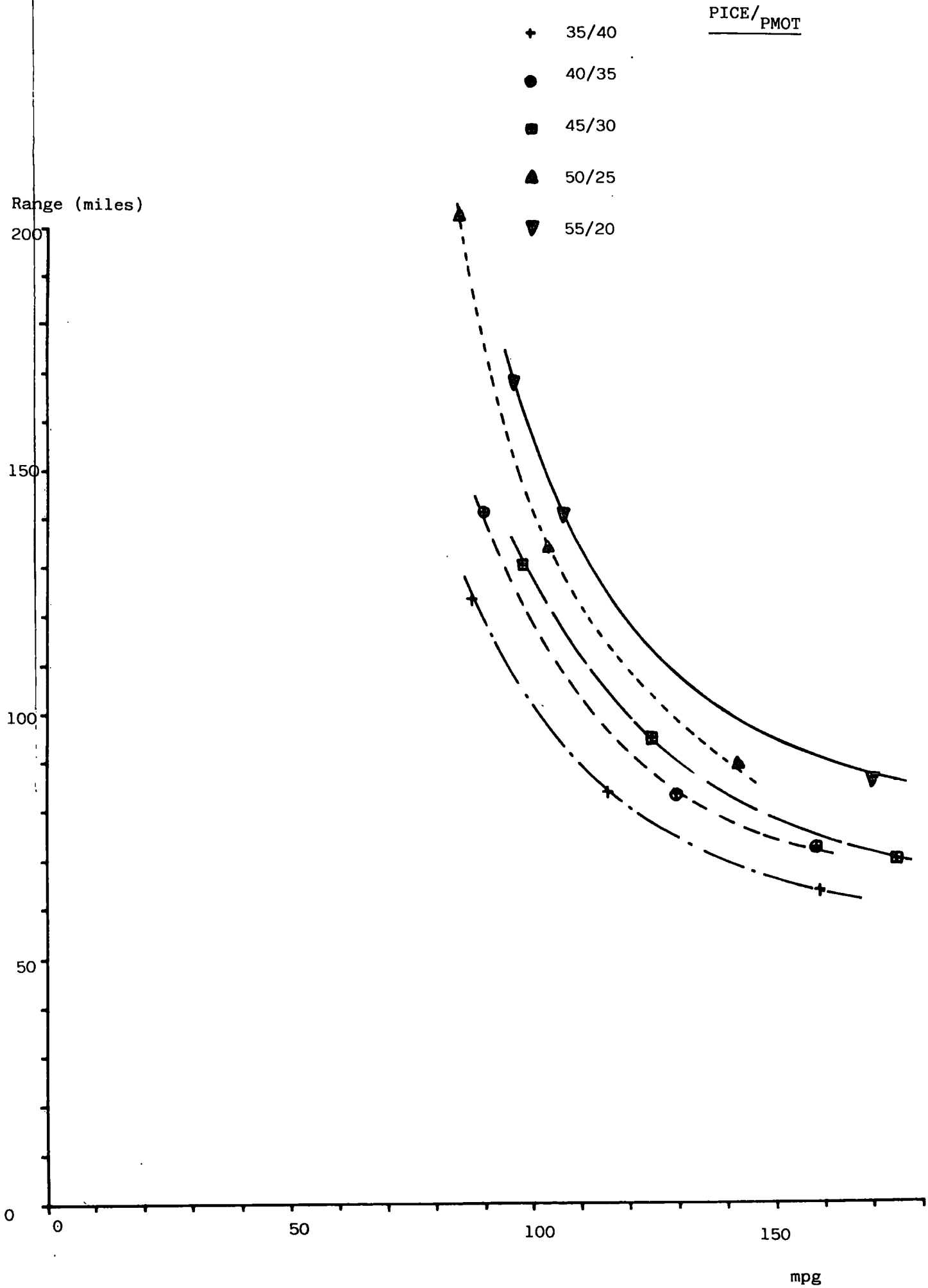

FIGURE 6.33b: The Base Hybrid of figure 6.21b but with an Advanced i.c. Engine

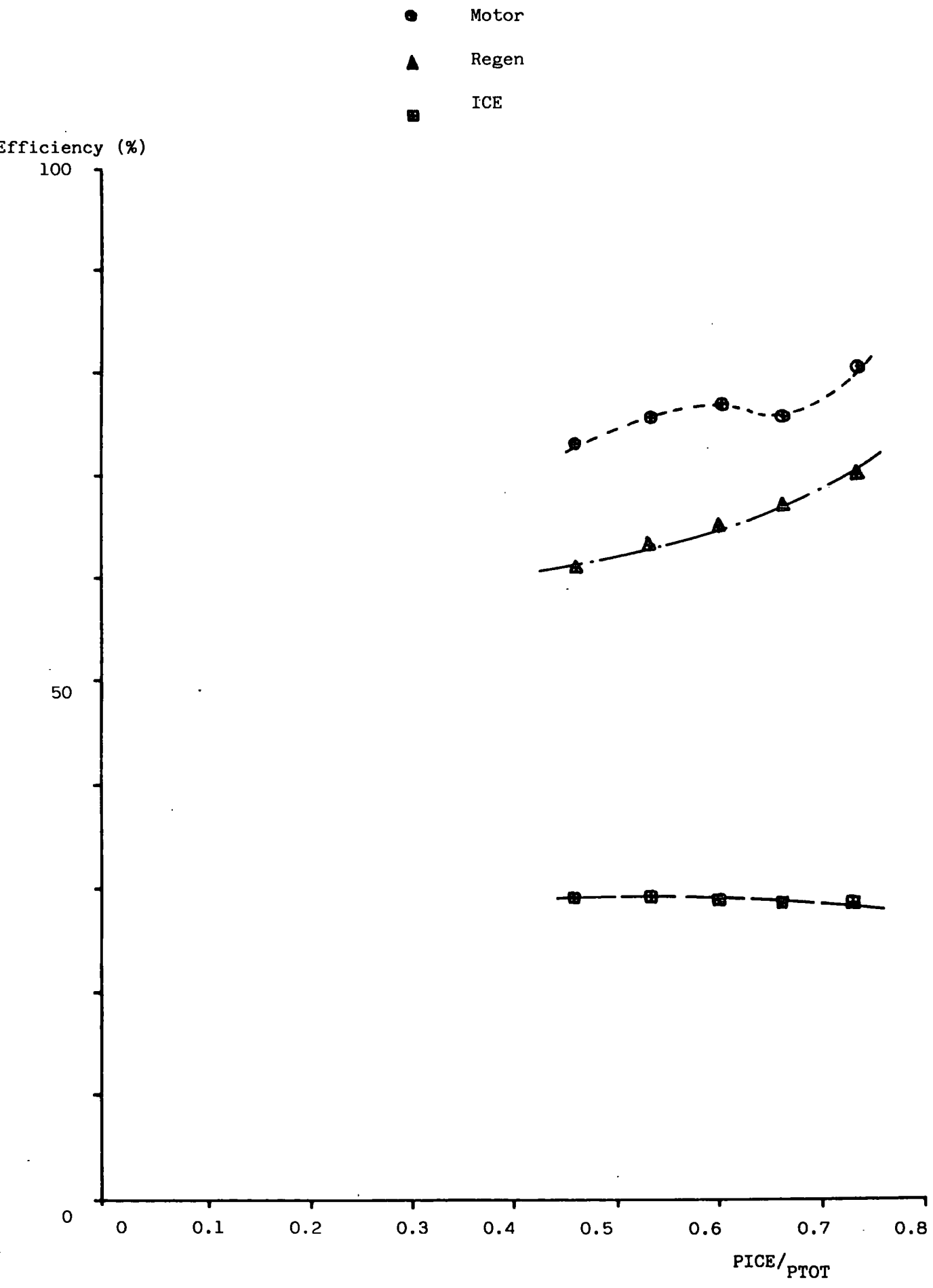

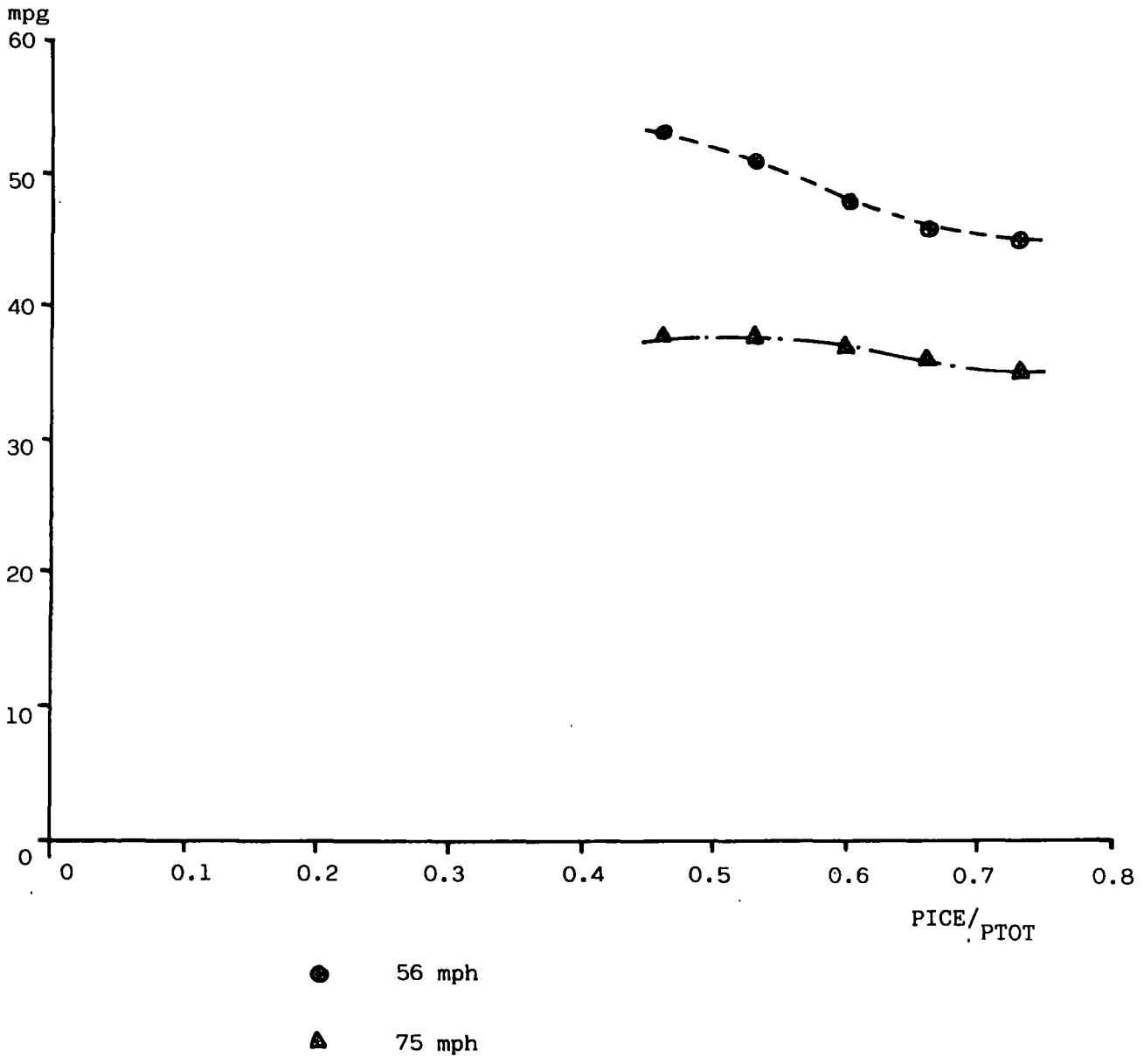

FIGURE 6.34a: The Base Hybrid of figure 6.27 but with an Advanced I.C. Engine for the 400 Kg Battery Size only

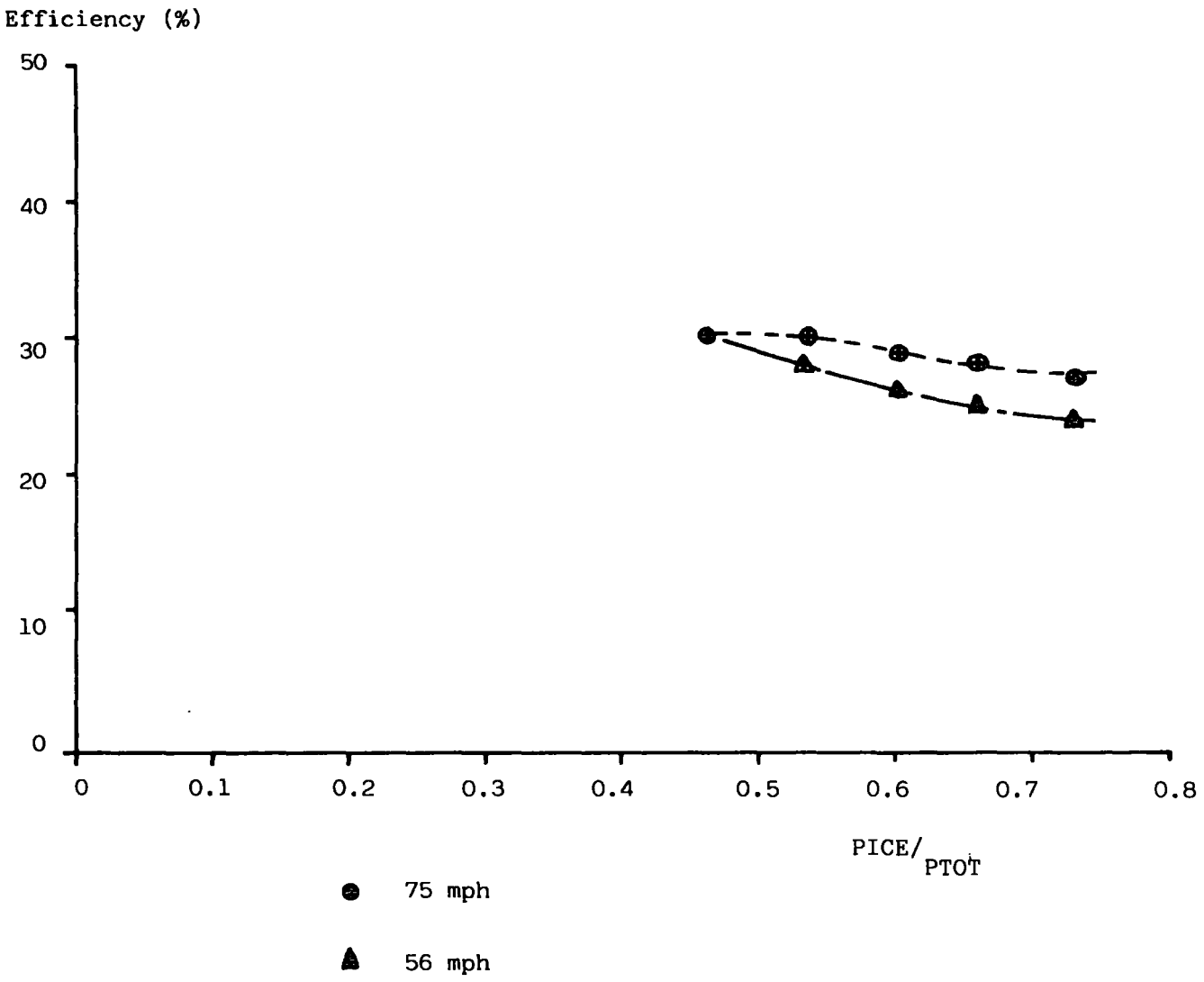

FIGURE 6.34b: The Effect of the Advanced I.C. Engine of figure 6.34a on Component Efficiency

FIGURE 6.35: The Base Hybrid of figure 6.21a showing the differences between spanning a given power range with 2 maps compared with 1 map.

PICE/PMOT

+ 45/30

▲ 55/20 - new map

▼ 55/20 - no map change from 45/30

■ 50/25 - new map

● 50/25 - no map change from 45/30

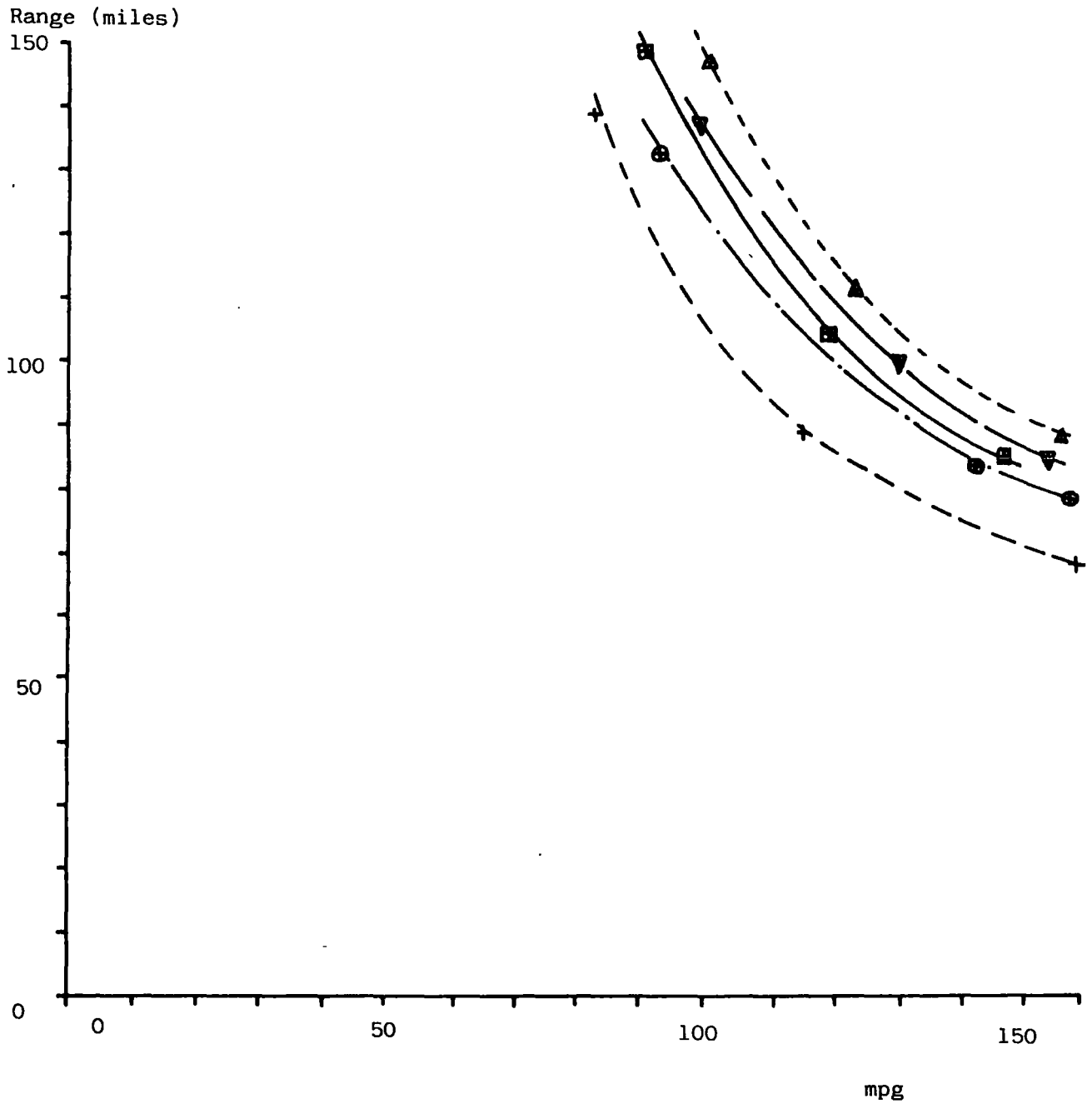

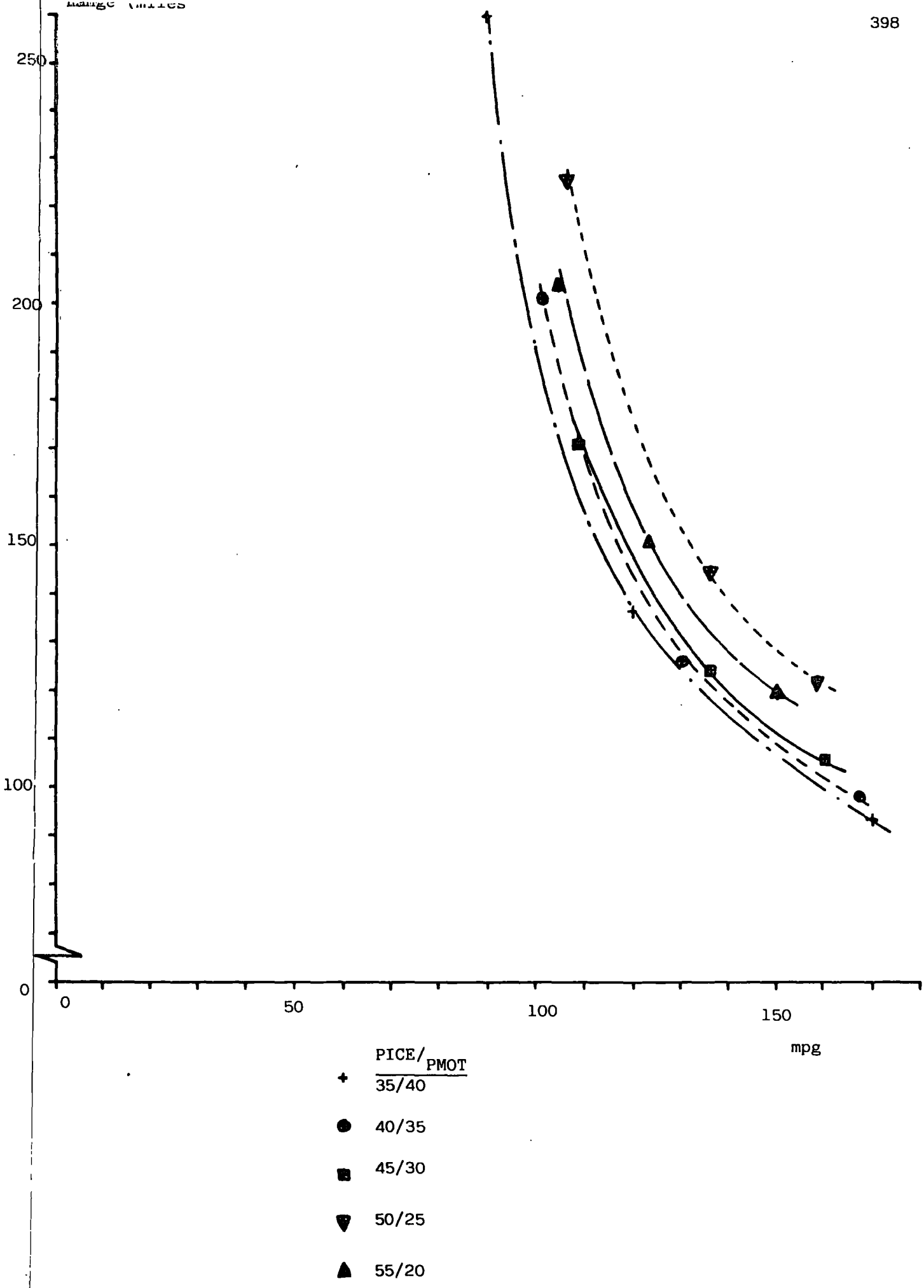

FIGURE 6.36a: The Base Hybrid of figure 6.21a but with an Advanced Traction Motor

FIGURE 6.36b: The Base Hybrid of figure 6.21b but with an Advanced Traction Motor

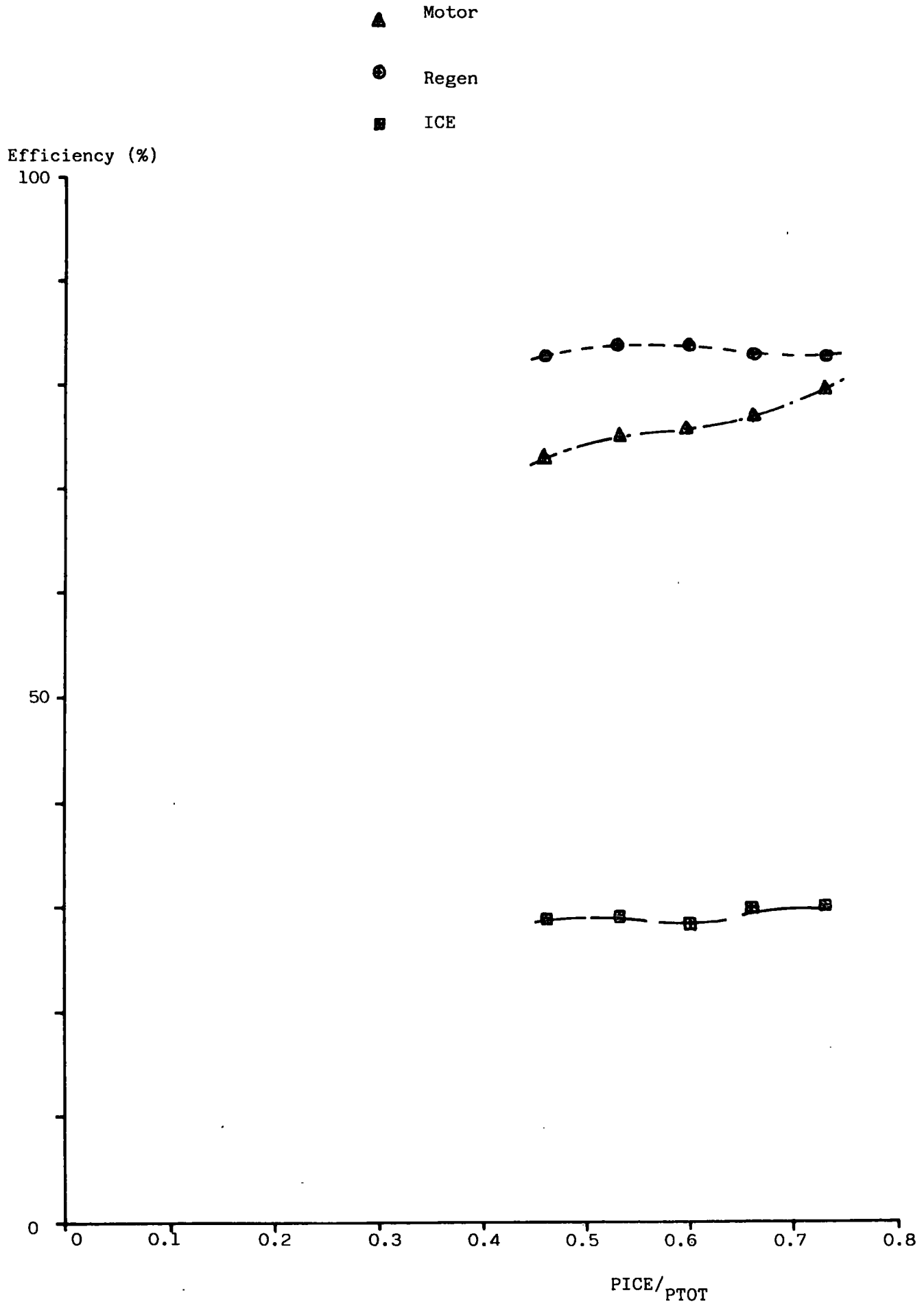

CHAPTER 7

Implementable Control of the Hybrid Electric Vehicle Derived from the Optimum Control Strategy

7.1 Introduction

The optimal control algorithm which was used in chapter 6 to study the parametric variations of the single parallel hybrid-electric configuration gives the best theoretical combination of control variables for each combination of vehicle parameters.

As was described in chapter 2, the algorithm as far as the simulation is concerned searches through the energy consumptions corresponding to each combination of control variable to find the minimum. However, this method of finding the optimum combination of control variables - here torque split,X, and transmission ratio, GR - cannot be implemented in practice as energy has to be consumed for the non-optimum cases, as well as the optimum case, before the optimum can be found.

An implementable control strategy has been suggested to control such variables as ignition timing and air-fuel-ratio for the i.c. engine (Rhodes et al., 1984) to achieve minimum SFC (maximum efficiency). A ' gradient' method (Fox,1971) is used to predict the minimum SFC by taking previous measurements of SFC and extrapolating. This could apply to the hybrid-electric vehicle by substitution of the required control variables, but, as was discussed in chapter 2, with this method, there is a definite possibility of locating 'local' rather than 'global' minima because of the complex nature of the objective function.

As alternative to developing a control strategy to resemble the 'method' of the optimum control algorithm, it is possible to study such control aspects as transmission ratio, i.e. engine behaviour and electrical system behaviour and formulate an implementable or sub-optimum control strategy from this.

This sub-optimum strategy may then be compared with, not only the optimum strategy from which it was derived - in terms of control strategy behaviour and vehicle energy consumption - but also with an existing

strategy implemented on a current hybrid-electric vehicle. Such a current control strategy is that employed on the Near-Term Hybrid Vehicle constructed in phase II by G.E. (Burke et al.1981)(Trummel et al.,1980).

The control strategy adopted in the G.E. vehicle used road speed as the control variable to determine when the vehicle should change from a "primary electric mode" to a "primary i.c. engine mode". In the primary electric mode, if the battery was within certain predefined state of charge limits, the traction motor would meet the road load with the i.c. engine being brought in to meet excess power demands. The power source roles would then be reversed when the primary i.c. engine mode was selected at a pre-determined road speed with the traction motor being brought in to meet excess power demands, but with the i.c. engine meeting the road load alone if it could do so rather than any excess power available being used to charge the battery.

7.2 Implementable Control Strategy Based on Optimum Control

In chapter 5, when the alternative drive-train configurations were discussed, the behaviour of the optimum control strategy, for both energy saving and petroleum substitution aims, using the single drive-train configuration selected was introduced.

Furthermore, in chapter 2, the operation of the sub-optimum control algorithm developed from the optimum control algorithm was also introduced in relation to other software developments for the simulation package.

In this section, therefore, it is proposed to embark upon a resume of the basis for developing the sub-optimum strategy, based on control behaviour for the optimum results.

As was stated in chapter 5, by looking at the i.c. engine 'usage' data on the fuel map for the energy saving aim and petroleum substitution aim using optimum control, an indication of what control variables, gear ratio

and torque split are trying to achieve can be obtained. This can also be reinforced if one considers the variation of torque split, X with cycle time.

For the usage data shown for the energy saving aim in Figure 5.19 and petroleum substitution aim in Figure 5.23, a number of basic points emerge over the ECE-15 urban cycle. Firstly, below a certain i.c. engine torque-load, all electic operation is desirable. Secondly, above a certain i.c. engine speed, again, all-electric operation is preferred. Finally, above about 80-90% of maximum i.c. engine torque, the hybrid mode should be used to meet the extra torque demanded.

If one looks at the torque split,X versus time plots for the two aims, shown in Figures 5.22 and 5.25, it is apparent that the use of one power source or the other is favoured, and the hybrid 'blend' only resorted to under heavy load demands - as seen at the end of the 3rd acceleration at 135-145 seconds. Furthermore, the i.c. engine is only used for the relatively heavy loading periods during acceleration, and with the exception of the 1st profile, at road speeds corresponding to i.c. engine speeds above its pre-deterimed minimum. During the 1st profile i.c. engine operation occurs in a high gear (low ratio) with a slipping clutch to enable the i.c. engine to be matched to road load - a practice which would drastically reduce the life of the clutch unit if prolonged.

As was described in chapters 5 and 6, of fundamental importance to the energy saving hybrid is the practice during vehicle deceleration of decoupling the i.c. engine, cutting its fuel flow and recovering vehicle braking energy regeneratively into the traction battery. If possible for the energy saving aim the practice must also be equally possible for the petroleum substitution aim. Furthermore, the practice of shutting off i.c. engine fuel flow during stationary periods should also be implemented for driving cycles having substantial vehicle idle periods.

In chapter 2, the plot of a typical hybrid-electric vehicle objective function with torque split, X - shown in Figure 2.39 - indicated that, due to the tortuous energy conversion route, charging the traction battery from the i.c. engine is inefficient and should be avoided unless a flat battery occurred for a hybrid with an inadequate i.c. engine power source.

From the above observations it is possible to deduce that i.c. engine only operation is favoured in a region bounded by the said maximum torque line, minimum torque line, maximum speed line and minimum speed line. In its simplest form, this region will take the form of a 'box' with straight edges at right angles to each other.

For torque loadings below i.c. engine maximum that do not occur inside this region, then all-electric operation is favoured, whereas for torque loadings above i.c. engine maximum, hybrid operation is necessary - using the traction motor to supplement the i.c. engine with the latter developing its maximum torque in order to maximise efficiency.

From the usage plots of Figures 5.19 - 5.23, it is seen that when moving from the energy saving aim to the petroleum substitution aim that the region, which encloses the area of maximum efficiency, contracts by movements in the minimum torque and maximum speed lines - so putting less emphasis on the i.c. engine. Therefore, the minimum load and maximum speed boundaries can be varied to dictate to what extent the i.c. engine is to be used throughout the given duty cycle, in a similar fashion to varying the value of λ_1/λ_2 for the optimum strategy.

The i.c. engine minimum speed and maximum torque lines, although variable within practical limits, tend to remain fixed as the usage data of Figures 5.19 and 5.23 show - which is explained if one considers that i.c. engine maximum efficiency occurs close to thse boundaries.

Therefore the basis of an implementable control strategy based on the optimum, as far as the i.c. engine is concerned will take the form of the

aforementioned box - which was shown in Figure 2.53 when superimposed upon the i.c. engine performance map. Also shown in Figure 2.53 is a typical traction motor map - indicating the all-electric operating regions in relation to the 'box' -, and also the combined traction motor and i.c. engine characteristics to show the hybrid operating region.

The algorithm developed for the simulation program to be used for sub-optimal control selects which, if any, of the available gear ratios put the driving cycle operating point at transmission output inside the pre-defined operating box when superimposed on the i.c. engine performance map. If more than one ratio satisfies this condtion, then the box is reduced in size towards the region of maximum i.c. engine efficiency, after which the test is repeated. If more than one ratio satisfies this second condtion, then the first ratio encountered in the search is selected.

It is also necessary for any control strategy to consider the efficiency of the electrical system components in the hybrid-electric vehicle - particularly in the all-electric mode.

Motor controller efficiency is generally at or above 90% of its maximum value even over urban cycle condtions and so can be considered to give a negligible contribution to vehicle losses. However, since, along with the i.c. engine, traction motor efficiency can fall as low as 60-70% of its maximum value over urban conditions, then the control strategy needs to consider gear shifting in relation to this power source also.

For all-electric operation, the sub-optimum control algorithm selects a transmission ratio that will put the operating point of transmission output as near to the motor break or base speed as possible, as it is here for the D.C. shunt machine that maximum efficiency occurs (Figure 2.13).

In the hybrid mode, however, a transmission ratio must be selected to satisfy the efficiency needs of both power sources. Because this is not possible, due to maximum efficiency for each not occurring at the same point when maps are superimposed, then the algorithm selects the lowest ratio (highest gear) possible in order to maximise i.c. engine efficiency

Finally, during regenerative braking, a gear ratio to achieve as high a motor speed as possible is selected in order to achieve a high efficiency.

The flow chart for the complete algorithm was shown in Figure 2.54 for the 'motoring' case, and in Figure 2.55 for the regeneration case.

From the prime mover characteristics of Figure 2.53, it may seem that given a suitable rating the traction motor may be capable of meeting loads over a region above i.c. engine maximum. However this would be an inefficient operating region for the motor and, whereas the hybrid mode, if selected, would result in the operating point occurring at medium loads and speeds on the motor map - so resulting in high efficiency.

Since, in chapter 5, results for the base parallel hybrid configuration selected were used to study the optimum strategy, so a comparison in terms of control behaviour may be made between optimum and sub-optimum using the same configuration.

Table 7.1 shows the energy consumption results for the base configuration in terms of mpg and range over the entire hybrid operating range - from all i.c. engine to all electric operation over the ECE-15 urban cycle. Also shown for each mpg and range combination are the parameter values defining the operating box - the lower torque bound, Tb, and the upper speed bound Nb. The corresponding charactertistic for the optimum strategy in terms of mpg and range versus λ_1/λ_2 was given in Figure 5.15 in chapter 5 and shows the sub-optimum strategy to give energy consumption of the order of 10% greater than the optimum case.

Figure 7.1 shows the i.c. engine usage data produced using the sub-optimum strategy and shows good agreement with the optimum results shown in Figure 5.19. Similarly Figures 7.2 and 5.20 show i.c. engine torque/time plots for sub-optimum and optimum cases and Figures 7.3 and 5.21 the gear ratio/time plots, again for sub-optimum and optimum cases

respectively. What is interesting to note about the torque/time plot is that the occasional rapid i.c. engine cutting in and out for the optimum case is now absent fo the sub-optimum case, whereas for the gear ratio/time plot the occasional rapid shifting for the optimum case is also absent for the sub-optimum case. The implications of these changes, which obviously occur at the expense of greater energy consumption for the sub-optimum case, are that control of the drive-train would be easier in terms of transient responses and also passenger comfort would be enhanced.

7.3 Comparison of Optimum and Sub-Optimum Control

Having derived a possible sub-optimum hybrid-electric control strategy it is now possible to assess its performance by comparing with the optimum strategy, upon which it is based, and the state of the art hybrid control strategy, applied to the G.E. Near-Term-Hybrid-Vehicle, described in section 7.1.

Again, as with the parametric study of chapter 6, the 'energy saving' and 'petroleum substitution' aims can be treated separately since it was shown in chapter 6 that they demand inherently different component sizes in terms of battery weight and knock-on effects.

Comparison is made possible between the 3 control strategies by the fact that it is possible to change the emphasis from one power/energy source to the other to enable the entire operating spectrum - from all i.c. engine to all electric operation - to be studied. As was described in chapters 2, 5 and 6, this is achieved using the optimum strategy by altering the power/engery source weighting factors relative to one another (in effect their ratio, λ_1/λ_2). For the sub-optimum strategy - described in section 7.2 - this can be achieved by altering the 'box' size using the lower torque and upper speed bounds. Finally, for the velocity control strategy the same effect can be obtained by altering the vehicle road speed at which the change from the primary electric to primary i.c. engine modes occurs.

However, in the case of the velocity control strategy, gear shifting is not implied, as the change velocity only specifies the change from one power source to the other. The G.E. hybrid using velocity control employed an additional control strategy for gear shifting, which although microcomputer based resembled the strategy employed in present day automatic transmissions in that shifting was controlled by vehicle speed but with a driver power demand input for vehicle acceleration requirements (the 'kick down').

For the comparison here, there are two alternatives as regards the vehicle speeds at which the velocity control strategy will specify gear shifting. Firstly, the standard ECE-15 gear shift points can be adhered to, or secondly some optimum velocity dependent gear shifting pattern can be implemented. The latter shift pattern simply up-shifts into the next gear as quickly as possible in order to maximise i.c. engine load-factor and hence efficiency, and down shifts into the next lowest gear as quickly as possible in order to maximise motor/generator speed and hence efficiency, and is similar to the ECE-15 shift pattern in that shifting is still dictated by vehicle speed - so emphasising the driving cycle dependency of the G.E. control strategy.

7.3.1 Energy Saving Aim

For the energy saving aim it is possible to condense the findings of the parametric study of chapter 6 and perform the comparison between the 3 control strategies over the range of battery sizes discussed (100 Kg - 500 Kg) but using the best relative power source fraction (PICE/PTOT) - as dictated by the optimum results - in each case.

As far as vehicle parameters are concerned, to be a consistent progression from chapter 6, the same configuration with the lead-acid battery type and 4-speed transmission is to be used with the argument that

since it formed the basis of the parametric study of chapter 6, it should also form the basis of the control strategy study here.

Unlike the study of chapter 6, however, a single fuel map will be adhered to throughout this study to span the required power range in order to prevent any of the i.c. engine efficiency changes, highlighted in chapter 6, creating discontinuities in results.

Comparison will be made over the ECE-15 urban cycle, at a steady 56 mph and at a steady 75 mph - as described in chapters 5 and 6.

7.3.1.1 Discussion of Results

Figure 7.4a shows a comparison of results for the optimum control strategy, the sub-optimum control strategy and simple velocity control strategy over the ECE-15 cycle. Results in each case are shown in terms of mpg over a range of battery sizes appropriate to the energy saving aim and using the best relative power source fraction dictated by the optimum results.

Although varying from battery size to battery size the value of relative power source fraction (PICE/PTOT) lies in the range 0.5 to 0.57 for the energy saving aim here.

Comparison over the ECE-15 cycle shows the optimum strategy to yield consistently higher mpg results than both the driving cycle dependent velocity control strategy and the implementable or sub-optimum control strategy - as would be expected. The implementable or sub-optimum strategy in turn yields consistently higher mpg results than both velocity control cases - of which the alternative employing optimum gear shift velocities shows higher mpg than that using ECE-15 gear shift velocities.

It is interesting to note that of the two non-optimum strategies, the sub-optimum strategy is unable to satisfy the energy saving aim (constant SOC) for the 100 Kg battery size, and the velocity control case is unable

to satisfy the energy saving aim for both 100 and 200 Kg battery sizes. This is because in the case of the sub-optimum control strategy i.c. engine operation with the clutch slipping is not permitted whereas, as was described in section 7.2, the optimum control strategy clearly favours this mode for the 1st portion of the ECE-15 cycle. Therefore the sub-optimum controlled vehicle has to run all-electic under such conditions with the result that for such a small battery (experiencing large average power densities) constant SOC operation is not possible. For the velocity control case, although i.c. engine operation with a slipping clutch is permitted, again, however, power density demand on the battery coupled with the fact that gear shifting is vehicle velocity dependent, rather than velocity and load dependent in the other cases, leads to cyclic discharge also.

The mpg/battery weight curve shown in Figure 7.4a for the optimum strategy indicates an optimum battery size for the energy saving aim. However, this can be explained by the effects of the ECE-15 cycle, discussed in chapter 6, in that, because of its mild nature, one or more of the 4 cruise regimes are being selected as the difference between range limited operation (significant discharge of the battery at the end of a cycle) and underusing the electrical system driving the cycle (all i.c. engine operation). The results for the more severe J227aD cycle in chapter 6 have indicated a steady trend of reducing fuel consumption as battery size decreases over this range battery size, so implying that there will be no optimum.

Results for the two cruise regimes are shown in Figure 7.4b and are identical for all 3 strategies. This is because, when using the same 4-speed discrete ratio transmission and assuming all i.c. engine operation for cruise, the task of selecting 1 from 4 possible ratios for a single operating point is relatively straightforward for even the velocity control case.

As has been indicated in chapters 5 and 6, the scope for improvement during vehicle cruise lies in the number and magnitude of the ratios available in a transmission - the ratio span.

As would be expected, for both 56 mph and 75 mph cases, from Figure 7.4b, mpg steadily rises as battery weight and hence vehicle weight decreases.

7.3.2 Petroleum Substitution Aim

Again, as with the energy saving aim, comparison of the optimum strategy, sub-optimum strategy and velocity control strategy can be made over the range of battery sizes, highlighted in chapter 6 as being appropriate to the petroleum substitution aim, and using the best relative power source fraction in each case as dictated by the optimum results - which is here 0.61 to 0.69.

The same driving cycles used for the energy saving comparison are also appropriate for the comparison here. Furthermore results for the velocity control case will also be presented here using ECE-15 gear shift points and also velocity shift points optimised for the ECE-15 cycle, and again, using a single i.c. engine fuel map to span the required power range.

Throughout the comparison, as was the case with the energy saving aim, the base parallel configuration used in chapter 6, comprising of a lead-acid battery and 4-speed discrete ratio transmission, will be used.

7.3.2.1 Discussion of Results

Figure 7.5a shows for the optimum control strategy the results presented for the petroleum substitution aim over the ECE-15 in terms of range to battery discharge and mpg over the range of battery sizes appropriate for petroleum substitution and using the best PICE/PTOT value in each case. Similarly Figures 7.6a, 7.7a and 7.7b show over the same

range of battery sizes an corresponding PICE/PTOT values the mpg/range results using the sub-optimum control strategy, the velocity control strategy using ECE-15 gear shift points and the velocity control strategy using gear shift points, optimised for the ECE-15 cycle, respectively.

The mpg/range curves for the optimum strategy in Figure 7.5a show a consistent increase in mpg for a given range over the range of battery sizes, 400 Kg to 700 Kg, although with the curves of the 500, 600 and 700 Kg battery sizes closer together, the implication is that above 500 Kg the rate of increase is reducing.

The results for the sub-optimum control strategy in Figure 7.6a show an improvement from 400 Kg to 500 Kg but with the 600 Kg and 700 Kg curves falling approximately coincident with the 500 Kg curve. Using the velocity control strategy, the same trend is observed, but with the difference when optimised ECE-15 gear shifts are used that the 600 Kg and 700 Kg curves fall below the 500 Kg curve - as shown in Figure 7.7b.

When comparing the average component efficencies over the range of battery sizes - as is shown in Figures 7.5b, 7.6b and 7.7c for optimum, sub-optimum and velocity control strategies respectively - it is seen that the curves show reasonably smooth trends. When compared in absolute value with the optimum results of Figure 7.5b, it is seen that the sub-optimum results are comprable in magnitude for both i.c. engine and traction motor (Figure 7.6b), whereas the velocity control results show i.c. engine efficiency to be of the order of 25% lower, traction motor 'motoring' efficiency to be about 5% higher but 10% lower on regeneration (Figure 7.7c).

It is clear, therefore, that there are no sudden efficiency changes occurring over the range of battery sizes to account for the trends in the mpg/range curves of Figures 7.5a, 7.6a, 7.7a and 7.7b, but as was suggested by the parametric study of chapter 6, there will be an ideal battery size

for the petroleum substitution hybrid aim, not only when in the all-electric mode, but also when in the hybrid mode. This ideal battery weight was found to be between 400 and 500 Kg and corresponded to a battery weight fraction of 0.2 -0.25.

The 600 Kg and 700 Kg battery sizes are clearly above this ideal battery weight fraction - given knock on effects such as weight propagation factors and total installed power changes - and therefore for these two larger battery sizes a greater proportion of the extra battery energy is being used to propel the extra battery weight.

This is best illustrated by the optimum case as the sub-optimum cases, have obviously shortfalls in control strategy clouding the trend, and shows the benefits in terms of mpg for a given range, in Figure 7.5a, to be diminishing above the 500 Kg battery size.

Generally, when comparing the absolute values of results from the 3 control strategies in terms of mpg for a given range, the same trend as was observed for the energy saving case is apparent here in Figure 7.5a, 7.6a, 7.7a and 7.7b in that the optimum yields the best results followed by the sub-optimum, which is in turn followed by the velocity control case. Again, as with the energy saving case, of the two velocity control gear-shifting alternatives, the case with gear shifting optimised for the ECE-15 cycle yields consistently higher mpg for a given range than the case using ECE-15 gear shift points.

As was the case with the energy saving aim, cruise results for the 3 control strategies are identical when using a discrete ratio transmission, as the selection of the correct ratios to satisfy the two single operating conditions from the 4 available is readily achievable, and these are shown in Figure 7.8.

7.4 Discussion

From the comparisons made in section 7.3 between the optimum, sub-optimum and simple velocity control strategies it has been shown that the results produced using the sub-optimum strategy lie consistently above those for the velocity control strategy but below those for the optimum strategy. The latter observation is to be expected since, by definition, a sub-optimum strategy can only ever approach the results produced by the optimum strategy from which it was derived. But the fact that the strategy derived from the optimum in this chapter shows consistently improved energy consumption results compared to the state-of-the art velocity control strategy, indicates an enouraging step in the right direction.

However, the discrepancy between optimum control results and sub-optimum control results - which is of the order of 10-20% for the energy saving aim and about 20% for the petroleum substitution aim - suggests significant improvements can still be made to the sub-optimum strategy.

7.4.1 Optimum Region Shape

As was described in section 7.2, the optimum region shape is in its present form a simple 'box' with straight edges at 90° to each other when superimposed upon the i.c. engine fuel map.

By using a box shape, having top and bottom edges that follow the curvature of the efficiency contours - shown in Figure 7.9 - will result in high and more easily controllable i.c. engine efficiency. In addition if the top edge of the region were to folow the curve at the full throttle

limit, then maximum engine torque at any given speed would also be made available. The present straight edge running from X to Y on Figure 2.53 leaves an area of the i.c. engine performance map unavailable.

Extending the region 'effectively' below the i.c. engine minimum speed line such that if an operating point falls in this region then i.c. engine only operation with a slipping clutch or torque converter - providing that it is only done for short periods - may give improved results, as has been shown, the optimum strategy favours this course combined with a low transmission ratio despite the reduced clutch efficiency.

7.4.2 All Electic Mode Gear Shifting

From the present all-electric mode gear shifting strategy of shifting into a ratio that brings the operating point closest to the break-speed can be improved upon by the use of a region of optimum efficiency here also. Figure 2.56 shows a region bounded by simple straight edges but if possible for the i.c. engine it would equally be possible for the motor to allow the region edges to follow the efficiency contours.

The strategy would take on a similar form to the electric vehicle gear shifting strategy, introduced in chapter 2 and then implemented in the electric vehicle study of chapter 4.

The limitations of using the present all-electric mode gear shifting strategy on motor types other than the D.C. shunt, upon which the strategy is based, become clear if one considers the A.C. induction motor type discussed in chapters 4 and 6 and shown in Figure 2.20.

Because the region of high efficiency is now in a speed range significantly above the break-speed, then simply shifting ratio to move the operating point close to the break speed will result in efficiencies during motoring lower than desired. However, during regeneration, the present policy of shifting ratio to move the operating point to as high a motor speed as possible will still result in the desired high motor efficiencies.

The above consideration of different motor types is important for the hybrid-electric vehicle - particularly the petroleum substitution aim since the traction motor is used for significant 'motoring' periods as well as during regeneration, but to a much lesser extent for the energy saving aim where typically the 'motoring' use of the traction motor is less than the regeneration use.

7.4.3 Hybrid Mode Gear Shifting

In the hybrid mode with the base configuration being considered throughout chapter 6 and this chapter, because of the single transmission acting for both power sources, ratio selection will be either a compromise of the needs of the power sources or a firm bias in favour of one of the power sources.

At present there is a bias in favour of the i.c. engine power source in that the hybrid mode gear shifting strategy seeks to use the lowest ratio possible in this mode - so achieving the lowest i.c. engine speed, which, with the i.c. engine torque being set on the upper torque bound, will achieve a high i.c. engine efficiency. The traction motor on the other hand requires the operating point to be moved to a high speed to achieve high efficiency.

However, since, as has been highlighted in section 7.2 by studying the behaviour of the optimum strategy, operation on one or other of the power sources is generally favoured, the hybrid mode will be seldom encountered.

The use of the two transmission configuration, discussed in chapter 5, would enable gear shifting in the hybrid mode to be achieved with both power sources in mind, but at the expense of added complexity and cost.

7.5 Conclusions

Although future development of the sub-optimum control strategy may cover the areas discussed in section 7.4, there also remains the study of the optimum strategy as a means of hybrid vehicle control. To achieve this, as was discussed in section 7.1 and in Chapter 2, a 'predictive' method would have to be adopted (as the simulation method presented here is unrealistic from the point of view of time taken and the measured variable used - i.e., energy consumed). The pitfalls associated with such methods when applied to complex non-linear systems have also been discussed in section 7.1 and Chapter 2.

FIGURE 7.1: I.C.Engine Usage Data for the Energy Saving Aim using Sub-Optimum Control over the ECE-15

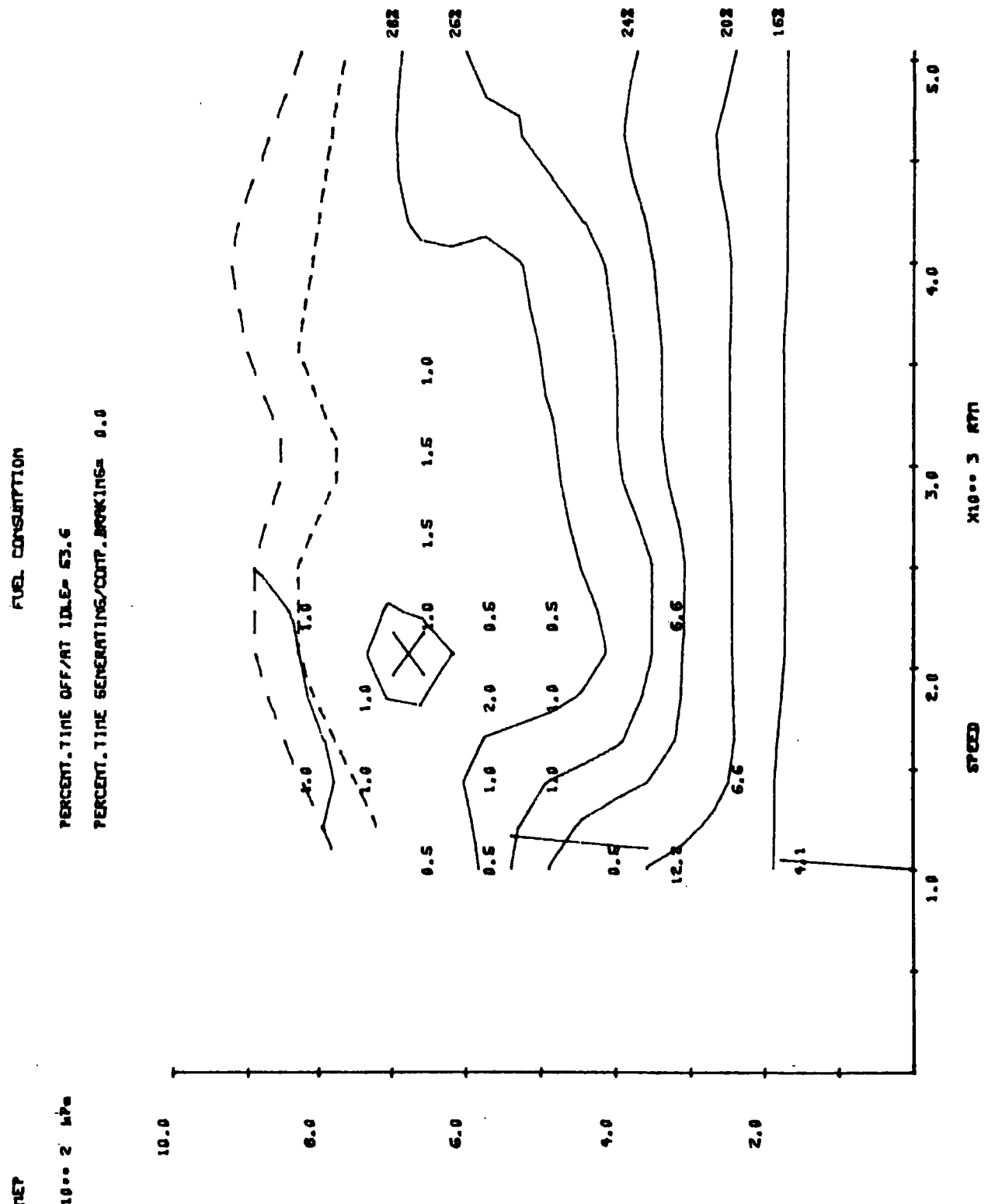

FIGURE 7.2: I.C.Engine Torque/time Profile for the Energy Saving Aim using Sub-Optimum Control over the ECE-15

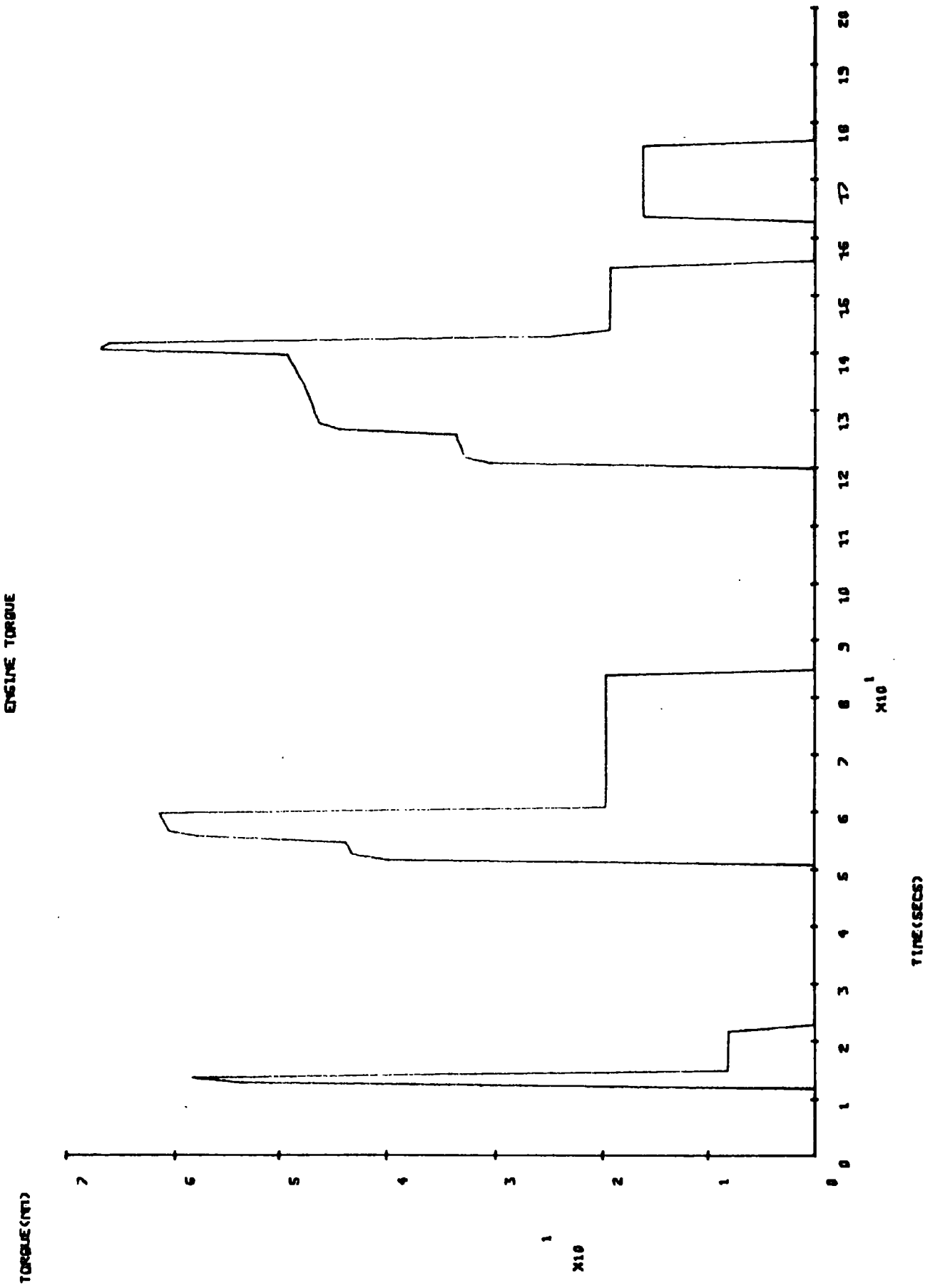

FIGURE 7.3: Transmission Ratio/Time Profile for the Energy Saving Aim Using Sub-Optimum Control over the ECE-15

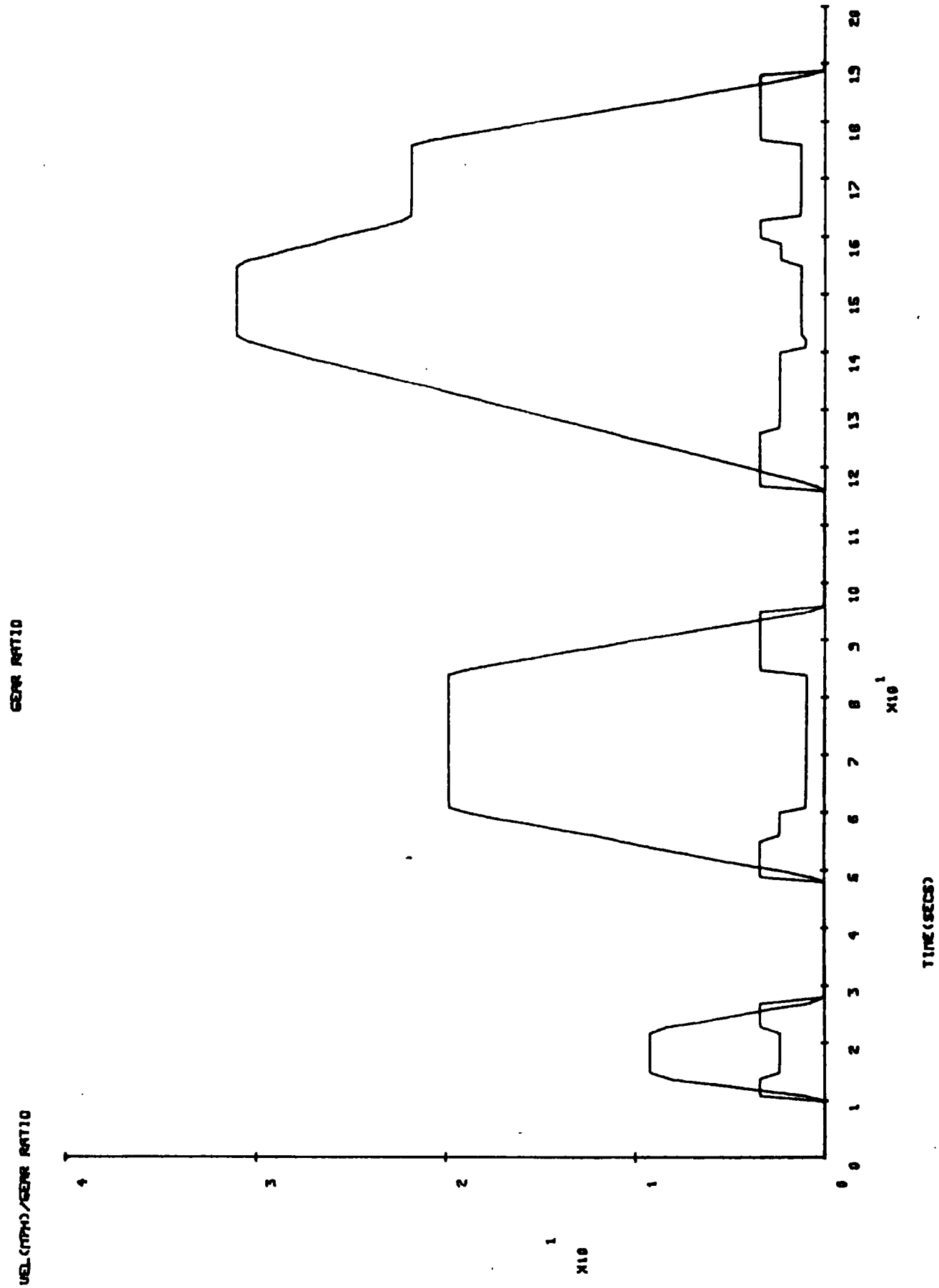

FIGURE 7.4a: Comparison of Optimum and Sub-Optimum Control Strategies for the Energy Saving Aim over the ECE-15 cycle with varying battery weight and fixed relative power source sizes

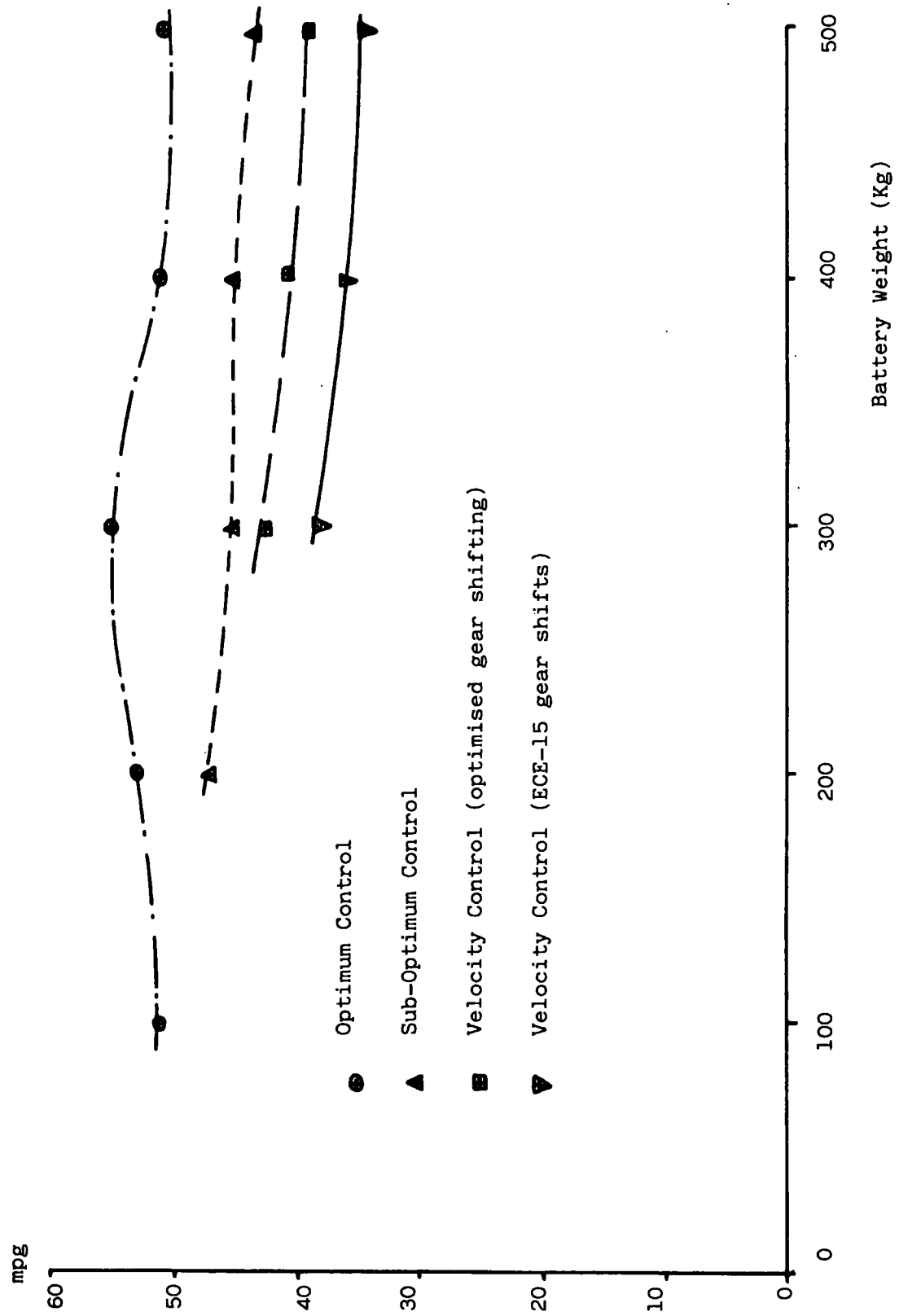

FIGURE 7.4b: As for figure 7.4a but at 56 mph and 75 mph cruises

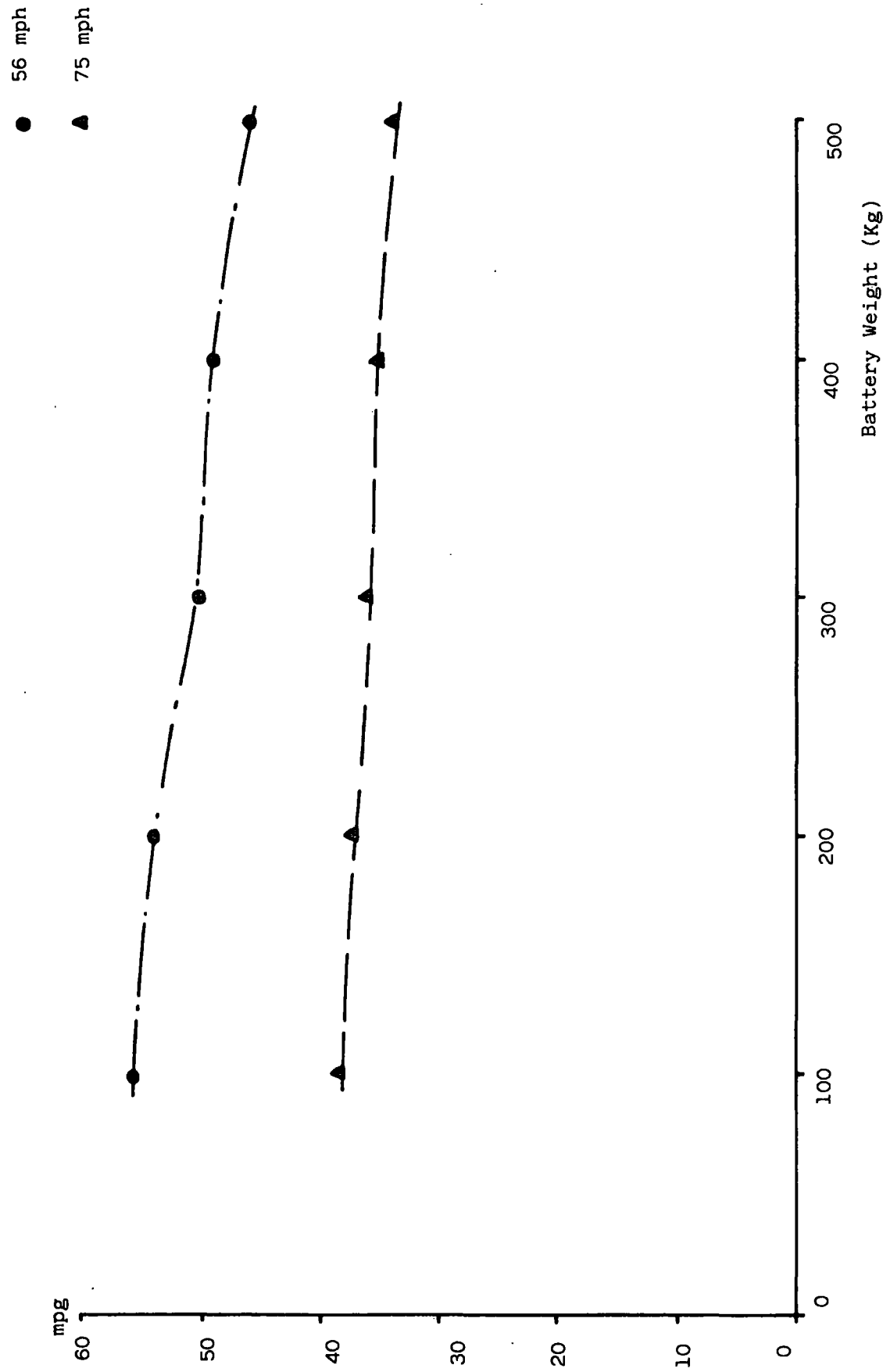

FIGURE 7.3a: Effect of battery weight on mpg/range curves for for petroelum substituion Aim using optimum control over the ECE-15 with the relative power source size fixed.

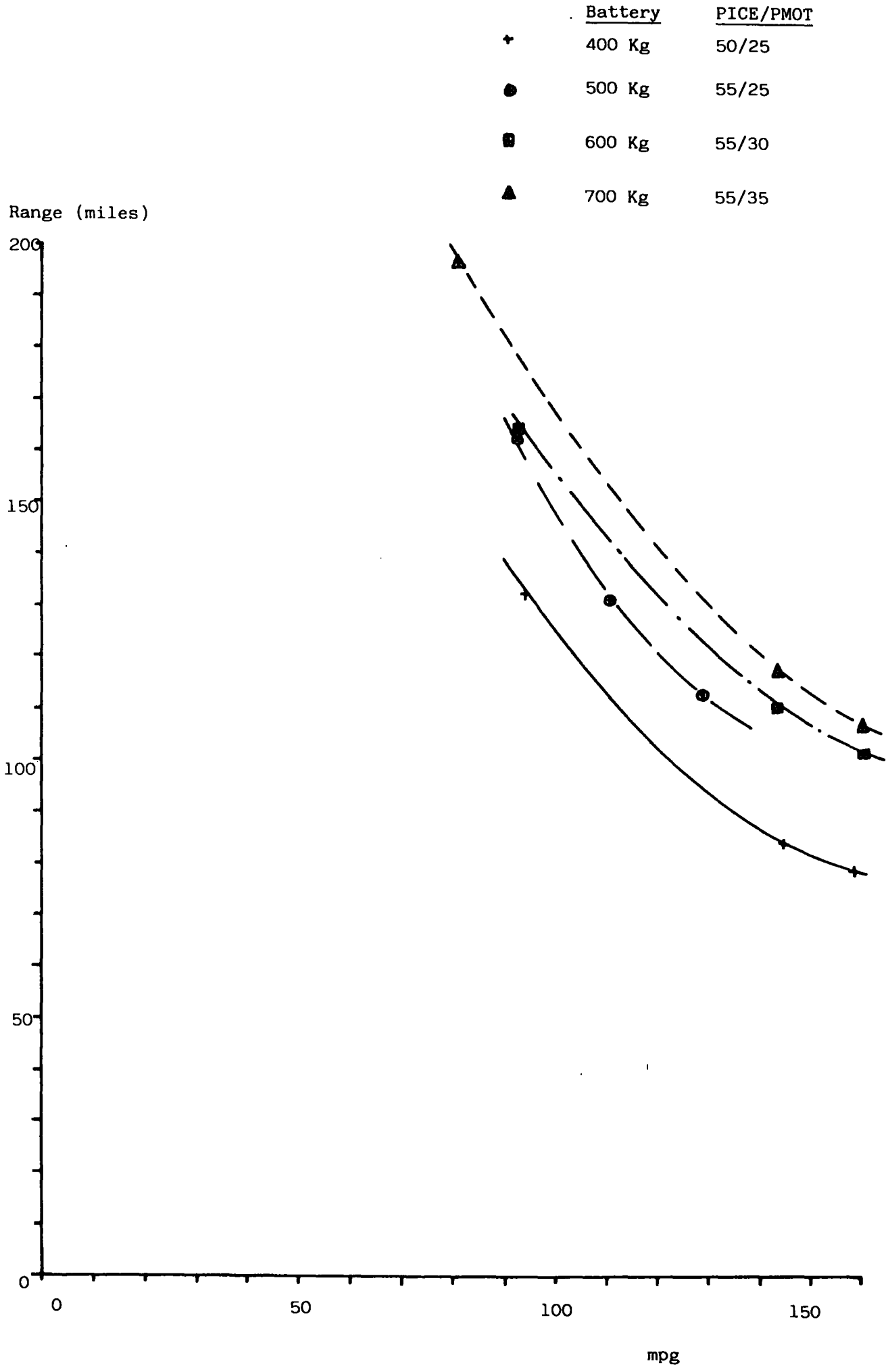

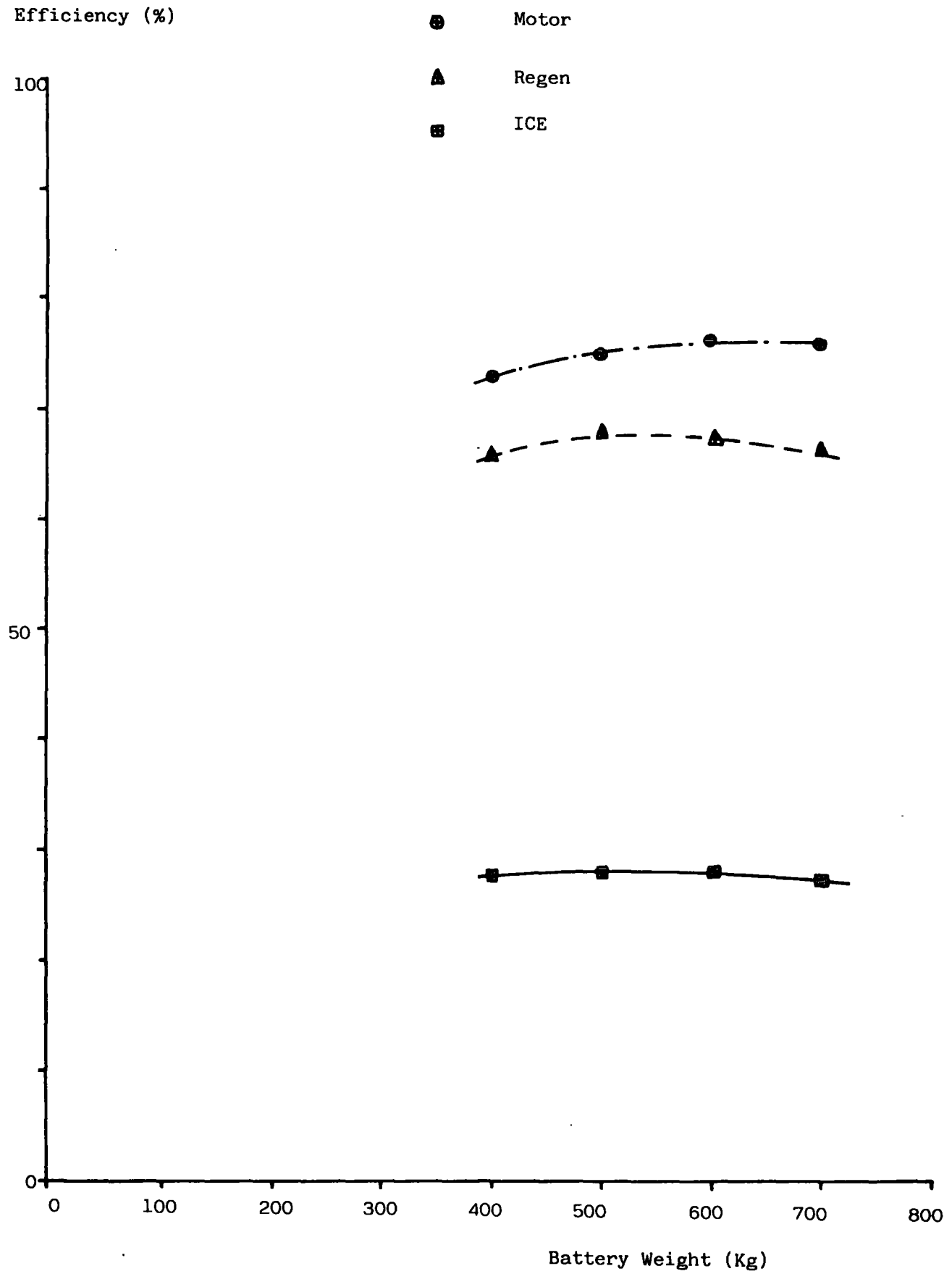

FIGURE 7.5b: As for Figure 7.5a but showing the Effect on component Efficiency

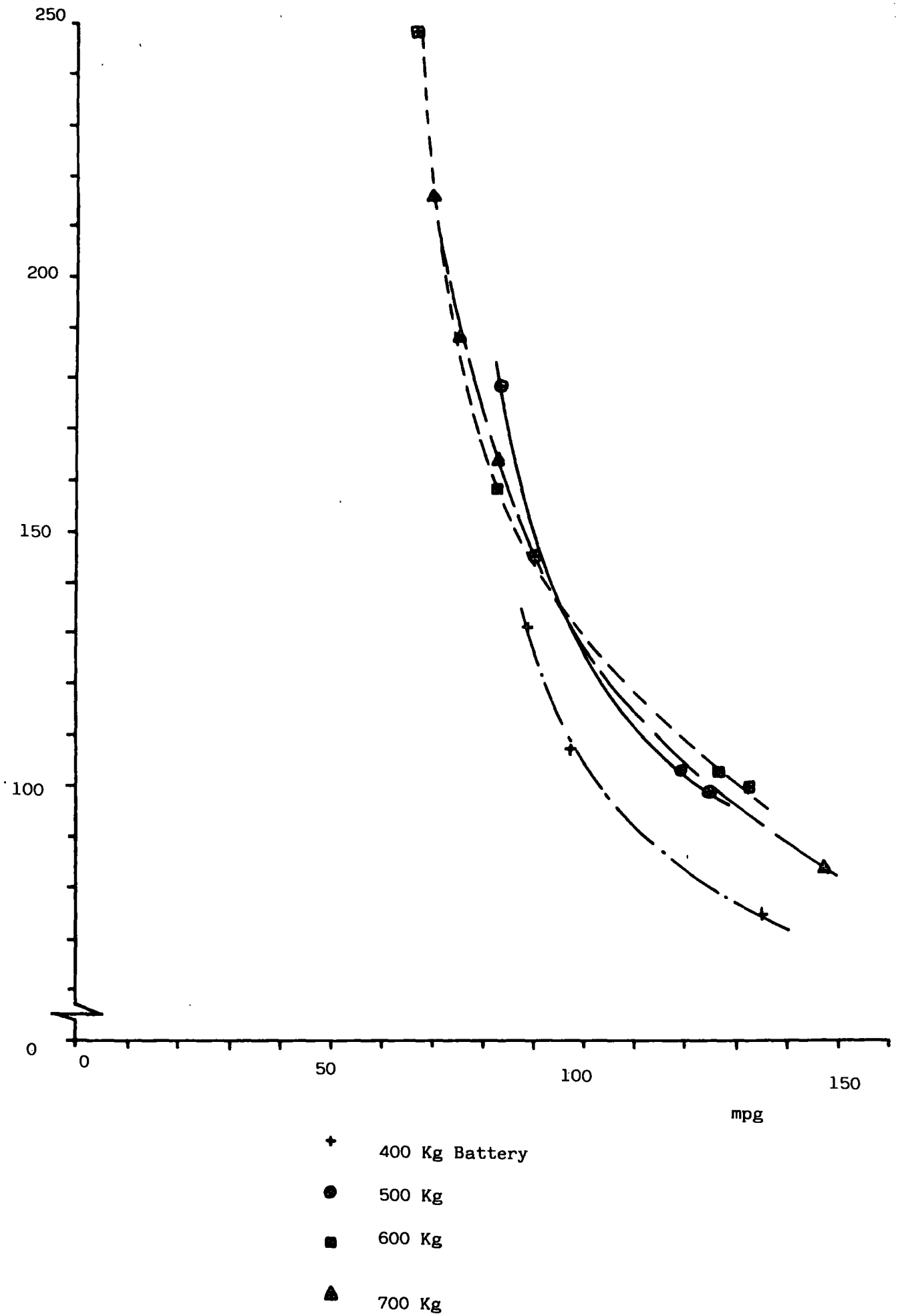

FIGURE 7.6a: As for Figure 7.5a but using sub-optimum control derived from

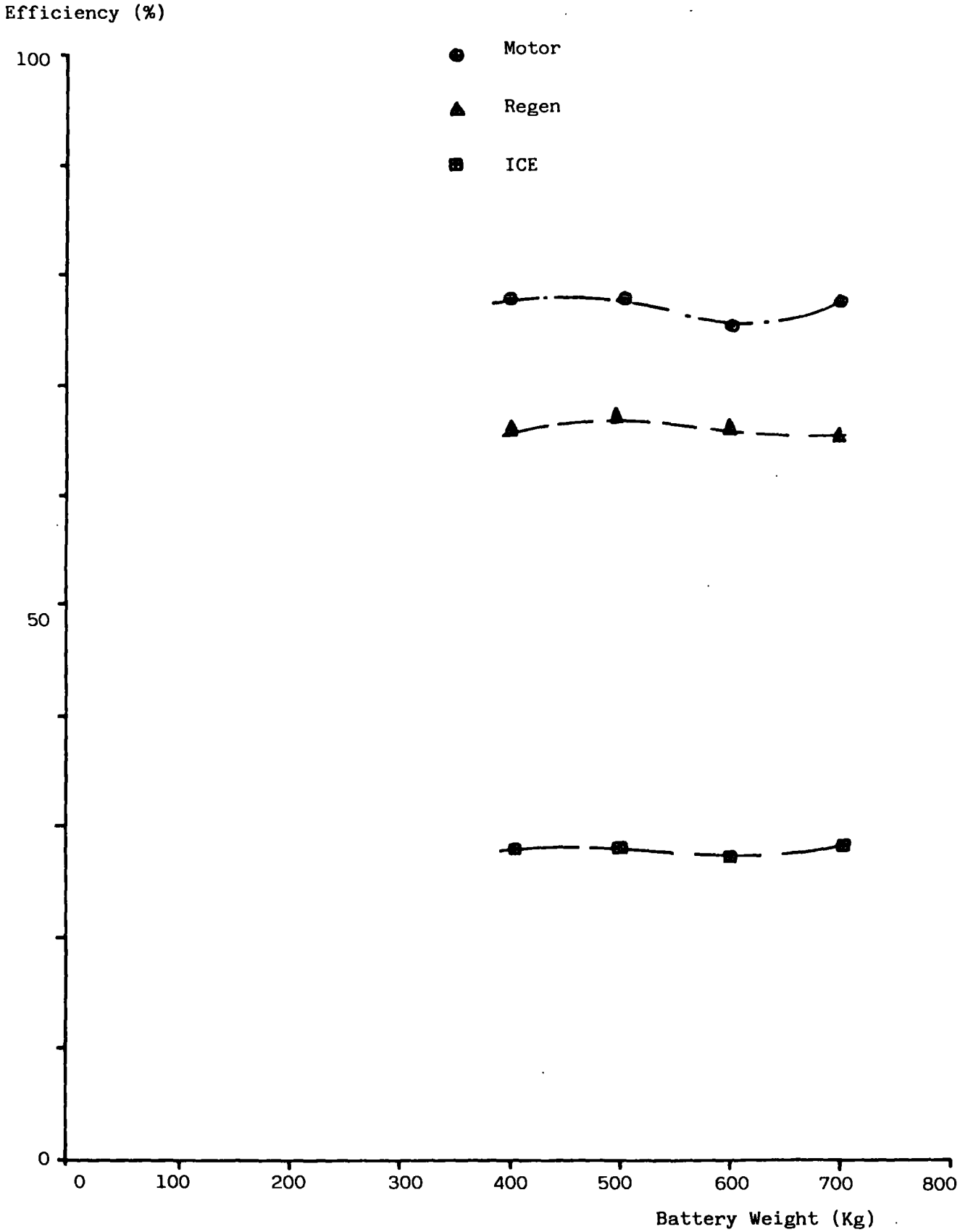

FIGURE 7.6b: As for Figure 7.5b but using sub-optimum control derived from the optimum

FIGURE 7.7a: As for Figure 7.5a but using velocity control with ECE-15 gear shifts

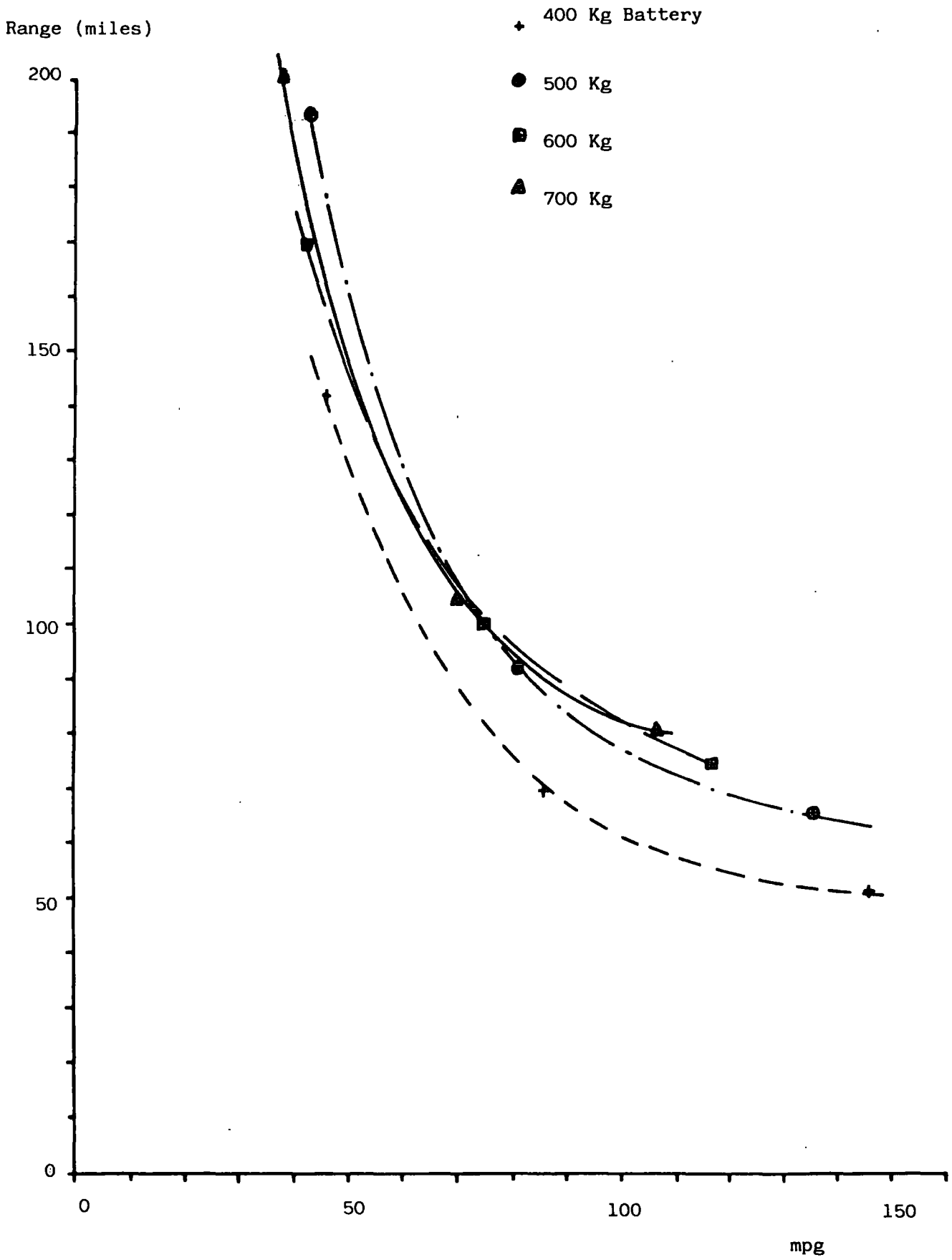

FIGURE 7.7b: As for Figure 7.5a but using velocity control and optimised ECE-15 gear shifts

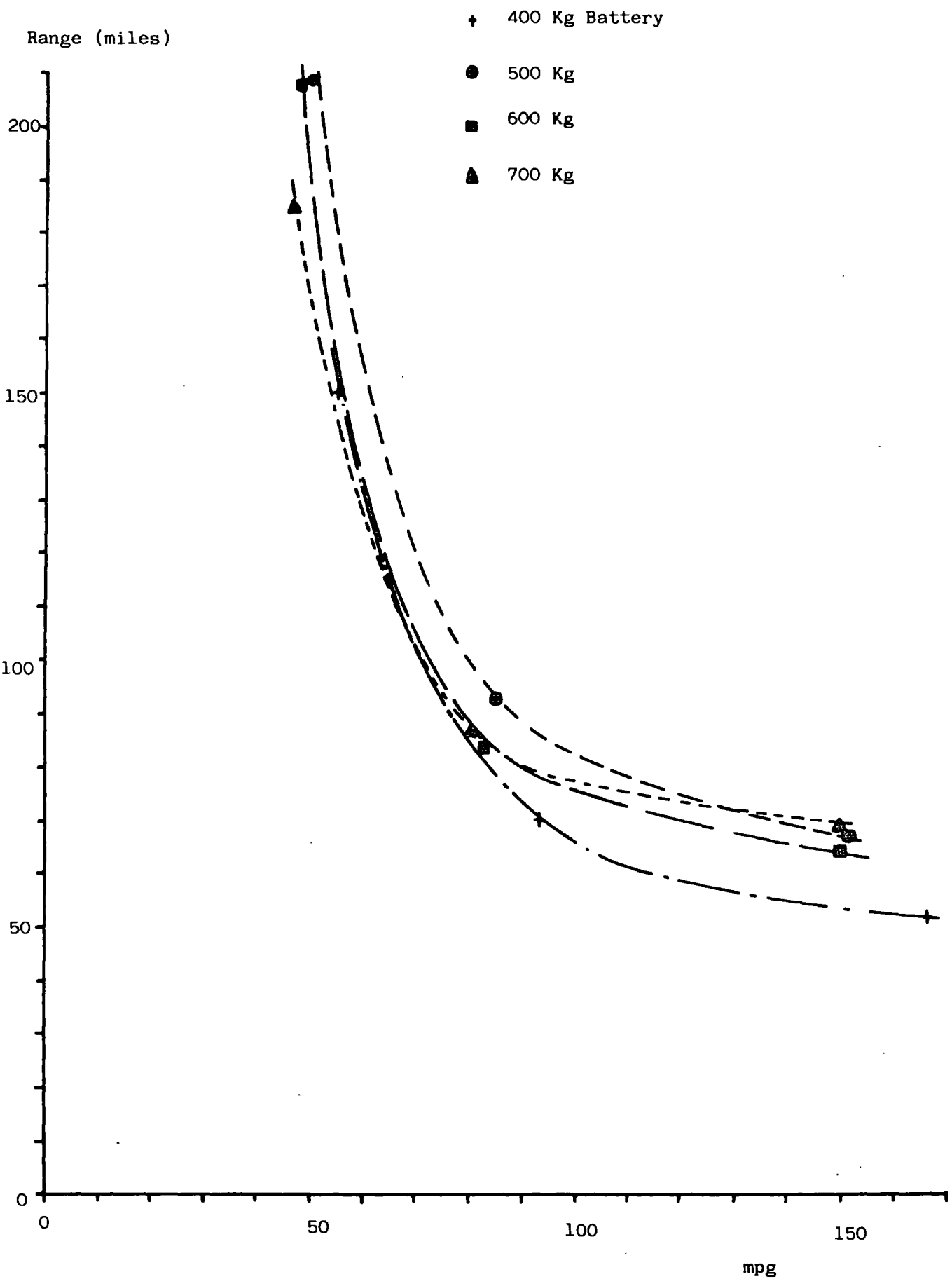

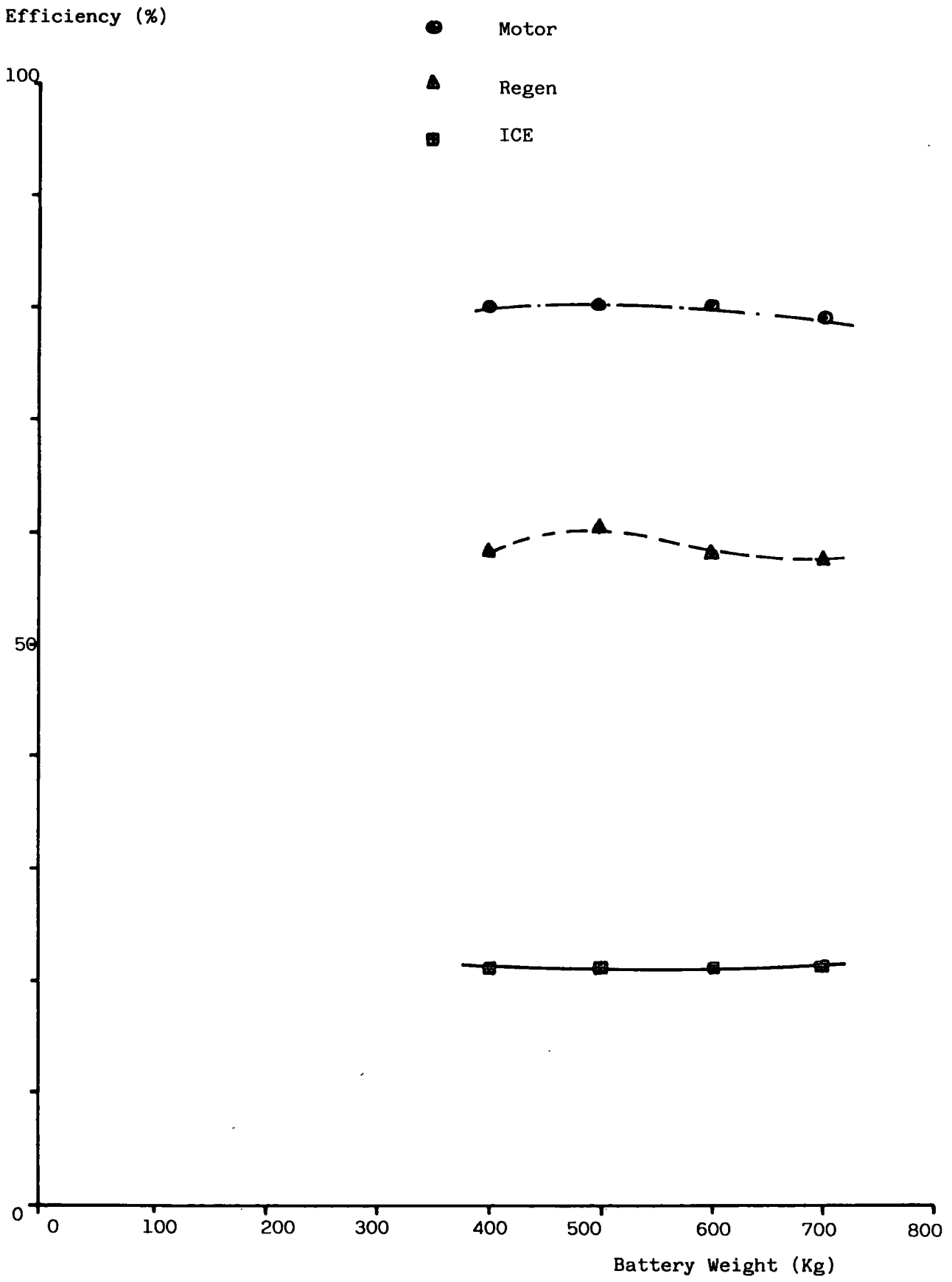

FIGURE 7.7c: As for Figure 7.5b but using velocity control

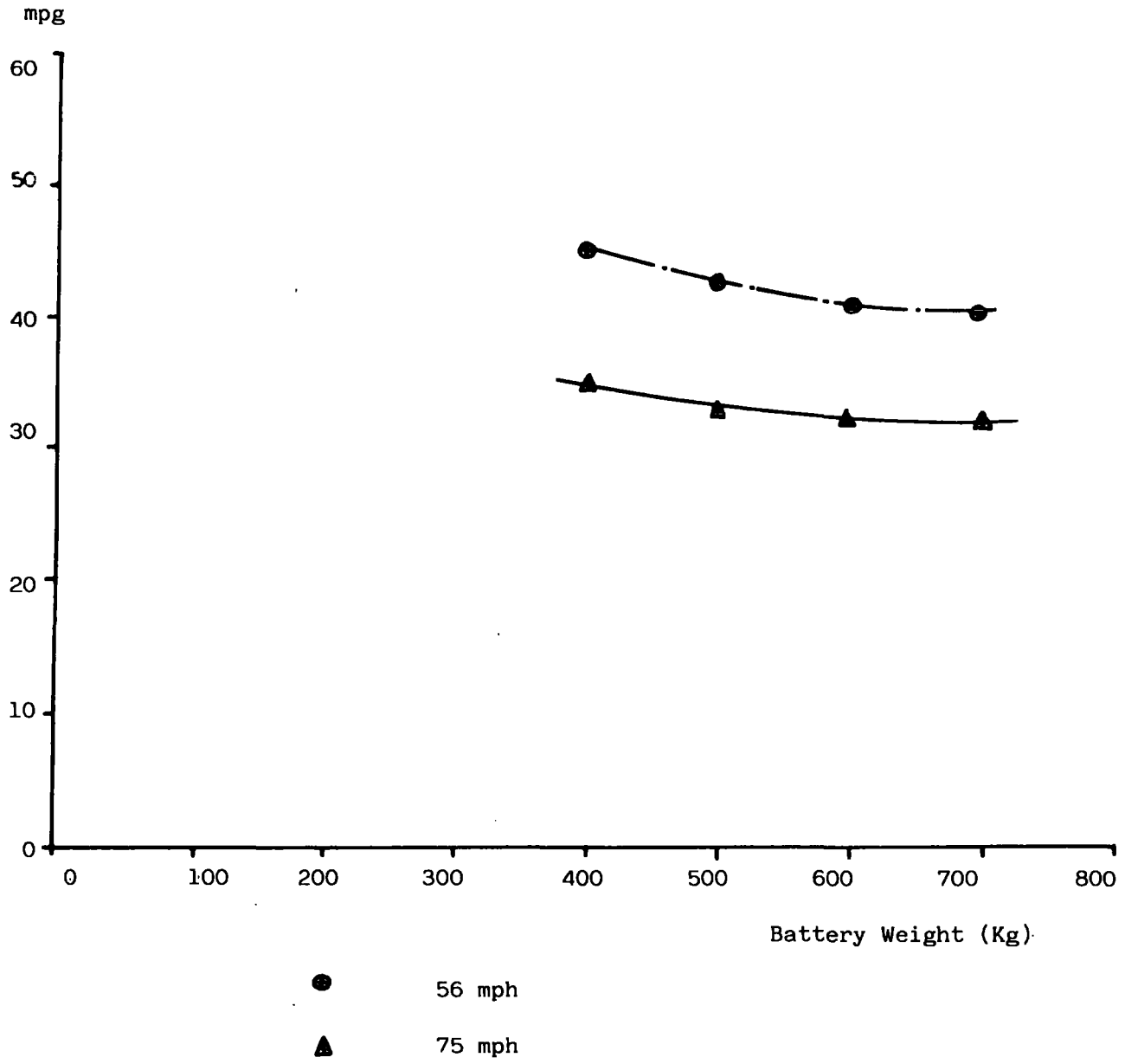

FIGURE 7.8: Effect of battery weight on 56 mph and 75 mph cruise mpg for optimum and sub-optimum control for the petroleum substitution Aim

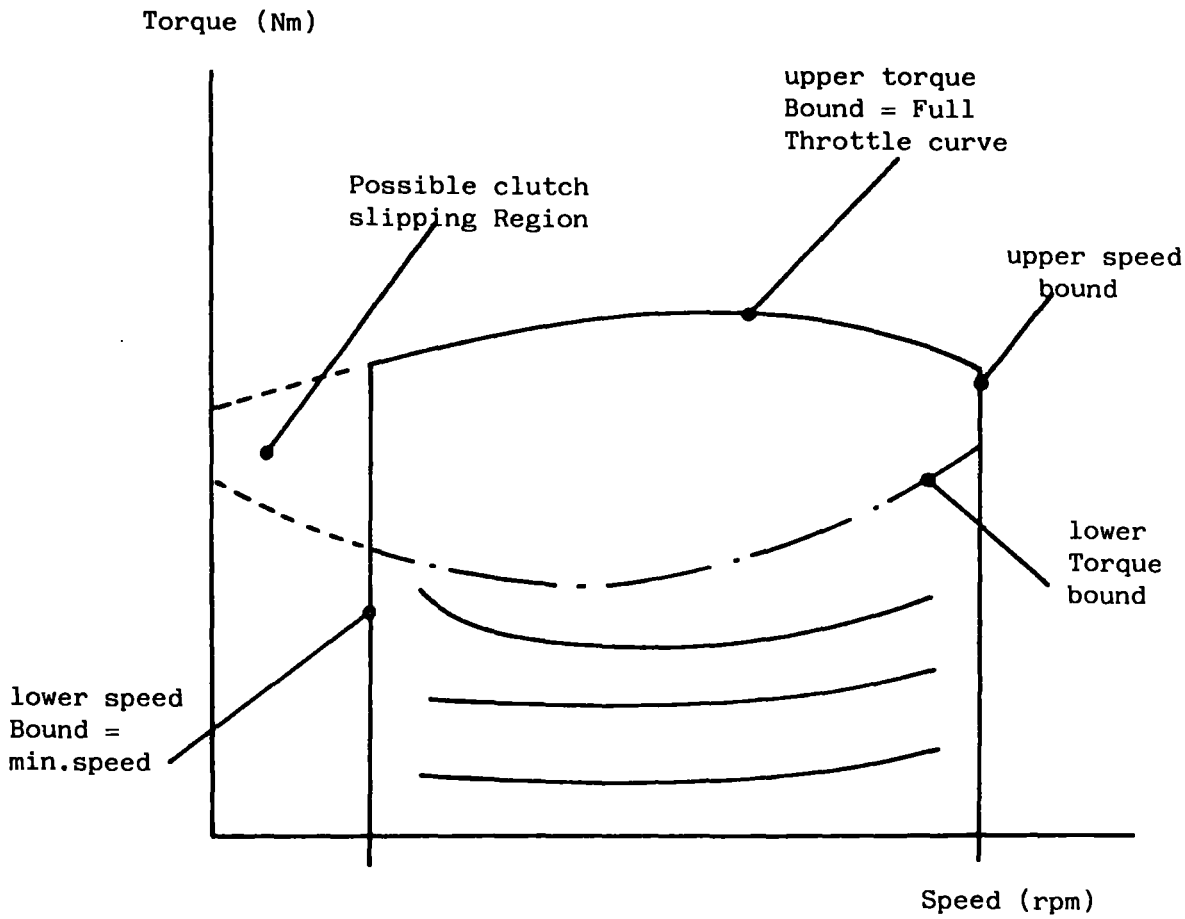

FIGURE 7.9: Improved Sub-Optimum I.C.Engine Operating Region Shape

TABLE 7.1: The Base Hybrid Configuration mpg and range Data using Sub-optimum Control

mpg	range (miles)	T_b	b
37.8	∞	0	1.0
44.9	∞	0.12	0.72
49.5	197.3	0.2	0.65
61.0	80.7	0.3	0.65
85.2	56.4	0.4	0.6
98.5	49.7	0.5	0.5
113.1	40.9	0.6	0.4
935	21.1	0.7	0.3
∞	21.1	1.0	1.0

T_b = lower torque bound

$_b$ = upper speed bound

CHAPTER 8

Comparison of Conventional I.C.Engined, Pure Electric and Hybrid Electric Drive Trains

8.1 Introduction

In chapter 5 the discussion of the hybrid-electric vehicle drive-train alternatives yielded two possible parallel configurations which, in terms of energy consumption and vehicle operating flexibility were the most attractive. Of the two alternatives, the simpler configuration was selected despite the shortfall in energy consumption.

Using this configuration, in chapter 6 a parametric study was performed in that vehicle parameters that could be sensibly varied for the hybrid were considered.

Finally, in chapter 7 the results from the parametric study were condensed to form a fixed set of vehicle parameters over a range of battery sizes in order to consider the effects of hybrid-electric vehicle control strategy, using the optimum control strategy as the basis for comparison.

In order to be a viable proposition in terms of energy consumption and/or petroleum dependence, the hybrid-electric concept must demonstrate significant improvements over the vehicles competing in the medium sized passenger car market. The hybrid must not only compete with the well established conventional i.c. engined vehicle, but also in terms of petroleum displacement, with the electric vehicle. Furthermore, as has been the case throughout chapters 5, 6 and 7, the energy saving aim must be treated separately from the petroleum substitution aim since, when the hybrid mode, the former consumes energy from only one of its on-board energy sources, whereas the latter consumes energy from both on-board energy sources.

The energy saving vehicle, in the hybrid mode shares the same energy conversion route as the conventional i.c.engined vehicle (petroleum to gasoline) and therefore can be compared in terms of mpg with this vehicle.

On the other hand, the petroleum substitution vehicle when in the hybrid mode, since it has removed energy from both on-board energy sources

at the end of a given duty cycle, has the two corresponding energy conversion routes (petroleum to gasoline and coal to battery energy). Therefore this hybrid vehicle aim must not only be compared with the i.c. engined vehicle but also the electric vehicle.

As a result, the petroleum substitution vehicle is less easy to compare with its competing vehicle types since as well as deciding upon the degree of substitutuion or displacement one must also consider the energy conversion route efficiencies, the energy source costs to the user, the energy source availability and any political pressure that may favour one source relative to the other.

For both hybrid-electric aims, when in their respective all i.c. engine and all-electric modes, comparison can be made directly with the conventional i.c. engined vehicle and the pure electric vehicle respectively as in each case only one on-board energy source is depleted.

The use of the computer simulation program in the comparison allows 'equivalent' vehicles with fundamentally differing drive-trains to be modelled and simulated by assembly in each case from the common set of base parameters described in chapters 5,6 and 7.

8.2 Vehicle Parameters

In order to get a sensible comparison between conventional i.c. engined, pure-electric and hybrid-electric vehicles, a common set of base vehicle parameters is to be used on to which the drive-train components appropriate to each vehicle type can be added.

The common base parameters are those used for the studies of chapters 5, 6 and 7 - thought to be typical of a near-term medium sized passenger car - and consist of drag and rolling resistance coefficients, frontal area, wheels radius, number of passengers, amount of payload and the basic bodyshell weight.

Using the automatic weight addition feature of the simulation program - described in chapter 2 - as drive-train components are added to the basic bodyshell weight for the three fundamentally different vehicle drive lines to be considered, the weight differences inherent will be accounted for.

Vehicle power source ratings were determined on the same basis as the hybrid-electric vehicle, which in the case of the i.c. engine vehicle was the ability to meet the acceleration requirement of 0-60 mph in 10-15 seconds and a maximum cruise speed requirement of >80 mph. However, for the pure-electric vehicle, due to the inherent power-to-weight disadvantage as a result of sizing the traction battery to return an adequate urban range to battery discharge of 40-50 miles, it was found necessary to use, instead, typial electric passenger car performance constraints of 0-30 mph in 10-15seconds and a maximum speed of 60 mph (Collie,1979)(Wilson et al,1982).

The vehicle parameters, which include the common base parameters, chosen for the equivalent i.c. engined and pure-electric vehicles to be the subject of the comparison in this chapter are shown in Tables 8.1 and 8.2 respectively, and their block diagrams in chapter 2.

In the control strategy study of chapter 7, the vehicle parameters used were condensed from the parametric study of chapter 6 but still covered a range of battery sizes and corresponding best PICE/PTOT values for both energy saving and petroleum substitution aims.

It is now possible in this chapter to use the battery sizes, indicated in the parametric study of chapter 6, as being ideal for both energy saving and petroleum substitution aims. Table 8.3 shows, along with the common base of vehicle parameters, for energy saving and petroleum substitution aims the resulting battery sizes and the corresponding power source ratings - as determined by the best PICE/PTOT value in each case.

Although the same basic component types will be used in this comparison - comprising of the gasoline i.c. engine, D.C.shunt traction

motor, the transistor chopper controller and the lead-acid traction battery - these may be varied in order to investigate the effects of various senarios that may exist in the near-term.

For the hybrid-electric vehicle, the implementable control strategy, derived and discussed in chapter 7, should be used throughout the comparison as the use of the optimum strategy would not yield a true comparison between practical vehicle types.

Again, as with the studies of chapters 5, 6 and 7, comparison between the i.c. engine, pure-electric and hybrid-electric drive trains can be made over the ECE-15 urban cycle, at a steady 56 mph cruise and also at a steady 75 mph cruise - although the latter speed is clearly not possible for the pure electric vehicle.

8.3 Energy Saving Aim

As was indicated in section 8.1, the energy saving hybrid, when in the hybrid mode, as it only uses liquid fuel energy can therefore be compared directly with the conventional i.c. engine. Furthermore, as it has been assumed that the concept of fuel-off at idle and overrun for the hybrid is possible in chapters 5, 6 and 7, then it can equally be assumed that the same concept is also possible for the conventional i.c. engined vehicle. Therefore this consideration must be included in the comparison.

The battery size chosen for the energy saving hybrid, shown in table 8.3, was 200 Kg as it was thought in the study of chapter 6 to give the best compromise between vehicle weight, stored energy for all-electric urban operation, mpg when in the hybrid mode and minimisation of battery power density demands.

In the parametric study of chapter 6, it was demonstrated how more advanced traction motor and traction battery types would affect hybrid performance in terms of energy consumption and all-electric urban range.

Since including such changes will affect the hybrid vehicle (when in its hybrid and all-electric modes) and the pure-electric vehicle but not the i.c. engined vehicle, then they should be considered here also. It was shown in Chapter 6, how an advanced i.c. engine type would affect hybrid energy consumption. This can be included for the hybrid in the study but must also be included for the conventional i.c. engine vehicle if it is assumed possible for the hybrid.

8.3.1 Discussion of Results

Table 8.4 shows in tabular form a comparison of the base hybrid configuration with the 200 Kg battery size and the conventional i.c. engined vehicle.

It is shown that as the i.c. engine control features that are necessary for the feasibility of the hybrid-electric concept are incorporated in the base i.c. engined vehicle of Table 8.1, plus the addition of such hardware features as 6-speed and continuously variable transmissions and an advanced i.c. engine map, the energy consumption is progressively reduced (mgp is increased) for both urban and cruise conditions.

The i.c. engine control features, such as fuel-off at idle and overrun or reduced idle fuel consumption, as would be expected, improve results only for the urban cycle (32% and 13% respectively) but only then if the cycle has significant vehicle idle and deceleration periods - as it has here.

Conversely the inclusion of the wide ratio 6-speed and continuously variable transmissions only significantly affect cruise results (urban results by about 5%) - up to 30% at 56 mph. Here, the i.c. engine load-factor is increased by the use of the overdrive ratios available, and hence i.c. engine efficiency also increases. High speed cruise improvements are more modest at 18% when using the 6-speed and CVT units as the lower/deeper overdrive ratios cannot be used because of the limits imposed by the i.c. engine full throttle curve.

It is seen that the significant improvements in i.c. engine efficiency due to the use of the CVT over the urban cycle, at 56 mph and at 75 mph are being offset by poorer transmission efficiency when compared to the discrete ratio units.

However there is an added benefit of the CVT in that because it is possible to make maximum i.c. engine power available for a greater proportion of a given vehicle speed range than for a discrete ratio unit, for a given acceleration rate, i.c. engine size may be reduced from 55 KW to 50 KW with the knock-on effect in terms of increased load factor and hence efficiency.

The use of the more advanced 3 cylinder i.c. engine performance map - discussed in chapter 6 - serves to improve i.c. engine efficiency and hence reduce fuel consumption for both urban and cruise conditions.

When the above developments in the i.c. engine vehicle are compared with the base energy saving hybrid over the urban cycle it is seen that any initial gain in mpg the hybrid has over the base i.c. engine vehicle is progressively erroded.

At the two cruise regimes, when comparing the base hybrid with the base i.c. engine vehicle, because of the inherently small i.c. engine used in the hybrid - which operates at relatively high load factors and hence efficiency - mpg as a result is higher for the hybrid despite its inherent weight disadvantage.

However if a 6-speed or CVT unit is included for the i.c. engined vehicle, it is seen that i.c. engine load factor and efficiency is raised sufficiently for the reverse to be true. But , if a 6-speed or CVT unit is included for the hybrid, no change in mpg is observed, since due to the inherently small power unit there is insufficient power available at the cruise speeds for the overdrive ratios available to be used.

By moving to the more advanced nickel-zinc battery type, table 8.4 shows there to be an improvement over the urban cycle only of the order of 15% due to the previously discussed improvements in electrical system efficiency (see chapter 6). Additionally, with this battery type, electric range to battery discharge is increased from 14 miles over the ECE-15 cycle using the lead-acid battery to 44 miles, so making it possible for this vehicle to run without using its i.c. engine for significant periods in urban conditions - perhaps amounting to an entire day's duty in the all electrice mode.

The effects of a more advanced traction motor type - here the A.C. induction type - are also shown in table 8.4, and due to improved component efficiency (particularly during regeneration - which is important for this aim) a gain of 20% above the base-line mpg is observed. The shortfall in motoring efficiency when using the sub-optimum strategy with the induction motor - as was discussed in chapter 7 - is clearly being offset by the improved regeneration efficiency.

Finally it is seen from Figure 8.1 how the use of the more advanced 3 cylinder i.c. engine map, used in the i.c. engine vehicle, similarly affects the energy consumption of the hybrid for both the urban and the two cruise regimes - giving gains in mpg of the order of 15% for the urban case at 5-10% for the cruise cases.

Although, as has been stressed throughout the hybrid studies, acceleration in the hybrid mode will be comparable with the conventional i.c. engined vehicle (0-60 mph in 10-15 seconds), acceleration in either the electric or the i.c. engine modes alone will be significantly reduced and will be comparable with electric passenger car performance. Table 8.5 shows the maximum speed and acceleration performance of the hybrid.

However, it must be borne in mind that for this hybrid aim the i.c. engine mode would only be used for constant speed motorway driving or as a

get-you-home measure after battery depletion in the electric mode, so would be used rarely under urban condtions. Nevertheless the inherently smaller i.c. engine for the hybrid does show a shortfall relative to the conventional i.c. engine vehicle in terms of gradeability. As table 8.5 shows, maximum speed up a 2% gradient as would be typically encountered on long distance motorway driving is reduced to 60 mph compared to over 90 mph for the conventional vehicle, shown in table 8.1. But with maximum speed limits in the UK of 70 mph this decrease in maximum vehicle speed would not appear to present any driveability problem.

Although there may be a signficiant amount of all-electric operation - particularly with an advanced battery and/or motor type - the majority of urban driving for this aim will be in the hybrid mode with the electrical system used as a load-leveller.

As the energy saving hybrid vehicle will never drive ECE-15 cycles day-in, day-out, if at all, a small amount of battery depletion will occur daily - depending upon the control strategy - so requiring a battery charge every few weeks.

8.4 Petroleum Substitution Aim

In section 8.1 it was indicated that because of the two energy conversion routes, the petroleum substitution hybrid is difficult to compare with the competing i.c. engine vehicle and electric vehicle. However, by taking a petroleum substitution result in terms of mpg and range to battery discharge such that the mpg is greater than that achieved by the equivalent i.c. engine vehicle, and the range is greater than that achieved by the equivalent electric vehicle, then substitution will be achieved.

The ideal battery size indicated by the parametric study of chapter 6 and the control strategy study of chapter 7, shown in table 8.3, was 500 Kg for the petroleum substitution aim.

As with the energy saving aim of section 8.3, although the base vehicle parameters - in terms of the gasoline engine, D.C. shunt motor, transistor chopper type motor controller and lead-acid traction battery - will be used, to study the effects of possible future developments an advanced battery type, an advanced traction motor type and an advanced i.c. engine type will also be considered.

8.4.1 Discussion of Results

Table 8.6a shows the acceleration and energy consumption performance of the petroleum substitution hybrid having the 500 Kg battery size in the all i.c. engine, all-electric and hybrid modes. The urban hybrid energy consumption in terms of mpg for a given range has been obtained from the mpg/range curve for the 500 Kg lead-acid battery - shown in Figure 8.1. The basis for selection was to give an urban range of about 60 miles to 70% battery depth at discharge with the argument that, as was shown in chapter 1, this will satisfy 95% of all journeys at a battery loading that will benefit the cyclic life.

Performance in all 3 of the modes described above is important for the petroleum substitution hybrid in that now, due to the larger battery, more significant urban all-electric ranges are possible than for the energy saving case. As was the case with the energy saving case, however, the all i.c. engine mode is important for long distance cruising, as is the hybrid mode as an alternative to running all-electric in urban areas or to be combined with the all-electric mode for urban areas.

The mpg figure of 140 to achieve an urban range of 60 miles to 70% DOD shows a significant degree of petroleum displacement when compared with the equivalent i.c. engine vehicle in table 8.4 and the electric vehicle of Figure 4.4. As the mpg/range curve of Figure 8.1 shows, the degree of petroleum displacement achieved will depend upon the urban range required to battery discharge.

Table 8.6a also shows how, by adding advanced component types such as a 6-speed transmission and the 3 cylinder i.c. engine map, petroleum displacement is affected for the given urban range. Over the urban cycle, only the 3 cylinder map gives an increase in displacement - from 140 to 150 mpg at 85 miles range - as there is insufficient power in the i.c. engine for the two overdrive ratios to be used. At cruise, the 3 cylinder map also gives a reduction in fuel consumption in the i.c. engine mode, as does the 6-speed transmission - but the latter only at 75 mph as due to the simplicity of the sub-optimum operating box (see chapter 7) a portion of the mid-speed maximum torque capability of the i.c. engine is lost, so preventing the overdrive ratios from being used.

Generally, when comparing the petroleum substitution hybrid cruise results with the conventional i.c. engine vehicle cruise results - shown in table 8.5 - it is seen that due to the inherent weight penalty of the hybrid - being roughly 100% heavier - fuel consumption even when compared to the base i.c. engine case is higher. This is so despite the inherently smaller i.c. engine for the hybrid - working to higher load factors and hence efficiency.

Another shortfall in the sub-optimum control strategy was highlighted when using an advanced traction motor - the A.C. induction type. Because maximum efficiency for this motor type falls in a significantly different load and speed range to that of the D.C. shunt motor type - upon which the sub-optimum motorng gear shifting strategy was based - no noticeable improvement is observed in terms of petroleum displacement. As was discussed in chapter 7, the regeneration gear shifting strategy for sub-optimum control does capitalise on the contour layout of the induction machine but regeneration for the substitution hybrid is not as significant as for the energy saving hybrid. This postulation is backed up if one considers another alternative traction motor type with improved efficiency

but a similar contour layout as that of the D.C. shunt motor - the D.C. switched reluctance motor described in chapter 4. Figure 8.2 shows the mpg/range characteristics of the hybrid when using the induction motor (which is coincident with that of the shunt motor) and the switched reluctance motor. Due to a contour layout that is favourable to the sub-optimum control strategy, the benefits of moving to a more advanced motor type can now be seen, which in terms of petroleum displacement over the urban cycle is an increase from 140 mpg to 180 mpg for 85 miles range.

The use of an advanced nickel-zinc battery type created an intersting effect in that using the 500 Kg battery size, all-electric range was pushed above the 85 miles to 100% DOD required for urban operation. This would enable one of two alternatives to be chosen. Firstly, with the battery size kept at 500 Kg, the said 95% of all vehicle journeys (urban) could be performed in the all-electric mode with the remainder - being journeys >60 miles - undertaken in the i.c. engine or hybrid modes. Secondly, to achieve the same urban all-electric range as with the lead-acid battery, battery size may be reduced with the knock-on effect in that total installed power may also be reduced to keep the same vehicle performance. A battery size of 200 Kg was found to give the same all-electric range of 50 miles as the 500 Kg lead-acid battery, and so total installed power could also be reduced from 80 KW to 65 KW. As was indicated by the parametric study of chapter 6 in the case of the petroleum substitution vehicle, as large a value of PICE/PTOT was favoured without impeding all-electric performance, which in this case yielded a traction motor power rating of 20 KW and an i.c engine power rating of 45 KW.

Results in terms of acceleration performance and energy consumption are shown in table 8.6b and over the ECE-15 urban cycle, a significant increase in displacement is observed in that for the given 85 miles range, mpg is increased from 140 to 165. The full mpg/range characteristic is,

again shown in Figure 8.1 along with the base-line 500 Kg lead-acid battery and the base-line wth the addition of the 3 cylinder map. An added benefit is observed for the cruise regimes shown in Table 8.6b in that because of both reduced vehicle weight and reduced i.c. engine size mpg is increased relative to the 500 Kg base-line.

Acceleration for the 3 modes is shown for the vehicle with the 500 Kg battery size in table 8.6a and for the vehicle with the 200 Kg battery size in table 8.6b. Because of the higher PICE/PTOT value than for the energy saving case, traction motor size for a given size of vehicle will be smaller and all electric performance more limited. As is shown though 0-30 mph acceleration when in the all-electric mode is still compatible with current electric vehicles - being 12 seconds for the 500 Kg vehicle and 14 seconds for the 200 Kg vehicle. Performance in the all i.c engine mode is also acceptable due to the high PICE/PTOT value with 0-30 mph times under 10 seconds and maximum speed on a 2% gradient at 89 mph for the 500 Kg vehicle, dropping to 79 mph for the 200 Kg vehicle.

It would be unrealistic to simply halt the comparison between the hybrid and the competing vehicle types at the base-line equivalent electric vehicle described in table 8.2, as a similar treatment that has been performed on the hybrid and i.c. engined vehicles can be performed here also.

The benefits of including an advanced battery type, advanced traction motor type or a variable ratio transmission (shown in Figure 4.5) have already been discussed in chapter 4, but table 8.2 shows how each of these developments in isolation will affect the equivalent electric vehicle range over two urban and two cruise regimes. Range increases are possible using the nickel-zinc battery due to the power-density/energy density characteristic compared with the lead-acid case and also due to the maximum energy density available. Similarly range increases are achieved using the induction motor by the improvements in electrical system efficiency with a knock-on effect in terms of reduced power density demands on the battery.

The use of the variable ratio transmission in the pure-electric drive line has several benefits associated with it. Firstly by the use of lower ratios in the transmission, vehicle maximum cruising speed will not be limited by the final drive ratio - as in the fixed ratio transmission case. Secondly, initial vehicle acceleration will be improved so enabling motor size to be reduced from 30 KW to 25 KW to achieve the same rate. Finally by arranging ratios and gear shifting to place the operating point at or above the break speed for maximum efficiency, motor efficiencies can be raised, and coupled with the reduction in motor size can offset the reduction in transmission efficiency - but as table 8.2 shows at cruise the gains in motor efficiency are in fact being offset by the poorer transmission efficiency.

It is seen in table 8.2 that the range improvements possible for the equivalent electric vehicle when considered in isolation will yield a maximum urban daily driving capability of 64 miles to 70% DOD. But the same electric drive-train refinements when applied to the hybrid will yield a greater mpg for a given range and vice versa - shown in Figures 8.1 and 8.2. Therefore, for the same liquid fuel consumption of 140 mpg, range to 100% DOD may be increased from 85 miles to 100 miles using a reduced size nickel-zinc battery, and to 110 miles using a switched reluctance traction motor.

As was indicated earlier, unlike the energy saving hybrid, performance in all 3 modes is important for the petroleum substitution aim because of the increased all-electric range as a result of the inherently larger traction battery necessary for substitution. As a result the vehicle may depend upon either power source for significant periods during urban operation or the i.c. engine only, all-electric and hybrid modes may be 'mixed' to achieve the desired daily range of 60 miles to 70% DOD.

Given that the i.c. engine mode is primarily intended for long distance motorway travel and is undesirable in urban areas due to noise and pollution except as a get-you-home measure after battery depletion, then there are four alternatives as to how the modes may be mixed. Firstly, there is the hybrid mode described for the base-line case so far which yields 140 mpg for a 60 mile range. Secondly, the vehicle can run all-electric to 70% DOD, which for the 500 Kg battery will be 35 miles, and the remaining 25 miles undertaken in the all i.c. engine mode at a fuel consumption rate of 30 mpg. Thirdly, the vehicle may run intermittently in the all-electric and all i.c. engine modes, but in the limit (optimum combination) this would simply amount to the hybrid mode. Finally, the vehicle could run to a prescribed DOD in the all electric mode, after which the hybrid mode would complete the journey. This latter alternative falls in between the first case where there is no all-electric mode and the second case where there is an electric mode up to battery discharge.

The energy consumptions of the first, second and fourth alternatives (the third tending to the first in the limit) are presented in table 8.7 in terms of the liquid fuel consumption in gallons necessary to complete the 60 mile range. Figure 8.3 also presents the results graphically in terms of fuel consumption in gallons versus battery DOD to which the vehicle is run in the all-electric mode, after which the hybrid mode is employed until battery discharge. It is seen that running all electric from 0% up to 30% DOD (the maximum being 70%) has no significant effect on fuel consumption - being between 0.4 and 0.45 gallons. This is due to the fact that the range demanded in the hybrid mode is relatively low and falls on a section of the mpg/range curve - shown in Figure 8.2 - where mpg falls significantly with increasing hybrid range (effectively the DOD to which the vehicle is run all electric). The result is that over the range of DOD, the increases in hybrid range are balanced by the reductions in mpg -

so the fuel consumption remains roughly constant. Above 30% DOD, however, with hybrid ranges demanded of >150 miles, as Figure 8.1 shows, mpg does not significantly reduce with increasing hybrid range and the result is that fuel consumption rises. The maximum fuel consumption occurs for the case when the vehicle is run all-electric to battery depletion (70% DOD) after which the all i.c. engine mode continues the journey.

8.5 Energy Consumption

So far in the comparison between hybrid-electric, pure-electric and conventional vehicles, energy consumption has only been considered in terms of the typical units associated with the two on-board energy sources. In the case of the liquid fuel tank, because it is easily and relatively quickly replenished and since it has no load-dependent characteristics, it is usual to regard it as infinite and hence quote energy consumption in terms of distance travelled - mpg. For the traction battery, however, because of the lower energy density when compared to liquid fuel, its load-dependent characteristics and since it is neither easily or quickly replenished, energy consumption is usually quoted in terms of a range when the source is exhausted.

Whereas for liquid fuel the rate of consumption in terms of mpg is implied, for the traction battery, the battery size needs to be considered when quoting a range in order to convert to a consumption rate per unit distance travelled.

Energy consumption per mile may be considered at the on-board energy sources - so implying the energy costs to the user if the costs per unit energy are known for the two energy sources.

Alternatively, energy consumption per mile may be considered at the point of extraction - which in the case of the wall-plug electricity may be

coal as a typical power generation fuel, and in the case of gasoline will be petroleum. This reference point for comparison is commonly referred to as the primary energy consumption.

The accuracy of calculating the on-board energy consumptions of the vehicles under consideration will depend upon the accuracy of the simulation program - which was analysed in chapter 3. However the accuracy of determining primary energy consumptions will depend upon not only the accuracy of the simulation program but also the accuracy of the conversion efficiencies of the conversion routes, petroleum to gasoline and coal to battery energy. Furthermore with the possible future senario of producing gasoline from coal a different conversion efficiency is likely (House of Lords, 1980) so adding another dimension to the study.

8.5.1 Energy Saving Aim

The energy saving hybrid in section 8.3 was compared in its hybrid mode with the i.c. engined vehicle only, as little or no battery energy would be consumed for this vehicle. As a result the units of energy consumption for both vehicles were mpg and therefore readily comparable at the fuel tank - in terms of cost to the user -, and also at the point of extraction. In the latter case, since the energy conversion routes are the same, the petroleum - gasoline or the coal - gasoline route energy consumptions will be implied.

From the results presented in table 8.4 for energy consumption at the fuel tank no significant difference in energy consumption between the energy saving hybrid and the conventional i.c engined vehicle is seen if it is assumed that the developments in latter vehicle will follow the course shown. It is implied, therefore, that there will be no significant saving in primary energy by the energy saving hybrid over the conventional vehicle.

8.5.2 Petroleum Substitution Aim

In section 8.4 it was shown how petroleum fuel could be displaced by on board stored electrical energy in the petroleum substitution hybrid - the degree of which would depend upon the range required of the vehicle as shown in Figure 8.2. However what was not considered was the impact to the user in terms of the energy taken from the traction battery and the fuel tank if the costs of these two energy sources per unit measure are known. Unlike the energy saving aim, the cost to the user will not be implied in the energy consumed at the on-board sources as they may have very different costs per unit measure associated with them. Similarly when considering the primary energy consumption of the petroleum substitution hybrid the conversion efficiencies must be considered - from petroleum to gasoline or coal to gasoline and from coal to battery energy.

Table 8.8a shows a detailed urban energy consumption breakdown of the conventional i.c. engine, pure-electric and hybrid-electric vehicles referenced both at the onboard energy sources and at the point of extraction - for the petroleum - gasoline route and coal-gasoline route. The conversion route efficiencies assumed are shown in table 8.8b along with the energy per unit measure for the liquid fuel and the battery energy - both lead-acid and nickel-zinc types.

The table shows how energy consumption is affected as the possible future developments in the 3 vehicle types are included. The developments for the i.c. engine vehicle are considered cumulatively, whereas for the electric and hybrid vehicles the developments are considered in isolation. This is because it is uncertain for the latter two cases if all improvements will come to fruition, whereas for the i.c. engined vehicle developments in all of the areas shown in the table are at such a stage that introduction in the near future is probable.

The hybrid mode is assumed when considering the hybrid vehicle as it was shown in section 8.4 for the base vehicle that a 'mix' of modes over the urban cycle did not significantly affect energy consumption in terms of liquid fuel consumption for a given battery charge.

It is seen that at the on-board energy source, the electric vehicle consumes the least amount of energy per mile with the hybrid consuming less than the i.c engine vehicle. However, this does not necessarily mean that the order in terms of running costs will be the same as the cost per unit energy of gasoline and wall-plug energy will determine this.

Energy consumption at the point of extraction is shown for both petroleum - gasoline and coal-gasoline routes and shows for the former for the i.c. engine vehicle to yield the lowest consumption per mile with the hybrid giving a lower consumption per mile than the electric vehicle. However, if gasoline were to be produced from coal, having a significantly lower conversion efficiency, then this would favour the electric vehicle. Table 8.8a shows that in this latter case, the positions have changed in that the electric and hybrid vehicles now consume roughly the same amount of energy per mile but still with the i.c. engined vehicle consuming the least amount of energy per mile.

Generally, it is seen from table 8.8a, that the battery traction motor conversion route is more efficient than the liquid fuel tank heat-engine conversion route - as characterised by i.c. engine efficiencies of the order of 25-30% maximum and motor/controller/battery efficiencies of the order of 75-85% maximum and shown in the on-board energy consumptions per mile of the pure-electric and conventional i.c. engine vehicles. This picture is reversed when considering the petroleum-gasoline and coal-battery energy conversion routes - having efficiencies of the order of 90% and 24% respectively - and is shown in the primary energy consumptions per mile of the two vehicles. Furthermore by producing

gasoline from coal with an estimated conversion efficiency of 60%, the primary energy consumption of the i.c. engine vehicle correspondingly increases.

The degree of substitution chosen for the hybrid, shown in table 8.8a shows the energy consumption at the on-board energy source per mile to be between that of the i.c. engined vehicle and the electric vehicle. It may be assumed, given a hybrid with identical road load energy demands and drive-train efficiencies as the other two vehicles, that whatever the degree of substitution the energy consumption at the on-board energy source would never be greater than the i.c. engined vehicle and never less than the electric vehicle. However, the hybrid has neither the same road-load energy demands (being inherently heavier) nor identical drive-train efficiency characteristics with load and speed than both i.c. engine and electric vehicles, and as table 8.8a also shows when the degree of substitution is altered with an i.c. engine power source bias the energy consumed is greater than the i.c. engined vehicle, whereas with a traction motor power source bias the energy consumed is greater than the electric vehicle.

When looking at the primary energy consumption of the hybrid for the 3 different degrees of substitution it is seen from table 8.8a that for the petroleum-gasoline route the lowest energy consumption is achieved when a bias is put on the i.c. engine - showing that the inherently smaller i.c. engine, running at high load factors is raising energy conversion route efficiency above that of the electric drive-train. However, when the coal to gasoline production route senario is considered, the hybrid with an i.c. engine bias is penalised more than that of the hybrid with a traction motor bias with the result that primary energy consumptions are now roughly the same.

8.6 Conclusions

In this chapter, the hybrid-electric vehicle has been compared in terms of vehicle acceleration and maximum speed performance and in terms of energy consumption with the competing conventional i.c. engine vehicle and the electric vehicle.

The study has considered the energy saving aim and the petroleum substitutuion aim separately but has included in each case several technological senarios that may exist over the near-term time scale necessary for hybrid introduction. Senarios such as advanced component types and the possibility of producing gasoline from a source other than petroleum have been considered for hybrid, pure-electric and conventional i.c. engined vehicles alike, where applicable.

When considering the hybrid electric vehicle in the energy saving role it has been assumed that to fully utilize the traction battery the vehicle must be capable of a significant all-electric range. With this in mind, it has been shown that, when compared with the advanced i.c. engined vehicle, a hybrid electric vehicle in this form will be unlikely to save energy.

For the petroleum substitution case in terms of energy consumption both at the on-board sources and at the point of extraction it was also shown that, given the technological advances, it would be unlikely to demonstrate any significant savings in energy consumption over both the conventional i.c. engine vehicle and the electric vehicle. The degree of substitution in favour of the i.c. engine power source (i.e., a reduction in substitition) was shown to yield the lowest primary energy consumption for the petroleum to gasoline route but the highest on-board energy consumption because of the efficiencies associated with the two conversion routes up to the on-board and primary frames of reference. However, when the senario of producing gasoline from coal was considered it was shown

that the change in conversion efficiency for the i.c. engine power source back to the point of extraction may now favour a degree of substitution with emphasis on the traction motor (increasing substitution).

The conclusion reached here that the petroleum substitution hybrid will be unlikely to save energy compared to the conventional i.c. engined and electric vehicles is in agreement by a study into hybrid vehicles performed by International Research and Development (IRD,1982).

In this study, however, what has not been considered so far when studying the on-board energy consumption of the petroleum substitution hybrid, that will influence degree of substitution, is the cost to the user of the energy consumed. This aspect has been purposely avoided so far since the costs of the two on-board energy sources per unit measure will depend upon such factors as the production efficiency (conversion route efficiency), the availability of the primary energy source and any political pressure that may be brought to bear to favour one source compared with the other, which may take the form of pollution and/or noise regulations.

At present, the costs to the potential user of gasoline, derived from petroleum, and battery energy, derived mainly from coal, are known per unit measure and current electric vehicle users enjoy significantly reduced energy costs per mile than i.c. engine vehicle users, so offsetting the higher capital costs of these vehicles.

In the future, however, due to dwindling petroleum reserves and/or the need to produce gasoline from other sources such as coal with reduced efficiency, gasoline costs it seems likely will increase per unit measure. As a result the electric drive-train would be favoured under these circumstances and the petroleum substitution hybrid would have a bias towards the traction motor power source (increased substitution). Similarly, if in the future political pressure and/or the use of a more expensive energy source to produce wall-plug electricity meant that battery

energy costs to the user were increased relative to gasoline costs, then the i.c. engine drive-train would be favoured and substitution would decrease.

Finally, therefore, as neither the energy saving nor petroleum substituion hybrid-electric vehicles will save either on-board or primary energy, then the only advantage foreseeable lies in the ability to displace a more costly and/or dwindling energy source by a cheaper and/or more abundant one. Because of the inherently larger traction battery present in the petroleum substitution vehicle compared with the energy saving vehicle, the latter is more able to achieve significant displacement of gasoline using battery energy and therefore will be the more technically viable of the two over the timescale being considered.

Table 8.1 Vehicle Parameters for an Equivalent Medium Sized Passenger car with a conventional i.c. engined drive-train

Drag Coefficient - 0.35

Frontal Area (m^2) - 1.95

Coefficient of Rolling Resistance - 0.010

Bodyshell Weight - 700 Kg

No. of passengers - 2 (70 Kg each)

Payload - 100 Kg

Wheel Radius (m) - 0.28

Wheel Inertia (Kg) - 20

Final Drive ratio - 3.5:1 (chain)

Transmission ratios

4 speed	6 speed	CVT (Perbury)
3.5:1	3.5:1	5.0:1
2.4:1	2.4:1	
1.3:1	1.3:1	
1.0:1	1.0:1	
	0.8:1	
	0.6:1	0.5:1

I.C. Engine rating - 55 KW at 5500 rpm
(50 KW at 5000 rpm for CVT)

Idle consumption - 0.15 gm/s (50-55 Kw)

Reduced Idle consumption - 0.075 gm/s

Performance

0.60mph in 13 sec for discrete ratio unit

0.60mph in 12.5 sec for CVT with 50 Kw ICE

Maximum speed > 90 mph

TABLE 8.2 Vehicle Parameters for an Equivalent Medium Sized Passenger Car with a Pure-Electric Drive-Train.

Drag Coefficient	0.35
Frontal Area (m^2)	1.95
Coefficient of Rolling Resistance	0.010
Bodyshell weight	700 Kg
No. of Passengers	2 (70 Kg each)
Payload	100 Kg
Wheel Radius (m)	0.28
Wheel Inertia	30 Kg
Final Drive Ratio	5.4:1 (chain)
DC Shunt Motor Rating	30 KW at 5000 rpm
Motor Voltage	100
Battery - Lead Acid	42 Whr/Kg
Battery Size	500 Kg

Performance

0.30 mph in 10.5 seconds
Maximum Speed - 60 mph

	ECE-15	J227aD	30 mph	56 mph
i) Base Configuration	44.9	48.4	131.3	62.2
i) + Ni/Zn Battery	97.9	129.5	230.6	148.9
i) + 4 speed transmission & 25 KW Motor	64.6	47.5	126.4	59.3
i) i) + Induction Motor	73.9	53.3	145.9	66.4

TABLE 8.3: Vehicle Parameters for the base Parallel Hybrid Electric Drive-train

Cd = 0.35
CR = 0.01
FA = 1.95m^2

Bodyshell wt = 700 Kg

No. of Passengers = 2 (70 Kg each)

Payload = 100 Kg

Wheel radius = 0.28m
Wheel inertia = 35Kg

Final Drive ratio = 3.5:1
Final Drive Type = chain

Transmission:

4 speed	6 speed	CVT
3.5:1	3.5:1	5.0:1
2.4:1	2.4:1	
1.3:1	1.3:1	
1.0:1	1.0:1	
	0.8:1	
	0.6:1	0.5:1

Electric machine drive ratio = 1.0:1 (chain)

A. Energy Saving Aim

i.c. engine size = 35 Kw at 5000 rpm
Idle consumption = 0.1 gm/s
Inertia = 0.1 Kgm^2

Traction motor = 30 KW at 5000 rpm
voltage = 100 volts

Motor controller type - transistor chopper

Battery Type - lead acid or nickel zinc

Battery size - 200 Kg

FIGURE 8.3 continued....

B. Petroleum substitution Aim

i.c. engine size = 55 KW at 5000 rpm

Idle consumption = 0.1 gm/s

Inertia = 0.1 Kg m^2

Traction motor = 25 KW at 5000 rpm

voltage = 100 volts

Motor Controller type = transistor chopper

Battery type = lead-acid or nickel zinc

Battery size = 500 Kg

TABLE 8.4: mpg and component efficiency comparison between the Energy saving Hybrid and the i.c. engined vehicle

Conventional I.C. Engined Vehicle

	ECE-15			56 mph			75 mph		
	mpg	ICE	LF	mpg	ICE	LF	mpg	ICE	LF
i) Base config	32	12	0.17	47	21	0.28	36	25	0.44
ii) i) + opt. shifts	36	13	0.23	47	21	0.28	36	25	0.44
iii) ii) + 6 speed	37	13	0.25	62	26	0.46	45	30	0.73
iv) ii) + CVT	37	15	0.28	64	30	0.75	43	31	0.85
v) iv) + reduced idle consumption	42	17	0.28	64	30	0.75	43	31	0.85
vi) iv) + fuel shut off	49	20	0.28	64	30	0.75	43	31	0.85
vii) vi) +reduced ICE size	53	21	0.3	63	29	0.8	44	31	0.88
viii) vii)+ 3 cylinder map	60	24	0.37	64	29	0.8	46	32	0.9

Energy Saving Parallel Hybrid

	ECE-15			56 mph			75 mph		
	mpg	ICE	LF	mpg	ICE	LF	mpg	ICE	LF
i) Base config	47	23	0.27	54	27	0.56	37	28	0.84
ii) i)+ 6 speed	47	23	0.38	54	27	0.56	37	28	0.84
iii) i) + Ni/Zn	53	24	0.43	54	27	0.56	37	28	0.84
iv) i)+ Induction motor	55	24	0.45	54	27	0.56	37	28	0.84
v) i) + 3 cylinder map	53	26	0.39	56	29	0.58	40	30	0.85

LF = load factor = load torque as a fraction of maximum torque

Table 8.5: Acceleration and Maximum Speed Performance of the Energy Saving Hybrid in modes

	Hybrid	All Electric	All ICE
Maximum speed	80mph	70mph	80mph
0-30 mph (sec)	NA	9	10.5
0-60 mph(sec)	14	NA	40
2% gradient	NA	NA	60 mph

Table 8.6a: Acceleration, maximum speed and energy consumption performance for the Petroleum Substitution Hybrid in modes with a 500 Kg Battery

Performance

	Hybrid	All Electric	All ICE
Max speed (mph)	90	70	90
0-30mph (sec)	NA	12	7.5
0-60mph (sec)	14	NA	27.3
2% grad.(mph)	NA	NA	89
Energy Cons.(4 speed)			
ECE-15	140	49	30
30 mph	NA	108	NA
56 mph	NA	52	42
75 mph	NA	NA	33
Energy Cons.(6 speed)			
ECE-15	140	49	30
30 mph	NA	108	NA
56 mph	NA	52	42
75 mph	NA	NA	37
Energy Cons.(3 cyl)			
ECE-15	150	49	33
30 mph	NA	108	NA
56 mph	NA	52	44
75 mph	NA	NA	34

NB:

All Electric ranges in miles
All ICE fuel consumption in mpg
Hybrid Urban mpg to give 85 miles range to 100% DOD

Table 8.6b As for figure 8.6a but for an advanced Battery - reduced to 200 Kg

Hybrid with a 200 Kg Ni/Zn battery

Performance

	Hybrid	All Electric	All ICE
max speed (mph)	90	70	90
0-30 mph (sec)	NA	13.8	8.3
0-60 mph (sec)	14	NA	31.3
2% grad. (mph)	NA	NA	79
Energy Cons (4 speed)			
ECE-15	165	52	37
30 mph	NA	93	NA
56 mph	NA	48	49
75 mph	NA	NA	37

NB: All Electric ranges in miles

All I.C. Engine fuel consumption in mpg

Hybrid Mode mpg to give 85 miles urban range to 100% DOD

Table 8.7 The Effects of a Mix of Control Modes for 60 mile urban range to 70% DOD - 500Kg Battery

i) Hybrid operation - 140 mpg 60 miles range - 0.43 gals

ii) All Elec to 35 miles (70% DOD) - 25 miles all ICE at 30 mpg urban - 0.833 gals.

iii) Intermittent all electric and all ICE operation - which in the limit ammounts to (i)

iv) Run all elec. to a certain DOD (0-70%) then hybrid operation

a) 10% - 5 miles all elec, 55 hybrid for remaining 60% charge. (91 miles at 130 mpg)-0.42 gals

b) 20% - 10 miles all elec., 50 hybrid for 50% charge (110 miles at 110 mpg) - 0.45 gals

c) 30% - 15 miles all elec, 45 hybrid for 40% charge (110 miles at 110 mpg) - 0.40 gals.

d) 40% - 20 miles all elec., 40 hybrid on 30% charge (133 miles at 95 mpg) - 0.43 gals.

e) 50% - 25 miles all elec, 35 hybrid on 20% charge (175 miles at 75 mpg) - 0.47 gals.

f) 60% - 30 Miles all elec, 30 hybrid on 10% charge (300 miles at 60 mpg) - 0.50 gals.

8.8a Comparison between the conventional i.c. engined, pure electric and petroleum substitution hybrid-electric drivetrains in terms of energy consumption over the ECE-15

Conventional ICE vehicle

		mpg	range (miles)	----Kwh/mile ----- Energy to user	Primary A	Primary B
i)	Base Config	32		1.283	1.426	2.138
ii)	i) + opt shifts	36		1.148	1.275	1.913
iii)	ii) + 6 speed	37		1.109	1.232	1.848
iv)	ii) + CVT	37		1.112	1.235	1.853
v)	iv) + reduced idle cons.	42		0.974	1.082	1.623
vi)	iv) + fuel cut off	49		0.833	0.926	1.388
vii)	vi) + reduced ICE size	53		0.785	0.872	1.308
viii)	vi) + 3 cylinder map	60		0.683	0.757	1.138

Electric Vehicle

i)	Base config.		44	0.468	1.950	1.950
ii)	Base+Ni/Zn		97	0.363	1.513	1.513
iii)	i)+transmission		64	0.325	1.354	1.354
iv)	i) +Induction motor		73	0.284	1.18	1.18

Petroleum Substitution Hybrid

i)	Base Config.	140	85	0.286+ 0.198	0.32+ 0.825	0.477+ 0.825
ii)	i)+Ni/Zn	range	>85 miles all electric			
iii)	i) + 200Kg Ni/Zn	165	85	0.252 +0.198	0.28 +0.825	0.42+ 0.825
iv)	i) + 3 cylinder	150	85	0.277 +0.198	0.308 +0.825	0.462+ 0.825
v)	i) +SR motor	180	85	0.230 +0.198	0.256 +0.825	0.383+ 0.825

Altered Substitution

vi)	liquid fuel bias	170	70	0.244+ 0.3	0.271+ 1.25	0.407+ 1.25
vii)	Wall plug bias	70	200	0.594+ 0.105	0.66+ 0.438	0.99+ 0.438

A = Gasoline from petroleum
B = Gasoline from coal
All Hybrid Energy consumptions quoted as "liquid fuel + wall plug"

8.8b Conversion Efficiencies and Conversion Factors used in the Comparison of Figure 8.8a.

	Petroleum-Gasoline	Coal - Gasoline	Coal - Battery Energy
Refining	90%	60%	NA
Generation	NA	NA	30%
Transmission	NA	NA	90%
Charging	NA	NA	90%
Total	90%	60%	24%

Conversion factors assumed for the on-board Energy sources in terms of energy stored per unit mass.

Gasoline - 44 MJ/Kg (=12222 whr/Kg)

Lead Acid Cell - 42 Whr/Kg

Nickel Zinc Cell - 70 Whr/Kg

FIGURE 8.1: Petroleum Substitution mpg/range curves using sub-optimum control showing the Effects of Technological Senarios over the ECE-15

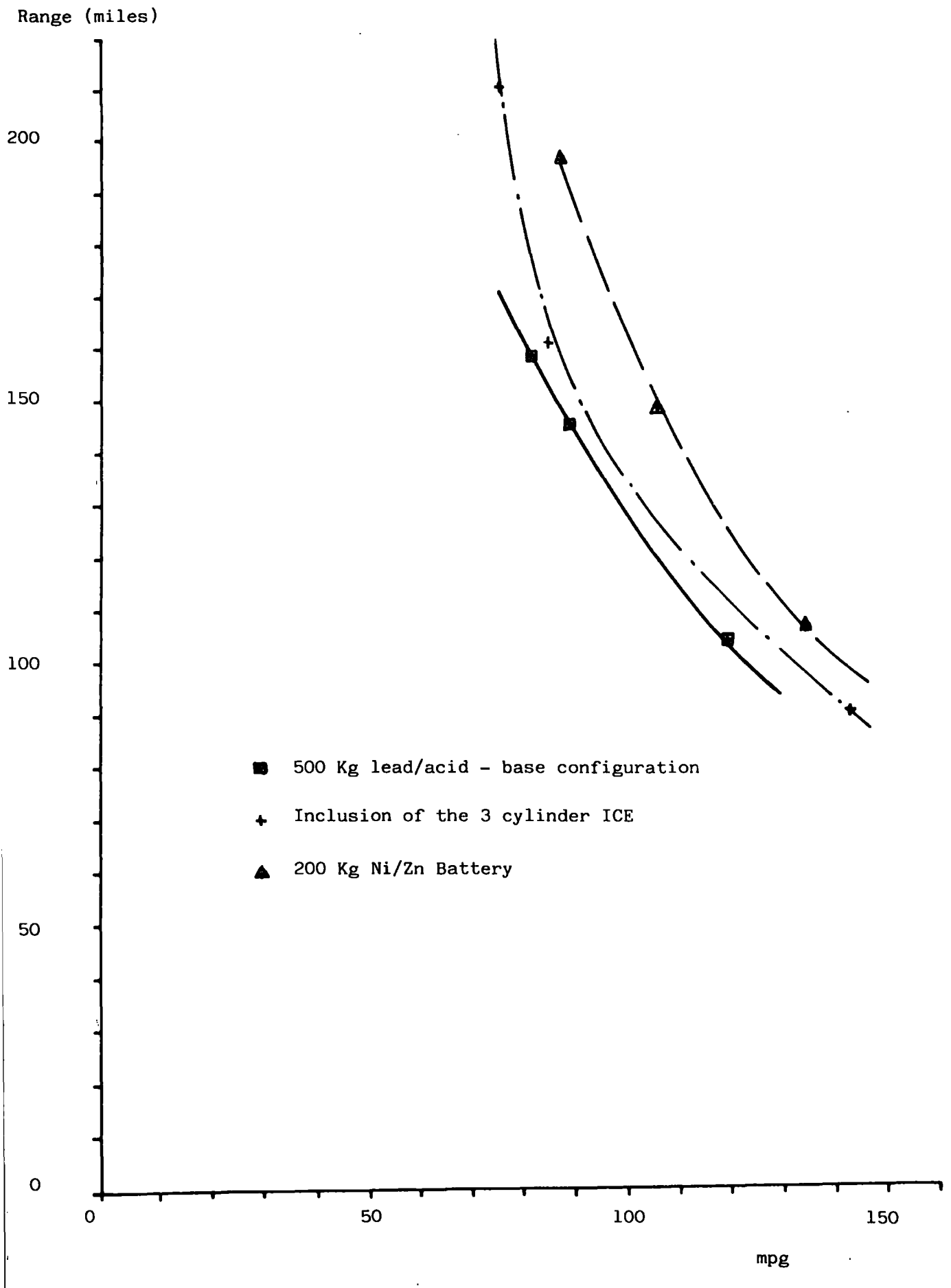

FIGURE 8.2: Petroleum Substitution mpg/range curves showing the Effects of Advanced Traction motor types over the ECE-15

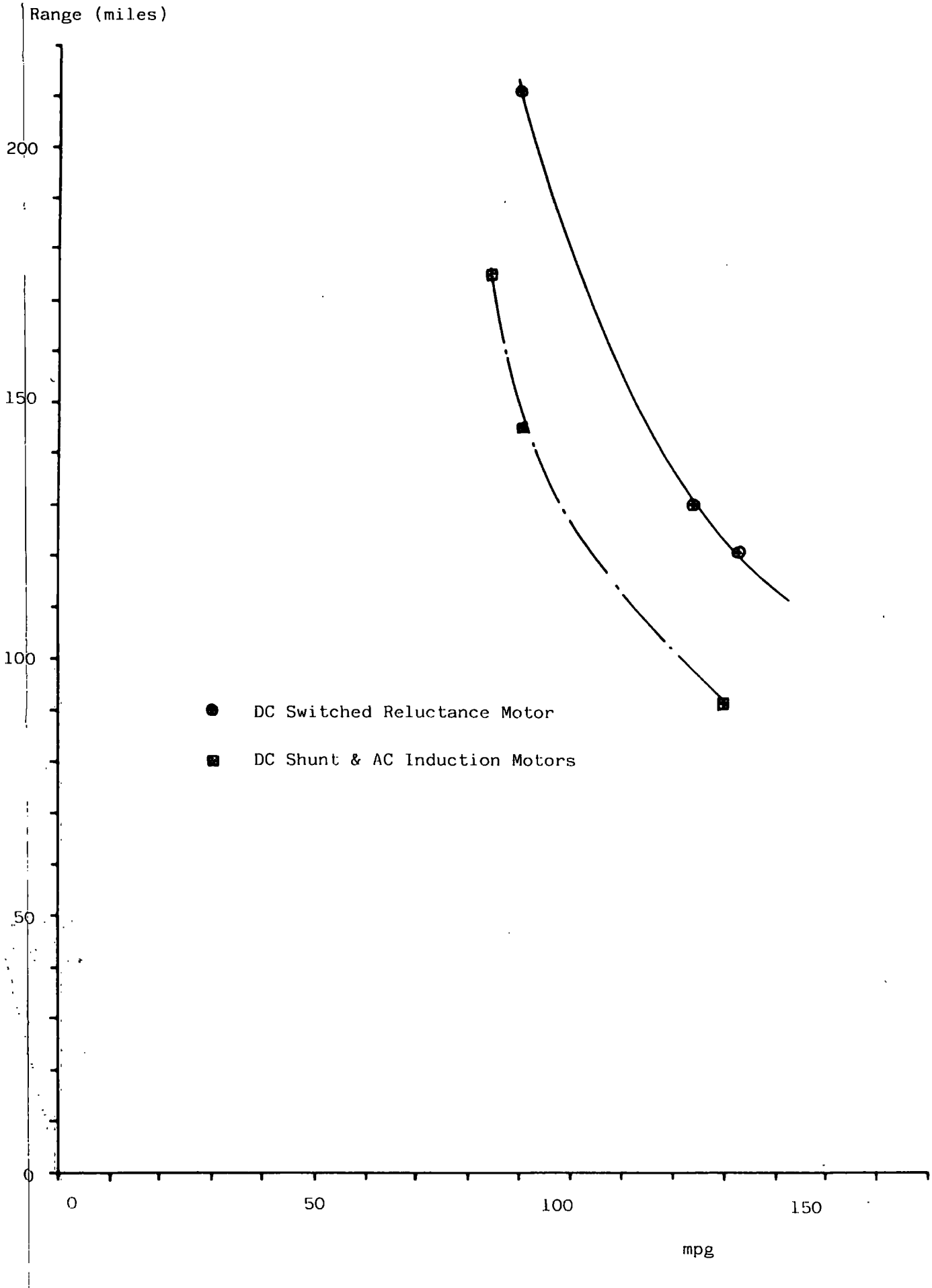

Figure 8.3: The Effect of a mix of All-Electric and Hybrid nodes for the Petroleum Substitution Aim to give an ECE-15 urban range of 60 miles to 70% DOD using a 500 Kg battery

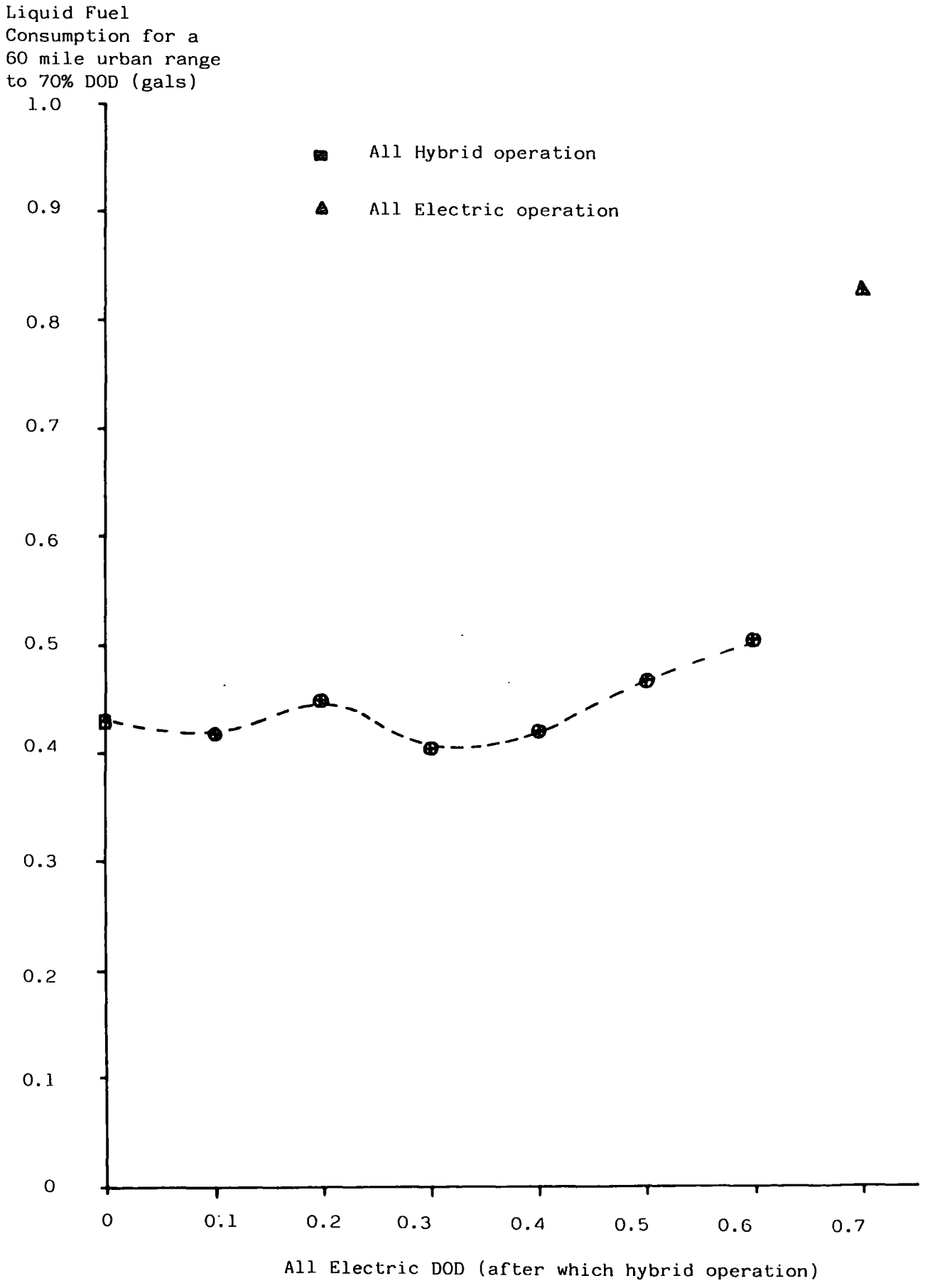

CHAPTER 9

General Conclusions

9.1 Concluding Remarks

The main thrust of the work presented here has been aimed at a study of the hybrid-electric concept as a means of reducing the world's dependency on a fast dwindling energy resource - petroleum or crude oil. But in doing so, the electric vehicle concept, highlighted in chapter 1 as a means of totally displacing petroleum in the road transport sector, has also been considered in terms of improving the inherent and well recognised range limitations in relation to the effectively infinite range enjoyed by i.c. engine vehicle users.

It may seem appropriate, therefore, that a similar study concerning the i.c. engined vehicle should also have been performed, but as was indicated in chapter 1, improvements to the efficiency of the conventional vehicle would not reduce the dependency on petroleum, and, given that the predictions in availability are valid, any reduction in the rate of consumption would only serve to forestall the time when extraction difficulties prohibited the use of petroleum as an energy source.

However, the study of future developments to the equivalent i.c. engined medium sized passenger car, performed as part of the comparison between the competing drive-trains of chapter 8, indicated that average mpg gains of up to 90% could be achievable in the near-term. This is in agreement with not only the estimates derived from the available literature in chapter 1, but also a study performed for several European passenger car classes, also using the JANUS simulation program (Bumby et al.,1984(b)).

The computer simulation program, described in chapter 2, has enabled a wide variety of variables to be studied, both in the pure-electric drive-train study of chapter 4 and the hybrid-electric drive-train studies of chapters 5, 6 and 7.

The electric vehicle drive-train study of chapter 4, although concentrating on a vehicle type that did not offer significant petroleum displacement, was intended by the consideration of a vehicle class that would lend itself to electric vehicle application in terms of daily usage and size, to show the impact of the technological advances possible in the future.

The study indicated that unless the buying public could be conditioned to expect a vehicle of limited range, as far as European car market conditions were concerned, the alternative to achieve petroleum displacement without limiting vehicle range would be the hybrid electric vehicle.

The subsequent hybrid-electric drive-train study has concentrated on a vehicle type with scope for significant petroleum displacement - the medium sized passenger car, highlighted in chapter 1 - and has moved from the basic drive-train concepts, to a study of hybrid vehicle parameters and then to consider the effects of control strategy.

In order to make a comparison between the hybrid, pure-electric and conventional i.c. engined drive-trains in chapter 8, the results of the parametric study have been condensed into a single vehicle design for each hybrid aim - energy saving and petroleum substitution.

It was subsequently shown in chapter 8, that although it seems unlikely that the hybrid-electric vehicle in the passenger car application will save energy, it will certainly displace petroleum by means of battery energy and in doing so offer a possible energy cost saving compared to the i.c. engined vehicle, if, as is likely the cost of petroleum based fuels compared to wall plug electricity increases as petroelum becomes more scarce. Relative to the electric vehicle, however, if the above state of affairs exists, the hybrid will offer greater energy costs, but these must be tempered by the ability of the hybrid to perform long distance journeys when required.

In order to be persuaded to purchase a hybrid vehicle in the future, in the event of a dramatic increase in the cost of petroleum fuels, the potential buyer must be shown that any future energy cost savings of the hybrid relative to the i.c. engine vehicle more than compensate for a likely increase in initial purchase cost (when spread over the lifetime of the vehicle) plus any additional maintenance costs inherent to the added complexity. Relative to the electric vehicle the hybrid will likely offer an increase in purchase, energy and maintenance costs but will have the unquantifiable asset of not being range limited.

A place for the hybrid-electric vehicle in the future will only exist if no suitable alternative to petroleum based fuels can be developed, and even though the hybrid will still be feasible in the event of the predicted future price increase of petroleum - since it only depends upon this energy source alone for infrequent long journeys - it may form an intermediate step in conditioning the buying public to accept a vehicle of limited daily range.

Although the absolute accuracy of the simulation program was verified in chapter 3, this was only possible for the conventional i.c. engine vehicle and the electric vehicle with the argument that when the two drive-trains were married together in the hybrid the accuracy would be assured here also. However, the optimum and sub-optimum hybrid-electric control strategies studied in chapter 7 have suggested certain aspects of hardware operation that it was not possible to include in the verification of the simulation program in chapter 3. Firstly, during restarting and synchronisation of the i.c. engine with the remainder of the drive-line, the time taken and the fuel consumption penalty incurred will be finite in practice whereas for the simulation study, both were assumed to be zero.

Secondly, the transient effects during gear shifting with a discrete ratio unit, in terms of any energy consumption penalty associated with i.c. engine and battery current transients, would also be finite in practice, but were again assumed to be zero in the simulation.

The aforementioned aspects of hybrid-electric vehicle control have been studied in the work performed by G.E. on the Near-Term-Hybrid-Vehicle (Burke et al.,1981)(Trummel et al.,1983).
In the case of the Near-Term Hybrid vehicle,
the rapid restarting and synchronising of the i.c. engine was studied along with the shifting transients experienced by the prime movers during gear shifting although no fuel penalties have been quoted in the G.E. work.

As well as the aspects of hybrid-electric vehicle control related to energy consumption, and therefore of direct relevance to the simulation study described here, there are those aspects of hybrid-electric vehicle control that introduce practical problems in terms of driveability and passenger comfort. Such aspects of control are, as with the aforementioned energy consumption implications related to, again, the problem of re-starting and synchronisation of the i.c. engine and also the transient effects during gear-shifting. As was described earlier, the time taken for the i.c. engine to be re-started and synchronised with the drive-line is important as the vehicle occupants would experience a 'lag' or noticeable break-in the continuity of vehicle acceleration if this time period was significant. The transient effects of gear shifting will manifest themselves in sudden accelerations or decelerations as far as the vehicle occupants are concerned. With the probability of more frequent use of the variable ratio transmission, as suggested by the results here, than is normally accepted, then the quality of the gear-shifting - particularly in the case of a discrete ratio unit - would be important.

There has already been significant interest shown in both the external (computer) control of friction clutches with a view to converting manual transmission into semi-automatic transmissions, (Falzoni,1983)(Tanaka,1984) and in the external computer control of variable ratio transmissions (Miller,1982 (Richardson et al.,1984)(Ono et al.,1983)(Morello,1977). So far, however the studies have been performed with the conventional i.c. engine vehicle in mind.

The work performed by G.E. on the Near-Term Hybrid-Vehicle did encompass the computer control of the i.c. engine friction clutch in terms of starting and synchronising with the drive-line, and also external control of a variable ratio transmission by means of a microcomputer. However, the vehicle was designed with the U.S. car market in mind - so resulting in a larger vehicle than is accepted in Europe - and also in the space of the 4 or 5 years since its construction the power and speed of microcomputers has progressed sufficiently to allow more sophisticated software algorithms to be used in the control of the hybrid vehicle.

Therefore the sub-optimum control algorithm - derived and studied in chapter 7, with the possible refinements suggested, may be implemented in microcomputer based control of a hybrid vehicle.

Although the drive-train configuration study of chapter 5 concluded by favouring an alternative, that, whilst not achieving the lowest energy consumption did benefit from relative simplicity it may be appropriate in the future to consider the drive-train alternatives that did achieve lower energy consumptions, such as in the use of 2 transmissions and/or the use of a coupling device on the traction motor when not in use.

If it was thought necessary to adopt either or both of the aforementioned drive-train alternatives then the parametric study of chapter 6 would still be of relevance as the parameters were varied independently of each other and therefore not dependent on the

configuration adopted. Furthermore, the sub-optimum control strategy of chapter 7 would still in the main be valid with the exception of the possibility of independent gear-shifting for both power sources simultaneously in the hybrid mode if the use of 2 transmissions was to be adopted.

9.2 Suggestions for Future Work

It is apparent that although the study presented here has covered a wide range of possibilities in order to reach the conclusions in terms of energy consumption for the hybrid-electric vehicle in chapter 8, several further questions would need to be answered in order for the concept to progress further. Firstly, the energy consumption penalties associated with the control of the hybrid drive-train need to be quanti fied. Secondly the driveability problems associated with hybrid-electric vehicle power-source blending and gear-shifting need to be somehow assessed.

When the aforementioned unknowns have been studied, then it may be possible - depending upon the outcome - to proceed on to the next step necessary for the near-term introduction of the hybrid-electric vehicle. As was indicated earlier in this chapter, this step would involve an assessment of the economic viability of the hybrid vehicle to the user in terms of weighing the possible future energy cost savings of the hybrid relative to the i.c. engine vehicle against increased initial purchase costs and maintenance costs.

The practical problems of the hybrid-electric drive-train indicated by the simulation study presented here will be best assessed by means of a drive-train test rig as this will enable the various hardware options to be constructed more easily than if a test-bed vehicle were to be used.

In the case of i.c. engine re-start, synchronisation and load pick up as well as the G.E. method of the conventional use of a friction clutch, there are two possible alternatives that may also be studied. Firstly the i.c. engine may be restarted by simply coupling it into the drive-line and using vehicle inertia to provide the starting torque. However, vehicle deceleration would result, which would be unacceptable in terms of driveability, but which may be overcome by the use of the traction motor to resist the retardation. Secondly, by the use of a free-wheel unit in between the i.c. engine and the drive-line, and providing that the drive-line speed is above i.c. engine minimum speed, then the i.c. engine may be re-started and only become coupled to the drive-line when its speed has reached the speed of the drive-line.

As far as the quality of variable ratio transmission gear shifting is concerned as no units, of either the ratio span or with the subsequent number of ratios, exist commercially, then the investigation would have to be performed by using a current 3 or 4 speed automatic unit modified for external computer control and with perhaps currently available overdrive units included in the drive-line in order to widen the ratio range and increase the number of ratios. The CVT may also be investigated in terms of shift quality on such a test rig but as has been shown consistently in the hybrid drive-train study of chapters 5 and 6, because of the inherently poorer transmission efficiency of current designs relative to the discrete ratio unit, the scope for gains (which is smaller for the hybrid relative to the conventional vehicle) is eroded.

Finally work using and developing the simulation package should continue where possible, and, as well as modelling improvements as a result of the aforementioned suggested hardware study, it may be now appropriate, having dismissed the hybrid-electric vehicle as regards the 'energy saving'

aim, to now consider the mechanical hybrid configurations discussed in chapter 1. Although lacking the ability to depend upon their secondary energy sources alone for significant periods, in a purely load-levelling role envisaged for the 'energy saving' vehicle, a lighter vehicle compared with the hybrid-electric configuration may result with a corresponding reduction in energy consumption.

REFERENCES

1. Alterndorf J.P. - An Electric Vehicle Drive Concept Using a Centrifugal Clutch - Volkswagenwerk A.G., Wolfsberg.1979

2. Anderson N.A., Loewenthal S.M. - Effect of Geometry and Operating Conditions on Spur Gear System Efficiency, Power loss - Journal of Mech.Design - Jan.1981 - Vol.103/151.

3. Argarwal P.D., Mooney P.J., Toepel R.R. - Stir-Lec I, A Stirling Electric Hybrid Car-Research Laboratories, General Motors Corp. 1967

4. Aston M.B., Chayanoff S.L., Chapman C.P. - Analytic Transmission Models for Electric and Hybrid Vehicle Simulation - EVC Symp VI, Baltimore, Oct.1981.

5. 'Autocar' - Buyer's Guide - w/e 17 Oct.1981.

6. Automotive Propulsion - Electric and Hybrid Systems - April 18-22 1977 - NATO/CCMS N.61 Vol.II, Feb.1978.

7. Bader C. - Electrical Propulsion Systems for Battery Driven Road Vehicles with Hydrodynamic Transmission of Power - SAE 750193 - 1975.

8. Bader C., Stephan W. - Comparison of Electrical Drives for Road Vehicles - IEEE,Vol.VT26 No.2 - May 1977.

9. Beachley N.H., Frank A.A. - Electric and Electric Hybrid Cars - Evaluation and Comparison - University of Wisconsin - SAE 730619 - 1973.

10. Beachley, N.H.,Frank A.A. - Improving Vehicle Fuel Economy with Hybrid Power Systems - SAE 780667 - 1978.

11. Bedford Vehicles, U.K.

12. Berman B., Gelb G.H. - Electric Car Drives - Design Considerations - TRW Systems Group - SAE 720111 - 1972.

13. Berman B., Gelb G.H. - Propulsion Systems for Electric Cars - IEEE Transactions on Vehicular Technology, Vol.VT23, No.3, Aug.1974.

14. Beven J., Weimburger, Metcalfe M.A - A Survey of Electric and Hybrid Vehicle Simulation Programs - J.P.L., Pass, CA - 1978.

15. B.L. Cars - U.K.

16. Blumberg P.N. - Powertrain Simulation : A Tool for the Design and Evaluation of Engine Control Strategies in Vehicles - Ford Motor Co. - SAE Progress 1976.

17. Bradford M., Knight D.E. - An Outline Investigation of a Hybrid (Combat) Trolley Bus - Electrical Research Association Ltd. 1978

18. Breig W.F., Oliver L.R., - Energy Loss and Efficiency of Power Transmission Belts - Advanced Engineering Research Belt Technical Centre - Dayco Corp., Springfield, Missouri. Proc.of National Conf.on Power Trans - Inst.of Tech.1980

19. Brusaglino G. - A Hybrid Electric Bus - Fiat Research Center.1981

20. Brusaglino G., Bertoldi F. - Outline Project of a Hybrid Bus - Fiat Research Center. 1974

21. Bucci G.D., Montalenti P. - Ni-Zn Battery Application to the Hybrid Gould Inc., Gould Center, Ill, & Fiat Research Center,Italy. 1981

22. Bujold M.P. - Small Passenger Car Transmission Tests - Eaton Corp.- EVC Symp VI, Baltimore, Oct.1981.

23. Bullock T. - Computer Simulation of a Series Hybrid, Electric Car - A Final Year Honours Project - May 1983 - University of Durham.

24. Bumby J.R., Clarke P.H. - The Role of the I.C. Engine/Battery Electric Hybrid Vehicle in the U.K. - Energy World 98.2. 1982.

25. Bumby J.R., Clarke P.H., Forster I. - Computer Modelling of Automotive Energy Requirements for I.C. Engine and Battery Electric Powered Vehicles - IEEE - 1985.

26(a) Bumby J.R., Clarke P.H., Forster I - The Evaluation of Hybrid Electric Road Vehicle Performance by Computer Simulation - Inf.Symp.Advanced and Hybrid Vehicles - 17-19 Sept. 1984.

26(b) Bumby J.R.,Clarke P.H., Forster I., Shakib N., - Computer Modelling of Spark Ignition Engined cars Showing What Fuel Economy is Feasible by the Year 2000 - Univ. of Durham - Passenger Car Meeting, Dearborn, Michigan, Oct. 2-4,1984.

28. Burke A.F., Somuah C.B. - Power Train Trade - Offs for Electric and Hybrid Vehicles - G.E. - Annual Conf. of the IEEE - Vehicular Tech.Soc. - Sept.1980.

29. Burke A.F., Smith G.E. - Impact of use - pattern on the Design of Electric and Hybrid Vehicles - SAE 810265 - 1981.

30. Burke A.F., Miersch R - Development of a Full Size, Hybrid (Electric/ICE) Passenger Car - G.E. Co. - 4th Int.Conf. - Hybrid, Dual Mode and Tracked Systems, London, Sept. 1981.

31. Burke A.F. - A Family of Hybrid (Electric/ICE) Passenger Cars - GE - EVC Symp VI, Baltimore, Oct.1981.

32. Burke A.F., Somuah C.G. - Computer Aided Design of Electric and Hybrid Vehicles - GE - Int J. of Veh.Design. SP2,1982.

33. Burris L., Nelson P.A. - Advanced Batteries for Vehicle Propulsion SAE 780458 - 1978.

34. Chang M. - Computer Simulation of an Advanced Hybrid Electric Powered Vehicle - SAE 789217 - 1978.

35. Chapman P., Aston M. - A Generic Battery Model for Electric and Hybrid Vehicle Simulation Performance Prediction - JPL - Int. J. of Veh.Design SP2 1982.

36. Coleman W. - Computing Efficiency for Bevel and Hypoid Gears - Machine Design - Aug.21 1975 - Vol.47 part 20 p 44-65.

37. Collie M.J.- Electric and Hybrid Vehicles - Energy Technology Review No.44 - 1979.

38. Cornell, C.P., Guess R.H., Turnbull F.G. - Advances Motor Developments for Electric Vehicles - IEEE Transactions on Vehicular Technology vol.26 No.2 - 1977.

39. Cummins Engine Co.Inc. - Guide to Lowest Cost per mile (LCPM) - Columbia, Indiana 1984.

40. Curtis - Application of a Stirling Engine to a City Bus - London Regional Transport - Int.Symp.Advanced & Hybrid Vehicles 17-19 Sept.1984.

41. Dabish S. - Ford Motor Company Automatic Overdrive Transmission - SAE 800004-1980.

42. Domann H., Renner S. - Experience with Electric Drives for Vehicles - 3rd Electric Vehicle Sympsoium and Exposition, Feb.1974, Wash.D.C.

43. Dovey R.E., Vaughan N.D. - The Computer Aided Investigation and Performance Evaluation of a Regenerative Hydrostatic Split Power Transmission for a City Bus - University of Bath - Int.Symp.Advanced & Hybrid Vehicles, University of Strathclyde, 17-19 Sept.1984.

44. Department of Energy - Energy Technologies for the UK : An Appraisal for R & D planning - Energy Paper No.39. Vols. I & II. London 1979.

45. D.O.T. - Official List of Results of Fuel Consumption Test on Passenger Cars - 1984.

46. Eshbach - Handbook of Engineering Fundamentals - 3rd Ed. - Wiley.

47. Falzoni G.L. - Microprocessor Clutch Control - SAE 830628 - 1983.

48. Firbank T.C. - Mechanical Efficiency Tests of Vee Belts and Flat Belts Drives - School of Mechanical and manufacturing Systems Engineering, University of Bradford. 1976.

49. Ford Motor Co. - U.K.

50. Ford Motor Co. - Ford Energy Report Vols.I, II & III, 1982.

51. Fox R.L. - Optimisation Methods for Engineering Design - 1971. Addison-Wesley Publishing Co.

52. Frank A.A., Ye Z., Yang D. - Some Flywheel Drive Applications in Motor Vehicles - College of Engineering, University of Wisconsin - Int.Symp.Advanced & Hybrid Vehicles - University of Strathclyde, 17-19 Sept.1984.

53. Frank H.A., Phillips A.M. - Evaluation of Battery Models for Prediction of Electric Vehicle Range - JPL - Cal.Inst. of Tech., Pass, Ca, 1977.

54. Fulton, N.N., Blake R.J.,Davies R.M.,Ray W.F., Lawrenson P.J., Stephenson J.M. - Switched Reluctance Motors for Battery Electric Road Vehicles - Int.Symp.Advanced & Hybrid Vehicles - University of Strathclyde - 17-19 Sept.1984.

55. Gates, D., Pocobello M. - Electric Van for Metropolitan Service - SAE 730249 - 1973.

56. Gurley A. - Towards a More Versatile Public Passenger Transport System Based on Experience with the Leyland/Bosch/Chloride Bus at Runcorn Cheshire - National Bus Company.1977

57. Hammond R.A., McGehee R.K., Users' Guide to the Hybrid and Electric Advanced Vehicles Systems (HEAVY) Simulation - Boeing Computer Services CO, Energy Technology Applications Division - US Dept. of Energy - DOE/NASA/0151-2-Nov.1981.

58. Hammond R.A., McGehee R.K. - Final Report. Hybrid and Electric Advanced Vehicle Systems (HEAVY) Simulation - Boeing Computer Services Co. - Nov.1981.

59. Hammerstrom L. - VTS Hydrostatic Transmission, Experiences from the First Field Tests - Volvo - Int.Symp. Advanced & Hybrid Vehicles - 17-19 Sept.1984 - University of Strathclyde.

60. Harding G.G., Phillips B.L., Hammond J.E. - The Lucas Hybrid Electric Car - Lucas Chloride Birmingham - SAE 8301113.- 1983.

61. Heitbrink E.H., Boak R.W.,Atkins L.P. - Electric Vehicle Road Tests of Ni/Zn Batteries - SAE 830110 - 1983.

62. Hoffman G.A. - Future Electric Cars - SAE 690073 - 1969.

63. Honda S., Hoshino C., Kawakitsu S., Tswkano H., YUamamoto T., Lida M. - Efficiency Studies About Daihatsu Engine/Electric Hybrid System - Daihatsu Motor Co.Ltd. (Japan). 1979

64. Hornfield M. - Weight Reduction - is it a Valid Concept - Materials and Design - April/May 1983 Vol.IV No.2.

65. House of Lords - Select Committee on Science and Technology - Electric Vehicles Session - 1979-1980.

66. Humphreys D.W., Harrow B.E., Howe J.W. - The 1978 State of the Art of In-Use Electric and Hybrid Vehicles - JPL - SAE 799120, 1979.,

67. Institution of Mechanical Engineers - Power Plants and Future Fuels - 1975.

68. International Research & Development Co.Ltd. (IRD) - Report to the Department of Industry on Hybrid and Electric Vehicles - May 1984.

69. Jamazadesh F.S., Frank A.A. - Optimal Control for Maximum Mileage of a Flywheel Energy Storage Vehicle - University of Wisconsin - SAE 820747 - 1982.

70. Jones, R.P., Holt M.J., Hughes M.T.G., Kuriger I.F., Marson S.J. - The Role of Simulation Modelling in Control Analysis and Design of Advanced Powertrains - Dept. of Eng., University of Warwick - Int.Sym.Advanced and Hybrid Vehicles, University of Strathclyde, 17-19 Sept.1984.

71. J.P.L. - Should we Have a New Engine - Jet Propulsion Laboratory, Pass., CA - 1975.

72. Katz, M.J. - The Department of Energy Battery Program: An Overview DOE, Washington DC - American Chemical Soc.1979.

73. King, C.S., - A Car for the Nineties : B.L.'s Energy Conservation Vehicle - B.L. Tech. - Proc.Inst'n of Mech.Eng. vol.198 No.3 1984.

74. Klink R. - Measures for Improving Efficiency of Vehicle Drive Units with Hydrodynamic Torque Converters - Int.Symp.Advanced & Hybrid Vehicles - 17-19 Sept.1984.

75. Koch L.G. - Powertrain Vehicle Modelling to Simulate Shifting Transients of off-Highway Vehicles - SAE 720044 - 1972.

76. Kose A.B., Hooker J.N., Roberts G.F., Hodgson J. - Data Based Simulation for Predicting Vehicle Fuel Consumption - Oakridge National Lab., TN (USA). 1982

77. Kugler G.C. - Electric Vehicle Hybrid Power Train - SAE 730254 - 1973.

78. Kutz D.W., Price T.W., Bryant J.A., - Performance Testing and System Evaluation of the DOE ETV-1 Electric Vehicle - Electric and Hybrid Vehicle Progress - SAE 810418 - 1981.

79. Kuzak D.M., Patil P.B., Bates B. - Regeneration Potential of Electric Vehicles - Ford Motor Co. - Int. J. of Veh.Design SP2 - 1982.

80. La France R.C., Schult R.W. - Electrical Systems for Hybrid Vehicles - IEEE Transactions on Vehicular Technology - Vol.VT22 No.1 - Feb.1973.

81. Lapedes D.E. - An Assessment of the Hybrid Heat Engine/Electric Powertrain for Use in Urban Buses - Staff Engineer, The Aerospace Corp.1971

82(a) Liddle S.G. - An Analytical Study of the Fuel Economy and Emissions of a Gas Turbine Electric Hybrid Vehicle - SAE 760122 - 1976.

82(b) Liddle S.G. - Emissions from Hybrid Vehicles - General Motors Research Ltd. - Int.Soc.Energy Conversion Eng. Conf. Aug. 1973.

84. Lucas Chloride, Birmingham, U.K.

85. Ludolph H.M.J. - Stepless Automatic Transmission for Cars - 10th Int.Automobile Tech.Congress. SAE of Japan 1964 - p262-76.

86. Magee C.L. - The Role of Weight Reducing Materials in Automotive Fuel Savings - Ford Motor Co. - SAE 820147 - 1982.

87. Martini S. - The M.A.N. Hydrobus - a Drive Concept with Hydrostatic Brake Energy Recovery - M.A.N. - Int. Symp.Advanced & Hybrid Vehicles - 17-19 Sept.1984, University of Strathclyde.

88. Martin K.F. - The Efficiency of Involute Spur Gears - Transtations of the ASME vol.103. Jan.1981.

89. McGehee R.K., Hammond R.A. - Comparison of Energy Management Strategies for a Heat Engine/Electric Hybrid Drive-Train - EVC Symp.VI - Baltimore - Oct.1981.

90. McKechnie R.M. - Generalised Vehicle Dynamics Program for Interactive Hybrid Computer Graphics - Proc.Summer Computer Simulation Conf. - Montreal July 17-19, 1973.

91. Mechanical Power Tansmission - Mech.Eng.Series. Macmillan - 1971.

92. Meyer E.W., Kershaw T.J., Barnes D. - An Electronic Fuel Control Carburrettor System - Austin Rover Group, Birmingham, U.K. 1983.

93. Miller, A.L. - Microcomputer Controlled Automatic Transmission - SAE 820394 - 1982.

94. Mitcham A.J., Bumby J.R. - A Survey of Hybrid Electric Vehicles, vol.1 - Technical Assessment and Recommendations - IRD Report 77/12 - April 1977.

95. Mitcham A.J. - Hybrid Electric Vehicles - An Assessment and Survey.

96. Morello L. - Optimising the Engine - Transmission System by Means of an Electronically Controlled Gearbox - Fiat Research Center - Proc. 4th Int.Symp. of Automatic Propulsion Systems - April 1977.

97. Morello L., Picolla R., Ipoolito L. - Fiat Research Center Hybrid Vehicle Prototype - SAE 790014 - 1979.

98. Mangan K.F., Griffith J.T. - Who Needs Electronics, Torque Converters can do the Job. 3rd Int.Elec.Veh.Symp.& Exp.1974

99. Mosbech H. - Optimal Control of a Hybrid Vehicle - Danish Technical University - Denmark.

100. Murphy G.J. - Regenerative Braking in Electric Vehicles - North Western University, 2145 Sheridan Road, Evanston, Ill., 60201. 1972

101. Murphy G.J. - considerations in the Design of Drive Systems for On-the-Road Electric Vehicles - IEEE Vol.60 No.12, Dec.1972.

102. Nasar S.A., Unnewehr L.E. - Electromechanics and Electric Machines - 1983 - John Wiley & Sons.

103. Nightingale M.R., Gorman D.G., Lawrence J.C. - Feasibility Study of a Hybrid Diesel - Electric Passenger Car - Int. Symp. Advanced & Hybrid Vehicles, 17-19 Sept.1984, University of Strathclyde.

104. Nix G.F. - Assessment of Hybrid Electric Vehicle Literature Survey- University of Manchester - 1982.

105. Ono H., Nakano J., Nakano Y., Takahasi Y. - Toyota's New Microprocessor Based Engine and Transmission Control System - SAE 830423 - 1983.

106. Pannier G., Laport A. - Electronic Control of Automobile Transmissions - SAE 820392 - 1982.

107. Pede and Richmond - Applied Thermodynamics Problems.

108. Peterson L.D., Holka T.C. - Engineering Development of the Probe IV Advanced Concept Vehicle -SAE 831002 - Ford Motor Co. - 1983.

109. Plunkett A.B., Kliman G.B. - Electric Vehicle A.C. Drive Development - SAE 8000061 - 1980.

110. Ratcliff J.E. - Torque Converters Make Electric Vehicles Competitive Advanced Vehicle Systems Ltd., Welwyn Garden City. 1976

111. Richardson R.M., Main T.J., Lindre J. - A 5-speed Microprocessor Controlled Economy Tranmission - Ford Motor Co. 1984

112. Rhodes D.M., Werson M.J. - The Petrol Engine. A Case for Closed Loop Control - ADAU, University of Southampton, UK and Moore Reed Ltd., U.K.1984

113. Rogers G.F.C., Mayhew Y.R. - Engineering Thermodynamics Work and Heat Transfer - Longman,1978.

114. Sampson H.T., Killian H.J. - Evaluation of Powertrains for Hybrid Heat/Engine Electric Vehicles - SAE 720194 - 1972.

115. Samuel J.M.G. - Range and Peformance Breakthrough - CVT with High Speed Shunt Motor - BT Advanced Vehicle Systems Ltd., Weybridge, Surrey. 3rd Int.Elec.Veh.Symp & Exp.1974

116. Sandberg J.J. - Trade off Studies and Preliminary Designs of Near-Term Hybrid Vehicles - J.P.L., Pass, CA, 1980.

117. Santer R.M., Gleason M.E. - The Aerodynamic Development of the Probe IV Advanced Concept Vehicle - Ford Motor Co. - SAE 831000 - 1983.

118. Sargent N.B., O'Dustin M. Results of the EV-1 Breadboard Tests Under Steady-State and Transient Conditions - EVC No.8123.1981

119. Schwartz R. - Design considerations for a Near-Term Hybrid Vehicle - South Coast Technology Inc., Santa Barbara, CA. Aug.1980

120. Scrinivasan K., Mattern D.L., Houser Dr.R., Kinzal G.I. - Microprocessor Controlled Continuously Variable Rubber V.Belt Transmission for an Automobile - SAE 820745 - 1982.

121. Sellner H.J. - Electronic Ignition with Closed Loop Knock Control - Audi NSU Auto Union AG, Federal Republic of Germany.

122. Shell Research - Thornton Research Centre, Chester, Cheshire.

123. Shepherd C.M. - Design of Primary and Secondary Cells.II. An Equation Describing Battery Discharge - US Naval Research Laboratory, Washington D.C. - 1965.

124. Slusser R.A., Brennand J. - Updates to the ELVEC Electric/Hybrid Vehicle Performance Computer Simulation Program - EVC Symp.VI, Baltimore, Oc.1981.

125. Slusser R.A.,Chapman P. Chazanoff S., - Electric/Hybrid Vehicle Simulation Program (ELVEC) User's Manual - J.P.L., Pass, Cal., 1981.

126. Stafford K.A. - Electric Vehicle Simulation for Design Optimisation - Air Force Inst. of Tech.1980

127. Steven R.C. - Electric Machines and Power Electronics - 1983 - Van Nostrand Reinhold.

128. Stieg R.F., Spencer-Worley W. - A Rubber Belt CVT for Front Wheel Drive Cars - SAE 820746 - 1982.

129. Stubbs P.W.R. - The Development of a Perbury Traction Transmission for Motor Car Applications - J. of Mech.Design.103.29.1981.

130. Tanaka H. - Proportional Clutch for Semi-Automatic Power Transmission - Int.Symp.Advanced & Hybrid Vehicles - 17-19 Sept.1984. University of Strathclyde.

131. Tanner J.C. - Some Aspects of New Car Registrations - T.R.R.L. Report No.1107.

132. Thring R.H. - Engine Transmission Matching - Ricardo Consulting Engineers Ltd. SAE 810446 - 1981.

133. Thring R.H. - Engine Transmission Matching to Improve Passenger Car Fuel Economy - SAE 820167 - 1982.

134. Thompson M.A., Walters L.A. - The Design of D.C. Commutator Motors for High Performance Electric Vehicles - Research Centre, Lucas Ltd., SAE 740169 - 1974.

135. Transport and Road Rsearch Laboratory - Sumposium on Energy and Road Transport - 12-13 April 1978 - TRRL Supplementary Report 447.

136. Traversi M. et al. - Phase 1 of the Near Term Hybrid Passenger Vehicle Development Program Appendix B : Trade-off Studies, vol.1 - Fiat Research Center. June 1980

137. Trummel M.C., Burke A.F. - Development History of the Hybrid Test Vehicle - IEEE Transactions on Vehicular Technology Vol.VT32 No.1 Feb.1983.

138. Unnerwehr L.E., Auiler J.E., Foote L.R., Moyer D.F., Stadler H.L. - Hybrid Vehicle for Fuel Economy - SAE 760121 - 1976.

139. van Donger I.A.M., van de Graff R., Visscher W.H.M. - Theoretical Prediction of Electric Vehicle Energy Consumption and Battery State of Charge during Arbitrary Driving Cycles - Eindhoven University of Technology - EVC Symp VI, Oct.1981, EVC No.8115.

140. Volkswagen - Audi - U.K. Ltd.

141. Wallace G.M. - The B & M Super Drive - an Aftermarket Torque Converter to Improve Fuel Economy of Large Engined Cars - SAE 820742 - 1982.

142. Waters W.C. - General Purpose Automotive Vehicle Performance and Economy Simulator - General Motors - SAE 720043 - 1972.

143. Watson J., Lee G.A. - Traffic Compatible Hybrid Electric Vehicles - an Outline of Development Work with Vans and Buses - Dept. of Mech.Eng. University of Swansea and Dragonfly Research Ltd.,U.K.

144. Watson J.F., Thomans G., Hooper A. - Computer Simulation and Test Rig Evaluation of a Hybrid Power System for a Light Goods Delivery Vehicle - University College, Swansea - Int.Symp.Advanced & Hybrid Vehicles, 17-19 Sept.1984, University of Strathclyde.

145. West Yorkshire P.T.E. - Alternative Traction Options - Project Report 81/1- 1981.

146. Wilson J.W.A. - The Drive System of the DOE Near-Term Electric Vehicle (ETV-1) - General Electric Co. - Schaectady, NY, SAE. 1981

147. Wilson J.W.A., Turnbull F.G. - A Review of Electrical Propulsion Systems for Battery Powered Passenger Vehicles - GE - Int.J. of Veh.Design SP2 1982.

148. Wolfson R.P., Gower J.H. - The Role of Computer Modelling and Simulation in Electric and Hybrid Vehicle Research and Development - IEEE Transactions on Vehicular Technology Vol.VT32 No.1.Feb.1983.

149. Wrangham D.A. - The Theory and Practice of Heat Engines - University Press Cambridge 1951.

Appendices

APPENDIX I

D.C. Shunt Motor Model. Mathematical Model

Basic Motor Model Defining Equations

A diagrammatic representation of the electrical and mechanical power paths in the DC shunt motor is shown in Figures 2.15 - 2.16. Working from the shaft to the terminals the basic defining equations can be written.

Shaft power:

$$PO = To.n/1000 \quad (KW) - \quad (46)$$

Mechanical losses:

$$Pm = C1.n + C2\,n^{1.5} + C3.n^{2.0} \quad (KW) - \quad (47)$$

$$Tm = Pm.1000/n \quad (Nm) - \quad (48)$$

Air gap power and torque:

$$Tag = K1\ Ia\ If = To + Tm \quad (Nm) - \quad (49)$$

$$Pag = Tag.\ n/1000 = E.Ia/1000 \quad (KW) - \quad (50)$$

Terminal input power:

$$Pi = Po/\eta_o \text{ motoring} = Po \quad o \text{ regeneration} \quad (KW) - (51)$$

also

$$Pi = Pa + Pf = (VaIa + Vf\ If)/1000 \quad (KW) - \quad (52)$$

Back emf:

$$E = K2\ Ifpu \quad (volts) \quad - \quad (53)$$

and $Ifpu = If/Ifmax \quad - \quad (54)$

Overall efficiency:

$$no = n\ mech\ nele \quad - \quad (55)$$

Saturation

The saturation effect of permitting no further increase in magnetic field strength above a certain field current value (Figure 2.18) is modelled by modification of the back emf constant K2, where, for no saturation present the back emf is:

$$E = K2\ Ifpu\ n \quad (volts) \quad - \quad (53)$$

With saturation included, the value of the constant K2 changes (decreases) as the field current increases:

$K2 = K2L\ (1 - KS.\ Ifpu^2)$ - (56); where constant K2L is a function of the unsaturated value of K2 and a user input constant KS:

$K2L = K2/(1-KS)$ - (57)

Break speed Variation

Break speed in Figure 2.17 varies due to the increasing IaRa voltage drop in the armature circuit as to increases (Ia)

$Va = E + IaRa$ (volts) - (58)

and $E = K_2\ Ifpu\ n\ b$ (volts) - (53)

If Va and Ifpu are constant at the breakpoint, as Ia increases so b decreases.

$n_b = n_{b2} - To/Tomax\ (n_{b2} - n_{b1})$ (rad/sec) - (59)

Where $_{b1}$ and $_{b1}$ are the break speed constants obtained from the motor map.

Rotor Inertia

Rotor inertia may be input manually if known or can be determined automatically by the motor model using a rate torque/inertia correlation based on empirical data.

Rated torque:

$T_{omnax} = KId^2$ (Bader et al,1977) (Nm)

(Thompson et al.,1974) - (60)

Rotor inertia for a thin disc or cylinder

$Rin = mr_m^2/2 = \rho\Pi\ 1d^2/32\ (Kgm^2)$ - (61)

Using data from Thompson in equation -

$KI = 27350$

Substituting back into equation (60) for;

$$d^2 = T_{omax}/K$$

Gives:

$$Rin = \frac{P \pi}{32KI^2 \ell} \cdot T^2 \qquad (Kgm^2) \quad - \quad (62)$$

Assuming is a constant

$$Rin = 4.9 \times 10^{-6} T_{omax}^2 \qquad (Kgm^2) \quad - \quad (63)$$

User Input Parameters

In order to determine constants for the motor model defining equations, the user must input certain parameters:

Pamax - maximum output shaft power (KW)

Nmax - maximum output shaft speed (rpm)

Vamax - maximum armature voltage (volts)

Vfmax - maximum field voltage (volts)

Pfrac - fraction of motor losses as mechanical loss at the break point.

Rin - rotor inertia (if known) (Kgm^2)

The input parameters shown are fairly self-explanatory with the exceptions of the saturation constant KS and mechanical loss fraction Pfrac. Typical values of KS lie in a range of 0-0.2 (Steven et al.,1983)(Unewehr et al.,1983). However because of the limited data available as regards mechanical losses, several values were compared with low load loss data for the Siemans machine (Van Donger et al.,1981). Figure I.1 shows that a value of 0.05 gives a reasonable comparison with the empirical data.

Calculation of Motor Constants

Maximum torque occurs at bi, so from (46):

$$To_{max} = Po_{max} \cdot 1000 / n_{b1} \quad (Nm)$$

maximum terminal input power at n_{b1} from (51):

$$Pi_{max} = Po_{max} / n_o \quad (Kw)$$

mechanical loss constants at n_{b1} (equation 47)

$$Pm = Pfrac\ (pimax - Pomax) \quad (Kw) \quad - \quad (64)$$

$$C1 = n_{b1}^{1.0} = C2\ n_{b1}^{1.5} = C3\ n_{b1}^{2.0} = Pm/3$$

$$C1 = 1/(Pm\ n_{b1}^{1.0})$$

$$C2 = 1/(Pm\ n_{b1}^{1.5})$$

$$C3 = 1/(Pm\ n_{b1}^{2.0})$$

Motor back emf constant at n_{b2}, using (53):

$$Ia \simeq 0 \ , \quad Ifpu = 1.0$$

$$E = Va_{max} = K2\ Ifpu\ n_{b2} \quad (volts)$$

$$K2 = E / n_{b2}$$

$$K2L = K2\ (1-KS)$$

Maximum airgap power and torque at n_{b1}:

$$Pagmax = Pomax + Pm \quad (Kw)$$

$$Tmax = Pagmax \times 1000 / n_{b1} \quad (Nm)$$

Maximum armature current at n_{b1} - (53) & (50):

$$E = K2\ n_{b1} \quad (volts)$$

$$Iamax = Pagmax \times 1000 / E \quad (Amps)$$

Maximum field power at nbl:

$$PFmax = Pi_{max} - Pa_{max} \quad (KW)$$

$$PFmax = Pi_{max} - Va_{max}Iamax/1000 \quad (KW)$$

Maximum held current at nbl:

$$Ifmax = PFmax\ 1000/VFmax \quad (Amps)$$

Field resistance:

$$Rf = Vfmax/Ifmax: \quad (ohms)$$

Motor torque constant at nbl from (49):

$$Kl = Tagmax/Iamax$$

Calculation of Motor Variables

Motor variables are calculated by dividing the motor performance map into 2 motoring and 2 generating regions shown in Figure 2.17.

Motoring Below the Break Speed Nb

With full field applied in this region

Ifpu = 1.o, If = Ifmax and VF = VFmax.

Back emf (53):

$$E = K2L(1-KS(Ifpu)^2)\ n \quad (volts)$$

Air-gap power:

$$Pag = Po + Pm \quad (KW)$$

Armature current (50):

$$Ia = Pag.1000/E \quad (Amps)$$

Terminal input power (Sl)

$$Pi = Po/\ o \quad (KW)$$

Field power:

$$P_f = VfIf/1000 \quad (KW)$$

Armature Power (52)

$$P_a = P_i - P_f \quad (KW)$$

Armature voltage:

$$Va = Pa.1000/Ia \quad (volts)$$

Motoring Above the Break Speed nb

Full armature voltage is applied in this region, Va = Vamax.

Assume a constant back emf from the break-point. So therefore calculating back emf at the break point where from (59):

$$nb = nb2 - To/Tomax\ (nb2 - nb) \quad (rad/sec)$$

and Ifpul = 1.0; and so from (53)

$$E = K2L\ (1-KS(Ifpu2)^2)\ nb \quad (volts)$$

Back at the operating point:

$$Ifpu = E/(K2\ n)$$

Compare Ifpu with Ifpul and if not equal modify Ifpul and repeat the calculation

Field current and power from (54):

$$If = Ifpu\ Ifmax \quad (Amps)$$

$$PF = (If)^2.Rf/1000 \quad (KW)$$

Terminal input power (51):

$$Pi = Po/n_o \quad (KW)$$

Armature power (52)

$$Pa = Pi - Pf \quad (KW)$$

Armature current:

$$Ia = Pm.1000/Va \quad (Amps)$$

Regenerating Above the break point nb:

Again, full armature voltage is applied in this region, Va= Vamax, and assume a constant back emf from the break point.

The calculation procedure is similar to motoring above the break speed with the exception that terminal power is now defined as the armature power (51):

$$Pi = Pa = Po\ _o\ (KW)$$

Regenerating Below the break point nb:

Full field and armature voltages are applied in this region, Vf = Vfmax, Va = Vamax, IPpu = 1.0 and Ip = Ipmax.

Back emf, using (53):

$$E = K2L.(1-KS(Ifpu)^2)\ n \quad \text{(volts)}$$

Air-gap power:

$$Pag = Po + Pm \quad \text{(KW)}$$

Armature current:

$$Ia = Pag.1000/E \quad \text{(Amps)}$$

Again in this region, terminal input power is defined as the armature power (51):

$$Pi = Pa = Po_{\ o} \quad \text{(KW)}$$

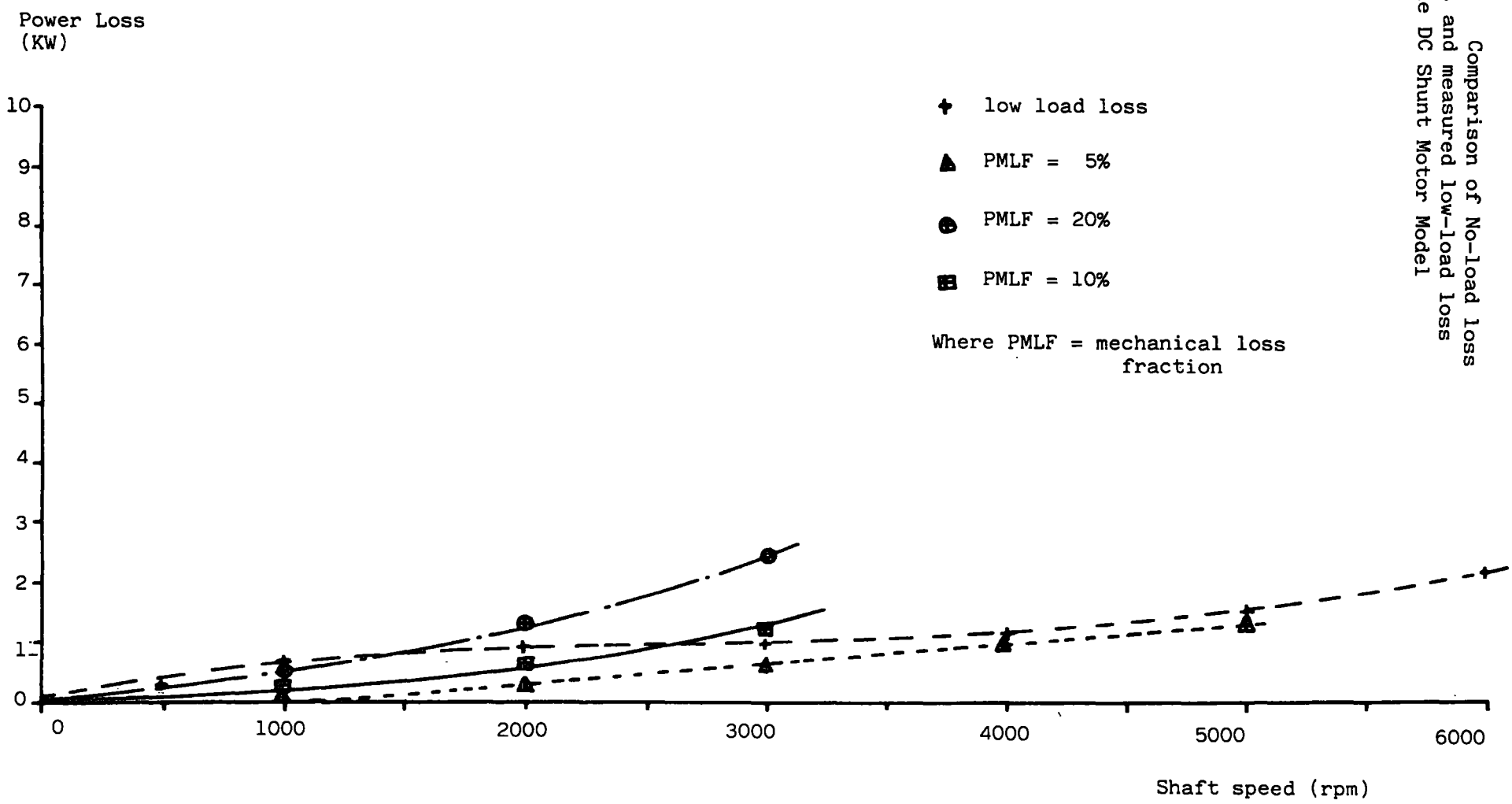

FIGURE I.1: Comparison of No-load loss Assumptions and measured low-load loss data for the DC Shunt Motor Model

APPENDIX II

Vehicle Braking Model

Ideal Braking with an Electric Drive-Train

From the diagrammatic representation of the electric drive-train, shown in Figure 2.32, if the regeneration limit is exceeded:

PI > PImax (modulii)

The power not recoverable by the motor is calculated and reflected back through the drive-train to be removed in the friction brakes (all power terms are negative):

$$PB = \frac{PI - PImax}{\eta_m . \eta_G . \eta_A} \quad (KW) - (65)$$

The power available for regeneration after the friction brakes is therefore:

PW = PDEC - PB (KW) - (66)

Working back through the drive-train, the power available at the motor terminals is recalculated but may not be equal to PIMAX because the reduced power through the drive line may result is significant efficiency changes (η_m, η_G and η_A)

The process is repeated until PI is within a few percent of PIMAX, upon which the system is now stable and the next deceleration time step is selected.

For a motor having no regeneration capability, PI = o and the absorbing loss in the motor becomes the mechanical losses, PML. Now the power not recoverable (or absorbed) by the motor, to be dissipated in friction brakes is when PG > PML :

$$PB = \frac{PG - PML}{\eta_G \ \eta_A} \quad (KW) - (67)$$

Note that no motor efficiency term appears as the power absorbing is at at the motor shaft and not the motor terminals.

Again, the iteration procedure occurs until a stable system results upon which the next deceleration time step is selected.

Ideal Braking with an I.C.Engine Drive Train

Figure 2.33 shows a diagrammatic representation of the conventional i.c. engine drive-train. The power absorbing mechanism in the i.c. engine is through compression braking, pumping losses, friction losses and accessory load. The model only models compression braking and accessory load (see appendix IV).

When the deceleration power available cannot be absorbed by the i.c. engine alone, as with the electric drive train, the amount that cannot be absorbed is reflected back through the drive-line and removed from the total available into friction braking:

$$PB = \frac{PE - PCB}{\eta_{CL} \cdot \eta_G \cdot \eta_A} \qquad (KW) - (68)$$

The power available at the final drive after the friction brakes is now:

$$PW = PDEC - PB$$

As with the electric drive-train the process is continually repeated until a stable operating system results, i.e the deceleration power available PE is equal to the power absorbing capabiltiy of the i.c. engine PCB, upon which the next decleration time step is selected.

I.C. Engine Compression Braking Model

Figure 2.34 shows the P-V diagram during the compression braking process and also the i.c. engine geometry required for the compression braking model.

Instantaneous compression braking torque is:

$$T_{comp\ braking} = PC\ Ar\ \cos \quad (Nm) \quad - \quad (69)$$

Average torque per crank revolution:

$$\bar{T}_{comp\ braking} = \bar{P}c\ A.\ \bar{r} \quad (Nm) \quad - \quad (70)$$

Average Effective Crank Radius

Effective crank radius varies at different points on the crank revolution, but as the crank revolution is made up of 4 equal segments, the variation can be considered over 90° or $\Pi/2$. Therefore average effective crank radius is:

$$\bar{r} = \int_{o}^{\Pi/2} l \cos \theta / (\Pi/2 / d\theta) \quad (m)$$

$$\bar{r} = \frac{2}{\Pi} \int_{o}^{\Pi/2} r \cos \theta d\theta = \left[\frac{2}{\Pi} (r \sin \theta) \right]_{o}^{\Pi/2}$$

$$\therefore \quad \bar{r} = \frac{2}{\Pi} r = 0.637.r \quad (m) \quad - \quad (71)$$

Also piston stroke S = 2r, and cylinder capacity cc = S.A. (cubic centimetres).

Therefore the average compression braking torque:

$$\bar{T}_{comp\ braking} = \bar{P}ccc \times 10^{-6} \ \frac{0.637}{2} = \bar{P}c.cc.0.318 \times 10^{-6} \quad (Nm) \quad - \quad (72)$$

Average Compression Braking Pressure

Average compression braking pressure above the piston:

APPENDIX III

I.C. Engine Compression and Accessory Braking Model

$$\bar{P} = (\bar{P}c_{compression} \quad \bar{P}c_{expansion}) \ (N/m^2) \ - \ (73)$$

From Figure III.1 for the compression stroke, the mean effective pressure:

$$\bar{P}c_{comp} = \frac{W1-2}{Vswept} \qquad (N/m^2) \qquad - \ (74)$$

For a polytropic compression (i.e. not isentropic due to the heat losses through the cylinder walls) the final pressure will be less and the work input greater than for the ideal isentropic case.

For an isentropic process:

Pv^{γ} = constant, where γ = 1.4 for air

For on polytropic process:

Pv^{nc} = constant; where n_c = 1.2 - 1.3 for air

Work done:

$$W_{1-2} = \int pdv = \int \frac{K}{V^{nc}} \, dv = \int_1^2 \frac{K}{V^{nc}} \, dv \quad (J)$$

This reduces to:

$$W_{1-2} = \frac{MR}{(1-nc)} \left(T_2 - T_1 \right) \qquad (J)$$

and if m = ρair & cc x 10^{-6} = $\frac{P1}{RT_1}$ x cc x 10^{-6}

$$W_{1-2} = \frac{P1 \ cc \ x \ 10^{-6}}{(1-nc)} \left(\frac{T2}{T1} - 1 \right) \qquad (J)$$

if V2/v1 = CR (compression ratio)

$$W_{1-2} = \frac{P1 \ cc \ x \ 10^{-6}}{(1-nc)} \left((CR)^{nc-1} - 1 \right) \ (J) \ - \ (75)$$

nc = 1.2 for compression (Wrangham 1951) (Rogers & Mayhew 1978)

Also from Figure III.1 for the expansion stroke

$$\bar{P}c_{expansion} = \frac{W2 - 3}{Vswept} \qquad (N/m^2) \ - \ (76)$$

For a polytropic process less work output and a higher final cylinder pressure and temperature results when compared to the isentropic process due to heat transfer through the cylinder walls.

Work done is therefore:

$$W_{2-3} = \int pdv = \int_2^3 \frac{Kc}{V^{ne}} \, dv \qquad (J)$$

This reduces to:

$$W_{2-3} = \left(\frac{mr}{1-nc}\right) (T3 - T2) \qquad (J)$$

and if $m = P_{gas}.cc \times 10^{-6} = \frac{p3}{T3\ R} \times cc \times 10^{-6}$ (Kg)

$$\therefore \quad W2\text{-}3 = \frac{P3\ cc \times 10^{-6}}{(n_e - 1)} \left(\frac{T2}{T3} - 1\right) \qquad (J)$$

and if $V3/V2 = CR$

$$W2\text{-}3 = \frac{P3\ cc \times 10^{-6}}{(n_e - 1)} \left((CR)^{ne-1} - 1\right) \qquad (J) \quad - \quad (77)$$

$n_e = 1.3$ for expansion and assuming exhaust gas cylinder contents (Wrangham 1951) (Rogers & Mayhew 1978).

Returning to the average compression braking torque equation and assuming a 4-stroke cycle, average torque occurs once every 2 revolutions, so combining equations (72) and (73):

$$\bar{T}_{\substack{comp \\ braking}} = \bar{P}\ c\ comp - \bar{P}c\ exp).\ cc.3.18 \times 10^{-7};$$

and from (74) and (76):

$$\bar{T}_{\substack{comp \\ braking}} = \left(\frac{W1\text{-}2 - W2\text{-}3}{Vswept}\right) .cc.\ 3.18 \times 10^{-7} \ (Nm)$$

Now substituting equations (75) & (77) and if Vswept = cc

$$\bar{T}_{\substack{comp \\ braking}} = \left(\frac{P1}{(n_c - 1)}\right) \left((CR)^{nc-1} - 1\right) - \frac{P3}{(nc-1)} \left((CR)^{ne-1} - 1\right)) \times cc \times 3.18 \times 10^{-7}/_2$$

If nc = ne and P1 = P3, then compression braking torque is zero

Now $P2 = P1\ (CR)^{nc}$ and $P3 = P2\ (\frac{1}{CR})^{ne}$

$\therefore\ P3 = P1\ CR^{(nc - ne)}$

Substituting for nc and ne in equation

$$\bar{T}_{\substack{comp \\ braking}} = Pl.cc.\ 1.59 \times 10^{-7} \left(\frac{1}{0.2}\ ((CR)^{0.3}-1)\right) \frac{-0.1}{-\frac{CR}{0.3}\ ((CR)^{0.3}-1)}$$

(Nm) = (78)

From accessory load power/speed data given in appendix - for the B.L. 3.5 litre engine at maximum speed, approximately 3 KW of engine power is lost to basic accessories out of a total available of 120 KW.

So 2.5% of maximum engine power is lost to accessories.

The power curve is also apparoximately straight (i.e. linear with speed) so load torque can be approximated to being constant with speed.

$$\bar{T}accessory = constant = \frac{0.025\ Pmax}{Rmax}\ (Nm) - (79)$$

Total i.c. engine braking torque is now compression braking torque plus accessory load torque:

$$\bar{T}_{brake} = \bar{T}_{\substack{comp \\ braking}} = \bar{T}accessory\ (Nm) - (80)$$

Braking power is therefore, assuming a 4-stroke cycle, i.e. compression braking torque once every 2 revolutions.

$$\bar{P}_{brake} = \bar{T}_{\substack{comp \\ braking}} . n/2 + \bar{T}accessory.\ n\ (W) - (81)$$

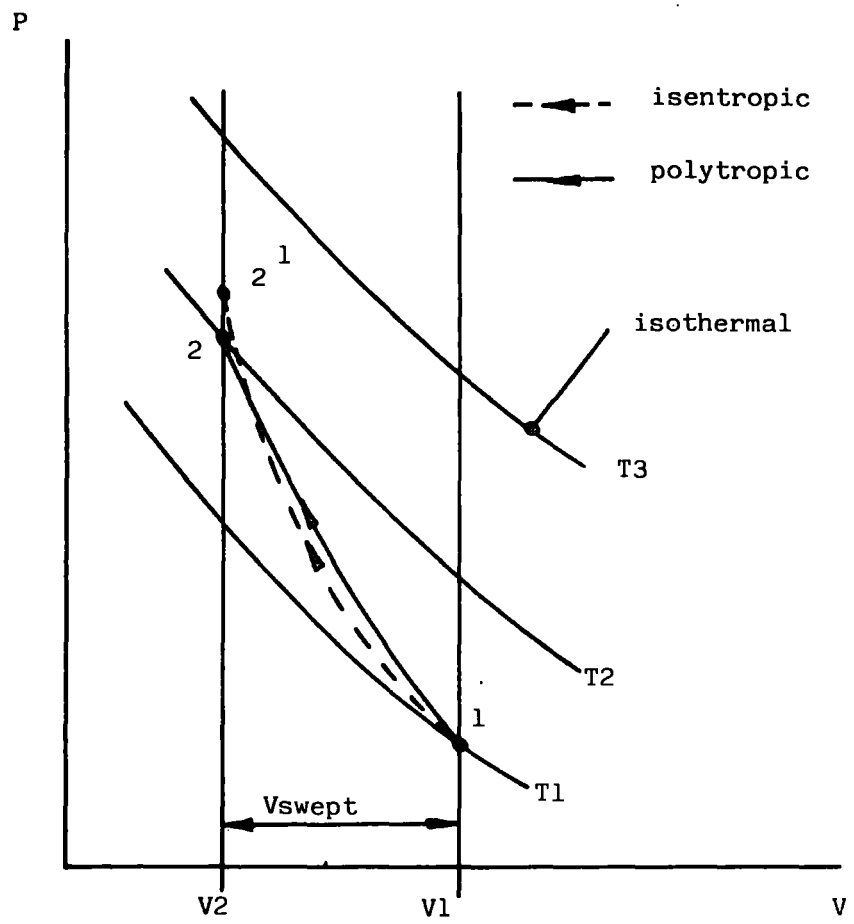

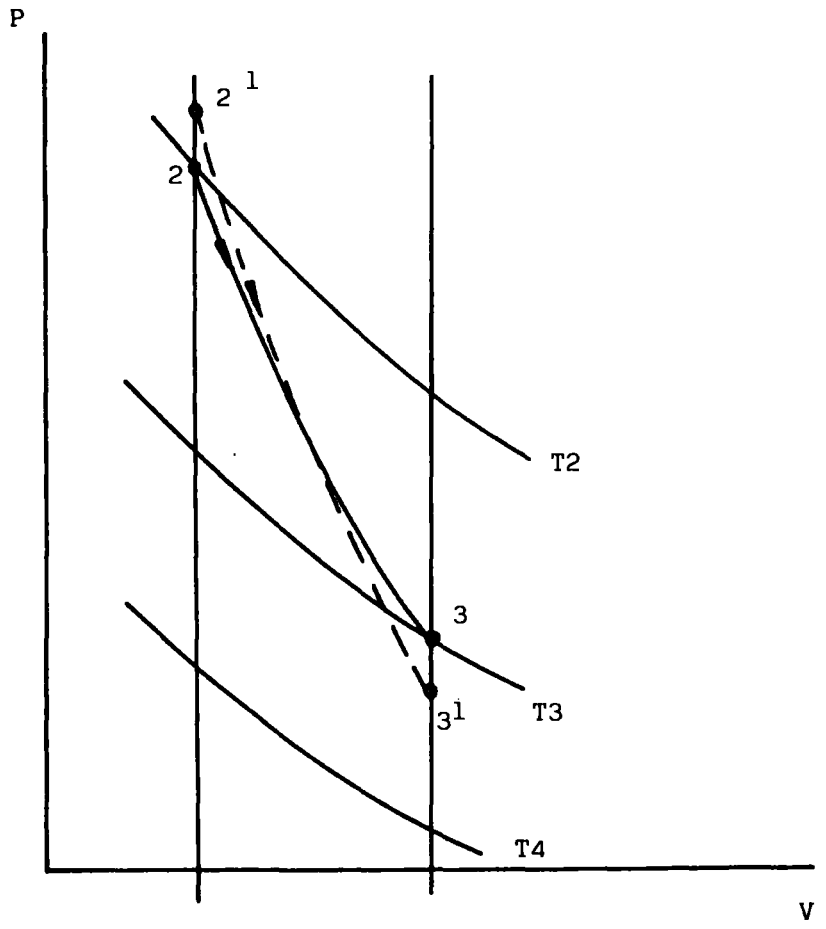

FIGURE III.1 : P-V Diagrams for compression and Expansion

APPENDIX IV

Accessory load for ICE vehicles and electric vehicles

TABLE IV.1

The effect of the idle fuel consumption on the overall fuel consumption, for an average small car, driven over the ECE-15 driving cycle:-

Cycle time - 195 (secs.)
Time at idle - 97 (secs) (= 50%)
Cycle length - 1 (Km)
AV vehicle fuel cons - 35 (mpg) (56 Km/gal)
Idle fuel cons - 1.0-2.0 (pts/hr)

1. Idle fuel cons/cycle (1.0 pts/hr):

$= 0.027 \text{ (pts)} = 3.38 \times 10^{-3} \text{ (gals)}$

2. Idle fuel cons/cycle (2.0 pts/hr)

$= 0.054 \text{ (pts)} - 6.75 \times 10^{-3} \text{ (gals)}$

3. Total fuel cons/cycle:

$= 1/56 \text{ (gals)} = 0.0179 \text{ (gals)}$

4. % of total fuel used at idle:

$$= \frac{3.38 \times 10^{-3}}{17.9 \times 10^{-3}} \times 100 \qquad \frac{6.75 \times 10^{-3}}{17.9 \times 10^{-3}} \times 100$$

$= 19\% - 38\%$

AV = 28.5% of total fuel used at idle

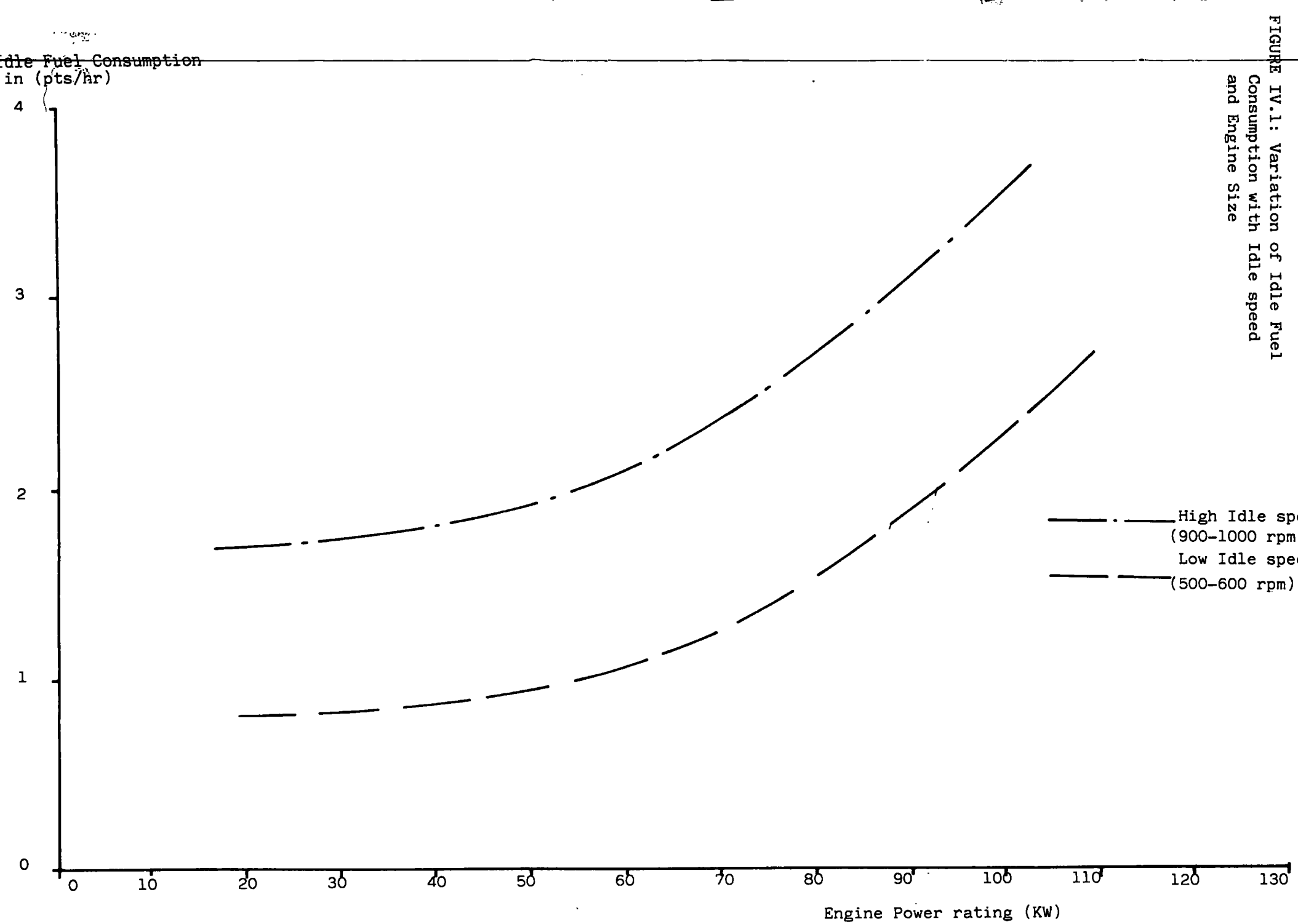

FIGURE IV.1: Variation of Idle Fuel Consumption with Idle speed and Engine Size

FIGURE IV.2: Accessory load versus Engine speed for various types of Accessory Loading

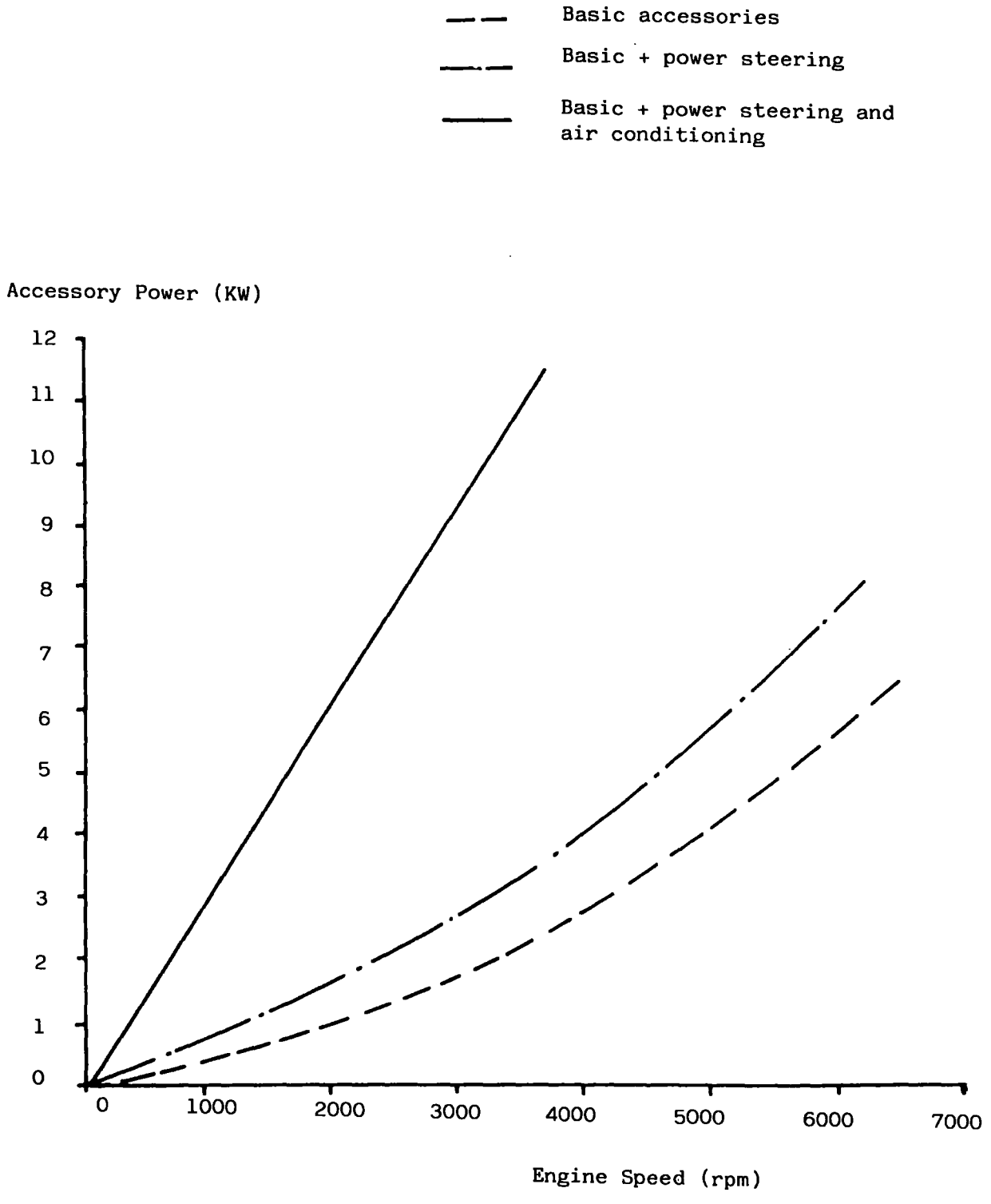

TABLE IV.2: Vehicle Data for the Power SD1 - V8 (B.L.) (Autocar 1981)

Vehicle Weight (kg) - 1360

Drag coefficient - 0.04

Frontal area (m^2) - 1.98

Coefficient of Rolling Resistance - 0.012

Wheel radius (m) - 0.36

Final Drive Ratio - 3.08:1

Final drive type - Bevel

Final Transmission drive ratios - 3.32:1

2.01:1

1.40:1

1.00:1

0.79:1

Engine max.power - 112 KW

Engine max.speed - 5250 rpm

FIGURE IV.3: Percentage of Engine Power to Accessories versus cruising speed

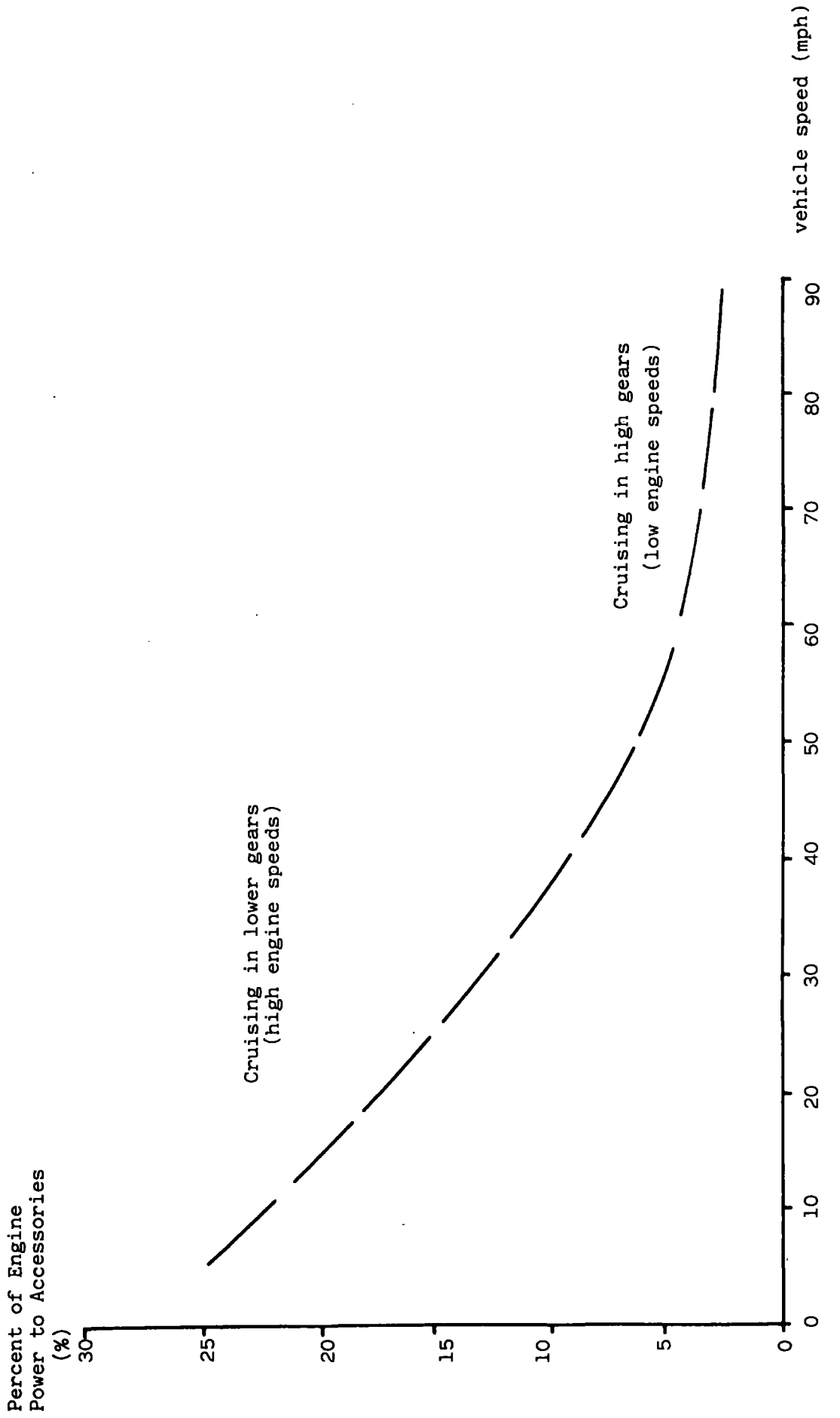

FIGURE IV.4: ETV-1 Accessory load variation with Cruising speed

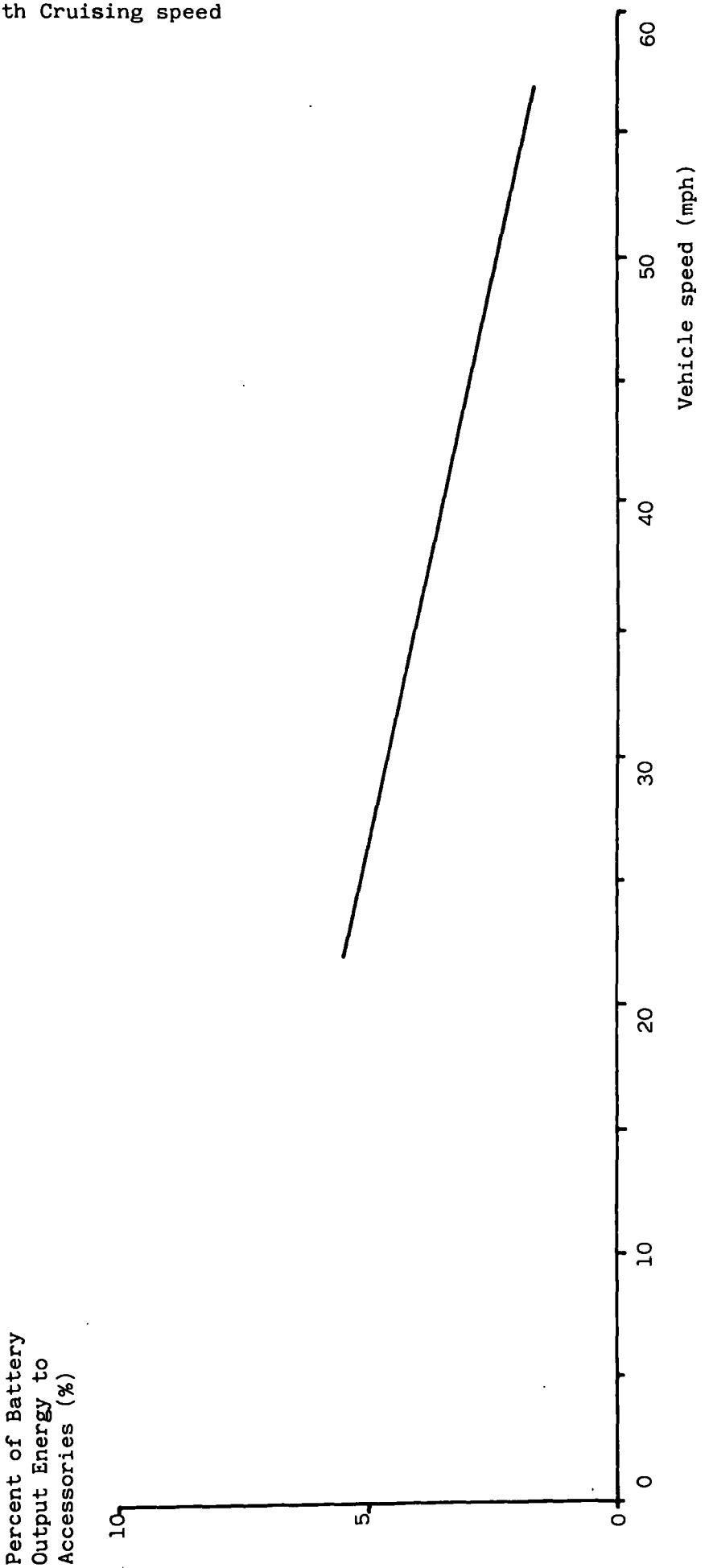

APPENDIX V

I.C.Engined Vehicle Test Weight

TABLE V.1 Vehicle test weight determination

Vehicle reference weight = unladen weight + 100Kg

100 Kg - represents: driver + tools + spares + fuel

driver = 70 Kg
fuel (full tank) = 25 Kg
tools and spare = 5 Kg

If the vehicle reference weight falls into a certain weight range. It is given a class weight:

	Class Weight
< 750 Kg	- 680 Kg
750 - 850	- 800
850 - 1020	- 910
1020 - 1250	- 1130
1250 - 1470	- 1360
1470 - 1700	- 1590
1700 - 1930	- 1810
1930 - 2150	- 2040

The class weight determined is used as the vehicle test weight.

APPENDIX VI

I.C.Engined Vehicle Estimated Aerodynamic Data

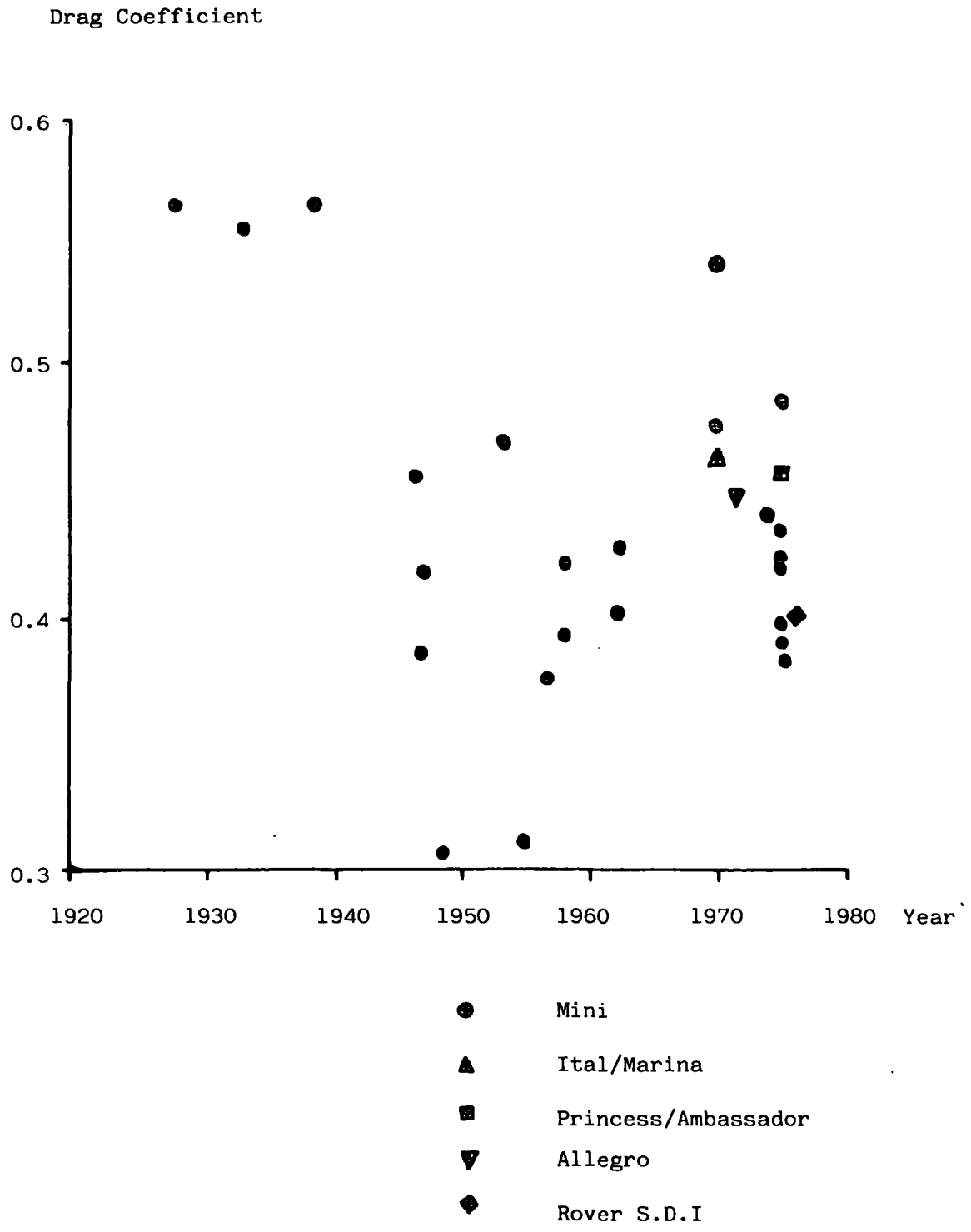

FIGURE VI.1 Vehicle Aerodynamic Development

TABLE VI.1 Correlation Between Vehicle Projected Frontal Area and Vehicle height multiplied by Vehicle Width

Car	Height x width - A (m^2) +	Projected Frontal-B Area (m^2) *	B/A
Metro	2.05	1.73	0.84
Rover	2.40	1.98	0.83
Ambassador	2.41	1.93	0.80

Average value of B/A = 0.824

Thereford Frontal Area Estimates :

$$FA_{est.} = 0.824 \times \text{height} \times \text{width} \ (m^2)$$

\+ Data obtained from Autocar

* Data obtained from B.L.

APPENDIX VII

Battery Depth of Discharge - Related to Discharge Current and Terminal Voltage

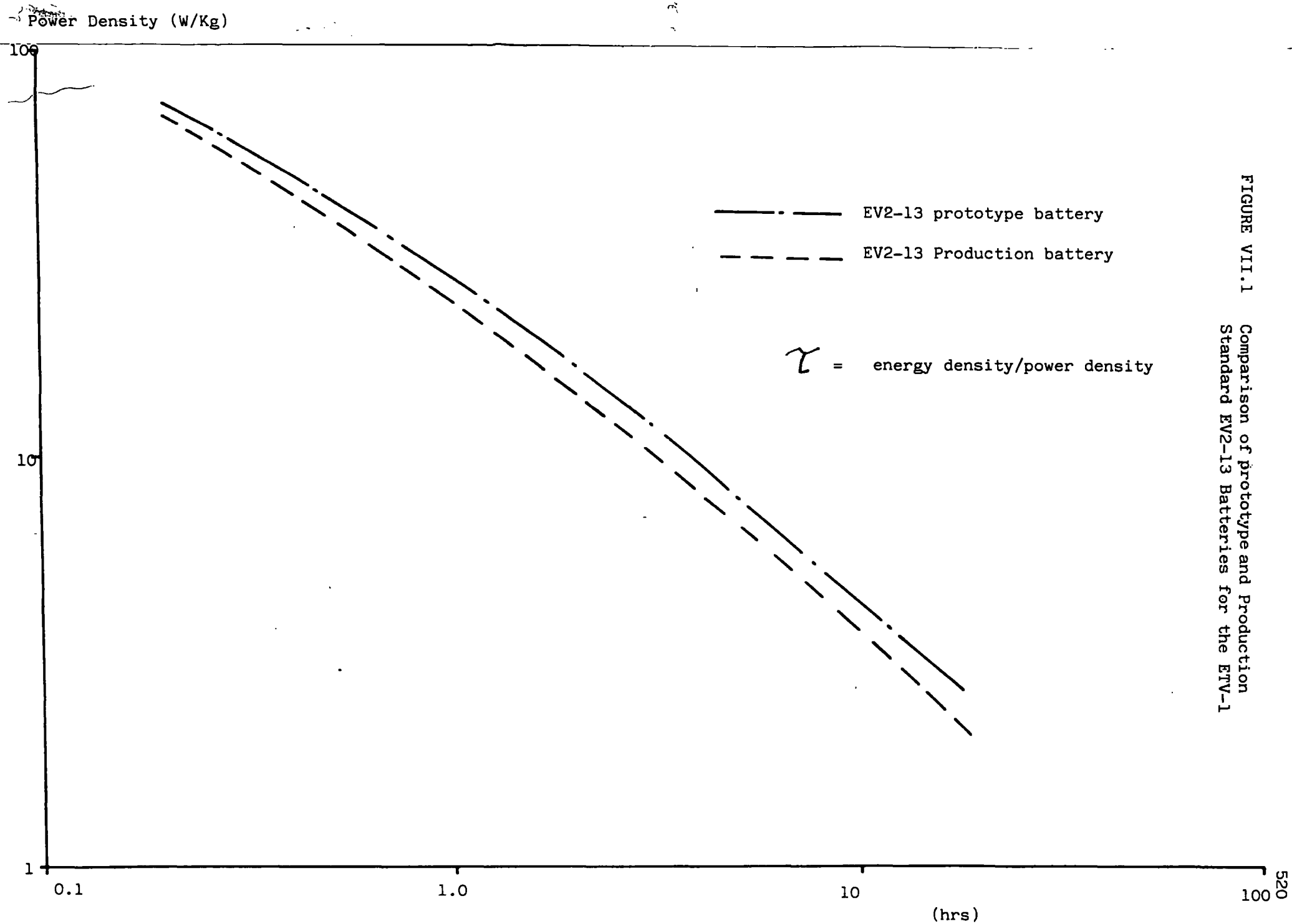

FIGURE VII.1 Comparison of prototype and Production Standard EV2-13 Batteries for the ETV-1

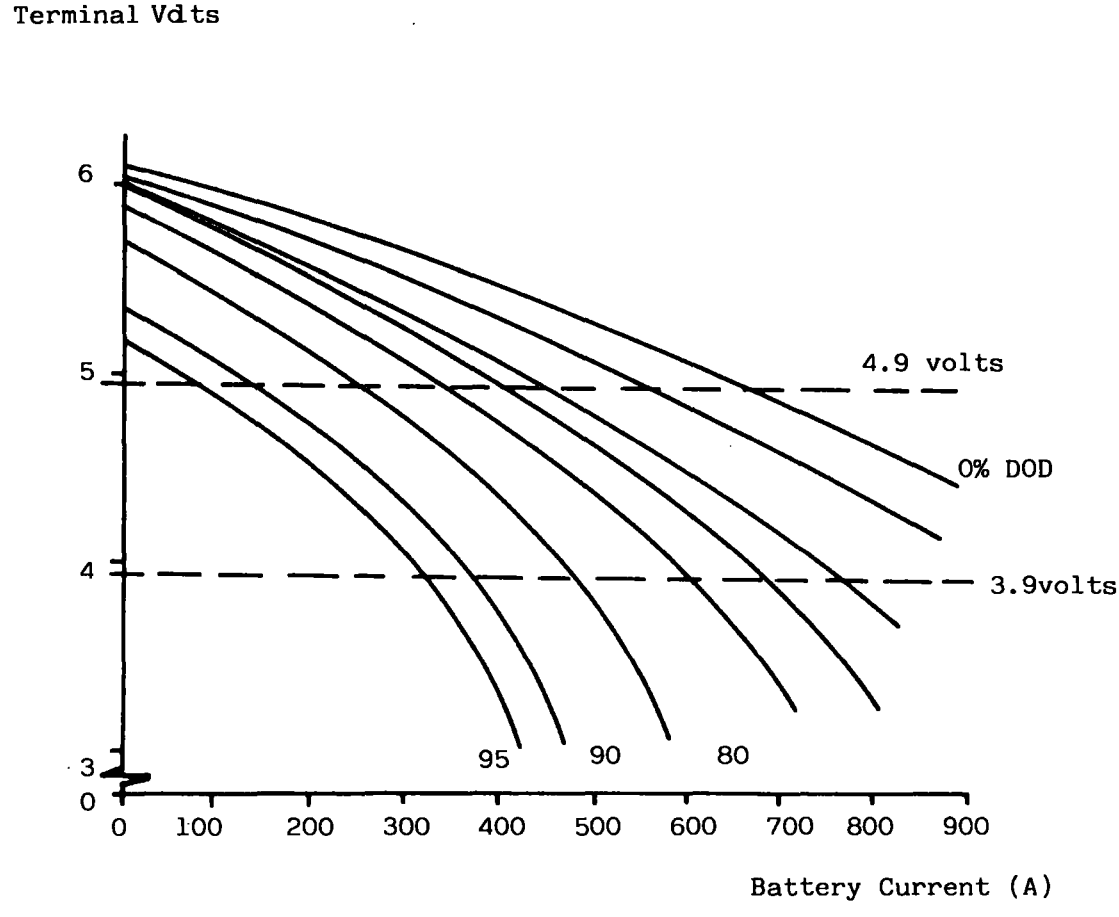

FIGURE VII.2: ETV-1 Battery (EV2-13) Characteristics - prototype

APPENDIX VIII

Comparison of Rolling Resistance Models - JANUS/JPL and ELVEC (Slusser et al)

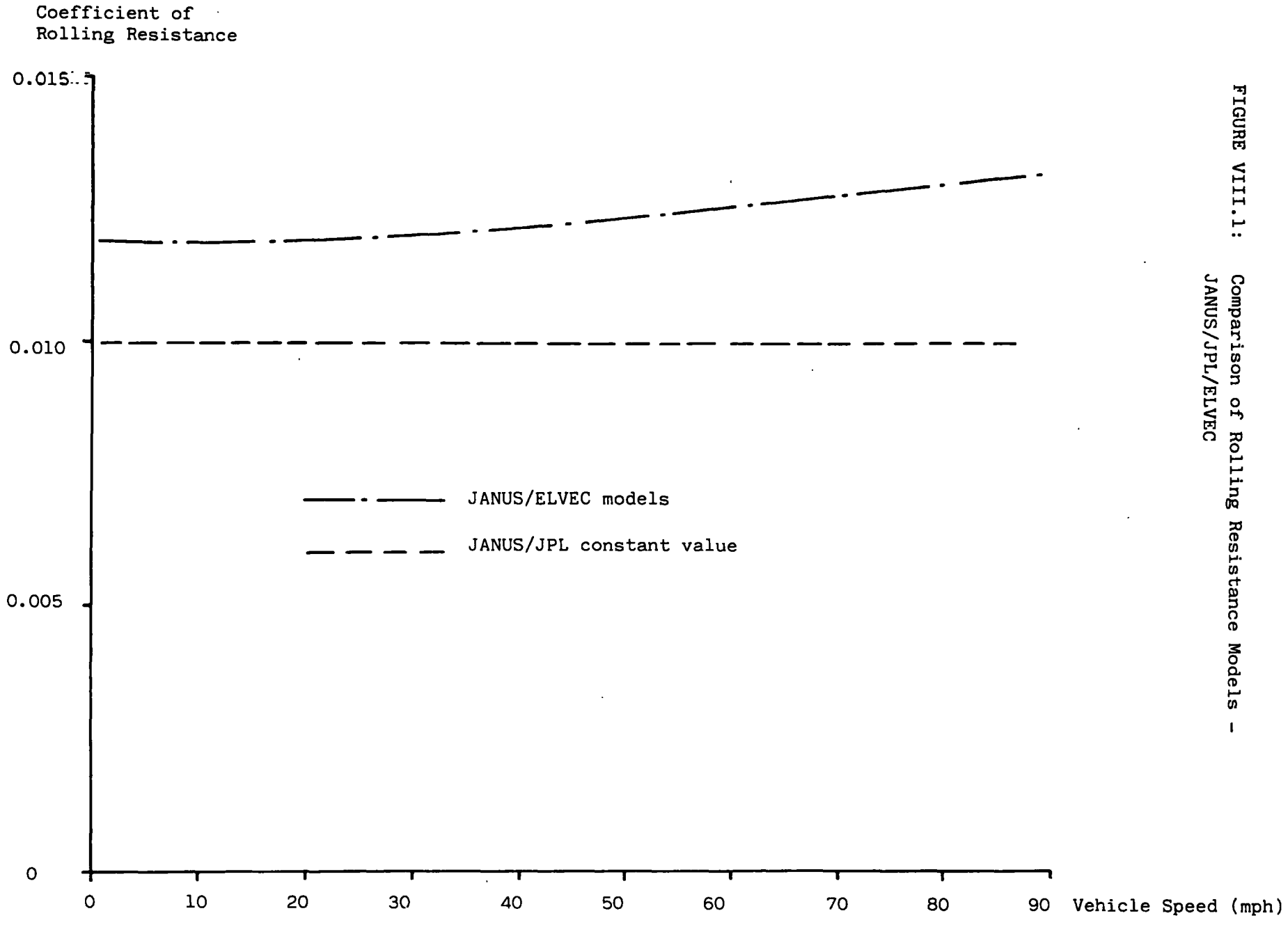

FIGURE VIII.1: Comparison of Rolling Resistance Models - JANUS/JPL/ELVEC

APPENDIX IX

Discrepancies, and Their Effects. Between JANUS and JPL/HEAVY J227aD Driving Cycle Interpretations

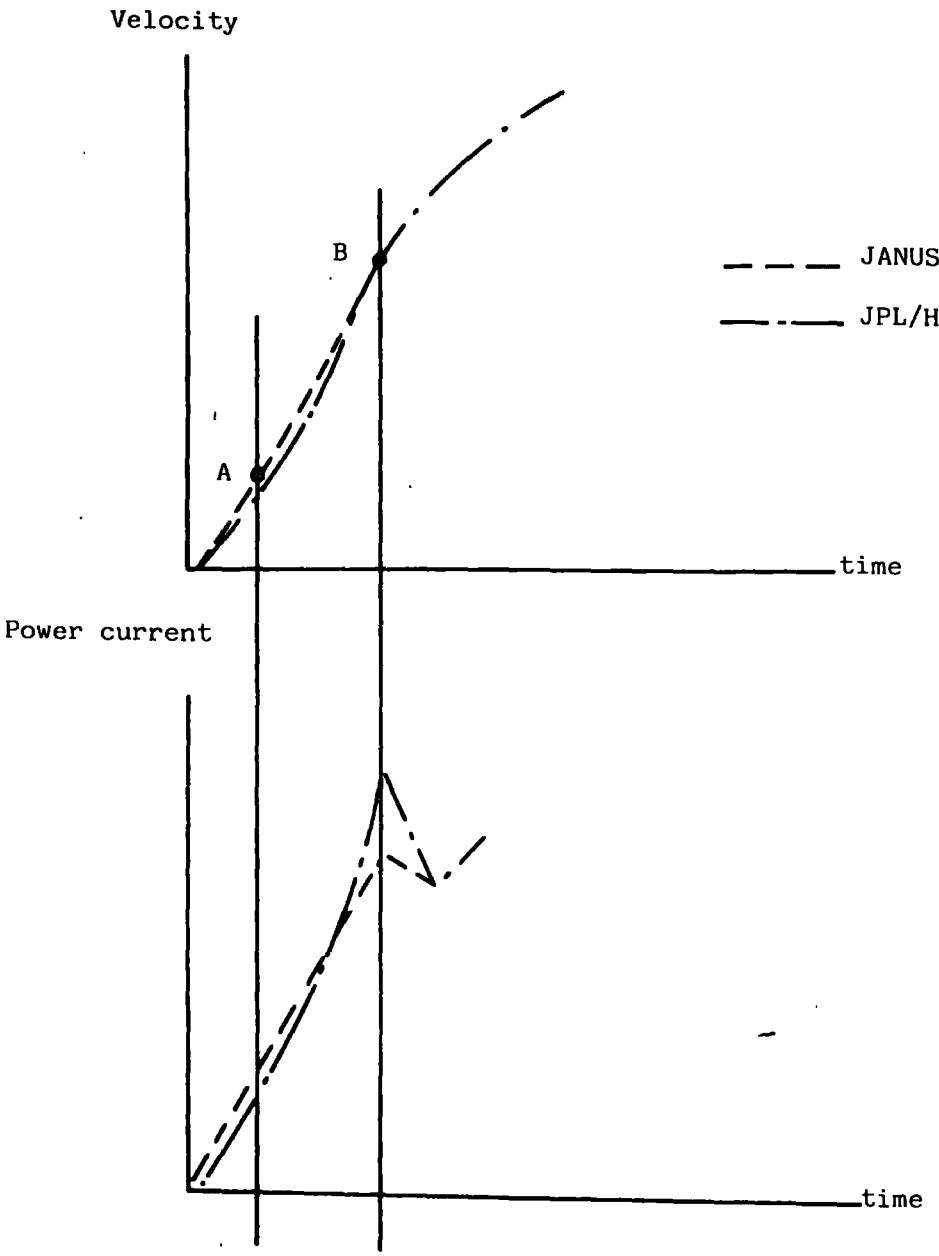

A - 1st occurrence of max. acceleration - JANUS

B - 1st occurrence of max. acceleration - JPL/HEAVY

Power acceleration x velocity

Current power

FIGURE IX.1: The Effect of Altering the position of the Maximum J227aD cycle acceleration

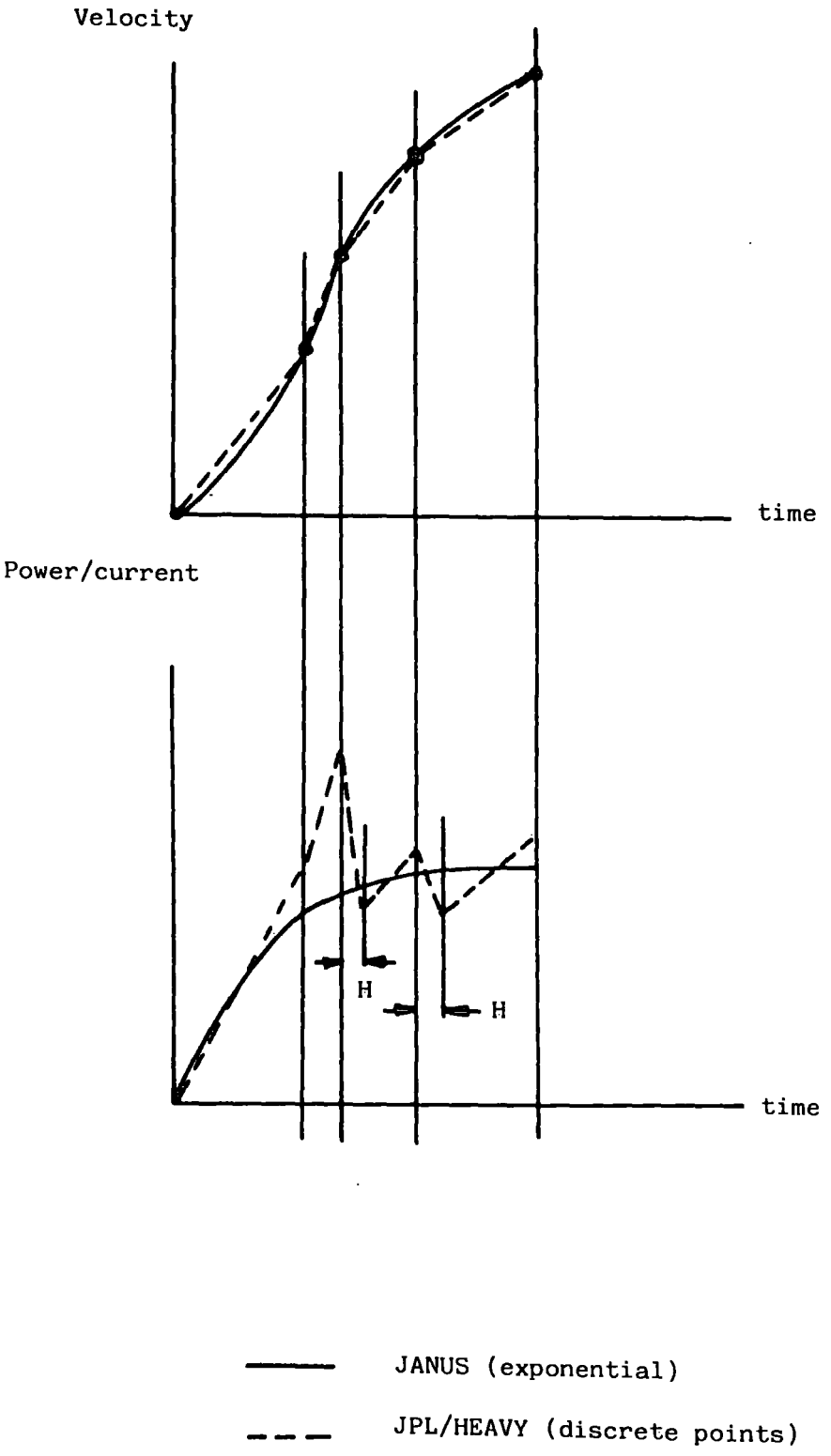

FIGURE IX.2: The Effect of using coarse Data Points to Represent a Smooth Velocity/time profile on the J227aD cycle.